A Stochastic Molecular Mechanism for the Thermodynamic Arrow of Time: Least Action, Equilibrium, and Dissipative Variational Dynamics

By Shipei Hu

hexagon:2611.00819v1

Abstract

How does macroscopic irreversibility emerge from time-reversible Hamiltonian dynamics? Microscopic equations preserve phase volume and are invariant under time reversal, yet a system coupled to a single isothermal reservoir shows a one-way arrow: entropy grows, or equivalently, nonequilibrium free energy decays monotonically. The puzzle is real. To resolve it, we shift from individual trajectories to probability laws and path ensembles; trajectory-level fluctuations remain possible. This shift is necessary because, under Poincaré recurrence, almost every state returns arbitrarily close to its initial state, and the full Hamiltonian ensemble preserves relative entropy against an invariant reference. Ensemble formation alone cannot select a direction. Directed relaxation therefore requires a specified preparation, observation, and effective limit.

The first step links two usually separate variational principles. Least action supplies the reversible Hamiltonian backbone; equilibrium statistical mechanics supplies the free-energy reference geometry needed for relaxation. A gap remains: least action describes orbit extremals, while equilibrium theory characterizes a reference state whose attraction needs dynamical estimates. The missing link is a molecular heat bath with controlled coarse-graining. In the Euclidean construction, harmonic oscillators couple linearly to the core system, and the bath is conditionally equilibrated with respect to the core's instantaneous initial configuration. Shifted bath modes become independent centred Gaussians. This removes the initial-slip force while retaining thermal fluctuations and memory.

With this preparation in hand, reduction proceeds through a fixed order: exact bath elimination gives a generalized Langevin equation with nonlocal memory; a Lorentzian spectrum and continuum limit give exponential memory; a short-memory limit gives instantaneous friction; a small-mass limit gives overdamped diffusion. The order is part of the theorem, not a convention. Crucially, no entropy-production inequality is assumed; it emerges from coarse-graining. On a torus, standard linear coupling fails globally, so periodic paired couplings are used to realize constant mobility. Even then, the dissipative direction is not automatic: it is fixed jointly by conditional preparation and retarded response, not by the bare Hamiltonian.

Having reduced the dynamics to overdamped diffusion, we ask what variational principle selects the probability current. The Onsager–Rayleigh principle minimizes current cost plus signed free-energy rate, equivalent to weighted Wasserstein gradient flow. Full kinetics adds hypocoercivity: reversible transport spreads local friction, while thermal diffusion prevents relative entropy from being preserved. Finally, the Markov data-processing inequality unifies the picture: relative entropy cannot increase. Equilibrium is not a transient endpoint but the persistent reference that organizes kinetic skeleton, dissipation geometry, and path asymmetry; it is the zero of relative entropy with respect to that reference. Thus the arrow is neither postulated nor hidden microscopically; it emerges from preparation, retarded response, and coarse-graining.

Keywords: second law of thermodynamics; stochastic dynamics; minimum dissipation; relative entropy; free energy; hypocoercivity; Bakry-Emery curvature; path space; Poincare recurrence; stochastic Navier-Stokes equations.

2020 Mathematics Subject Classification: 60H10; 60J60; 60J75; 58J65; 82B31; 82C31.

Contents

1. Introduction 3
2. Microscopic Dynamics and Temporal Orientation 15
3. Reduction of the dissipative current 21
4. Microscopic implementation and the emergence of a variational time direction 31
5. A conditional microscopic bridge and the scope of the arrow of time 53
6. Stochastic Dynamics and Variational Thermodynamics 63
7. Entropy Dissipation and Convergence to Equilibrium 81
8. Time Reversal, Path Entropy, and Recurrence 93
9. Infinite-Dimensional Extensions 113
10. Exact Models and Testable Diagnostics 125
11. Stochastic Control and the Common Variational Framework 146
12. A conditional thermodynamic reduction of the regulated mother process 154
13. A concrete four-dimensional interacting regulator and its thermodynamic reduction 158
14. Identifiable finite models, constrained motion, and positive quantum evolution 164
15. Cross-sector response and independent validation 205
16. Three-layer invariant-measure and regulator-limit theorem 256
17. Spatial correlation, inverse geometry, and an interacting mode limit 260
18. Equilibrium, evolution, and the calibration of time 265
19. Conclusion 268
Appendix A. Notation and Variational Identities 272
Appendix B. Supplementary Entropy and Convergence Arguments 278
Appendix C. Infinite-Dimensional Geometry and Fluid Estimates 285
Appendix D. Perturbation Expansion for the Driven Ring 289
Use of AI tools 291
References 292

1. Introduction

An equilibrium law fixes occupation probabilities but does not fix the rate of relaxation. Section 17 gives a spatially correlated coframe example with a nonlinear mode limit and uniform inverse bounds. Section 18 separates thermal populations from the independent observation that calibrates an evolution rate. It shows why physical heat rates require a calibrated clock in addition to a stationary reference. The spatial reference is explicitly chosen, while the heat interpretation continues to use the stated reservoir and physical time.

The second law of thermodynamics is among the most robust empirical regularities in physics. In autonomous isothermal relaxation, it states that the appropriate nonequilibrium free energy cannot increase; convergence to equilibrium requires additional dynamical conditions. Everyday experience offers familiar illustrations of relaxation: hot tea cools, a compressed gas expands, and ink diffuses through still water. Yet this macroscopic picture becomes conceptually delicate at the microscopic level. For a Hamiltonian with the appropriate time-reversal symmetry, reversing a valid microscopic trajectory, including the momenta and any time-odd external parameters, yields another admissible trajectory. If these equations have no preference for one temporal direction, where does the observed irreversibility enter?

This tension between macroscopic relaxation and microscopic reversibility is a foundational problem of statistical physics. It imposes a precise logical requirement: the dynamical premises connecting the two descriptions must be stated without assuming the entropy inequality that is to be derived. We therefore ask under which microscopic, stochastic, and thermodynamic hypotheses an entropy-production inequality follows, and which parts of that implication survive observation and time reversal.

To address this question, we place the probability current at the center of the analysis. A probability current is the local flux of probability through state space. It connects the motion specified by a stochastic equation to the transport of an ensemble. Our framework admits two complementary starting points. In the fundamental interpretation, a stochastic law is specified as the microscopic model, together with its physical time reversal; that law may or may not break stationary reversal symmetry. In the effective interpretation, conservative Hamiltonian mechanics, a specified reservoir preparation, and an ordered sequence of limits produce dissipative dynamics after unresolved variables are eliminated. The latter interpretation tests whether a proposed dissipative structure has a concrete mechanical realization.

We organize the construction around three connected variational ideas. First, the principle of least action provides the reversible dynamical skeleton. Here “least action” means Hamilton’s stationary-action principle, $\delta S = 0$; a physical trajectory need not minimize the action globally. Second, equilibrium supplies the free-energy reference for nonequilibrium evolution. Minimization of the calibrated free energy identifies the Gibbs law; attraction to that law is a separate dynamical

result. Third, the Onsager–Rayleigh principle characterizes the dissipative current by balancing its quadratic cost against the associated free-energy change. This is the meaning of the minimum-dissipation principle used below. It minimizes a Rayleighian, not dissipation alone, and its physical sign is supplied by the prepared reservoir and retarded response in the mechanically realized branch.

The guiding idea can therefore be stated directly: least action provides the variational foundation of microscopic motion, while equilibrium supplies the free-energy reference for nonequilibrium evolution. We connect these structures through a specified molecular reservoir and controlled reduction, obtaining dissipative variational dynamics and identifying when free-energy loss represents total entropy production. The equilibrium reference remains part of the description throughout relaxation; it is not used only to name a possible final state.

The irreversible statement concerns evolving probability laws and forward–reverse path comparisons. It does not assert that every microscopic orbit is individually irreversible. A stochastic entropy production can be assigned to a trajectory once its forward and reverse path laws have been specified, and individual values can fluctuate in sign. Likewise, a dissipative generator can satisfy equilibrium detailed balance even while a nonequilibrium initial law relaxes. These distinctions allow reversible microscopic motion, equilibrium fluctuations, and irreversible relaxation to be treated within the same description.

1.1. *From microscopic reversible motion to the thermodynamic arrow.* The directional content of the second law has its thermodynamic origins in Clausius's work [18] and its statistical interpretation in Boltzmann's work [12]. For autonomous isothermal relaxation at a fixed reservoir temperature $T > 0$, one convenient form is

$$\frac{\mathrm{d}F}{\mathrm{d}t} \leq 0. \tag{1.1}$$

When the energy, entropy, and reservoir heat satisfy the balance specified below, this implies

$$\dot{S}_{\mathrm{tot}} \geq 0. \tag{1.2}$$

The connection is thermodynamic, not merely a consequence of calling an invariant density an equilibrium law. The isothermal free-energy statement also differs from the microcanonical formulation for an isolated system. We specify the reference measure, free energy, and reservoir conditions before applying either interpretation.

The microscopic tension has a simple mathematical form. Let $z = (q, p)$ be a phase-space point and Φ_t an autonomous Hamiltonian flow, defined for the times in question. Its group property gives

$$\Phi_{t+s} = \Phi_t \circ \Phi_s, \qquad \Phi_t^{-1} = \Phi_{-t}. \tag{1.3}$$

For a time-reversal-symmetric Hamiltonian without time-odd external parameters, the physical parity transformation is

$$\Theta(q, p) = (q, -p), \tag{1.4}$$

and reversibility reads

$$\Theta\Phi_t\Theta^{-1} = \Phi_{-t}. \tag{1.5}$$

A time-reversal-even scalar cannot be strictly increasing along every such trajectory and its reverse. Loschmidt's objection [65] therefore concerns the identification of a macroscopic monotonic law with a pointwise property of every microscopic orbit. It does not contradict relaxation observed under a specified preparation.

Poincaré's recurrence theorem [86] and Zermelo's thermodynamic objection [106] raise a different issue. Recurrence applies to a measure-preserving evolution with a finite invariant measure. Liouville's theorem supplies volume preservation for Hamiltonian mechanics, but it does not make the volume of an unbounded phase space finite. A finite invariant probability or a finite-volume invariant region must be supplied separately. Changing from a finite state description to a history space does not, by itself, remove recurrence. Our nonrecurrence result concerns nonequilibrium probability laws under strict entropy contraction; individual trajectories may still revisit previously occupied regions.

These observations lead to the central question:

> *Under which microscopic stochastic and thermodynamic hypotheses does probability evolution have the Lyapunov structure needed for the second law, and how does that structure coexist with conservative motion and well-defined reverse processes?*

The relevant objects are the generator, invariant reference, variable parities, preparation, and path-probability comparison. Specifying them turns the apparent conflict into a set of distinct mathematical questions. The physical motivation is the tension between two descriptions of time. At the microscopic level, a Hamiltonian system can obey an exact reversal law; at the macroscopic level, prepared systems relax and produce entropy. The central task is therefore to identify the precise operation that connects these descriptions rather than to assume that equilibrium alone supplies a time direction. We eliminate unresolved variables in a declared order, fix the reference measure, match mobility with noise covariance, and then derive the free-energy and path-space statements for the observed law.

The unified-field interface asks whether the same regulated state description can also account for the coefficients entering the thermodynamic reduction. Its physical identification requires the stated matching conditions in addition to the thermodynamic proof. The Lorentzian geometric sector supplies constraints and reversible transport; a positive dissipative mobility arises only after the declared reduction and projection. The finite four-dimensional branch developed below makes this distinction concrete. A single shared regulated functional produces the gauge, coframe, and order-parameter contributions, while the Gibbs and entropy identities follow from the positive reduced generator. Thus the interface is tested by an explicit calculation rather than by assigning the same symbol to two unrelated actions.

The resulting architecture has a controlled scope. It proves a finite, regulated thermodynamic reduction under a fixed parameter registry and the stated positivity, coercivity, boundary, and local-detailed-balance assumptions. It does not silently promote that result to a theorem about the complete Lorentzian field or its quantum completion. This distinction is essential: a finite regulator can verify the mechanism while leaving the continuum constraint algebra, removal of the regulator, and construction of the physical Hilbert space open. The standalone stochastic statements are therefore read at their own level, whereas the field interpretation is conditional on the interface hypotheses made explicit below.

Section 14 develops the finite construction further. It gives a response-based inverse map, an explicit energy-scale ambiguity, and a constrained nonlinear example. An alternative symmetric temporal regulator then gives a positive interacting quantum model at fixed spatial resolution. The distinction between this model, physical gravitational constraints, and a spatial continuum limit determines the order of the remaining analysis.

Two further questions make the interface physically testable. First, does a geometric probability law control the inverse coframes that enter observables? A finite covariant logarithmic model answers this question together with an explicit free-energy balance (Section 14.11). Second, does preserving an equilibrium family identify the physical evolution? The time-change calculation shows why the generator and clock must also be matched (Section 14.14). Exact temporal normalization and a finite-time backreaction estimate then quantify two errors that would otherwise be hidden in the interface. Synthetic comparisons use a fixed parameter registry and distinguish transient trajectories from periodic frequency measurements. The resulting statements strengthen the finite thermodynamic connection while specifying the estimates still required for a field limit.

1.2. *Fundamental dynamics and effective reduction.* The fundamental interpretation treats stochastic dynamics as primitive within the chosen model class. The effective interpretation derives a stochastic equation by eliminating unresolved microscopic variables. These routes can give the same reduced equation while assigning different physical meanings to its assumptions.

The Mori–Zwanzig formalism [75] and [108] and analyses of memory in coarse-grained Hamiltonian systems [29] explain why elimination and a Markov limit are separate operations. When only a slow variable is observed, hidden variables can retain information and later return it to the observed system. Accordingly, the exact projected equation generally contains memory and fluctuating forces. Schematically, a resolved observable A_t satisfies

$$\frac{\mathrm{d}A_t}{\mathrm{d}t} = \mathcal{R}(A_t) + \int_0^t K(t-s, A_s)\,\mathrm{d}s + F_t. \tag{1.6}$$

Here K denotes a memory kernel and F_t the fluctuating force defined by the chosen projection; these symbols are local to this schematic equation. A memoryless approximation requires an additional limit or closure argument.

Section 4 supplies a concrete effective realization. A harmonic reservoir is prepared in its canonical distribution conditional on the initial system coordinate. Exact Hamiltonian elimination first produces a memory equation and its fluctuation–dissipation relation. Ordered reservoir, short-memory, and small-mass limits then give the overdamped diffusion. Periodic paired couplings realize the constant-mobility model on a torus. Conditional equilibration here specifies the initial bath distribution; it does not assert that a finite isolated harmonic bath is itself an attractor. The preparation temperature is an input to the construction.

Section 5 identifies the scope of this connection. A finite oscillator gives recurring observed relative entropy, so reversibility alone cannot imply monotone reduced relaxation. The positive bridge theorem states the reservoir and convergence assumptions that do yield the Rayleighian diffusion. A separate symmetry argument shows why time-reversal-invariant premises alone cannot select an absolute temporal orientation. The forward thermodynamic direction in the constructed branch belongs to the preparation and response protocol. Exact reversal retains system–reservoir correlations that are absent when a fresh equilibrium bath is prepared.

The probability-current formulation also makes observation part of the argument. Section 3 proves an exact quadratic contraction, calculates the conditional force left by hidden coordinates, and bounds the resulting defect in observed free-energy dissipation. A current minimum, an instantaneous marginal balance, and an autonomous Markov law are three different results. A hidden Gaussian example shows how information can return to a measured coordinate while the full relative entropy decreases.

1.3. *Main results and their physical interpretation.* The results are organized into four levels. Each adds a conclusion only after the assumptions needed for that conclusion have been supplied. The relative entropy $D(\nu\|\mu)$ measures the difference between a probability law ν and its reference μ: for $\nu = f\mu$, it is $\int f \log f \, \mathrm{d}\mu$, and it is infinite when ν is not absolutely continuous with respect to μ. It is nonnegative and vanishes precisely when the measures coincide.

Level I: Markov contraction. If $(P_t)_{t\geq 0}$ is a Markov semigroup and μ is invariant, then data processing gives

$$D(\nu P_t\|\mu) \leq D(\nu\|\mu)\,. \tag{1.7}$$

This statement requires neither detailed balance nor a differential generator formula. It applies in finite and infinite dimensions, but invariance alone does not identify μ as a thermal equilibrium.

Level II: Differential entropy dissipation. For the diffusion generators considered here, the stated domain, integrability, and chain-rule assumptions refine contraction to

$$\frac{\mathrm{d}}{\mathrm{d}t} D(\nu_t\|\mu) = -\mathcal{I}_\mu(f_t), \qquad \mathcal{I}_\mu(f_t) \geq 0, \tag{1.8}$$

where $\nu_t = f_t\mu$. The functional $\mathcal{I}_\mu$ includes the diffusion coefficients and therefore has units of inverse time. It quantifies the rate at which the law loses relative entropy. Jump processes require their own logarithmic dissipation expression.

Level III: Thermodynamic identification. For a Gibbs equilibrium law μ_{eq}, with energy and temperature fixed independently of the entropy calculation,

$$F[\nu] - F[\mu_{\mathrm{eq}}] = k_B T D(\nu\|\mu_{\mathrm{eq}})\,. \tag{1.9}$$

Thus the equilibrium reference fixes the free-energy minimum, and relative entropy measures the excess above that minimum. Combining Equations (1.8) and (1.9) yields

$$\frac{\mathrm{d}F[\nu_t]}{\mathrm{d}t} = -k_B T \mathcal{I}_{\mu_{\mathrm{eq}}}(f_t) \le 0. \tag{1.10}$$

To identify the right-hand side with physical entropy production, we use a single ideal thermal bath, a time-independent energy function, and no external work, and compatible heat and local-detailed-balance conventions [95], [30], and [100]. With heat positive into the bath, the first law gives $\dot{Q}_{\mathrm{bath}} = -\dot{E}$, and hence

$$\dot{S}_{\mathrm{tot}} = \dot{S}_{\mathrm{sys}} + \frac{\dot{Q}_{\mathrm{bath}}}{T} = -\frac{\dot{F}}{T} = k_B \mathcal{I}_{\mu_{\mathrm{eq}}}(f_t) \ge 0. \tag{1.11}$$

Here $S_{\mathrm{sys}} = -k_B \int \rho \log \rho \,\mathrm{d}x$ uses a fixed reference volume, and kinetic energy is included when momenta are retained. These physical identifications require more than Gibbs invariance. A maintained stationary current can produce heat even though the one-time probability law and its relative entropy remain constant.

Level IV: Convergence and its rate. Free-energy decay does not by itself prove attraction to equilibrium. A separate coercive estimate must prevent entropy from remaining in undamped directions. For example, a logarithmic Sobolev inequality [41], normalized as $\mathcal{I}_{\mu_{\mathrm{eq}}}(f) \ge 2\lambda_{\mathrm{LS}} D(f\mu_{\mathrm{eq}}\|\mu_{\mathrm{eq}})$ with $\lambda_{\mathrm{LS}} > 0$, implies

$$D(\nu_t\|\mu_{\mathrm{eq}}) \le e^{-2\lambda_{\mathrm{LS}} t} D(\nu_0\|\mu_{\mathrm{eq}})\,. \tag{1.12}$$

In kinetic models, thermal noise usually acts directly on momenta but not on positions. Hypocoercivity uses the coupling between this diffusion and conservative transport to obtain relaxation of the full law. For the specified quadratic kinetic branch, an explicit Gaussian factorization gives the optimal finite-time entropy-contraction factor and a computable exponential bound. More general models require their own coercivity or mixing estimates.

Variational characterization of the current. For constant symmetric positive mobility K, the overdamped probability current minimizes the Onsager–Rayleigh functional

$$\mathscr{R}_\rho[j] = \frac{1}{2}\int \frac{j^{\mathsf{T}}\mathsf{K}^{-1}j}{\rho}\,\mathrm{d}x + \int j\cdot\nabla\frac{\delta F}{\delta\rho}\,\mathrm{d}x. \tag{1.13}$$

The first term is a quadratic cost for transporting probability; the second is the resulting free-energy rate under the continuity equation and compatible boundary conditions. At a fixed positive

density, the unique minimizer in the stated current space is

$$j_\star = -\rho \mathsf{K} \nabla \frac{\delta F}{\delta \rho}. \tag{1.14}$$

Indeed, completing the square gives

$$\mathscr{R}_\rho[j] - \mathscr{R}_\rho[j_\star] = \frac{1}{2} \int \frac{(j - j_\star)^{\mathsf{T}} \mathsf{K}^{-1} (j - j_\star)}{\rho} \, \mathrm{d}x.$$

This identity proves the variational statement without assuming entropy monotonicity. Minimizing the quadratic cost alone would give zero current; minimizing the free-energy rate alone, without a cost or a speed constraint, would generally have no finite minimum. The physical statement is the balance of these terms at the calibrated mobility. In the effective branch, it is an equivalent characterization of the derived diffusion.

The constant-mobility formulation connects to Wasserstein gradient flow and the Jordan–Kinderlehrer–Otto minimizing-movement scheme [52], as well as Onsager–Rayleigh formulations [26]. Conservative motion remains in a separate antisymmetric generator component. Hamilton's stationary action, Onsager reciprocal relations [80] and [81], Onsager–Machlup path actions [82] and [68], and Freidlin–Wentzell rate functionals [33] refer to different variational objects. Keeping them distinct preserves the physical meaning of the connection made here.

Relation to previous work. Variational descriptions of irreversible dynamics have several distinct origins. Onsager's reciprocal relations and variational ideas provide a near-equilibrium force–flux description [80] and [81]. Prigogine's minimum-entropy-production principle concerns a particular near-equilibrium stationary regime [88]. Onsager–Machlup and Freidlin–Wentzell theories describe stochastic trajectory likelihoods and small-noise large deviations [82], [68], [33], and [93]. For gradient-drift Fokker–Planck equations, Jordan–Kinderlehrer–Otto identify the dynamics as free-energy gradient flow [52]; related structures are available for discrete Markov chains and jump processes [67] and [28]. The GENERIC framework organizes the reversible and irreversible sectors of nonequilibrium dynamics [39], [84], and [83].

Stochastic thermodynamics connects heat, work, local detailed balance, path-probability ratios, absolute irreversibility, and excess and housekeeping contributions [20], [51], [60], [94], [95], [30], [100], [76], and [54]. These connections require attention to the level of description: local detailed balance can fail after coarse graining even when the reduced dynamics is Markovian [44]. Results for one-dimensional response, stationary diffusions, and jump diffusions also distinguish transport response, path entropy production, and time reversal [35], [21], and [107].

The question pursued here is whether a specified variational dynamics and equilibrium law imply an autonomous isothermal second law, and how that implication is compatible with time reversal and recurrence. The direction of this implication matters. In the variational construction of Vaquero del Pino et al. [101], nonnegative average total entropy production is imposed to obtain constitutive restrictions and generalized fluctuation–dissipation relations. In Theorem 6.17, the

thermally matched mobility and current variational principle are the inputs, and the free-energy dissipation inequality is derived from them. These constructions have different hypotheses and model classes. Mohite and Rieger [74] develop a minimum-action description of discrete-state transition dynamics, relating nonquadratic dissipation to entropy production and fluctuation and uncertainty relations. The diffusion current functional used here has a different domain and a quadratic mobility cost. The present argument connects it to Gibbs invariance, strict contraction of nonequilibrium laws, and the obstruction to an equilibrium-preserving Markov inverse. Separate hypotheses govern convergence, regulator limits, and physical interpretation.

1.3.1. *Mechanical origins and observation.* The mechanical origin of dissipation is a separate question from the variational description of a diffusion already specified. Zwanzig's nonlinear oscillator-reservoir construction gives conditional canonical preparation, a memory equation and its fluctuation–dissipation relation [109]. Our reservoir calculation belongs to that tradition. The paired trigonometric coupling used on the torus also has a one-dimensional antecedent in dissipative ring models [31]. The claims considered here concern the stated matrix realization and the specified sequence of limits, rather than the invention of an oscillator bath or of paired sine and cosine forces.

Microscopic fluctuation costs have also been related to variational dissipation. Adams et al. connect a Brownian-particle large-deviation principle to Wasserstein gradient flow [1]. Mielke, Peletier and Renger identify conditions relating large deviations and generalized gradient structures [72]; Kraaij et al. derive GENERIC structure from a generalized fluctuation symmetry [55]. These works address the origin of thermodynamic structure, not merely an inequality after it has been postulated. They also involve different microscopic classes and do not supply an unrestricted derivation from every reversible mechanical system.

Mielke, Peletier and Zimmer derive a GENERIC system by coupling a finite-dimensional resolved Hamiltonian system to an infinite-dimensional linear bath [73]. Their special compression assumption produces closed projected dynamics and, at positive temperature, an exact multivariate Ornstein–Uhlenbeck bath process. Projection and closure are therefore central to their construction. The present observation calculation asks a complementary question: for a given joint thermal diffusion and a coordinate observation that need not close, which conditional terms remain in the marginal free-energy rate? The answer is the force defect of Theorem 3.3 and its extension including transport in Theorem 3.4.

The conditional-force estimate has a direct quantitative precursor in Legoll and Lelièvre [61]; related vector coarse-graining estimates appear in Duong et al. [27]. Equation (3.20) identifies the shared mean-force term exactly. Consequently, quantitative control of hidden forces is not presented as absent from the preceding literature.

Ding and Cates propose a microscopic dynamical entropy and obtain a second-law implication when the resolved density evolves independently of hidden details, up to a model-dependent autonomy error [25]. Their condition concerns changes of hidden preparation over an evolution interval. Vanishing of an instantaneous conditional force does not establish that property. The distinction is demonstrated below by a stationary Gaussian observation with zero defect at every time and a non-Markov path law. The correspondence between their entropy and our marginal relative entropy is stated only when the temperature and effective energy defining both references agree.

Earlier analyses already distinguish entropy changes under preparation, time reversal, and Markov approximation [69], as well as conserved fine-grained Hamiltonian entropy and irreversible macroscopic entropy [38]. Xing's microcanonical construction supplies another route to stochastic thermodynamic relations under its declared assumptions, including a Markov coarse-grained description [104]. Against this background, the physical question pursued here is how the specified reservoir, variational current, observation and reversal protocol fit together in one model. A general statement that the second law has previously only been assumed would be too broad.

1.4. *Four aspects of time irreversibility.* The probability-law formulation separates four complementary aspects of irreversibility. They address different questions rather than forming a chain in which every property implies the next.

Generator structure and physical reversal. The dissipative part of a generator and the breaking of stationary time-reversal symmetry are distinct. For time-odd variables such as momentum, generalized detailed balance reads $L^{\dagger_\mu} = \Theta L \Theta^{-1}$, with the same boundary and domain conventions on both sides. An equilibrium kinetic process can satisfy this relation while containing friction and thermal noise.

An inverse Markov evolution. If a step strictly decreases finite relative entropy, no μ-preserving positive Markov map can recover the initial law from the final law. Otherwise, applying data processing to that recovery would reverse the strict inequality. The restriction on the reference and recovery class is essential.

Ordering and nonrecurrence of laws. Under strict entropy contraction, a nonequilibrium law cannot return exactly to an earlier law. This concerns an ensemble distribution, not the recurrence of individual trajectories. A stationary law itself is unchanged and is excluded from the strict statement.

Paths and observed histories. Forward–reverse path relative entropy, relative entropy of a moving history, and one-time relative entropy compare different measures. For a fixed finite window of the same Markov process, once the prescribed prehistory has left the window, the history relative entropy equals that of its oldest endpoint. This identity transfers endpoint convergence without an additional history-space decay assumption. Infinite memory and delayed feedback require a

separate construction. Together these distinctions explain the scope in which the classical reversal and recurrence objections are addressed.

1.5. *Applications and physical tests.* The current formulation can be tested wherever a physical model supplies a resolved state, thermal calibration, and an observation protocol. The applications below retain those inputs and ask which identities remain valid after the model is reduced or extended.

Molecular and fluid dynamics. The molecular examples compare relaxation rates with those predicted from the energy, mobility, and bath temperature. In a fluid regulator, only finitely many spatial modes are retained. Matching a projected drift does not suffice: the noise covariance, physical clock, and reservoir balance must also agree with the proposed thermal generator. Section 9.2 treats the stated two-dimensional stochastic Navier–Stokes setting, while Section 14.23 gives a thermal Galerkin counterexample. Its dimension-independent entropy-decay estimate coexists with failure of energy-space tightness. Thus convergence of probability laws at each resolution does not alone control the energy carried by increasingly fine spatial modes.

The unified-field interface. The common-energy programme [50] asks whether one regulated state description can constrain both field dynamics and stochastic transport. In the notation used by that programme, the thermodynamic energy entering the Gibbs law is obtained only after the reference measure has been fixed. More precisely, on a regulated chart with reference density m_r, the identification is

$$S_r = E_r - \theta s_r + C_r, \qquad \pi_r(x) = Z_r^{-1} m_r(x) \exp\left[s_r(x) - \frac{E_r(x)}{\theta}\right] = Z_r^{-1} m_r(x) e^{-S_r(x)/\theta},$$

where C_r is state independent. Thus S_r in the present paper is the energy-normalized reduced master functional, not the unscaled Lorentzian action. In an affine chart with $m_r \equiv 1$, this reduces to the simpler density used in the displayed finite-regulator theorem; otherwise the corresponding reference-volume drift correction must be retained. The function s_r is fixed as part of the regulated state description (for example as a degeneracy or entropy potential); it is not the evolving Shannon entropy of p_t. This prevents the Gibbs reference from depending on the distribution whose dissipation is being evaluated. In the corresponding finite free-energy identity, S_r is the Hamiltonian-like function relative to $m_r \, \mathrm{d}x$; E_r and s_r are not separately varied with the evolving law.

The finite interface is therefore the following conditional map. The positive symmetric part of the master mobility supplies M_r and the fluctuation covariance $2\theta M_r$; a reversible or maintained circulation supplied by the master transport sector is represented by c_r, subject to $\nabla\cdot(\pi_r c_r) = 0$ and the stated boundary condition; and the declared projection, constraint surface, parity map, and physical clock transport these data to the observed process. Section 12 then proves the relative-free-energy decay for that finite generator. The proof uses these matching conditions and does not by itself derive the full gauge-constrained field mobility, its bath, or its continuum limit.

A nonzero circulation has a separate stationary path-entropy rate. The Schwarzschild comparison [49] makes the scope concrete: statistical equilibrium of field labels cannot replace local gravitational constraints or the quantum state needed for radiation. A rotating reservoir also requires energy–angular-momentum work accounting. These are requirements for transferring the thermodynamic statement to a physical field sector, rather than consequences of a shared symbol for the action or the Gibbs density.

Calibration and independent observations. The control and observation sections derive the HJB/Cole–Hopf relations, the stochastic conservation criterion, and the conditions for information projection onto a prescribed drift family. An explicit rank condition is needed for identifiable coefficients. The calibration and holdout observables must use the same physical parameters, reference volume, and clock; agreement after refitting is a different claim. Sampling, discretization, and finite-horizon errors are kept separate [105], [36], [78], and [85].

Stochastic control and observation. Section 11.2 derives an exact cost–generator compatibility identity for a specified stochastic-control realization. It states when a chosen energy, drift, diffusion, and cost describe the same evolution. Compatibility does not uniquely determine a physical cost or eliminate unresolved memory. The observation results then calculate the conditional-force and transport terms omitted by a reduced description. They distinguish fitting a trajectory from predicting an independently observed one with frozen parameters.

Solvable models and numerical comparisons. The Ornstein–Uhlenbeck model, optical-trap quench, and driven ring in Section 10 connect the abstract quantities to an evolving variance, a heat balance, and a maintained current. The coupled realization in Section 14.22 uses the same mechanical coefficients at equilibrium and under heat transport. Section 15.31 proves boundary inaccessibility, invariance, and entropy convergence for a coupled positive-coordinate diffusion; an added circulation preserves its stationary law but changes path-reversal entropy. Numerical data generated from these models are synthetic. They test the stated calculations and finite-resolution predictions.

1.6. *Organization of the paper.* The remainder of the paper is organized as follows. We first establish the microscopic and observational setting. Section 2 distinguishes the orientation of a dynamical law from reversal of a prepared experiment and relaxation of its probability distribution. Section 3 then studies what an observer retains after hidden variables are eliminated: it derives the contracted current cost, the conditional-force and transport defects, and the additional condition needed for an autonomous observed process.

With these distinctions in place, Section 4 constructs the Hamiltonian system–reservoir model and follows its exact memory equation through the ordered bath-spectrum, short-memory, and small-mass limits. Section 5 collects the assumptions and states the resulting conditional bridge,

including the periodic realization on the torus and the role of the preparation in selecting a forward description. The stochastic law obtained in this way becomes the starting point for the thermodynamic analysis.

Section 6 develops the stochastic molecular models, their Gibbs references, and the Onsager–Rayleigh current principle. Section 7 proves entropy dissipation and separates this monotonicity from the further estimates needed for convergence. Section 8 examines time reversal, path-space entropy, maintained stationary currents, and the recurrence objections. Section 9 turns to moving histories and stochastic fluid dynamics, identifying the additional domain and noise conditions needed beyond finite dimensions.

Section 10 makes these structures explicit in solvable models and numerical comparisons. Section 11 then relates the variational description to stochastic control and the associated conservation and balance laws. Section 12 states the compatibility conditions under which the mother process admits the thermodynamic reduction, including the $S_r = E_r - \theta s_r + C_r$ reference-measure identification and the finite-regulator mapping of mobility and circulation. Section 13 then gives a concrete four-dimensional gauge–coframe–order-parameter regulator. It proves the finite Gibbs and entropy identities from one frozen interacting action and records exactly which Lorentzian, continuum, and quantum statements remain outside that theorem. This explicit branch is included to test the interface constructively; it is not counted as a proof of the complete unified field. The oriented coframe barrier branch immediately following it makes the nondegenerate-sector assumption explicit, proves finite inverse-coframe moments at fixed regulator, and quantifies the loss of uniformity when the barrier is removed. The finite extensions in Section 14 then examine identification, local rotation covariance, temporal normalization, observation-scale nondegeneracy, and dynamical response. Section 14.15 supplies the finite-time estimate and its synthetic comparisons. Section 15 develops cross-sector response and independent validation with a fixed parameter registry. Section 16 separately treats existence, uniqueness, attraction, and passage to a regulator limit. Section 19 presents the conclusions and further questions. Appendices A–D provide the notation and the longer variational, entropy, operator, fluid, and driven-ring calculations.

1.7. *Summary and outlook.* The construction connects least-action mechanics, an equilibrium free-energy reference, and dissipative variational dynamics within a specified stochastic molecular description. Its physical content lies in the connection: the reservoir preparation determines the effective response, the current determines the free-energy rate, and compatible heat accounting gives the thermodynamic entropy production. Observation introduces additional conditions because hidden variables can carry both force and memory.

The results also distinguish the questions that remain. In continuum fluid limits, uniform moment estimates, compact containment, generator convergence, and preservation of the reservoir balance are needed in addition to entropy decay. The thermal Galerkin example makes this requirement concrete. For non-Markovian dynamics, a reduced model must retain or control the

memory produced by microscopic elimination; a finite-window observation of a Markov process does not solve that problem. A quantum extension would require a physical quantum generator, a suitable reference state, and a separately justified heat and work balance. In a gravitational application, this would also require a specified quantum state and observation map; equilibrium of classical field labels does not provide them. These questions identify the additional mechanisms and estimates needed to extend the present results while retaining their physical interpretation.

2. **Microscopic Dynamics and Temporal Orientation**

An evolution equation specifies how a preparation changes as a clock is advanced; it answers the dynamical question of how the system changes as physical time progresses. A thermodynamic statement adds a further claim: a particular ensemble quantity decreases along that evolution. Establishing this claim requires the energy, probability law, and dissipative response to be specified together. We first formulate their connection before studying a Hamiltonian reservoir that realizes one of its branches. A stochastic law may be either a microscopic modelling premise or an effective law obtained by eliminating a reservoir. When the generators, their domains, and the initial laws agree and the evolution is uniquely defined, these interpretations have the same probabilistic consequences but different physical premises. This distinction runs through the section and is developed in Section 2.7.

2.1. *Orientation, Reversal, and Relaxation.* A deterministic equation can contain a dissipative direction. For example, $\dot{x} = -M\nabla U(x)$ with $M = M^{\mathsf{T}} > 0$ gives $\dot{U} = -|\nabla U|_M^2$. The gradient flow therefore moves toward decreasing U. Reversing a nonstationary solution changes the vector field: the reversed orbit does not satisfy the original equation. This observation does not directly determine the reversal of a stochastic equation, because reversed fluctuations contribute a density-dependent drift. The distinction matters even at equilibrium. Deterministic reversal cannot simply be carried over to the stochastic setting.

Let Θ be a measurable involution preserving an invariant probability π, and let $\mathcal{T}f = f \circ \Theta$ be its action on observables. Then $\mathcal{T}^2 = I$ and $\mathcal{T}$ is unitary in $L^2(\pi)$. For a stationary Markov process, the generator of physical reversal is

$$L^{\mathrm{R}} = \mathcal{T}L^{\dagger_\pi}\mathcal{T}, \qquad \Delta_\Theta L = L - L^{\mathrm{R}}. \tag{2.1}$$

These identities concern the appropriate generator domains as well as the formal expressions on a core. They assume that external parameters are held fixed; reversing a magnetic field or another odd external parameter requires the corresponding family of generators.

Generalized detailed balance is $L^{\mathrm{R}} = L$. A nonzero $\Delta_\Theta L$ describes stationary path asymmetry relative to the specified parity and external parameters. We call such asymmetry *intrinsic to the declared stochastic model* when it belongs to its fixed generator rather than its nonequilibrium initial distribution. This terminology describes the fixed model structure rather than a transient

effect of the initial preparation. It does not establish the stochastic model as a fundamental law of nature.

The third property is relaxation of a nonequilibrium ensemble. Drift describes the local motion, stationary path asymmetry compares forward and reversed histories, and relaxation describes the evolution of the ensemble distribution. For example, the scalar Ornstein–Uhlenbeck equation

$$\mathrm{d}X_t = -\gamma X_t\,\mathrm{d}t + \sqrt{2\gamma\theta}\,\mathrm{d}W_t, \qquad \gamma,\theta > 0,$$

has the reversible stationary law $N(0,\theta)$ and contracts relative entropy from nonequilibrium initial laws. Thus microscopic drift, stationary path asymmetry, and thermodynamic relaxation are distinct statements. The stochastic formulation below allows an asymmetry in the generator, but the relaxation theorem does not require it. This example explains why relaxation and stationary reversal breaking must be examined separately.

2.2. *A Thermally Calibrated Microscopic Law.* To obtain a concrete theorem, we work on a flat torus $\mathbb{T}^d$ with its declared coordinate volume. The periodic domain removes boundary fluxes and permits the physical balance to be examined before boundary and nonconfinement issues are introduced. Let U, M, c be smooth, $\theta = k_B T_{\mathrm{bath}} > 0$, and

$$M = M^{\mathsf{T}}, \qquad m_- I \preceq M(x) \preceq m_+ I, \qquad m_- > 0.$$

Here M is a mobility, not the mass matrix used in kinetic equations. Put $\pi = Z^{-1}e^{-U/\theta}$ and require $\nabla\cdot(\pi c) = 0$. In this subsection π is a density relative to coordinate volume; integrals against it define the reference measure. Choose a smooth matrix σ with $\sigma\sigma^{\mathsf{T}} = M$. The Itô equation and its backward generator are

$$\mathrm{d}X_t = [c - M\nabla U + \theta\,\mathrm{div}\,M](X_t)\,\mathrm{d}t + \sqrt{2\theta}\,\sigma(X_t)\,\mathrm{d}W_t, \tag{2.2}$$

$$Lf = [c - M\nabla U + \theta\,\mathrm{div}\,M]\cdot\nabla f + \theta M : D^2 f. \tag{2.3}$$

We use $(\mathrm{div}\,M)_i = \sum_j \partial_j M_{ij}$. All coefficients are independent of the evolving density. Smoothness and compactness give a unique conservative diffusion. On a noncompact space, nonexplosion, normalizability, and integration by parts need separate conditions. Compactness supplies a sufficient setting for the present argument; it is not necessary for every diffusion with the same entropy identity. The Euclidean example in Section 2.6 verifies its own well-posedness and integrability conditions.

The covariance is $a = 2\theta M$. The current in the forward equation is $j_i = b_i\rho - \frac{1}{2}\partial_j(a_{ij}\rho)$. Expanding each term gives

$$\begin{aligned} j_i &= \rho c_i - \rho M_{ij}\partial_j U + \theta\rho\partial_j M_{ij} - \theta(\partial_j M_{ij})\rho - \theta M_{ij}\partial_j\rho,\\ j_\rho &= \rho c - \theta\rho M\nabla\log(\rho/\pi), \qquad \partial_t\rho = -\nabla\cdot j_\rho. \end{aligned} \tag{2.4}$$

The divergence correction is indispensable when M varies in space. At $\rho = \pi$ the current is πc, so the well-posed forward equation establishes invariance. When $c \neq 0$ and all variables are even, the same Gibbs density carries a stationary current and need not describe a thermal equilibrium experiment. This distinction will reappear when the entropy rate is separated into relaxation and maintained circulation.

THEOREM 2.1 (Thermal relaxation from a specified microscopic law). *Under the compact hypotheses above, let ρ_0 be a smooth strictly positive probability density. The resulting densities satisfy*

$$\frac{\mathrm{d}}{\mathrm{d}t} D(\rho_t \| \pi) = -\theta \int \rho_t |\nabla \log(\rho_t/\pi)|_M^2 \, \mathrm{d}x, \tag{2.5}$$

$$\mathcal{F}[\rho] - \mathcal{F}[\pi] = \theta D(\rho \| \pi), \qquad \mathcal{F}[\rho] = \int U \rho \, \mathrm{d}x + \theta \int \rho \log \rho \, \mathrm{d}x, \tag{2.6}$$

$$\frac{\mathrm{d}}{\mathrm{d}t} \mathcal{F}[\rho_t] = -\theta^2 \int \rho_t |\nabla \log(\rho_t/\pi)|_M^2 \, \mathrm{d}x \leq 0. \tag{2.7}$$

The circulation drops out of these identities. For $c = 0$, with an autonomous single thermal reservoir and the heat convention below, the mean total entropy-production rate is $-\dot{\mathcal{F}}/T_{\mathrm{bath}}$. For a maintained circulation, the relaxation rate and the total entropy-production rate must be distinguished.

Proof. Uniform parabolicity on the compact torus preserves smoothness and positivity, and justifies differentiating the entropy on every finite interval. Set $f_t = \rho_t/\pi$. Mass conservation removes the derivative of the linear term in $\rho \log \rho$, giving

$$D'(t) = -\int (\nabla \cdot j_{\rho_t}) \log f_t \, \mathrm{d}x = \int j_{\rho_t} \cdot \nabla \log f_t \, \mathrm{d}x.$$

Substitution of the current yields

$$D'(t) = \int \pi c \cdot \nabla f_t \, \mathrm{d}x - \theta \int \rho_t |\nabla \log f_t|_M^2 \, \mathrm{d}x.$$

The first integral is $-\int f_t \nabla \cdot (\pi c) \, \mathrm{d}x = 0$. Next $\log \pi = -U/\theta - \log Z$ gives $\mathcal{F}[\rho] = \theta D(\rho \| \pi) - \theta \log Z$ and $\mathcal{F}[\pi] = -\theta \log Z$. This proves all three formulas.

For $c = 0$, define the system entropy $S_{\mathrm{sys}} = -k_B \int \rho \log \rho \, \mathrm{d}x$ and the mean energy $E = \int U \rho \, \mathrm{d}x$. In autonomous relaxation with no applied work, the first law reads $\dot{Q}_{\mathrm{bath}} = -\dot{E}$, with heat positive into the reservoir. Hence

$$\dot{S}_{\mathrm{tot}} = \dot{S}_{\mathrm{sys}} + \dot{Q}_{\mathrm{bath}}/T_{\mathrm{bath}} = -\dot{\mathcal{F}}/T_{\mathrm{bath}}.$$

The thermal noise calibration and this energy balance supply the physical interpretation. They are independent of the entropy differentiation. □

2.3. *The Two Operator Decompositions.* The Hilbert-space adjoint and physical reversal answer different questions. The first uses an inner product weighted by the invariant law; the second also

uses the physical parity of the variables. On a common core define

$$L_{\mathrm{s}} = \tfrac{1}{2}(L + L^{\dagger_\pi}), \qquad L_{\mathrm{a}} = \tfrac{1}{2}(L - L^{\dagger_\pi}).$$

These expressions are symmetric and skew symmetric on that core. For (2.3),

$$L_{\mathrm{s}} f = \theta \pi^{-1} \nabla \cdot (\pi M \nabla f), \qquad L_{\mathrm{a}} f = c \cdot \nabla f.$$

$$-\langle g, L_{\mathrm{s}} h \rangle_\pi = \theta \int \nabla g^{\mathsf{T}} M \nabla h \, \pi \, \mathrm{d}x.$$

In contrast, $(L - L^{\mathrm{R}})/2$ and $(L + L^{\mathrm{R}})/2$ are not generally skew symmetric and symmetric in $L^2(\pi)$. For example, equilibrium kinetic Langevin dynamics has a nonzero Hamiltonian transport operator, yet $L^{\mathrm{R}} = L$ under momentum reversal. Its reversal defect vanishes while its Hilbert-space skew part does not. Physical reversibility and Hilbert-space symmetry therefore cannot be substituted for one another. They are not logically unrelated: for all-even variables the physical reverse is precisely the weighted adjoint.

Even Hilbert-space skew symmetry alone does not imply $\langle Af, \log f \rangle_\pi = 0$. The diffusion proof uses the additional fact that $A = c \cdot \nabla$ is a derivation and preserves π:

$$(c \cdot \nabla)(f \log f) = (1 + \log f) c \cdot \nabla f.$$

For the skew-symmetric part of a jump generator this chain rule fails. For instance, on three states with uniform π, let

$$A = \begin{pmatrix} 0 & 1 & -1 \\ -1 & 0 & 1 \\ 1 & -1 & 0 \end{pmatrix}, \qquad f = \tfrac{3}{7}(1, 2, 4)^{\mathsf{T}}.$$

Then $\pi f = 1$ and direct multiplication gives $\langle Af, \log f \rangle_\pi = (\log 2)/7 \neq 0$. Here A is not itself a Markov generator, because some off-diagonal entries are negative. It is the skew part of the valid generator

$$Q = \begin{pmatrix} -4 & 3 & 1 \\ 1 & -4 & 3 \\ 3 & 1 & -4 \end{pmatrix}, \qquad A = \tfrac{1}{2}(Q - Q^{\mathsf{T}}),$$

whose off-diagonal rates are positive and whose row and column sums vanish. Thus the uniform reference is invariant. Jump-process entropy contraction remains valid by data processing, but its differential calculation cannot use this diffusion cancellation.

2.4. *What the Variational Principle Selects.* Let $\mu_\rho = U + \theta \log \rho$, with a fixed reference volume understood inside the logarithm. For smooth positive ρ, take currents in the Hilbert space with norm squared $\int j^{\mathsf{T}} M^{-1} j / \rho$. Completing the square yields

$$\mathscr{R}_\rho[j] = \tfrac{1}{2} \int \frac{j^{\mathsf{T}} M^{-1} j}{\rho} \, \mathrm{d}x + \int j \cdot \nabla \mu_\rho \, \mathrm{d}x,$$

$$= \tfrac{1}{2}\int \frac{|j+\rho M\nabla\mu_\rho|^2_{M^{-1}}}{\rho}\,\mathrm{d}x - \tfrac{1}{2}\int \rho|\nabla\mu_\rho|^2_M\,\mathrm{d}x. \tag{2.8}$$

The unique minimizer is $j_{\mathrm{d}} = -\rho M\nabla\mu_\rho$. There is no prescribed endpoint or prescribed $\partial_t\rho$ in this instantaneous minimization. The transport ρc is added separately. In other words, the principle selects the current that minimizes the Rayleighian for the given density and mobility. It does not minimize the quadratic dissipation term alone, which would select zero current, and it does not prescribe an entire trajectory. Conservative transport requires its own operator, particularly when momentum is retained.

Changing the sign of the entire linear term produces $j = +\rho M\nabla(U+\theta\log\rho)$. Its continuity equation has a negative diffusion tensor and cannot define a positive forward Markov semigroup on arbitrary smooth densities. To test the positive maximum principle, choose a smooth function with a negative-definite Hessian at its maximum. On the period-one torus, for example,

$$\psi(x) = \sum_{i=1}^{d}\cos(2\pi(x_i - x_{0,i})), \qquad L_-\psi(x_0) = 4\pi^2\theta\,\mathrm{Tr}\,M(x_0) > 0.$$

The drift term vanishes at x_0 and the negative diffusion coefficient reverses the sign of the Hessian term. This contradicts the positive maximum principle. A strict maximum alone would not ensure a strictly positive generator value, since its Hessian could vanish. This observation concerns reversal of the *entire* dissipative current. Merely replacing $-M\nabla U$ by $+M\nabla U$ while retaining positive noise still defines a diffusion on the torus, but generally changes its invariant law and fails to dissipate the original free energy. Reversing the force and reversing the entire dissipative current are therefore different operations: the first retains positive diffusion, whereas the second fails the maximum-principle test above.

For all-even variables, the actual nonstationary reverse drift on a window $[0,\tau]$ is

$$b^{\leftarrow}_s = -b + 2\theta\,\mathrm{div}\,M + 2\theta M\nabla\log\rho_{\tau-s}. \tag{2.9}$$

It has positive covariance $2\theta M$. At stationarity this becomes $-c - M\nabla U + \theta\,\mathrm{div}\,M$; in particular the gradient part is unchanged when $c = 0$. Thus choosing a forward stochastic model is not a proof that its stationary law breaks time reversal. Stationary asymmetry is characterized by the declared generator, parity, and path law; a relaxation direction can exist even when that asymmetry vanishes.

2.5. *Relaxation and Maintained Entropy Production.* In the all-even convention, assume the usual finite path-energy and absolute-continuity conditions for a stationary reversal with external forcing held fixed. The drift difference is $2c$. Girsanov's quadratic cost per unit time is therefore

$$e_{\mathrm{path}} = \frac{1}{\theta}\int \pi c^{\mathsf{T}}M^{-1}c\,\mathrm{d}x. \tag{2.10}$$

For a nonstationary density, expansion of the current square gives

$$\frac{1}{\theta}\int \frac{j_\rho^{\mathsf{T}} M^{-1} j_\rho}{\rho}\,\mathrm{d}x = \theta\int \rho|\nabla\log(\rho/\pi)|_M^2\,\mathrm{d}x + \frac{1}{\theta}\int \rho|c|_{M^{-1}}^2\,\mathrm{d}x. \tag{2.11}$$

The cross term is proportional to $\int \pi c\cdot\nabla(\rho/\pi) = 0$. The first term is $-D'(t)$. The second can remain positive at stationarity. Multiplication by k_B gives physical entropy units only when a thermal force and reservoir balance have been supplied. With odd variables one must instead use the parity-correct reverse law; Hamiltonian transport must not be counted as dissipative by this all-even formula. At $\rho = \pi$ the relaxation term is zero, whereas a nonzero smooth circulation gives a positive maintained term. Mere weak convergence of densities to π does not by itself imply convergence of the gradient-dependent dissipation. The displayed decomposition holds under the stated model and reversal conditions.

2.6. *A Finite Model Separating the Statements.* Take $U(x) = |x|^2/2$, $\theta = 1$, $M = \mathrm{diag}(1,2)$, and

$$\Omega = \begin{pmatrix} 0 & 1 \\ -1 & 0 \end{pmatrix}, \qquad B_\omega = -M + \omega\Omega, \qquad \mathrm{d}X_t = B_\omega X_t\,\mathrm{d}t + \sqrt{2M}\,\mathrm{d}W_t.$$

Although the theorem above was stated on the torus, this linear Euclidean example is globally well posed and all Gaussian integrations are finite. Since $B_\omega + B_\omega^{\mathsf{T}} + 2M = 0$, its invariant law is $N(0, I_2)$. For $X_0 \sim N(m_0, I_2)$, independent of future increments,

$$\begin{aligned} m_t &= e^{B_\omega t} m_0, \qquad & D(\rho_t\|\pi) &= \tfrac{1}{2}|m_t|^2, \\ D'(t) &= -m_t^{\mathsf{T}} M m_t, \qquad & e_{\mathrm{path}} &= \omega^2\,\mathrm{Tr}(\Omega^{\mathsf{T}} M^{-1}\Omega) = \tfrac{3}{2}\omega^2. \end{aligned} \tag{2.12}$$

The covariance stays I_2 by its Lyapunov equation. With $\omega = 0$ the stationary law is reversible but nonequilibrium means relax. With $\omega \neq 0$, declaring both coordinates even gives positive stationary path asymmetry. With the energy and mobility fixed, these cases show that relaxation does not require generator-level reversal breaking. Moreover, a process started at its invariant law has no change in its one-time density, even when the circulating model has positive stationary path asymmetry. The example separates these properties; it does not prove that every pair of dynamical properties is logically independent.

2.7. *Physical Interpretation of the Two Starting Points.* Returning to the distinction raised at the beginning of the section, we can now state the physical meaning of the two starting points. The primitive stochastic interpretation takes the complete generator, temperature, parity, and physical clock as model inputs. Its microscopic temporal asymmetry, when present, is tested by (2.1); the free-energy theorem follows from invariance and the positive diffusion form. The reservoir interpretation instead derives a specific diffusion from a Hamiltonian model, preparation, and ordered finite-time limits. Its scope is the specified reservoir class.

Neither interpretation requires a monotonic entropy along each sample path. A relative-entropy inequality orders ensemble laws. Exact reversal of a prepared Hamiltonian system retains hidden correlations, whereas a new canonical preparation resets them. These facts explain why the probability-law theorem can coexist with reversible microscopic trajectories and with trajectory recurrence.

A common local relaxation direction also requires a common physical clock if several sectors are to be compared. Positive calibrated clock changes preserve their orientation, subject to the corresponding change of stationary sampling law. Choosing such clocks is not a proof of a global cosmological time function. The finite theory fixes the thermodynamic implication once its physical inputs are declared; the origin of a universal microscopic clock or a cosmological boundary condition remains a separate physical question. The stochastic molecular framework therefore supplies conditional thermodynamic statements that can be tested within their specified physical preparations.

3. **Reduction of the dissipative current**

Macroscopic measuring instruments typically record only a fraction of the underlying microscopic motion. In molecular dynamics, for instance, we often track a few characteristic slow variables of a large molecule, while many atomic coordinates remain outside the observational window. For the coordinate observations considered here, this loss of information means that the observed probability current is obtained by projecting the microscopic current and integrating over the hidden coordinates.

This raises a question that no static equilibrium density can answer on its own: does minimizing a dissipative Rayleighian before observation give the same current as minimizing its effective counterpart after the hidden coordinates have been eliminated? The question concerns whether coordinate reduction and variational current selection commute. If they do not, the current predicted by the proposed reduced constitutive law differs from the projection of the microscopic current. This is a statement about ensemble currents, rather than an assertion that an individual molecular trajectory minimizes a dissipation functional.

To address this question, we proceed in three steps. First, we solve the contraction of a positive quadratic cost in finite dimensions. For a specified observation map, this determines the effective mobility and the unique minimizing lift. Second, we extend the calculation to current fields on a product torus and identify the conditional force left by hidden coordinates. Third, we derive the observed free-energy balance, including both force and transport defects. A separate generator condition then determines when the observed path law is autonomous and Markovian. The distinction between these questions is essential: an instantaneous variational identity does not determine the law of an entire observed history.

3.1. *Quadratic cost contraction in finite dimensions.* Before considering current fields, it is useful to build a clear algebraic picture. Let $\mathbb{R}^n$ be the microscopic current space, and let $H = H^{\mathsf{T}} > 0$ be its mobility matrix. The quadratic cost of a current J is $\frac{1}{2}J^{\mathsf{T}}H^{-1}J$. An $m \times n$ observation matrix C, with $m < n$, records $j = CJ$. We require C to have full row rank: every direction in the declared observed current space can be represented by a microscopic current.

For a prescribed j, we minimize the quadratic cost over the fibre $\{J : CJ = j\}$. This is a constrained variational problem; its solution does not imply that an arbitrary microscopic current is the minimizing lift. The next identity measures the difference exactly.

Proposition 3.1 (Contraction of a positive quadratic cost). *The effective mobility and unique minimizing lift are*

$$H_{\mathrm{eff}} = CHC^{\mathsf{T}}, \qquad J_* = HC^{\mathsf{T}}H_{\mathrm{eff}}^{-1}j. \tag{3.1}$$

For every J with $CJ = j$,

$$\tfrac{1}{2}J^{\mathsf{T}}H^{-1}J = \tfrac{1}{2}j^{\mathsf{T}}H_{\mathrm{eff}}^{-1}j + \tfrac{1}{2}(J - J_*)^{\mathsf{T}}H^{-1}(J - J_*). \tag{3.2}$$

Proof. For nonzero $v \in \mathbb{R}^m$, full row rank gives $C^{\mathsf{T}}v \neq 0$, so $v^{\mathsf{T}}H_{\mathrm{eff}}v > 0$. The proposed lift has $CJ_* = j$. Writing $J = J_* + K$ gives $CK = 0$ and $K^{\mathsf{T}}H^{-1}J_* = K^{\mathsf{T}}C^{\mathsf{T}}H_{\mathrm{eff}}^{-1}j = 0$. Expanding the square proves the identity and uniqueness. □

The decomposition separates the cost needed to realize the measured current from a nonnegative cost carried by unresolved directions. The latter is lost when one retains only the minimum over the fibre; it is not additional dissipation generated by observation. Nor is this quadratic cost automatically a physical entropy-production rate: that identification requires a thermally calibrated dynamical model.

The separation of costs does not automatically extend to driving forces. If the microscopic force is the pullback $C^{\mathsf{T}}g$ of an observed force g, then $J^{\mathsf{T}}C^{\mathsf{T}}g = j^{\mathsf{T}}g$ on every constraint fibre. Consequently the contracted Rayleighian is

$$\inf_{CJ=j}\{\tfrac{1}{2}J^{\mathsf{T}}H^{-1}J + J^{\mathsf{T}}C^{\mathsf{T}}g\} = \tfrac{1}{2}j^{\mathsf{T}}H_{\mathrm{eff}}^{-1}j + j^{\mathsf{T}}g.$$

Its minimizer is $-H_{\mathrm{eff}}g$. For a general force h, the unconstrained microscopic minimizer projects instead to $-CHh$. Equality with the proposed thermodynamic current therefore requires the separate force-matching condition $CH(h - C^{\mathsf{T}}g) = 0$. Positive quadratic contraction alone does not establish force compatibility.

When C selects a coordinate block, CHC^{T} is the corresponding mobility block. Its inverse is also the Schur complement obtained by eliminating the unobserved block in H^{-1}. A Schur complement of a mobility under a different constraint is a different operation; the constraint must be stated before either formula is used.

3.2. *Contraction along hidden coordinates.* The linear calculation extends to current fields when observation retains some coordinates and integrates out the others. Work on the product torus $\mathbb{T}^m_y \times \mathbb{T}^k_z$, and let $P = (I_m, 0)$ select the observed coordinates. Let $\rho(y,z) > 0$ be smooth, and let $M(y,z) = M(y,z)^{\mathsf{T}}$ be smooth and uniformly positive. Define

$$p(y) = \int \rho(y,z)\,\mathrm{d}z, \qquad \overline{M}_\rho(y) = \frac{1}{p(y)} \int \rho(y,z) P M(y,z) P^{\mathsf{T}}\,\mathrm{d}z.$$

For a microscopic current $J(y,z)$, its observed current is $j(y) = \int PJ(y,z)\,\mathrm{d}z$. Let

$$\Phi_\rho[J] = \tfrac{1}{2} \int J^{\mathsf{T}} M^{-1} J/\rho \;\mathrm{d}y\,\mathrm{d}z.$$

THEOREM 3.2 (Exact current contraction). *For every smooth observed current j,*

$$\inf_{\int PJ\;\mathrm{d}z = j} \Phi_\rho[J] = \tfrac{1}{2} \int j^{\mathsf{T}} \overline{M}_\rho^{-1} j/p \;\mathrm{d}y, \tag{3.3}$$

$$J_*(y,z) = \frac{\rho(y,z)}{p(y)} M(y,z) P^{\mathsf{T}} \overline{M}_\rho(y)^{-1} j(y). \tag{3.4}$$

The minimum is unique in the weighted current space. Moreover,

$$\Phi_\rho[J] - \Phi_\rho[J_*] = \tfrac{1}{2} \int |J - J_*|^2_{M^{-1}}/\rho \;\mathrm{d}y\,\mathrm{d}z.$$

Proof. Uniform positivity passes to $\overline{M}_\rho$. Integrating PJ_* over z gives j. For $K = J - J_*$, the constraint implies $\int PK\;\mathrm{d}z = 0$. The cross term is

$$\int K^{\mathsf{T}} M^{-1} J_*/\rho \;\mathrm{d}y\,\mathrm{d}z = \int \left(\int PK\;\mathrm{d}z \right)^{\mathsf{T}} \overline{M}_\rho^{-1} j/p \;\mathrm{d}y = 0.$$

The same integration gives the stated cost of J_*. Expansion and positivity finish the proof. □

This is an instantaneous contraction at a fixed density. Once j is chosen, its observed density derivative is $-\nabla_y \cdot j$; no independently prescribed hidden density derivative is imposed. If a hidden derivative or an endpoint law is also fixed, the admissible currents form a smaller set and the displayed unconstrained lift need not be admissible. The theorem therefore gives an instantaneous optimum, rather than an optimum over a prescribed density history. Path autonomy and memory introduce further questions beyond this difference in admissible sets.

3.3. *The thermodynamic force left by hidden variables.* Instantaneous contraction determines the least quadratic cost at a given joint density. It does not yet determine whether hidden variables leave a residual force when only the observed density is specified. Let $\pi(y,z) > 0$ be the Gibbs reference density, and write

$$\bar{\pi}(y) = \int \pi(y,z)\,\mathrm{d}z, \quad r(z \mid y) = \rho(y,z)/p(y), \quad s(z \mid y) = \pi(y,z)/\bar{\pi}(y).$$

The exact relative-entropy chain rule is

$$D(\rho\|\pi) = D(p\|\bar{\pi}) + \int p(y) D(r(\cdot \mid y)\|s(\cdot \mid y))\,\mathrm{d}y. \tag{3.5}$$

It follows by inserting $\log(\rho/\pi) = \log(p/\bar{\pi}) + \log(r/s)$ into the full integral. Thus the full relative entropy equals the marginal mismatch plus an average of the conditional mismatch. This decomposition also separates the thermodynamic forces. Define the observed force and the residual hidden force by

$$g = \nabla_y \log(p/\bar{\pi}), \qquad R_\rho(y) = \int r(z \mid y) PM(y,z) \nabla_{y,z} \log(r/s)\, \mathrm{d}z. \tag{3.6}$$

The term R_ρ is determined by the conditional densities and the mobility. Given these quantities it can be computed directly; it is not an entropy-production coefficient fitted after the calculation. Estimating it from observations nevertheless requires information about the hidden conditional distribution.

THEOREM 3.3 (Projected dissipation and its defect). *Suppose the smooth joint density evolves with current*

$$J = \rho c - \theta \rho M \nabla \log(\rho/\pi), \qquad \nabla \cdot (\pi c) = 0.$$

Set $\bar{c}_\rho(y) = \int r(z \mid y) Pc(y,z)\, \mathrm{d}z$. *Then the marginal current and marginal free-energy rate satisfy*

$$j = p\bar{c}_\rho - \theta p \overline{M}_\rho g - \theta p R_\rho, \tag{3.7}$$

$$\frac{\mathrm{d}}{\mathrm{d}t}\{\theta D(p\|\bar{\pi})\} = \theta \int p\bar{c}_\rho \cdot g\, \mathrm{d}y - \theta^2 \int p|g|^2_{\overline{M}_\rho}\, \mathrm{d}y - \theta^2 \int p\, g \cdot R_\rho\, \mathrm{d}y. \tag{3.8}$$

If $\nabla_y \cdot (\bar{\pi}\bar{c}_\rho) = 0$, *then for every* $0 < \delta < 1$,

$$\frac{\mathrm{d}}{\mathrm{d}t}\{\theta D(p\|\bar{\pi})\} \le -\theta^2(1-\delta) I_{\overline{M}_\rho} + \frac{\theta^2}{4\delta} \int p|R_\rho|^2_{\overline{M}_\rho^{-1}}\, \mathrm{d}y, \tag{3.9}$$

where $I_{\overline{M}_\rho} = \int p|g|^2_{\overline{M}_\rho}\, \mathrm{d}y$.

Proof. Differentiate the logarithmic factorization:

$$\nabla_{y,z} \log(\rho/\pi) = P^{\mathsf{T}} g + \nabla_{y,z} \log(r/s).$$

Projecting and integrating the current gives (3.7). Integration of the hidden divergence on the torus gives $\partial_t p = -\nabla_y \cdot j$. Differentiation of the marginal entropy therefore gives $\theta \int j \cdot g$, which is (3.8). Under the weighted-solenoidal condition the transport integral vanishes: $\int p\bar{c}_\rho \cdot g = \int \bar{\pi}\bar{c}_\rho \cdot \nabla(p/\bar{\pi}) = 0$. Finally,

$$|g \cdot R_\rho| \le |g|_{\overline{M}_\rho} |R_\rho|_{\overline{M}_\rho^{-1}} \le \delta |g|^2_{\overline{M}_\rho} + (4\delta)^{-1} |R_\rho|^2_{\overline{M}_\rho^{-1}}.$$

Multiplying by $p\theta^2$ and integrating proves the estimate. □

Conditional equilibrium $r = s$ implies $R_\rho = 0$. In that case $\overline{M}_\rho = \int sPMP^{\mathsf{T}}\, \mathrm{d}z$ depends on the reference law rather than on the evolving marginal. Also $\bar{\pi}\bar{c}_\rho = \int \pi Pc\, \mathrm{d}z$ is divergence-free after integration over hidden coordinates. The marginal instantaneous Rayleighian then agrees exactly with the contracted microscopic one. Conditional equilibrium is a sufficient condition, not a necessary one: the weaker projected force condition $R_\rho = 0$ can also hold. Neither condition is

automatically preserved by the joint dynamics. Conditional equilibrium is therefore not a one-time check that remains valid throughout the experiment; its persistence needs a dynamical argument.

For $\delta = 1/2$ and compatible transport, integration gives the useful finite-window bound

$$\theta D(p_\tau\|\bar\pi) + \frac{\theta^2}{2}\int_0^\tau I_{\overline{M}_{\rho_t}}\,\mathrm{d}t \le \theta D(p_0\|\bar\pi) + \frac{\theta^2}{2}\int_0^\tau\int p_t|R_{\rho_t}|^2_{\overline{M}^{-1}_{\rho_t}}\,\mathrm{d}y\,\mathrm{d}t.$$

This estimate quantifies the accuracy required of a proposed conditional-equilibration or scale-separation argument. Once the conditional force is controlled over the time window, its effect on the observed balance is bounded explicitly.

3.4. *A balance including the transport defect.* Theorem 3.3 isolates the conditional thermodynamic force when the averaged transport preserves the observed reference. That additional transport condition is automatic at conditional equilibrium, but it need not hold away from it. To treat both effects together, average the transport against the reference conditional density first. Define

$$\bar c_{\mathrm{eq}} = \int sPc\,\mathrm{d}z, \qquad A_\rho = \bar c_\rho - \bar c_{\mathrm{eq}}, \qquad B_\rho = R_\rho - \theta^{-1}A_\rho. \tag{3.10}$$

Here A_ρ is the transport change caused by replacing the reference conditional density s with the actual conditional density r. The factor θ^{-1} converts this velocity contribution to the units of R_ρ, so that B_ρ combines the two effects in a single current defect. The subscript eq denotes averaging with the reference conditional law. It does not assert that the joint process satisfies detailed balance: the reference may carry a stationary current.

THEOREM 3.4 (Complete observed balance). *Under the smoothness, positivity and periodic hypotheses of Theorem 3.3, define*

$$F_{\mathrm{obs}} = \theta D(p\|\bar\pi), \qquad I = \int p|g|^2_{\overline{M}_\rho}\,\mathrm{d}y, \qquad E_B = \int p|B_\rho|^2_{\overline{M}^{-1}_\rho}\,\mathrm{d}y.$$

Then $\nabla_y\cdot(\bar\pi\bar c_{\mathrm{eq}}) = 0$, *and*

$$j = p\bar c_{\mathrm{eq}} - \theta p\overline{M}_\rho g - \theta p B_\rho, \tag{3.11}$$

$$F'_{\mathrm{obs}} = -\theta^2 I - \theta^2\int p\, g\cdot B_\rho\,\mathrm{d}y. \tag{3.12}$$

No condition on $\nabla_y\cdot(\bar\pi\bar c_\rho)$ *is needed. For every* $0<\delta<1$,

$$F'_{\mathrm{obs}} \le \theta^2(-I + \sqrt{IE_B}), \tag{3.13}$$

$$F'_{\mathrm{obs}} \le -\theta^2(1-\delta)I + \frac{\theta^2}{4\delta}E_B, \tag{3.14}$$

$$F'_{\mathrm{obs}} \le \frac{\theta^2}{4}E_B. \tag{3.15}$$

These are instantaneous statements. If the hypotheses and integrability hold on $[0,\tau]$, *then*

$$F_{\mathrm{obs}}(\tau) - F_{\mathrm{obs}}(0) \le \frac{\theta^2}{4}\int_0^\tau E_B(t)\,\mathrm{d}t, \tag{3.16}$$

$$F_{\mathrm{obs}}(\tau) + \frac{\theta^2}{2}\int_0^\tau I(t)\,\mathrm{d}t \le F_{\mathrm{obs}}(0) + \frac{\theta^2}{2}\int_0^\tau E_B(t)\,\mathrm{d}t. \tag{3.17}$$

Proof. Since $\bar{\pi}\bar{c}_{\mathrm{eq}} = \int \pi P c\,\mathrm{d}z$, integrate $\nabla\cdot(\pi c) = 0$ over the hidden torus. The integral of its hidden divergence is zero. The remaining observed divergence is precisely $\nabla_y\cdot(\bar{\pi}\bar{c}_{\mathrm{eq}})$. Substitute $\bar{c}_\rho = \bar{c}_{\mathrm{eq}} + A_\rho$ in (3.7) to obtain (3.11). The reference is time independent and mass is conserved, so differentiation and integration by parts give

$$F'_{\mathrm{obs}} = \theta\int j\cdot g\,\mathrm{d}y, \qquad \int p\bar{c}_{\mathrm{eq}}\cdot g\,\mathrm{d}y = \int \bar{\pi}\bar{c}_{\mathrm{eq}}\cdot\nabla_y(p/\bar{\pi})\,\mathrm{d}y = 0.$$

This proves (3.12). Weighted Cauchy–Schwarz gives

$$\left|\int p\,g\cdot B_\rho\,\mathrm{d}y\right| \le \left(\int p|g|^2_{\overline{M}_\rho}\,\mathrm{d}y\right)^{1/2}\left(\int p|B_\rho|^2_{\overline{M}_\rho^{-1}}\,\mathrm{d}y\right)^{1/2}.$$

Apply $uv \le \delta u^2 + v^2/(4\delta)$ to get (3.14). For the last pointwise bound use $-u^2+uv = v^2/4-(u-v/2)^2$ with $u=\sqrt{I}$ and $v=\sqrt{E_B}$. Integration gives (3.16); choosing $\delta = 1/2$ before integration gives (3.17). □

In particular $E_B \le I$ is sufficient for instantaneous observed monotonicity. The condition $B_\rho = 0$ is stronger and is not necessary. If $E_B(t) \le \varepsilon^2$ throughout a time window, the possible increase is at most $\theta^2\varepsilon^2\tau/4$. This ε measures a conditional current defect, with units fixed by E_B. It is not automatically a memory time, a path-space approximation error, or an error in a microscopic limit. Each of those errors requires its own definition and estimate. When $A_\rho = 0$, $B_\rho = R_\rho$ and the previous force estimate is recovered. Under the weaker transport condition of Theorem 3.3, its estimate in terms of R_ρ continues to apply directly, whether or not A_ρ vanishes.

Corollary 3.5 (Bounds from conditional information). *Suppose additionally $M \ge \lambda I$ and $|Pc| \le C_c$ uniformly, with $\lambda > 0$. Put*

$$H_{\mathrm{cond}} = \int pD(r\|s)\,\mathrm{d}y, \qquad J_{\mathrm{cond}} = \int \rho|\nabla_{y,z}\log(r/s)|^2_M\,\mathrm{d}y\,\mathrm{d}z.$$

Then for every $\eta > 0$,

$$E_B \le (1+\eta)J_{\mathrm{cond}} + \frac{2(1+\eta^{-1})C_c^2}{\theta^2\lambda}H_{\mathrm{cond}}. \tag{3.18}$$

Proof. Fix y and write $h = \nabla_{y,z}\log(r/s)$. For any $v\in\mathbb{R}^m$, weighted Cauchy–Schwarz gives

$$|v\cdot R_\rho|^2 = \left|\int r(P^{\mathsf{T}}v)^{\mathsf{T}}Mh\,\mathrm{d}z\right|^2 \le (v^{\mathsf{T}}\overline{M}_\rho v)\int r|h|^2_M\,\mathrm{d}z.$$

Take $v = \overline{M}_\rho^{-1}R_\rho$, treating $R_\rho = 0$ separately, to obtain $|R_\rho|^2_{\overline{M}_\rho^{-1}} \le \int r|h|^2_M\,\mathrm{d}z$. For the transport term, total variation and Pinsker's inequality give

$$|A_\rho| = \left|\int (r-s)Pc\,\mathrm{d}z\right| \le C_c\int|r-s|\,\mathrm{d}z \le C_c\sqrt{2D(r\|s)}.$$

Since $\overline{M}_\rho \geq \lambda I$, integration yields $\int p|A_\rho|^2_{\overline{M}_\rho^{-1}}\,\mathrm{d}y \leq 2C_c^2 H_{\mathrm{cond}}/\lambda$. Finally apply the Hilbert-space inequality $|u-v|^2 \leq (1+\eta)|u|^2 + (1+\eta^{-1})|v|^2$ to $B_\rho = R_\rho - A_\rho/\theta$ and integrate. □

The conditional Fisher term contains observed as well as hidden derivatives. Small conditional entropy alone does not bound those derivatives. A conditional logarithmic Sobolev inequality gives an entropy bound by a Fisher quantity, not the reverse estimate needed to discard J_{cond}. The corollary therefore identifies the derivative control needed to turn a conditional-equilibration assertion into a quantitative observed balance. A small mismatch of conditional densities is not, by itself, enough to make their thermodynamic forces close.

The factor $1/4$ is sharp for the stated information I, E_B. Equality in the two inequalities requires $B_\rho = -2\overline{M}_\rho g$ in the weighted space. An admissible diffusion realizes this equality at an instant, as the next example shows. Thus the bound measures possible observed recovery; it does not assert that a nonzero defect always causes recovery or that the complete system violates its entropy balance.

3.4.1. *A transport defect with no conditional force defect.* The product-torus theorem also holds on Euclidean space when all displayed integrals are finite and integration by parts has vanishing boundary terms. The following Gaussian example has these properties. Set $\theta = 1$, $\pi = N(0, I_2)$, $M = I_2$, and $c(y,z) = (\omega z, -\omega y)$ with $\omega \neq 0$. Then

$$\nabla \cdot (\pi c) = \omega z(-y\pi) - \omega y(-z\pi) = 0.$$

The joint diffusion has drift $(-y + \omega z, -z - \omega y)$ and noise $\sqrt{2}I_2$. For $\rho = N((m_1, m_2)^{\mathsf{T}}, I_2)$, $r = N(m_2, 1)$ and $s = N(0,1)$ do not depend on y. Consequently

$$R_\rho = 0, \quad A_\rho = \omega m_2, \quad B_\rho = -\omega m_2, \quad F'_{\mathrm{obs}} = -m_1^2 + \omega m_1 m_2. \tag{3.19}$$

The covariance stays equal to I_2, since the skew transport cancels from the covariance equation. Meanwhile $m_1' = -m_1 + \omega m_2$ and $m_2' = -m_2 - \omega m_1$, so

$$\frac{\mathrm{d}}{\mathrm{d}t}\frac{|m|^2}{2} = -|m|^2, \qquad I = m_1^2, \qquad E_B = \omega^2 m_2^2.$$

At $m_1 = 1, m_2 = 2, \omega = 1$, the observed rate is $1 = E_B/4$. It is positive despite $R_\rho = 0$, while the full rate is -5. This example does not contradict Theorem 3.3: its additional condition fails because $\partial_y(\bar{\pi}\bar{c}_\rho) = -\omega m_2 y \bar{\pi}$.

3.5. *Connection with conditional mean-force estimates.* The conditional-force term has a direct antecedent in effective molecular dynamics. To make the comparison explicit, take $M = I$ and $c = 0$, and let $\pi = Z^{-1}e^{-U/\theta}$. Denote the potential of mean force by $\mathcal{A}(y) = -\theta \log \int e^{-U(y,z)/\theta}\,\mathrm{d}z$. Differentiating its defining integral gives

$$\nabla_y \mathcal{A} = \int s \nabla_y U\,\mathrm{d}z, \qquad \nabla_y \log s = -\theta^{-1}\nabla_y U + \theta^{-1}\nabla_y \mathcal{A}.$$

Normalization of r gives $\int \nabla_y r \, \mathrm{d}z = 0$. Therefore

$$\theta R_\rho = \int r \nabla_y U \, \mathrm{d}z - \int s \nabla_y U \, \mathrm{d}z. \tag{3.20}$$

Thus in this special case the defect is the instantaneous conditional mean force minus its equilibrium counterpart, divided by θ. Legoll and Lelièvre derive this mean-force discrepancy and a quadratic entropy estimate in their conditional-expectation construction [61]. Vector coarse-graining and quantitative relative-entropy and Wasserstein error estimates for Langevin and overdamped Langevin dynamics are developed by Duong et al. [27]. The conditional-force square and Young estimate are accordingly used here with their prior context. The present formulation records the simultaneous current contraction, general mobility, transport mismatch and separate requirement of path autonomy. These distinctions specify the result used here, while the cited works provide the earlier conditional mean-force and coarse-graining estimates on which the comparison rests.

3.6. *The additional requirement for a Markov law.* A current identity alone does not identify the observed path law. For an autonomous projected diffusion, a sufficient generator condition is

$$L(f \circ P) = (\bar{L} f) \circ P \quad \text{for all smooth } f, \tag{3.21}$$

with a well-posed conservative martingale problem for $\bar{L}$. For a coordinate projection this requires $Pb(y,z) = \bar{b}(y)$ and $Pa(y,z)P^{\mathsf{T}} = \bar{a}(y)$, including the common physical clock. The full martingale problem then gives

$$f(Y_t) - f(Y_0) - \int_0^t \bar{L} f(Y_s) \, \mathrm{d}s$$

as a martingale in the full filtration. Because this expression is adapted to the observed filtration, the tower property makes it a martingale there as well. Uniqueness identifies the law of $Y = PX$ with the claimed Markov diffusion. This proof establishes path-law closure, rather than only equality of one-time Fokker–Planck equations. The stationary example in Section 3.8 explains why this extra step is necessary even when the instantaneous defect vanishes.

3.7. *A hidden variable can restore observed relative entropy.* There is a simple counterexample to inferring marginal monotonicity from full monotonicity. On $\mathbb{R}^2$, put

$$M_* = \begin{pmatrix} 1 & \alpha \\ \alpha & 1 \end{pmatrix}, \quad 0 < |\alpha| < 1, \quad \mathrm{d}X_t = -M_* X_t \, \mathrm{d}t + \sqrt{2M_*} \, \mathrm{d}W_t.$$

The stationary covariance is I_2. Start from $N((0,a)^{\mathsf{T}}, I_2)$, where $a \neq 0$, and observe $Y = X_1$. Then

$$m_1(t) = -ae^{-t}\sinh(\alpha t), \qquad m_2(t) = ae^{-t}\cosh(\alpha t).$$

The full entropy $D_{\text{full}} = \frac{1}{2}(m_1^2 + m_2^2)$ decreases, whereas

$$D_Y(t) = \tfrac{1}{2} a^2 e^{-2t} \sinh^2(\alpha t) \tag{3.22}$$

starts at zero and becomes positive. Here $R_\rho = \alpha m_2$, $g = m_1$, and $\overline{M}_\rho = 1$, so

$$D'_Y(t) = -m_1^2 - \alpha m_1 m_2.$$

This agrees exactly with the defect formula. It shows why the instantaneous marginal free energy can increase even though the complete process is a reversible dissipative diffusion.

The same projection is not a scalar stationary Gaussian Markov process. Its stationary covariance at lag $t \geq 0$ is $C(t) = e^{-t}\cosh(\alpha t)$. A centered scalar stationary Gaussian Markov process with $C(0) = 1$ must satisfy $C(t+s) = C(t)C(s)$: Gaussian regression and conditional independence give this identity. Here the difference is $e^{-(t+s)}\sinh(\alpha t)\sinh(\alpha s)$, which is nonzero for positive s, t. Force defect and memory are therefore both visible in this exact example. The same model displays an increase of marginal relative entropy and a failure of the observed Markov property, with both effects traced to the hidden coordinate.

3.8. *Zero defect does not establish autonomy.* The hidden Gaussian model also distinguishes a statement about a density from a statement about paths. Start that model at its stationary law $N(0, I_2)$, rather than at the displaced law above. At every time $\rho = \pi$, $r = s$, $R_\rho = 0$ and $B_\rho = 0$. The observed density is constant and its relative entropy is zero. Nevertheless its stationary covariance is $C(t) = e^{-t}\cosh(\alpha t)$, and

$$C(2t) - C(t)^2 = e^{-2t}\sinh^2(\alpha t) > 0 \qquad (t > 0). \tag{3.23}$$

For a centered scalar stationary Gaussian Markov process, Gaussian regression gives $\mathbb{E}[Y_{s+t} \mid Y_s] = C(t)Y_s/C(0)$. Taking its covariance with Y_0 and using the Markov property yields $C(s+t) = C(s)C(t)/C(0)$. Equation (3.23) violates this necessary condition, since $C(0) = 1$. Thus even zero defect throughout a stationary experiment does not imply a Markov observed law. Changing the hidden initial displacement while leaving the initial observed marginal fixed also changes its later mean. Independence from hidden preparation is therefore stronger than cancellation of a force at one evolving density. The preceding displaced example shows that a defect can restore marginal relative entropy; the stationary example shows that zero defect does not imply Markovianity. Together they establish the need to check force matching and path autonomy separately, rather than a general logical independence theorem for arbitrary observations.

3.9. *Relation to microscopic dynamical entropy.* For comparison with Ding and Cates [25], take the dimensionless entropy convention $k_B = 1$. For readers unfamiliar with that construction, the comparison concerns the entropy functional on matching model data. Their microscopic dynamical entropy has the form

$$S^{\mathrm{md}} = S_X^G - \beta\langle H_X\rangle + S_Y^\Omega(E).$$

Suppose $\beta = \theta^{-1}$ is fixed, the effective energy used in that definition is H_X, and the observed reference in the present calculation is exactly $\bar{\pi} = Z_X^{-1} e^{-\beta H_X}$. Expansion gives

$$D(p\|\bar{\pi}) = \int p \log p \, \mathrm{d}y + \beta \langle H_X \rangle + \log Z_X, \qquad S^{\mathrm{md}} = S_Y^{\Omega}(E) + \log Z_X - D(p\|\bar{\pi}).$$

For fixed total energy and a fixed bath reference, the first two terms in the last expression are constants. On this common reference the complete-defect estimate implies, for the specified joint diffusion,

$$\frac{\mathrm{d}S^{\mathrm{md}}}{\mathrm{d}t} = \theta \left(I + \int p \, g \cdot B_\rho \, \mathrm{d}y \right) \geq -\frac{\theta}{4} E_B.$$

The correspondence is between functionals with the same energy and reference measure. It does not identify the diffusion with the finite Hamiltonian bath of Ding and Cates. Different strong-coupling energies, varying temperatures, or changing reference measures add terms and require a separate calculation. The autonomy error in their microscopic construction likewise cannot be identified with E_B without a dynamical approximation theorem.

3.10. *Finite baths, exact memory and the limiting balance.* There is a simple consistency check on every microscopic interpretation. Let Φ_t be an invertible Hamiltonian flow preserving a reference probability π_{tot}, and let $\rho_0 = f_0 \pi_{\mathrm{tot}}$ with finite relative entropy. The evolved density ratio is $f_t = f_0 \circ \Phi_{-t}$. A change of variables gives

$$D((\Phi_t)_{\#}\rho_0 \| \pi_{\mathrm{tot}}) = \int f_0 \circ \Phi_{-t} \log(f_0 \circ \Phi_{-t}) \, \mathrm{d}\pi_{\mathrm{tot}} = D(\rho_0 \| \pi_{\mathrm{tot}}). \tag{3.24}$$

Observation can lower this entropy by data processing, but it does not by itself make the observed entropy monotone in time. The reversible oscillator and hidden Gaussian examples illustrate the distinction. Disintegrating the reference over the observed coordinate identifies the unobserved contribution as conditional relative entropy. A product reference is a special case, not a requirement for this chain rule. If the full Hamiltonian relative entropy is constant, a rise in the observed relative entropy is balanced by a fall in that conditional term.

The bath construction takes its continuum-spectrum, short-memory and small-mass limits in the stated order on finite time windows. The entropy identity is proved for the resulting diffusion. Weak path convergence alone does not imply convergence of relative entropy, its time derivative or its dissipation. A transfer of a quantitative entropy statement from a finite bath would additionally need convergence or uniform integrability of the density ratios, control of the relevant conditional gradients, and a stated time interval. Such estimates must precede an interchange of a reservoir limit with an infinite-time limit. Finite-system recurrence and effective-law contraction therefore refer to different evolutions; a limiting theorem must specify their relation.

Within the declared diffusion class, the generator, Gibbs law, current minimization, and entropy balance are connected by the stated proofs. These results concern a specified preparation and effective evolution. Whether a broader class of microscopic systems has the same limit, and whether cosmological boundary data select a universal orientation, are separate physical questions.

3.11. *Limits require an additional theorem.* The exact contractions above do not assert a general Γ-limit. For a sequence of mobilities, density laws, or observation maps, a limiting variational statement needs a specified topology, a liminf inequality, a recovery sequence, and sufficient compactness to pass minimizers. A limiting diffusion additionally needs tightness and identification of its martingale problem. These obligations have different roles.

A conditional limiting argument can transfer an integrated entropy balance when the required convergence is available. Suppose, for fixed times, $\rho_t^n \Rightarrow \rho_t$ and $\pi_n \Rightarrow \pi$, with convergent initial relative entropies, and

$$D(\rho_t^n \| \pi_n) + \int_0^t \mathcal{D}_n(\rho_s^n)\,\mathrm{d}s \le D(\rho_0^n \| \pi_n).$$

If the integrated dissipation has a liminf bound by a nonnegative limiting functional, joint lower semicontinuity of relative entropy yields

$$D(\rho_t \| \pi) + \int_0^t \mathcal{D}(\rho_s)\,\mathrm{d}s \le D(\rho_0 \| \pi).$$

Indeed, apply the liminf to the nonnegative left-hand terms and use the convergence of the right-hand side. Equality of entropy derivatives requires stronger convergence of the dissipation, not merely weak path convergence. The Hamiltonian limits established later determine a specific limiting generator; their entropy identity is then proved for that limiting generator on its own regularity domain.

4. **Microscopic implementation and the emergence of a variational time direction**

This section develops the reversible-reservoir interpretation introduced in Section 2. The underlying Hamiltonian equations retain their physical time-reversal symmetry. The effective diffusion is obtained from a specified initial preparation and an ordered reduction of the unresolved variables.

The appearance of a negative gradient drift does not by itself imply stationary time-reversal breaking. The current-reduction results of Section 3 also show why a static equilibrium density does not determine an autonomous observed law. A microscopic realization must specify four related inputs: the system–reservoir coupling, the initial conditional bath distribution, the response spectrum, and the scales on which memory and momentum are removed.

We use a system coupled to unresolved harmonic oscillators. Their initial coordinates and momenta are sampled from a conditional canonical law, while the full evolution remains Hamiltonian. Eliminating the oscillators produces a memory force that records past motion and a fluctuating force inherited from the bath preparation. Their relation is derived before a memoryless approximation is made.

The mechanical starting point is Hamilton's stationary-action principle for the total system–reservoir coordinates,

$$\delta \int_{t_0}^{t_1} \left[p \cdot \dot{q} + \sum_{a=1}^{N} P_a \dot{x}_a - H_N(q,p,x,P) \right] \mathrm{d}t = 0,$$

where (q,p) are the resolved variables, (x_a, P_a) are the reservoir coordinates and momenta, and H_N is the total Hamiltonian specified below. Configuration endpoints are fixed in the variation. This gives Hamiltonian equations, which are reversible for the Hamiltonian used here; the effective relaxation direction additionally uses the initial preparation and retarded response. We first identify why these inputs are needed, then construct the reservoir and take the limits in the declared order. Throughout, $\theta = k_B T$, $G = G^{\mathsf{T}} > 0$ is friction, $K = G^{-1}$ is mobility, and F denotes nonequilibrium free energy rather than mechanical action or control cost.

4.1. *The logical target and the two variational signs.* An arbitrary reversible system may be uncoupled, periodic, or retain persistent memory. Reversibility alone therefore does not guarantee a particular coarse-grained behavior. The following elementary calculation rules out, by an explicit counterexample, an unrestricted inference from microscopic reversibility to monotone reduced entropy.

Proposition 4.1 (A reversible system with recurring observed entropy). *Consider $H(q,p) = (p^2 + \omega^2 q^2)/2$, $\omega > 0$, and temperature parameter $\theta > 0$. Let $q_0 \sim N(a, \theta/\omega^2)$ and $p_0 \sim N(0,\theta)$ be independent, with $a \neq 0$. The observed position law satisfies*

$$D\big(\mathrm{Law}(q_t) \big\| N(0, \theta/\omega^2)\big) = \frac{\omega^2 a^2}{2\theta} \cos^2(\omega t).$$

It reaches zero and subsequently returns to its initial positive value. The relative entropy of the full phase-space law against the canonical phase-space law is constant.

Proof. Hamilton's equations give

$$q_t = q_0 \cos(\omega t) + \frac{p_0}{\omega} \sin(\omega t), \qquad p_t = -\omega q_0 \sin(\omega t) + p_0 \cos(\omega t).$$

The mean of q_t is $a\cos(\omega t)$ and its variance is $\theta\omega^{-2}(\cos^2 + \sin^2) = \theta/\omega^2$. For Gaussians with the same covariance, relative entropy is one half the squared mean in the inverse covariance. This proves the formula. The energy of the phase-space mean is $[\omega^2 a^2 \cos^2 + \omega^2 a^2 \sin^2]/2 = \omega^2 a^2/2$. This is the excess energy over the centered canonical state; the total expected energy also includes the constant thermal contribution θ. The covariance remains the canonical covariance, so the full relative entropy is $\omega^2 a^2/(2\theta)$ and is constant. Equivalently, its constancy follows from the invertible Hamiltonian flow preserving the canonical reference. □

This example shows that the observed law can return to its initial state rather than follow a monotone relaxation. It motivates a closer look at the dynamical information supplied by the variational sign.

4.1.1. *Two convex functionals of opposite sign and the selection of orientation.* To make the sign question explicit, consider two convex functionals with opposite signs in their linear term. Let $K = K^T > 0$ be a constant mobility matrix, $\theta = k_B T$, and define the free energy and its chemical potential, up to an irrelevant additive constant, by

$$F[\rho] = \int U\rho \,\mathrm{d}q + \theta \int \rho \log \rho \,\mathrm{d}q, \qquad \mu_\rho = U + \theta \log \rho.$$

All logarithms in physical coordinates use a fixed reference volume; writing $\log \rho$ suppresses only the resulting additive constant. This constant does not change a functional derivative gradient or a free-energy difference. For smooth positive densities and currents with no boundary flux,

$$\partial_t \rho + \nabla \cdot j = 0 \quad \Longrightarrow \quad \dot{F} = \int j \cdot \nabla \mu_\rho \,\mathrm{d}q.$$

Define

$$\Phi_\rho[j] = \frac{1}{2} \int \frac{j^T K^{-1} j}{\rho} \,\mathrm{d}q, \qquad \mathscr{R}^{\pm}_\rho[j] = \Phi_\rho[j] \pm \dot{F}.$$

The quadratic cost is the same in the two functionals. At a fixed positive density it makes each functional strictly convex on the weighted current space, although their linear terms have opposite signs. Direct differentiation gives

$$j_+ = -\rho K \nabla \mu_\rho, \qquad j_- = +\rho K \nabla \mu_\rho. \tag{4.1}$$

Consequently,

$$\dot{F}[j_+] = -\int \rho |\nabla \mu_\rho|^2_K \,\mathrm{d}q, \qquad \dot{F}[j_-] = +\int \rho |\nabla \mu_\rho|^2_K \,\mathrm{d}q.$$

Positive definiteness makes the quadratic cost nonnegative and ensures uniqueness. It does not select between these two signs. The free-energy functional supplies an equilibrium reference, but it is also unchanged when a history is read in the opposite direction. The sign in $\Phi + \dot{F}$ therefore specifies a dynamical orientation when adopted as a constitutive principle. To connect that algebraic choice to a physical process, we must also require a positive, probability-preserving evolution. The next proposition excludes the opposite constitutive branch as a forward diffusion; the subsequent reservoir construction identifies the preparation and response that produce the admissible branch.

Proposition 4.2 (Why the opposite sign is not a forward diffusion). *The current j_- in (4.1) would give*

$$\partial_t \rho = -\nabla \cdot (\rho K \nabla U) - \theta \nabla \cdot (K \nabla \rho).$$

Its formal backward generator is $L_- f = K \nabla U \cdot \nabla f - \theta K : D^2 f$. It cannot generate a conservative positive forward Markov semigroup on an unrestricted smooth class of initial probability laws.

Proof. A positive Markov semigroup has the positive maximum principle: at a global maximum x_* of a function in its generator domain, $Lf(x_*) \le 0$. This follows by differentiating $P_t f(x_*) \le f(x_*)$ at $t = 0+$. Choose a smooth function with a strict maximum at x_*, zero gradient there, and negative-definite Hessian. Then $L_- f(x_*) = -\theta K : D^2 f(x_*) > 0$, a contradiction. The same problem is visible for a Fourier mode of the backward heat equation: its amplitude grows like $e^{\theta k^T K k\, t}$. □

This result explains why a probability-preserving diffusion with positive noise covariance uses the dissipative sign in a chosen forward time. It does not establish which temporal orientation the entire universe must adopt. A time-reversed diffusion still has positive covariance; its drift contains a density-dependent correction, computed in Section 4.5.

4.1.2. *Equilibrium does not uniquely determine the dynamics: circulation currents.* Even after fixing a positive diffusion covariance and a Gibbs invariant law, the drift retains freedom. Equilibrium constrains the divergence of the stationary current, rather than necessarily making that current vanish. For constant $K = K^T > 0$, all smooth drifts of the form

$$b = -K\nabla U + \ell, \qquad \nabla \cdot (\pi \ell) = 0, \qquad \pi = Z^{-1} e^{-U/\theta},$$

preserve π, subject to a conservative realization and boundary conditions. Their stationary current is $\pi\ell$, which need not vanish. Its zero divergence preserves the density, but does not require every flow line to be a closed orbit. For example, in dimension at least two, let $A^T = -A$ be a constant matrix and choose $\ell = A\nabla U$. Then

$$\nabla \cdot (\pi A \nabla U) = -\frac{\pi}{\theta} \nabla U^T A \nabla U + \pi A : D^2 U = 0.$$

For a regular density its current is $j = -\rho K \nabla \mu_\rho + \rho \ell$. The extra contribution to the free-energy rate also vanishes:

$$\int \rho \ell \cdot \nabla \mu_\rho \, \mathrm{d}q = \theta \int \pi \ell \cdot \nabla(\rho/\pi) \, \mathrm{d}q = 0.$$

Thus the same Gibbs reference law and even the same free-energy dissipation identity need not select the pure gradient current. The current variational principle specifies additional dynamical structure. For the position-only diffusion with fixed constant K, zero equilibrium current, equivalently detailed balance on the regular conservative realization, sets $\ell = 0$. Detailed balance is stronger than invariance. In the proposed realization the microscopic model and its preparation, rather than the equilibrium density alone, supply that additional information. With momentum, the appropriate reversal includes odd parity and cannot be replaced by the position-only zero-current test.

4.2. *Exact elimination of a reversible Hamiltonian reservoir and the origin of memory.* Equilibrium and covariance alone leave the drift undetermined. We now specify the mechanical system whose reduction selects the required drift. The resolved particle is linearly coupled to a Hamiltonian bath of harmonic oscillators, an established construction in statistical mechanics [32] and [109].

This model gives an explicit mechanism for energy exchange through the coupling forces. It contains no molecular collision law. At finite bath size, the eliminated dynamics retains memory and can return energy or information to the resolved system. A Markov description will require the additional spectral limit and estimates developed below.

4.2.1. *Hamiltonian, variational assumptions, and conditional preparation.* Let $q, p \in \mathbb{R}^d$, let the resolved mass be $m > 0$, and let $U \in C^3(\mathbb{R}^d)$ satisfy

$$\lambda I \le D^2 U(q) \le \Lambda I, \qquad 0 < \lambda \le \Lambda < \infty. \tag{4.2}$$

Higher smoothness can be imposed for the later classical density calculations. Bounded Hessian makes ∇U globally Lipschitz; the lower bound supplies confinement and a finite canonical partition function. This is a specific nonlinear class, not an arbitrary molecular interaction with collisions or singular forces.

For reservoir oscillators $(x_a, P_a) \in \mathbb{R}^2$, with masses $M_a > 0$, frequencies $\omega_a > 0$, and coupling vectors $c_a \in \mathbb{R}^d$, set

$$H_N = \frac{|p|^2}{2m} + U(q) + \sum_{a=1}^{N} \left\{ \frac{P_a^2}{2M_a} + \frac{M_a \omega_a^2}{2} \left(x_a - \frac{c_a^T q}{M_a \omega_a^2} \right)^2 \right\}. \tag{4.3}$$

The quadratic counterterm inside the square is essential. Without it, integrating over the reservoir generally changes the resolved potential and may even destroy stability. Expanding the square gives

$$\frac{M_a \omega_a^2 x_a^2}{2} - x_a c_a^T q + \frac{(c_a^T q)^2}{2 M_a \omega_a^2}.$$

The counterterm compensates the static potential shift produced by the linear coupling. Consequently the reduced equilibrium potential can be checked directly by integration, rather than inferred from a desired invariant density.

Once the mechanical model is fixed, its statistical interpretation also requires a preparation protocol. Prepare the resolved state with law $\nu_0(\,\mathrm{d}q\,\mathrm{d}p)$ and prepare the reservoir conditionally on $q_0 = q$. The shifted bath coordinates are

$$y_a = x_a - \frac{c_a^T q}{M_a \omega_a^2}.$$

The conditional reservoir law has density proportional to

$$\exp\left[-\frac{1}{\theta} \sum_a \left(\frac{P_a^2}{2M_a} + \frac{M_a \omega_a^2 y_a^2}{2} \right) \right]. \tag{4.4}$$

Equivalently, the $y_a(0)$ and $P_a(0)$ are independent centered Gaussians, independent of (q_0, p_0) in these shifted variables, with

$$\mathbb{E} y_a(0)^2 = \frac{\theta}{M_a \omega_a^2}, \qquad \mathbb{E} P_a(0)^2 = M_a \theta.$$

This puts the bath in conditional equilibrium at the preparation time. The physical coordinates $x_a(0)$ are not independent of q_0. An unshifted product preparation changes the initial transient and adds the initial-slip force computed below. Conditional preparation removes that particular term; it does not remove fluctuations, eliminate all initial layers, or by itself establish a Markov limit.

4.2.2. *A static canonical limit from a finite-energy reservoir.* The canonical preparation has a further statistical-mechanical interpretation. Integrating a specified microcanonical energy-shell measure over a large harmonic bath yields a canonical resolved marginal in the limit. This geometric calculation requires no entropy monotonicity. It explains the limiting exponential weight for that ensemble, rather than proving that every initial bath state thermalizes.

Introduce energy coordinates $a_i = \sqrt{M_i}\omega_i y_i$ and $b_i = P_i/\sqrt{M_i}$. The reservoir energy is $\frac{1}{2}\sum_i(a_i^2 + b_i^2)$. The density of states of N oscillators is, up to a positive constant,

$$\Omega_N(E) = E^{N-1}\mathbf{1}_{\{E>0\}}.$$

This follows by differentiating the volume of a ball of radius $\sqrt{2E}$ in $2N$ dimensions; its volume is proportional to E^N. The linear coordinate Jacobian does not depend on q because of the counterterm and the shift used in (4.3).

For a full microcanonical equilibrium at energy $E_N = N\theta$, the resolved marginal is proportional to

$$\left(1 - \frac{H_S(q,p)}{N\theta}\right)_+^{N-1}, \qquad H_S = U(q) + |p|^2/(2m),$$

after shifting the minimum of U to zero. At each fixed resolved state, this tends to $e^{-H_S/\theta}$. For $N \geq 2$ its value is at most $e^{-H_S/(2\theta)}$, because $\log(1-x) \leq -x$ on $[0,1)$. The upper bound is integrable under (4.2). Dominated convergence therefore proves convergence of the normalizing constants and of the marginal densities in L^1.

For an isolated harmonic bath at energy E_B, its kinetic temperature parameter is E_B/N. At a fixed resolved state in the full microcanonical ensemble, $E_B = E_N - H_S$; thus the conditional bath temperature is $\theta - H_S/N$, rather than exactly θ at finite N. If the derivative of the surface density-of-states entropy is used instead, its temperature parameter is $E_B/(N-1)$ for $N > 1$. Both tend to θ at each fixed resolved state. The separate fixed-bath-energy preparation used below has $E_B = N\theta$ exactly. This equilibrium calculation derives the canonical limiting weight from a specified uniform energy-shell ensemble; it does not derive the choice of that ensemble from Hamilton's principle.

More generally, a reservoir entropy $S_B(E) = k_B \log \Omega_B(E)$ gives

$$\log \Omega_B(E-h) - \log \Omega_B(E) = -\frac{h}{k_B T} - \frac{h^2}{2k_B T^2 C_B} + \text{higher terms},$$

when the required derivatives exist, $C_B > 0$, and h is small compared with the reservoir's energy scale. Here $S_B' = 1/T$ and $S_B'' = -1/(T^2 C_B)$. For the harmonic example the preceding exact calculation replaces this expansion and its unquantified remainder.

4.2.3. *Canonical marginal decoupling before dissipation.* Before deriving the dynamical reduction, we check the static marginal directly. Integration over each x_a uses a translation and gives

$$\int_{\mathbb{R}} \exp\left[-\frac{M_a\omega_a^2}{2\theta}\left(x_a - \frac{c_a^T q}{M_a\omega_a^2}\right)^2\right] \mathrm{d}x_a = \sqrt{\frac{2\pi\theta}{M_a\omega_a^2}}.$$

The result is independent of q. The momentum integral is $\sqrt{2\pi M_a\theta}$. Hence the full canonical law Π_N has resolved marginal

$$\pi_m(\,\mathrm{d}q\,\mathrm{d}p) = Z_m^{-1} \exp\left[-\frac{U(q) + |p|^2/(2m)}{\theta}\right] \mathrm{d}q\,\mathrm{d}p. \tag{4.5}$$

Integrating out p gives $\pi(\,\mathrm{d}q) = Z^{-1}e^{-U/\theta}\,\mathrm{d}q$. Thus the equilibrium marginal depends on U and the temperature, with the bath normalization absorbed into the partition function. This does not make the physical bath coordinates independent of q, nor does it put an arbitrarily prepared resolved state in equilibrium. These are static integrations; they do not use a free-energy decay law. We next eliminate the bath from the equations of motion to determine how a nonequilibrium preparation evolves.

4.2.4. *Hamilton equations and the retarded solution.* Hamilton's equations from (4.3) are

$$\begin{aligned} \dot q &= p/m, \\ \dot p &= -\nabla U(q) + \sum_a c_a\left(x_a - \frac{c_a^T q}{M_a\omega_a^2}\right), \\ \dot x_a &= P_a/M_a, \qquad \dot P_a = -M_a\omega_a^2 x_a + c_a^T q. \end{aligned} \tag{4.6}$$

For finite N these are globally well posed under (4.2). The full flow preserves phase volume and H_N. Its physical reversal changes (p, P) to $(-p, -P)$ and leaves (q, x) unchanged.

Solving the oscillator equation with data at 0 gives

$$x_a(t) = x_a(0)\cos\omega_a t + \frac{P_a(0)}{M_a\omega_a}\sin\omega_a t + \int_0^t \frac{\sin\omega_a(t-s)}{M_a\omega_a} c_a^T q_s\,\mathrm{d}s. \tag{4.7}$$

The lower limit is a boundary condition: this is the solution in terms of the prepared initial state. It has not been selected by minimizing entropy production.

For $f(s) = c_a^T q_s$, integration by parts gives

$$\int_0^t \frac{\sin\omega_a(t-s)}{M_a\omega_a} f(s)\,\mathrm{d}s = \frac{f(t) - f(0)\cos\omega_a t}{M_a\omega_a^2} - \int_0^t \frac{\cos\omega_a(t-s)}{M_a\omega_a^2}\dot f(s)\,\mathrm{d}s.$$

The endpoint term at $s = t$ cancels the counterterm in (4.6). The endpoint at 0 combines with $x_a(0)$ to produce the centered variable $y_a(0)$.

THEOREM 4.3 (Exact generalized Langevin equation). *For the finite Hamiltonian model and conditional preparation above, the resolved motion satisfies*

$$m\ddot{q}_t = -\nabla U(q_t) - \int_0^t \Gamma_N(t-s)\dot{q}_s \,\mathrm{d}s + \eta_N(t), \tag{4.8}$$

where

$$\Gamma_N(t) = \sum_a \frac{c_a c_a^T}{M_a \omega_a^2} \cos \omega_a t, \tag{4.9}$$

$$\eta_N(t) = \sum_a c_a \left[y_a(0) \cos \omega_a t + \frac{P_a(0)}{M_a \omega_a} \sin \omega_a t \right]. \tag{4.10}$$

The force η_N is a stationary centered Gaussian process, independent of the resolved initial state, with

$$\mathbb{E}[\eta_N(t)\eta_N(s)^T] = \theta \Gamma_N(t-s). \tag{4.11}$$

Proof. Substitution of (4.7) and the integration-by-parts identity proves (4.8). Independence removes the terms with different oscillator indices and the mixed position–momentum terms in the covariance. The remaining terms for oscillator a are

$$\frac{\theta c_a c_a^T}{M_a \omega_a^2} [\cos \omega_a t \cos \omega_a s + \sin \omega_a t \sin \omega_a s] = \frac{\theta c_a c_a^T}{M_a \omega_a^2} \cos \omega_a (t-s).$$

Summation gives (4.11). A centered Gaussian process is determined by its covariance, so dependence on $t-s$ proves stationarity. □

This derives the fluctuation–dissipation relation for this reservoir from its Hamiltonian and preparation. It is a more specific result than assuming an Einstein relation after writing a Langevin equation. General linear-response versions require their own hypotheses [56].

If instead $x_a(0)$ is centered at zero independently of q_0, the same calculation produces an additional force $-\Gamma_N(t)q_0$. This initial-slip term must either be retained or removed by changing the preparation. The proposed theorem removes it by the explicit conditional law (4.4).

4.2.5. *What is positive, and what is not.* The even matrix kernel need not be positive at every nonzero time: a cosine can be negative. Its positivity is covariance positivity. For any vector-valued test function v,

$$\iint v(t)^T \Gamma_N(t-s) v(s) \,\mathrm{d}t \,\mathrm{d}s = \frac{1}{\theta} \mathbb{E} \left(\int v(t)^T \eta_N(t) \,\mathrm{d}t \right)^2 \geq 0.$$

Replacing this positive-type statement by the stronger assertion $\Gamma_N(t) > 0$ for every t would be an error. Neither statement implies a memoryless evolution or monotone reduced entropy at finite N.

For a prescribed deterministic velocity protocol v on $[0, \tau]$, the mean work of the retarded reservoir friction on the resolved coordinate is

$$W_{\mathrm{fric}} = -\int_0^\tau \int_0^t v(t)^T \Gamma_N(t-s) v(s) \,\mathrm{d}s \,\mathrm{d}t$$

$$= -\frac{1}{2}\int_0^\tau \int_0^\tau v(t)^T \Gamma_N(t-s) v(s)\,\mathrm{d}s\,\mathrm{d}t \le 0.$$

The second equality uses evenness and matrix symmetry of the kernel; the sign uses the covariance identity, not an entropy inequality. The centered random force does zero mean work against this prescribed deterministic protocol. This is an equilibrium passivity statement relative to an initially prepared retarded response. It does not assert that instantaneous frictional power has a fixed sign at finite memory, or that a randomly evolving coupled subsystem loses energy monotonically. For its random velocity, the force and velocity become correlated, and the fluctuating-force work cannot be dropped.

4.2.6. *The finite model stores the information that a Markov limit loses.* Let f_t be the full evolved law and let ν_t be its resolved phase-space marginal. Since the Hamiltonian flow is invertible and preserves Π_N,

$$D(f_t\|\Pi_N) = D(f_0\|\Pi_N). \tag{4.12}$$

This follows by changing variables under the flow in the KL integral; it holds whenever the initial relative entropy is finite. Disintegration against the conditional canonical reservoir gives the exact chain rule

$$D(f_t\|\Pi_N) = D(\nu_t\|\pi_m) + C_N(t), \tag{4.13}$$

where

$$C_N(t) = \int D(f_t(\,\mathrm{d}B \mid s)\|\Pi_N(\,\mathrm{d}B \mid s))\,\nu_t(\,\mathrm{d}s) \ge 0.$$

Here $s = (q,p)$ and $B = (x,P)$. The initial preparation gives $C_N(0) = 0$, so

$$D(\nu_t\|\pi_m) + C_N(t) = D(\nu_0\|\pi_m). \tag{4.14}$$

The conditional term includes reservoir disturbance and correlations relative to its equilibrium conditional law. Because the canonical reservoir coordinates depend on q, it should not automatically be identified with ordinary mutual information in the original coordinates.

Equation (4.14) bounds the marginal entropy by its initial value but does not make it monotone in time. $C_N(t)$ can increase and later decrease. A finite reservoir can return information to the system. This exact accounting is the appropriate starting point for discussing the relation between microscopic reversibility and effective dissipation.

4.3. *Continuum limit of the bath spectrum and controlled Markov reduction.* The exact memory equation is not yet an overdamped Markov diffusion. The latter requires selecting a bath spectrum and supplying a convergence argument. A Lorentzian spectral weight is particularly useful because its force covariance is exponential and its memory has a finite Markovian realization. This choice is a model specification, not a consequence of equilibrium alone.

4.3.1. *A bath spectrum with a computable memory kernel.* Let $G = G^T > 0$ be the target friction matrix and $\varepsilon > 0$ the memory time. Specify the matrix-valued spectral weight

$$S_\varepsilon(\omega) = \frac{2}{\pi}\frac{G}{1+\varepsilon^2\omega^2}, \qquad \omega \geq 0. \tag{4.15}$$

The cosine transform identity gives

$$\Gamma_\varepsilon(t) = \int_0^\infty S_\varepsilon(\omega)\cos(\omega t)\,\mathrm{d}\omega = \frac{G}{\varepsilon}e^{-|t|/\varepsilon}. \tag{4.16}$$

In particular,

$$\int_0^\infty \Gamma_\varepsilon(t)\,\mathrm{d}t = G, \qquad \int_{-\infty}^\infty \Gamma_\varepsilon(t)\,\mathrm{d}t = 2G.$$

The factor of two is important. The causal memory convolution converges to $G\dot{q}$, whereas the two-sided force covariance converges to $2\theta G\delta$. Treating these two integrals as the same would produce the wrong Einstein coefficient.

To realize the spectrum with finite baths, diagonalize G and use oscillators in each eigenvector direction. Approximate the positive spectral measure in each direction by positive point masses w_a at frequencies $\omega_a > 0$ and choose, for example, $M_a = 1$ and $c_a = \omega_a\sqrt{w_a}\,e_a$. Then $c_a c_a^T/(M_a\omega_a^2) = w_a e_a e_a^T$, exactly the weight required in (4.9). First let the frequency mesh tend to zero on a bounded interval, then let its cutoff tend to infinity, at a fixed ε.

4.3.2. *A sufficient Gaussian convergence argument.* Covariance convergence at individual times establishes only convergence of finite-dimensional Gaussian distributions. It does not by itself establish convergence in a continuous-path space. Add the following explicit tightness condition for every fixed horizon τ:

$$\mathbb{E}|\eta_N(t) - \eta_N(s)|^{2r} \leq C_{\varepsilon,\tau,r}|t-s|^r, \qquad r > 1. \tag{4.17}$$

For the continuous spectral truncations this bound follows from

$$\mathbb{E}|\eta(t) - \eta(s)|^2 = 2\theta\,\mathrm{Tr}[\Gamma_\varepsilon(0) - \Gamma_\varepsilon(t-s)] \leq C_\varepsilon|t-s|.$$

Truncation only removes a nonnegative contribution to the scalar increment variance in each eigenvector direction. Gaussian moment identities then give (4.17).

For a discrete frequency approximation, take mesh size at most one and put each bin's exact positive spectral mass at a representative frequency. For $h = t - s$, the estimate

$$|e^{i\omega_a h} - 1|^2 \leq 2|e^{i\omega h} - 1|^2 + 2|\omega_a - \omega|^2 h^2$$

gives the same bound, uniformly along the mesh/cutoff sequence, up to $C_\varepsilon h^2$. Together with convergence of the covariance this proves tightness and weak convergence in $C([0,\tau];\mathbb{R}^d)$. The solution map of the Volterra equation is continuous under uniform force convergence and L^1 kernel convergence on this finite interval: subtract the two integral equations, use the Lipschitz constant of ∇U, and apply Gronwall's inequality. Thus the resolved paths converge in law at fixed m, ε.

No assertion is needed that the infinite reservoir has a finite total canonical energy. Typically it does not. The rigorous object is the finite-bath sequence and its resolved finite-time limit. A normalized infinite-dimensional Lebesgue density $e^{-H/\theta}$ must not be introduced to bypass this issue.

4.3.3. *The same force limit from a microcanonical bath preparation.* The Gaussian bath variables in (4.4) can be replaced by a uniform conditional energy-shell preparation, keeping the resolved nonequilibrium initial law independent of the standardized bath variables. In the energy coordinates (a, b), sample uniformly on the sphere of radius $\sqrt{2N\theta}$ in $2N$ dimensions. This preparation has fixed bath energy $N\theta$ and covariance θI, so the finite-bath fluctuation–dissipation covariance (4.11) still holds exactly. Its force is not exactly Gaussian at finite N.

Let g_N be a standard Gaussian vector in $\mathbb{R}^{2N}$. The uniform sphere vector has the representation

$$\sqrt{2N\theta}\,\frac{g_N}{|g_N|} = R_N\sqrt{\theta}\,g_N, \qquad R_N = \frac{\sqrt{2N}}{|g_N|} \longrightarrow 1 \quad \text{in probability.}$$

The last statement follows from $|g_N|^2/(2N) \to 1$ in probability, for example by its mean and variance. Since the exact reservoir force is linear in (a, b), this coupling gives

$$\eta_N^{\mathrm{mc}} = R_N \eta_N^{\mathrm{can}}.$$

The Gaussian force sequence at fixed ε is tight in $C([0,\tau])$. Therefore $|R_N - 1|\,\|\eta_N^{\mathrm{can}}\|_\infty \to 0$ in probability; independence of the two factors is not required. The microcanonical and canonical preparations have the same limiting force process and, by continuity of the Volterra solution map, the same resolved finite-time limit. This is an explicit ensemble-equivalence argument for the dynamical force, not just for one equilibrium marginal.

The energy-shell measure is singular relative to the finite canonical bath density. Consequently the finite relative-entropy identity (4.14), which used a canonical conditional preparation and finite initial KL, cannot be applied to this singular ensemble with $C_N(0) = 0$. One may use the canonical preparation for that identity, or a finite-width energy shell with its nonzero initial conditional relative entropy retained. The limiting diffusion's entropy theorem is unaffected by this finite-ensemble distinction. Also, an integrable harmonic bath is not claimed to drive every arbitrary initial bath state to a microcanonical ensemble. The uniform sphere law is a specified preparation.

4.3.4. *An exact exponential-memory realization.* Let η^ε be the stationary Ornstein–Uhlenbeck force

$$\mathrm{d}\eta_t^\varepsilon = -\varepsilon^{-1}\eta_t^\varepsilon\,\mathrm{d}t + \varepsilon^{-1}\sqrt{2\theta G}\,\mathrm{d}W_t, \qquad \eta_0^\varepsilon \sim N(0, \theta G/\varepsilon). \tag{4.18}$$

It is independent of the resolved initial state and has covariance $\theta G\varepsilon^{-1}e^{-|t-s|/\varepsilon}$, equal to the limiting force covariance derived from the Hamiltonian bath. Define

$$z_t^\varepsilon = \eta_t^\varepsilon - \int_0^t \frac{G}{\varepsilon}e^{-(t-s)/\varepsilon}\frac{p_s^\varepsilon}{m}\,\mathrm{d}s.$$

Differentiation of the convolution gives the exact system

$$\begin{aligned} \mathrm{d}q_t^\varepsilon &= p_t^\varepsilon \,\mathrm{d}t/m, \\ \mathrm{d}p_t^\varepsilon &= -\nabla U(q_t^\varepsilon)\,\mathrm{d}t + z_t^\varepsilon \,\mathrm{d}t, \\ \mathrm{d}z_t^\varepsilon &= -z_t^\varepsilon \,\mathrm{d}t/\varepsilon - G p_t^\varepsilon \,\mathrm{d}t/(m\varepsilon) + \sqrt{2\theta G}\,\mathrm{d}W_t/\varepsilon. \end{aligned} \tag{D}$$

Here $z_0^\varepsilon = \eta_0^\varepsilon$. This stochastic embedding is used because its law equals that of the Gaussian continuum reservoir force. Starting by postulating (D) without the preceding Hamiltonian elimination would not constitute a microscopic derivation.

Its equilibrium density is proportional to

$$\exp\left[-\frac{1}{\theta}\left(U(q) + \frac{|p|^2}{2m} + \frac{\varepsilon}{2} z^T G^{-1} z\right)\right]. \tag{4.19}$$

The conservative coupling cancels in the energy derivative: $(p/m)^T z + \varepsilon z^T G^{-1}[-Gp/(m\varepsilon)] = 0$. The remaining z-OU part has covariance $\theta G/\varepsilon$. The correct parity is $(q,p,z) \mapsto (q,-p,z)$; the force variable is even. Thus the equilibrium embedding is reversible under this parity, despite the appearance of a friction and a noise term.

4.3.5. *White-memory limit at a fixed positive mass.*

Theorem 4.4 (Controlled white-memory limit). *Assume (4.2), fix $m > 0$ and a finite horizon τ, and give (q_0, p_0) finite second moments. Couple (D) and the kinetic Langevin equation*

$$\mathrm{d}q_t = p_t\,\mathrm{d}t/m, \qquad \mathrm{d}p_t = -\nabla U(q_t)\,\mathrm{d}t - G p_t\,\mathrm{d}t/m + \sqrt{2\theta G}\,\mathrm{d}W_t \tag{4.20}$$

with the same initial resolved state and Brownian motion. Then

$$\mathbb{E} \sup_{0\le t\le\tau} (|q_t^\varepsilon - q_t|^2 + |p_t^\varepsilon - p_t|^2) \longrightarrow 0.$$

In fixed dimensionless coordinates a bound of order $C_{m,\tau}\varepsilon[1+\log(1+\tau/\varepsilon)]$ is sufficient. Its constant is not asserted to be uniform as $m \downarrow 0$.

Proof. Multiplying the last equation of (D) by ε and integrating gives

$$\int_0^t z_s^\varepsilon \,\mathrm{d}s = -G(q_t^\varepsilon - q_0) + \sqrt{2\theta G} W_t - \varepsilon(z_t^\varepsilon - z_0^\varepsilon).$$

Therefore

$$p_t^\varepsilon = p_0 - \int_0^t \nabla U(q_s^\varepsilon)\,\mathrm{d}s - G(q_t^\varepsilon - q_0) + \sqrt{2\theta G} W_t + r_t^\varepsilon, \quad r_t^\varepsilon = -\varepsilon(z_t^\varepsilon - z_0^\varepsilon). \tag{4.21}$$

The same equation for (4.20) has zero remainder.

We first control the force maximum rather than replacing colored noise by white noise pointwise. On $[0,\tau]$, a stationary OU process (4.18) satisfies

$$\mathbb{E} \sup_{t\le\tau} |\varepsilon \eta_t^\varepsilon|^2 \le C\theta\,\|G\|\,\varepsilon[1 + \log(1+\tau/\varepsilon)]. \tag{4.22}$$

One direct proof partitions time into intervals of length ε. The values at the endpoints have Gaussian tails with variance $O(\varepsilon)$ after multiplication by ε. A union bound over at most $2+\tau/\varepsilon$ endpoints yields an expected squared maximum $O(\varepsilon \log(2+\tau/\varepsilon))$. On one interval the OU increment is a deterministic decay plus a Gaussian stochastic integral. After scaling time by ε, the latter has a maximal tail bounded by $C\exp[-u^2/(C\varepsilon)]$, obtained from the Brownian maximal inequality after its deterministic time change. A second union bound and integration of this tail give the same order for the interval maxima. Summation over the fixed number of coordinate directions proves (4.22).

The convolution representation of z^ε gives

$$\varepsilon \sup_{s\le t} |z_s^\varepsilon| \le \varepsilon \sup_{s\le t} |\eta_s^\varepsilon| + \frac{\varepsilon \|G\|}{m} \sup_{s\le t} |p_s^\varepsilon|. \tag{4.23}$$

Let $V(t) = \sup_{s\le t}(|q_s^\varepsilon| + |p_s^\varepsilon|)$. The integral equations, linear growth of ∇U, and (4.23) imply, with constants depending on m, τ, G, U,

$$V(t) \le C\left(1 + |q_0| + |p_0| + \sup_{s\le t}|W_s| + \varepsilon \sup_{s\le t}|\eta_s^\varepsilon|\right) + C\int_0^t V(s)\,\mathrm{d}s + C\varepsilon V(t).$$

For sufficiently small ε, absorb the last term. Gronwall's inequality, the Brownian maximal second moment, and (4.22) give $\sup_{\varepsilon\le\varepsilon_0} \mathbb{E}V(\tau)^2 < \infty$. Equations (4.23)–(4.21) now imply

$$\mathbb{E}\,\|r^\varepsilon\|_\infty^2 \le C_{m,\tau}\varepsilon[1 + \log(1+\tau/\varepsilon)].$$

Finally, subtract the zero-remainder equation, and use $\delta q_t = \int_0^t \delta p_s\,\mathrm{d}s/m$ and the Lipschitz bound on ∇U. A second Gronwall estimate gives $\|\delta q\|_\infty + \|\delta p\|_\infty \le C_{m,\tau}\|r^\varepsilon\|_\infty$. Taking squares and expectations proves the assertion. □

This proof derives both the damping sign and the matching white-noise amplitude without assuming an entropy inequality. It also explains why η_t^ε itself has no finite pointwise white noise limit: its stationary variance diverges like $1/\varepsilon$. Only its time integral, or the resolved dynamics, has the stated limit.

4.3.6. *Physical meaning of friction positivity.* For a stationary force with integrable covariance $C(t)$ and the required equilibrium symmetry, the Green–Kubo candidate is

$$G = \frac{1}{\theta}\int_0^\infty C(t)\,\mathrm{d}t.$$

For every $v \in \mathbb{R}^d$,

$$v^T G v = \lim_{T\to\infty} \frac{1}{2\theta T}\mathbb{E}\left(\int_0^T v^T \eta_s\,\mathrm{d}s\right)^2 \ge 0.$$

To verify the equality, expand the variance as $2\int_0^T (T-u)v^T C(u)v\,\mathrm{d}u$ and use integrability to pass to the limit. Strict positivity requires nonzero zero-frequency fluctuation power in every retained direction; it is not automatic. In the chosen spectrum it is exactly the hypothesis $G > 0$. This

gives a physical covariance origin for the positive metric. It does not assign a temporal orientation to that metric by itself.

4.4. *Overdamped reduction and variational characterization.* The white-memory limit retains momentum, whereas the present Rayleighian describes an overdamped position law. Removing momentum is therefore a second limiting step, with its own preparation and estimate. Deleting $m\ddot{q}$ from the equation would miss the initial momentum layer and does not justify that limit.

4.4.1. *Small mass with a thermally scaled initial momentum.* Set $K = G^{-1}$. Let q_0 have finite second moment and take $p_0^m \sim N(0, m\theta I)$ independently. This momentum scaling keeps the mean kinetic energy $d\theta/2$ finite and gives $\mathbb{E}|p_0^m|^2 = dm\theta \to 0$.

THEOREM 4.5 (Small-mass realization of the overdamped diffusion). *Under (4.2), the position in (4.20) converges, on every fixed $[0,\tau]$, to the unique strong solution*

$$\mathrm{d}Q_t = -K\nabla U(Q_t)\,\mathrm{d}t + \sqrt{2\theta K}\,\mathrm{d}W_t, \qquad Q_0 = q_0. \tag{4.24}$$

With the coupling just specified, $\mathbb{E}\sup_{t\le\tau}|q_t^m - Q_t|^2 \to 0$.

Proof. Integrating the momentum equation gives the exact identity

$$q_t^m = q_0 - \int_0^t K\nabla U(q_s^m)\,\mathrm{d}s + \sqrt{2\theta K}W_t - K(p_t^m - p_0^m). \tag{4.25}$$

We used $K\sqrt{G} = \sqrt{K}$, valid because G is symmetric positive definite. For a nonsymmetric friction, the noise matrix must be handled separately; it is not obtained by this identity.

Variation of constants gives

$$p_t^m = \xi_t^m - \int_0^t e^{-G(t-s)/m}\nabla U(q_s^m)\,\mathrm{d}s,$$

where

$$\xi_t^m = e^{-Gt/m}p_0^m + \int_0^t e^{-G(t-s)/m}\sqrt{2\theta G}\,\mathrm{d}W_s.$$

The chosen p_0^m makes ξ^m stationary with covariance $m\theta I$. The interval-maximal argument of (4.22), now with correlation time proportional to m, gives in fixed dimensionless units

$$\mathbb{E}\sup_{t\le\tau}|\xi_t^m|^2 \le Cm[1+\log(1+\tau/m)].$$

If $g_0 > 0$ is the smallest eigenvalue of G, the convolution satisfies

$$\sup_{t\le\tau}\left|\int_0^t e^{-G(t-s)/m}\nabla U(q_s^m)\,\mathrm{d}s\right| \le \frac{m}{g_0}\sup_{t\le\tau}|\nabla U(q_t^m)|.$$

Linear growth of ∇U and (4.25) yield a Gronwall bound on $\mathbb{E}\sup|q^m|^2$, uniformly for sufficiently small m, after the $Cm\sup|q^m|$ term is absorbed. Thus

$$\mathbb{E}\sup_{t\le\tau}|p_t^m|^2 \le C_\tau\{m[1+\log(1+\tau/m)] + m^2\} \longrightarrow 0.$$

Subtracting the integral equation for Q from (4.25) gives

$$|q_t^m - Q_t| \le \|K\|\,\Lambda \int_0^t |q_s^m - Q_s|\,\mathrm{d}s + \|K\|\,(|p_t^m| + |p_0^m|).$$

Gronwall and the preceding maximal estimate finish the proof. □

If a fixed nonzero initial momentum is used instead, the last term in (4.25) can produce a nonvanishing initial displacement during the momentum boundary layer. Uniform convergence from the same initial position cannot then be asserted without a modified statement. General state-dependent-friction limits have additional drift terms [48]; the constant-friction theorem above avoids that extra complication.

4.4.2. *The order of limits is part of the theorem.* The proven construction has the order

$$\lim_{m\downarrow 0}\ \lim_{\varepsilon\downarrow 0}\ \lim_{\text{bath mesh}\downarrow 0,\,\text{cutoff}\uparrow\infty} \mathrm{Law}(q_{[0,\tau]}^{N,\varepsilon,m}) = \mathrm{Law}(Q_{[0,\tau]}). \tag{4.26}$$

The inner bath limit is at fixed ε, m. The estimates for the next limit may depend on m. The last limit uses the thermal momentum scaling. These statements do not establish commutation of limits, a simultaneous scaling for arbitrary parameter ratios, or uniform convergence as $\tau \to \infty$. A diagonal sequence can be chosen for each fixed finite-time weak-convergence criterion, but no uniform physical rate follows merely from a diagonal argument.

Finite-bath recurrence is therefore not contradicted: a finite-time reservoir limit is taken before an unbounded observation horizon. Long-time and reservoir-size limits are consequently not interchanged without an additional estimate.

4.4.3. *Generator, current, and equilibrium obtained from the limits.* Equation (4.24) has generator

$$Lf = -K\nabla U \cdot \nabla f + \theta K : D^2 f.$$

Its forward equation and current are

$$\partial_t \rho = -\nabla \cdot j_\rho, \qquad j_\rho = -\rho K \nabla U - \theta K \nabla \rho. \tag{4.27}$$

The positive covariance $2\theta K$ fixes the sign of the second-order term. The restoring drift was obtained from the Hamiltonian potential and the retarded reservoir response. Neither sign was inferred from a desired entropy-production inequality.

For $\pi = Z^{-1}e^{-U/\theta}$, $\theta\nabla\pi = -\pi\nabla U$ gives $j_\pi = 0$. The globally Lipschitz drift defines a unique conservative diffusion; the corresponding well-posed forward equation identifies π as an invariant probability. Equivalently, integration by parts gives

$$\int f L g\,\pi\,\mathrm{d}q = -\theta \int \nabla f^T K \nabla g\,\pi\,\mathrm{d}q$$

on a suitable core, followed by the conservative realization. The formal equation $L^*\pi = 0$ alone is not substituted for that realization.

4.4.4. *The Rayleighian becomes a derived characterization.* For each fixed smooth positive density,

$$j_\rho = -\rho K \nabla(U + \theta \log \rho) = -\rho K \nabla \mu_\rho.$$

Assume $\int \rho |\nabla \mu_\rho|_K^2 \, \mathrm{d}q < \infty$ and minimize over the weighted Hilbert space of measurable currents with $\int j^T K^{-1} j / \rho \, \mathrm{d}q < \infty$. The linear term is continuous on this space by Cauchy–Schwarz. No prescribed density derivative or two-endpoint constraint is imposed in this instantaneous constitutive minimum. Completing the square gives

$$\mathscr{R}_\rho[j] = \frac{1}{2} \int \frac{|j + \rho K \nabla \mu_\rho|_{K^{-1}}^2}{\rho} \, \mathrm{d}q - \frac{1}{2} \int \rho |\nabla \mu_\rho|_K^2 \, \mathrm{d}q. \tag{4.28}$$

The Hamiltonian reservoir reduction already determined j_ρ. Equation (4.28) shows that the same current uniquely minimizes $\Phi + \dot{F}$. In this microscopic realization, the Rayleighian need not be an independent dynamical postulate. This complements the mesoscopic route in which it is postulated and its consequences are proved. Onsager–Rayleigh formulations and free-energy gradient flows have established antecedents [26] and [52].

4.4.5. *Free-energy identity and physical entropy balance.* Work on the class of smooth positive probability densities with finite absolute energy and entropy integrals and with integrable current boundary terms. One convenient initial class is a smooth bounded positive perturbation of π with controlled derivatives; the corresponding diffusion and cutoff estimates justify the integrations. If only weak convergence is available, use the appropriate entropy inequality instead of silently asserting a differentiated identity.

Since $\log \pi = -U/\theta - \log Z$,

$$\theta D(\rho \| \pi) = \theta \int \rho \log \rho \, \mathrm{d}q + \int U \rho \, \mathrm{d}q + \theta \log Z.$$

Also $F[\pi] = -\theta \log Z$. Thus

$$F[\rho] - F[\pi] = \theta D(\rho \| \pi). \tag{4.29}$$

Using mass conservation and (4.27),

$$\begin{aligned} \dot{F} &= \int \mu_\rho \partial_t \rho \, \mathrm{d}q = \int \nabla \mu_\rho \cdot j_\rho \, \mathrm{d}q \\ &= -\int \rho |\nabla \mu_\rho|_K^2 \, \mathrm{d}q = -\theta^2 \int \rho |\nabla \log(\rho/\pi)|_K^2 \, \mathrm{d}q. \end{aligned} \tag{4.30}$$

No entropy sign was used to obtain the diffusion in the preceding sections. Equation (4.30) is now a consequence. Positivity of K and connectedness imply that a vanishing integrand forces $\rho = \pi$.

For an autonomous system in contact with one isothermal reservoir and no work input, declare heat into the reservoir by $\dot{Q}_{\mathrm{bath}} = -\,\mathrm{d}\mathbb{E}U/\,\mathrm{d}t$ after the kinetic reduction. Let $S_{\mathrm{sys}} = -k_B \int \rho \log \rho$. Then direct algebra yields

$$\dot{S}_{\mathrm{sys}} + \frac{\dot{Q}_{\mathrm{bath}}}{T} = -\frac{\dot{F}}{T} = k_B \theta \int \rho |\nabla \log(\rho/\pi)|_K^2 \, \mathrm{d}q \geq 0. \tag{4.31}$$

The use of Q/T as reservoir entropy assumes the isothermal reservoir limit. It is not an exact assertion that a finite disturbed oscillator bath remains in equilibrium. Before the small-mass reduction, the resolved energy is $U + |p|^2/(2m)$ and the corresponding kinetic entropy dissipation acts in momentum. These two balances must not be mixed.

For the kinetic SDE, the Stratonovich energy identity is

$$\mathrm{d}\left(U(q) + \frac{|p|^2}{2m}\right) = \frac{p^T}{m}\left(-\frac{Gp}{m}\,\mathrm{d}t + \sqrt{2\theta G} \circ \mathrm{d}W_t\right).$$

The equivalent Itô mean energy rate contains $\theta\,\mathrm{Tr}(G)/m$ in addition to $-\mathbb{E}[p^T G p]/m^2$. The fluctuation term compensates friction at equilibrium; friction alone must not be interpreted as positive stationary total entropy production.

4.4.6. *Two extensions requiring different statements.*

Position-dependent mobility. For an isothermal symmetric $K(q)$, the Gibbs-preserving Itô drift is

$$b_i(q) = -K_{ij}(q)\partial_j U(q) + \theta\partial_j K_{ij}(q). \tag{4.32}$$

Indeed the current is $J_i = b_i\rho - \theta\partial_j(K_{ij}\rho) = -K_{ij}(\rho\partial_j U + \theta\partial_j\rho)$. Leaving out the second term in (4.32) leaves an unwanted current $-\theta\pi\,\partial_j K_{ij}$ at π. Thus a state-dependent-friction generalization needs an additional limit theorem, not a symbol replacement in the constant-matrix proof.

A periodic configuration space. The linear coupling $c_a^T q$ in (4.3) is globally defined on $\mathbb{R}^d$, not on $\mathbb{T}^d$. Therefore this microscopic realization directly supports the confined Euclidean model above. It does not establish a microscopic realization on a torus. Such a realization needs periodic coupling functions, or a separately defined lifted/quotient model, and its own limiting calculation. Section 5.7 supplies that calculation using periodic paired couplings and a separate fixed-mass convergence estimate. The Euclidean and periodic proofs therefore keep their distinct couplings and hypotheses.

4.5. *Where the effective time direction enters.* The sign question can now be answered explicitly. The positive metric is generated by equilibrium force fluctuations. The free-energy reference is generated by the canonical marginal. Their positivity and static form do not alone orient time. The effective orientation arises when initial preparation is propagated by a retarded response and the reservoir memory is removed in a specified forward description.

4.5.1. *Physical inputs and their consequences.* The inputs in the microscopic realization are:

(1) A reversible Hamiltonian, specified potential, and resolved system–reservoir split.
(2) A conditional canonical reservoir distribution at the preparation time and an independently specified nonequilibrium resolved distribution.
(3) A reservoir spectrum with a positive integrated response and a finite correlation time, followed by the stated scale limits.

(4) Evolution from the preparation time using the retarded oscillator solution, with no separately arranged future system–reservoir correlations.
(5) The choice of retained variables and the time resolution at which a Markov description is asserted.

The drift, diffusion coefficient, current, Rayleighian characterization, and entropy inequality are consequences for this model. Temperature, spectral shape, preparation, and the resolved variables remain physical inputs. Describing these inputs as if they had all been deduced from equilibrium would create a new unsupported claim.

4.5.2. *The reverse experiment has a different preparation.* At a later time τ, the full state is $f_\tau = \Phi_{\tau *} f_0$. A reversed microscopic experiment starts from $\Theta_* f_\tau$. It contains the reservoir conditional disturbance measured by $C_N(\tau)$ in (4.13). It generally does not have the fresh conditional canonical bath preparation used at 0. Resetting the bath to that canonical conditional law discards the information needed for exact reversal. This is a physically specified change of preparation, not a contradiction in Hamiltonian mechanics.

An equilibrium bath by itself is time-reversal symmetric. If the full initial preparation is invariant under Θ, an even resolved observable has the same law at t and $-t$ under the exact reversible flow. Thus a prepared nonequilibrium state at a distinguished time does not identify an absolute orientation of all microscopic time. It can support relaxation away from that preparation time in either temporal direction when the two experiments are posed with the corresponding boundary data. A cosmological initial-condition theory or a fundamental time-asymmetric law is an additional problem.

4.5.3. *Why reverse diffusion is not anti-diffusion.* For the derived overdamped SDE with $b = -K\nabla U$ and covariance $2\theta K$, use smooth positive densities on $[0, \tau]$ for which the score and the reversed SDE are well defined, nonexplosive, and in the uniqueness class of the forward equation. The nonstationary time reverse over $[0, \tau]$ then has drift

$$b_s^R(q) = -b(q) + 2\theta K \nabla \log \rho_{\tau - s}(q). \tag{4.33}$$

The reversed initial law is ρ_τ. Its diffusion covariance remains $2\theta K$, and its current is

$$b_s^R \rho_{\tau - s} - \theta K \nabla \rho_{\tau - s} = -b\rho_{\tau - s} + \theta K \nabla \rho_{\tau - s} = -j_{\rho_{\tau - s}}.$$

This verifies the reversal at the level of the continuity equation. For path-law reversal, the same formula follows from the reversed transition density $p(s, x; t, y)\rho_s(x)/\rho_t(y)$ by expanding its conditional first and second moments; regularity is needed for this expansion. A reversed one-time density equation alone would not determine a path law without the Markov and uniqueness hypotheses. At equilibrium, $\nabla \log \pi = -\nabla U/\theta$, so $b^R = b$. Away from equilibrium the reverse drift depends on the forward marginal family and generally differs from the original autonomous drift.

Merely changing $K\nabla U$ to its negative while retaining the same score term would not describe this reversal.

The equilibrium-preserving Markov-inverse obstruction has a precise meaning. If $D(\rho_\tau\|\pi) < D(\rho_0\|\pi)$, no positive Markov kernel R can simultaneously satisfy $\pi R = \pi$ and $\rho_\tau R = \rho_0$, because

$$D(\rho_0\|\pi) = D(\rho_\tau R\|\pi R) \le D(\rho_\tau\|\pi) < D(\rho_0\|\pi).$$

This does not exclude a reverse experiment with a changed drift, reservoir correlations, control, or preparation. It identifies which information-losing reduced operation cannot be undone within the same equilibrium-preserving Markov class.

4.5.4. *Recurrence and the order of the physical limits.* For every finite N, (4.3) has a finite canonical invariant probability. Poincaré recurrence applies to almost every microscopic state under the usual measure-preserving-flow formulation. This prevents a claim of irreversible settling of almost every full trajectory. Recurrence alone does not rule out mixing or weak convergence of observed probability laws: recurrent measure-preserving systems can be mixing. In the completely quadratic finite model the resolved means are finite sums of oscillatory normal modes, providing an explicit obstruction to a universal monotone relaxation claim. The oscillator example in Proposition 4.1 displays the simplest such information return. A large number of finite oscillators alone is not a proof of a Markov entropy law.

The reservoir limit in (4.26) compares resolved paths on a fixed finite horizon. The final Markov diffusion has an entropy contraction theorem on its own state space. The two statements are compatible. They do not provide an estimate that a fixed finite bath agrees with the Markov model through its recurrence time. Discarded information can return before the ideal reservoir limit is appropriate.

4.5.5. *Equilibrium reversibility is a required check.* A model cannot explain an irreversible stationary heat current in a single equilibrium reservoir merely by displaying nonzero friction. At the canonical law the thermodynamic entropy-production rate in (4.31) is zero. The overdamped gradient diffusion is reversible; the kinetic and exponential-memory embeddings are reversible with the declared odd momentum parity. This check prevents a false identification of dynamical damping with positive stationary total entropy production.

4.5.6. *Exact memory criterion for information loss.* For the finite prepared Hamiltonian model, define a reduced transition kernel by preparing a fresh conditional canonical bath at 0, evolving the full system for time t, and observing the resolved state. Each such kernel preserves π_m, because a full canonical preparation evolves to the same full canonical law. However, in general

$$K_{s+t} \ne K_s K_t.$$

The right side inserts a fresh preparation between the two intervals; the left side retains the correlations created during the first interval. The difference explains why data processing yields $D(\nu_0 K_t\|\pi_m) \le D(\nu_0\|\pi_m)$ for every t, but does not yield monotonicity between arbitrary two later times. The Markov limit is a substantive replacement of these correlated reduced maps by a semigroup, justified here by an explicit scale limit.

4.5.7. *Initial layers and two-sided preparation.* For a finite bath in the conditional equilibrium preparation, the instantaneous conditional mean reservoir force at 0 is zero. The initial resolved derivative is Hamiltonian, and the first derivative of its phase-space relative entropy is zero under regularity. An effective Markov friction can have a nonzero initial dissipative derivative for an initially nonequilibrium momentum law. Similarly, the position entropy for a displaced thermal kinetic Gaussian has zero derivative at 0 for every positive mass, whereas its overdamped limit has a strictly negative initial derivative. There is no contradiction: uniform path or density convergence does not justify interchanging the derivative at 0 with a singular limit. The memory and momentum layers are precisely where that interchange fails. Any stronger derivative-convergence claim needs a separate estimate away from 0 or a matched initial-layer analysis.

This distinction can also be seen in a two-sided preparation. In the harmonic example with an even thermal momentum law, the exact position mean is even in microscopic time. Its overdamped mean on the two outgoing branches tends to $a_0 e^{-k|t|/g}$. The limiting function has a cusp at the preparation time, although each finite-mass mean has zero derivative there. Each outgoing branch can be described by a forward relaxation equation in its own elapsed time. Neither branch establishes a preferred absolute orientation of the full time axis.

4.6. *Deriving the variational sign from a drift-change cost.* The microscopic calculation explains how the forward stochastic law arises. A second calculation explains why its current minimizes the particular Rayleighian used below. The appropriate object is a dimensionless relative-entropy cost between diffusion laws. It is not the real-time Hamilton action or an unqualified Onsager–Machlup path-density formula.

4.6.1. *Admissible changes of drift.* Use the already derived reference diffusion

$$\mathrm{d}X_t = b(X_t)\,\mathrm{d}t + \sqrt{2\theta K}\,\mathrm{d}W_t, \qquad b = -K\nabla U,$$

on a fixed $[0,\tau]$, with an assigned initial law. Consider a changed law Q with an additional drift v_t adapted to the canonical filtration of the observed diffusion path. Work first with bounded drifts satisfying the usual Girsanov martingale condition, and with enough regularity for the expectations below. The diffusion covariance is unchanged. Girsanov's formula then gives

$$D(Q\|P) = \frac{1}{4\theta}\mathbb{E}_Q \int_0^\tau v_t^T K^{-1} v_t\,\mathrm{d}t. \tag{4.34}$$

To see the factor, write the Brownian drift change as $(\sqrt{2\theta K})^{-1}v$. The expectation of the stochastic integral in the logarithmic likelihood vanishes under Q, leaving one half its squared norm. Hence the factor is $1/(4\theta)$. If the initial law is changed as well, add its initial relative entropy. Formula (4.34) does not apply to a change of diffusion covariance through the same argument.

4.6.2. *Density and current determine the optimal Markov drift.* Let ρ_t denote the marginal density under Q and define $\bar{v}_t(x) = \mathbb{E}_Q[v_t \mid X_t = x]$. For a smooth vector test field, the expected Stratonovich current is

$$j_t = (b + \bar{v}_t)\rho_t - \theta K \nabla \rho_t.$$

This follows either from the forward equation or by converting the Stratonovich test integral to Itô form and integrating its $\theta K : DF$ correction by parts. Consequently

$$\bar{v}_t = \frac{j_t - j_{\rho_t}}{\rho_t}, \qquad j_\rho = b\rho - \theta K \nabla \rho.$$

Conditional Jensen's inequality in (4.34) gives

$$D(Q\|P) \geq \mathcal{A}[\rho, j] := \frac{1}{4\theta} \int_0^\tau \int \frac{|j - j_\rho|^2_{K^{-1}}}{\rho} \, \mathrm{d}x \, \mathrm{d}t. \tag{4.35}$$

For a prescribed smooth positive history (ρ, j) satisfying the continuity equation, suppose $u = (j - j_\rho)/\rho$ is bounded and uniformly Lipschitz in space, and that the displayed density is in the uniqueness class of its forward equation. The Markov-controlled diffusion with additional drift $u(t, X_t)$ has exactly these marginals and current, by uniqueness of that forward equation. It attains equality in both Jensen and (4.34). Thus (4.35) is the exact minimum entropy cost among this declared class of admissible drift changes. Extending it to unbounded controls requires martingale and uniform-integrability estimates, not just a formal substitution.

This derivation proves a precise variational statement without claiming that a single realized Brownian trajectory minimizes an ordinary differentiable-path action. A typical trajectory is not differentiable. The current is an ensemble object.

4.6.3. *Expansion gives the sign in the Rayleighian.* Because $j_\rho = -\rho K \nabla \mu_\rho$, the numerator in (4.35) is $|j + \rho K \nabla \mu_\rho|^2_{K^{-1}}$. Expanding gives

$$\frac{|j + \rho K \nabla \mu_\rho|^2_{K^{-1}}}{\rho} = \frac{|j|^2_{K^{-1}}}{\rho} + 2j \cdot \nabla \mu_\rho + \rho |\nabla \mu_\rho|^2_K. \tag{4.36}$$

At a fixed instantaneous density the last term is independent of j. The current-dependent part is exactly $2\mathscr{R}_\rho[j]$. Thus the forward zero-cost current is the minimizer of $\Phi + \dot{F}$. The plus sign has been recovered from the drift-change cost relative to the forward diffusion that the reservoir reduction produced.

There is an important constraint qualification. If an entire density history, including its derivative, is fixed, the admissible currents must also satisfy its continuity equation. The pointwise

unconstrained minimizer need not satisfy that constraint for an arbitrary history. The local constitutive principle chooses the current and hence the density derivative together. Minimizing the full path cost with two fixed endpoint laws is a different boundary-value control problem.

Integration of the cross term in (4.36) yields

$$\mathcal{A}[\rho, j] = \frac{1}{4\theta} \int_0^\tau \int \left(\frac{|j|^2_{K^{-1}}}{\rho} + \rho |\nabla \mu_\rho|^2_K \right) \mathrm{d}x \, \mathrm{d}t + \frac{F[\rho_\tau] - F[\rho_0]}{2\theta}. \tag{4.37}$$

This is an energy–dissipation decomposition of a nonnegative relative-entropy cost. It must not be confused with a Boltzmann factor formed from $\mathcal{S}_H/\theta$.

4.6.4. *Time reversal and the cost of an uphill history.* For position variables, set $\rho^R_t = \rho_{\tau-t}$ and $j^R_t = -j_{\tau-t}$. The two quadratic terms in (4.37) are unchanged; the endpoint term changes sign. Therefore

$$\mathcal{A}[\rho, j] - \mathcal{A}[\rho^R, j^R] = \frac{F[\rho_\tau] - F[\rho_0]}{\theta}. \tag{4.38}$$

If (ρ, j) is a zero-cost relaxation, its reversed history costs

$$\mathcal{A}[\rho^R, j^R] = \frac{F[\rho_0] - F[\rho_\tau]}{\theta} \geq 0.$$

An uphill fluctuation is not forbidden. Its cost differs from that of the typical prepared relaxation. In particular, this calculation does not claim monotonic entropy along individual noisy trajectories.

Including the equilibrium initial cost gives

$$D(\rho_0 \| \pi) + \mathcal{A}[\rho, j] = D(\rho_\tau \| \pi) + \mathcal{A}[\rho^R, j^R]. \tag{4.39}$$

Equation (4.39) shows explicitly how an equilibrium path ensemble can remain reversible while conditioned nonequilibrium relaxation has a directed free-energy decrease. Suppressing the initial-law contribution would hide this reconciliation. Stochastic heat and path-ratio interpretations should be matched to the declared reversal and reservoir convention [95].

4.6.5. *A completely computable one-dimensional example.* Let $U(x) = kx^2/2$, $K = 1/g$, and use Gaussian density histories with variance θ/k and mean $a(t)$. Their translation current is $j = \dot{a}\,\rho$, while $j_\rho = -(k/g)a\rho$. Thus

$$\mathcal{A}[a] = \frac{g}{4\theta} \int_0^\tau (\dot{a} + ka/g)^2 \, \mathrm{d}t. \tag{4.40}$$

The mean $a(t) = a_0 e^{-kt/g}$ has zero cost. Its reverse has $\dot{a}^R = (k/g)a^R$, giving

$$\mathcal{A}[a^R] = \frac{k^2}{g\theta} \int_0^\tau (a^R)^2 \, \mathrm{d}t = \frac{k}{2\theta}(a_0^2 - a_\tau^2).$$

The free-energy difference is exactly $k(a_0^2 - a_\tau^2)/2$. This verifies the sign, the factor of two, and the temperature normalization without an asymptotic expansion.

4.7. *The combined microscopic-realization theorem.*

THEOREM 4.6 (Microscopic realization of variational isothermal relaxation). *Let U satisfy (4.2), let $\theta = k_B T > 0$, and let $G = G^T > 0$. Consider the finite reversible Hamiltonians (4.3), prepared with a resolved position law ρ_0 of finite second moment, thermal momentum $N(0, m\theta I)$, and the conditional canonical bath (4.4). Choose their positive spectral weights to approximate (4.15), with the covariance convergence and path tightness described in Section 4.3. Then, on every fixed finite time interval, the resolved position laws converge in the order (4.26) to*

$$\mathrm{d}Q_t = -K\nabla U(Q_t)\,\mathrm{d}t + \sqrt{2\theta K}\,\mathrm{d}W_t, \qquad K = G^{-1}.$$

The limiting invariant law is $\pi = Z^{-1}e^{-U/\theta}\,\mathrm{d}q$. For every smooth positive density in the stated finite-energy, finite-entropy and integration-by-parts class, with $\int \rho|\nabla\mu_\rho|_K^2\,\mathrm{d}q < \infty$, the limiting current uniquely minimizes

$$\mathscr{R}_\rho[j] = \frac{1}{2}\int \frac{j^T K^{-1} j}{\rho}\,\mathrm{d}q + \int j\cdot\nabla(U + \theta\log\rho)\,\mathrm{d}q.$$

For its regular density evolution,

$$F[\rho_t] - F[\pi] = \theta D(\rho_t\|\pi), \qquad \dot F[\rho_t] = -\theta^2\int \rho_t|\nabla\log(\rho_t/\pi)|_K^2\,\mathrm{d}q.$$

With the autonomous single-isothermal-reservoir heat convention, the associated mean total entropy-production rate is $-\dot F/T \geq 0$. No entropy monotonicity assumption is used in the Hamiltonian elimination or either stochastic limit. The assertion concerns this preparation, reservoir class, order of limits, and density domain.

Proof. The canonical integration gives (4.5). The exact Hamiltonian elimination is Theorem 4.3. The positive spectral approximation converges to the Gaussian exponential-memory force and its Volterra solution. Theorem 4.4 then gives the kinetic SDE at each fixed mass, and Theorem 4.5 gives the position diffusion. Its well-posed forward equation and zero Gibbs current establish invariance. Equation (4.28) gives the current minimizer; (4.29) and (4.30) give the entropy conclusions on the stated regularity class. Finally (4.31) gives the heat-bath interpretation. The roles of the finite-time limits and the density-domain hypotheses are distinct; weak path convergence alone has not been used to pass an entropy derivative through a limit. □

5. A conditional microscopic bridge and the scope of the arrow of time

The reservoir construction above has two logically distinct tasks. The first is constructive: under a specified preparation, spectrum, and order of limits, it produces the overdamped diffusion used in the variational calculation. The second concerns scope: whether the same conclusion follows from reversibility alone for every microscopic system. The oscillator example shows that it does not. We now collect the hypotheses and conclusions to make this distinction precise.

5.1. *Why reversibility alone cannot imply the proposed diffusion.* The following proposition is a logical obstruction, rather than a technical limitation of the harmonic construction. A finite,

smooth, exactly reversible model already disproves a universal inference from reversibility to overdamped diffusion.

PROPOSITION 5.1 (No universal bridge from reversibility alone). *There is no implication of the form*

$$\textit{every finite reversible Hamiltonian system} \quad \Longrightarrow \quad \mathrm{d}Q_t = -K\nabla U(Q_t)\,\mathrm{d}t + \sqrt{2\theta K}\,\mathrm{d}W_t$$

for a fixed positive matrix K and a strictly decreasing observed relative entropy. In particular, the harmonic oscillator of Proposition 4.1 is a counterexample: its microscopic flow is reversible, its full relative entropy is constant, and its observed position relative entropy is periodic.

Proof. The oscillator has

$$D(\mathrm{Law}(q_t)\|\pi_q) = \frac{\omega^2 a^2}{2\theta}\cos^2(\omega t).$$

At $t = \pi/(2\omega)$ this quantity is zero, whereas at $t = \pi/\omega$ it equals its strictly positive initial value. A strictly decreasing Lyapunov function cannot have this behaviour. The contradiction arises before any issue about differentiating an entropy through a limit; it is a finite, smooth, exactly reversible model. Therefore additional conditions on the system–reservoir split, preparation, response kernel, observation scale, and limiting procedure are logically necessary. □

The counterexample identifies the scope of the constructive result: the proposed diffusion follows from an admissible reservoir realization, with the additional hypotheses stated next.

5.2. *The admissible class for the positive bridge.* We collect the assumptions used by the positive construction so that each can be checked in a concrete model. They specify the dynamics, preparation, and limit procedure without using the entropy-production conclusion.

Assumption 5.2 (Admissible reversible-reservoir bridge). Fix a finite horizon $\tau < \infty$. A sequence of finite Hamiltonian models of the form (4.3) is called admissible on $[0, \tau]$ if the following conditions hold.

(A1) The Hamiltonian flow Φ_t^N is globally well posed, preserves phase volume and the Hamiltonian, and has a time-reversal involution Θ with $\Theta\Phi_t^N\Theta^{-1} = \Phi_{-t}^N$.

(A2) The resolved potential satisfies the regularity and confinement assumptions in (4.2); the resolved initial position has finite second moment, and the initial momentum has the thermal scaling $p_0^m \sim N(0, m\theta I)$.

(A3) At the preparation time the reservoir is conditionally canonical in the shifted variables of (4.4). Consequently the eliminated force is centered, independent of the resolved initial state in those variables, and satisfies the finite-bath fluctuation–dissipation identity (4.11).

(A4) At fixed memory time ε the positive bath spectra converge to (4.15). The force laws are tight in $C([0,\tau];\mathbb{R}^d)$ and their bounded–Lipschitz distance from the exponential-memory force tends to zero. No rate is assumed for this bath-discretisation error.

(A5) The white-memory and small-mass estimates are uniform on the fixed horizon in the form proved in Theorems 4.4 and 4.5. The limits are taken in the order (4.26).

Condition (A4) is deliberately stated in terms of path laws. Covariance convergence at finitely many times is insufficient for a path-space result, whereas the tightness estimate (4.17) supplies the missing compactness for the present harmonic realization. Condition (A5) also prevents a finite-time estimate from being silently promoted to a long-time statement. For a non-Gaussian reservoir, verifying (A4) is the place where a central-limit, martingale, or homogenisation theorem must be proved; it is not supplied by the fluctuation–dissipation identity alone.

5.3. *Conditional bridge theorem.* Let d_{BL} denote the bounded–Lipschitz distance on probability laws over $C([0,\tau];\mathbb{R}^d)$, with the supremum norm truncated at one. Write $q^{N,\varepsilon,m}$ for the resolved path of a finite bath, $q^{\varepsilon,m}$ for the exponential-memory realization, q^m for the white-memory kinetic process, and Q for the overdamped limit.

THEOREM 5.3 (Conditional microscopic bridge to the Rayleighian diffusion). *Under Assumption 5.2, let $G = G^{\mathsf{T}} > 0$ and $K = G^{-1}$. Then, for every fixed $\tau < \infty$,*

$$\mathrm{Law}(q^{N,\varepsilon,m}_{[0,\tau]}) \Longrightarrow \mathrm{Law}(Q_{[0,\tau]})$$

in the ordered limits

$$N \to \infty, \qquad \varepsilon \downarrow 0, \qquad m \downarrow 0,$$

where

$$\mathrm{d}Q_t = -K\nabla U(Q_t)\,\mathrm{d}t + \sqrt{2\theta K}\,\mathrm{d}W_t. \tag{5.1}$$

The limiting invariant law is

$$\pi(\,\mathrm{d}q) = Z^{-1}e^{-U(q)/\theta}\,\mathrm{d}q,$$

and the forward current for every density in the regularity class of Theorem 4.6 is

$$j_\rho = -\rho K\nabla U - \theta K\nabla\rho = -\rho K\nabla(U + \theta\log\rho).$$

It is the unique minimizer of

$$\mathscr{R}_\rho[j] = \frac{1}{2}\int \frac{j^{\mathsf{T}}K^{-1}j}{\rho}\,\mathrm{d}q + \int j\cdot\nabla(U+\theta\log\rho)\,\mathrm{d}q.$$

Consequently,

$$\frac{\mathrm{d}}{\mathrm{d}t}\left[\theta D(\rho_t\|\pi)\right] = -\theta^2\int \rho_t\left|\nabla\log\frac{\rho_t}{\pi}\right|_K^2\,\mathrm{d}q \le 0. \tag{5.2}$$

No entropy monotonicity assumption is used in the Hamiltonian elimination, the white-memory limit, or the small-mass limit. The theorem is conditional on (A1)–(A5) and does not assert the implication for systems outside this class.

Proof. The shifted canonical preparation gives the exact generalized Langevin equation and the fluctuation–dissipation identity in Theorem 4.3. By (A4), the finite-bath force and the exponential-memory force have the same path-law limit at fixed (ε, m). The Volterra solution map is continuous on the fixed horizon, so the corresponding resolved paths have the same limit.

For fixed $m > 0$, Theorem 4.4 gives the kinetic Langevin equation. Its remainder estimate is obtained directly from

$$\int_0^t z_s^\varepsilon \, \mathrm{d}s = -G(q_t^\varepsilon - q_0) + \sqrt{2\theta G} W_t - \varepsilon(z_t^\varepsilon - z_0^\varepsilon),$$

and the stationary OU maximum bound (4.22); no sign of an entropy derivative enters this estimate. Theorem 4.5 then gives the overdamped equation (5.1), with the thermal momentum scaling removing the initial momentum layer.

The limiting generator is

$$Lf = -K\nabla U \cdot \nabla f + \theta K : D^2 f.$$

Since $\theta \nabla \pi = -\pi \nabla U$, its equilibrium current is zero. For $\mu_\rho = U + \theta \log \rho$, completing the square gives

$$\mathscr{R}_\rho[j] = \frac{1}{2} \int \frac{|j + \rho K \nabla \mu_\rho|^2_{K^{-1}}}{\rho} \, \mathrm{d}q - \frac{1}{2} \int \rho |\nabla \mu_\rho|^2_K \, \mathrm{d}q.$$

Thus the displayed current is the unique minimizer. Finally,

$$F[\rho] - F[\pi] = \theta D(\rho \| \pi), \qquad \dot{F}[\rho_t] = \int j_{\rho_t} \cdot \nabla \mu_{\rho_t} \, \mathrm{d}q,$$

and substitution of the current yields (5.2). The proof uses the Hamiltonian equations, covariance convergence, and positive quadratic forms; the entropy sign appears only in this last calculation. □

5.4. *Finite-scale error decomposition.* The ordered-limit theorem is qualitative unless a bath approximation rate is also established. The following decomposition records exactly what is and is not available from the estimates above. Define

$$\delta_{N,\varepsilon,m,\tau} := \mathsf{d}_{\mathrm{BL}}\big(\mathrm{Law}(q^{N,\varepsilon,m}_{[0,\tau]}), \mathrm{Law}(q^{\varepsilon,m}_{[0,\tau]})\big).$$

Then $\delta_{N,\varepsilon,m,\tau} \to 0$ for fixed (ε, m, τ) by (A4), but no numerical rate is assigned without a specified quadrature or spectral discretisation theorem. The proved white- memory and small-mass estimates imply

$$\begin{aligned} \mathsf{d}_{\mathrm{BL}}\big(\mathrm{Law}(q^{N,\varepsilon,m}_{[0,\tau]}), \mathrm{Law}(Q_{[0,\tau]})\big) \le \delta_{N,\varepsilon,m,\tau} &+ C_{m,\tau} \sqrt{\varepsilon\big[1 + \log(1 + \tau/\varepsilon)\big]} \\ &+ C_\tau \sqrt{m\big[1 + \log(1 + \tau/m)\big] + m^2}. \end{aligned} \tag{5.3}$$

The first term is a model-dependent bath error; the second is the proved white-memory error at fixed mass; the third is the proved small-mass error. The constants may depend on the displayed horizon and coefficients. In particular, (5.3) does not claim a uniform rate in m, a simultaneous

scaling, or convergence of relative entropies and Fisher informations. Weak path convergence does not by itself justify passing an entropy derivative through either singular limit.

5.5. *No absolute cosmic orientation from symmetric premises.* The preceding bridge selects a direction relative to a preparation time and a retarded response convention. It cannot select an absolute orientation from premises that are themselves invariant under time reversal.

PROPOSITION 5.4 (No absolute arrow from time-reversal-symmetric premises). *Let $\mathcal{P}$ be a class of microscopic model descriptions invariant under the reversal operation*

$$\mathcal{R}(\Phi)_t = \Theta \Phi_{-t} \Theta^{-1}.$$

Suppose an orientation selector $a : \mathcal{P} \to \{-1, 0, +1\}$ depends only on the reversal-invariant premises, so that $a(\mathcal{R}\Phi) = a(\Phi)$, while physical covariance of an oriented statement requires

$$a(\mathcal{R}\Phi) = -a(\Phi).$$

Then $a(\Phi) = 0$ for every $\Phi \in \mathcal{P}$. Hence a nonzero absolute time orientation requires additional time-asymmetric data, such as a boundary preparation, a retarded-response condition, an explicitly time-asymmetric microscopic law, or a cosmological boundary condition.

Proof. The two transformation rules give

$$a(\Phi) = a(\mathcal{R}\Phi) = -a(\Phi).$$

Therefore $2a(\Phi) = 0$. Since the codomain is discrete, $a(\Phi) = 0$. The conclusion is a symmetry statement and does not depend on the particular form of the entropy or on the existence of a Markov limit. □

This proposition does not deny a time arrow in a prepared experiment. It states that the arrow cannot be an output of premises that contain no datum capable of distinguishing the two orientations. Positive dissipation and a positive mobility are compatible with both orientations until the preparation and response convention are fixed.

5.6. *Conditional thermodynamic orientation.* We can now state precisely what the reservoir construction does select. Let f_0 be the full prepared Hamiltonian law and let $f_\tau = \Phi_{\tau *} f_0$. The exact reverse experiment starts from $\Theta_* f_\tau$. A fresh forward experiment at the observed state instead uses

$$\widehat{f}_0^R(\,\mathrm{d}s\,\mathrm{d}B) = \nu_\tau(\,\mathrm{d}s)\,\Pi_N(\,\mathrm{d}B \mid s),$$

whereas the exact reverse contains the hidden reservoir disturbance and correlations inherited from $\Theta_* f_\tau$. The KL chain rule gives

$$D(f_\tau \| \Pi_N) = D(\nu_\tau \| \pi_m) + C_N(\tau), \qquad C_N(\tau) \geq 0. \tag{5.4}$$

THEOREM 5.5 (Conditional selection of the thermodynamic orientation). *Assume the admissible bridge hypotheses and prepare the reservoir at time* 0 *by the conditional canonical law. Evolve the full Hamiltonian system with the retarded solution, observe the resolved coordinate, and take the ordered finite-time limits of Theorem 5.3. Then the forward effective law satisfies*

$$\frac{\mathrm{d}}{\mathrm{d}t}\left[\theta D(\rho_t\|\pi)\right] = -\theta^2 \int \rho_t \left|\nabla \log(\rho_t/\pi)\right|_K^2 \, \mathrm{d}q \le 0.$$

The selected orientation is therefore the composite protocol

$$\boxed{\begin{array}{c} \textit{preparation} + \textit{retarded response} \\ + \textit{hidden correlations} + \textit{ordered Markov limit} \end{array}}$$

The exact microscopic reverse is obtained from $\Theta_* f_\tau$ *and retains the conditional information in* (5.4). *If* $C_N(\tau) > 0$, *a fresh canonical reverse preparation is a different experiment and cannot be identified with the exact reverse. The theorem does not assert an absolute cosmic time direction.*

Proof. The first assertion is exactly the conclusion of the conditional bridge theorem. For the second assertion, Hamiltonian reversibility gives

$$\Phi_{t*}(\Theta_* f_\tau) = \Theta_* f_{\tau - t},$$

so the exact reverse must carry the hidden conditional law at the final time. Replacing it by $\widehat{f}_0^R$ resets that conditional law. By the chain rule (5.4), a positive value of $C_N(\tau)$ records a nonzero discrepancy in the full relative-entropy accounting. The replacement is therefore not a reversal of the same prepared Hamiltonian trajectory ensemble. The forward entropy sign follows only after the response and ordered limits have produced the autonomous diffusion; it is not used to justify the preparation or the limits. □

The construction therefore identifies the data that select a forward thermodynamic description: a preparation time, a retarded response, and the stated effective limit. It does not derive these data from time-reversal symmetry alone. Extending the result to other microscopic systems requires verifying their coupling, preparation, and convergence hypotheses; a cosmological orientation requires additional boundary or dynamical information.

5.7. *A periodic microscopic realization of the compact model.* The linear coupling used above is not a globally defined function on a torus. A periodic coupling supplies a separate realization of the compact current model. This construction permits any constant symmetric positive friction matrix; no convexity of the periodic potential is required. Write $\mathbb{T}^d = \mathbb{R}^d/\mathbb{Z}^d$ in fixed period-one coordinates and use normalized Haar volume. Let $U \in C^\infty(\mathbb{T}^d)$, $\theta = k_B T > 0$, and $G = G^T > 0$.

5.7.1. *Periodic couplings with a constant friction matrix.*

LEMMA 5.6 (Positive integer-direction decomposition). *There are finitely many $k_\ell \in \mathbb{Z}^d \setminus \{0\}$ and $a_\ell > 0$ such that $G = \sum_{\ell=1}^{L} a_\ell k_\ell k_\ell^T$. Consequently there are $J = 2L$ smooth periodic scalar functions h_α whose gradient matrix $B(q) = (\nabla h_1(q), \dots, \nabla h_J(q))$ satisfies $B(q)B(q)^T = G$ at every q.*

Proof. Choose an invertible rational matrix R sufficiently close to $G^{1/2}$. The matrix $C = R^{-1}GR^{-T}$ is then sufficiently close to I that $C_{ii} > \sum_{j\neq i} |C_{ij}|$ for every i. This choice is possible by continuity of matrix inversion and density of rational matrices. The identity

$$C = \sum_i \left(C_{ii} - \sum_{j\neq i} |C_{ij}| \right) e_i e_i^T + \sum_{i<j : C_{ij}\neq 0} |C_{ij}| (e_i + \operatorname{sgn}(C_{ij}) e_j)(e_i + \operatorname{sgn}(C_{ij}) e_j)^T$$

is checked entry by entry. Its coefficients are positive. Conjugating by R expresses G as a finite positive sum of vv^T with rational nonzero vectors v. For each such vector choose a positive integer n with $k = nv \in \mathbb{Z}^d$ and replace its weight a by a/n^2. This proves the first assertion.

For each resulting direction define

$$h_{\ell,1}(q) = \frac{\sqrt{a_\ell}}{2\pi} \sin(2\pi k_\ell \cdot q), \qquad h_{\ell,2}(q) = \frac{\sqrt{a_\ell}}{2\pi} \cos(2\pi k_\ell \cdot q).$$

Their gradients are $\sqrt{a_\ell} k_\ell \cos(2\pi k_\ell \cdot q)$ and $-\sqrt{a_\ell} k_\ell \sin(2\pi k_\ell \cdot q)$. Thus

$$\sum_{r=1}^{2} \nabla h_{\ell,r} \nabla h_{\ell,r}^T = a_\ell k_\ell k_\ell^T (\cos^2 + \sin^2) = a_\ell k_\ell k_\ell^T.$$

Summing proves $BB^T = G$. All derivatives of B are bounded. □

The periodic functions, including the factor $1/(2\pi)$, fix the normalization of the coupling. The positive weights are parameters of the reservoir realization, rather than quantities inferred from an entropy-decay curve. The coupling family is chosen to realize the specified matrix G. This proves existence of a microscopic realization; it does not assert that arbitrary molecular interactions have this coupling structure.

5.7.2. *A reversible Hamiltonian and its exact memory equation.* Compared with the linear-coupling construction in Section 4.2, the coupling gradients now form a position-dependent matrix $B(q)$. The identity $B(q)B(q)^T = G$ will fix the limiting friction, but the finite-memory equation retains both $B(q_t)$ and $B(q_s)$. This dependence must be kept throughout the elimination and controlled before taking the short-memory limit.

Give each channel $\alpha = 1, \dots, J$ an independent oscillator bath with the same positive masses M_a, frequencies ω_a, and scalar couplings κ_a. For a scalar resolved mass $m > 0$, set

$$H_N = \frac{|p|^2}{2m} + U(q) + \sum_{\alpha=1}^{J} \sum_{a=1}^{N} \left[\frac{P_{\alpha a}^2}{2M_a} + \frac{M_a \omega_a^2}{2} \left(x_{\alpha a} - \frac{\kappa_a h_\alpha(q)}{M_a \omega_a^2} \right)^2 \right]. \tag{5.5}$$

This is globally defined on $T^*\mathbb{T}^d$ times the reservoir phase space. Its reversal changes p, P to $-p, -P$. Smoothness, periodicity, and energy conservation give a complete finite-dimensional flow: on each energy surface p and the shifted reservoir coordinates are bounded, and the position remains on a compact space.

Prepare q_0 with an assigned probability law, p_0 thermally when taking the small-mass limit, and the bath conditionally on q_0 by independent centered Gaussian variables

$$y_{\alpha a} = x_{\alpha a} - \frac{\kappa_a h_\alpha(q_0)}{M_a\omega_a^2}, \qquad \mathbb{E}y_{\alpha a}^2 = \frac{\theta}{M_a\omega_a^2}, \qquad \mathbb{E}P_{\alpha a}^2 = M_a\theta.$$

In these shifted coordinates the bath variables are independent of (q_0, p_0). Translation in each $x_{\alpha a}$ shows directly that the finite canonical marginal is proportional to $\exp[-(U(q) + |p|^2/(2m))/\theta]$.

Solving each driven oscillator and integrating its convolution by parts, now with $h_\alpha(q_s)$ in place of a linear coordinate, gives

$$\begin{aligned}
\dot{q}_t &= p_t/m, \\
\dot{p}_t &= -\nabla U(q_t) + B(q_t)\eta_N(t) - B(q_t)\int_0^t \gamma_N(t-s)B(q_s)^T\frac{p_s}{m}\,\mathrm{d}s, \qquad (5.6)\\
\gamma_N(t) &= \sum_a \frac{\kappa_a^2}{M_a\omega_a^2}\cos(\omega_a t), \\
(\eta_N)_\alpha(t) &= \sum_a \kappa_a\left[y_{\alpha a}(0)\cos(\omega_a t) + \frac{P_{\alpha a}(0)}{M_a\omega_a}\sin(\omega_a t)\right].
\end{aligned}$$

The endpoint containing $h_\alpha(q_t)$ cancels the quadratic counterterm. The endpoint at zero combines with the prepared shift. Since $dh_\alpha(q_s)/ds = \nabla h_\alpha(q_s)^T p_s/m$, the remaining convolution is exactly the displayed one. Independence and $\cos u\cos v + \sin u\sin v = \cos(u-v)$ give

$$\mathbb{E}[\eta_N(t)\eta_N(s)^T] = \theta\gamma_N(t-s)I_J.$$

The memory force is nonlinear in the resolved path; it is not replaced by a constant kernel before taking the short-memory limit.

Approximate the positive scalar spectrum $2/[\pi(1+\varepsilon^2\omega^2)]$ by positive point masses and set $\kappa_a^2/(M_a\omega_a^2)$ equal to those masses. At fixed m, ε, the force converges in $C([0,\tau];\mathbb{R}^J)$ to the stationary Gaussian force with covariance $\theta\varepsilon^{-1}e^{-|t-s|/\varepsilon}I_J$. Covariance convergence is accompanied by the Gaussian increment bound $\mathbb{E}|\eta_N(t) - \eta_N(s)|^{2r} \le C|t-s|^r$, $r > 1$. Positive spectral truncation and frequency quantization give this bound as in the preceding scalar-kernel construction.

For completeness, the nonlinear Volterra solution map remains continuous in the force and in the L^1 kernel on a fixed interval. Boundedness of B and ∇U gives

$$|p_t| \le |p_0| + C\tau + C\int_0^\tau |\eta(s)|\,\mathrm{d}s + \frac{C}{m}\|\gamma\|_{L^1(0,\tau)}\int_0^t |p_s|\,\mathrm{d}s.$$

Gronwall bounds p for bounded force and kernel sets. Subtracting two equations on that bounded set, using the bounded derivatives of B and ∇U, and applying Gronwall again proves continuity.

Thus continuous-path convergence of the Gaussian forces transfers to weak convergence of the resolved paths at fixed m, ε.

5.7.3. *The short-memory limit with periodic coupling.* The limiting memory equation has the exact embedding

$$\begin{aligned} \mathrm{d}q_t^\varepsilon &= p_t^\varepsilon \,\mathrm{d}t/m, \\ \mathrm{d}p_t^\varepsilon &= -\nabla U(q_t^\varepsilon)\,\mathrm{d}t + B(q_t^\varepsilon) z_t^\varepsilon \,\mathrm{d}t, \\ \mathrm{d}z_t^\varepsilon &= -z_t^\varepsilon \,\mathrm{d}t/\varepsilon - B(q_t^\varepsilon)^T p_t^\varepsilon \,\mathrm{d}t/(m\varepsilon) + \sqrt{2\theta}\,\mathrm{d}W_t/\varepsilon, \end{aligned} \tag{5.7}$$

where W is J dimensional and $z_0^\varepsilon \sim N(0, \theta I_J/\varepsilon)$ is independent of the resolved initial state and future Brownian increments. The extended Gibbs energy is $U + |p|^2/(2m) + \varepsilon|z|^2/2$. The conservative coupling cancels in its derivative and has zero phase-space divergence. The remaining z part is an OU thermostat. The equilibrium parity is $(q, p, z) \mapsto (q, -p, z)$.

Proposition 5.7 (Fixed-mass periodic short-memory limit). *At fixed $m > 0$ and finite horizon τ, the resolved paths of (5.7) converge in probability, under the same Brownian motion and resolved initial state, to*

$$\mathrm{d}q_t = p_t \,\mathrm{d}t/m, \qquad \mathrm{d}p_t = -\nabla U(q_t)\,\mathrm{d}t - G p_t \,\mathrm{d}t/m + \sqrt{2\theta} B(q_t)\,\mathrm{d}W_t. \tag{5.8}$$

The initial momentum has finite second moment. The law of this kinetic limit is the law of constant-friction Langevin dynamics with momentum noise covariance $2\theta G$.

Proof. Write $z^\varepsilon = \eta^\varepsilon - \int_0^t \varepsilon^{-1} e^{-(t-s)/\varepsilon} B(q_s^\varepsilon)^T p_s^\varepsilon/m \,\mathrm{d}s$, where η^ε is stationary OU. Multiplication of the last equation in (5.7) by $\varepsilon B(q_t^\varepsilon)$, and the product rule, give

$$\begin{aligned} p_t^\varepsilon &= p_0 - \int_0^t \nabla U(q_s^\varepsilon)\,\mathrm{d}s - G\int_0^t p_s^\varepsilon \,\mathrm{d}s/m + \sqrt{2\theta}\int_0^t B(q_s^\varepsilon)\,\mathrm{d}W_s + r_t^\varepsilon, \\ r_t^\varepsilon &= -\varepsilon B(q_t^\varepsilon) z_t^\varepsilon + \varepsilon B(q_0) z_0^\varepsilon + \varepsilon \int_0^t DB(q_s^\varepsilon)[p_s^\varepsilon/m] z_s^\varepsilon \,\mathrm{d}s. \end{aligned} \tag{5.9}$$

Here $BB^T = G$. There is no quadratic-covariation correction in this product: at positive mass q^ε is a finite-variation path. The derivative term in the remainder cannot simply be discarded without an estimate.

Lift positions continuously to $\mathbb{R}^d$ from the same initial representative. Stop both equations when either momentum reaches radius R, and denote this time by τ_R. With $B_* = \sup \|B\|$,

$$\sup_{t \le \tau \wedge \tau_R} \varepsilon |z_t^\varepsilon| \le \varepsilon \sup_{t \le \tau} |\eta_t^\varepsilon| + \varepsilon B_* R/m.$$

The stationary OU maximal bound is

$$\mathbb{E} \sup_{t \le \tau} |\varepsilon \eta_t^\varepsilon|^2 \le C\varepsilon[1 + \log(1 + \tau/\varepsilon)].$$

It follows by dividing time into intervals of length ε, using Gaussian endpoint tails and time-changed Brownian maximal tails within each interval, and integrating the union bound over $O(1+\tau/\varepsilon)$ intervals. Therefore

$$\mathbb{E}\sup_{t\le\tau\wedge\tau_R}|r_t^\varepsilon|^2 \le C_{R,m,\tau}\varepsilon[1+\log(1+\tau/\varepsilon)] + C_{R,m,\tau}\varepsilon^2 \longrightarrow 0.$$

All derivatives of B are bounded, and $|p^\varepsilon| \le R$ on the stopped interval. Subtract (5.8) from (5.9). The drift terms are Lipschitz; the Burkholder–Davis–Gundy inequality bounds the stopped noise difference by a constant times $\int_0^\tau \mathbb{E}\sup_{u\le s\wedge\tau_R}|q_u^\varepsilon - q_u|^2\,\mathrm{d}s$. Together with $q_t^\varepsilon - q_t = \int_0^t (p_s^\varepsilon - p_s)\,\mathrm{d}s/m$, Gronwall yields

$$\mathbb{E}\sup_{t\le\tau\wedge\tau_R}(|q_t^\varepsilon - q_t|^2 + |p_t^\varepsilon - p_t|^2) \longrightarrow 0.$$

The limiting equation has globally Lipschitz coefficients on the lift and is nonexplosive. On the event $\sup_{t\le\tau}|p_t| < R/2$, an exit of p^ε at radius R forces the stopped momentum error to reach $R/2$. For each fixed R, the probability of that error tends to zero. Letting $R\to\infty$ removes the stopping and proves convergence in probability, without assuming an unstopped uniform moment bound for the memory process.

Finally, $\beta_t = G^{-1/2}\int_0^t B(q_s)\,\mathrm{d}W_s$ is a continuous martingale with quadratic variation tI_d. Lévy's characterization makes it a d-dimensional Brownian motion. Thus the momentum noise is $\sqrt{2\theta G}\,\mathrm{d}\beta_t$. Uniqueness in law for the globally Lipschitz kinetic equation proves the last assertion. Equivalently, its generator is the constant-covariance kinetic generator. No position-noise correction is introduced at this fixed-mass step. □

5.7.4. *The small-mass limit and the compact second law.*

THEOREM 5.8 (Microscopic realization on the torus). *Let $U \in C^\infty(\mathbb{T}^d)$, $G = G^T > 0$, and $\theta > 0$. Use the periodic Hamiltonians (5.5), the conditional canonical bath preparation, the positive spectral approximation just stated, and an independent initial momentum $N(0, m\theta I_d)$. On every fixed finite interval, the resolved position laws converge, first in the bath mesh and cutoff, next as $\varepsilon \downarrow 0$ at fixed m, and finally as $m \downarrow 0$, to the law of*

$$\mathrm{d}Q_t = -K\nabla U(Q_t)\,\mathrm{d}t + \sqrt{2\theta K}\,\mathrm{d}\beta_t \quad \text{on } \mathbb{T}^d, \qquad K = G^{-1}. \tag{5.10}$$

For a smooth positive initial position density, its invariant density is $\pi = Z^{-1}e^{-U/\theta}$ and its current uniquely minimizes $\Phi + \dot{F}$ in the finite weighted-current space. Moreover,

$$F[\rho_t] - F[\pi] = \theta D(\rho_t\|\pi), \qquad \dot{F}[\rho_t] = -\theta^2\int \rho_t|\nabla\log(\rho_t/\pi)|_K^2\,\mathrm{d}q \le 0.$$

The corresponding mean total entropy-production rate is $-\dot{F}/T$ under the autonomous single-isothermal-reservoir heat convention.

Proof. The finite-bath elimination and force convergence give the memory embedding, and Proposition 5.7 gives its fixed-mass kinetic limit. That kinetic law equals the additive-noise

Langevin law. It remains to justify the momentum reduction for a periodic potential; a confining Euclidean Gibbs density is unnecessary.

Use the periodic lift of U, whose gradient is bounded and globally Lipschitz. In the additive kinetic representation the exact integral identity is

$$q_t^m = q_0 - \int_0^t K\nabla U(q_s^m)\,\mathrm{d}s + \sqrt{2\theta K}\beta_t - K(p_t^m - p_0^m).$$

Variation of constants gives

$$p_t^m = \xi_t^m - \int_0^t e^{-G(t-s)/m}\nabla U(q_s^m)\,\mathrm{d}s, \qquad \mathbb{E}[\xi_t^m(\xi_t^m)^T] = m\theta I_d,$$

where ξ^m is stationary because the initial momentum has the thermal law. If $g_* > 0$ is the least eigenvalue of G, then

$$\sup_{t\le\tau}|p_t^m| \le \sup_{t\le\tau}|\xi_t^m| + \frac{m}{g_*}\|\nabla U\|_\infty.$$

The OU maximal estimate, with its momentum correlation time of order m, gives in fixed dimensionless units

$$\mathbb{E}\sup_{t\le\tau}|p_t^m|^2 \le C_\tau m[1+\log(1+\tau/m)] + C_\tau m^2 \longrightarrow 0.$$

Subtract the lifted integral equation for Q. Lipschitz continuity of ∇U and Gronwall give

$$\mathbb{E}\sup_{t\le\tau}|q_t^m - Q_t|^2 \le C_\tau\mathbb{E}\left[\sup_{t\le\tau}|p_t^m|^2 + |p_0^m|^2\right] \longrightarrow 0.$$

Projection to $\mathbb{T}^d$ gives the claimed final path-law limit. The bath and short-memory limits are taken first; no commutation or infinite-horizon uniformity has been used.

The forward current of (5.10) is $j_\rho = -\rho K\nabla U - \theta K\nabla\rho$. Its value at π is zero. Smooth coefficients and ellipticity on the compact torus give a unique conservative diffusion and a smooth positive density evolution. Completing the weighted square gives the unique Rayleighian minimizer, and integration by parts on the torus gives the displayed free-energy identity. For the heat convention $\dot{Q}_{\mathrm{bath}} = -d\mathbb{E}U/dt$ and $S_{\mathrm{sys}} = -k_B\int\rho\log\rho$, direct algebra gives $\dot{S}_{\mathrm{sys}} + \dot{Q}_{\mathrm{bath}}/T = -\dot{F}/T$. The stochastic limits were established before this entropy calculation. □

This result supplies a microscopic realization of the compact constant-mobility current model, using globally periodic couplings. Its preparation, bath spectrum and sequential scale limits remain physical assumptions. Exact reverse preparation retains the correlations created during the forward evolution. The construction neither selects an absolute cosmic orientation from equilibrium alone nor realizes arbitrary interacting reservoirs or constrained continuum fields.

6. **Stochastic Dynamics and Variational Thermodynamics**

The reservoir calculation has supplied one effective stochastic law. We now ask which features of that law are needed for a thermodynamic description. The energy specifies the conservative forces, the mobility specifies the response to those forces, and the bath temperature fixes the fluctuation

scale. Their compatibility determines whether the Gibbs law is preserved. We first state these inputs, then derive the probability current and its variational form. The overdamped and kinetic models are treated separately because removing momentum changes the way dissipation acts on the state. Appendix A collects the notation and units.

The physical content of this chain is an accounting of exchange. Friction transfers energy from a resolved degree of freedom to the reservoir, while reservoir fluctuations return energy to it. At thermal equilibrium these exchanges continue, although the probability law is stationary. Away from equilibrium, their net effect is expressed by a probability current. The equilibrium reference identifies the free-energy excess carried by that current; the local heat balance determines whether its loss is the physical entropy gain of system plus reservoir. Thus the stationary-action skeleton specifies admissible reversible motion, and the prepared reservoir supplies the direction of the effective dissipative response. The next hypotheses make each part of this interpretation explicit before the variational identity is used.

6.1. *Assumption Hierarchy.* The paper does not use a single monolithic axiom. Instead, assumptions are modular and are invoked only where needed.

Assumption 6.1 (M1: Markov well-posedness). The microscopic stochastic equation under consideration admits a conservative Markov solution and a transition semigroup $(P_t)_{t\geq 0}$. Standard finite-dimensional diffusion background is used in the form summarized by Pavliotis [85]; infinite-dimensional stochastic evolution and ergodic background are invoked only under hypotheses compatible with Da Prato–Zabczyk theory [22] and [23]; and Harris-type Markov-chain stability statements are invoked only in the scope covered by Meyn–Tweedie theory [71].

Assumption 6.2 (M2: thermodynamic calibration). In equilibrium molecular models, conservative forces and stochastic dissipation satisfy the stated Hamiltonian and fluctuation-dissipation structure. In particular, the thermal covariance is matched to the friction or mobility at temperature T.

Assumption 6.3 (M3: normalizability). The candidate equilibrium Gibbs measure has finite nonzero partition function.

Assumption 6.4 (M4: invariant equilibrium law). The equilibrium law μ_{eq} satisfies $\mu_{\mathrm{eq}} P_t = \mu_{\mathrm{eq}}$. Whenever possible this property is proved from Theorem 6.2 rather than assumed.

Assumption 6.5 (M5: entropy regularity). For the diffusion entropy identity, the dissipative form is strongly local and has the stated diffusion chain rule; any antisymmetric part acts as a first-order derivation on the common core. For regular solutions, the common-domain and integrability conditions below permit differentiation of entropy and integration in time. For a weak-solution passage, one must instead verify an approximation with convergent endpoint entropies and convergence in L^1 in time of the Fisher-information terms. Lower semicontinuity alone gives an inequality, not

necessarily an identity. Closed symmetric and quasi-regular Dirichlet-form issues are interpreted in the sense of [34] and [92]; closedness alone does not establish these extra properties.

Assumption 6.6 (M6: physical time reversal). There exists a measurable involution Θ such that $\Theta^2 = I$ and $\Theta_{\#}\mu_{\mathrm{eq}} = \mu_{\mathrm{eq}}$.

Assumption 6.7 (M7: irreducibility or hypoelliptic mixing). Whenever uniqueness or strict long-time convergence is asserted, the system satisfies the corresponding irreducibility, positivity-improving, Harris, Hormander, or hypocoercive hypothesis explicitly cited in the theorem. Elliptic positivity and support arguments are not assumed silently; when used, they must be traced to results of Aronson type or Stroock–Varadhan type [5] and [98].

Assumption 6.8 (M8: coercivity). A quantitative convergence theorem uses a separately stated logarithmic Sobolev, Bakry-Emery, Harris, spectral, or hypocoercive estimate. The existence of an energy or action minimum is never used as a substitute for coercivity.

Assumption 6.9 (M9: path-space consistency). When a family of finite-window trajectory measures is interpreted as restrictions of one stochastic process, the family is projectively consistent. Stationarity is separately established by time-shift invariance.

Assumption 6.10 (M10: history-space generation). The physical moving-history process is described by its actual shift-boundary generator. An abstract Gibbs sampler on path space is not identified with the physical history generator unless that equality is independently proved.

Assumption 6.11 (M11: Navier-Stokes trace regularity). The noise covariance in the $\mathcal{H}$-valued 2D stochastic Navier-Stokes model satisfies the trace assumptions stated in Section 9.2; in particular, enstrophy estimates require $\mathrm{Tr}(A_{\mathrm{St}}Q) < \infty$.

Assumption 6.12 (M12: experimental protocol). Each experimental prediction is conditioned on the specified calibration, time-scale separation, measurement model, and post-driving protocol. Work performed by external parameter changes is not absorbed into autonomous relaxation entropy production.

Assumption 6.13 (M13: local detailed balance when physical entropy is inferred from paths). Whenever a path likelihood ratio is interpreted as physical medium or total entropy production, the microscopic transition mechanism satisfies a model-specific local-detailed-balance relation. For jump channels this includes a declared channel involution $\nu \mapsto \bar{\nu}$, support equivalence of forward and reversed channels, and cancellation of the corresponding holding-time terms. For diffusions this includes the declared stochastic convention, parity map, covariance, endpoint initialization, and heat sign.

6.2. *Dependency Map.* The proof structure is summarized by the following implications:

$$\text{Markovity} + \text{invariance} \Longrightarrow \text{relative-entropy contraction}, \tag{6.1}$$

$$\text{Dirichlet regularity} \Longrightarrow \text{entropy-dissipation identity}, \tag{6.2}$$

$$\text{Gibbs thermodynamic identification} \Longrightarrow F - F_{\mathrm{eq}} = k_B T D(\nu \| \mu_{\mathrm{eq}})\,, \tag{6.3}$$

$$\text{coercivity/hypocoercivity} \Longrightarrow \text{quantitative convergence}, \tag{6.4}$$

$$\text{strict contraction} \Longrightarrow \begin{cases} \text{no equilibrium-preserving positive Markov inverse}, \\ \text{no exact recurrence of a non-equilibrium law}. \end{cases} \tag{6.5}$$

These implications are deliberately one-directional. In particular, neither invariance nor the existence of a free-energy minimum uniquely determines the physical generator.

The complete proof chain used for the central theorem is

$$\begin{array}{c} \text{open-system stochastic model} \\ \Downarrow \\ \text{thermal calibration } (\mathsf{D} = k_B T \mathsf{K}) \text{ and ideal-bath interpretation} \\ \Downarrow \\ \text{Gibbs invariant law and free-energy identity} \\ \Downarrow \\ \text{Onsager–Rayleigh characterization of the dissipative current} \\ \Downarrow \\ \text{Markov relative-entropy contraction and class-dependent dissipation} \\ \Downarrow \\ \text{autonomous unforced isothermal second law} \\ \Downarrow \\ \text{convergence in law only after an additional coercive theorem.} \end{array} \tag{6.6}$$

Every arrow in Equation (6.6) is either proved in the paper, imported with explicit hypotheses, or stated as a constitutive modeling premise. The sign of $\dot{S}_{\mathrm{tot}}$ is never used as a premise for the relative-entropy contraction that later proves it in the autonomous Gibbs class. For the confined constant-mobility branch, Section 4 also supplies the preceding Hamiltonian-reservoir realization. Its finite-time path convergence is distinct from the entropy identity of the limiting diffusion; no convergence of entropy derivatives is inferred from weak path convergence.

6.3. *Microscopic Stochastic Molecular Dynamics.* The choice of state is physical. If momentum relaxes on a much shorter time scale than position, an overdamped model records position alone. If that separation is unavailable, momentum remains part of the state: forces change momentum,

momentum transports position, and the reservoir acts through friction and momentum fluctuations. The two models below therefore share a thermal interpretation but have different generators.

6.3.1. *Overdamped and Underdamped Model Classes.* The finite-dimensional molecular state may be represented either by configuration variables alone or by full phase-space variables. The distinction is essential because the associated entropy-dissipation mechanisms are different.

For an overdamped system with configuration $X_t \in \mathbb{R}^n$, the prototype is

$$\mathrm{d}X_t = b(X_t)\,\mathrm{d}t + \sigma(X_t)\,\mathrm{d}W_t. \tag{6.7}$$

When the mobility is constant and the force is conservative, the thermally calibrated equilibrium model takes the form

$$\mathrm{d}X_t = -\mathsf{K}\nabla U(X_t)\,\mathrm{d}t + \sqrt{2k_BT\mathsf{K}}\;\mathrm{d}W_t, \qquad \mathsf{K} = \mathsf{K}^{\mathsf{T}} > 0. \tag{6.8}$$

When momentum relaxation must be resolved, the molecular model retains momentum. Let $q_t, p_t \in \mathbb{R}^{dN}$, let $\mathsf{M} = \mathsf{M}^{\mathsf{T}} > 0$ be the mass matrix, and let $\mathsf{G} = \mathsf{G}^{\mathsf{T}} > 0$ denote the friction matrix. The underdamped Langevin equation is

$$\mathrm{d}q_t = \mathsf{M}^{-1}p_t\,\mathrm{d}t, \tag{6.9}$$

$$\mathrm{d}p_t = -\nabla U(q_t)\,\mathrm{d}t - \mathsf{G}\mathsf{M}^{-1}p_t\,\mathrm{d}t + \sqrt{2k_BT\mathsf{G}}\;\mathrm{d}W_t. \tag{6.10}$$

The molecular Hamiltonian is

$$\mathcal{H}(q,p) = \frac{1}{2}p^{\mathsf{T}}\mathsf{M}^{-1}p + U(q). \tag{6.11}$$

The noise in Equation (6.10) acts only in the momentum directions. Thus the kinetic diffusion is degenerate in the full (q,p) state space and cannot be treated by a naive uniformly elliptic argument.

6.3.2. *Fluctuation-Dissipation Calibration.* The noise covariance and friction are not independent parameters in the equilibrium model. This calibration is the stochastic analogue of the fluctuation-dissipation structure developed in linear-response theory [13] and [56]. In the kinetic normalization of Equation (6.10),

$$\sigma_p\sigma_p^{\mathsf{T}} = 2k_BT\mathsf{G}. \tag{6.12}$$

Similarly, for the overdamped model Equation (6.8),

$$\sigma\sigma^{\mathsf{T}} = 2k_BT\mathsf{K}. \tag{6.13}$$

These identities are fluctuation-dissipation calibrations. They do not by themselves imply Gibbs equilibrium: the conservative form of the drift is also required. For example, if a nonconservative force $F_{\mathrm{nc}}(q)$ is added to Equation (6.10), then the canonical Gibbs density generally ceases to be invariant.

PROPOSITION 6.14 (Conservative force plus fluctuation-dissipation calibration yields Gibbs invariance). *Assume $U \in C^2(\mathbb{R}^{dN})$ is bounded below, has compact sublevel sets, and has globally Lipschitz gradient. Keep the fixed positive mass and friction matrices specified above, and assume*

$$Z = \int_{\mathbb{R}^{2dN}} \exp[-\beta \mathcal{H}(q,p)]\, \mathrm{d}q\, \mathrm{d}p < \infty, \qquad \beta = (k_B T)^{-1}. \tag{6.14}$$

Then the probability measure

$$\pi_{\mathrm{eq}}(\,\mathrm{d}q\,\mathrm{d}p) = Z^{-1} \exp[-\beta \mathcal{H}(q,p)]\, \mathrm{d}q\, \mathrm{d}p \tag{6.15}$$

is invariant for Equations (6.9) and (6.10).

Proof. The backward generator is decomposed as

$$L = A + S, \tag{6.16}$$

where

$$A = \mathsf{M}^{-1} p \cdot \nabla_q - \nabla U(q) \cdot \nabla_p \tag{6.17}$$

and

$$S = -\mathsf{G}\mathsf{M}^{-1} p \cdot \nabla_p + k_B T \mathsf{G} : \nabla_p^2. \tag{6.18}$$

Let $\pi(q,p)$ denote the density in Equation (6.15). Differentiating gives

$$\nabla_q \pi = -\beta \nabla U(q) \pi, \tag{6.19}$$

$$\nabla_p \pi = -\beta \mathsf{M}^{-1} p\, \pi. \tag{6.20}$$

The Lebesgue adjoint of A is

$$A^* = -\mathsf{M}^{-1} p \cdot \nabla_q + \nabla U(q) \cdot \nabla_p, \tag{6.21}$$

because the Hamiltonian vector field has zero Euclidean divergence. Applying Equation (6.21) to π and using Equations (6.19) and (6.20),

$$\begin{aligned} A^* \pi &= -\mathsf{M}^{-1} p \cdot (-\beta \nabla U \pi) + \nabla U \cdot (-\beta \mathsf{M}^{-1} p\, \pi) \\ &= \beta \mathsf{M}^{-1} p \cdot \nabla U\, \pi - \beta \nabla U \cdot \mathsf{M}^{-1} p\, \pi \\ &= 0. \end{aligned} \tag{6.22}$$

The forward dissipative operator is

$$S^* \rho = \nabla_p \cdot \left(\mathsf{G}\mathsf{M}^{-1} p\, \rho + k_B T \mathsf{G} \nabla_p \rho \right). \tag{6.23}$$

Substituting Equation (6.20), the vector field inside the divergence is

$$\begin{aligned} \mathsf{G}\mathsf{M}^{-1} p\, \pi + k_B T \mathsf{G} \nabla_p \pi &= \mathsf{G}\mathsf{M}^{-1} p\, \pi - k_B T \beta \mathsf{G}\mathsf{M}^{-1} p\, \pi \\ &= 0, \end{aligned} \tag{6.24}$$

since $k_B T\beta = 1$. Hence $S^*\pi = 0$. Combining this identity with Equation (6.22) gives

$$L^*\pi = (A^* + S^*)\pi = 0, \tag{6.25}$$

This establishes infinitesimal stationarity. To pass from it to invariance of the actual semigroup, we also need a conservative well-posed realization; the global Lipschitz hypothesis supplies it. One direct argument avoids identifying a formal adjoint solution with an invariant probability without this step.

Let H_t be the deterministic Hamiltonian transition and O_t the Ornstein–Uhlenbeck transition acting only on momentum. The Hamiltonian flow is complete, preserves $\mathcal{H}$, and has unit Jacobian because its vector field is divergence free. Thus $\pi_{\mathrm{eq}} H_t = \pi_{\mathrm{eq}}$. The momentum covariance $C_p = k_B T \mathsf{M}$ satisfies

$$(\mathsf{G}\mathsf{M}^{-1})C_p + C_p(\mathsf{M}^{-1}\mathsf{G}) = 2k_B T \mathsf{G}.$$

Consequently O_t preserves the Maxwell momentum factor while leaving the position factor unchanged, and $\pi_{\mathrm{eq}} O_t = \pi_{\mathrm{eq}}$. Every product $(H_{t/n} O_{t/n})^n$ therefore preserves π_{eq} exactly.

For globally Lipschitz drift, these split transitions converge to the Langevin transition P_t from each fixed initial state. To see the ingredients, expand each deterministic step to first order and use the exact Gaussian momentum step. Its conditional drift is the momentum drift times $t/n + O(n^{-2})$, its conditional covariance is $2k_B T \mathsf{G}\, t/n + O(n^{-2})$, and the deterministic part supplies the Hamiltonian drift. Global linear-growth moment bounds give tightness of the interpolations. Their martingale limits have generator $A + S$; global Lipschitz uniqueness identifies that limit with P_t. Equivalently, the usual coupled time-discretization estimate proves convergence on a finite interval. For every bounded continuous f, dominated convergence now gives

$$\int P_t f \, d\pi_{\mathrm{eq}} = \lim_{n\to\infty} \int (H_{t/n} O_{t/n})^n f \, d\pi_{\mathrm{eq}} = \int f \, d\pi_{\mathrm{eq}}.$$

No energy moment of the equilibrium is needed for this last passage, because the test is bounded and convergence holds pointwise in the initial state. This proves invariance. □

The global Lipschitz condition is a transparent sufficient condition, not a necessary one. Singular molecular forces or faster-growing smooth forces need a separate conservative-realization and convergence argument; normalizability of a formal Gibbs density alone does not supply that argument.

Remark 6.15 (Why fluctuation-dissipation calibration alone is insufficient). Suppose a force $F_{\mathrm{nc}}(q)$ is added to the momentum equation. The additional forward operator is

$$\mathcal{N}^*\rho = -\nabla_p \cdot (F_{\mathrm{nc}}\rho). \tag{6.26}$$

Because F_{nc} is independent of p,

$$\begin{aligned} \mathcal{N}^*\pi &= -F_{\mathrm{nc}} \cdot \nabla_p \pi \\ &= \beta F_{\mathrm{nc}} \cdot \mathsf{M}^{-1} p \, \pi, \end{aligned} \tag{6.27}$$

which is generally nonzero. Thus Gibbs invariance is produced by the joint conservative-force and fluctuation-dissipation structure, not by stochasticity or the covariance relation alone.

6.3.3. *The Itô Convention and the Stratonovich Correction.* Whenever an explicit finite-dimensional calculation is required, the manuscript uses Itô form. If a model is originally written as

$$\mathrm{d}X_i = b_i^{\mathrm{S}}(X)\,\mathrm{d}t + \sigma_{ik}(X) \circ \mathrm{d}W_k, \tag{6.28}$$

then the corresponding Itô drift is

$$b_i^{\mathrm{I}} = b_i^{\mathrm{S}} + \frac{1}{2}\sum_{j,k} \sigma_{jk}\partial_j \sigma_{ik}. \tag{6.29}$$

In general this is not equal to $b_i^{\mathrm{S}} + \frac{1}{2}\partial_j(\sigma\sigma^{\mathsf{T}})_{ij}$ because

$$\begin{aligned} \partial_j(\sigma\sigma^{\mathsf{T}})_{ij} &= \sum_k \partial_j(\sigma_{ik}\sigma_{jk}) \\ &= \sum_k \sigma_{jk}\partial_j\sigma_{ik} + \sum_k \sigma_{ik}\partial_j\sigma_{jk}. \end{aligned} \tag{6.30}$$

The second term in Equation (6.30) is not part of the general Stratonovich-to-Itô correction.

6.3.4. *Why Stochasticity Is Not Identical to Time-Reversal Breaking.* The equilibrium Ornstein-Uhlenbeck process already provides a decisive counterexample to the statement that noise by itself generates a physical arrow of time. The stationary process is stochastic and dissipative, but its stationary law is reversible. Physical time reversal must therefore be formulated relative to the parity involution and the stationary law, as developed in Section 8.1.

6.4. *Stochastic Actions and the Minimum-Dissipation Principle.* Least action and variational dissipation concern different objects. Hamilton's principle varies a mechanical trajectory with prescribed endpoint data. The principle used here varies an ensemble current at a fixed density. The free-energy gradient provides the thermodynamic force, and the mobility fixes how much current that force produces. The Rayleighian combines the free-energy rate with a positive transport cost, so that its minimizer reproduces the already specified dissipative dynamics. A comparison with path-action formulations is needed before writing this current principle mathematically.

6.4.1. *Three Inequivalent Action Concepts.* The word "action" is used in several branches of mechanics and probability, but the corresponding objects are not interchangeable. Confusing them creates both dimensional and logical errors.

Hamilton Action. The classical real-time Hamilton action is

$$\mathcal{S}_H[q] = \int_0^T \left[\frac{1}{2}m|\dot{q}_t|^2 - U(q_t)\right] \mathrm{d}t. \tag{6.31}$$

Its variational condition is stationarity,

$$\delta\mathcal{S}_H = 0, \tag{6.32}$$

not a universal monotone descent law. The resulting Euler-Lagrange or Hamilton equations are conservative under the usual assumptions and do not by themselves imply entropy production.

There is also a dimensional obstruction to using $\exp(-\beta\mathcal{S}_H)$ as a classical thermal path weight. The dimensions are

$$[\mathcal{S}_H] = \mathrm{J\,s}, \qquad [\beta] = \mathrm{J}^{-1}, \tag{6.33}$$

so $\beta\mathcal{S}_H$ has units of time rather than being dimensionless. Accordingly, the final theory never inserts the real-time Hamilton action directly into a Boltzmann factor.

Girsanov Relative Path Action. Consider, as an elliptic prototype, two path measures generated by diffusions with the same constant invertible diffusion matrix σ and the same initial law. The reference process is

$$\mathrm{d}X_t = \sigma\,\mathrm{d}W_t, \tag{6.34}$$

and the drifted process is

$$\mathrm{d}X_t = b(X_t)\,\mathrm{d}t + \sigma\,\mathrm{d}W_t. \tag{6.35}$$

Set

$$u(x) = \sigma^{-1}b(x). \tag{6.36}$$

Under Novikov's condition

$$\mathbb{E}_{\mathbb{P}_0}\exp\left[\frac{1}{2}\int_0^T |u(X_t)|^2\,\mathrm{d}t\right] < \infty, \tag{6.37}$$

Here the expectation is under the reference law and the stochastic integral below uses its Brownian motion W^0. Girsanov's theorem gives

$$\frac{\mathrm{d}\mathbb{P}_b}{\mathrm{d}\mathbb{P}_0} = \exp\left[\int_0^T u(X_t)\cdot\,\mathrm{d}W_t^0 - \frac{1}{2}\int_0^T |u(X_t)|^2\,\mathrm{d}t\right]. \tag{6.38}$$

The relative path action is therefore defined by

$$\mathcal{A}_T^G = -\log\frac{\mathrm{d}\mathbb{P}_b}{\mathrm{d}\mathbb{P}_0}. \tag{6.39}$$

This quantity is dimensionless by construction. It is a logarithmic likelihood ratio between path measures; it is not automatically a most-probable-path action. Under the drifted law, $W^b = W^0 - \int_0^{\cdot} u(X_s)\,\mathrm{d}s$ is Brownian. If $\mathbb{E}_{\mathbb{P}_b}\int_0^T |u(X_t)|^2\,\mathrm{d}t < \infty$, taking the expectation of the log likelihood under that law gives

$$D(\mathbb{P}_b\|\mathbb{P}_0) = \frac{1}{2}\mathbb{E}_{\mathbb{P}_b}\int_0^T |u(X_t)|^2\,\mathrm{d}t. \tag{6.40}$$

This expectation condition and the reference Novikov condition serve different purposes. The drifted-law expectation of $\mathcal{A}_T^G$ is the negative of this KL divergence.

If the initial distributions differ, $\nu_0 \ll \mu_0$, the path Radon-Nikodym derivative acquires the initial contribution

$$\log\frac{\mathrm{d}\mathbb{P}_b^{\nu_0}}{\mathrm{d}\mathbb{P}_0^{\mu_0}} = \log\frac{\mathrm{d}\nu_0}{\mathrm{d}\mu_0}(X_0) + \int_0^T u(X_t)\cdot\,\mathrm{d}W_t^0 - \frac{1}{2}\int_0^T |u(X_t)|^2\,\mathrm{d}t. \tag{6.41}$$

Remark 6.16 (Degenerate kinetic diffusions). The full underdamped Langevin diffusion matrix is degenerate in the (q, p) state space, so a full inverse σ^{-1} does not exist. The elementary derivation Equations (6.36) and (6.38) is therefore only an elliptic prototype. A kinetic Girsanov comparison is legitimate only when the drift difference belongs to the range of the noise operator, for example when two kinetic processes share the same position kinematics and differ only in suitably integrable momentum-direction drifts.

Onsager-Machlup and Freidlin-Wentzell Functionals. The Onsager-Machlup functional characterizes small-tube probabilities of smooth comparison paths for appropriate diffusion models, whereas the Freidlin-Wentzell functional is a small-noise large-deviation rate functional. They need not coincide with Equation (6.39); divergence, geometry, normalization, and limiting procedures matter. Accordingly, the manuscript uses separate notations $\mathcal{A}^G$, $\mathcal{A}^{OM}$, and I_{FW} and never replaces one by another without a theorem.

6.4.2. *Overdamped Free-Energy Gradient Flow.* For the constant-mobility equilibrium diffusion Equation (6.8), the Fokker-Planck equation is

$$\partial_t \rho = \nabla \cdot [\mathsf{K} (\rho \nabla U + k_B T \nabla \rho)] . \tag{6.42}$$

Define the nonequilibrium free-energy functional relative to Lebesgue measure for the present finite-dimensional calculation by

$$F[\rho] = \int_{\mathbb{R}^n} U(x)\rho(x)\,\mathrm{d}x + k_B T \int_{\mathbb{R}^n} \rho(x) \log \rho(x)\,\mathrm{d}x. \tag{6.43}$$

The reference-measure refinement needed for physical dimensional consistency is given in Section 6.5. Its first variation is

$$\frac{\delta F}{\delta \rho} = U + k_B T(1 + \log \rho). \tag{6.44}$$

Therefore

$$\nabla \frac{\delta F}{\delta \rho} = \nabla U + k_B T \nabla \log \rho. \tag{6.45}$$

Using $\rho \nabla \log \rho = \nabla \rho$, we obtain

$$\rho \mathsf{K} \nabla \frac{\delta F}{\delta \rho} = \mathsf{K}(\rho \nabla U + k_B T \nabla \rho). \tag{6.46}$$

Consequently Equation (6.42) can be written as

$$\partial_t \rho = \nabla \cdot \left[\rho \mathsf{K} \nabla \frac{\delta F}{\delta \rho} \right] . \tag{6.47}$$

6.4.3. *Rayleighian Minimization of the Dissipative Current.* The sign of the linear free-energy term is part of this characterization. Both $\Phi + \dot{F}$ and $\Phi - \dot{F}$ are convex in the current, and their minimizers have opposite signs. In the microscopic realization of Section 4, equilibrium force covariance gives the positive metric, while the retarded response of the prepared reservoir gives the

forward dissipative drift. The drift-change cost in Section 4.6 recovers the same sign. In a model without that derivation, the variational sign remains a constitutive premise.

Write the continuity equation as

$$\partial_t \rho + \nabla \cdot j = 0. \tag{6.48}$$

For a fixed density ρ, define the extended Rayleighian

$$\mathscr{R}_\rho[j] = \frac{1}{2}\int_{\mathbb{R}^n} \frac{j^{\mathsf{T}}\mathsf{K}^{-1}j}{\rho}\,\mathrm{d}x + \int_{\mathbb{R}^n} j\cdot\nabla\frac{\delta F}{\delta\rho}\,\mathrm{d}x, \tag{6.49}$$

with the convention

$$\frac{j^{\mathsf{T}}\mathsf{K}^{-1}j}{\rho} = \begin{cases} 0, & \rho = 0 \text{ and } j = 0, \\ +\infty, & \rho = 0 \text{ and } j \neq 0. \end{cases} \tag{6.50}$$

Boundary conditions are assumed periodic, no-flux, or sufficiently decaying so that all integrations by parts below have no boundary contribution.

THEOREM 6.17 (Minimum-dissipation current). *Assume $\mathsf{K} = \mathsf{K}^{\mathsf{T}} > 0$ is constant, ρ is positive almost everywhere, and $\int \rho\,\nabla(\delta F/\delta\rho)^{\mathsf{T}}\mathsf{K}\nabla(\delta F/\delta\rho)\,\mathrm{d}x < \infty$. Use the Hilbert space of currents with finite $\int j^{\mathsf{T}}\mathsf{K}^{-1}j/\rho\,\mathrm{d}x$, with no additional pointwise current constraints. If a physical boundary is present, assume the displayed minimizing current has the required zero normal trace. Then Equation (6.49) is strictly convex and attains its unique minimum at*

$$j_\star = -\rho\mathsf{K}\nabla\frac{\delta F}{\delta\rho}. \tag{6.51}$$

Substitution into Equation (6.48) yields the Fokker-Planck equation Equation (6.47).

Proof. Let h be any admissible variation and set $j_\varepsilon = j + \varepsilon h$. The domain assumptions give the complete-square identity

$$\mathscr{R}_\rho[j] = \frac{1}{2}\int \frac{\big(j+\rho\mathsf{K}\nabla(\delta F/\delta\rho)\big)^{\mathsf{T}}\mathsf{K}^{-1}\big(j+\rho\mathsf{K}\nabla(\delta F/\delta\rho)\big)}{\rho}\,\mathrm{d}x - \frac{1}{2}\int\rho\left(\nabla\frac{\delta F}{\delta\rho}\right)^{\mathsf{T}}\mathsf{K}\nabla\frac{\delta F}{\delta\rho}\,\mathrm{d}x. \tag{6.52}$$

It proves attainment as well as uniqueness; strict convexity alone would prove only the latter. Equivalently, the first variation is

$$\begin{aligned}\frac{\mathrm{d}}{\mathrm{d}\varepsilon}\mathscr{R}_\rho[j_\varepsilon]\Big|_{\varepsilon=0} &= \int h^{\mathsf{T}}(\rho\mathsf{K})^{-1}j\,\mathrm{d}x + \int h\cdot\nabla\frac{\delta F}{\delta\rho}\,\mathrm{d}x \\ &= \int h\cdot\left[(\rho\mathsf{K})^{-1}j + \nabla\frac{\delta F}{\delta\rho}\right]\mathrm{d}x.\end{aligned} \tag{6.53}$$

For this expression to vanish for every admissible h, the bracket must vanish almost everywhere:

$$(\rho\mathsf{K})^{-1}j + \nabla\frac{\delta F}{\delta\rho} = 0. \tag{6.54}$$

Multiplication by $\rho\mathsf{K}$ gives Equation (6.51). The second variation is

$$\delta^2\mathscr{R}_\rho[j](h,h) = \int \frac{h^{\mathsf{T}}\mathsf{K}^{-1}h}{\rho}\,\mathrm{d}x, \tag{6.55}$$

which is strictly positive for nonzero admissible h on the support of ρ. Therefore the stationary point is the unique minimizer. Finally, substituting Equation (6.51) into Equation (6.48) gives Equation (6.47). □

The same structure yields free-energy dissipation directly. Using Equation (6.48) and integrating by parts,

$$\begin{aligned}\frac{\mathrm{d}F}{\mathrm{d}t} &= \int \frac{\delta F}{\delta \rho}\partial_t \rho \,\mathrm{d}x \\ &= -\int \frac{\delta F}{\delta \rho}\nabla \cdot j_\star \,\mathrm{d}x \\ &= \int j_\star \cdot \nabla \frac{\delta F}{\delta \rho}\,\mathrm{d}x \\ &= -\int \rho \left(\nabla \frac{\delta F}{\delta \rho}\right)^{\mathsf{T}} \mathsf{K} \left(\nabla \frac{\delta F}{\delta \rho}\right) \mathrm{d}x \le 0. \end{aligned} \tag{6.56}$$

6.4.4. *Weighted Wasserstein Form of the JKO Step.* For $\mathsf{K} = I$, the Jordan-Kinderlehrer-Otto scheme uses the standard 2-Wasserstein metric. When $\mathsf{K} \neq I$ is a constant symmetric positive-definite matrix, the correct transport geometry is the metric induced by K^{-1}. Define

$$W_{\mathsf{K}}^2(\rho_0, \rho_1) = \inf_{\Pi \in \Gamma(\rho_0, \rho_1)} \int (x-y)^{\mathsf{T}} \mathsf{K}^{-1} (x-y)\, \mathrm{d}\Pi(x,y), \tag{6.57}$$

where $\Gamma(\rho_0, \rho_1)$ denotes the set of transport plans with the prescribed marginals. The corresponding minimizing-movement step is

$$\rho_{n+1} \in \arg\min_{\rho} \left\{ F[\rho] + \frac{1}{2\tau} W_{\mathsf{K}}^2(\rho, \rho_n) \right\}. \tag{6.58}$$

If $y = \mathsf{K}^{-1/2} x$, then the cost in Equation (6.57) becomes the ordinary Euclidean quadratic cost. Thus Equation (6.58) is the constant-mobility coordinate transform of the standard Wasserstein scheme. The JKO theorem is used here only for the gradient-drift Fokker-Planck class for which its hypotheses apply; it is not promoted to a theorem for arbitrary molecular SDEs.

6.4.5. *State-Dependent Mobility and the Itô Drift Correction.* If the mobility depends on position, $\mathsf{K} = \mathsf{K}(x)$, the Itô equation must include a thermal drift correction to generate the desired free-energy gradient flow. Let

$$\sigma(x)\sigma(x)^{\mathsf{T}} = 2k_B T \mathsf{K}(x). \tag{6.59}$$

Then the Itô drift should be

$$b_i(x) = -\mathsf{K}_{ij}(x)\partial_j U(x) + k_B T \partial_j \mathsf{K}_{ij}(x). \tag{6.60}$$

Indeed, the Itô Fokker-Planck equation is

$$\partial_t \rho = -\partial_i (b_i \rho) + k_B T \partial_i \partial_j (\mathsf{K}_{ij} \rho). \tag{6.61}$$

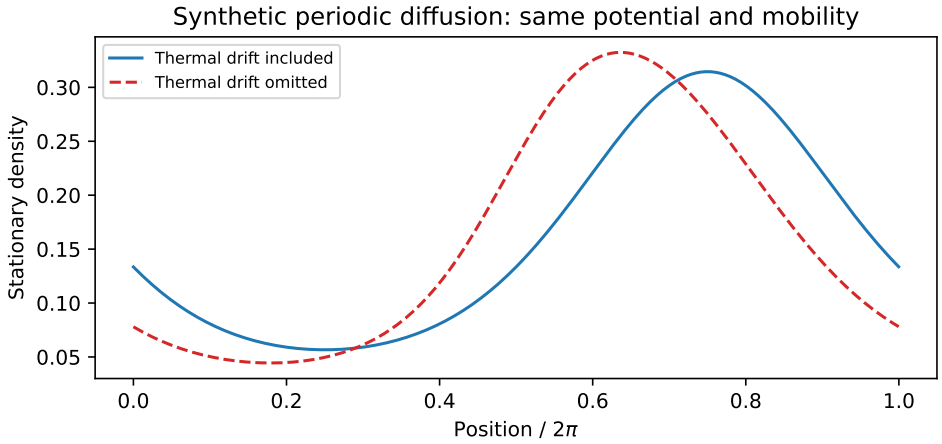


Figure 1. Synthetic stationary-density comparison on a periodic domain. Both curves use the same potential, mobility, and temperature. The additional factor K^{-1} is the consequence of omitting the thermal Itô drift; no experimental data are used.

Substituting Equation (6.60) and expanding the second derivative gives cancellation of the terms containing $\partial_j \mathsf{K}_{ij}$ and yields

$$\partial_t \rho = \nabla \cdot \left[\mathsf{K}(x) \left(\rho \nabla U + k_B T \nabla \rho \right) \right]. \tag{6.62}$$

The constant-mobility theorem is retained as the clean foundational case; Equation (6.60) records the precise modification required for state-dependent mobility.

The consequence of omitting this term is visible without solving a time-dependent equation. On a periodic one-dimensional domain, write $\theta = k_B T$, take smooth $K(x) > 0$, and use periodic U. The corrected drift has stationary density $\pi \propto e^{-U/\theta}$. If the Itô drift is instead $-KU'$, its zero-current equation is $0 = -KU'\widetilde{\pi} - \theta(K\widetilde{\pi})'$, and therefore

$$\widetilde{\pi}(x) = \widetilde{Z}^{-1} K(x)^{-1} e^{-U(x)/\theta}.$$

Spatially varying mobility then changes the equilibrium populations even though the intended potential and temperature have been held fixed. For the synthetic dimensionless choice $K = 1 + \frac{1}{2}\cos x$, $U = 0.6 \sin x$, and $\theta = 0.7$, the total-variation distance between the two normalized stationary laws is approximately 0.16397. This is a change of model, not a time-discretization error. Figure 1 shows the resulting redistribution of probability.

6.4.6. *Conservative Transport Plus Dissipative Minimization.* The preceding gradient-flow structure does not imply that every physical generator is symmetric. A more realistic representation is

$$L = A + S, \tag{6.63}$$

where A is conservative or circulatory transport and S is dissipative. The minimum-dissipation principle applies to the dissipative probability current generated by S; it does not force A to vanish.

This separation is closely related to Onsager's variational ideas and to the GENERIC framework of reversible-irreversible coupling. Accordingly, the decomposition itself is not claimed as novel. The contribution sought here lies in connecting this structure to the exact Markov relative-entropy theorem, the thermodynamic free-energy identity, the positive-Markov-inverse obstruction, law-level nonrecurrence, and history-space formulations.

6.5. *Equilibrium Gibbs Measures and Thermodynamic Free Energy.* Equilibrium supplies a reference throughout the motion, not just a name for its possible endpoint. For a time-independent energy function and bath temperature, the Gibbs law fixes the minimum of the nonequilibrium free energy. A different law has an excess free energy measured by relative entropy. This static comparison does not specify a relaxation time or guarantee that the dynamics reach the minimum; those questions also involve the mobility and the accessible states. We first fix the reference volume so that logarithms of densities and free-energy differences have unambiguous meanings.

6.5.1. *Reference Measures and Dimensional Consistency.* A continuous probability density generally has physical units, so an expression such as $\log \rho$ should be interpreted relative to a fixed reference measure. Let m be a reference phase-space measure and assume $\nu \ll m$ with density

$$r = \frac{\mathrm{d}\nu}{\mathrm{d}m}. \tag{6.64}$$

Define the entropy relative to m by

$$\mathrm{Ent}_m(\nu) = \int r \log r \, \mathrm{d}m. \tag{6.65}$$

Any fixed dimensional normalization, such as a classical phase-space cell factor, changes the absolute free energy by an additive constant but does not change the dissipation identities proved below.

Let $\mathcal{H}$ be a measurable real-valued energy function and define the canonical equilibrium measure

$$\mu_{\mathrm{eq}}(\,\mathrm{d}x) = Z^{-1} e^{-\beta \mathcal{H}(x)} m(\,\mathrm{d}x), \qquad Z = \int e^{-\beta \mathcal{H}} \, \mathrm{d}m, \tag{6.66}$$

where $0 < Z < \infty$, $k_B T > 0$, and $\beta = (k_B T)^{-1}$.

The nonequilibrium Helmholtz-type free energy is

$$F[\nu] = \int \mathcal{H} \, \mathrm{d}\nu + k_B T \, \mathrm{Ent}_m(\nu). \tag{6.67}$$

Theorem 6.18 (Exact Gibbs free-energy identity). *Assume additionally* $\int |\mathcal{H}| \, d\mu_{\mathrm{eq}} < \infty$. *Use the finite-term class*

$$\mathcal{A}_F = \left\{ \nu \ll \mu_{\mathrm{eq}} : \int |\mathcal{H}| \, d\nu < \infty, \ \int r |\log r| \, dm < \infty, \quad r = d\nu/dm \right\}.$$

For every probability $\nu \in \mathcal{A}_F$,

$$F[\nu] - F[\mu_{\mathrm{eq}}] = k_B T D(\nu \| \mu_{\mathrm{eq}}) \, . \tag{6.68}$$

In particular, $\mu_{\mathrm{eq}} \in \mathcal{A}_F$ *and is the unique minimizer of* F *in this class.*

Proof. Put $w = e^{-\beta\mathcal{H}}$. Since $w > 0$ and $\int w\, dm = Z < \infty$, the measurable sets $B_n = \{w \geq 1/n\}$, $n \geq 1$, cover the state space and satisfy $m(B_n) \leq nZ$. Thus m is σ-finite; no separate volume assumption is needed. The Gibbs density is strictly positive, so m and μ_{eq} have the same null sets. The finite-term assumptions make every logarithmic identity below integrable with respect to ν. Let $r = \mathrm{d}\nu/\,\mathrm{d}m$. From Equation (6.66),

$$\log \frac{\mathrm{d}\mu_{\mathrm{eq}}}{\mathrm{d}m} = -\beta\mathcal{H} - \log Z. \tag{6.69}$$

Therefore

$$\begin{aligned} \log \frac{\mathrm{d}\nu}{\mathrm{d}\mu_{\mathrm{eq}}} &= \log r - \log \frac{\mathrm{d}\mu_{\mathrm{eq}}}{\mathrm{d}m} \\ &= \log r + \beta\mathcal{H} + \log Z. \end{aligned} \tag{6.70}$$

Integrating with respect to ν yields

$$D(\nu\|\mu_{\mathrm{eq}}) = \mathrm{Ent}_m(\nu) + \beta \int \mathcal{H}\, \mathrm{d}\nu + \log Z. \tag{6.71}$$

Multiplying by $k_B T$ gives

$$k_B T D(\nu\|\mu_{\mathrm{eq}}) = F[\nu] + k_B T \log Z. \tag{6.72}$$

For $\nu = \mu_{\mathrm{eq}}$, the relative entropy vanishes, so

$$F[\mu_{\mathrm{eq}}] = -k_B T \log Z. \tag{6.73}$$

The added energy moment and $\log(d\mu_{\mathrm{eq}}/dm) = -\beta\mathcal{H} - \log Z$ show that the equilibrium entropy term is absolutely integrable. Thus substituting $\nu = \mu_{\mathrm{eq}}$ above is legitimate. Substituting Equation (6.73) into Equation (6.72) proves Equation (6.68). Relative entropy is nonnegative and vanishes only for equal measures, which proves uniqueness. □

There is a useful extension, but it must be defined explicitly:

$$F_{\mathrm{rel}}[\nu] = -k_B T \log Z + k_B T D(\nu\|\mu_{\mathrm{eq}}).$$

This expression is meaningful as an extended-real functional and agrees with F on $\mathcal{A}_F$. Finite relative entropy alone need not make the separate energy and reference-entropy integrals finite. In particular, $D(\mu_{\mathrm{eq}}\|\mu_{\mathrm{eq}}) = 0$ even when the equilibrium energy moment is infinite. For example, use counting measure on $n \geq 2$, dimensionless $k_B T = 1$, and $\mathcal{H}(n) = \log n + 2\log\log n$. Then $Z = \sum_{n\geq 2}[n(\log n)^2]^{-1} < \infty$, whereas $\sum_n \mathcal{H}(n)e^{-\mathcal{H}(n)} = \infty$, by comparison with $\sum_{n\geq 2}[n\log n]^{-1}$. The Gibbs relative entropy is zero, but the two separate terms in (6.67) do not define a finite sum.

6.5.2. *Why a Minimum Does Not Imply Convergence.* The existence of the minimizer in Theorem 6.18 is not sufficient to prove that an arbitrary dynamics converges to that minimizer. A simple deterministic counterexample makes the logical point explicit. Let

$$V(x, y) = x^2 + y^2, \tag{6.74}$$

whose unique minimizer is $(0,0)$, and consider the rotational dynamics

$$\dot{x} = -y, \qquad \dot{y} = x. \tag{6.75}$$

Then

$$\begin{aligned} \frac{\mathrm{d}}{\mathrm{d}t} V(x_t, y_t) &= 2x_t\dot{x}_t + 2y_t\dot{y}_t \\ &= -2x_t y_t + 2y_t x_t = 0. \end{aligned} \tag{6.76}$$

Thus the system moves forever on a level set of a function possessing a unique minimum. A quantitative sufficient condition for convergence is

$$\begin{aligned} H'(t) = -\mathcal{I}(t), \qquad \mathcal{I}(t) \geq 2\rho H(t), \quad \rho > 0, \quad H(0) < \infty \\ \implies \quad H(t) \leq e^{-2\rho t} H(0), \end{aligned} \tag{6.77}$$

where $H(t) = D(\nu_t \| \mu_{\mathrm{eq}})$. The dissipation inequality, rather than existence of a minimum alone, is the estimate that must be proved for the chosen dynamics.

6.5.3. *Autonomous and Driven Thermodynamic Balances.* Throughout this subsection heat is counted positive when it enters the system, $T > 0$ is fixed unless explicitly varied, and the mobility K and diffusion $\mathsf{D} = k_B T \mathsf{K}$ are interpreted in the same stochastic convention as the Fokker-Planck current. If an externally controlled potential $U(x,t)$ is present, the protocol work rate performed on the system is

$$\dot{W}_t = \int \rho_t(x) \partial_t U(x,t) \, \mathrm{d}x. \tag{6.78}$$

If no protocol is present, $\dot{W}_t = 0$. If the overdamped current has the force-driven form

$$j_t = \rho_t \mathsf{K} \left[f_{\mathrm{nc}} - \nabla \frac{\delta F}{\delta \rho}(\rho_t) \right], \tag{6.79}$$

then the nonconservative work rate is

$$\dot{W}_{\mathrm{nc}}(t) = \int f_{\mathrm{nc}}(x,t) \cdot j_t(x) \, \mathrm{d}x. \tag{6.80}$$

Combining Equation (6.79) with the free-energy rate induced by the continuity equation gives

$$\begin{aligned} \dot{W}_t + \dot{W}_{\mathrm{nc}}(t) - \dot{F}_t &= \int \left[f_{\mathrm{nc}} - \nabla \frac{\delta F}{\delta \rho}(\rho_t) \right] \cdot j_t \, \mathrm{d}x \\ &= \int \frac{j_t^{\mathsf{T}} \mathsf{K}^{-1} j_t}{\rho_t} \, \mathrm{d}x \\ &= k_B T \int \frac{j_t^{\mathsf{T}} \mathsf{D}^{-1} j_t}{\rho_t} \, \mathrm{d}x \geq 0. \end{aligned} \tag{6.81}$$

Thus the unforced Lyapunov identity is a special case of the driven balance, not a replacement for it. Time homogeneity alone is not enough: an autonomous nonequilibrium steady state can have $\dot{F} = 0$ and $\dot{W}_{\mathrm{nc}} > 0$.

For autonomous unforced relaxation with a single ideal bath at fixed temperature, assume in addition that the effective dynamics obey local detailed balance with the heat convention stated above. Define $S_{\mathrm{sys}} = -k_B \operatorname{Ent}_m(\nu_t)$ relative to the fixed reference volume, and $\dot{S}_{\mathrm{tot}} = \dot{S}_{\mathrm{sys}} - \dot{Q}_{\mathrm{in}}/T$. The first law gives $\dot{E} = \dot{Q}_{\mathrm{in}}$, while $F = E - TS_{\mathrm{sys}}$. Consequently

$$T\dot{S}_{\mathrm{tot}} = -\dot{F}. \tag{6.82}$$

If an externally controlled potential $U(x,t)$ is present, the free-energy change contains the mechanical or parametric work defined in Equation (6.78). The appropriate nonequilibrium balance becomes

$$T\dot{S}_{\mathrm{tot}} = \dot{W}_t + \dot{W}_{\mathrm{nc}}(t) - \dot{F}_t \geq 0. \tag{6.83}$$

The optical-trap quench in Section 10.2 is interpreted using this distinction: the rapid switching stage performs work, whereas the subsequent fixed-parameter relaxation is autonomous.

A scalar harmonic calculation fixes the sign convention. Consider

$$\mathrm{d}X_t = -K\kappa(t)X_t\,\mathrm{d}t + \sqrt{2Kk_BT}\,\mathrm{d}W_t, \tag{6.84}$$

where $K > 0$, $\kappa(t) > 0$, and $y(t) = \mathbb{E}[X_t^2]$. Itô's formula gives

$$\dot{y} = -2K(\kappa y - k_BT). \tag{6.85}$$

Up to an additive constant independent of y, the centered Gaussian free energy is

$$F(t) = \frac{1}{2}\kappa(t)y(t) - \frac{k_BT}{2}\log y(t). \tag{6.86}$$

The work rate performed on the system is $\dot{W}_t = \dot{\kappa}\,y/2$, and differentiation yields

$$\begin{aligned}\dot{F}_t &= \frac{1}{2}\dot{\kappa}\,y + \frac{1}{2}\left(\kappa - \frac{k_BT}{y}\right)\dot{y} \\ &= \dot{W}_t - K\frac{(\kappa y - k_BT)^2}{y}.\end{aligned} \tag{6.87}$$

Consequently,

$$T\dot{S}_{\mathrm{tot}} = \dot{W}_t - \dot{F}_t = K\frac{(\kappa y - k_BT)^2}{y} \geq 0. \tag{6.88}$$

At the dimensionless regression point $K = k_BT = y = 1$, $\kappa = 2$, and $\dot{\kappa} = 10$, this gives

$$\dot{W}_t = 5, \qquad T\dot{S}_{\mathrm{tot}} = 1, \qquad \dot{F}_t = 4 > 0. \tag{6.89}$$

This example shows explicitly why a driven process may increase nonequilibrium free energy even though the total entropy production is nonnegative.

6.5.4. *Local Detailed Balance as an Additional Physical Bridge.* The free-energy identity compares probability laws; a heat measurement records energy transferred to a reservoir. To connect them, the forward and reversed transition weights must encode the same reservoir energy exchange.

Local detailed balance supplies this relation. The sign convention is fixed below so that heat entering the system is the negative of heat entering the bath. This is the additional physical step that turns an information inequality into a thermodynamic balance.

The equality between a path likelihood ratio and physical entropy production is not a consequence of Markovity or Jensen's inequality alone. It requires a model-specific local-detailed-balance relation connecting elementary forward and reversed transition weights to reservoir heat [94], [95], and [107]. This premise is separate from relative-entropy contraction: data processing is information-theoretic, whereas local detailed balance assigns thermodynamic meaning to the logarithm of a path probability ratio.

For a jump $i \to j$ through reservoir channel ν, declare the dynamically reversed channel $\bar{\nu}$. The support condition is

$$k_{ij}^{(\nu)} > 0 \quad \Longleftrightarrow \quad k_{ji}^{(\bar{\nu})} > 0. \tag{6.90}$$

When the same channel label is physically valid in both directions, $\bar{\nu} = \nu$, the local detailed-balance convention reads

$$\log \frac{k_{ij}^{(\nu)}}{k_{ji}^{(\nu)}} = \frac{\Delta s_{\mathrm{med}}^{(\nu)}(i \to j)}{k_B} = -\beta_\nu Q_{\mathrm{in}}^{(\nu)}(i \to j), \tag{6.91}$$

where Q_{in} is heat entering the system. For one bath and no mechanical or chemical work, Equation (6.91) reduces to

$$\frac{k_{ij}}{k_{ji}} = \exp[-\beta(E_j - E_i)], \tag{6.92}$$

which is the Gibbs detailed-balance ratio.

For a complete jump-path likelihood ratio, the rate ratio is not enough. Let $r_i^F(t) = \sum_{j,\nu} k_{ij}^{F,(\nu)}(t)$ be the forward escape rate and let $r_i^R(t)$ be the escape rate in the reversed protocol. The holding-time contribution cancels only under the declared convention, for example when

$$r_i^R(\tau - t) = r_i^F(t) \tag{6.93}$$

along the reversed path. If Equation (6.90) fails, the logarithm in Equation (6.91) is an extended value and singular path components may appear. In that case the ordinary finite path-KL and ordinary integral fluctuation theorem must be replaced by an absolute-continuity statement with the appropriate singular correction [76].

For diffusion paths in the Stratonovich convention, the corresponding work and heat increments are

$$\delta W_{\mathrm{on}} = \partial_t U_t(X_t)\,\mathrm{d}t + f_{\mathrm{nc}}(X_t, t) \circ \mathrm{d}X_t, \tag{6.94}$$

$$\delta Q_{\mathrm{bath}} = [-\nabla U_t(X_t) + f_{\mathrm{nc}}(X_t, t)] \circ \mathrm{d}X_t, \qquad \delta Q_{\mathrm{in}} = -\delta Q_{\mathrm{bath}}. \tag{6.95}$$

The Stratonovich chain rule gives the first-law convention

$$\mathrm{d}U = \delta W_{\mathrm{on}} - \delta Q_{\mathrm{bath}} = \delta W_{\mathrm{on}} + \delta Q_{\mathrm{in}}. \tag{6.96}$$

With a declared reverse protocol, parity map, endpoint initialization, and common covariance, the conditional path calculation may identify the medium entropy with a path likelihood ratio,

$$\log \frac{\mathrm{d}P_F(\cdot \mid x_0)}{\mathrm{d}P_R(\Theta\cdot \mid \vartheta x_\tau)} = \beta Q_{\mathrm{bath}}[\omega] = \frac{\Delta s_{\mathrm{med}}[\omega]}{k_B}. \tag{6.97}$$

Only after the endpoint density term is restored does this become total entropy production. Local detailed balance fixes the time-antisymmetric ratio of forward and backward transition weights. It does not fix the time-symmetric kinetic activity and therefore does not uniquely determine the generator; moreover, coarse graining can destroy local detailed balance even when the reduced process remains Markovian [44].

6.5.5. *Optional Microcanonical Ensemble Formulation.* For a genuinely isolated ensemble, suppose the stochastic dynamics preserves the energy shell

$$\Sigma_E = \{x : \mathcal{H}(x) = E\} \tag{6.98}$$

and admits a normalized invariant microcanonical reference measure μ_E on that shell. For ensemble laws $\nu \ll \mu_E$ define the information-theoretic microcanonical entropy

$$S_E[\nu] = S_E^{\mathrm{eq}} - k_B D(\nu\|\mu_E)\,. \tag{6.99}$$

If $\mu_E P_t = \mu_E$, Markov data processing implies

$$S_E[\nu P_t] \geq S_E[\nu]. \tag{6.100}$$

This is an ensemble theorem relative to the chosen microcanonical measure. It is not assigned to singular point masses for which the relative entropy may be infinite, and it is not used as a substitute for the canonical theorem.

7. **Entropy Dissipation and Convergence to Equilibrium**

The preceding current calculation gives an instantaneous free-energy balance. We now follow an entire probability law through time. Three questions must be distinguished: does relative entropy decrease, can its rate be computed, and must it eventually reach zero? Markov data processing answers the first, diffusion calculus answers the second under its domain assumptions, and coercive or hypocoercive estimates answer the third. For a particle cloud in a trap, these correspond to the direction of relaxation, its instantaneous rate, and the time needed to approach the equilibrium cloud. The equilibrium reference is the same in all three questions, but the required dynamical information is different.

7.1. *Markov Relative-Entropy Contraction and Differential Dissipation.*

7.1.1. *Relative Entropy.* Let ν and μ be probability measures on a measurable state space $(\mathcal{X}, \mathcal{B})$ and assume $\nu \ll \mu$. Write

$$f = \frac{\mathrm{d}\nu}{\mathrm{d}\mu}. \tag{7.1}$$

The Kullback-Leibler relative entropy is

$$D(\nu\|\mu) = \int f \log f \, \mathrm{d}\mu. \tag{7.2}$$

If $\nu \not\ll \mu$, the relative entropy is defined to be $+\infty$.

7.1.2. *Dimension-Free Markov Data Processing.*

THEOREM 7.1 (Invariant-measure relative-entropy contraction). *Let P be a Markov kernel and let μ be a probability measure satisfying*

$$\mu P = \mu. \tag{7.3}$$

Then for every probability measure ν,

$$D(\nu P\|\mu) \le D(\nu\|\mu)\,. \tag{7.4}$$

Consequently, if $(P_t)_{t\ge 0}$ is a Markov semigroup preserving μ, then $t \mapsto D(\nu P_t\|\mu)$ is nonincreasing.

Proof. If $D(\nu\|\mu) = +\infty$, the inequality is immediate. Assume therefore that $\nu \ll \mu$ and define f by Equation (7.1). Introduce two probability measures on $\mathcal{X} \times \mathcal{X}$:

$$Q(\mathrm{d}x, \mathrm{d}y) = \nu(\mathrm{d}x)P(x, \mathrm{d}y), \tag{7.5}$$

$$R(\mathrm{d}x, \mathrm{d}y) = \mu(\mathrm{d}x)P(x, \mathrm{d}y). \tag{7.6}$$

The two joint laws possess the same conditional transition kernel, hence

$$\frac{\mathrm{d}Q}{\mathrm{d}R}(x, y) = f(x). \tag{7.7}$$

Therefore

$$\begin{aligned} D(Q\|R) &= \int \log f(x)\, Q(\mathrm{d}x, \mathrm{d}y) \\ &= \int f(x) \log f(x) \mu(\mathrm{d}x) \\ &= D(\nu\|\mu)\,. \end{aligned} \tag{7.8}$$

Project the pair (x, y) onto its second coordinate. The second marginal of Q is νP, while the second marginal of R is $\mu P = \mu$. Relative entropy cannot increase under a measurable map, so

$$D(\nu P\|\mu) \le D(Q\|R) = D(\nu\|\mu)\,, \tag{7.9}$$

which proves the theorem. □

7.1.3. *Exact Equality Condition.* The equality case has an exact interpretation as recoverability of the initial likelihood ratio from the output.

PROPOSITION 7.2 (Equality in the Markov data-processing inequality). *Assume* $0 \le D(\nu\|\mu) < \infty$ *and use the stationary joint law* R *from Equation (7.6). Let* X *and* Y *denote the first and second coordinates. Equality in Equation (7.4) holds if and only if*

$$f(X) = \mathbb{E}_R[f(X) \mid Y] \qquad R\text{-almost surely.} \tag{7.10}$$

Equivalently, there exists a measurable function g *such that* $f(X) = g(Y)$ R*-almost surely.*

Proof. Let

$$g(Y) = \mathbb{E}_R[f(X) \mid Y]. \tag{7.11}$$

For every bounded measurable φ,

$$\begin{aligned} \int \varphi(y)g(y)\mu(\,\mathrm{d}y) &= \mathbb{E}_R[\varphi(Y)g(Y)] \\ &= \mathbb{E}_R[\varphi(Y)f(X)] \\ &= \int \varphi(y)(\nu P)(\,\mathrm{d}y). \end{aligned} \tag{7.12}$$

Hence $g = \mathrm{d}(\nu P)/\,\mathrm{d}\mu$. Let $\Psi(r) = r\log r$. Since

$$\Psi''(r) = \frac{1}{r} > 0 \qquad (r > 0), \tag{7.13}$$

conditional Jensen gives

$$\Psi(g(Y)) = \Psi(\mathbb{E}[f(X) \mid Y]) \le \mathbb{E}[\Psi(f(X)) \mid Y]. \tag{7.14}$$

After taking expectations, Equation (7.14) is precisely the data-processing inequality. Strict convexity gives equality if and only if $f(X)$ is almost surely constant conditional on Y, which is exactly Equation (7.10).

The value $\Psi(0) = 0$ is defined by continuity. Strict convexity extends to $[0,\infty)$: when $s > 0$ and $0 < t < 1$, $\Psi(ts) = t\Psi(s) + ts\log t < t\Psi(s) + (1-t)\Psi(0)$. Thus the equality condition also allows an initial density that vanishes. For a direct check, put $R_\nu(\,\mathrm{d}x,\,\mathrm{d}y) = \nu(\,\mathrm{d}x)P(x,\,\mathrm{d}y) = f(x)R(\,\mathrm{d}x,\,\mathrm{d}y)$ and $\widehat{R}_\nu(\,\mathrm{d}x,\,\mathrm{d}y) = g(y)R(\,\mathrm{d}x,\,\mathrm{d}y)$. Both are probability laws. On $\{g(Y) = 0\}$, nonnegativity and the conditional-expectation identity imply $f(X) = 0$, R-almost surely. Hence $R_\nu \ll \widehat{R}_\nu$, even when $R \not\ll R_\nu$. The logarithmic density chain rule and the finite-entropy assumption give

$$D(\nu\|\mu) = D(\nu P\|\mu) + D\left(R_\nu \middle\| \widehat{R}_\nu\right).$$

All terms are finite, so no subtraction of infinities occurs. Equality in data processing is equivalent to $R_\nu = \widehat{R}_\nu$, hence to $f(X) = g(Y)$, R-almost surely. This argument also covers zero likelihoods without an additional reverse absolute-continuity hypothesis. □

Remark 7.3 (Strictness requires more than Markovity). Theorem 7.1 gives nonincrease, not automatic strict decrease. To conclude that equality forces $\nu = \mu$, one needs an additional property such as positivity improvement, irreducibility combined with a suitable smoothing theorem, or a

direct characterization of the fixed density class. This distinction is particularly important in degenerate kinetic diffusions.

7.1.4. *Generators, Adjoints, and Carre du Champ.* For a sufficiently regular diffusion on $\mathbb{R}^n$,

$$L\varphi = b_i\partial_i\varphi + \frac{1}{2}a_{ij}\partial_i\partial_j\varphi, \qquad a = \sigma\sigma^{\mathsf{T}}. \tag{7.15}$$

The carre du champ is

$$\begin{aligned}\Gamma_L(\varphi,\psi) &= \frac{1}{2}\left[L(\varphi\psi) - \varphi L\psi - \psi L\varphi\right] \\ &= \frac{1}{2}\nabla\varphi^{\mathsf{T}} a \nabla\psi.\end{aligned} \tag{7.16}$$

In particular,

$$\Gamma_L(\varphi) = \frac{1}{2}\left\|\sigma^{\mathsf{T}}\nabla\varphi\right\|^2. \tag{7.17}$$

The diffusion chain rule yields

$$L\Phi(f) = \Phi'(f)Lf + \Phi''(f)\Gamma_L(f). \tag{7.18}$$

For $\Phi(r) = \log r$,

$$L\log f = \frac{Lf}{f} - \Gamma_L(\log f). \tag{7.19}$$

If $\nu_t = f_t\mu$ and $L^{\dagger_\mu}$ denotes the $L^2(\mu)$ adjoint of L, then the relative density evolves according to

$$\partial_t f_t = L^{\dagger_\mu} f_t. \tag{7.20}$$

This formula must not be confused with the Lebesgue Fokker-Planck equation unless μ itself is Lebesgue measure.

7.1.5. *Symmetric and Antisymmetric Generator Components.* Define

$$S_\mu = \frac{1}{2}\left(L + L^{\dagger_\mu}\right), \tag{7.21}$$

$$A_\mu = \frac{1}{2}\left(L - L^{\dagger_\mu}\right). \tag{7.22}$$

Then

$$S_\mu^{\dagger_\mu} = S_\mu, \qquad A_\mu^{\dagger_\mu} = -A_\mu. \tag{7.23}$$

With the usual Markov-generator sign convention, the dissipative Dirichlet form is

$$\mathcal{E}_{S,\mu}(g,h) = -\left\langle g, S_\mu h\right\rangle_{L^2(\mu)}, \tag{7.24}$$

and

$$\mathcal{E}_{S,\mu}(g,g) \geq 0. \tag{7.25}$$

Thus S_μ is nonpositive and $-S_\mu$ is the nonnegative operator associated with dissipation.

7.1.6. *Dirichlet-Form Entropy Dissipation.* For a closed symmetric form $\mathcal{E}_{S,\mu}$, define the relative Fisher information by

$$\mathcal{I}_\mu(f) = 4\mathcal{E}_{S,\mu}(\sqrt{f}, \sqrt{f}), \tag{7.26}$$

whenever $\sqrt{f} \in \mathrm{Dom}(\mathcal{E}_{S,\mu})$. For smooth positive densities in a diffusion setting,

$$\mathcal{I}_\mu(f) = \int f \Gamma_L(\log f)\, \mathrm{d}\mu \tag{7.27}$$

when the antisymmetric part is a first-order derivation and the carre du champ is generated by the dissipative second-order part.

THEOREM 7.4 (Integrated entropy-dissipation identity). *Assume Theorems 6.1, 6.4 and 6.5 in the diffusion setting, with finite entropy at s. Suppose either the regular common-domain calculation below applies with an absolutely continuous entropy, or the approximation and convergence conditions in Theorem 6.5 hold. Then, for $0 \le s \le t$,*

$$D(\nu_t\|\mu) + \int_s^t \mathcal{I}_\mu(f_r)\, \mathrm{d}r = D(\nu_s\|\mu)\,. \tag{7.28}$$

Proof. Under the regular hypotheses, the calculation in Equations (7.32) and (7.35) gives $H'(r) = -\mathcal{I}_\mu(f_r)$ almost everywhere. Absolute continuity permits integration on $[s,t]$. For a weak limit, apply this equality to the regular approximations; convergence of the two endpoint entropies and of the time-integrated Fisher information passes each term to the limit. If only lower semicontinuity of the dissipative integral is known, the same argument yields $H(t) + \int_s^t \mathcal{I}_\mu(f_r)\, dr \le H(s)$. □

The integrated form is the preferred rigorous formulation because it remains meaningful for densities that need not lie pointwise in a strong generator domain. Its diffusion identity is not the corresponding formula for an arbitrary jump process. For a finite reversible chain with rates q_{ij}, positive invariant law π, and positive relative density f,

$$-H' = \frac{1}{2}\sum_{i,j} \pi_i q_{ij}(f_j - f_i)(\log f_j - \log f_i) \ge 4\mathcal{E}(\sqrt{f}, \sqrt{f}).$$

The inequality follows from $(a-b)(\log a - \log b) \ge 4(\sqrt{a} - \sqrt{b})^2$. For the two-state unit-rate chain and $f = (3/2, 1/2)$, the left side equals $\frac{1}{2}\log 3$, whereas the right side is $4 - 2\sqrt{3}$; they are not equal.

7.1.7. *Strong Differential Proof under Explicit Common-Domain Assumptions.* For completeness, suppose in addition that, for almost every $t > 0$,

$$f_t \in \mathrm{Dom}(L) \cap \mathrm{Dom}(L^{\dagger_\mu}), \qquad \log f_t \in \mathrm{Dom}(L), \tag{7.29}$$

and that every pairing below is integrable. Define

$$H(t) = D(\nu_t\|\mu)\,. \tag{7.30}$$

Then normalization gives

$$\int \partial_t f_t\, \mathrm{d}\mu = 0. \tag{7.31}$$

Hence

$$\begin{aligned} H'(t) &= \int (\partial_t f_t) \log f_t \, \mathrm{d}\mu \\ &= \int (L^{\dagger_\mu} f_t) \log f_t \, \mathrm{d}\mu \\ &= \int f_t L \log f_t \, \mathrm{d}\mu. \end{aligned} \tag{7.32}$$

Using Equation (7.19),

$$H'(t) = \int L f_t \, \mathrm{d}\mu - \int f_t \Gamma_L(\log f_t) \, \mathrm{d}\mu. \tag{7.33}$$

Invariance gives

$$\int L f_t \, \mathrm{d}\mu = 0, \tag{7.34}$$

so

$$H'(t) = -\int f_t \Gamma_L(\log f_t) \, \mathrm{d}\mu. \tag{7.35}$$

7.1.8. *Why the Antisymmetric Part Does Not Directly Dissipate State Relative Entropy.* Suppose A_μ is a first-order derivation on a common algebra core. Let

$$\Psi(r) = r \log r - r, \tag{7.36}$$

so that $\Psi'(r) = \log r$. The derivation property gives

$$A_\mu \Psi(f) = (A_\mu f) \log f. \tag{7.37}$$

Since $A_\mu 1 = 0$ and $A_\mu^{\dagger_\mu} = -A_\mu$,

$$\int A_\mu g \, \mathrm{d}\mu = \langle 1, A_\mu g \rangle_{L^2(\mu)} = -\langle A_\mu 1, g \rangle_{L^2(\mu)} = 0. \tag{7.38}$$

Applying this identity to $g = \Psi(f)$ yields

$$\int (A_\mu f) \log f \, \mathrm{d}\mu = 0. \tag{7.39}$$

Thus the antisymmetric derivation transports probability without directly contributing to the state-relative-entropy dissipation. This statement is an entropic statement; it is not by itself a statement of physical reversibility.

7.1.9. *Jump Generators and the Scope of the Antisymmetric Cancellation.* The conclusion of Equation (7.39) is local. It relies on the first-order derivation property $A_\mu \Psi(f) = \Psi'(f) A_\mu f$. A nonlocal jump generator does not satisfy this chain rule, and its antisymmetric part may contribute nontrivially to the derivative of state relative entropy. Discrete entropy decay therefore uses jump-process Dirichlet forms and modified logarithmic Sobolev inequalities rather than the local diffusion square-root identity [14], [10], and [28].

For a finite-state generator

$$(Lg)_i = \sum_{j \neq i} q_{ij}(g_j - g_i), \qquad \mu L = 0, \tag{7.40}$$

assume $\mu_i > 0$, $q_{ij} < \infty$, and $f_i(t) > 0$. Then

$$\begin{aligned} \frac{\mathrm{d}}{\mathrm{d}t} \operatorname{Ent}_\mu(f_t) &= \langle f_t, L \log f_t \rangle_{L^2(\mu)} \\ &= \sum_i \mu_i f_i \sum_{j \neq i} q_{ij} \log \frac{f_j}{f_i}. \end{aligned} \tag{7.41}$$

Equivalently, using stationarity of μ,

$$-\frac{\mathrm{d}}{\mathrm{d}t} \operatorname{Ent}_\mu(f_t) = \sum_{i \neq j} \mu_i q_{ij} \left[f_i \log \frac{f_i}{f_j} - f_i + f_j \right]. \tag{7.42}$$

This directed Bregman sum is nonnegative under the Markov contraction theorem, but it is not the same object as the physical housekeeping entropy production of a stationary nonequilibrium jump process.

Even in the reversible two-state case, the square-root expression is generally only a lower bound. For

$$L = \begin{pmatrix} -1 & 1 \\ 1 & -1 \end{pmatrix}, \qquad \mu = \left(\frac{1}{2}, \frac{1}{2} \right), \qquad f = (1.6, 0.4), \tag{7.43}$$

one obtains

$$\mathcal{E}(f, \log f) = -\langle f, L \log f \rangle_{L^2(\mu)} = 0.6 \log 4 = 0.8317766166719344\ldots, \tag{7.44}$$

whereas

$$4\mathcal{E}(\sqrt{f}, \sqrt{f}) = 4(\sqrt{1.6} - \sqrt{0.4})^2 \frac{1}{2} = 0.8. \tag{7.45}$$

Thus the inequality

$$(a - b)(\log a - \log b) \geq 4(\sqrt{a} - \sqrt{b})^2 \tag{7.46}$$

must not be silently replaced by equality.

For a nonreversible three-state cycle, take

$$L = \begin{pmatrix} -2.3 & 2 & 0.3 \\ 0.3 & -2.3 & 2 \\ 2 & 0.3 & -2.3 \end{pmatrix}, \qquad \mu = \left(\frac{1}{3}, \frac{1}{3}, \frac{1}{3} \right), \qquad f = (1.5, 1, 0.5). \tag{7.47}$$

Since μ is uniform, $L^{\dagger_\mu} = L^{\mathsf{T}}$. With

$$S_\mu = \frac{1}{2}(L + L^{\mathsf{T}}), \qquad A_\mu = \frac{1}{2}(L - L^{\mathsf{T}}), \tag{7.48}$$

direct multiplication gives

$$\langle f, L \log f \rangle_{L^2(\mu)} = -0.5909471057201607\ldots, \tag{7.49}$$

$$\langle f, S_\mu \log f\rangle_{L^2(\mu)} = -0.6317020659841630\ldots, \tag{7.50}$$

$$\langle f, A_\mu \log f\rangle_{L^2(\mu)} = 0.04075496026400233\ldots. \tag{7.51}$$

The final number is nonzero. It does not contradict Equation (7.39), because the finite-state A_μ is not a first-order derivation on a local algebra. It only rules out the unqualified statement that every antisymmetric generator component makes zero direct contribution to the state-entropy derivative.

7.2. *Coercivity, Hypocoercivity, and Convergence to Equilibrium.* An entropy identity gives a rate of loss, but the rate could become small while the law remains far from equilibrium. A coercive estimate rules this out by bounding the entropy itself in terms of its dissipation. In kinetic dynamics the noise acts only on momentum, so the missing control of position must come from transport between the two variables. This transfer is the physical role of hypocoercivity. The curvature and functional inequalities below quantify these two routes to relaxation.

7.2.1. *Bakry-Emery Curvature in the Elliptic Reversible Prototype.* For a diffusion generator L with carre du champ Γ_L, define

$$\Gamma_{2,L}(g) = \frac{1}{2}L\Gamma_L(g) - \Gamma_L(g, Lg). \tag{7.52}$$

The Bakry-Emery curvature condition $BE(\rho,\infty)$ [6] and [7] is

$$\Gamma_{2,L}(g) \geq \rho\Gamma_L(g) \qquad \text{for all admissible } g, \tag{7.53}$$

with $\rho > 0$.

For the weighted Riemannian diffusion

$$L = \Delta - \nabla V\cdot\nabla, \tag{7.54}$$

the Bochner identity gives

$$\Gamma_{2,L}(g) = \|\nabla^2 g\|_{\mathrm{HS}}^2 + \left(\mathrm{Ric} + \nabla^2 V\right)(\nabla g, \nabla g). \tag{7.55}$$

Consequently,

$$\mathrm{Ric} + \nabla^2 V \geq \rho I \tag{7.56}$$

is a sufficient curvature condition.

7.2.2. *A Minimum Is Not a Curvature Bound.* The distinction between minimization and positive curvature is elementary but foundational. Consider

$$V(x) = x^4 - x^2. \tag{7.57}$$

The function possesses global minima, but

$$V''(x) = 12x^2 - 2, \tag{7.58}$$

and hence

$$V''(0) = -2. \tag{7.59}$$

Therefore the statement "the action has a minimum" cannot be used to infer a positive Bakry-Emery constant.

7.2.3. *Logarithmic Sobolev Inequality and Exponential Entropy Decay.* Assume the invariant measure μ satisfies the logarithmic Sobolev inequality

$$\mathrm{Ent}_\mu(g^2) \le \frac{2}{\rho}\mathcal{E}_{S,\mu}(g,g), \qquad \rho > 0, \tag{7.60}$$

where

$$\mathrm{Ent}_\mu(g^2) = \int g^2 \log g^2 \,\mathrm{d}\mu - \left(\int g^2 \,\mathrm{d}\mu\right) \log\left(\int g^2 \,\mathrm{d}\mu\right). \tag{7.61}$$

Set $g = \sqrt{f}$ for a normalized density f. Then

$$\mathrm{Ent}_\mu(f) = D(f\mu\|\mu)\,, \tag{7.62}$$

and by Equation (7.26),

$$D(f\mu\|\mu) \le \frac{1}{2\rho}\mathcal{I}_\mu(f). \tag{7.63}$$

Equivalently,

$$\mathcal{I}_\mu(f) \ge 2\rho D(f\mu\|\mu)\,. \tag{7.64}$$

Combining Equation (7.64) with the entropy-dissipation identity yields

$$H'(t) \le -2\rho H(t). \tag{7.65}$$

Gronwall's inequality therefore gives

$$H(t) \le e^{-2\rho(t-s)}H(s) \qquad t \ge s. \tag{7.66}$$

Pinsker's inequality then implies

$$\|\nu_t - \mu\|_{\mathrm{TV}} \le \sqrt{\frac{H(s)}{2}}e^{-\rho(t-s)}. \tag{7.67}$$

7.2.4. *The Second Law in the Autonomous Isothermal Class.* Combining Theorems 6.18 and 7.4 gives the central thermodynamic statement.

THEOREM 7.5 (Autonomous unforced isothermal stochastic second law). *Assume Theorems 6.1 to 6.5. Suppose μ_{eq} is the thermodynamic Gibbs law, $\nu_s \in \mathcal{A}_F$, and the finite-term free-energy identity holds at the times considered. Require the regularity or convergent approximation hypotheses of Theorem 7.4; a weak-limit inequality alone does not imply the equality below. Throughout this theorem the reservoir temperature $T > 0$, the mobility/noise calibration, and the potential are time independent, and no nonconservative work source is present. Then*

$$F[\nu_t] + k_B T \int_s^t \mathcal{I}_{\mu_{\mathrm{eq}}}(f_r)\,\mathrm{d}r = F[\nu_s], \tag{7.68}$$

and therefore

$$F[\nu_t] \le F[\nu_s] \qquad (t \ge s). \tag{7.69}$$

Whenever the differential identity is valid and the physical heat-bath interpretation in Theorem 6.13 is available,

$$\dot{S}_{\mathrm{tot}}(t) = k_B \mathcal{I}_{\mu_{\mathrm{eq}}}(f_t) \ge 0. \tag{7.70}$$

If, in addition, Theorem 6.8 supplies an LSI of constant $\rho > 0$, then

$$F[\nu_t] - F[\mu_{\mathrm{eq}}] \le e^{-2\rho(t-s)} \left[F[\nu_s] - F[\mu_{\mathrm{eq}}]\right]. \tag{7.71}$$

Proof. By Equation (6.68),

$$F[\nu_r] - F[\mu_{\mathrm{eq}}] = k_B T D(\nu_r \| \mu_{\mathrm{eq}}) \tag{7.72}$$

for every admissible time r. Apply Equation (7.28) with $\mu = \mu_{\mathrm{eq}}$:

$$D(\nu_t \| \mu_{\mathrm{eq}}) + \int_s^t \mathcal{I}_{\mu_{\mathrm{eq}}}(f_r)\, \mathrm{d}r = D(\nu_s \| \mu_{\mathrm{eq}}). \tag{7.73}$$

Multiply by $k_B T$ and use Equation (7.72) at $r = s, t$. The equilibrium constant cancels, giving Equation (7.68). Since the integral is nonnegative, Equation (7.69) follows. For autonomous isothermal relaxation, the thermodynamic balance Equation (6.82) gives

$$\dot{S}_{\mathrm{tot}} = -T^{-1}\dot{F} = k_B \mathcal{I}_{\mu_{\mathrm{eq}}}(f_t), \tag{7.74}$$

which proves Equation (7.70). Finally, the LSI estimate Equation (7.66) multiplied by $k_B T$ gives Equation (7.71). □

7.2.5. *Kinetic Entropy Dissipation and the Failure of Instantaneous Strictness.* For the underdamped generator Equation (6.16), the carre du champ is generated entirely by the momentum diffusion:

$$\Gamma_L(g) = k_B T (\nabla_p g)^{\mathsf{T}} \mathsf{G} \nabla_p g. \tag{7.75}$$

Hence, under the corresponding entropy regularity,

$$\frac{\mathrm{d}}{\mathrm{d}t} D(f_t \pi_{\mathrm{eq}} \| \pi_{\mathrm{eq}}) = -k_B T \int f_t (\nabla_p \log f_t)^{\mathsf{T}} \mathsf{G} \nabla_p \log f_t \, \mathrm{d}\pi_{\mathrm{eq}}. \tag{7.76}$$

Now let

$$f(q,p) = g(q) \tag{7.77}$$

with g nonconstant and normalized. Then

$$\nabla_p \log f = 0, \tag{7.78}$$

so the right-hand side of Equation (7.76) vanishes at that instant even though $f \ne 1$. Therefore the implication

$$\mathcal{I}(f) = 0 \Longrightarrow f = 1 \tag{7.79}$$

is not valid as an instantaneous statement for the degenerate kinetic diffusion.

7.2.6. *Hypocoercive Transfer of Information.* The missing mechanism is coupling. Hamiltonian transport differentiates in both q and p, while the noise differentiates only in p. Commutators transfer regularity and decay between these directions. This is the essence of hypocoercivity, for which Villani [102] develops a systematic framework. For a quadratic potential the transition can be computed exactly; the following theorem derives explicit entropy bounds without assuming a kinetic decay estimate.

THEOREM 7.6 (Explicit entropy convergence for a quadratic kinetic branch). *Fix dimensionless coordinates and time, and let $k, \gamma, \theta > 0$. Consider the one-coordinate Langevin system*

$$dq_t = p_t\,dt, \qquad dp_t = (-kq_t - \gamma p_t)\,dt + \sqrt{2\gamma\theta}\,dW_t.$$

Its unique invariant probability is $\pi_{\mathrm{eq}} = N(0, \mathrm{diag}(\theta/k, \theta))$. For every initial law ν_0 with finite relative entropy, put

$$B = \begin{pmatrix} 0 & \sqrt{k} \\ -\sqrt{k} & -\gamma \end{pmatrix}, \qquad R_t = e^{tB}, \qquad r_t = \|R_t\|_{\mathrm{op}},$$

$$\mathsf{P} = \begin{pmatrix} \gamma^{-1} + \gamma/(2k) & 1/(2\sqrt{k}) \\ 1/(2\sqrt{k}) & \gamma^{-1} \end{pmatrix}.$$

Let p_- and p_+ be the smallest and largest eigenvalues of P. Then $0 < r_t < 1$ for every $t > 0$, and

$$D(\nu_t\|\pi_{\mathrm{eq}}) \le r_t^2 D(\nu_0\|\pi_{\mathrm{eq}}) \le \min\{1, (p_+/p_-)e^{-t/p_+}\} D(\nu_0\|\pi_{\mathrm{eq}})\,. \tag{7.80}$$

Thus relative entropy converges to zero with explicit constants, and $\|\nu_t - \pi_{\mathrm{eq}}\|_{\mathrm{TV}} \le \sqrt{D(\nu_t\|\pi_{\mathrm{eq}})/2}$.

Proof. In the normalized variables $x = (\sqrt{k/\theta}\,q, p/\sqrt{\theta})$, the invariant covariance is the identity and the diffusion covariance is $A = \mathrm{diag}(0, 2\gamma)$. Direct substitution gives $B + B^{\mathsf{T}} + A = 0$. The characteristic polynomial of B is $z^2 + \gamma z + k$, whose roots have negative real part. The exact transition is therefore the Gaussian channel

$$x_t = R_t x_0 + \xi_t, \qquad \xi_t \sim N(0, Q_t),$$
$$Q_t = \int_0^t e^{sB} A e^{sB^{\mathsf{T}}}\,ds = I - R_t R_t^{\mathsf{T}},$$

with ξ_t independent of x_0. The two columns e_2 and $Be_2 = (\sqrt{k}, -\gamma)^{\mathsf{T}}$ span $\mathbb{R}^2$. More explicitly, if $v^{\mathsf{T}} Q_t v = 0$, continuity and nonnegativity of the integrand give $v^{\mathsf{T}} e^{sB} e_2 = 0$ on $[0, t]$. Its value and derivative at zero imply $v_2 = 0$ and $\sqrt{k} v_1 = 0$. Thus $Q_t > 0$, and $r_t < 1$. Invertibility of the matrix exponential gives $r_t > 0$. The same transition shows convergence to $N(0, I)$ and uniqueness: in the stationary characteristic-function identity, let t tend to infinity to obtain the Gaussian characteristic function.

For any matrix U with $\|U\|_{\mathrm{op}} \le 1$, the channel

$$\mathcal{K}_U(x, \cdot) = N(Ux, I - UU^{\mathsf{T}})$$

preserves $N(0, I)$, including when its noise covariance is singular. At a fixed positive time set $U_t = R_t/r_t$. Applying first $\mathcal{K}_{U_t}$ and then the scalar channel $\mathcal{K}_{r_t I}$ has mean $R_t x$ and covariance $r_t^2(I - U_t U_t^{\mathsf{T}}) + (1 - r_t^2)I = Q_t$. Hence it is exactly the transition above. Data processing bounds entropy after the first channel by the initial entropy. The second is the standard Gaussian Ornstein–Uhlenbeck semigroup at time $s = -\log r_t$; Gross's logarithmic Sobolev inequality [41], with generator $\Delta - x \cdot \nabla$, gives the further factor $e^{-2s} = r_t^2$. The conclusion extends from regular densities to every finite-entropy law by entropy approximation and the semigroup contraction. Relative entropy is unchanged by the invertible coordinate normalization.

Finally, $\mathsf{P} > 0$, since its first diagonal entry is positive and $\det \mathsf{P} = \gamma^{-2} + (4k)^{-1} > 0$. Matrix multiplication gives

$$B^{\mathsf{T}}\mathsf{P} + \mathsf{P}B = -I.$$

Along $\dot{z} = Bz$,

$$\frac{d}{dt}(z^{\mathsf{T}}\mathsf{P}z) = -|z|^2 \le -p_+^{-1} z^{\mathsf{T}}\mathsf{P}z.$$

Norm equivalence and Gronwall yield $\|R_t\|_{\mathrm{op}}^2 \le (p_+/p_-)e^{-t/p_+}$. Combining this with $r_t \le 1$ proves the estimate. Pinsker's inequality gives the total-variation bound in the convention $\|\nu - \pi\|_{\mathrm{TV}} = \sup_A |\nu(A) - \pi(A)|$. □

Remark 7.7. The theorem derives a rate for the specified quadratic branch using the established Gaussian logarithmic Sobolev inequality after an explicit channel factorization. The finite-time factor r_t^2 is optimal among bounds of this form: a translated $N(m, I)$ has input entropy $|m|^2/2$ and output entropy $|R_t m|^2/2$, with equality when m is a maximizing right singular vector of R_t. For $k = \gamma = 1$, $p_\pm = (5 \pm \sqrt{5})/4$, so the coarse prefactor is $(3 + \sqrt{5})/2$ and the exponential rate is $4/(5 + \sqrt{5})$. For an initial position displacement, the entropy derivative at zero still vanishes; the prefactor cannot in general be replaced by one while retaining a positive uniform exponential rate from time zero. Nonquadratic confinement requires a separate theorem with its actual Hessian, regularity, and functional-inequality assumptions.

The corresponding numerical diagnostic is shown in Figure 2.

Remark 7.8. For a nonquadratic kinetic model, quantitative decay depends on confinement, Hessian growth, and the functional inequalities available for its invariant law. A rate for the quadratic model cannot be transferred to that setting without verifying the hypotheses of an appropriate theorem.

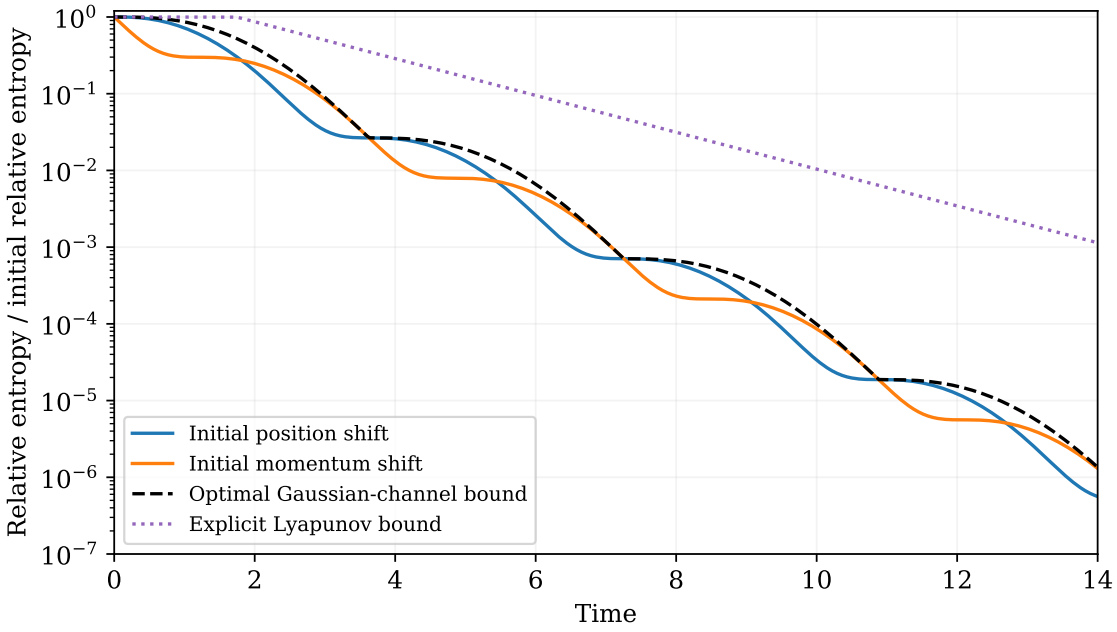


Figure 2. Exact entropy relaxation in the normalized quadratic kinetic model with $k = \gamma = \theta = 1$. The two translated Gaussian initial laws have mean e_1 or e_2 and identity covariance. The solid curves show their entropy divided by its initial value; the dashed curve is the optimal all-input factor $\|e^{tB}\|_{\mathrm{op}}^2$. The dotted curve is the explicit Lyapunov bound. These are analytic model evaluations, not experimental data.

8. **Time Reversal, Path Entropy, and Recurrence**

An experiment that lets a prepared system relax and an experiment that reverses its complete microscopic motion are different preparations. Reversing velocities is only part of the second operation: reservoir correlations, driving, and time-odd parameters must also be specified. We therefore compare explicit forward and reverse laws before assigning an entropy production to their difference. This explains how a nonequilibrium ensemble can relax even when its equilibrium dynamics obey detailed balance, and why recurrence of an individual trajectory does not imply recurrence of the relaxing probability law.

8.1. *Four Complementary Manifestations of Time Irreversibility.*

8.1.1. *Level I: Generator Structure and Generalized Detailed Balance.* Physical time reversal must account for odd variables. Under Theorem 6.6, define generalized equilibrium reversibility by

$$L^{\dagger_\mu} = \Theta L \Theta^{-1}. \tag{8.1}$$

The generalized reversal defect is

$$\mathfrak{R} = L^{\dagger_\mu} - \Theta L \Theta^{-1}. \tag{8.2}$$

Thus $\mathfrak{R} = 0$ characterizes generalized detailed balance on the relevant domain.

For the kinetic equilibrium model, $\Theta(q,p) = (q,-p)$. The Hamiltonian transport obeys

$$\Theta A \Theta^{-1} = -A, \tag{8.3}$$

and the dissipative component obeys

$$\Theta S \Theta^{-1} = S. \tag{8.4}$$

Since $A^{\dagger_{\pi_{\mathrm{eq}}}} = -A$ and $S^{\dagger_{\pi_{\mathrm{eq}}}} = S$,

$$L^{\dagger_{\pi_{\mathrm{eq}}}} = S - A = \Theta(S+A)\Theta^{-1}. \tag{8.5}$$

Hence an equilibrium stochastic process can possess both nonzero dissipation and nonzero antisymmetric transport while remaining reversible in the physically correct generalized sense. This observation prevents the false identification

$$S \neq 0 \quad \Longleftrightarrow \quad \text{stationary time-reversal breaking.} \tag{8.6}$$

8.1.2. *Level II: Strict Contraction Excludes a Physical Positive Markov Inverse.*

THEOREM 8.1 (No invariant-measure-preserving positive Markov inverse). *Let P be a Markov kernel preserving μ, and suppose*

$$D(\nu P \| \mu) < D(\nu \| \mu) < \infty. \tag{8.7}$$

Then there is no Markov kernel Q satisfying simultaneously

$$(\nu P)Q = \nu, \tag{8.8}$$

$$\mu Q = \mu. \tag{8.9}$$

Proof. If such Q existed, data processing under Q would give

$$\begin{aligned} D(\nu\|\mu) &= D((\nu P)Q \| \mu Q) \\ &\leq D(\nu P \| \mu)\,, \end{aligned} \tag{8.10}$$

which contradicts Equation (8.7). Therefore no such positive Markov recovery map exists. □

Remark 8.2 (Reverse process versus inverse semigroup). Theorem 8.1 does not say that a time-reversed diffusion cannot be mathematically constructed. A reverse process may exist and may itself be Markov under suitable regularity. The theorem excludes a much stronger object: a positive μ-preserving Markov recovery map that undoes a strictly information-losing forward step on the specified law.

8.1.3. *Level III: Thermodynamic-Law Ordering and Nonrecurrence.*

THEOREM 8.3 (No exact recurrence of a non-equilibrium law under strict exponential contraction). *Suppose that* $D(\nu_s\|\mu) < \infty$ *and that for* $t > s$,

$$D(\nu_t\|\mu) \le e^{-2\rho(t-s)} D(\nu_s\|\mu)\,, \qquad \rho > 0. \tag{8.11}$$

If

$$\nu_t = \nu_s, \tag{8.12}$$

then $\nu_s = \mu$.

Proof. Let

$$H = D(\nu_s\|\mu) \ge 0. \tag{8.13}$$

By Equation (8.12), the left-hand side of Equation (8.11) equals H. Hence

$$H \le e^{-2\rho(t-s)} H. \tag{8.14}$$

Since $t > s$ and $\rho > 0$,

$$0 < e^{-2\rho(t-s)} < 1. \tag{8.15}$$

Subtracting the right-hand side of Equation (8.14) from the left gives

$$\left[1 - e^{-2\rho(t-s)}\right] H \le 0. \tag{8.16}$$

Both factors are nonnegative and the first is strictly positive, so $H = 0$. Relative entropy vanishes only at equality of the measures; hence $\nu_s = \mu$. □

This theorem does not exclude an individual stochastic trajectory from returning to a previously visited region. It excludes exact recurrence of the full non-equilibrium probability law under the stated strict contraction. The finite-entropy assumption is necessary for the subtraction in the proof: $+\infty \le c(+\infty)$, with $0 < c < 1$, gives no information. For example, identity evolution on $[0, 1]$, Lebesgue invariant probability μ, and $\nu_t = \delta_0$ satisfies that extended-real inequality and exact recurrence without $\nu_t = \mu$.

8.1.4. *Level IV: Path Asymmetry and History Relaxation.* Let $\mathbb{P}_{[0,T]}$ be the forward path law and let $\mathbb{P}^R_{[0,T]}$ be the correctly parity-reversed path law. Define

$$\Sigma_{[0,T]} = D\left(\mathbb{P}_{[0,T]} \middle\| \mathbb{P}^R_{[0,T]}\right). \tag{8.17}$$

This quantity measures distinguishability of forward and reversed histories. It is conceptually different from the state relative entropy

$$D(\nu_t\|\mu_{\mathrm{eq}}) \tag{8.18}$$

and also from a history-ensemble relaxation functional

$$D\left(\nu_t^{\Omega} \middle\| \mu_{\mathrm{eq}}^{\Omega}\right). \tag{8.19}$$

The three quantities coincide only in special structures that must be proved separately.

The endpoint convention is part of the definition. If the forward law starts from ν_0 and ends at ν_T, the endpoint-matched reversed law starts from $\Theta_{\#}\nu_T$ and evolves under the reversed protocol. Let ρ_0, ρ_T be densities relative to the same parity-invariant physical phase volume. Under Theorems 6.6 and 6.13, local detailed balance with the stated bath-heat convention, and mutual absolute continuity on the finite window,

$$\log \frac{\mathrm{d}\mathbb{P}_{[0,T]}}{\mathrm{d}\mathbb{P}^{R,\Theta}_{[0,T]}}(\omega) = \log \rho_0(X_0) - \log \rho_T(X_T) + \beta Q_{\mathrm{bath}}[\omega]. \tag{8.20}$$

The right-hand side is

$$\frac{\Delta s_{\mathrm{sys}}[\omega] + \Delta s_{\mathrm{med}}[\omega]}{k_B}. \tag{8.21}$$

If the reversed law instead starts from a density g_T relative to that same phase volume and is not endpoint matched, then the calculation contains the explicit boundary mismatch

$$\log \rho_0(X_0) - \log g_T(\Theta X_T) + \beta Q_{\mathrm{bath}}[\omega], \tag{8.22}$$

which must not be suppressed. In particular, if $\rho_t = f_t \pi$ for a fixed Gibbs reference $\pi \propto e^{-\beta U}$, the endpoint difference is $\log f_0(X_0) - \log f_T(X_T) + \beta \Delta U$. Using Gibbs-relative densities without this energy term would count heat incorrectly. A full derivation is given in Section 8.2. If the forward and reversed path laws are not mutually absolutely continuous, the ordinary integral fluctuation relation requires a singular correction. Write $Q = Q_{\mathrm{ac}} + Q_{\mathrm{s}}$ for the reversed comparison law decomposed relative to the forward law P, and set $\lambda_{\mathrm{S}} = Q_{\mathrm{s}}(\Omega)$. With $\Delta s_{\mathrm{tot}}/k_B = -\log(dQ_{\mathrm{ac}}/dP)$,

$$\mathbb{E}[\exp(-\Delta s_{\mathrm{tot}}/k_B)] = 1 - \lambda_{\mathrm{S}}, \tag{8.23}$$

where a zero density gives infinite production and zero exponential weight [76]. The identity follows by integrating dQ_{ac}/dP; Theorem 8.4 gives the precise measure-theoretic statement. This is why the comparison law must be named.

8.2. *Endpoint measures, fluctuation identities, and three distinct arrows.*

8.2.1. *The reverse experiment is part of the observable.* A statement about the direction of time requires two specified experiments. Let P be the forward law on a finite interval $[0,T]$, let $\widetilde{P}$ be a declared reverse experiment, and set $Q = \mathcal{R}_{\#}\widetilde{P}$, where $(\mathcal{R}\omega)_t = \Theta\omega_{T-t}$ and Θ changes the sign of odd variables. The reversed driving protocol, initial law, and parity of external fields belong to this definition. Comparing two unspecified "directions" has no invariant thermodynamic meaning.

Proposition 8.4 (Path likelihood and absolute irreversibility). *Suppose P and Q are equivalent probability measures and put $\Sigma = \log(dP/dQ)$. Then*

$$\mathbb{E}_P e^{-\Sigma} = 1, \qquad \mathbb{E}_P \Sigma = D(P\|Q) \geq 0, \qquad P(\Sigma \leq -s) \leq e^{-s} \quad (s \geq 0). \tag{8.24}$$

The mean may be infinite; equality of the finite mean to zero holds exactly when $P = Q$. More generally let $Q = Q_{\mathrm{ac}} + Q_{\mathrm{s}}$ be the Lebesgue decomposition with respect to P, write $q = dQ_{\mathrm{ac}}/dP$, and let $\lambda = Q_{\mathrm{s}}(\Omega)$. With $\Sigma = -\log q$, including $+\infty$ on $\{q = 0\}$,

$$\mathbb{E}_P e^{-\Sigma} = 1 - \lambda. \tag{8.25}$$

When $P \ll Q$, this Σ is $\log(dP/dQ)$, P-almost surely. Its negative part is integrable, so its mean is well defined with values in $(-\infty, +\infty]$. If $\lambda < 1$, $\mathbb{E}_P\Sigma \geq -\log(1-\lambda)$. For arbitrary $0 \leq \lambda \leq 1$, the sharper tail bound is $P(\Sigma \leq -s) \leq (1-\lambda)e^{-s}$, $s \geq 0$.

Proof. For equivalent laws, integrating dQ/dP gives the fluctuation identity, while the definition of relative entropy gives $\mathbb{E}_P\Sigma = D(P\|Q)$, including the infinite case. Gibbs' inequality gives nonnegativity and the stated equality condition.

In the general case, $\int q\, dP = Q_{\mathrm{ac}}(\Omega) = 1 - \lambda$. Write $\Sigma^- := \max\{-\Sigma, 0\}$. Since $\Sigma^- = \max\{\log q, 0\} \leq q$, its integral is finite. Thus $\mathbb{E}_P\Sigma = \mathbb{E}_P\Sigma^+ - \mathbb{E}_P\Sigma^-$ is well defined and can equal $+\infty$; no subtraction of two infinite integrals occurs. If $P(q = 0) > 0$, the mean is $+\infty$. For $a = 1 - \lambda > 0$, the claimed lower bound is immediate when the positive part has infinite integral. In the remaining case $q > 0$ almost surely and $-\log q$ is integrable. The pointwise inequality $\log(q/a) \leq q/a - 1$, after integration, yields $\mathbb{E}_P[-\log q] \geq -\log a$. Finally, $e^{-\Sigma} = q$, with $e^{-\infty} = 0$, so Markov's inequality gives $P(\Sigma \leq -s) \leq e^{-s}\mathbb{E}_P q = (1-\lambda)e^{-s}$. This also covers $\lambda = 1$, for which $q = 0$ almost surely. Setting $\lambda = 0$ recovers the equivalent-law bound. □

Nonnegative mean production permits negative production on individual finite histories. Identifying $k_B\Sigma$ with physical total entropy requires local detailed balance and a specified reservoir; the measure identity alone does not supply a thermometer, a heat variable, or a microscopic bath.

8.2.2. *A reference-density correction in the heat formula.* To display every endpoint term, use even variables on a torus, a constant positive diffusion matrix D, a smooth time-independent drift b, and the equation $dX = b(X)dt + \sqrt{2D}\, dW$. Let p_0, p_T denote positive densities relative to coordinate volume. The reverse experiment uses the same drift and starts from p_T. Under the finite-window absolute-continuity assumptions, the path ratio is

$$\Sigma = \log \frac{p_0(X_0)}{p_T(X_T)} + \int_0^T (D^{-1}b)(X_t) \circ dX_t. \tag{8.26}$$

One way to verify the sign is to compare midpoint transition weights. The difference of the two quadratic actions for increments dX and $-dX$ is $b^T D^{-1} \circ dX$; their divergence terms cancel. Multiplication by the initial densities gives the two endpoint terms. Equivalently, the diffusion time-reversal theorem and Girsanov's formula give the same expression. In a thermal realization $b = DF/\theta$, $\theta = k_B T_{\mathrm{bath}}$, the integral is Q_{bath}/θ, with $Q_{\mathrm{bath}} = \int F \circ dX$.

Now introduce a Gibbs reference $\pi = Z^{-1}e^{-U/\theta}$ and write $p_t = f_t\pi$. Merely changing the reference density gives

$$\log\frac{p_0(X_0)}{p_T(X_T)} = \log\frac{f_0(X_0)}{f_T(X_T)} + \frac{U(X_T)-U(X_0)}{\theta},$$
$$\Sigma = \log\frac{f_0(X_0)}{f_T(X_T)} + \frac{\Delta U + Q_{\mathrm{bath}}}{\theta}. \tag{8.27}$$

Consequently a Gibbs-relative endpoint logarithm cannot simply be added to the full bath heat. For a conservative undriven force $F = -\nabla U$, $Q_{\mathrm{bath}} = -\Delta U$ and those energy terms cancel. With work $W = \Delta U + Q_{\mathrm{bath}}$, the last term is W/θ. Time-dependent reference potentials also require their partition-function change and the prescribed protocol reversal; they are not covered by the fixed-reference simplification above.

8.2.3. *Relaxation, stationary circulation, and information loss.*

Proposition 8.5 (Endpoint-matched relaxation identity). *Let a Markov diffusion have invariant probability π and be reversible under the declared measurable parity involution Θ, with $\Theta_{\#}\pi = \pi$. Write $R = P_\pi$ for its stationary path law, so $\mathcal{R}_{\#}R = R$. Let $p_T = (X_T)_{\#}P_{p_0}$ and set $Q = \mathcal{R}_{\#}P_{\Theta_{\#}p_T}$. Assume $p_0 = f_0\pi$ and $p_T = f_T\pi$, where f_0, f_T are measurable, finite and positive π-almost everywhere, and $\int |\log f_i|\, dp_i < \infty$ for $i = 0, T$. Then the path laws are equivalent, all three relative entropies below are finite, and*

$$\log\frac{dP_{p_0}}{dQ} = \log f_0(X_0) - \log f_T(X_T), \qquad D(P_{p_0}\|Q) = D(p_0\|\pi) - D(p_T\|\pi). \tag{8.28}$$

Proof. Let K_x denote the conditional path law started at x. It is concentrated on $\{X_0 = x\}$, and $P_p = \int K_x\, p(dx)$. For every nonnegative measurable path function g,

$$\int g\, dP_{p_0} = \int f_0(x)\Big(\int g\, dK_x\Big)\,\pi(dx) = \int g\, f_0(X_0)\, dR.$$

Thus the initial-density change is derived from the path kernel. Parity invariance gives $d(\Theta_{\#}p_T)/d\pi = f_T \circ \Theta$. Reversing this path law and using $\Theta X_0 = X_T \circ \mathcal{R}$ and $\mathcal{R}_{\#}R = R$ gives $dQ/dR = f_T(X_T)$. Both densities are positive R-almost everywhere because the two stationary endpoint marginals are π. Their Radon–Nikodym ratio therefore gives the first identity. The prescribed endpoint logarithmic moments make both terms integrable under P_{p_0}, since its endpoint laws are exactly p_0, p_T. Integrating their difference proves the second identity with finite terms; no subtraction of two infinite entropies is used. □

Thus stationary equilibrium has zero path production while relaxation from a nonequilibrium law can have positive endpoint-matched path production. There is no contradiction between reversible equilibrium dynamics and a strictly decreasing nonequilibrium free energy.

For a complementary maintained process, retain even variables and set

$$b = D\nabla\log\pi + c, \qquad \nabla\cdot(\pi c) = 0, \qquad f = p/\pi, \qquad J = pc - Dp\nabla\log f. \tag{8.29}$$

Integration by parts, with periodic conditions or vanishing boundary terms, gives

$$-\frac{d}{dt}D(p\|\pi) = \int p\,\nabla\log f^T D\nabla\log f =: \mathcal{I}_D(p),$$
$$\int \frac{J^T D^{-1} J}{p} = \mathcal{I}_D(p) + \int p\,c^T D^{-1} c. \tag{8.30}$$

Indeed the transport contribution is $\int \pi c\cdot\nabla f = 0$; the same expression removes the cross term in the second line. The first formula expresses free-energy decay since $F(p) - F(\pi) = \theta D(p\|\pi)$. Under the thermal interpretation of (8.26), the second formula is the expected rate of total entropy production in units of k_B: the mean medium rate is $\int J\cdot D^{-1}b$, and the Shannon entropy rate is $-\int J\cdot\nabla\log p$.

At $p=\pi$, the state KL is constant and the stationary path rate is $\int \pi c^T D^{-1}c$. Directly, the reversed stationary drift is $b^R = -b + 2D\nabla\log\pi$; Girsanov's quadratic cost is $\frac{1}{2}(2c)^T(2D)^{-1}(2c) = c^T D^{-1}c$. This calculation requires the stated all-even fixed-drive reversal. An odd Hamiltonian transport current must not be counted as dissipative by this formula without its parity decomposition and noise-range test.

Finally, suppose a Markov evolution K_t preserves π and strictly decreases $D(p\|\pi)$ for a particular nonequilibrium p. There is no positive Markov kernel R_t preserving π with $R_tK_tp = p$: data processing would give

$$D(p\|\pi) = D(R_tK_tp\|R_t\pi) \le D(K_tp\|\pi) < D(p\|\pi). \tag{8.31}$$

This is an information-recovery obstruction, not a prohibition on defining a reverse diffusion. Exponential decay, if needed, requires a functional inequality such as $\mathcal{I}_D(p) \ge \lambda D(p\|\pi)$. Invariance alone does not give that inequality or cosmic convergence.

8.2.4. *What can be inferred across physical sectors.* The common origin supplies a testable statement only after the energy, mobility, noise, physical time, and observation map have been fixed. For an observation $Y = P(X)$ on standard Borel path spaces, disintegration gives the following decomposition when $P_X \ll Q_X$ and $D(P_X\|Q_X) < \infty$:

$$D(P_X\|Q_X) = D(P_Y\|Q_Y) + \int D(P_X(\cdot\mid y)\|Q_X(\cdot\mid y))P_Y(dy). \tag{8.32}$$

An observed arrow is therefore bounded by the full arrow. Under these finite-entropy hypotheses, the deficit is the integral of nonnegative conditional relative entropies. It vanishes if and only if $P_X(\cdot\mid y) = Q_X(\cdot\mid y)$ for P_Y-almost every y, because relative entropy is zero exactly for identical probability laws. Data processing remains valid with extended values, but an equality $+\infty = +\infty$ does not imply equality of hidden conditional laws. Small simulation error does not establish this equality criterion. Convergence of a regulated probability law likewise does not establish bounded spacetime curvature, preservation of a physical constraint, or regularity after removal of

the regulator. Those statements need their own dynamical estimates. The distinction makes the proposed common origin falsifiable without assigning the same evidential meaning to every sector.

8.3. *Nonequilibrium Steady States and Path Entropy Production.* Stationarity means that the density no longer changes; it does not mean that matter or probability has stopped circulating. A particle driven around a ring can have a stationary position distribution while the drive continually supplies work that is released as heat. The state relative entropy is then constant, but the forward and reversed path laws differ. The following formulas distinguish these two observations and identify the additional heat accounting required for a physical entropy-production rate.

8.3.1. *Stationary Current Decomposition.* Consider an overdamped diffusion on a compact domain or a periodic torus with constant positive-definite diffusion matrix D. Let the Fokker-Planck equation be

$$\partial_t \rho = -\nabla \cdot J, \tag{8.33}$$

with current

$$J = b\rho - \mathsf{D}\nabla\rho. \tag{8.34}$$

Let π be a stationary density and define

$$J_{\mathrm{ss}} = b\pi - \mathsf{D}\nabla\pi, \qquad \nabla \cdot J_{\mathrm{ss}} = 0. \tag{8.35}$$

Set

$$f = \frac{\rho}{\pi}, \qquad v_{\mathrm{ss}} = \frac{J_{\mathrm{ss}}}{\pi}. \tag{8.36}$$

Because $\rho = f\pi$,

$$\begin{aligned} J &= bf\pi - \mathsf{D}(\pi\nabla f + f\nabla\pi) \\ &= f(b\pi - \mathsf{D}\nabla\pi) - \pi\mathsf{D}\nabla f \\ &= fJ_{\mathrm{ss}} - \pi\mathsf{D}\nabla f. \end{aligned} \tag{8.37}$$

Dividing by $\rho = f\pi$ gives

$$\frac{J}{\rho} = v_{\mathrm{ss}} - \mathsf{D}\nabla \log f. \tag{8.38}$$

8.3.2. *Housekeeping and Nonadiabatic Entropy Production.* Define the dimensionless total entropy-production rate by

$$\sigma_{\mathrm{tot}} = \int \frac{J^{\mathsf{T}}\mathsf{D}^{-1}J}{\rho}\,\mathrm{d}x. \tag{8.39}$$

Substitute Equation (8.38):

$$\begin{aligned} \sigma_{\mathrm{tot}} = &\int \rho v_{\mathrm{ss}}^{\mathsf{T}}\mathsf{D}^{-1}v_{\mathrm{ss}}\,\mathrm{d}x \\ &- 2\int \rho v_{\mathrm{ss}} \cdot \nabla \log f\,\mathrm{d}x \\ &+ \int \rho(\nabla \log f)^{\mathsf{T}}\mathsf{D}\nabla \log f\,\mathrm{d}x. \end{aligned} \tag{8.40}$$

The cross term vanishes because

$$\begin{aligned}\int \rho v_{\mathrm{ss}} \cdot \nabla \log f \,\mathrm{d}x &= \int f\pi \frac{J_{\mathrm{ss}}}{\pi} \cdot \frac{\nabla f}{f} \,\mathrm{d}x \\ &= \int J_{\mathrm{ss}} \cdot \nabla f \,\mathrm{d}x \\ &= -\int f \nabla \cdot J_{\mathrm{ss}} \,\mathrm{d}x = 0. \end{aligned} \tag{8.41}$$

Hence

$$\sigma_{\mathrm{tot}} = \sigma_{\mathrm{hk}} + \sigma_{\mathrm{na}}, \tag{8.42}$$

where

$$\sigma_{\mathrm{hk}} = \int \rho v_{\mathrm{ss}}^{\mathsf{T}} \mathsf{D}^{-1} v_{\mathrm{ss}} \,\mathrm{d}x, \tag{8.43}$$

$$\sigma_{\mathrm{na}} = \int \rho (\nabla \log f)^{\mathsf{T}} \mathsf{D} \nabla \log f \,\mathrm{d}x. \tag{8.44}$$

The relative entropy with respect to the stationary density is

$$D(\rho \| \pi) = \int \rho \log f \,\mathrm{d}x. \tag{8.45}$$

Differentiating, using $\partial_t \rho = -\nabla \cdot J$, and integrating by parts yields

$$\begin{aligned}\frac{\mathrm{d}}{\mathrm{d}t} D(\rho_t \| \pi) &= \int (\partial_t \rho) \log f \,\mathrm{d}x \\ &= \int J \cdot \nabla \log f \,\mathrm{d}x \\ &= \int \rho v_{\mathrm{ss}} \cdot \nabla \log f \,\mathrm{d}x \\ &\quad - \int \rho (\nabla \log f)^{\mathsf{T}} \mathsf{D} \nabla \log f \,\mathrm{d}x \\ &= -\sigma_{\mathrm{na}}. \end{aligned} \tag{8.46}$$

Thus state relative-entropy decay measures the nonadiabatic contribution, not the entire NESS entropy production.

8.3.3. *Exact Driven Ring Counterexample.* Consider the diffusion on a ring of circumference $L > 0$, with $D > 0$ and $b \neq 0$,

$$\mathrm{d}X_t = b \,\mathrm{d}t + \sqrt{2D} \,\mathrm{d}W_t \pmod{L}. \tag{8.47}$$

The stationary density is

$$\pi(x) = \frac{1}{L}, \tag{8.48}$$

and the stationary current is

$$J_{\mathrm{ss}} = \frac{b}{L}. \tag{8.49}$$

At stationarity the state relative entropy is

$$D(\pi\|\pi) = 0, \tag{8.50}$$

but the total entropy-production rate is

$$\begin{aligned}\sigma_{\mathrm{tot}} &= \int_0^L \frac{(b/L)^2}{D/L}\,\mathrm{d}x \\ &= \frac{b^2}{D} > 0.\end{aligned} \tag{8.51}$$

This exact calculation proves that stationary state KL dissipation and total NESS entropy production cannot be universally identified.

8.3.4. *Forward-Reverse Path KL on the Ring.* For the stationary ring process, the time-reversed stationary drift is $-b$. The drift difference is therefore $2b$. Since the covariance in the SDE is $2D$, the Girsanov relative-entropy rate between the forward and reversed path laws is

$$\begin{aligned}D\Big(\mathbb{P}_{[0,T]}\Big\|\mathbb{P}^R_{[0,T]}\Big) &= \frac{1}{2}\int_0^T \frac{(2b)^2}{2D}\,\mathrm{d}t \\ &= \frac{b^2}{D}T.\end{aligned} \tag{8.52}$$

Combining Equations (8.50) and (8.52) gives the explicit inequality

$$D\Big(\mathbb{P}_{[0,T]}\Big\|\mathbb{P}^R_{[0,T]}\Big) \neq D(\nu_0\|\pi) - D(\nu_T\|\pi) \tag{8.53}$$

in general.

8.4. *Loschmidt, Poincare, and Zermelo.*

8.4.1. *What the Stochastic Theory Does and Does Not Claim about Loschmidt.* The finite Hamiltonian realization gives an explicit preparation-level comparison. If f_τ is its full evolved law, exact reversal starts from $\Theta_* f_\tau$, including its system–reservoir correlations. A fresh conditional thermal bath is a different preparation. The chain rule in (4.14) locates the discarded conditional information; its return is allowed before memory is removed. The nonstationary reverse diffusion in (4.33) retains positive covariance and changes its drift through the forward density. It is not a negative-diffusion equation.

Loschmidt's argument constructs a reverse trajectory within a reversible microscopic group. In the present framework, the relevant irreversible theorem is instead Theorem 8.1: once a probability law has undergone strict relative-entropy contraction, the information lost by that law cannot be recovered by another positive Markov evolution that preserves the same invariant reference measure. This is a probability-dynamical obstruction, not a denial of the mathematical existence of a reverse diffusion. Rigorous time reversal under finite-entropy assumptions is treated, for example,

in [45] and [15], and stationary diffusion entropy production is analyzed from a complementary generator/path-space viewpoint in [21].

For an equilibrium reversible diffusion, the stationary forward and reverse path laws may coincide. Therefore the implication

$$\text{stochastic noise} \Longrightarrow \text{forward/reverse path asymmetry} \tag{8.54}$$

is false in general. The arrow relevant to autonomous thermodynamic relaxation is the ordering of non-equilibrium probability laws by free energy and relative entropy.

8.4.2. *Correct Statement of Poincare Recurrence.* Let $(X, \mathcal{B}, \mu)$ be a finite measure space and let $T : X \to X$ be measure preserving:

$$\mu(T^{-1}A) = \mu(A) \tag{8.55}$$

for all measurable A. Poincare recurrence states, in one standard form, that almost every point of any measurable set of positive measure returns to that set infinitely often. The theorem does not require finite dimensionality.

This point can be illustrated by an explicitly infinite-dimensional example. Let

$$\Omega = \mathbb{R}^{\mathbb{Z}}, \qquad \mu = \bigotimes_{n\in\mathbb{Z}} N(0,1), \tag{8.56}$$

and define the shift

$$(\theta\omega)_n = \omega_{n+1}. \tag{8.57}$$

Then

$$\theta_{\#}\mu = \mu, \qquad \mu(\Omega) = 1. \tag{8.58}$$

Thus infinite-dimensional probability spaces can satisfy the hypotheses of abstract recurrence.

8.4.3. *Absence of a Flat Infinite-Dimensional Liouville Analogue.* A different statement is true and is useful for understanding why finite-dimensional Liouville volume does not extend naively to Banach trajectory space.

THEOREM 8.6 (No nonzero locally finite translation-invariant Borel measure). *Let E be an infinite-dimensional separable Banach space. There is no nonzero locally finite Borel measure λ satisfying*

$$\lambda(A + h) = \lambda(A) \tag{8.59}$$

for every Borel set $A \subset E$ and every $h \in E$.

Proof. Assume for contradiction that such a nonzero locally finite measure exists. We first extract a ball with both positive and finite measure. Local finiteness means that every point has an open neighbourhood of finite λ-measure. Since E is separable, every open cover has a countable subcover, so E is covered by countably many finite-measure open sets. Because λ is nonzero, one

member U of this countable cover satisfies $\lambda(U) > 0$. The separability of E gives a countable base of open balls. Therefore, if every open ball contained in U had zero measure, countable subadditivity would imply $\lambda(U) = 0$, a contradiction. Hence there exist $x_0 \in E$ and $R > 0$ such that $B(x_0, R) \subset U$ and

$$0 < \lambda(B(x_0, R)) < \infty. \tag{8.60}$$

By translation invariance,

$$0 < \lambda(B(0, R)) < \infty, \tag{8.61}$$

after replacing $B(x_0, R)$ by its translate $B(0, R)$.

Choose any $0 < r < R/8$. Separability gives a countable dense set $(z_j)_{j\geq 1}$ in E, and hence

$$B(0, R) \subset \bigcup_{j=1}^{\infty} B(z_j, r). \tag{8.62}$$

If $\lambda(B(0, r)) = 0$, translation invariance would give $\lambda(B(z_j, r)) = 0$ for every j, and countable subadditivity would contradict Equation (8.61). Hence

$$\lambda(B(0, r)) > 0. \tag{8.63}$$

Because E is infinite dimensional, Riesz's lemma [90] gives a sequence of unit vectors $(u_n)_{n\geq 1}$ with $\|u_n - u_m\| \geq 1/2$ whenever $n \neq m$. Set $x_n = (R/2)u_n$. Then the open balls $B(x_n, R/8)$ are pairwise disjoint, because two points lying in the same intersection would force the centre distance to be strictly smaller than $R/4$, while

$$\|x_n - x_m\| = \frac{R}{2}\|u_n - u_m\| \geq \frac{R}{4}. \tag{8.64}$$

Moreover, $B(x_n, R/8) \subset B(0, 5R/8) \subset B(0, R)$. Translation invariance and Equation (8.63) give

$$\begin{aligned} \lambda(B(0, R)) &\geq \sum_{n=1}^{\infty} \lambda(B(x_n, R/8)) \\ &= \sum_{n=1}^{\infty} \lambda(B(0, R/8)) = +\infty, \end{aligned} \tag{8.65}$$

contradicting the finiteness in Equation (8.61). Therefore no such nonzero measure exists. □

Remark 8.7. Theorem 8.6 rules out a flat translation-invariant analogue of finite-dimensional Lebesgue volume. It does not rule out Gaussian measures, Gibbs measures, invariant stationary probabilities, or Poincare recurrence for finite invariant measures on infinite-dimensional spaces.

8.4.4. *Resolution of the Zermelo Objection at the Probability-Law Level.* The strongest no-recurrence statement in this paper is therefore not an infinite-dimensional volume argument. It is Theorem 8.3. If the thermodynamic law satisfies strict exponential relative-entropy contraction, exact return of the same non-equilibrium law is impossible. An individual sample path may nevertheless return, and an equilibrium stationary process may itself be recurrent in an appropriate

sense. This separation removes the logical overreach that would result from claiming that "history itself cannot recur because path space is infinite dimensional."

8.5. *Causal order, clock duration, and a statistical arrow.* Time enters this construction in three distinct ways. A Lorentzian metric specifies which events can be connected by causal signals. A material clock measures duration along a timelike trajectory. A path law specifies whether forward histories can be distinguished statistically from physically reversed histories. The last property does not define either of the first two. In signature $(-+++)$ and coordinates $x^0 = ct$, proper time satisfies

$$d\tau^2 = -c^{-2} g_{\mu\nu}\, dx^\mu dx^\nu.$$

This formula applies to timelike worldlines, not to an arbitrary Brownian path in a configuration space. An auxiliary sampling parameter acquires a physical interpretation only after a clock map has been supplied.

The following result makes the effect of a clock map explicit. It is an application of the standard time-change construction for Markov processes, not a derivation of relativistic proper time from a probability law.

PROPOSITION 8.8 (A state-dependent clock changes the invariant law). *Let X_s be a conservative diffusion on a connected compact smooth manifold without boundary, with smooth uniformly elliptic generator*

$$Lf = b^i \partial_i f + D^{ij} \partial_i \partial_j f, \qquad D = D^{\mathsf{T}} > 0.$$

Suppose that it has invariant probability π and a unique martingale problem. Let a be smooth and $0 < a_- \le a(x) \le a_+ < \infty$. Define $T(s) = \int_0^s a(X_v)\, dv$, its inverse $S(t) = T^{-1}(t)$, and $Y_t = X_{S(t)}$. Then the generator and invariant law of Y are

$$\widetilde{L} = a^{-1} L, \qquad \widetilde{\pi}(dx) = \frac{a(x)}{Z_a} \pi(dx), \qquad Z_a = \int a\, d\pi. \tag{8.66}$$

The invariant probability is unique. Reversibility is preserved under this clock change, with respect to the new invariant probability.

Proof. For a smooth f, the process $f(X_s) - f(X_0) - \int_0^s Lf(X_v)\, dv$ is a local martingale. Substituting $s = S(t)$ and using $dS/dt = 1/a(Y_t)$ gives the martingale problem for $\widetilde{L}$. The bounds on a prevent clock explosion or stopping. The smooth uniformly elliptic diffusion on the compact connected state space has a conservative, irreducible, smoothing semigroup. Its invariant probability is therefore unique. Integration gives

$$\int \widetilde{L} f\, d\widetilde{\pi} = Z_a^{-1} \int Lf\, d\pi = 0.$$

Smooth elliptic well-posedness identifies this infinitesimal identity with invariance. Finally,

$$\langle f, \widetilde{L} g \rangle_{\widetilde{\pi}} = Z_a^{-1} \langle f, Lg \rangle_\pi.$$

Thus symmetry of one generator is equivalent to symmetry of the other on their smooth cores, and hence of their closed realizations. □

The identity extends to compatible reflecting realizations when the time-changed martingale problem, conormal boundary condition, and invariant measure criterion are established. An unbounded clock, a vanishing lapse, or a singular boundary requires a separate theorem. In particular, this compact uniformly elliptic result cannot be extended to a black-hole horizon by substitution.

8.6. *Entropy rates and relaxation after calibration.* For an explicit calculation take a flat torus and assume all state variables are even under time reversal. Write $\pi(x)$ for the smooth positive stationary density and

$$J_i = b_i\pi - \partial_j(D_{ij}\pi).$$

Assume the stationary forward and reversed laws satisfy the usual finite path-energy and absolute-continuity hypotheses. Their relative entropy per unit s is

$$e_s = \int \frac{J^{\mathsf{T}} D^{-1} J}{\pi}\, dx.$$

Under (8.66), direct substitution yields

$$\widetilde{D} = D/a, \qquad \widetilde{J} = J/Z_a, \qquad e_t = \int \frac{\widetilde{J}^{\mathsf{T}} \widetilde{D}^{-1} \widetilde{J}}{\widetilde{\pi}}\, dx = \frac{e_s}{Z_a}.$$

The cancellation follows from $\partial_j[(D_{ij}/a)(a\pi/Z_a)] = Z_a^{-1}\partial_j(D_{ij}\pi)$. This also proves that a positive clock change cannot turn a reversible diffusion into an irreversible one. For odd variables the reversal must include their parity; preservation of generalized detailed balance requires a parity-even clock and the corresponding operator domains.

On a finite path window the informational asymmetry is $D(P_F\|P_R\circ\mathcal{T}^{-1})$. Under mutual absolute continuity, normalization gives

$$\mathbb{E}_F \exp(-\Sigma/k_B) = 1, \qquad \mathbb{E}_F\Sigma = k_B D(P_F\|P_R\circ\mathcal{T}^{-1}) \geq 0,$$

where $\Sigma = k_B \log[dP_F/d(P_R\circ\mathcal{T}^{-1})]$. The equality of Σ with thermodynamic total entropy requires local detailed balance, reservoir bookkeeping, and the specified endpoint laws. It does not follow solely from normalization.

An invariant Gibbs law can support irreversible relaxation from a prepared nonequilibrium distribution while its stationary process is reversible. Conversely, a stationary circulating law can have positive path entropy production even though its state relative entropy is constant. Thus duration, relaxation, and stationary path asymmetry are different physical quantities.

Proposition 8.9 (A calibrated spectral-gap bound). *Under Proposition 8.8, suppose that L is reversible and obeys* $\mathrm{Var}_\pi f \leq C_P\mathcal{E}(f,f)$, *where* $\mathcal{E}(f,f) = -\langle f, Lf\rangle_\pi$. *Then*

$$\mathrm{Var}_{\widetilde{\pi}} f \leq a_+ C_P\, \widetilde{\mathcal{E}}(f,f), \qquad \widetilde{\mathcal{E}}(f,f) = Z_a^{-1}\mathcal{E}(f,f).$$

In particular the new spectral gap is at least $(a_+C_P)^{-1}$.

Proof. Use the variational characterization of variance and choose the old mean:

$$\operatorname{Var}_{\widetilde{\pi}} f \le \int (f-\pi f)^2 \, d\widetilde{\pi} \le (a_+/Z_a) \operatorname{Var}_{\pi} f.$$

Insert the old Poincare inequality and the displayed Dirichlet-form identity. The spectral theorem gives exponential $L^2(\widetilde{\pi})$ relaxation for densities initially in that space. This argument does not claim uniform total-variation convergence from every singular initial law. □

8.7. *An exactly normalized clock experiment.* Consider $dX_s = b\,ds + \sqrt{2D}\,dW_s$ modulo 2π, with $D > 0$, and $a(x) = a_0(1 + \eta\cos x)$, where $a_0 > 0$ and $|\eta| < 1$. The original invariant density is $1/(2\pi)$, whereas

$$\widetilde{\pi}(x) = \frac{1+\eta\cos x}{2\pi}, \qquad \widetilde{J} = \frac{b}{2\pi a_0}, \qquad e_t = \frac{b^2}{Da_0}.$$

Consequently equilibrium histograms alone cannot identify the clock or the current: changing b preserves this histogram and changes the arrow. The example is dimensionless; a_0 converts its two declared time units.

For an integer $N \ge 3$, set $h = 2\pi/N$ and $q_\pm = D/h^2 \pm b/(2h) > 0$, and divide the two outgoing rates at node i by $a_i = a(ih)$. The resulting Markov chain has $\widetilde{\pi}_i = a_i/\sum_j a_j$. Its stationary oriented edge flows are $q_\pm/\sum_j a_j$, so its entropy rate is exactly

$$e_{t,N} = \frac{b}{a_0 h} \log \frac{D/h^2 + b/(2h)}{D/h^2 - b/(2h)} = \frac{b^2}{Da_0} + \frac{b^4h^2}{12D^3a_0} + O(h^4). \tag{8.67}$$

The restriction $N \ge 3$ keeps the two neighbours distinct. For $N = 2$, clockwise and counterclockwise jumps reach the same state, so the state-observed off-diagonal rate is $(q_+ + q_-)/a_i$. The stationary flux in either direction is then $(q_+ + q_-)/\sum_{j=0}^{1} a_j$, and the state-path entropy production is zero. Formula (8.67) can still describe the two-state system if jump orientations are recorded as distinct channels; it is not the entropy rate of the state path alone. The series uses $\log[(1+z)/(1-z)] = 2z + 2z^3/3 + O(z^5)$, with $|z| = |b|h/(2D) < 1$. Thus positivity and second-order entropy-rate convergence can be checked independently of a stochastic sampling error. The matrix-exponential experiment uses $(b, D, a_0, \eta) = (0.7, 0.4, 1.6, 0.5)$. It compares transient densities with the exact stationary law and checks relative-entropy contraction toward that law. It is a synthetic clock calibration example, not an observation of fundamental time. The corresponding numerical values are reported in Table 1.

The corresponding numerical diagnostic is shown in Figure 3.

8.8. *A finite-state proof of the three entropy statements.* A clock orders events and measures duration. Entropy production asks a different question: how well can the statistics of a history be distinguished from those of its specified reverse? The distinction can be proved without a continuum limit. Throughout this subsection all variables are even under reversal, and rates refer to one fixed

Table 1. Synthetic clock experiment. The exact continuum entropy rate is 0.76562500; the invariant residual is the maximum component of $Q^{\mathsf{T}}\widetilde{\pi}$.

N	Entropy rate	Absolute error	Invariant residual
16	0.79809013	3.25e-02	8.33e-17
32	0.77329434	7.67e-03	1.11e-16
64	0.76751664	1.89e-03	1.67e-16
128	0.76609634	4.71e-04	4.44e-16
256	0.76574274	1.18e-04	8.88e-16

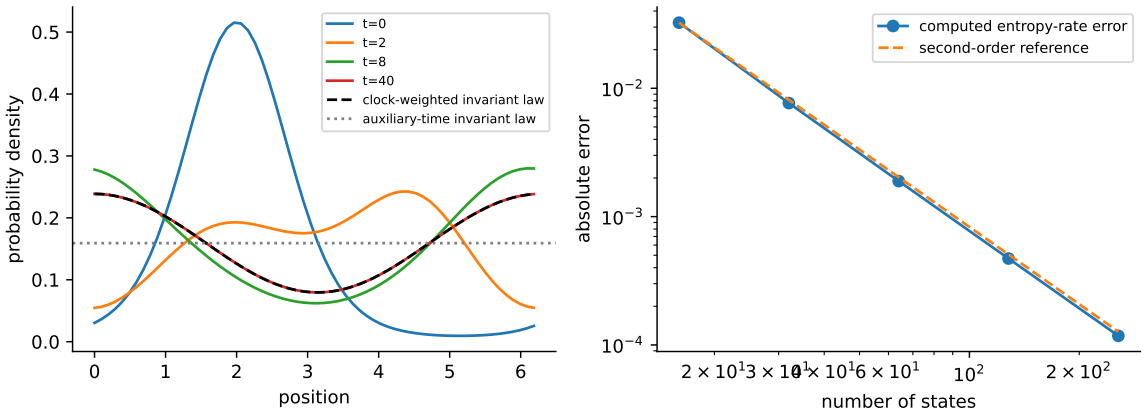


Figure 3. A state-dependent clock reweights the invariant density. The left panel shows deterministic Markov-semigroup evolution and its exact target. The right panel compares discrete stationary path entropy rates with the continuum value. The calculation tests a clock transformation, not a derivation of a spacetime metric.

physical clock. Odd variables, magnetic protocols, and time-dependent reservoirs require their corresponding reversed dynamics.

Proposition 8.10 (Relaxation and stationary path asymmetry). *Let q_{ij}, $i \neq j$, be the rates of an irreducible finite continuous-time Markov chain. Assume reciprocal support: $q_{ij} > 0$ if and only if $q_{ji} > 0$. Let π be its unique stationary probability, and let $p(t) > 0$ solve the master equation. Put $f_i = p_i/\pi_i$. Sums below run over directed edges with positive rate. Then*

$$\sigma_{\mathrm{tot}} = \sum_{i\neq j} p_i q_{ij} \log \frac{p_i q_{ij}}{p_j q_{ji}}, \tag{8.68}$$

$$\sigma_{\mathrm{hk}} = \sum_{i\neq j} p_i q_{ij} \log \frac{\pi_i q_{ij}}{\pi_j q_{ji}}, \tag{8.69}$$

$$\sigma_{\mathrm{na}} = \sum_{i\neq j} p_i q_{ij} \log \frac{f_i}{f_j} = -\frac{d}{dt} D(p(t)\|\pi). \tag{8.70}$$

All three rates are nonnegative and $\sigma_{\mathrm{tot}} = \sigma_{\mathrm{hk}} + \sigma_{\mathrm{na}}$. These rates have units of inverse time. Multiplication by k_B gives entropy units, but their physical reservoir interpretation additionally requires a thermodynamic identification of the rates.

Proof. Stationarity gives $\sum_{j\neq i}\pi_j q_{ji} = \pi_i \sum_{j\neq i} q_{ij}$. Define $q^\dagger_{ij} = \pi_j q_{ji}/\pi_i$. Thus the original and adjoint chains have the same escape rate at every state. Since $x\log(x/y) \geq x - y$ for $x, y > 0$,

$$\sigma_{\mathrm{hk}} = \sum_i p_i \sum_{j\neq i} q_{ij}\log(q_{ij}/q^\dagger_{ij}) \geq \sum_i p_i \sum_{j\neq i}(q_{ij} - q^\dagger_{ij}) = 0.$$

The same inequality yields

$$\sigma_{\mathrm{na}} = \sum_{i\neq j} \pi_i q_{ij} f_i \log(f_i/f_j) \geq \sum_{i\neq j} \pi_i q_{ij}(f_i - f_j) = 0,$$

where the final cancellation uses stationarity after summing over i. Equivalently, with $w_{ij} = \pi_i q_{ij}$, the relaxation rate is

$$\sigma_{\mathrm{na}} = \sum_{i\neq j} w_{ij}\left[f_i\log(f_i/f_j) - f_i + f_j\right].$$

Each bracket is nonnegative and vanishes exactly when $f_i = f_j$. Thus zero relaxation production forces equal relative densities along every positive-rate edge. Irreducibility and normalization then give $f_i = 1$ at every state. This equality criterion requires connectivity; nonnegativity alone does not establish a unique equilibrium. Differentiate $D(p\|\pi) = \sum_i p_i \log f_i$ and use $\sum_i \dot p_i = 0$:

$$\frac{d}{dt}D(p\|\pi) = \sum_i \dot p_i \log f_i = \sum_{i\neq j} p_i q_{ij}(\log f_j - \log f_i).$$

Splitting the logarithm in σ_{tot} proves the decomposition. Alternatively, pairing opposite edges gives

$$\sigma_{\mathrm{tot}} = \frac{1}{2}\sum_{i\neq j}(p_i q_{ij} - p_j q_{ji})\log\frac{p_i q_{ij}}{p_j q_{ji}} \geq 0.$$

This last formula also fixes the factor-of-two convention. □

At $p = \pi$, the state relative entropy and σ_{na} vanish, but σ_{hk} can remain positive. Detailed balance, $\pi_i q_{ij} = \pi_j q_{ji}$, makes $\sigma_{\mathrm{hk}} = 0$. In a reversible chain prepared away from π, σ_{na} is instead generally positive during relaxation. Consequently an invariant law, relaxation to that law, and a stationary arrow are three distinct properties.

8.9. *The initial law is part of the reversal experiment.* Let $\mathcal{T}_T\omega(t) = \omega(T - t)$ and let $P_\pi^{[0,T]}$ be the stationary path law of the preceding chain. Reciprocal rates and positive π ensure mutual absolute continuity of forward and reversed laws. For a history with jumps $i_0 \to i_1 \to \cdots \to i_n$, the waiting-time factors cancel and

$$\log\frac{dP_\pi}{d(P_\pi\circ\mathcal{T}_T^{-1})} = \log\frac{\pi_{i_0}}{\pi_{i_n}} + \sum_{\alpha=1}^{n}\log\frac{q_{i_{\alpha-1}i_\alpha}}{q_{i_\alpha i_{\alpha-1}}}.$$

Taking its expectation, the endpoint term has zero mean by stationarity. Expected jump counts are $T\pi_i q_{ij}$. Hence

$$D(P_\pi\|P_\pi\circ\mathcal{T}_T^{-1}) = T\sigma_{\mathrm{tot}}(\pi). \tag{8.71}$$

Detailed balance is therefore equivalent to vanishing stationary path asymmetry in this finite irreducible setting. Motion does not cease: a reversible chain still jumps.

The word *stationary* cannot be omitted. Consider two states with $q_{12} = q_{21} = 1$ and initial law $p(0) = (0.8, 0.2)$. The generator is reversible with $\pi = (1/2, 1/2)$, while $p_1(T) = 1/2 + 0.3e^{-2T}$. Reversing the same nonstationary path law gives

$$D(P_{p(0)} \| P_{p(0)} \circ \mathcal{T}_T^{-1}) = [0.8 - p_1(T)] \log 4 > 0 \quad (T > 0).$$

To prove this formula, detailed balance reduces the path log ratio to $\log f_0(X_0) - \log f_0(X_T)$; take expectations with the two endpoint laws. This is not the same comparison as an experiment whose reverse is initialized in $p(T)$. With that reverse initialization and the same reversible rates, the expected log ratio is instead $D(p(0)\|\pi) - D(p(T)\|\pi)$. Thus the self-reversed path law and a thermodynamic reverse protocol must not be silently exchanged.

8.10. *Local detailed balance supplies the physical interpretation.* If an edge represents one resolved reservoir mechanism and Q_{ij} is heat delivered to the system on a jump, one common convention is

$$\log(q_{ij}/q_{ji}) = -Q_{ij}/(k_B T_b).$$

This local detailed-balance law must follow from, or be imposed as, the specified system–bath model. Internal degeneracies, particle exchange, and multiple mechanisms add their own entropy and chemical terms. For several reservoirs one must retain the reservoir label on a jump; aggregating the rates can hide physical entropy production. The endpoint contribution is the change in stochastic system entropy, and the rate ratio accounts for the bath contribution under this convention. Only after these identifications does a path log ratio equal the total thermodynamic entropy change.

For mutually absolutely continuous forward and specified reverse path laws, write $\Sigma = k_B \log(dP_F/dP_R^{\mathrm{rev}})$. Normalization gives

$$\mathbb{E}_F e^{-\Sigma/k_B} = 1, \qquad \mathbb{E}_F \Sigma = k_B D(P_F \| P_R^{\mathrm{rev}}) \geq 0.$$

The first identity follows by integrating dP_R^{rev}/dP_F; the second follows from the definition of relative entropy. Neither identity creates a light cone, determines a proper-time metric, or proves a thermodynamic interpretation without the specified bath and reversal data.

8.11. *Existence, uniqueness, and convergence are separate claims.* Even in finite dimension, a normalizable formal Gibbs expression must be compatible with the realized generator and its boundary before it is an invariant law. Irreducibility establishes uniqueness for the finite chain above, and a finite irreducible continuous-time chain then converges to that law. The corresponding diffusion results require their own nonexplosion, domain, boundary, and mixing hypotheses.

In particular, existence does not imply uniqueness: two disconnected communicating classes have distinct invariant laws. Uniqueness alone does not imply relaxation for a general dynamical

semigroup: a deterministic rotation at nonzero speed on a circle has a unique probability invariant under the full continuous-time flow, but a point mass remains a point mass and does not converge weakly to the uniform law. Entropy decay alone need not establish a strict rate. Spectral-gap, Harris, or other suitable mixing estimates are additional arguments. These logical distinctions persist when a finite regulator is removed.

8.12. *Shared definitions, clocks, and the scope of recovery.* The primitive configuration, action, measure, mobility, covariance, and constraints are defined in the mother paper [50]. That paper's operational branch record also includes the operator boundary, projection, physical clock, and observation map. This branch retains that source of definitions. A quantity is derived only after the primitive model and the relevant realization are fixed; a further physical identification is a matching condition; a remaining fitted or chosen coefficient is an input. In particular, a unique response for specified couplings does not select unique physical couplings. Control cost, Palatini normalization, horizon surface gravity, trap stiffness, and a proposed shared coupling are different quantities even when historical notation uses variants of the same Greek letter.

There are three time structures. The physical metric determines causal order. A material clock on a timelike worldline measures, in signature $(-+++)$,

$$d\tau = \frac{1}{c}\sqrt{-g_{\mu\nu}\,dx^\mu dx^\nu}.$$

Path reversal compares the statistics of histories. An auxiliary stochastic parameter s_{aux} is identified with a laboratory time only through a specified clock map. If $dt_{\mathrm{lab}} = a(X_{s_{\mathrm{aux}}})\,ds_{\mathrm{aux}}$ with a control-independent positive clock, then the generator, drift, and covariance become L/a, b/a, and A/a, respectively; the noise amplitude is divided by $\sqrt{a}$. A running cost per unit s_{aux} is divided by a. Existence and integrability of the time change must be checked, especially at a horizon or on an unbounded state space.

Detailed balance eliminates stationary path asymmetry when the initial law is stationary and the reversal includes the correct variable parities. It does not stop the motion, nor does it make the self-reversal of every prepared nonstationary path law identical to that law. State relative-entropy decay, stationary entropy production, and thermodynamic reservoir entropy are distinct statements. The last requires local detailed balance, heat and work conventions, and a physical clock. None defines the metric light cone or creates proper time.

Finite-regulator statements include their fixed domain and boundary. Physical recovery additionally includes its matching and limiting hypotheses. Existence, uniqueness, and convergence of an invariant law are separate claims. The continuum limit needs uniform estimates, tightness, limiting-generator identification, and control of energy and entropy defects. A real independent test further requires a completed forward map and a parameter vector frozen before the test data are examined. A simulation of the specified equations establishes neither this observational test nor an unconditional physical completion.

8.13. *A state-dependent clock changes stationary sampling.* Changing a clock changes the duration assigned to the same sequence of states. If the clock runs at a state-dependent rate, it also changes the fraction of recorded time spent in each region. The stationary sampling law and entropy-production rate must therefore be transformed together. This operation calibrates a physical rate; by itself it neither breaks detailed balance nor determines a spacetime metric.

Changing the unit of time by a constant rescales rates. A state-dependent clock also changes the fraction of observed time spent in each state. This distinction matters when a stochastic parameter is compared with a laboratory clock. The following finite calculation fixes the convention without domain issues for unbounded diffusion generators.

PROPOSITION 8.11 (Clock change of a finite stationary chain). *Let q_{ij} be the rates of a finite irreducible chain with stationary law π. Assign $a_i > 0$ and set $d\tau = a_{X_t}\,dt$. The chain observed in τ has rates $\widetilde{q}_{ij} = q_{ij}/a_i$, and its stationary law is*

$$\widetilde{\pi}_i = \frac{a_i \pi_i}{\langle a \rangle_\pi}, \qquad \langle a \rangle_\pi = \sum_i a_i \pi_i.$$

If the rates have reciprocal support and all states are even under the chosen reversal, its stationary path entropy rate satisfies

$$\widetilde{\sigma}_{\mathrm{stat}} = \sigma_{\mathrm{stat}} / \langle a \rangle_\pi.$$

Detailed balance is preserved by this clock change.

Proof. While the chain is in state i, multiplication of the exponential holding time by a_i divides its escape rate by a_i. The jump destination probabilities are unchanged. The stationary edge fluxes obey

$$\widetilde{\pi}_i \widetilde{q}_{ij} = \pi_i q_{ij} / \langle a \rangle_\pi.$$

Summing incoming and outgoing fluxes proves stationarity; irreducibility and normalization give uniqueness. Every forward-to-reverse stationary flux ratio is unchanged. Substitution into $\sigma_{\mathrm{stat}} = \sum_{i \neq j} \pi_i q_{ij} \log(\pi_i q_{ij} / \pi_j q_{ji})$ proves the rate formula. Pairwise flux equality is likewise preserved. □

For example, $q_{12} = q_{21} = 1$ and $(a_1, a_2) = (1, 2)$ give $\pi = (1/2, 1/2)$ but $\widetilde{\pi} = (1/3, 2/3)$. Both chains satisfy detailed balance. Identifying their two stationary laws would therefore be incorrect even though their ordered jump paths are the same.

A nonreversible example is the three-state ring with clockwise rate 2 and counterclockwise rate 1. Its stationary law is uniform and $\sigma_{\mathrm{stat}} = \log 2$. Taking $(a_1, a_2, a_3) = (1, 2, 3)$ gives $\widetilde{\pi} = (1/6, 1/3, 1/2)$ and $\widetilde{\sigma}_{\mathrm{stat}} = \frac{1}{2} \log 2$. Direct summation of the six directed stationary flux contributions gives approximately 0.6931471806 and 0.3465735903, respectively. This finite example checks the physical-clock scaling while retaining nonzero path asymmetry; no reservoir heat interpretation is assumed without additional matching.

For a diffusion the formal invariant candidate for L/a is similarly $a\pi/\int a\,d\pi$. To use it as an invariant probability one must also check normalization, conservative realization, boundary conditions and an appropriate generator core or semigroup argument. On an unbounded state space these requirements do not follow from writing the density. If a is not integrable, the displayed probability does not exist.

8.14. *Entropy balances and regulator limits.* Relative-entropy contraction, stationary path asymmetry and reservoir entropy have separate roles. In particular, a driven invariant state may produce entropy at a positive rate even though its density is unchanged. A fixed-bath isothermal relaxation result does not describe all driven turbulent or accreting states. Each physical application requires a heat, work and particle-exchange convention, together with the time-reversed reservoir protocol and the parity of its state variables.

A family of finite chains or diffusions can satisfy the same entropy identity while failing to converge as its regulator is removed. Passing to that limit requires tightness in a stated path topology, identification of the limiting generator, and sufficient control of the entropy and energy terms. Lower semicontinuity may yield an inequality with a defect; it does not establish equality or a regulator-independent mixing rate. These requirements are distinct from the already finite-dimensional nonnegativity argument.

9. **Infinite-Dimensional Extensions**

A history records many times of one process; a fluid configuration contains many spatial degrees of freedom. These are two different reasons for using an infinite-dimensional state space. For a finite history window of a Markov process, the conditional future law is already fixed by the oldest endpoint. A continuum fluid instead requires control of the energy and noise in arbitrarily fine spatial modes. We develop these extensions separately, retaining the process, reference measure, and generator domain needed by each entropy identity. Dimension-independent algebra alone does not supply the missing spatial compactness.

9.1. *Infinite-Dimensional Trajectory and Physical History Space.*

9.1.1. *Why Path Space Is Used.* A Markov diffusion does not need its entire past to predict its future conditional law. Nevertheless, trajectory space is indispensable for several distinct reasons:

(i) stochastic actions and likelihood ratios are path functionals;
(ii) physical time reversal compares path laws;
(iii) entropy production may depend on currents or complete histories;
(iv) genuinely non-Markovian systems can be made Markov by enlarging the state to include memory variables;

(v) a moving-history state provides a natural physical-time realization of path-dependent observables.

They distinguish a path-dependent observable from a process whose future dynamics depends on its whole past.

9.1.2. *Abstract Wiener Space.* Let (E, H, γ) be an abstract Wiener space in the sense initiated by Gross [40]; modern Gaussian-measure background is provided by [11]. Here E is a separable Banach path space, H is its Cameron-Martin Hilbert space, and γ is a centered Gaussian probability measure. For the classical Wiener model one may take

$$E = C_0([0,T];\mathbb{R}^m), \tag{9.1}$$

and

$$H = \left\{h : h(0) = 0,\ h \text{ absolutely continuous},\ \dot{h} \in L^2([0,T];\mathbb{R}^m)\right\}, \tag{9.2}$$

with inner product

$$\langle h, k\rangle_H = \int_0^T \dot{h}(s)\cdot\dot{k}(s)\,\mathrm{d}s. \tag{9.3}$$

The reference measure is γ, not a nonexistent flat symbol $\mathcal{D}\omega$.

9.1.3. *Finite-Window Gibbs Path Measures.* Let

$$\Phi_T : E_T \to (-\infty, +\infty] \tag{9.4}$$

be a measurable dimensionless finite-window path cost, and assume

$$0 < Z_T = \int_{E_T} e^{-\Phi_T(\omega)}\gamma_T(\,\mathrm{d}\omega) < \infty. \tag{9.5}$$

Define

$$\mu_T^{\Omega}(\,\mathrm{d}\omega) = Z_T^{-1} e^{-\Phi_T(\omega)}\gamma_T(\,\mathrm{d}\omega). \tag{9.6}$$

This construction is mathematically meaningful because the exponential weight is taken relative to a genuine probability measure.

The equilibrium path measure is not obtained by minimizing Φ_T over individual trajectories. The correct finite-temperature variational problem is over probability measures.

Theorem 9.1 (Path-space Gibbs variational identity). *Assume, in addition to Equation (9.5), that*

$$\int |\Phi_T| e^{-\Phi_T}\, d\gamma_T < \infty.$$

The integrand is assigned value zero where $\Phi_T = +\infty$. For every probability measure $\nu \ll \gamma_T$ with $D(\nu\|\gamma_T) < \infty$ and $\int |\Phi_T|\, d\nu < \infty$, define

$$\mathscr{J}_T[\nu] = D(\nu\|\gamma_T) + \int \Phi_T\,\mathrm{d}\nu. \tag{9.7}$$

Then

$$\mathscr{J}_T[\nu] - \mathscr{J}_T[\mu_T^\Omega] = D\big(\nu\big\|\mu_T^\Omega\big) \geq 0. \tag{9.8}$$

Thus μ_T^Ω is the unique minimizer among probability measures in the stated finite-term class.

Proof. Let $A_T = \{\Phi_T < +\infty\}$. This set is measurable, and $\int |\Phi_T|\, d\nu < \infty$ implies $\nu(A_T^c) = 0$. On A_T, the Gibbs density is finite and strictly positive. Consequently $\nu \ll \gamma_T|_{A_T} \ll \mu_T^\Omega$, so the logarithmic density ratio is well defined ν-almost everywhere. Moreover,

$$\int |\Phi_T|\, d\mu_T^\Omega = Z_T^{-1} \int_{A_T} |\Phi_T| e^{-\Phi_T}\, d\gamma_T < \infty.$$

The identity $\log(d\mu_T^\Omega/d\gamma_T) = -\Phi_T - \log Z_T$ on A_T therefore has an integrable right-hand side under μ_T^Ω. In particular, the equilibrium law belongs to the same finite-term class as the competitors. All subsequent logarithmic identities are taken on A_T, hence almost everywhere for both laws. From Equation (9.6),

$$\log \frac{\mathrm{d}\mu_T^\Omega}{\mathrm{d}\gamma_T} = -\Phi_T - \log Z_T. \tag{9.9}$$

Therefore

$$\begin{aligned} D\big(\nu\big\|\mu_T^\Omega\big) &= \int \log \frac{\mathrm{d}\nu}{\mathrm{d}\gamma_T}\, \mathrm{d}\nu + \int \Phi_T\, \mathrm{d}\nu + \log Z_T \\ &= \mathscr{J}_T[\nu] + \log Z_T. \end{aligned} \tag{9.10}$$

For $\nu = \mu_T^\Omega$, the left-hand side vanishes, hence

$$\mathscr{J}_T[\mu_T^\Omega] = -\log Z_T. \tag{9.11}$$

Subtracting Equation (9.11) from Equation (9.10) proves Equation (9.8). □

The additional moment assumption ensures that μ_T^Ω belongs to the stated finite-term admissible class. It is automatic for a nonnegative Φ_T, since $xe^{-x} \leq e^{-1}$ for $x \geq 0$. Normalizability alone does not suffice for a cost unbounded below: on $\mathbb{N}$, the reference law $\gamma(n) = 2^{-n}$ and cost $\Phi(n) = -n \log 2 + 2 \log n$ give finite $Z = \sum_{n\geq 1} n^{-2}$, but the Gibbs law has infinite $\int |\Phi|\, d\mu$ and infinite relative entropy with respect to γ. Their formal difference cannot be used as a finite variational objective.

Define the trajectory-space Gibbs free energy by

$$\mathcal{F}_{\Omega,T}[\nu] = k_B T\, \mathscr{J}_T[\nu]. \tag{9.12}$$

Then

$$\mathcal{F}_{\Omega,T}[\nu] - \mathcal{F}_{\Omega,T}[\mu_T^\Omega] = k_B T D\big(\nu\big\|\mu_T^\Omega\big)\,. \tag{9.13}$$

This functional is a trajectory-space Gibbs free energy. It is not automatically identical to the ordinary Helmholtz free energy of a one-time marginal.

9.1.4. *Projective Consistency and Stationarity.* A collection of finite-window measures does not automatically define one stochastic process. For $0 < S < T$, let

$$R_{T,S} : E_T \to E_S \tag{9.14}$$

be the restriction map. A necessary consistency condition is

$$(R_{T,S})_{\#}\mu_T^{\Omega} = \mu_S^{\Omega}. \tag{9.15}$$

If this consistency is established for all compatible windows, an extension theorem may be used to construct a process law on a larger time axis.

For an equilibrium stationary path process, one must additionally prove invariance under the time-shift map θ_s:

$$(\theta_s\omega)(t) = \omega(t+s), \tag{9.16}$$

and

$$(\theta_s)_{\#}\mu_{\mathrm{eq}}^{\Omega} = \mu_{\mathrm{eq}}^{\Omega}. \tag{9.17}$$

The safest construction in the molecular setting is often to start from a stationary microscopic SDE, construct its stationary path law, and then take finite-window restrictions. Projective consistency and time-shift stationarity then follow from the underlying stationary process rather than being guessed from unrelated finite-window Gibbs weights.

9.1.5. *Finite-Window Absolute Continuity versus Infinite-Horizon Singularity.* Finite-window path measures may be mutually absolutely continuous while their infinite-horizon extensions are singular. Consequently, the identity

$$\frac{\mathrm{d}\mathbb{P}}{\mathrm{d}\mathbb{Q}} = Z^{-1}e^{-\Phi} \tag{9.18}$$

should not be asserted on an infinite time axis merely because analogous identities hold for every finite T.

For stationary nonequilibrium processes the path relative entropy often grows linearly with observation time. The natural long-time quantity is then an entropy rate,

$$h(\mathbb{P}\|\mathbb{Q}) = \lim_{T\to\infty} \frac{1}{T} D\big(\mathbb{P}_{[0,T]}\big\|\mathbb{Q}_{[0,T]}\big)\,, \tag{9.19}$$

when the limit exists. The theory therefore distinguishes finite-window Gibbs/Radon-Nikodym formulas from infinite-horizon stationary path measures.

9.1.6. *Cameron-Martin Derivative and the Abstract Symmetric Gibbs Generator.* For a cylinder functional F on E, the Cameron-Martin gradient $D_H F$ is defined by

$$\frac{\mathrm{d}}{\mathrm{d}\varepsilon} F(\omega + \varepsilon h)\Big|_{\varepsilon=0} = \langle D_H F(\omega), h\rangle_H\,. \tag{9.20}$$

For a Gibbs perturbation $\mu_\Phi \propto e^{-\Phi}\gamma$, the formal symmetric Dirichlet form is

$$\mathcal{E}_\Omega(F,G) = \int \langle D_H F, D_H G\rangle_H \, \mathrm{d}\mu_\Phi. \tag{9.21}$$

If this form is closable, its self-adjoint generator is formally

$$L_\Phi F = L_\gamma F - \langle D_H \Phi, D_H F\rangle_H \,, \tag{9.22}$$

on an appropriate cylinder core. Equation Equation (9.22) defines the canonical symmetric Gibbs sampler associated with the weighted Gaussian measure. It does not prove that this sampler is the physical moving-history generator of the original molecular SDE.

9.1.7. *Moving-History Process and Physical Time.* Fix a memory horizon $\tau > 0$ and define

$$Y_t(\theta) = X_{t+\theta}, \qquad -\tau \le \theta \le 0. \tag{9.23}$$

Then

$$Y_t \in E_\tau = C([-\tau, 0]; \mathbb{R}^n). \tag{9.24}$$

The outer variable t is physical time; the coordinate θ labels the location within the retained history. For $-\tau < \theta < 0$, one has the formal shift relation

$$\partial_t Y_t(\theta) = \partial_\theta Y_t(\theta), \tag{9.25}$$

whereas the newest endpoint obeys

$$\mathrm{d}Y_t(0) = b(Y_t(0))\,\mathrm{d}t + \sigma(Y_t(0))\,\mathrm{d}W_t. \tag{9.26}$$

Thus the physical history generator contains a left-shift part and a boundary drift/noise part. Schematically,

$$\mathcal{L}_{\mathrm{hist}} = \mathcal{S}_{\mathrm{shift}} + \mathcal{B}_{\mathrm{bdry}} + \mathcal{Q}_{\mathrm{bdry}}. \tag{9.27}$$

The covariance acts only at the newest endpoint, making the full history dynamics degenerate. Standard uniformly elliptic Bakry-Emery estimates therefore cannot be assumed.

THEOREM 9.2 (Entropy transfer to a finite moving history). *Let X be a time-homogeneous Markov process with continuous paths in a Polish state space and invariant probability π. Fix $\tau > 0$, and let $K_\tau(x,\cdot)$ be the law of its path segment of duration τ, including the initial point x, parametrized on $[-\tau, 0]$. Suppose that future evolution from time zero, conditional on the initial history, uses the same transition law and depends only on its endpoint X_0. Write ν_0 for that endpoint law and $\mu_{\mathrm{hist}} = \pi K_\tau$. Then*

$$D\Big(\nu_t^{\mathrm{hist}}\Big\|\mu_{\mathrm{hist}}\Big) = D(\nu_0 P_{t-\tau}\|\pi)\,, \qquad t \ge \tau,$$

including the value $+\infty$. If the endpoint process satisfies $D(\nu_0 P_s\|\pi) \le Ce^{-\lambda s}\mathscr{H}(\nu_0)$ for $s \ge 0$, with $C, \lambda > 0$ and finite $\mathscr{H}(\nu_0)$, then

$$D\Big(\nu_t^{\mathrm{hist}}\Big\|\mu_{\mathrm{hist}}\Big) \le Ce^{-\lambda(t-\tau)}\mathscr{H}(\nu_0), \qquad t \ge \tau. \tag{9.28}$$

Proof. For $t \geq \tau$, the Markov property gives $\nu_t^{\mathrm{hist}} = (\nu_0 P_{t-\tau})K_\tau$. Stationary initialization gives the segment law πK_τ; time shifts preserve it. Let $\alpha = \nu_0 P_{t-\tau}$. Applying data processing to K_τ gives

$$D(\alpha K_\tau \| \pi K_\tau) \leq D(\alpha \| \pi)\,.$$

The initial-point map $e_{-\tau}(\omega) = \omega(-\tau)$ is measurable and satisfies $(e_{-\tau})_\#(\alpha K_\tau) = \alpha$ and $(e_{-\tau})_\#(\pi K_\tau) = \pi$. Applying data processing to this map gives the reverse inequality, hence equality. Substitution of the endpoint estimate proves Equation (9.28). For a finite-entropy density $f = d\alpha/d\pi$, the same argument can be read directly from $d(\alpha K_\tau)/d(\pi K_\tau) = f \circ e_{-\tau}$. □

Remark 9.3. Theorem 9.2 transfers an endpoint theorem to the actual finite segment process without assuming a new history-space entropy chain rule or positive curvature. For the quadratic kinetic model, Theorem 7.6 supplies the explicit factor $r_{t-\tau}^2$. Before $t = \tau$, the segment still contains the prescribed past, which can be singular with respect to stationary history; no such bound is asserted. Dynamics with delayed feedback depending on the whole past, growing observation windows, and infinite histories require different arguments. A physical-history Gibbs weight not equal to πK_τ also requires a separate matching proof.

9.2. *Two-Dimensional Stochastic Navier-Stokes as an Infinite-Dimensional Stress Test.* The purpose of this section is diagnostic rather than rhetorical. The two-dimensional stochastic Navier-Stokes equation is sufficiently structured to display energy cancellation and invariant-measure phenomena, but sufficiently infinite dimensional that finite-dimensional ellipticity, phase volume, and uniform nondegenerate-noise intuition can fail. Rigorous ergodicity and hypoellipticity results for stochastic Navier-Stokes equations require model-specific forcing and controllability assumptions, as illustrated by [42] and [43].

9.2.1. *Functional Setting.* Let

$$\mathbb{T}^2 = (\mathbb{R}/2\pi\mathbb{Z})^2. \tag{9.29}$$

Define the divergence-free mean-zero Hilbert space

$$\mathcal{H} = L^2_{\sigma,0}(\mathbb{T}^2;\mathbb{R}^2) \tag{9.30}$$

and the energy space

$$V = H^1_{\sigma,0}(\mathbb{T}^2;\mathbb{R}^2). \tag{9.31}$$

The standard Gelfand triple is

$$V \subset \mathcal{H} \equiv \mathcal{H}^* \subset V^*. \tag{9.32}$$

Let $\mathbb{P}_\sigma$ be the Leray projection and define the positive Stokes operator

$$A_{\mathrm{St}} = -\mathbb{P}_\sigma \Delta. \tag{9.33}$$

The convective bilinear form is

$$B(u,v) = \mathbb{P}_\sigma[(u \cdot \nabla)v]. \tag{9.34}$$

At the natural energy regularity,

$$B : V \times V \to V^*. \tag{9.35}$$

It is generally incorrect to declare $B : V \to \mathcal{H}$ at this level without additional regularity.

9.2.2. *Fourier Form and Leray Projection.* For

$$u(x) = \sum_{k \in \mathbb{Z}^2 \setminus \{0\}} \widehat{u}_k e^{ik\cdot x}, \qquad k \cdot \widehat{u}_k = 0, \tag{9.36}$$

define

$$P_k = I - \frac{k \otimes k}{|k|^2}. \tag{9.37}$$

Then the nonlinear Fourier coefficient has the form

$$\widehat{B(u,u)}_k = iP_k \sum_{\ell+m=k} (m \cdot \widehat{u}_\ell)\widehat{u}_m. \tag{9.38}$$

The projector P_k must be retained; omitting it generally destroys the divergence-free constraint.

9.2.3. *Stochastic Equation and Admissible Noise.* The $\mathcal{H}$-valued SPDE is

$$\mathrm{d}u_t + [\nu A_{\mathrm{St}} u_t + B(u_t, u_t)]\,\mathrm{d}t = Q^{1/2}\,\mathrm{d}W_t. \tag{9.39}$$

For the main $\mathcal{H}$-valued theory assume at least

$$\operatorname{Tr} Q < \infty. \tag{9.40}$$

A trace-class covariance cannot satisfy

$$Q \geq cI \qquad (c > 0) \tag{9.41}$$

on an infinite-dimensional $\mathcal{H}$, because for any orthonormal basis (e_n),

$$\operatorname{Tr} Q = \sum_n \langle Qe_n, e_n\rangle \geq \sum_n c = \infty. \tag{9.42}$$

Similarly, space-time white noise corresponds formally to $Q = I$ and is not trace class on $\mathcal{H}$. It therefore requires a different distributional state space and is not silently included in Equation (9.40).

9.2.4. *Energy Cancellation.* For divergence-free u, define

$$b(u, v, w) = \int_{\mathbb{T}^2} (u \cdot \nabla)v \cdot w\,\mathrm{d}x. \tag{9.43}$$

Integration by parts gives

$$\begin{aligned} b(u, v, w) + b(u, w, v) &= \int u \cdot \nabla(v \cdot w)\,\mathrm{d}x \\ &= -\int (\nabla \cdot u)(v \cdot w)\,\mathrm{d}x = 0. \end{aligned} \tag{9.44}$$

Setting $v = w = u$ yields

$$\langle B(u, u), u\rangle = 0. \tag{9.45}$$

9.2.5. *Energy Estimate.* Applying Itô's formula to $\|u_t\|_{\mathcal{H}}^2$ gives

$$\begin{aligned} \mathrm{d}\|u_t\|_{\mathcal{H}}^2 = &-2\nu \langle A_{\mathrm{St}} u_t, u_t\rangle \,\mathrm{d}t - 2\langle B(u_t,u_t), u_t\rangle \,\mathrm{d}t \\ &+ \operatorname{Tr} Q \,\mathrm{d}t + 2\left\langle u_t, Q^{1/2}\,\mathrm{d}W_t\right\rangle. \end{aligned} \tag{9.46}$$

Using Equation (9.45) and

$$\langle A_{\mathrm{St}} u, u\rangle = \left\|A_{\mathrm{St}}^{1/2} u\right\|_{\mathcal{H}}^2, \tag{9.47}$$

we obtain

$$\mathrm{d}\|u_t\|_{\mathcal{H}}^2 + 2\nu \left\|A_{\mathrm{St}}^{1/2} u_t\right\|_{\mathcal{H}}^2 \,\mathrm{d}t = \operatorname{Tr} Q \,\mathrm{d}t + 2\left\langle u_t, Q^{1/2}\,\mathrm{d}W_t\right\rangle. \tag{9.48}$$

Taking expectation yields

$$\frac{\mathrm{d}}{\mathrm{d}t}\mathbb{E}\|u_t\|_{\mathcal{H}}^2 + 2\nu\mathbb{E}\left\|A_{\mathrm{St}}^{1/2} u_t\right\|_{\mathcal{H}}^2 = \operatorname{Tr} Q. \tag{9.49}$$

If $\lambda_1 > 0$ is the smallest nonzero Stokes eigenvalue, then

$$\left\|A_{\mathrm{St}}^{1/2} u\right\|^2 \geq \lambda_1 \|u\|_{\mathcal{H}}^2, \tag{9.50}$$

and Gronwall gives

$$\mathbb{E}\|u_t\|_{\mathcal{H}}^2 \leq e^{-2\nu\lambda_1 t}\mathbb{E}\|u_0\|_{\mathcal{H}}^2 + \frac{\operatorname{Tr} Q}{2\nu\lambda_1}\left(1 - e^{-2\nu\lambda_1 t}\right). \tag{9.51}$$

9.2.6. *Enstrophy Estimate.* The correct enstrophy estimate requires the stronger noise condition

$$\operatorname{Tr}(A_{\mathrm{St}} Q) < \infty. \tag{9.52}$$

For sufficiently regular two-dimensional solutions one has the enstrophy cancellation

$$\langle B(u,u), A_{\mathrm{St}} u\rangle = 0. \tag{9.53}$$

Applying Itô's formula to $\left\|A_{\mathrm{St}}^{1/2} u_t\right\|^2$ gives

$$\begin{aligned} &\mathrm{d}\left\|A_{\mathrm{St}}^{1/2} u_t\right\|^2 + 2\nu \|A_{\mathrm{St}} u_t\|^2 \,\mathrm{d}t \\ &\qquad = \operatorname{Tr}(A_{\mathrm{St}} Q)\,\mathrm{d}t + 2\left\langle A_{\mathrm{St}}^{1/2} u_t, A_{\mathrm{St}}^{1/2} Q^{1/2}\,\mathrm{d}W_t\right\rangle. \end{aligned} \tag{9.54}$$

Therefore

$$\frac{\mathrm{d}}{\mathrm{d}t}\mathbb{E}\left\|A_{\mathrm{St}}^{1/2} u_t\right\|^2 + 2\nu\mathbb{E}\|A_{\mathrm{St}} u_t\|^2 = \operatorname{Tr}(A_{\mathrm{St}} Q). \tag{9.55}$$

Using

$$\|A_{\mathrm{St}} u\|^2 \geq \lambda_1 \left\|A_{\mathrm{St}}^{1/2} u\right\|^2, \tag{9.56}$$

we obtain

$$\begin{aligned} \mathbb{E}\left\|A_{\mathrm{St}}^{1/2} u_t\right\|^2 \leq &\, e^{-2\nu\lambda_1 t}\mathbb{E}\left\|A_{\mathrm{St}}^{1/2} u_0\right\|^2 \\ &+ \frac{\operatorname{Tr}(A_{\mathrm{St}} Q)}{2\nu\lambda_1}\left(1 - e^{-2\nu\lambda_1 t}\right). \end{aligned} \tag{9.57}$$

9.2.7. *Generator and Carre du Champ.* For a smooth cylinder function F, the formal Kolmogorov generator is

$$L_{NS}F(u) = -\langle \nu A_{\mathrm{St}} u + B(u,u), DF(u)\rangle + \frac{1}{2}\operatorname{Tr}[QD^2F(u)]. \tag{9.58}$$

Therefore

$$\Gamma_{NS}(F) = \frac{1}{2}\left\|Q^{1/2}DF\right\|_{\mathcal{H}}^2. \tag{9.59}$$

There is no additional independent viscosity term in the carre du champ; viscosity appears in the first-order drift of the Kolmogorov generator, whereas Γ_{NS} is determined by the second-order stochastic part.

9.2.8. *Unconditional Relative-Entropy Contraction.* Assume the stochastic Navier-Stokes Markov semigroup admits an invariant probability measure μ_{NS}. Then Theorem 7.1 immediately yields

$$D\left(\nu P_t^{NS}\middle\|\mu_{NS}\right) \le D(\nu\|\mu_{NS}). \tag{9.60}$$

This is the robust infinite-dimensional result. It does not require a Galerkin identification of the nonlinear full law with the projection of a truncated law.

9.2.9. *Conditional Differential NS Identity.* If a closed form and generator-domain theory is available such that the logarithmic chain rule is justified, then for $\nu_t = f_t\mu_{NS}$,

$$\frac{\mathrm{d}}{\mathrm{d}t}D(\nu_t\|\mu_{NS}) = -\frac{1}{2}\int f_t\left\|Q^{1/2}D\log f_t\right\|_{\mathcal{H}}^2 \mathrm{d}\mu_{NS}. \tag{9.61}$$

Equation Equation (9.61) is explicitly conditional on the infinite-dimensional closability, domain, and chain-rule hypotheses. It is stronger than Equation (9.60) and should not be presented as an assumption-free consequence of Markovity.

9.2.10. *OU Reference Covariance.* For the corresponding linear stochastic Stokes equation

$$\mathrm{d}X_t = -\nu A_{\mathrm{St}}X_t\,\mathrm{d}t + Q^{1/2}\,\mathrm{d}W_t, \tag{9.62}$$

a stationary covariance C satisfies the Lyapunov equation

$$\nu A_{\mathrm{St}}C + \nu C A_{\mathrm{St}} = Q. \tag{9.63}$$

If A_{St}, Q, and C are diagonal in the same orthonormal basis,

$$A_{\mathrm{St}}e_k = \lambda_k e_k, \qquad Qe_k = q_k e_k, \qquad Ce_k = c_k e_k, \tag{9.64}$$

then

$$c_k = \frac{q_k}{2\nu\lambda_k}. \tag{9.65}$$

The Gaussian covariance therefore depends on the forcing spectrum.

9.2.11. *Modal Gaussian LSI in a Compatible Diagonal Truncation.* For a single forced mode

$$\mathrm{d}X_k = -\nu\lambda_k X_k\,\mathrm{d}t + \sqrt{q_k}\,\mathrm{d}W_k, \qquad q_k > 0, \tag{9.66}$$

the invariant variance is $c_k = q_k/(2\nu\lambda_k)$. The one-dimensional Gaussian LSI reads

$$\mathrm{Ent}_{\mu_k}(g^2) \le 2c_k \int |g'|^2\,\mathrm{d}\mu_k. \tag{9.67}$$

Since

$$\Gamma_k(g) = \frac{q_k}{2}|g'|^2, \tag{9.68}$$

we have

$$|g'|^2 = \frac{2}{q_k}\Gamma_k(g). \tag{9.69}$$

Substituting c_k gives

$$\mathrm{Ent}_{\mu_k}(g^2) \le \frac{2}{\nu\lambda_k}\int \Gamma_k(g)\,\mathrm{d}\mu_k. \tag{9.70}$$

Thus the modal curvature/LSI rate in this convention is

$$\rho_k = \nu\lambda_k. \tag{9.71}$$

A uniform rate $\nu\lambda_1$ is justified only in compatible finite-dimensional structures in which every retained stochastic direction satisfies the required covariance and nondegeneracy assumptions.

9.2.12. *Conservative transport: weighted skew-symmetry and operator domains.* Consider a finite-dimensional vector field $N(x)$ and the first-order generator

$$L_{\mathrm{conv}}F = N\cdot\nabla F. \tag{9.72}$$

Let

$$\rho(x) = Z^{-1}e^{-\beta E(x)}. \tag{9.73}$$

For smooth compactly supported or periodic F, G,

$$\begin{aligned}\int G(N\cdot\nabla F)\rho\,\mathrm{d}x = &-\int F(N\cdot\nabla G)\rho\,\mathrm{d}x\\ &-\int FG\nabla\cdot(\rho N)\,\mathrm{d}x.\end{aligned} \tag{9.74}$$

Hence skew-symmetry on this test domain is equivalent to

$$\nabla\cdot(\rho N) = 0. \tag{9.75}$$

Using $\nabla\rho = -\beta\rho\nabla E$,

$$\nabla\cdot(\rho N) = \rho\left[\nabla\cdot N - \beta N\cdot\nabla E\right]. \tag{9.76}$$

Therefore the two structural conditions

$$\nabla\cdot N = 0, \tag{9.77}$$

$$N\cdot\nabla E = 0 \tag{9.78}$$

are sufficient for the weighted-divergence identity. Energy conservation alone does not ensure that identity; phase-space volume preservation is an additional sufficient condition. The identity above establishes skew-symmetry on the chosen test functions. A skew-adjoint operator additionally requires a dense operator domain and equality with the negative of its Hilbert-space adjoint, including equality of domains. The following realization makes that additional requirement explicit.

PROPOSITION 9.4 (A skew-adjoint realization of conservative transport). *Let N be a C^1 vector field on $\mathbb{R}^d$ with a complete C^1 flow Φ_t, defined for every $t \in \mathbb{R}$. Suppose $\rho > 0$ is C^1, $\int \rho\, dx = 1$, and* $\operatorname{div}(\rho N) = 0$. *Then*

$$U_t f = f \circ \Phi_t$$

is a strongly continuous unitary group on the complex Hilbert space $L^2(\rho\, dx)$. Its generator A is skew-adjoint and satisfies $Af = N \cdot \nabla f$ for $f \in C_c^\infty(\mathbb{R}^d)$. The same conclusion holds on a torus, with smooth periodic test functions. This identifies a skew-adjoint realization; identifying it with the closure of a particular smaller test domain additionally requires that domain to be a core.

Proof. Write $J_t(x) = \det D\Phi_t(x) > 0$. The Jacobian equation and the chain rule imply

$$\frac{d}{dt}\{\rho(\Phi_t(x))J_t(x)\} = \operatorname{div}(\rho N)(\Phi_t(x))J_t(x) = 0.$$

Thus $\rho(\Phi_t(x))J_t(x) = \rho(x)$. Changing variables gives $\|U_t f\|_{L^2(\rho)} = \|f\|_{L^2(\rho)}$; completeness gives $U_t^{-1} = U_{-t}$ and the group law. For continuous compactly supported f, pointwise convergence $f(\Phi_t(x)) \to f(x)$ and the integrable bound $4\|f\|_\infty^2 \rho(x)$ give strong continuity at zero. Density and the isometry property extend it to every L^2 function.

The generator has the domain

$$D(A) = \left\{ f \in L^2(\rho) : \lim_{t\to 0} \frac{U_t f - f}{t} \text{ exists in } L^2(\rho) \right\}.$$

Stone's theorem gives $A^* = -A$ on this domain [96]. For a smooth compactly supported f, the flow identity gives

$$\frac{U_t f - f}{t} = \frac{1}{t}\int_0^t U_s(N \cdot \nabla f)\, ds \longrightarrow N \cdot \nabla f \quad \text{in } L^2(\rho).$$

The last convergence follows from strong continuity and $N \cdot \nabla f \in L^2(\rho)$. This proves that the group generator realizes the stated differential expression. On a torus, the same argument applies with compactness replacing compact support. □

Completeness is verifiable in a useful finite thermal branch. If E has compact sublevel sets, N is C^1, and $N \cdot \nabla E = 0$, every trajectory stays in the compact set $\{E \le E(x_0)\}$. The local ODE continuation theorem therefore extends the trajectory in both time directions. Together with $\operatorname{div} N = 0$, this gives the preceding realization for the normalizable Gibbs density. Compact sublevels alone do not ensure normalizability; the separate condition $Z < \infty$ remains.

The distinction cannot be removed by integration by parts. On $L^2(0,1)$, the operator $A_0 f = f'$ with domain $C_c^\infty(0,1)$ is skew-symmetric and satisfies the weighted-divergence identity with $N = \rho = 1$. Nevertheless, its closure has domain $H_0^1(0,1)$, whereas its adjoint acts as $-f'$ on the larger domain $H^1(0,1)$. It is therefore not skew-adjoint. The periodic realization instead uses $\{f \in H^1(0,1) : f(0) = f(1)\}$ and is skew-adjoint. Boundary conditions and operator domains are consequently part of the transport model, even when the formal differential expression has already been fixed.

9.2.13. *Invariant-measure equivalence and functional inequalities.* For the mean-zero, divergence-free equation on $\mathbb{T}^2$, Coe, Hairer and Tolomeo [19, Theorem 1.1] prove equivalence of the unique invariant measure with the corresponding OU invariant measure for the specific forcing family $\sqrt{2}|\nabla|^{-\alpha_{\mathrm{ref}}}\xi_0$, where $\alpha_{\mathrm{ref}} > 0$ and ξ_0 is divergence-free, mean-zero space–time white noise. Here α_{ref} denotes the spatial smoothing exponent in that reference, whose viscosity is normalized to one. The result is not asserted for an arbitrary covariance Q or arbitrary boundary conditions. Mutual absolute continuity does not imply a bounded Radon–Nikodym ratio and therefore does not by itself give a Holley–Stroock [47] transfer of LSI constants.

A separate recent result for a fluctuation-dissipation-completed, spectrally truncated Navier-Stokes Fokker-Planck model on $\mathbb{T}^3$ [103] establishes a self-adjoint OU part plus an antisymmetric convective part and proves an LSI with the same optimal constant as the OU model. That theorem relies on energy conservation together with finite-dimensional phase-volume preservation. It is not used as a proof of a general infinite-dimensional 2D colored-noise LSI.

The positive rate $\nu\lambda_1$ also requires fixing or removing the zero Fourier mode. Viscous drift and the stated thermal noise both vanish in that mode, and the spatial integral of the convective term is zero on the torus. Consequently the mean velocity is conserved. If a stationary law assigns a nonzero variance to that mean, a nonconstant square-integrable function of it has zero Dirichlet energy but positive variance; a positive Poincaré gap on the whole state space is then impossible. The finite decay statements here concern a fixed-mean sector, with strictly positive retained Stokes eigenvalues.

9.2.14. *Nonlinear Galerkin approximation and entropy limits.* Let u_t solve the full nonlinear equation and let $u_t^{(N)}$ solve the N-mode truncated equation. In general,

$$u_t^{(N)} \neq P_N u_t, \tag{9.79}$$

because nonlinear evolution and projection do not commute. Consequently,

$$\mathrm{Law}(u_t^{(N)}) \neq (P_N)_{\#}\,\mathrm{Law}(u_t) \tag{9.80}$$

in general. Thus one cannot identify truncated relative entropies with projected full relative entropies without an independent theorem.

Moreover, an LSI has the direction

$$H_N \le \frac{1}{2\rho} I_N, \tag{9.81}$$

which is equivalent to

$$I_N \ge 2\rho H_N, \tag{9.82}$$

not an upper bound on I_N. Finally, weak convergence of probability laws does not imply convergence of Fisher information. A legitimate infinite-dimensional passage would require substantially stronger tools such as Mosco convergence of Dirichlet forms, strong density convergence, uniform integrability, or an appropriate recovery-sequence argument. These complications are unnecessary for the unconditional Markov contraction Equation (9.60).

10. **Exact Models and Testable Diagnostics**

The preceding results become physically testable when probability laws are connected to measured quantities. In a harmonic trap, the position variance determines both the excess free energy and its relaxation rate. On a driven ring, a time-independent density can coexist with a sustained current and heat production. The examples below use these observables to separate relaxation from maintained dissipation and to compare exact formulas with numerical calculations. Each comparison retains its stated temperature, coefficients, preparation, and observation interval.

10.1. *Exact Ornstein-Uhlenbeck Benchmark.* A linear restoring force and Gaussian thermal fluctuations give a model in which the evolving mean and covariance can be calculated exactly. The mean tracks displacement of the cloud; the covariance tracks its width and correlations. Their contributions to relative entropy can therefore be separated, making this example a direct check of the free-energy normalization and relaxation coefficients.

10.1.1. *Exact Solution and Invariant Measure.* Consider

$$\mathrm{d}X_t = -\gamma X_t \,\mathrm{d}t + \sqrt{2\gamma}\,\mathrm{d}W_t, \qquad \gamma > 0. \tag{10.1}$$

Multiplying by $e^{\gamma t}$ and applying Itô's product rule gives

$$\mathrm{d}(e^{\gamma t} X_t) = \sqrt{2\gamma} e^{\gamma t}\,\mathrm{d}W_t. \tag{10.2}$$

Integrating from 0 to t,

$$X_t = e^{-\gamma t} X_0 + \sqrt{2\gamma} \int_0^t e^{-\gamma(t-s)}\,\mathrm{d}W_s. \tag{10.3}$$

The stochastic integral is centered Gaussian with variance

$$\begin{aligned} 2\gamma \int_0^t e^{-2\gamma(t-s)}\,\mathrm{d}s &= 2\gamma \int_0^t e^{-2\gamma r}\,\mathrm{d}r \\ &= 1 - e^{-2\gamma t}. \end{aligned} \tag{10.4}$$

Therefore

$$X_t \mid X_0 = x \sim N\left(e^{-\gamma t}x, 1 - e^{-2\gamma t}\right). \tag{10.5}$$

The invariant measure is

$$\mu = N(0,1). \tag{10.6}$$

10.1.2. *Gaussian Initial Data.* Assume

$$\nu_0 = N(m_0, v_0), \qquad v_0 > 0. \tag{10.7}$$

Then Equation (10.3) implies

$$m_t = m_0 e^{-\gamma t}, \tag{10.8}$$

$$v_t = 1 + (v_0 - 1)e^{-2\gamma t}. \tag{10.9}$$

The relative entropy of $N(m_t, v_t)$ with respect to $N(0,1)$ is

$$H(t) = \frac{1}{2}\left[v_t + m_t^2 - 1 - \log v_t\right]. \tag{10.10}$$

Since

$$\dot{m}_t = -\gamma m_t, \tag{10.11}$$

$$\dot{v}_t = -2\gamma(v_t - 1), \tag{10.12}$$

we obtain

$$\begin{aligned}\dot{H}(t) &= \frac{1}{2}\left[\dot{v}_t + 2m_t\dot{m}_t - \frac{\dot{v}_t}{v_t}\right] \\ &= -\gamma m_t^2 - \gamma(v_t - 1)\left(1 - \frac{1}{v_t}\right) \\ &= -\gamma\left[m_t^2 + \frac{(v_t-1)^2}{v_t}\right].\end{aligned} \tag{10.13}$$

Thus the exact relative Fisher information is

$$\mathcal{I}_\mu(\nu_t) = \gamma\left[m_t^2 + \frac{(v_t-1)^2}{v_t}\right], \tag{10.14}$$

and

$$\dot{H}(t) = -\mathcal{I}_\mu(\nu_t). \tag{10.15}$$

10.1.3. *Direct Fisher-Information Verification.* The density ratio is

$$\log\frac{\mathrm{d}\nu}{\mathrm{d}\mu}(x) = -\frac{1}{2}\log v - \frac{(x-m)^2}{2v} + \frac{x^2}{2}. \tag{10.16}$$

Differentiating,

$$\partial_x \log\frac{\mathrm{d}\nu}{\mathrm{d}\mu} = x\left(1 - \frac{1}{v}\right) + \frac{m}{v}. \tag{10.17}$$

If $X \sim N(m, v)$, then a direct expansion gives

$$\mathbb{E}\left[X\left(1-\frac{1}{v}\right)+\frac{m}{v}\right]^2 = m^2 + \frac{(v-1)^2}{v}. \tag{10.18}$$

The generator of Equation (10.1) is

$$L\varphi = \gamma(\varphi'' - x\varphi'), \tag{10.19}$$

so

$$\Gamma_L(\varphi) = \gamma(\varphi')^2. \tag{10.20}$$

Equations Equations (10.17), (10.18) and (10.20) therefore reproduce Equation (10.14) exactly.

10.1.4. *Bakry-Emery Constant of the Normalized OU Process.* For completeness, compute

$$\Gamma_{2,L}(f) = \frac{1}{2}L\Gamma_L(f) - \Gamma_L(f, Lf). \tag{10.21}$$

Since

$$\Gamma_L(f) = \gamma(f')^2, \tag{10.22}$$

we obtain

$$\frac{1}{2}L\Gamma_L(f) = \gamma^2\left[(f'')^2 + f'f''' - xf'f''\right], \tag{10.23}$$

$$\Gamma_L(f, Lf) = \gamma^2\left[f'f''' - (f')^2 - xf'f''\right]. \tag{10.24}$$

Subtracting gives

$$\Gamma_{2,L}(f) = \gamma^2\left[(f'')^2 + (f')^2\right] \geq \gamma\Gamma_L(f). \tag{10.25}$$

Thus the Bakry-Emery curvature constant in this normalization is $\rho = \gamma$.

10.1.5. *Finite Entropy Does Not Imply a Bounded Density Ratio.* Let

$$\mu = N(0,1), \qquad \nu = N(0, v), \qquad v > 1. \tag{10.26}$$

Then

$$\frac{\mathrm{d}\nu}{\mathrm{d}\mu}(x) = v^{-1/2}\exp\left[\frac{x^2}{2}\left(1-\frac{1}{v}\right)\right]. \tag{10.27}$$

Because $1 - 1/v > 0$,

$$\frac{\mathrm{d}\nu}{\mathrm{d}\mu}(x) \longrightarrow +\infty \qquad \text{as } |x| \to \infty. \tag{10.28}$$

Nevertheless,

$$D(\nu\|\mu) = \frac{1}{2}(v - 1 - \log v) < \infty. \tag{10.29}$$

Therefore finite relative entropy does not imply an essentially bounded relative density, Gaussian decay of that relative density, or ultracontractivity.

10.2. *Experimental and Exactly Solvable Tests.* Changing the stiffness of an optical trap changes the energy assigned to the same particle position. The switch performs work; the subsequent

relaxation at fixed stiffness exchanges heat with the bath. Distinguishing these stages is necessary before interpreting a change in free energy as dissipation. We use the measured variance as the link between the stochastic dynamics and the heat balance.

This section collects checks that can be evaluated without appealing to the full abstract theory. When the formulas are tested by simulation, standard Monte Carlo error control and sampling diagnostics remain necessary [78]; numerical agreement is evidence for a model prediction only after calibration, discretization bias, and estimator variance have been separately controlled.

10.2.1. *Optical-Trap Quench.* Consider a colloidal particle in a one-dimensional harmonic trap. After a rapid change of trap stiffness to κ_2, the post-quench dynamics is

$$\mathrm{d}X_t = -\frac{\kappa_2}{\gamma} X_t \,\mathrm{d}t + \sqrt{\frac{2k_B T}{\gamma}}\,\mathrm{d}W_t, \qquad t > 0. \tag{10.30}$$

Here $\gamma = 6\pi\eta a$ is the Stokes friction coefficient for a spherical particle of radius a in a fluid of viscosity η.

Assume the particle was equilibrated before the switch at stiffness κ_1. Then

$$y_1 = \mathbb{E}[X_0^2] = \frac{k_B T}{\kappa_1}, \tag{10.31}$$

and the new equilibrium variance is

$$y_2 = \frac{k_B T}{\kappa_2}. \tag{10.32}$$

Let

$$y(t) = \mathbb{E}[X_t^2]. \tag{10.33}$$

Itô's formula gives

$$\mathrm{d}(X_t^2) = 2X_t \,\mathrm{d}X_t + (\,\mathrm{d}X_t)^2. \tag{10.34}$$

Substituting Equation (10.30),

$$\mathrm{d}(X_t^2) = -\frac{2\kappa_2}{\gamma} X_t^2 \,\mathrm{d}t + 2\sqrt{\frac{2k_B T}{\gamma}} X_t \,\mathrm{d}W_t + \frac{2k_B T}{\gamma}\,\mathrm{d}t. \tag{10.35}$$

Taking expectations,

$$\dot{y} = -\frac{2\kappa_2}{\gamma}(y - y_2). \tag{10.36}$$

Hence

$$y(t) = y_2 + (y_1 - y_2)e^{-2\kappa_2 t/\gamma}. \tag{10.37}$$

10.2.2. *Trap Relative Entropy and Entropy Production.* At every time the state is centered Gaussian. Therefore

$$D(N(0,y)\|N(0,y_2)) = \frac{1}{2}\left[\frac{y}{y_2} - 1 - \log\frac{y}{y_2}\right]. \tag{10.38}$$

Set

$$r(t) = \frac{y(t)}{y_2}. \tag{10.39}$$

Then

$$H(t) = \frac{1}{2}[r(t) - 1 - \log r(t)]. \tag{10.40}$$

From Equation (10.36),

$$\dot{r} = -\frac{2\kappa_2}{\gamma}(r-1). \tag{10.41}$$

Therefore

$$\begin{aligned} \dot{H} &= \frac{1}{2}\left(1 - \frac{1}{r}\right)\dot{r} \\ &= -\frac{\kappa_2}{\gamma}\frac{(r-1)^2}{r}. \end{aligned} \tag{10.42}$$

The autonomous post-quench total entropy-production rate is

$$\dot{S}_{\mathrm{tot}}(t) = k_B \frac{\kappa_2}{\gamma}\frac{(r(t)-1)^2}{r(t)}. \tag{10.43}$$

Equivalently,

$$\dot{S}_{\mathrm{tot}}(t) = \frac{\kappa_2^2}{\gamma T} y(t)\left[1 - \frac{y_2}{y(t)}\right]^2. \tag{10.44}$$

10.2.3. *Numerical Prediction.* Take

$$a = 1 \times 10^{-6}\ \mathrm{m}, \tag{10.45}$$

$$\eta = 1 \times 10^{-3}\ \mathrm{Pa\,s}, \tag{10.46}$$

$$T = 300\ \mathrm{K}, \tag{10.47}$$

$$\kappa_1 = 1 \times 10^{-6}\ \mathrm{N\,m^{-1}}, \tag{10.48}$$

$$\kappa_2 = 2 \times 10^{-6}\ \mathrm{N\,m^{-1}}. \tag{10.49}$$

Then

$$\begin{aligned} \gamma &= 6\pi\eta a \\ &= 1.8849556 \times 10^{-8}\ \mathrm{kg\,s^{-1}}. \end{aligned} \tag{10.50}$$

Using the exact SI value of k_B,

$$k_B T = 4.141947 \times 10^{-21}\ \mathrm{J}. \tag{10.51}$$

Hence

$$y_1 = 4.141947 \times 10^{-15}\ \mathrm{m^2}, \tag{10.52}$$

$$y_2 = 2.0709735 \times 10^{-15}\ \mathrm{m^2}. \tag{10.53}$$

Thus $r(0) = 2$, so

$$\begin{aligned} -\dot{H}(0) &= \frac{\kappa_2}{2\gamma} \\ &= 53.0516\ \mathrm{s^{-1}}. \end{aligned} \tag{10.54}$$

Therefore

$$\dot{S}_{\mathrm{tot}}(0) = 53.0516\, k_B\, \mathrm{s}^{-1} = 7.32457 \times 10^{-22}\ \mathrm{J\,K^{-1}s^{-1}}. \tag{10.55}$$

The position-correlation time and variance-relaxation time are respectively

$$\tau_x = \frac{\gamma}{\kappa_2} = 9.4248\ \mathrm{ms}, \tag{10.56}$$

$$\tau_y = \frac{\gamma}{2\kappa_2} = 4.7124\ \mathrm{ms}. \tag{10.57}$$

10.2.4. *Work Performed during the Quench.* The formulas above describe the relaxation for $t > 0$ after κ_2 has become fixed. The rapid parameter switch itself performs work. For a finite-time protocol $\kappa(t)$ with potential $U(x,t) = \kappa(t)x^2/2$, the average work rate is

$$\dot{W}_t = \frac{1}{2}\dot{\kappa}(t)\mathbb{E}[X_t^2]. \tag{10.58}$$

The complete driven thermodynamics therefore obeys Equation (6.83); the post-quench formula Equation (10.43) is the autonomous part of that protocol.

10.2.5. *Sampling Uncertainty.* For N independent Gaussian samples from $N(0,y)$, the unbiased sample variance $\widehat{y}$ satisfies

$$\frac{(N-1)\widehat{y}}{y} \sim \chi^2_{N-1}. \tag{10.59}$$

Therefore

$$\mathrm{Var}(\widehat{y}) = \frac{2y^2}{N-1}, \tag{10.60}$$

and the relative standard error is

$$\frac{\mathrm{SD}(\widehat{y})}{y} = \sqrt{\frac{2}{N-1}}. \tag{10.61}$$

For $N = 10^5$,

$$\frac{\mathrm{SD}(\widehat{y})}{y} \approx 0.004472 = 0.4472\%. \tag{10.62}$$

Near equilibrium the first derivative of the entropy-production estimator with respect to $y - y_2$ vanishes, so a first-order delta method becomes degenerate. A second-order delta method, parametric bootstrap, or direct likelihood treatment is preferable.

10.2.6. *Periodically Perturbed Driven Ring.* Consider

$$\mathrm{d}X_t = [b + \varepsilon_r \sin(kX_t)]\,\mathrm{d}t + \sqrt{2D}\,\mathrm{d}W_t \pmod{L}. \tag{10.63}$$

For the sinusoidal perturbation to be single-valued on the ring of circumference L, we assume throughout this example that

$$k = \frac{2\pi n}{L} \quad \text{for some integer } n \geq 1. \tag{10.64}$$

The zero mode is separate: if $k = 0$, the sine perturbation vanishes, so the density and current retain their unperturbed values for every ε_r. The formulas containing $1/k$ below concern only the

nonzero modes. The exact stationary-current calculation is the primary benchmark; the perturbative calculation below is retained as a sign and coefficient cross-check. Let

$$B_{\varepsilon_r}(x) = b + \varepsilon_r \sin(kx), \qquad \Phi_{\varepsilon_r}(x) = \int_0^x \frac{B_{\varepsilon_r}(z)}{D}\,\mathrm{d}z = \frac{bx}{D} + \frac{\varepsilon_r}{Dk}[1-\cos(kx)]. \tag{10.65}$$

The stationary equation $J_{\varepsilon_r} = B_{\varepsilon_r}\rho_{\varepsilon_r} - D\rho'_{\varepsilon_r}$ implies

$$\frac{\mathrm{d}}{\mathrm{d}x}\left(e^{-\Phi_{\varepsilon_r}(x)}\rho_{\varepsilon_r}(x)\right) = -\frac{J_{\varepsilon_r}}{D}e^{-\Phi_{\varepsilon_r}(x)}. \tag{10.66}$$

For $b \neq 0$, integration from x to $x+L$, periodicity of ρ_{ε_r}, and

$$\Phi_{\varepsilon_r}(x+L) = \Phi_{\varepsilon_r}(x) + \frac{bL}{D} \tag{10.67}$$

give

$$\rho_{\varepsilon_r}(x) = \frac{J_{\varepsilon_r}}{D(1-e^{-bL/D})}e^{\Phi_{\varepsilon_r}(x)}\int_x^{x+L} e^{-\Phi_{\varepsilon_r}(y)}\,\mathrm{d}y. \tag{10.68}$$

At $b = 0$, Equation (10.68) is a $0/0$ representation and must not be evaluated literally. The continuous equilibrium branch is

$$J_{\varepsilon_r} = 0, \qquad \Sigma_{\varepsilon_r} = 0, \qquad \rho_{\varepsilon_r}(x) = \frac{e^{\Phi_{\varepsilon_r}(x)}}{\displaystyle\int_0^L e^{\Phi_{\varepsilon_r}(y)}\,\mathrm{d}y}. \tag{10.69}$$

For $b \neq 0$, normalization in Equation (10.68) yields

$$J_{\varepsilon_r} = \frac{D(1-e^{-bL/D})}{\displaystyle\int_0^L e^{\Phi_{\varepsilon_r}(x)}\int_x^{x+L} e^{-\Phi_{\varepsilon_r}(y)}\,\mathrm{d}y\,\mathrm{d}x}. \tag{10.70}$$

This is the classical stationary-current quadrature for a one-dimensional tilted periodic diffusion, written in the present probability-current convention [97], [91], [89], and [59]. Therefore the quadrature itself is a benchmark, not a standalone novelty claim.

Set $y = x + s$. The identity

$$\cos(k(x+s)) - \cos(kx) = -2\sin\left(kx + \frac{ks}{2}\right)\sin\left(\frac{ks}{2}\right) \tag{10.71}$$

and the integral representation of the modified Bessel function I_0 reduce the denominator in Equation (10.70) to

$$L\int_0^L e^{-bs/D} I_0\left(\frac{2\varepsilon_r}{Dk}\sin\frac{ks}{2}\right)\,\mathrm{d}s. \tag{10.72}$$

Define

$$\alpha = \frac{b}{D}, \qquad \mathscr{H}_{\mathrm{ring}}(\varepsilon_r) = \frac{\alpha}{1-e^{-\alpha L}}\int_0^L e^{-\alpha s} I_0\left(\frac{2\varepsilon_r}{Dk}\sin\frac{ks}{2}\right)\,\mathrm{d}s, \tag{10.73}$$

with the continuous interpretation

$$\frac{\alpha}{1-e^{-\alpha L}} = \frac{\alpha}{-\operatorname{expm1}(-\alpha L)} \longrightarrow \frac{1}{L} \quad (\alpha \to 0). \tag{10.74}$$

Then

$$J_{\varepsilon_r} = \frac{b}{L\mathscr{H}_{\mathrm{ring}}(\varepsilon_r)} \qquad (b \neq 0). \tag{10.75}$$

Expanding

$$I_0(z) = \sum_{m=0}^{\infty} \frac{(z^2/4)^m}{(m!)^2} \tag{10.76}$$

and evaluating the weighted trigonometric moments gives the all-even series

$$\mathscr{H}_{\mathrm{ring}}(\varepsilon_r) = \sum_{m=0}^{\infty} \frac{\binom{2m}{m}}{4^m} \frac{\varepsilon_r^{2m}}{\prod_{\ell=1}^{m}(b^2 + \ell^2 D^2 k^2)}. \tag{10.77}$$

The empty product in Equation (10.77) is one. The moment identity used in the calculation is

$$\frac{\alpha}{1 - e^{-\alpha L}} \int_0^L e^{-\alpha s} \sin^{2m}\left(\frac{ks}{2}\right) \mathrm{d}s = \frac{(2m)! k^{2m}}{4^m \prod_{\ell=1}^{m}(\alpha^2 + \ell^2 k^2)}. \tag{10.78}$$

It follows that $\mathscr{H}_{\mathrm{ring}}$ is entire and even as a function of ε_r, whereas $1/\mathscr{H}_{\mathrm{ring}}$ is used only as a real-analytic local reciprocal on parameter ranges where $\mathscr{H}_{\mathrm{ring}} \neq 0$.

The stationary entropy-production functional is

$$\Sigma_{\varepsilon_r} = \int_0^L \frac{J_{\varepsilon_r}^2}{D\rho_{\varepsilon_r}(x)} \mathrm{d}x. \tag{10.79}$$

Since

$$\frac{J_{\varepsilon_r}}{D\rho_{\varepsilon_r}} = \frac{B_{\varepsilon_r}}{D} - \partial_x \log \rho_{\varepsilon_r}, \tag{10.80}$$

the logarithmic derivative and the sinusoidal part of B_{ε_r} integrate to zero over the ring. Hence

$$\Sigma_{\varepsilon_r} = \frac{bLJ_{\varepsilon_r}}{D} = \frac{b^2}{D\mathscr{H}_{\mathrm{ring}}(\varepsilon_r)} \qquad (b \neq 0). \tag{10.81}$$

With

$$R_\ell = b^2 + \ell^2 D^2 k^2, \qquad A = \frac{1}{2R_1}, \qquad B = \frac{3}{8R_1 R_2}, \tag{10.82}$$

the expansion of Equation (10.81) begins as

$$\frac{\Sigma_{\varepsilon_r}}{\Sigma_0} = 1 - A\varepsilon_r^2 + (A^2 - B)\varepsilon_r^4 + O(\varepsilon_r^6), \qquad \Sigma_0 = \frac{b^2}{D}. \tag{10.83}$$

More explicitly,

$$A^2 - B = \frac{5D^2k^2 - b^2}{8R_1^2 R_2}. \tag{10.84}$$

If $|\varepsilon_r| \leq \varepsilon_0$ and

$$q_2 = \frac{\varepsilon_0^2}{R_3} < 1, \tag{10.85}$$

then the nonnegative tail of $\mathscr{H}_{\mathrm{ring}}$ gives the checkable fourth-order reciprocal bound

$$\left| \frac{1}{\mathscr{H}_{\mathrm{ring}}(\varepsilon_r)} - (1 - A\varepsilon_r^2) \right| \leq \left[A^2 + \frac{B}{1 - q_2}(1 + A\varepsilon_0^2) \right] |\varepsilon_r|^4. \tag{10.86}$$

This bound replaces any unqualified odd-order remainder. At $b = D = k = 1$ and $L = 2\pi$, the sixth-order coefficient of Σ_{ε_r} cancels and

$$\Sigma_{\varepsilon_r} = 1 - \frac{\varepsilon_r^2}{4} + \frac{\varepsilon_r^4}{40} - \frac{69\varepsilon_r^8}{217600} + O(\varepsilon_r^{10}). \tag{10.87}$$

For a nonzero sixth-order regression one may instead use $b = 2$, $D = k = 1$, for which

$$\Sigma_{\varepsilon_r} = 4 - \frac{2}{5}\varepsilon_r^2 + \frac{1}{400}\varepsilon_r^4 + \frac{57}{52000}\varepsilon_r^6 + O(\varepsilon_r^8). \tag{10.88}$$

If the drift is thermally parametrized by $b = \mathsf{K} f_{\mathrm{nc}}$ and $D = \mathsf{K} k_B T$, then

$$\dot{W}_{\mathrm{nc}} = f_{\mathrm{nc}} L J_{\varepsilon_r} = \frac{b L J_{\varepsilon_r}}{\mathsf{K}} = k_B T \Sigma_{\varepsilon_r} = T \dot{S}_{\mathrm{tot}}. \tag{10.89}$$

Let

$$\pi_0 = \frac{1}{L} \tag{10.90}$$

be the unperturbed stationary density. Write

$$\rho_{\varepsilon_r} = \pi_0 + \delta\rho + O(\varepsilon_r^2). \tag{10.91}$$

At first order, stationarity of the current gives

$$b\,\delta\rho + \varepsilon_r \pi_0 \sin(kx) - D\,\delta\rho' = 0. \tag{10.92}$$

Set

$$\delta\rho = C_1 \cos(kx) + C_2 \sin(kx). \tag{10.93}$$

Then

$$\delta\rho' = -kC_1 \sin(kx) + kC_2 \cos(kx). \tag{10.94}$$

Equating cosine and sine coefficients gives

$$bC_1 - DkC_2 = 0, \tag{10.95}$$

$$bC_2 + DkC_1 + \varepsilon_r \pi_0 = 0. \tag{10.96}$$

Solving,

$$C_1 = -\frac{\varepsilon_r \pi_0 D k}{b^2 + D^2 k^2}, \tag{10.97}$$

$$C_2 = -\frac{\varepsilon_r \pi_0 b}{b^2 + D^2 k^2}. \tag{10.98}$$

Hence

$$\delta\rho(x) = -\frac{\varepsilon_r \pi_0}{b^2 + D^2 k^2}\left[Dk \cos(kx) + b \sin(kx)\right]. \tag{10.99}$$

A consistent second-order expansion of

$$\Sigma_{\varepsilon_r} = \int_0^L \frac{J_{\varepsilon_r}^2}{D \rho_{\varepsilon_r}}\, \mathrm{d}x \tag{10.100}$$

yields

$$\Delta\Sigma = \Sigma_{\varepsilon_r} - \Sigma_0 = -\frac{b^2\varepsilon_r^2}{2D(b^2 + D^2k^2)} + R_4(\varepsilon_r), \tag{10.101}$$

where R_4 is even and satisfies the explicit local fourth-order bound implied by Equation (10.86). Because

$$\Sigma_0 = \frac{b^2}{D}, \tag{10.102}$$

For $b \neq 0$, we obtain

$$\frac{|\Delta\Sigma|}{\Sigma_0} = \frac{\varepsilon_r^2}{2(b^2 + D^2k^2)} + O(\varepsilon_r^4). \tag{10.103}$$

For $\varepsilon_r = 0.1b$ and $Dk \ll b$,

$$\frac{|\Delta\Sigma|}{\Sigma_0} \approx 0.005. \tag{10.104}$$

The negative sign in Equation (10.101) is a property of this perturbation direction and is not promoted to a universal minimum-entropy-production theorem.

10.2.7. *Measurement of Current on the Ring.* An overdamped Brownian path is almost surely nondifferentiable, so an "instantaneous velocity" estimated by $\Delta X/\Delta t$ at arbitrarily small Δt is not a well-defined microscopic velocity. Instead, unwrap the angular coordinate to $\widetilde{X}_t \in \mathbb{R}$ and estimate the long-time winding current by

$$\widehat{J}_T = \frac{\widetilde{X}_T - \widetilde{X}_0}{LT}. \tag{10.105}$$

Local currents can be reconstructed from transition statistics at a controlled temporal coarse-graining scale.

10.3. *Numerical illustrations of state and path entropy.* To test the distinction between a relaxing state law and a maintained path arrow, use a ring of circumference 2π, diffusivity $D = 0.3$, and drift $v = 0.6$. Starting from $p_0(x) = [1 + 0.6\cos x]/(2\pi)$, its exact law is

$$p_t(x) = \frac{1 + 0.6e^{-Dt}\cos(x - vt)}{2\pi}. \tag{10.106}$$

Translation does not change its state KL relative to the uniform law. The state KL is evaluated by periodic quadrature with 4096 points. The stationary fixed-drive path KL is Tv^2/D, with rate 1.2. The state-relaxation rate is transient and tends to zero, whereas the maintained path rate remains positive. These data reproduce an exact finite-model distinction; they are not new laboratory measurements.

A second test constructs a reflecting two-coordinate finite-volume chain from a smooth potential, a positive diagonal mobility, and a fluctuation scale $\theta = 0.12$. Detailed balance holds on each edge. The independent formulas for the time derivative of discrete KL, from $Q^T p$ and from edge dissipation, agree to floating-point accuracy. Grid refinement tracks the spectral gap and probability-law decay. The two coordinates serve as a synthetic regulated mass–spin example; their coefficients

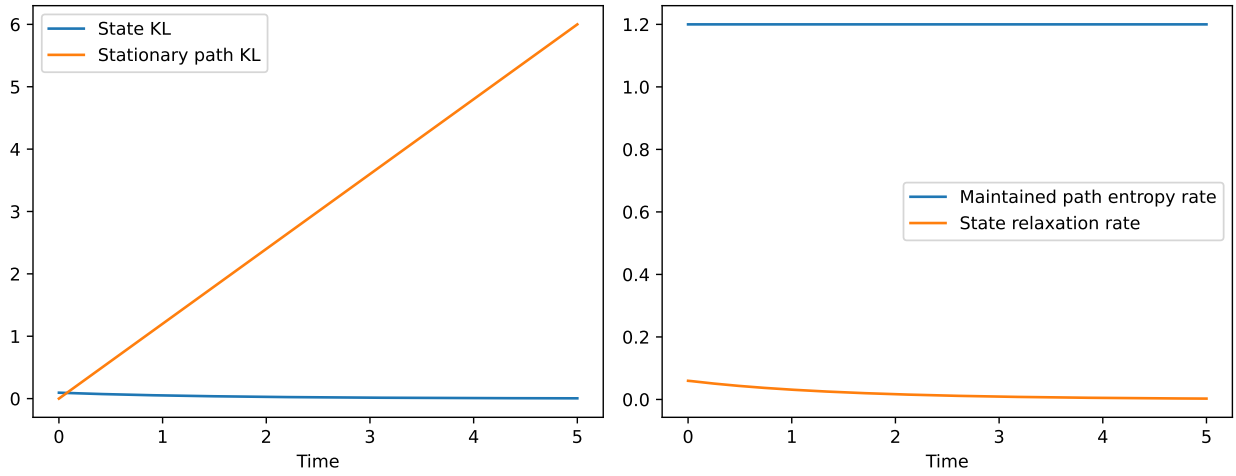


Figure 4. Computed state and stationary path ledgers for the declared ring. The plotted state curve uses a nonequilibrium initial law; the linear path curve refers to the separately specified stationary process. The common drift and diffusivity are fixed in both calculations.

are supplied effective inputs, and their stationary law does not establish spacetime regularity or a quantum thermal state.

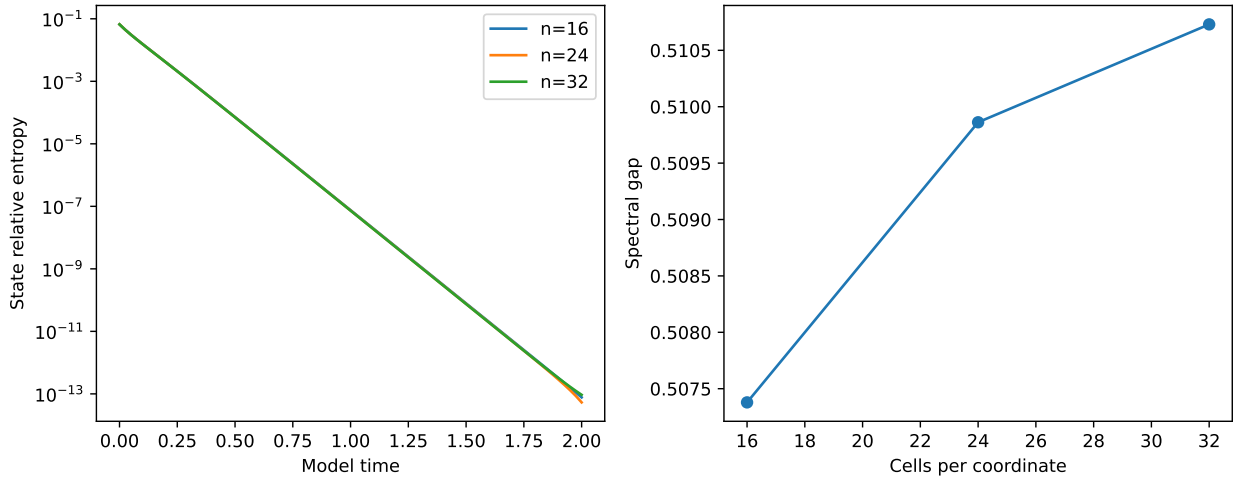


Figure 5. Synthetic finite-volume law relaxation and spectral-gap refinement. The data test a specified positive Gibbs generator, not a physical black-hole equilibrium measurement.

A finite likelihood comparison illustrates the quantitative observation bound in Proposition 11.2. The reference law is uniform on $\{-1,1\}^2$, the tilted law is proportional to $e^{0.4y+\varepsilon z}$, and only y is observed. Direct summation of the four probabilities, for 101 values of ε from zero to two, gives the hidden relative entropy $\varepsilon \tanh \varepsilon - \log \cosh \varepsilon$. The direct sum and closed expression differ by at most 4.5×10^{-16}. The comparison illustrates a finite information bound; no reservoir identification or physical entropy measurement is assumed in this binary example.

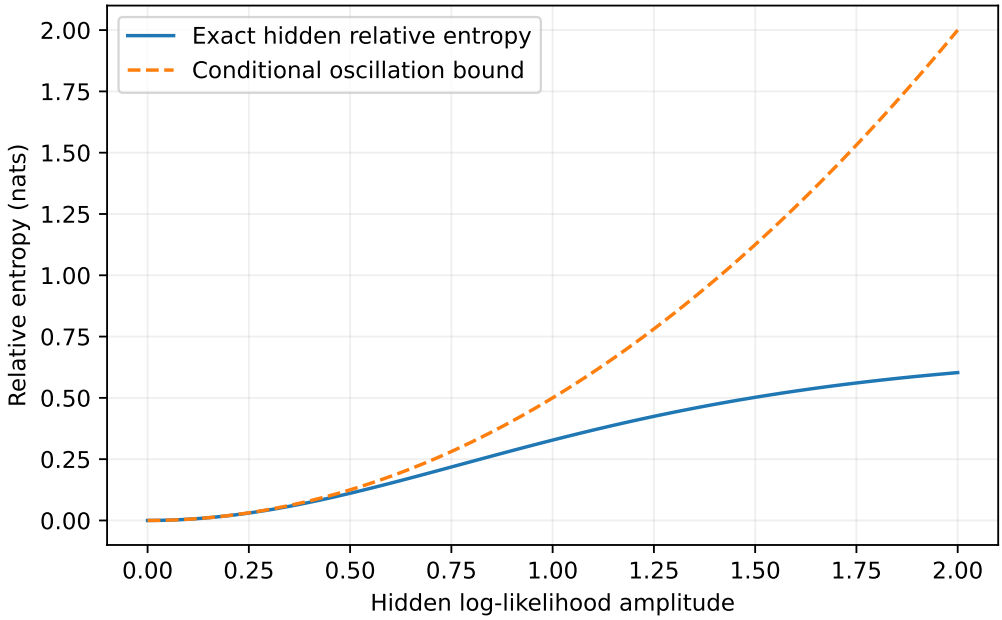


Figure 6. Hidden relative entropy in the finite likelihood example and the conditional-oscillation upper bound. The two curves agree to leading quadratic order for small hidden likelihood amplitude.

These examples also illustrate how the mother model is to be compared with a declared projection: the same coefficients must be used in the current, noise, equilibrium reference, and cost verification. A good plot produced by independently retuning each one would not check that common-origin claim.

10.4. *Exact Gaussian reservoir comparisons.* The following comparisons evaluate exact Gaussian mean dynamics and stationary covariances numerically. They test the normalization of the reservoir realization and display the effect of retained memory. They are deterministic finite-model calculations, not experimental data or an additional stochastic convergence theorem.

10.4.1. *A Gaussian model with three resolved embedding variables.* Take $U(q) = kq^2/2$ and the scalar version of (D). Its drift, stationary covariance, and diffusion covariance are

$$A_\varepsilon = \begin{pmatrix} 0 & 1/m & 0 \\ -k & 0 & 1 \\ 0 & -g/(m\varepsilon) & -1/\varepsilon \end{pmatrix},$$

$$C_\varepsilon = \operatorname{diag}(\theta/k, m\theta, \theta g/\varepsilon), \quad Q_\varepsilon = \operatorname{diag}(0, 0, 2\theta g/\varepsilon^2).$$

Symbolic matrix multiplication gives

$$A_\varepsilon C_\varepsilon + C_\varepsilon A_\varepsilon^T + Q_\varepsilon = 0.$$

The conservative part, obtained by removing the last diagonal damping, is antisymmetric in the inverse-covariance metric and changes sign under $\mathrm{diag}(1,-1,1)$ conjugation. These identities check both equilibrium calibration and momentum parity.

Initialize the covariance at C_ε and the mean at $(1,0,0)$. The covariance then stays constant and the mean is $\bar{X}_t = e^{A_\varepsilon t}(1,0,0)^T$. Consequently the full embedding and resolved phase-space KL divergences are

$$H_{\mathrm{ext}}(t) = \frac{k\bar{q}^2 + \bar{p}^2/m + \varepsilon\bar{z}^2/g}{2\theta}, \qquad H_{\mathrm{sys}}(t) = \frac{k\bar{q}^2 + \bar{p}^2/m}{2\theta}.$$

Differentiating these expressions with the mean equations gives

$$\dot{H}_{\mathrm{ext}} = -\frac{\bar{z}^2}{\theta g}, \qquad \dot{H}_{\mathrm{sys}} = \frac{\bar{p}\bar{z}}{m\theta}. \tag{10.107}$$

The second sign is not fixed. With $k = g = m = \theta = 1$ and $\varepsilon = 2$, the calculated maximum of $\dot{H}_{\mathrm{sys}}$ over the stated time grid is $0.09521305805 > 0$. The embedding entropy is nonincreasing. This is a concrete warning against assuming a closed monotone entropy law after discarding a memory variable.

10.4.2. *Two independently controlled finite-model limits.* For the memory comparison fix $m = 1$ and compare the exact three-variable mean against the kinetic Langevin mean. For the small-mass comparison compare the kinetic position mean with e^{-t}, the overdamped mean for the same $k = g = 1$. The horizon is 8 and the grid has 1601 points. The errors in the table are maxima over that grid, not certified continuous-time suprema or stochastic strong-error estimates.

Small parameter	Memory-limit mean error	Small-mass mean error
0.50	0.18895958	0.21682690
0.20	0.06835685	0.11945087
0.10	0.03248375	0.07094532
0.05	0.01586866	0.04008173
0.02	0.00626588	0.01776884
0.01	0.00311999	0.00931330

For the declared Gaussian path, the computed reverse action is 0.490842180556, and the independently evaluated free-energy difference divided by θ is 0.490842180556. Their difference is $5.55e-17$.

The monotone reduction of these mean errors is consistent with the two proved limits, but does not replace their path estimates. The memory and mass parameter in a given row have the same numerical value in dimensionless units; the two columns describe different comparisons. The small-mass initial mean momentum is zero, consistent with the declared thermal initial momentum law.

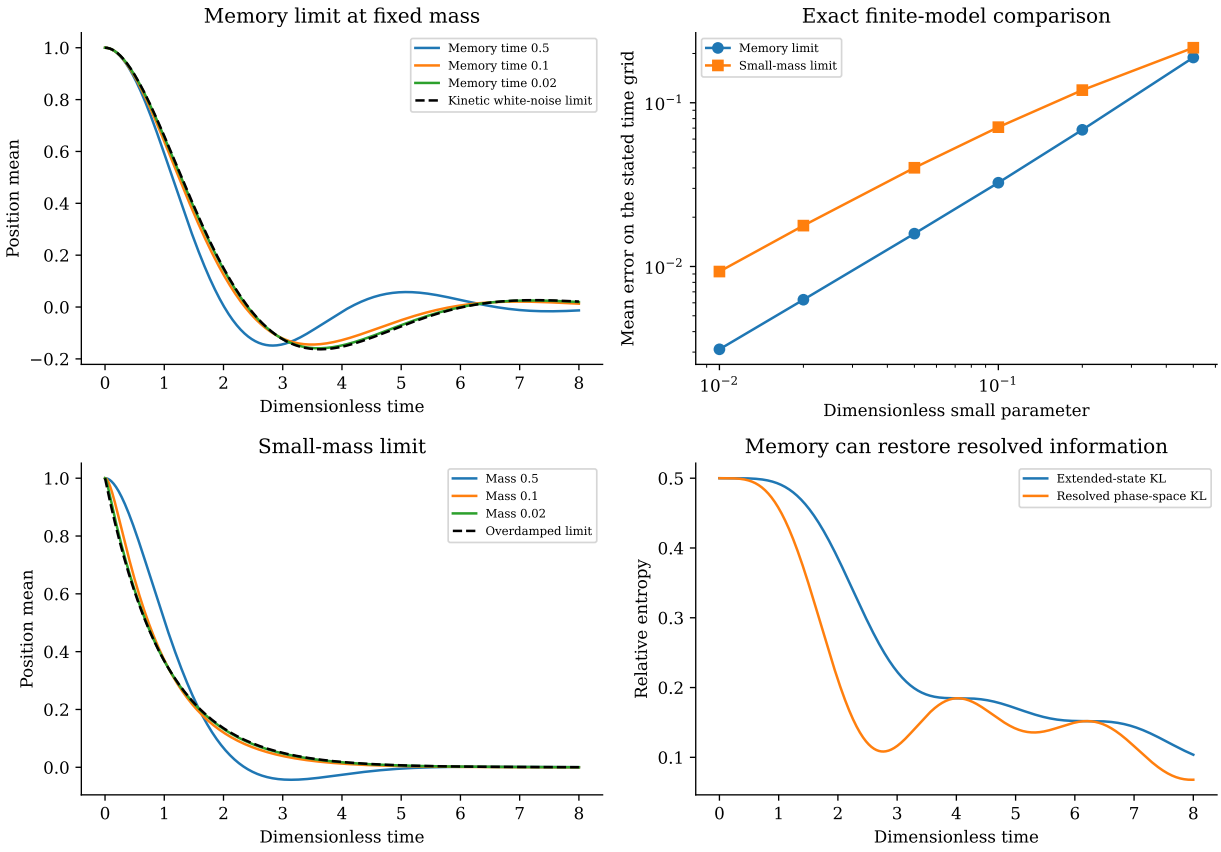


Figure 7. Exact Gaussian comparisons. The upper-left panel shows the memory limit at fixed mass, the upper-right panel the finite-grid mean errors, and the lower-left panel the small-mass limit. The lower-right panel displays a resolved entropy rebound while the extended-state KL continues to decrease. All coefficients are declared model inputs.

10.4.3. *Reversal cost and the nonuniversal counterexample.* For $a_0 = k = g = \theta = 1$ and $\tau = 2$, the Gaussian relaxation has zero action. Direct quadrature of the reversed action and independent evaluation of its free-energy rise both give approximately 0.490842180556. Their agreement tests the normalization in (4.38), not a newly measured thermodynamic law. The second figure also plots the exactly recurring position entropy of Proposition 4.1.

All displayed means follow from the stated drift matrices and initial data. The covariance is stationary by the Lyapunov identity, so the relative entropies are the corresponding explicit Gaussian quadratic forms. The two parameter comparisons concern finite-grid mean errors; the stochastic path limits rely on the preceding analytical estimates.

10.5. *Numerical tests of orientation and reduction.* The explicit models in Sections 2 and 3 allow the theoretical distinctions to be tested without fitting a physical dataset. All data in this

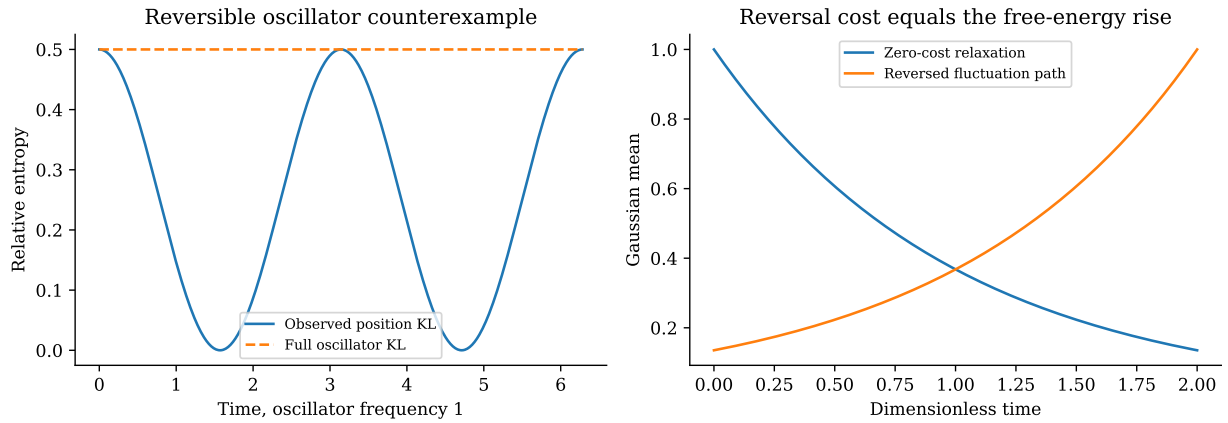


Figure 8. A reversible oscillator provides an explicit counterexample to an unrestricted dissipative-reduction claim. For the derived Gaussian diffusion, the reverse of a zero-cost relaxation has a positive cost equal to its free-energy rise divided by θ. These statements concern different models and are labeled separately.

subsection are synthetic. We compare stochastic sampling with analytic values, and use a separate hidden-coordinate example to test a closure claim that would otherwise be easy to assume.

For the Gaussian model (2.12), take $m_0 = (1, 0)$, $\omega = 0$ or 0.8, and $X_0 \sim N(m_0, I_2)$. On a grid of spacing $h = 0.05$, use the exact transition

$$X_{k+1} = E_h X_k + \zeta_k, \qquad E_h = e^{B_\omega h}, \qquad \zeta_k \sim N(0, I_2 - E_h E_h^{\mathsf{T}}).$$

The covariance formula follows by integrating $e^{B_\omega s} 2M e^{B_\omega^{\mathsf{T}} s}$ and using the Lyapunov identity. Its positivity follows from that integral. The increments and initial draws are independent. Thus no Euler bias is present in this sampling experiment.

For $N = 50{,}000$ independent trajectories, the sample mean satisfies $\widehat{m}_t \sim N(m_t, I_2/N)$. The bias-corrected estimator

$$\widehat{D}_{\mathrm{mean}}(t) = \tfrac{1}{2}|\widehat{m}_t|^2 - \frac{1}{N}$$

has expectation $D(\rho_t \| \pi)$ in this known-covariance Gaussian family and variance

$$\mathrm{Var}(\widehat{D}_{\mathrm{mean}}(t)) = |m_t|^2/N + 1/N^2.$$

It can take a negative value near equilibrium because it is an unbiased estimate of a nonnegative quantity. It is not an empirical-density relative entropy estimator. Error bars show 1.96 times this standard deviation at each time; they are pointwise uncertainty indicators, not a simultaneous confidence band.

The run used seed 20261030, a final time of 3, and both values of ω. The largest absolute errors over the reported times were 0.004763 and 0.004363, respectively. The stationary rate was estimated independently from 100,000 samples of $N(0, I_2)$ by averaging $c(X)^{\mathsf{T}} M^{-1} c(X)$. The resulting values are

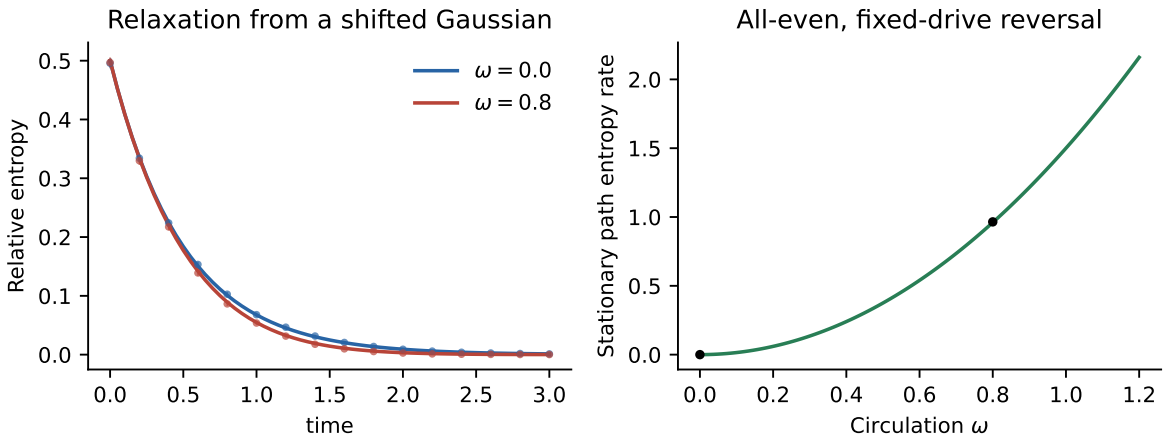


Figure 9. Exact-transition Gaussian simulations. Left: analytic relative entropy (curves) and unbiased mean estimates with pointwise uncertainty bars. Right: analytic stationary path entropy rate and independent stationary estimates. Both coordinates are even under reversal and the circulation is held fixed in the reversed experiment.

ω	Exact rate	Estimated rate	Standard error
0.0	0.000000	0.000000	0.000000
0.8	0.960000	0.964666	0.003229

The second estimate differs from 0.96 by approximately 1.45 of its sample standard errors. Sampling supports the specified finite-model calculation; it does not establish the theorem for other parameters or constitute physical experimental evidence.

The corresponding numerical diagnostic is shown in Figure 9.

For the hidden-coordinate example take $\alpha = 0.6$ and $a = 1$ in (3.22). Figure 10 shows the analytically evaluated full and observed relative entropies, the observed derivative, and the upper bound $-\frac{1}{2}m_1^2 + \frac{1}{2}\alpha^2 m_2^2$ from (3.9). The marginal entropy starts at zero, rises, and later decays while the full entropy decreases throughout. Every value in this figure follows from the explicit two-dimensional matrix exponential. No Markov approximation is used for the observed coordinate.

The algebraic contraction can also be checked without discretization. For

$$H = \begin{pmatrix} 2 & 1 & 0 \\ 1 & 3 & 1 \\ 0 & 1 & 2 \end{pmatrix}, \qquad C = \begin{pmatrix} 1 & 0 & 1 \\ 0 & 1 & 0 \end{pmatrix}, \qquad j = (1,2)^{\mathsf{T}},$$

the principal minors of H are $2, 5, 8$, so it is positive definite. Then

$$H_{\mathrm{eff}} = \begin{pmatrix} 4 & 2 \\ 2 & 3 \end{pmatrix}, \qquad J_* = (1/2, 2, 1/2)^{\mathsf{T}}, \qquad \Phi(J_*) = 11/16.$$

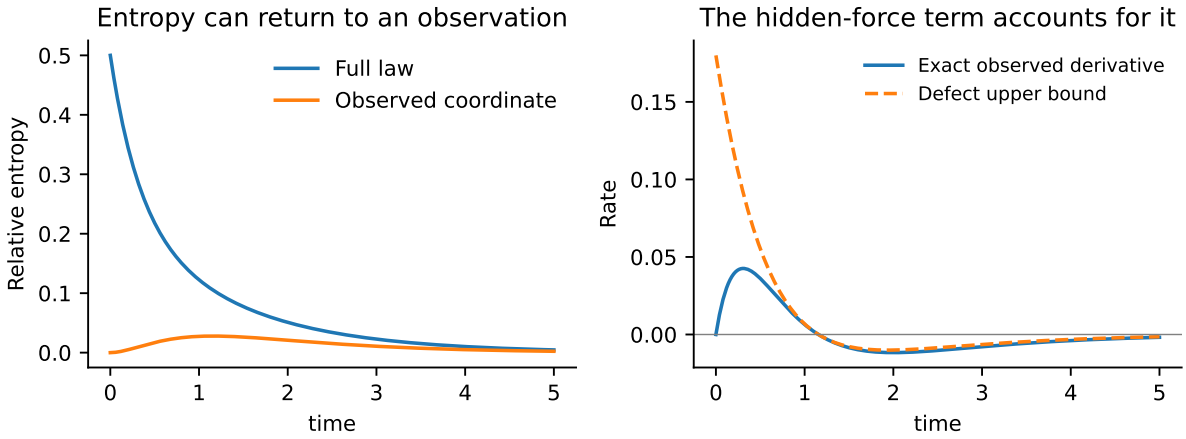


Figure 10. Exact hidden-coordinate calculation. The transfer of a hidden initial displacement to the measured coordinate produces an increase of observed relative entropy. The conditional-force defect accounts for that increase and satisfies the stated upper bound. The complete reversible diffusion still dissipates its full relative entropy.

The family $J_* + u(1, 0, -1)^{\mathsf{T}}$ has the same observed current. Its cost is $11/16 + u^2/2$, verifying the exact orthogonal cost gap. These finite comparisons test distinct ingredients: covariance calibration, ensemble relaxation, stationary reversal, and current contraction. Their agreement does not replace the separate hypotheses needed for a physical projection or a continuum limit.

10.6. *Force and transport defects in Gaussian observations.* The complete observed balance separates two mechanisms that the preceding force-only example cannot distinguish. We use a dimensionless family with $\theta = 1$, reference $N(0, I_2)$, and

$$M_\alpha = \begin{pmatrix} 1 & \alpha \\ \alpha & 1 \end{pmatrix}, \qquad \Omega_\omega = \begin{pmatrix} 0 & \omega \\ -\omega & 0 \end{pmatrix}, \qquad \mathsf{B} = -M_\alpha + \Omega_\omega.$$

The process is $\mathrm{d}X = \mathsf{B}X\,\mathrm{d}t + \sqrt{2M_\alpha}\,\mathrm{d}W$. Since $\mathsf{B} + \mathsf{B}^{\mathsf{T}} + 2M_\alpha = 0$, an initial covariance I_2 remains I_2 and $m(t) = e^{\mathsf{B}t}m(0)$. Hence

$$D_{\mathrm{full}} = \tfrac{1}{2}|m|^2, \quad D_Y = \tfrac{1}{2}m_1^2, \quad R_\rho = \alpha m_2, \quad A_\rho = \omega m_2, \quad B_\rho = (\alpha - \omega)m_2. \tag{10.108}$$

The distinct symbol B denotes the joint drift matrix; B_ρ denotes the observed conditional defect. The full entropy rate is $-m^{\mathsf{T}}M_\alpha m$, while the observed rate is $-m_1^2 - (\alpha - \omega)m_1m_2$.

Three preparations isolate the mechanisms. The force case uses $(\alpha, \omega, m(0)) = (0.6, 0, (0, 1)^{\mathsf{T}})$; the transport case uses $(0, 1, (1, 2)^{\mathsf{T}})$; the mixed case uses $(0.6, 0.8, (0, 1)^{\mathsf{T}})$. The following table gives analytic values from the matrix exponential, rounded to six decimal places.

Case	t	D_{full}	D_Y	D'_Y
Force	0.0	0.500000	0.000000	-0.000000
Force	0.5	0.218054	0.017057	0.036149
Force	1.0	0.122523	0.027428	0.006430
Force	2.0	0.050890	0.020866	-0.011696
Transport	0.0	2.500000	0.500000	1.000000
Transport	0.5	0.919699	0.620335	-0.378797
Transport	1.0	0.338338	0.334469	-0.596986
Transport	2.0	0.045789	0.018012	-0.080760
Mixed	0.0	0.500000	0.000000	0.000000
Mixed	0.5	0.173158	0.001797	0.003425
Mixed	1.0	0.052888	0.002463	-0.000469
Mixed	2.0	0.003196	0.000994	-0.001396

Observed relative entropy can increase in each experiment even though the full relative entropy decreases. In the transport experiment the force defect is identically zero. At $t = 0$ the recovery bound is attained: $D'_Y = 1 = E_B/4$, whereas $D'_{\mathrm{full}} = -5$.

For an independent stochastic comparison, we sample the exact Gaussian transition at spacing $h = 0.025$ on $[0, 4]$:

$$X_{k+1} = E_h X_k + \zeta_k, \qquad E_h = e^{\mathsf{B}h}, \qquad \zeta_k \sim N(0, I_2 - E_h E_h^{\mathsf{T}}).$$

All initial draws and transition increments are independent as specified by the model. Each case has $N = 30{,}000$ trajectories, generated from seed 20261030. With the known unit covariance, the unbiased estimates are $|\widehat{m}|^2/2 - 1/N$ for the full relative entropy and $\widehat{m}_1^2/2 - 1/(2N)$ for the observed one. Their variances are $|m|^2/N + 1/N^2$ and $m_1^2/N + 1/(2N^2)$, respectively. These are Gaussian-family moment estimates, not relative entropies of atomic empirical measures. Their largest observed-entropy absolute errors on the grid are 0.001412, 0.008852 and 0.000696 in the three cases. The plotted markers are selected from those generated data.

The corresponding numerical diagnostic is shown in Figure 11.

The analytic rate identity has a largest absolute floating-point residual below 2×10^{-16} on the reported grid. A separate adaptive ODE integration agrees with the matrix-exponential means to 1.1×10^{-11}. Trapezoidal integration on a grid of 4001 points gives a largest balance error below 3.1×10^{-7}. These are numerical residuals for the stated finite models. The proofs do not depend on a numerical tolerance. Figure 12 also displays the strictly positive covariance gap for the stationary zero-defect observation of Section 3.8. That gap concerns a path law; a constant marginal density alone would not reveal it.

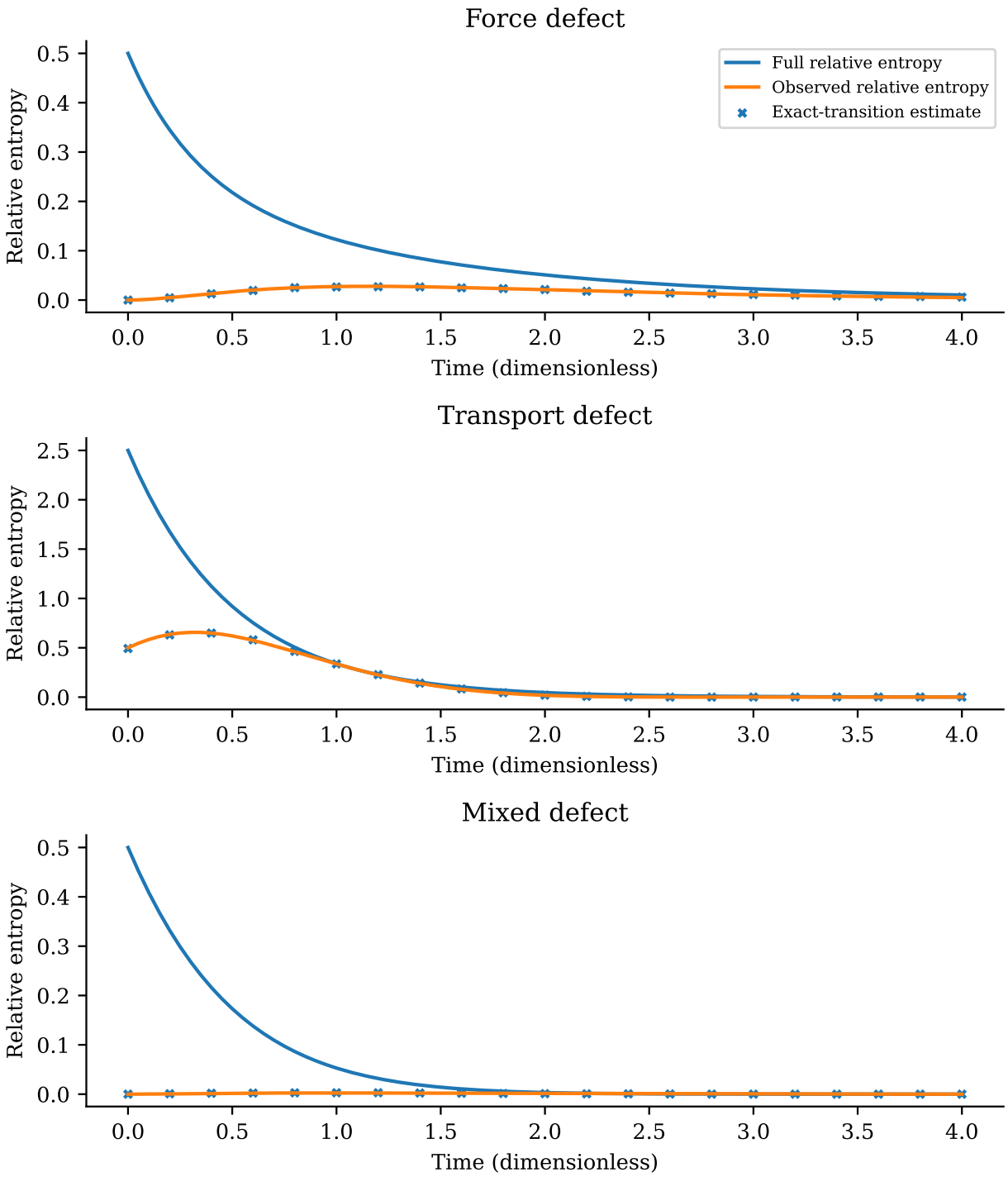


Figure 11. Synthetic Gaussian observations. Exact full and observed relative entropies are compared with estimates from exact-transition sampling. From top to bottom, the panels separate a conditional-force defect, a transport defect, and their combined effect. All axes use dimensionless model units.

10.6.1. *A periodic check of conditional regularity.* The role of conditional gradients can be seen without a Gaussian law. On the period-one two-dimensional torus set $\pi = p = 1$ and

$$r(z \mid y) = 1 + \epsilon \sin(2\pi k y) \sin(2\pi z),$$
$$M = \operatorname{diag}(2 + \sin(2\pi z), 1), \qquad c = (\sin(2\pi z), 0).$$

Here $0 < \epsilon < 1$, k is a positive integer, $M \geq I$, and $\nabla \cdot c = 0$. Direct integration gives

$$\overline{M}_\rho = 2 + \tfrac{\epsilon}{2} \sin(2\pi k y), \quad R_\rho = \epsilon \pi k \cos(2\pi k y), \quad A_\rho = \tfrac{\epsilon}{2} \sin(2\pi k y).$$

At $\theta = 1$, $B_\rho = R_\rho - A_\rho$. Evaluating the displayed integrals on a 512×512 periodic grid with $\epsilon = 0.2$ gives

k	H_{cond}	J_{cond}	E_B
1	0.005019	1.193387	0.101263
3	0.005019	7.558115	0.891325
7	0.005019	39.381756	4.841637

These values satisfy (3.18) with $\eta = 1$, $\lambda = 1$ and $C_c = 1$. The conditional entropy is independent of the positive integer frequency by periodic change of variables, while the force square grows as k^2. Thus small conditional entropy alone does not provide the required gradient control. Write $u = r - 1$. Taylor's formula for $(1 + u)\log(1 + u) - u$, whose second derivative is $1/(1 + u)$, and $|u| \leq \epsilon$ give

$$H_{\mathrm{cond}} \leq \frac{\epsilon^2}{8(1 - \epsilon)}, \qquad E_R := \int \frac{|R_\rho|^2}{\overline{M}_\rho} \, \mathrm{d}y \geq \frac{\epsilon^2 \pi^2 k^2}{4 + \epsilon}.$$

Here the averages of u and u^2 are 0 and $\epsilon^2/4$; the force bound uses $\overline{M}_\rho \leq 2 + \epsilon/2$ and the average $\cos^2(2\pi k y) = 1/2$. Taking $\epsilon = k^{-1/2}$ for integers $k \geq 2$ makes $H_{\mathrm{cond}} \to 0$ while $E_R \to \infty$. This proves the absence of an entropy-only force bound in this class. The table is a deterministic quadrature of a prepared density, not a time-discretized simulation of its evolution. At this preparation $g = 0$, so its instantaneous observed free-energy rate is zero; the nonzero defect measures a conditional current and is not itself an entropy-production rate.

The simulations and exact calculations therefore check a specific physical distinction: information returning to a resolved coordinate need not be generated by the thermodynamic force alone. A hidden transport contribution can produce the same effect. Neither mechanism invalidates the complete thermal balance, and neither a zero marginal rate nor zero conditional defect by itself establishes memoryless observed dynamics.

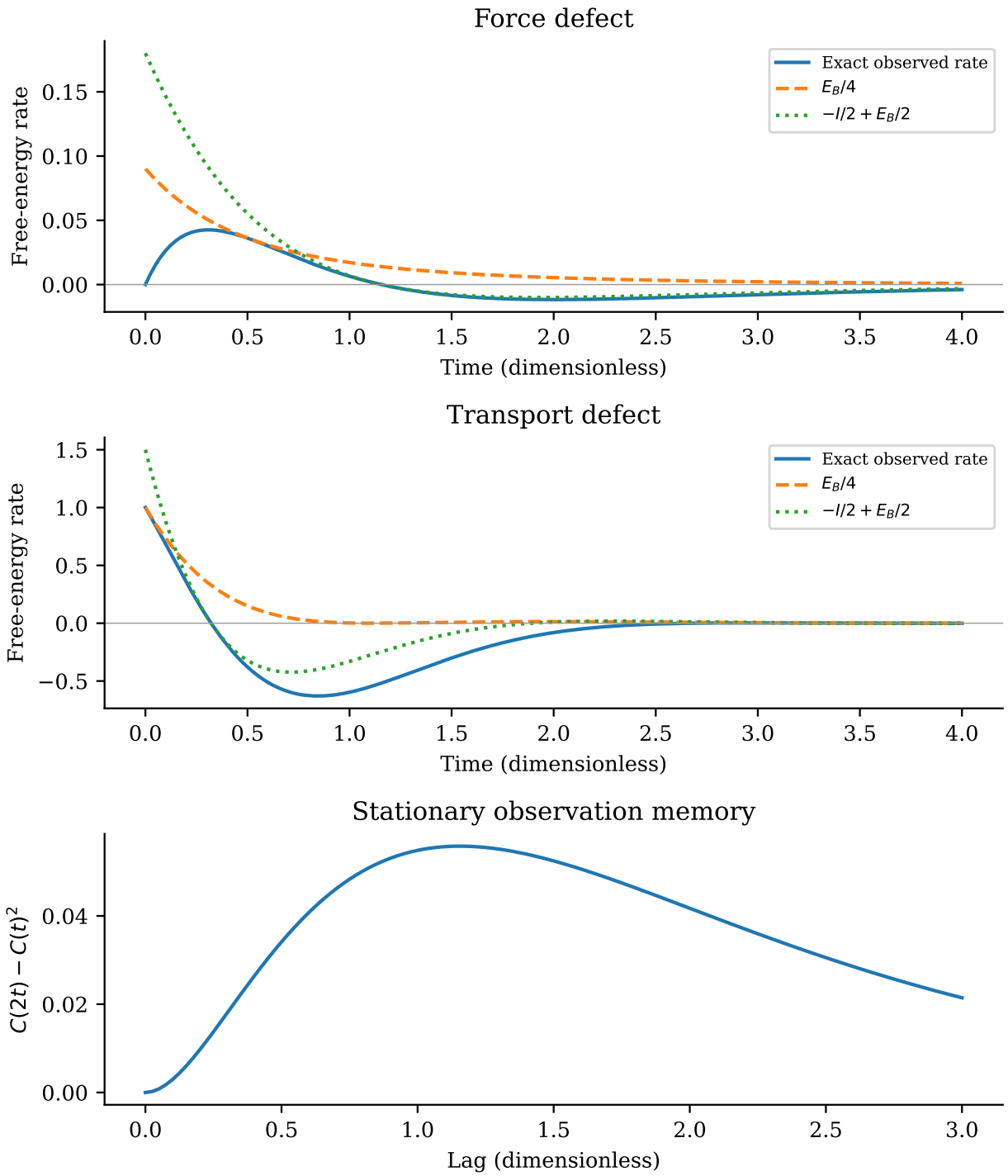


Figure 12. Exact observed rates and complete-defect bounds for the force and transport experiments (top and middle). The bottom panel shows $C(2t) - C(t)^2$ for the stationary force model with $\alpha = 0.6$. It is positive for positive lags, although the conditional defect vanishes at every time in that stationary preparation. Curves in this figure are analytic evaluations rather than Monte Carlo estimates.

11. **Stochastic Control and the Common Variational Framework**

A variational description of probability transport can also be expressed as a stochastic-control problem. The control specifies a change in drift, and its running cost assigns a price to that change. A thermodynamic interpretation requires that this cost, the noise covariance, the energy, and the boundary conditions describe the same evolution. We derive the Hamilton–Jacobi–Bellman equation and the corresponding compatibility identity before using the control representation. Constructing a cost for a known generator and independently determining a physical cost are different tasks.

11.1. *Dynamic Programming and Related Variational Structures.*

11.1.1. *Hamilton-Jacobi-Bellman Structure.*

Consider the controlled diffusion

$$\mathrm{d}X_t = [b(X_t) + u_t]\,\mathrm{d}t + \sqrt{2D}\,\mathrm{d}W_t. \tag{11.1}$$

For the quadratic running cost

$$J_{t,x}(u) = \mathbb{E}_{t,x}\left[\int_t^T \left(\frac{1}{2}|u_s|^2 + V(X_s)\right)\,\mathrm{d}s + G(X_T)\right], \tag{11.2}$$

define

$$\phi(t,x) = \inf_u J_{t,x}(u). \tag{11.3}$$

Under standard dynamic-programming assumptions, as in standard stochastic-control treatments such as [105], the Hamilton-Jacobi-Bellman equation is

$$-\partial_t\phi = D\Delta\phi + b\cdot\nabla\phi - \frac{1}{2}|\nabla\phi|^2 + V. \tag{11.4}$$

For $b = 0$ and the Cole-Hopf substitution

$$\phi = -2D\log\psi, \tag{11.5}$$

one obtains

$$\partial_t\psi = -D\Delta\psi + \frac{V}{2D}\psi. \tag{11.6}$$

This is a real heat-type equation. It is not the real-time Schrodinger equation. Any Wick rotation is a formal analytic continuation and does not constitute a physical derivation of quantum mechanics.

11.1.2. *Nelson Stochastic Mechanics.*

Nelson's stochastic mechanics [77] uses a real positive Brownian diffusion coefficient proportional to

$$\frac{\hbar}{2m}. \tag{11.7}$$

The diffusion is real and positive. Its relation to $\hbar$ is part of the stochastic-mechanics construction, not a consequence of the classical thermal model studied here.

11.1.3. *Measurable Selection in Stochastic Control.* The existence of a value function and the existence of a measurable exact optimizer are distinct issues. Let U be a Polish control space and let

$$J : \Omega \times U \to \mathbb{R} \cup \{+\infty\} \tag{11.8}$$

be jointly measurable. A safe exact-selection framework additionally assumes that $u \mapsto J(\omega, u)$ is lower semicontinuous and that the sublevel sets are compact or inf-compact. If the argmin multifunction is nonempty and measurably selectable, one can choose a measurable optimizer. Without exact attainment one instead works with measurable ε-optimal controls satisfying

$$J(\omega, u_\varepsilon(\omega)) \le \inf_{u \in U} J(\omega, u) + \varepsilon. \tag{11.9}$$

Coercivity alone does not imply continuity, and no such implication is used.

11.1.4. *Relation to GENERIC.* The decomposition of nonequilibrium dynamics into reversible and irreversible sectors has a substantial prior literature. In particular, the GENERIC framework explicitly couples reversible and irreversible evolution and discusses thermal fluctuations [39] and [84]. Therefore the present manuscript does not claim novelty for the abstract decomposition $L = A + S$ itself. The proposed contribution is the theorem architecture connecting molecular stochastic dynamics, a precisely formulated minimum-dissipation sector, Gibbs invariance, Markov relative-entropy contraction, thermodynamic free energy, four distinct irreversibility statements, path/history geometry, recurrence obstructions, and infinite-dimensional tests.

11.2. *A common variational origin with a closed stochastic realization.*

11.2.1. *What must be shared before a claim of unification is meaningful.* An action determines stationary field configurations; a stochastic generator determines a law of evolving configurations. These are different mathematical objects. To connect them, fix a finite regulator, a gauge treatment, and local coordinates z on the admissible configuration space. Let $S(z)$ be the regulated master energy, $\theta > 0$ the energy scale of fluctuations, and $M(z) = M(z)^T$ a positive mobility. Positivity refers to the physical reduced directions, not to the indefinite gravitational DeWitt form. The reference volume is declared before a probability density is written. In this section it is coordinate Lebesgue volume; a volume weight is included below.

For a joint residual $R(z, u)$, a single running cost may be defined by

$$q(z, u) = R(z, u)^T H(z) R(z, u), \qquad \ell_0(z, u) = \frac{1}{4} q(z, u), \qquad H = H^T \succ 0. \tag{11.10}$$

The components of R must first be divided by their physical scales so that q has consistent units. Cross blocks are permitted only between compatible representations. For $H = \left(\begin{smallmatrix} H_1 & C \\ C^T & H_2 \end{smallmatrix}\right)$ with positive diagonal blocks, completing the square gives

$$r^T H r = \big(r_2 + H_2^{-1} C^T r_1\big)^T H_2 \big(r_2 + H_2^{-1} C^T r_1\big)$$

$$+ r_1^T \big(H_1 - C H_2^{-1} C^T\big) r_1. \tag{11.11}$$

Thus positivity is equivalent to a positive Schur complement. Eliminating the second residual changes the first sector's stiffness. This is a real cross-sector restriction after H has been fixed; it does not determine H from a symmetry that leaves several invariant metrics possible.

For the direct product of two distinct simple gauge algebras, a bilinear invariant pairing between their adjoint representations vanishes: invariance under the first factor forces every cross-functional to annihilate its commutators, and a simple algebra equals its commutator algebra. Shared scalars, spacetime geometry, matter representations, and the reduced mobility can couple the sectors without violating this restriction.

11.2.2. *An exact compatibility theorem for cost, drift, and Gibbs law.* The following construction supplies a precise version of the statement that one cost can produce dynamics and statistical equilibrium. Its strength is an exact calculation; its restriction is that the cost and generator must satisfy the displayed compatibility relation. Work on a compact torus, or on a smooth bounded domain with reflecting conditions. All coefficients are smooth, M is uniformly positive, and

$$\pi = Z^{-1} e^{-S/\theta}, \qquad \nabla \cdot (\pi c) = 0, \qquad c \cdot n = 0 \tag{11.12}$$

at a reflecting boundary. An admissible gradient must also satisfy the boundary condition of the value equation.

Proposition 11.1 (Cost–generator compatibility). *Consider the controlled generator*

$$L^u f = (c + \theta \nabla \cdot M + u) \cdot \nabla f + \theta M : D^2 f \tag{11.13}$$

and the cost $\ell = W + \frac{1}{2} u^T M^{-1} u$. *If*

$$W = \lambda + \frac{1}{2} \nabla S^T M \nabla S - c \cdot \nabla S - \theta \nabla \cdot (M \nabla S), \tag{11.14}$$

then $V = S$ *solves the ergodic HJB equation* $\lambda = \inf_u \{\ell + L^u V\}$, *and the minimizing feedback is* $u_* = -M \nabla S$. *Subject to the usual verification integrability, transversality, and boundary conditions, this is optimal. Its invariant law is* π, *and its density current is*

$$j_p = pc - \theta p M \nabla \log(p/\pi). \tag{11.15}$$

Proof. Substitution of $V = S$ gives

$$\ell + L^u S - \lambda = \frac{1}{2} (u + M \nabla S)^T M^{-1} (u + M \nabla S). \tag{11.16}$$

The unique minimizer follows from positive definiteness. Applying Itô's formula and taking expectations makes the integrated right side the excess cost, up to the endpoint term $-\mathbb{E}[S(Z_T) - S(Z_0)]$. On a compact space that endpoint divided by T tends to zero; on a noncompact space it is a separate transversality condition. The noise covariance is $2\theta M$. Its forward current is $bp - \theta \nabla \cdot (Mp)$, which simplifies to (11.15). At $p = \pi$ this is πc, whose divergence vanishes by (11.12). □

Section 4 gives an independent Hamiltonian realization of constant-mobility branches on the torus and in a confined Euclidean space, with no circulation. It does not derive arbitrary $M(z)$, the circulation c, or the residual metric H from the master action. In particular, solving (11.14) for W after choosing S and M is an inverse construction. It verifies a compatible control realization, but does not independently explain why the physical running cost has that form. Identical notation cannot replace the bath preparation, scale limits, constraint propagation and independently fixed physical clock needed for a field realization. A Lorentzian action is not a thermal energy, and its indefinite kinetic form is not a positive bath mobility.

The potential W in this proposition is constructed, not independently derived from a microscopic field theory. Therefore the result closes a specified realization and gives a test for any proposed independently derived cost. It cannot prove that arbitrary residual costs automatically generate the same Gibbs law. In particular, the master energy, running cost, value function, and mechanical Hamiltonian may coincide only through an explicit relation. At a reflecting endpoint this distinction is essential: for the half-line potential $\Phi(M) = M$, the candidate $V = \Phi$ fails the Neumann condition $V'(0) = 0$. Its Gibbs diffusion is well defined, but the displayed reflected HJB verification cannot use that candidate. A compatible value must obey the boundary condition, or the cost must include the appropriate boundary-local-time term. Boundary data are part of the common-origin test.

If the reference volume is $w(z)\,dz$, replace the coordinate energy in this calculation by $U = S - \theta \log w$. The probability density relative to dz is then $Z^{-1} w e^{-S/\theta}$. Equivalently one can formulate the generator in weighted divergence form. This correction prevents a change of coordinates from being mistaken for a change of physical equilibrium.

11.2.3. *Free-energy loss and maintained irreversibility.* Let $f = p/\pi$, let $\mathcal{D}(p\|\pi) = \int p \log f \, dz$, and assume positive smooth densities with finite weighted Fisher information. A direct integration by parts yields

$$\begin{aligned} \frac{d}{dt}\mathcal{D}(p_t\|\pi) &= \int j_p \cdot \nabla \log f \, dz \\ &= -\theta \int p \, \nabla \log f^T M \nabla \log f \, dz. \end{aligned} \tag{11.17}$$

Indeed, the circulation contribution is $\int \pi c \cdot \nabla f = -\int f \nabla \cdot (\pi c) = 0$. Expanding the current square gives a second, distinct identity:

$$\begin{aligned} \frac{1}{\theta} \int \frac{j_p^T M^{-1} j_p}{p} \, dz &= \frac{1}{\theta} \int p \, c^T M^{-1} c \, dz \\ &\quad + \theta \int p \, \nabla \log f^T M \nabla \log f \, dz. \end{aligned} \tag{11.18}$$

The two terms measure maintained circulation and relaxation, respectively. The excess free energy is $\theta \mathcal{D}(p\|\pi)$; it decreases even when the limiting law carries a nonzero circulation. At stationarity its derivative is zero while the first term may remain positive.

For even state variables, a stationary law and a fixed-drive reversal, assume the forward and reverse path laws are mutually absolutely continuous and the Girsanov energy is finite. The reversed drift differs by $2c$. Consequently the path relative-entropy rate is

$$\lim_{T\to\infty}\frac{1}{T}\mathcal{D}(P_{[0,T]}\|P^R_{[0,T]})=\frac{1}{\theta}\int \pi c^T M^{-1}c\,dz. \tag{11.19}$$

The factor follows from $\frac{1}{2}(2c)^T(2\theta M)^{-1}(2c)=c^TM^{-1}c/\theta$. For odd variables or reversed external parameters, the reverse generator must first be conjugated by the declared parity map; c alone is no universal irreversible current. Singular noise limits may destroy absolute continuity.

If a logarithmic Sobolev inequality has the convention $\mathcal{D}(p\|\pi)\le C_{\mathrm{LS}}I_M(p\|\pi)/2$, (11.17) implies decay at rate $2\theta/C_{\mathrm{LS}}$. Gibbs invariance, attraction of laws, nonzero stationary path asymmetry, and regularity of individual spacetime geometries remain separate claims. This separation permits an irreversible realization without incorrectly declaring every equilibrium diffusion irreversible.

11.2.4. *Two nonlinear objectives that must not be confused.* For a dimensionless residual square and $\kappa\ge 0$, the nonlinear running penalty

$$\varphi_\kappa(q)=\frac{e^{\kappa q}-1}{4\kappa},\qquad \varphi_0(q)=\frac{q}{4} \tag{11.20}$$

has derivative $e^{\kappa q}/4$. Its ordinary expected-integral objective therefore changes both the feedback and the variational field equations. In particular,

$$\delta\int\varphi_\kappa(q)=\frac{1}{4}\int e^{\kappa q}\,\delta q, \tag{11.21}$$

with variations of the measure and state dependence of H added where present. The factor cannot be silently omitted in a low-energy recovery. For bounded $0\le q\le Q$, the expansion $\varphi_\kappa(q)=q/4+\kappa q^2/8+O(\kappa^2Q^3e^{\kappa Q})$ specifies a controlled weak-nonlinearity regime.

By contrast, for $\kappa>0$ the entropic risk objective

$$V_\kappa(t,z)=\frac{1}{\kappa}\log\inf_u\mathbb{E}_{t,z}\exp\left[\kappa\left(\int_t^T\ell\,ds+G(Z_T)\right)\right] \tag{11.22}$$

has, when finite and smooth, the equation

$$0=\partial_tV_\kappa+\inf_u\left\{\ell+b^u\cdot\nabla V_\kappa+\tfrac{1}{2}a:D^2V_\kappa+\tfrac{\kappa}{2}\nabla V_\kappa^Ta\nabla V_\kappa\right\}. \tag{11.23}$$

The extra gradient square comes from differentiating $e^{\kappa V}$, not from putting $e^{\kappa q}$ in the running cost. These models may be studied together, but they are not equivalent. Neither entails a new radiated particle species or a Hawking-spectrum correction without a field equation, a quantized state, and a detector observable. Here κ is scaled so that its product with the accumulated cost is dimensionless. At $\kappa=0$ the objective is defined separately as the ordinary expected cost, when the exponential-moment bounds justify the limit. For $\kappa<0$, minimizing the entropic cost instead requires $\kappa^{-1}\log\sup_u\mathbb{E}e^{\kappa C_u}$, where $C_u=\int_t^T\ell\,ds+G(Z_T)$: the negative prefactor reverses the order. The displayed logarithm of an infimum is therefore restricted to $\kappa>0$.

If a residual contains $\nabla \log p_t$, it depends on the evolving law. A conventional state-space HJB can then be used only with a frozen declared law, followed by a consistency problem, or within an explicitly derived mean-field control system on probability measures. The variation through p_t is part of that system. Treating a score-dependent cost as a law-independent cost would omit a functional derivative.

11.2.5. *Independent projection and observable restrictions.* Let $\mathcal{O}$ be a measurable observation of a path and suppose it commutes with the specified reversal. On standard Borel path spaces, disintegration gives the exact chain rule

$$\begin{aligned}\mathcal{D}(P\|P^R) &= \mathcal{D}(\mathcal{O}_*P\|\mathcal{O}_*P^R)\\ &\quad + \int \mathcal{D}\big(P(\,\cdot\mid y)\|P^R(\,\cdot\mid y)\big)\,(\mathcal{O}_*P)(dy).\end{aligned} \tag{11.24}$$

Finite entropy and the corresponding conditional absolute continuity are assumed. The nonnegative conditional term is hidden irreversibility. An observed fluid current therefore supplies a lower bound on the mother path entropy, not an equality unless conditional sufficiency is proved. This result does not identify information filtering with gravitational holography: no area entropy bound or bulk–boundary algebra follows from disintegration.

Proposition 11.2 (A conditional bound on hidden relative entropy). *Let P, Q be equivalent probability laws on a standard Borel space, let Y be a measurable observation, and assume $D(P\|Q) < \infty$. Write $\Lambda = \log(dP/dQ)$. Suppose that, for Q_Y-almost every y, the conditional essential range of Λ under $Q(\,\cdot\mid y)$ lies in an interval $[a(y), b(y)]$, with measurable finite endpoints. If $\mathbb{E}_P[(b(Y)-a(Y))^2] < \infty$, then*

$$0 \le D(P\|Q) - D(P_Y\|Q_Y) \le \frac{1}{8}\mathbb{E}_P[(b(Y)-a(Y))^2]. \tag{11.25}$$

The statement does not require the observed process to be Markovian.

Proof. Disintegrate Q and define, conditionally on $Y = y$,

$$K_y(t) = \log \int e^{t\Lambda}\, Q(d\omega \mid y), \qquad 0 \le t \le 1.$$

The conditional bound makes this function twice differentiable. At $t = 1$, $e^{K_y(1)} = dP_Y/dQ_Y(y)$, and the tilted conditional law $e^{\Lambda - K_y(1)}Q(d\omega \mid y)$ is $P(d\omega \mid y)$. Thus its relative entropy is $K_y'(1) - K_y(1)$, since $K_y(0) = 0$. For the intermediate tilt $Q_{y,t}$, differentiation gives

$$K_y'(t) = \mathbb{E}_{Q_{y,t}}\Lambda, \qquad K_y''(t) = \mathrm{Var}_{Q_{y,t}}\,\Lambda.$$

Every probability law supported in $[a, b]$ has variance at most $(b-a)^2/4$. To verify this bound, average $(X-a)(b-X) \ge 0$, subtract the square of the mean, and maximize $(\mathbb{E}X - a)(b - \mathbb{E}X)$

over the interval. Integration by parts consequently gives

$$K_y'(1) - K_y(1) = \int_0^1 tK_y''(t)\,dt \le \frac{(b(y)-a(y))^2}{8}.$$

The relative-entropy chain rule and integration with respect to P_Y prove the assertion. Nonnegativity follows from the conditional relative entropy, rather than from a sign assumption on Λ. □

In a time-reversal application Q is the specified reversed experiment, and the observation must commute with the declared reversal. The result quantifies approximate sufficiency of an observation: little variation of the full log likelihood among hidden states with the same observation implies little hidden entropy. It does not establish that variation bound from a small error in a one-time density or a fitted drift. Gaussian path likelihoods often have unbounded conditional range, so the proposition is not asserted to apply to every diffusion.

If $\Lambda = g(Y) + r$ and $|r| \le \varepsilon$, the bound becomes $\varepsilon^2/2$. This is a finite-time statement. A rate conclusion requires a bound on $\mathbb{E}_P[(b_T - a_T)^2]/T$; dividing a bound that grows as T^2 by T does not give uniform long-time control.

For a finite check, let Q be uniform on $(y,z) \in \{-1,1\}^2$ and let $P(y,z) \propto \exp(\gamma y + \varepsilon z)Q(y,z)$. Observation of y alone gives

$$D(P\|Q) - D(P_Y\|Q_Y) = \varepsilon\tanh\varepsilon - \log\cosh\varepsilon \le \varepsilon^2/2.$$

Summing the four probabilities proves the equality directly. Its expansion is $\varepsilon^2/2 - \varepsilon^4/4 + O(\varepsilon^6)$, so the leading quadratic coefficient in the general bound cannot be improved. This finite likelihood example checks the information estimate; it is not an experimental measurement of thermodynamic entropy production.

A second bridge concerns evolution. If P_N is a field projection, L the mother generator, and L_N a proposed reduced generator, define

$$\mathfrak{d}_N\phi = L(\phi\circ P_N) - (L_N\phi)\circ P_N. \tag{11.26}$$

For $v(s,y) = e^{(T-s)L_N}\phi(y)$, Dynkin's formula gives

$$\mathbb{E}\phi(P_N Z_T) - \mathbb{E}\phi(Y_T) = \int_0^T \mathbb{E}\big[\mathfrak{d}_N v(s,\cdot)(Z_s)\big]ds, \tag{11.27}$$

for matching projected initial data and adequate domain and martingale conditions. A uniform bound δ_N on the integrand gives $T\delta_N$. Independent microscopic derivation means controlling this defect with coefficients fixed from the mother model. A fitted fluid closure is a different, useful, task.

11.2.6. *Dynamic programming, the maximum principle, and stochastic symmetry.* For a finite-horizon cost $\mathbb{E}[\int \ell\,dt + G]$, the HJB equation is $V_t + \inf_u\{\ell + b\cdot V_z + \frac{1}{2}a : D^2V\} = 0$. Under differentiability and verification assumptions, the maximum principle uses the same ℓ, b, σ, with

Hamiltonian $H_{\mathrm{SMP}} = \ell + p^T b + \mathrm{tr}(q^T \sigma)$, and

$$dp = -\partial_z H_{\mathrm{SMP}}\, dt + q\, dW, \qquad p_T = \nabla G(Z_T). \tag{11.28}$$

For control-independent σ and a sufficiently smooth value function, $p_t = \nabla V(t, Z_t)$ and $q_t = D^2 V(t, Z_t)\sigma(Z_t)$. The stochastic symmetry formulation has a prior Bellman/contact-symmetry theory [24]. These identities require a third spatial derivative in a classical Itô proof. They do not identify the adjoint with physical momentum.

For example, suppose a constant translation direction η leaves the drift, covariance, running cost, and admissible controls invariant on a domain without boundary. Differentiate the HJB equation along η; the envelope condition cancels derivatives of the optimizing control. Then

$$(\partial_t + L^{u_*})(\eta \cdot \nabla V) = 0. \tag{11.29}$$

Itô's formula makes $\eta \cdot \nabla V(t, Z_t)$ a local martingale. Square integrability makes it a true martingale. Reflection adds its normal derivative times the boundary regulator; a vanishing value-function normal derivative does not by itself eliminate the derivative of this charge. Hence a symmetry charge may have an explicit boundary balance.

The deterministic limit gives the corresponding control symmetry statement. It recovers the usual mechanical Noether charge only after the control problem is shown equivalent to a regular mechanical Lagrangian problem with its physical time and boundary data. The existence of this stochastic symmetry theorem cannot uniquely select a common scalar coupling: many distinct symmetry-invariant positive costs satisfy the same regularity conditions.

11.2.7. *From local consistency to a physical completion.* On a low-energy covariant branch, gauge invariance gives the appropriate current identities and diffeomorphism invariance gives the matter conservation identity on the coupled field equations. With external driving, the reservoir stress or work flux must be included. A path-cost minimizer, by itself, is not a solution of the gravitational constraints. These constraints must either be imposed on the admissible state space or propagated by the proposed generator. If $C(z) = 0$ defines a smooth constraint and the noise vector fields are σ_α, Itô invariance requires

$$DC\, \sigma_\alpha = 0, \qquad DC\, b + \tfrac{1}{2} a : D^2 C = 0 \quad \text{on } \{C = 0\}. \tag{11.30}$$

The first relation prevents Brownian escape; the second includes the noise-induced drift of a curved constraint surface.

The completion problem consequently has a definite order. Specify a single action and its allowed residual couplings; derive or match a tangent positive generator; prove its invariant law and coercivity; control the physical projection; and determine which measurements identify the remaining inputs. A classical probability model may satisfy all these steps while retaining the Bell-local CHSH bound. Complex quantum amplitudes, noncommuting observables, physical states,

and a four-dimensional interacting limit require additional construction. Likewise, convergence of a probability law on Schwarzschild or Kerr parameters does not change the curvature of a sample geometry.

For a bounded stopping rate $0 \le h \le h_*$ up to a finite geometric endpoint τ, conditional survival is $\exp[-\int_0^\tau h(Z_s)ds] \ge e^{-h_*\tau} > 0$. Thus killing a controlled path cannot supply a regular interior extension. An extension needs local field equations, a regular metric, matching data, and an extendibility or geodesic-completeness argument. This is a structural requirement, not a matter of choosing a larger penalty.

12. **A conditional thermodynamic reduction of the regulated mother process**

The thermodynamic paper uses the same logical architecture as the unified field and fluid papers, but it proves the thermodynamic statement only on a declared stochastic class. Let $r = (a, N, V)$ denote the finite regulator, let S_r be the regulated master energy, and let $M_r = M_r^{\mathsf{T}} \succ 0$ be the mobility inherited from the master field metric. The correspondence with the unified-field notation is conditional and is fixed before the thermodynamic calculation. If $m_r(x)\,\mathrm{d}x$ is the reduced reference volume and E_r, s_r are the energy and dimensionless entropy components, then the Gibbs identification is

$$S_r = E_r - \theta s_r + C_r, \qquad \pi_r(x) = Z_r^{-1} m_r(x) e^{-S_r(x)/\theta}.$$

Here s_r is a fixed state function (for example, a regulated degeneracy or entropy potential) determined before the evolving probability p_t is introduced; it is not the Shannon entropy of p_t. This distinction keeps the Gibbs reference independent of the law whose dissipation is being proved. Accordingly, in the free-energy identity below the Hamiltonian-like quantity is S_r relative to the fixed reference $m_r\,\mathrm{d}x$; E_r and s_r are not separately varied with p_t. The formulas below use an affine reduced chart with $m_r \equiv 1$. In a non-flat chart one must replace $\operatorname{div} M_r$ by $\beta_{r,i} = m_r^{-1}\partial_j(m_r M_r^{ij})$, and all densities and boundary terms must be interpreted with respect to $m_r\,\mathrm{d}x$. This is the finite-coordinate specialization of the master generator, not an additional field equation. Likewise, c_r denotes the projection of a reversible or maintained transport drift only after the projection has been shown to preserve the reduced Gibbs measure. A candidate such as the $\mathbb{L}_r \nabla E_r$ sector is admissible only when its projected drift satisfies the weighted invariance condition below; antisymmetry of $\mathbb{L}_r$ alone is insufficient if s_r, the reference density, or the projection is nontrivial. The common process is

$$\mathrm{d}X_t = \big[-M_r \nabla S_r + \theta \operatorname{div} M_r + c_r\big](X_t)\,\mathrm{d}t + \sqrt{2\theta M_r(X_t)}\,\mathrm{d}W_t. \tag{12.1}$$

Assume $\pi_r = Z_r^{-1} e^{-S_r/\theta}$, finite normalization, the stated periodic or reflecting boundary conditions, and $\nabla \cdot (\pi_r c_r) = 0$. Direct substitution gives the current

$$j_r[p] = p c_r - \theta p M_r \nabla \log(p/\pi_r). \tag{12.2}$$

Consequently, for smooth positive densities in the generator domain,

$$\frac{\mathrm{d}}{\mathrm{d}t}\left[\theta\,\mathrm{KL}(p_t\|\pi_r)\right] = -\theta^2\int p_t\nabla\log(p_t/\pi_r)^{\mathsf{T}}M_r\nabla\log(p_t/\pi_r)\,\mathrm{d}x \le 0. \tag{12.3}$$

The circulation term drops out by weighted incompressibility. Equation (12.3) is therefore the second-law reduction of the common process, not a separate entropy penalty appended after the fluid or geometric calculation.

The statement remains an ensemble theorem. It does not say that every sample path has a monotonically increasing entropy, nor that a stationary Gibbs density is necessarily an equilibrium path law. If $c_r \neq 0$, the same stationary density can support a maintained current. Under a declared physical parity map and pathwise absolute continuity, the forward–reverse entropy-rate calculation gives the housekeeping contribution

$$\sigma_r = \frac{1}{\theta}\int \pi_r c_r^{\mathsf{T}} M_r^{-1} c_r\,\mathrm{d}x \ge 0 \tag{12.4}$$

in the all-even convention; the parity-corrected expression must be used when momenta or rotation variables are odd.

For the constant-mobility branches with $c_r = 0$, both on the torus and in the stated confined Euclidean setting, the reservoir construction of Section 4 supplies a microscopic realization. The same calculation does not yet produce the full state-dependent, circulating, gauge-constrained field process. Its covariance, response, normalizable equilibrium measure and projection must be derived on the physical state space before the finite identity is interpreted as a microscopic field-theory result. Preparation at a distinguished boundary time explains a conditional relaxation direction; it does not select an absolute orientation from an equilibrium density alone.

The mother-process interpretation is thus a conditional bridge. It becomes a physical unification only if S_r, M_r, c_r, the bath temperature, the clock and the observation map are fixed by the same model and are not reselected for each reduced experiment. The continuum and quantum limits are not implied by the finite-regulator identity.

12.1. *The projected second law and its physical normalization.* The Galerkin energy budget and the projected entropy law require different calculations. Suppose the mother process has invariant probability π_r, the observation $U = \Pi_N(X)$ is autonomous Markov, and its well-posed martingale problem has the generator fixed by the drift and covariance matching identities. Write $\pi_N = (\Pi_N)_{\#}\pi_r$. If $X_0 \sim \pi_r$, then $X_t \sim \pi_r$ and $U_t \sim \pi_N$; hence π_N is invariant for the projected semigroup. The same Markov kernel acts on every admissible initial law, so data processing gives

$$\mathrm{KL}(p_t^N\|\pi_N) \le \mathrm{KL}(p_s^N\|\pi_N), \qquad t \ge s. \tag{12.5}$$

This conclusion needs neither detailed balance nor a quadratic Gibbs law for the resolved velocity.

For a projected diffusion with covariance $Q_N(U)$, let $f_t = dp_t^N/d\pi_N > 0$. Assume that the logarithmic chain rule, generator adjoint relation, and boundary integrations are valid, with finite

entropy and Fisher integral. Invariance and

$$L_N(f\log f) = (1+\log f)L_N f + \frac{1}{2f}\nabla f^{\mathsf{T}} Q_N \nabla f$$

give, using $\partial_t f_t = L_N^\dagger f_t$ in $L^2(\pi_N)$,

$$\frac{d}{dt}\,\mathrm{KL}(p_t^N\|\pi_N) = -\frac{1}{2}\int f_t\,\nabla\log f_t^{\mathsf{T}} Q_N \nabla\log f_t\,d\pi_N \le 0. \tag{12.6}$$

Indeed, $\int f_t L_N \log f_t\,d\pi_N$ is the entropy derivative, and $L_N\log f = f^{-1}L_N f - (2f^2)^{-1}\nabla f^{\mathsf{T}} Q_N \nabla f$, whose first term integrates to zero after multiplication by f. This derivation avoids an unjustified assumption that the projected generator is symmetric.

If $\pi_N = Z_N^{-1} e^{-E_N/(k_B T)}$ relative to the declared reference measure at a calibrated constant temperature, the excess isothermal free energy is $k_B T\,\mathrm{KL}(p^N\|\pi_N)$. Thus $-T^{-1}d\mathcal{F}_N/dt \ge 0$ is the corresponding relaxation contribution to the entropy-production rate. For a maintained nonequilibrium stationary law, that contribution need not equal total entropy production: external work and housekeeping production must also be included. A stationary law need not be a Gibbs law for the kinetic energy. Marginalizing a Gibbs measure generally produces a potential of mean force, not the original microscopic energy evaluated at a projection.

These results establish a finite Galerkin second law when the projected generator, covariance, and invariant measure really are inherited from the same mother process. They do not establish an unconditional second law for arbitrary reversible microscopic dynamics or a continuum turbulence theorem. The latter would require a compatible family of generators, uniform bounds, tightness, and control of entropy and boundary terms in the limit.

12.2. *Constraint, clock, and projection compatibility.* A common master energy becomes a physical interface only after the admissible state space and the observed dynamics have been fixed. The current-contraction theorem supplies a positive quadratic cost for a specified observation map. It does not prove that a proposed field equation preserves its constraints or has the same observed noise. We state the additional finite-regulator conditions explicitly.

Let a regular constraint surface be $\mathcal{C}_r = \{x : \chi_r(x) = 0\}$, where $D\chi_r$ has full rank on $\mathcal{C}_r$. For an Itô equation $\mathrm{d}X = b_r\,\mathrm{d}t + \Sigma_r\,\mathrm{d}W$ with $a_r = \Sigma_r\Sigma_r^{\mathsf{T}}$, preservation of each constraint requires

$$D\chi_r\,\Sigma_r = 0, \qquad D\chi_r\,b_r + \tfrac{1}{2}a_r : D^2\chi_r = 0 \quad \text{on } \mathcal{C}_r. \tag{12.7}$$

The contraction in the second equation is taken separately for each component of χ_r. These identities follow by applying Itô's formula to $\chi_r(X_t)$ and setting its quadratic variation and drift to zero. Under smooth local Lipschitz coefficients on a regular embedded manifold, they are the tangency conditions for stochastic invariance, with completeness or nonexplosion supplied separately. For a unit-sphere constraint $\chi(x) = |x|^2 - 1$, they become $x^{\mathsf{T}}\Sigma = 0$ and $2x\cdot b + \mathrm{Tr}\,a = 0$. Tangent noise without the normal drift correction is insufficient.

On the physical reduced manifold with volume measure vol_r, a coordinate-independent thermal generator has the divergence form

$$L_r f = c_r \cdot \nabla f + \theta \pi_r^{-1} \operatorname{div}(\pi_r M_r \nabla f), \qquad \pi_r = Z_r^{-1} e^{-S_r/\theta}. \tag{12.8}$$

Here M_r is positive on the tangent space, and both gradient and divergence use the declared geometry and volume. If $\operatorname{div}(\pi_r c_r) = 0$, integration by parts gives

$$\frac{\mathrm{d}}{\mathrm{d}t} D(\rho_t \| \pi_r) = -\theta \int \rho_t |\nabla \log(\rho_t/\pi_r)|^2_{M_r} \, \mathrm{dvol}_r.$$

This finite identity requires a conservative realization and the appropriate boundary conditions. It does not identify a positive tangent mobility with an indefinite Lorentzian field metric.

For a smooth physical observation $Y = \Pi_r(X)$, Itô's formula gives the drift and covariance

$$\beta_r = D\Pi_r \, b_r + \tfrac{1}{2} a_r : D^2 \Pi_r, \qquad \alpha_r = D\Pi_r \, a_r (D\Pi_r)^{\mathsf{T}}. \tag{12.9}$$

To claim an autonomous observed diffusion, these coefficients must depend only on Y, and the resulting martingale problem must be well posed. Otherwise they are hidden-state-dependent coefficients. Conditional averaging can produce a one-time marginal equation, but does not generally identify the observed path law with a Markov law. The explicit hidden Gaussian example in Section 3 demonstrates the distinction.

The physical clock is an additional part of the specification. If $dt = a(X_s)\, ds$ with $0 < a_- \le a \le a_+ < \infty$, the generator in the new clock is $a^{-1} L_r$. Its stationary probability is proportional to $a\pi_r$, not generally π_r. Consequently a field interface cannot change the clock and retain an unchanged Gibbs reference without checking this transformation. For generalized detailed balance the clock must also respect the declared parity. These conditions link the present microscopic discussion to the later clock calculations.

The tuple $(S_r, M_r, c_r, \theta, \Theta_r, \Pi_r)$, its volume, constraints, and clock must therefore remain fixed across the experiments claimed to have a common origin. The cost–generator compatibility identity is a precise test of such a tuple. Choosing the running cost after specifying the target generator establishes a compatible control realization, while an independent physical derivation must still explain that cost. Likewise, finite current contraction proves an elimination identity; it does not supply a continuum limit or a universal choice of couplings.

12.2.1. *Observation without exact field closure.* The finite-regulator interface also has an intermediate regime between an autonomous projection and an unspecified reduction. In a regular product coordinate chart with the stated volume and boundary conditions, Theorem 3.4 provides the marginal balance even when the observed process is not Markov. The force and transport terms must both be computed from the same conditional mother law. A force-only cancellation is insufficient when the averaged circulation changes with that law. The resulting bound controls observed free-energy recovery for the regulated diffusion; it does not turn an unclosed field observation

into a closed stochastic field theory. For nonlinear observations or nonproduct constraint volumes, the conditional geometry and its Jacobian must be included before applying the corresponding calculation. The coordinate theorem is not silently extended to all gauge quotients.

The microscopic reservoir realization and the field interface therefore meet at a precisely specified finite generator. Their identification requires the same energy, mobility, parity, clock, volume, observation and noise covariance. A continuum or quantum identification requires additional estimates beyond this finite statement. These conditions preserve the physical content of the proposed common origin while making each necessary comparison testable.

13. **A concrete four-dimensional interacting regulator and its thermodynamic reduction**

The preceding construction is abstract until one declares a finite branch on which every integration variable, coefficient, and boundary condition is visible. This section supplies such a branch. Its purpose is deliberately limited: it gives a fully specified four-dimensional Euclidean regulator with interacting gauge, coframe, and order-parameter variables, and proves the finite-regulator thermodynamic theorem on that branch. It does not identify this regulator with the complete Lorentzian gravitational theory, and it does not claim a regulator-independent quantum limit.

13.1. *Finite four-dimensional state space and mother-data registry.* Let Λ_h be a finite periodic hypercubic lattice approximating the four-dimensional torus $\mathbb{T}^4$. Write $\mathcal{V}_h$, $\mathcal{E}_h$, and $\mathcal{P}_h$ for its vertices, oriented links, and oriented plaquettes. The compact gauge group used at the finite regulator is

$$K = \mathrm{SO}(5) \times \mathrm{SU}(3) \times \mathrm{SU}(2) \times \mathrm{U}(1), \qquad \mathcal{X}_h = K^{\mathcal{E}_h} \times \mathbb{R}^{16|\mathcal{V}_h|} \times \mathbb{R}^{|\mathcal{V}_h|}. \tag{13.1}$$

The first factor contains link variables U_ℓ. The second contains the four-by-four coframe coefficients e_v at each vertex, flattened into $\mathbb{R}^{16}$, and the last contains the scalar/order-parameter values σ_v. The coframe variables in this section are Euclidean regulator coordinates. The oriented nondegenerate sector and its Lorentzian continuation are treated as additional matching conditions below. In this particular finite model, e_v and σ_v are invariant under link gauge transformations. The differences $e_v - e_w$ below are ordinary differences, not covariant differences of local Lorentz vectors. Thus the sixteen variables at a vertex are coordinates for a proposed geometric sector; identifying them with a gravitational coframe requires a further covariant construction. The finite thermal argument does not assume that identification.

All numerical coefficients are recorded before any evolution or comparison with data. The registry is

$$\mathscr{R}_h = \big(\beta_a, \alpha, \eta, \kappa_e, m_e, \lambda_e, f, m_\sigma, \theta, e_\star, \sigma_\star, \Gamma_h\big), \tag{13.2}$$

where $\beta_a, \kappa_e, m_e, \lambda_e, f, m_\sigma, \theta > 0$, $\eta, \alpha \geq 0$, and Γ_h is a fixed positive mobility matrix. In the unified-field interpretation each entry of $\mathscr{R}_h$ must be the value of a specified pairing, regulator, vacuum datum, or bath coupling in the mother data. A value selected after inspecting an observable is a fit and is not counted as a mother prediction. The graph, the positive symmetric edge weights a_{vw}, and the unitary representations R_a of dimensions d_a are also fixed data. Each geometric plaquette is assigned one orientation and one anchor vertex $v(p)$.

For a plaquette p let $U_{p,a}$ be the ordered product in the ath group factor and define

$$k_p(U) = \sum_a \beta_a \big[d_a - \operatorname{Re}\operatorname{tr} R_a(U_{p,a}) \big] \geq 0. \tag{13.3}$$

Let

$$w_v(e, \sigma) = \exp(-\alpha\sigma_v) \left[1 + \eta \, \frac{\|e_v - e_\star\|^2}{1 + \|e_v - e_\star\|^2} \right]. \tag{13.4}$$

The coframe factor lies in $[1, 1+\eta]$. The full weight is positive but is unbounded as $\sigma_v \to -\infty$ when $\alpha > 0$. Its multiplication by $k_p \geq 0$ preserves the lower bound on the action; boundedness of the full weight is not needed for the partition integral. With each unoriented edge counted once, set

$$\begin{aligned} S_h(U, e, \sigma) = {} & \sum_{p \in \mathcal{P}_h} w_{v(p)}(e, \sigma) k_p(U) + \frac{\kappa_e}{2} \sum_{\{v,w\}} \|e_v - e_w\|^2 \\ & + \frac{m_e^2}{2} \sum_v \|e_v - e_\star\|^2 + \frac{\lambda_e}{4} \sum_v \|e_v - e_\star\|^4 \\ & + \frac{f^2}{2} \sum_{\{v,w\}} a_{vw} (\sigma_v - \sigma_w)^2 + \frac{m_\sigma^2 f^2}{2} \sum_v (\sigma_v - \sigma_\star)^2. \end{aligned} \tag{13.5}$$

This is a specified finite candidate for matching to the positive norm-square branch of the extended curvature. The plaquette term is the gauge-curvature block, the coframe terms are the regulated geometric block, and the scalar terms are the order-parameter block. The common weight in (13.4) is the retained mixed interaction. Equality with the primitive mother norm is a matching condition on the selected pairing and regulator; it is not obtained merely by reusing the word "action". If that matching condition is established, the displayed terms must all be accounted for by the same primitive pairing. The finite theorem below holds for the displayed action without presupposing that the matching has been proved.

13.2. *Exact finite generator and Gibbs law.* Equip $K^{\mathcal{E}_h}$ with the product bi-invariant metric and use the Euclidean metric on the coframe and scalar factors. Let ∇_h and div_h denote the corresponding gradient and divergence. For the fixed temperature parameter $\theta > 0$ define

$$\mathcal{L}_h F = \theta \operatorname{div}_h(\Gamma_h \nabla_h F) - \langle \Gamma_h \nabla_h S_h, \nabla_h F \rangle_h, \qquad \Gamma_h = \Gamma_h^{\mathsf{T}} \succ 0. \tag{13.6}$$

The intrinsic form includes the metric-volume drift; writing an Itô equation in local coordinates without that drift would change the invariant measure. Here a fixed matrix on the group factors

means its components in a fixed product frame of left-invariant and Euclidean vector fields. More generally, Γ_h may be a smooth symmetric bundle map satisfying $\gamma_- I \le \Gamma_h \le \gamma_+ I$ for fixed positive constants. These are assumptions at a fixed regulator, not bounds uniform in h.

THEOREM 13.1 (Finite four-dimensional interacting equilibrium). *For every fixed finite lattice, every registry satisfying* (13.2) *and the fixed geometric data above, the diffusion generated by* (13.6) *is nonexplosive and has the unique invariant probability*

$$\pi_h(\,\mathrm{d}U\ \mathrm{d}e\ \mathrm{d}\sigma) = Z_h^{-1}\exp[-S_h(U,e,\sigma)/\theta]\,\mathrm{d}U\ \mathrm{d}e\ \mathrm{d}\sigma, \qquad 0 < Z_h < \infty. \tag{13.7}$$

It is reversible with respect to π_h, and all polynomial moments of the Euclidean variables are finite.

Proof. The compact gauge factor has finite Haar volume. Since $k_p \ge 0$ and the quadratic and quartic coframe terms are nonnegative, the integrand in (13.7) is bounded above by a product of Gaussian–quartic integrable factors in (e,σ). Restricting these variables to a compact box gives a strictly positive lower bound, so $0 < Z_h < \infty$. Smoothness and uniform ellipticity on each bounded coordinate domain give local existence and pathwise uniqueness. For nonexplosion, we use an energy argument that does not require an unproved comparison between exponential derivatives and polynomial confinement. Write $z = (e - e_\star, \sigma - \sigma_\star)$ and choose smooth cutoffs $\chi_R(z) = \chi(z/R)$ with $0 \le \chi_R \le 1$, $\chi_R \to 1$, and $|\nabla\chi_R| \le C/R$. The gradient form on $L^2(\pi_h)$ is closable because its density is smooth and positive and its coefficients are locally uniformly elliptic. For its closure $\mathcal{E}_h$, finite total mass gives

$$\|1 - \chi_R\|_{L^2(\pi_h)} \to 0, \qquad \mathcal{E}_h(\chi_R,\chi_R) \le \theta\gamma_+ C^2/R^2 \to 0. \tag{13.8}$$

Consequently 1 belongs to the closed form domain with zero energy. The associated symmetric semigroup preserves 1, so its diffusion has no killing or explosion for π_h-almost every initial state. Local smooth ellipticity upgrades this to every starting point. Indeed, the minimal diffusion has an absolutely continuous transition law before its lifetime; the Markov property at time $\varepsilon > 0$ then rules out an explosion after ε, and local existence rules out explosion at time zero. The local strong solution therefore extends globally. This is the conservative-form criterion of [34]. Integration by parts gives

$$\int F\mathcal{L}_h G\ \mathrm{d}\pi_h = -\theta\int \langle \nabla_h F, \Gamma_h \nabla_h G\rangle_h\ \mathrm{d}\pi_h, \tag{13.9}$$

which proves reversibility and invariance. Strict positivity of the finite dimensional heat kernel and connectedness imply uniqueness by the standard irreducibility argument. □

13.3. *Second-law identity on the declared branch.* For a law $\rho_t \ll \pi_h$, let $r_t = \mathrm{d}\rho_t/\,\mathrm{d}\mu_h$ and $f_t = \mathrm{d}\rho_t/\,\mathrm{d}\pi_h$, where $\mu_h = \mathrm{d}U\ \mathrm{d}e\ \mathrm{d}\sigma$. Define $F_h[\rho] = \int S_h\ \mathrm{d}\rho + \theta\int \log r\ \mathrm{d}\rho$. Then

Table 2. Synthetic finite-regulator quadrature check. The numbers are not experimental data and are not a continuum test.

Quantity	Value
Estimated partition integral Z_h	12.0485034910
Left side $\int g\mathcal{L}_h g \, \mathrm{d}\pi_h$	−0.3744077978
Right side $-\theta \int \nabla g^{\mathsf{T}} \Gamma \nabla g \, \mathrm{d}\pi_h$	−0.3744077978
Absolute discrepancy	5.6×10^{-17}

THEOREM 13.2 (Finite-regulator entropy production). *For every smooth positive solution of the Fokker–Planck equation generated by (13.6), with finite Fisher information,*

$$F_h[\rho_t] - F_h[\pi_h] = \theta D(\rho_t \| \pi_h), \tag{13.10}$$

$$\frac{\mathrm{d}}{\mathrm{d}t} D(\rho_t \| \pi_h) = -\theta \int r_t \left(\nabla_h \log \frac{\rho_t}{\pi_h} \right)^{\mathsf{T}} \Gamma_h \left(\nabla_h \log \frac{\rho_t}{\pi_h} \right) \mathrm{d}\mu_h \le 0. \tag{13.11}$$

For a physical heat interpretation, additionally assume $\theta = k_B T$ and that S_h is the effective energy in fixed units. The Euclidean regulator and its sampling parameter do not by themselves specify a physical bath or physical time. If the bath coupling obeys local detailed balance and the heat convention is $\dot{Q}_{\mathrm{bath}} = -\,\mathrm{d}\mathbb{E}[S_h]/\,\mathrm{d}t$, then

$$\dot{S}_{\mathrm{tot}} = -T^{-1} \frac{\mathrm{d}F_h[\rho_t]}{\mathrm{d}t} \ge 0. \tag{13.12}$$

Proof. Equation (13.9) gives the symmetric Dirichlet form. Applying it to $f_t = \rho_t/\pi_h$ yields the second line of (13.11); positive definiteness of Γ_h gives the sign. The first line is the exact Gibbs identity and follows by expanding $\log(d\rho_t/d\pi_h)$. The final statement uses the first-law balance and local detailed balance; it is not inferred from Gibbs invariance alone. □

13.4. *Reproducible finite diagnostic.* As a numerical check of the analytic identity, we evaluated the one-plaquette U(1) subbranch with one coframe and one scalar coordinate. The potential was the restriction of (13.5) with $(\theta, \beta, \alpha, \eta, m_e^2, \lambda_e, m_\sigma^2) = (0.8, 1, 0.3, 0.2, 1, 0.1, 1)$ and $\Gamma = \mathrm{diag}(0.7, 0.5, 0.4)$. A tensor-product quadrature on $64 \times 161 \times 161$ points was applied to a smooth test function $g(\vartheta, e, \sigma) = \sin\vartheta + 0.2e^2 + 0.1\sigma e$. The two sides of the Dirichlet identity were computed independently: The corresponding numerical values are reported in Table 2. The angular reference measure in this table is $\mathrm{d}\vartheta$ with total mass 2π; normalizing Haar measure changes Z_h but not either expectation. The discrepancy is a floating-point residual, not a certified bound on quadrature or truncation error. The calculation checks the finite integration-by-parts identity only; it supplies no evidence for a regulator-independent or quantum theory.

13.5. *Relation to Lorentzian and continuum dynamics.* The use of polynomially confined matrix coordinates leaves a geometric integrability issue even at fixed resolution. A matrix can be invertible almost surely while its inverse has no finite first moment.

PROPOSITION 13.3 (Inverse-coframe moments in the finite reference law). *For the Gibbs law* (13.7)*, at every vertex* v *and for every* $r \geq 1$*,*

$$\mathbb{E}_{\pi_h} |\det e_v|^{-r} = \infty, \qquad \mathbb{E}_{\pi_h} \|e_v^{-1}\|_{\mathrm{F}}^r = \infty.$$

These statements persist on conditioning on $\det e_v > 0$*.*

Proof. Choose a rank-three matrix E_0. At least one cofactor is nonzero, so the determinant has nonzero differential there. The inverse function theorem gives local coordinates $(u, y) \in \mathbb{R} \times \mathbb{R}^{15}$ with $u = \det e_v$, with a smooth nonzero change-of-volume factor. Restrict y and all remaining noncompact variables to small compact boxes and the group variables to a set of positive Haar measure. The Gibbs density is continuous and strictly positive on this compact set, including $u = 0$. Its contribution to the first expectation is therefore bounded below by $c \int_{-\varepsilon}^{\varepsilon} |u|^{-r} du = \infty$. The selected cofactor remains bounded away from zero on a smaller box. The inverse-matrix formula consequently bounds one inverse entry below in magnitude by $c'/|u|$, proving the second assertion. On the positive orientation sector the same argument uses $\int_0^{\varepsilon} u^{-r} du$; conditioning divides by a finite positive probability and cannot remove the divergence. □

The singular matrices themselves have zero probability. The divergence comes from their neighborhoods and is compatible with finiteness of all polynomial moments proved above. Interpreting this reference law as a measure on fluctuating nondegenerate geometry therefore requires additional control near singular coframes. A change of measure or action for that purpose must be matched to the mother data and its quantum positivity checked separately.

On this fixed four-dimensional lattice, the same declared action supplies the gauge-curvature energy, the coframe/order-parameter coupling, the Gibbs law, and the entropy-production identity. It is not a proof of the full unified theory. In particular, the following implications remain to be established before a continuum or quantum claim is made:

(1) the oriented nondegenerate coframe sector and Lorentzian continuation must be selected without changing the registry;
(2) the nonlinear Hamiltonian and gauge constraints must close and be preserved for all lattice modes;
(3) estimates uniform in h must give a regulator-independent limit;
(4) a physical interacting Hilbert space, positive inner product, and anomaly-free quantum constraint algebra must be constructed.

The finite theorem connects the declared energy, probability law, and dissipation on the same state space. The next section examines which additional structures can be constructed explicitly and which require further matching to the gravitational theory.

13.6. *An oriented nondegenerate coframe branch.* The inverse-coframe obstruction in Proposition 13.3 is a structural diagnostic of the unconstrained Gaussian-like coframe coordinates. It does

not invalidate the finite Gibbs identity, but it shows that the unconstrained reference law cannot itself be interpreted as a law of integrable inverse geometry. We therefore record one explicit extension that removes this obstruction at fixed regulator. The extension is a new, registered branch of the model; it is not a consequence of the original polynomial action.

Let

$$\mathcal{E}_+ = \{e \in \mathbb{R}^{16} : \det e > 0\}, \qquad \mathcal{X}_{h,+} = K^{\mathcal{E}_h} \times \mathcal{E}_+^{\mathcal{V}_h} \times \mathbb{R}^{|\mathcal{V}_h|}.$$

For a fixed barrier strength $\zeta > 0$, define on this oriented sector

$$B_\zeta(e) = \zeta \sum_{v \in \mathcal{V}_h} (\det e_v)^{-2}, \qquad S_{h,\zeta} = S_h + B_\zeta, \tag{13.13}$$

with $B_\zeta = +\infty$ outside $\mathcal{X}_{h,+}$. The corresponding registry is obtained by appending ζ to (13.2). In particular, fixing ζ is part of the model specification; it is not a posterior correction chosen after looking at an inverse-coframe observable. The barrier is a simple analytic device. A mother-functional construction would have to derive or independently calibrate it.

THEOREM 13.4 (Finite oriented branch and inverse-moment control). *For every fixed finite lattice and every $\zeta > 0$, the measure*

$$\pi_{h,\zeta}(\,\mathrm{d}x) = Z_{h,\zeta}^{-1} \exp[-S_{h,\zeta}(x)/\theta]\,\mathrm{d}x, \qquad x \in \mathcal{X}_{h,+}, \tag{13.14}$$

has $0 < Z_{h,\zeta} < \infty$. The symmetric generator obtained from $S_{h,\zeta}$ and the same positive mobility is conservative on the oriented sector and has $\pi_{h,\zeta}$ as its unique invariant law on the connected component. Every inverse-coframe moment is finite:

$$\mathbb{E}_{\pi_{h,\zeta}}\left[\,|\det e_v|^{-r} + \|e_v^{-1}\|_{\mathrm{F}}^r\,\right] < \infty \qquad (r > 0). \tag{13.15}$$

The entropy identity (13.11) *remains valid with S_h, π_h, and Z_h replaced by $S_{h,\zeta}$, $\pi_{h,\zeta}$, and $Z_{h,\zeta}$.*

Proof. The polynomial confinement in S_h controls the Euclidean variables at infinity, while the factor $\exp[-\zeta(\det e_v)^{-2}/\theta]$ suppresses every approach to the singular hypersurface. In a local chart in which $u = \det e_v$ is one coordinate, the potentially singular integral is bounded by a constant multiple of

$$\int_0^\varepsilon u^{-r} \exp\!\left(-\frac{\zeta}{\theta u^2}\right) \mathrm{d}u = \frac{1}{2}\left(\frac{\zeta}{\theta}\right)^{(1-r)/2} \Gamma\!\left(\frac{r-1}{2}, \frac{\zeta}{\theta\varepsilon^2}\right), \tag{13.16}$$

which is finite for every $r > 0$ (the case $r = 1$ is the finite incomplete Gamma function $\Gamma(0,\cdot)$). A finite atlas and the polynomial tail bound prove both normalization and the determinant part of (13.15). The adjugate formula $e^{-1} = (\operatorname{cof} e)^{\mathsf{T}}/\det e$, together with polynomial moments of the cofactors, gives the Frobenius-norm assertion by Cauchy–Schwarz with a slightly higher determinant moment.

The associated weighted gradient form is locally uniformly elliptic. Cutoff functions that vanish near $\det e = 0$ and outside a large Euclidean ball have both $L^2(\pi_{h,\zeta})$ tails and Dirichlet energy tending to zero. The closed form is therefore conservative, and integration by parts gives the

same Dirichlet identity as in (13.9). Strict positivity of the finite-dimensional heat kernel on the connected oriented sector gives uniqueness. Applying the proof of Theorem 13.2 to this new action proves the final entropy statement. □

The barrier branch has a precise relation to the unbarriered positive-orientation law. Let π_h^+ denote π_h conditioned on $D_h = \{\det e_v > 0 \text{ for every } v\}$, and put

$$a_\zeta = \frac{Z_{h,\zeta}}{Z_{h,0}^+} = \mathbb{E}_{\pi_h^+}[\exp(-B_\zeta/\theta)]\,.$$

Dominated convergence gives $a_\zeta \to 1$ and $\pi_{h,\zeta} \Rightarrow \pi_h^+$ as $\zeta \downarrow 0$. For every bounded observable φ,

$$\left|\mathbb{E}_{\pi_{h,\zeta}}\varphi - \mathbb{E}_{\pi_h^+}\varphi\right| \le 2\|\varphi\|_\infty(1-a_\zeta). \tag{13.17}$$

This convergence is not uniform for inverse observables. In the determinant coordinate, for $r > 1$,

$$\mathbb{E}_{\pi_{h,\zeta}}|\det e_v|^{-r} \asymp \zeta^{(1-r)/2}, \qquad \zeta \downarrow 0, \tag{13.18}$$

up to finite nonzero chart factors; for $r = 1$ the divergence is logarithmic. Thus the barrier provides a finite, geometrically interpretable branch and a controlled weak removal for bounded observables, while explicitly proving that inverse-coframe estimates cannot be passed to the unbarriered limit without a new uniform-integrability argument. This is the exact point at which the finite interface still falls short of a regulator-independent Lorentzian theory.

14. **Identifiable finite models, constrained motion, and positive quantum evolution**

A common variational structure becomes predictive only after its parameters, admissible motions, and observation rules have been fixed. Recovering coefficients from responses does not select those coefficients from first principles. Preserving a constraint does not identify it with a gravitational constraint. Likewise, constructing positive quantum evolution at fixed spatial resolution leaves a separate problem of removing that resolution. We develop explicit constructions that provide a starting point for these three distinct extensions.

14.1. *What the finite responses determine.* Fix the graph, its edge weights and representations, the reference fields $e_\star, \sigma_\star$, and units of field amplitude, energy, and time. Consider (13.2) with constant mobility in the specified product frame. We ask whether different coefficients can give the same complete responses. This inverse problem within a selected model differs from whether primitive mother data select one model and one registry.

An actual configuration variation avoids treating plaquette energies as independent coordinates. Choose a link ℓ contained in $n_\ell > 0$ distinct plaquettes and X_a in one Lie-algebra factor, with $c_a = \operatorname{tr}[dR_a(X_a)^\dagger dR_a(X_a)] > 0$. Vary $U_{\ell,a}(t) = \exp(tX_a)$, set all other links to the identity, and

take constant fields $\sigma = s$ and $\|e - e_\star\|^2/(1 + \|e - e_\star\|^2) = r$. Then

$$Q_a(r,s) := \frac{1}{n_\ell c_a} \frac{\mathrm{d}^2}{\mathrm{d}t^2} S_h(U(t), e, s)\Big|_{t=0} = \beta_a e^{-\alpha s}(1 + \eta r). \tag{14.1}$$

Indeed, either orientation of an incident plaquette gives $d_a - \operatorname{Re}\operatorname{tr} R_a(e^{\pm tX_a}) = c_a t^2/2 + O(t^4)$; the remaining energy terms are independent of t. Consequently

$$\beta_a = Q_a(0,0), \qquad \alpha = -\partial_s \log Q_a(0,s)|_{s=0}, \qquad \eta = \partial_r \log Q_a(r,0)|_{r=0+}. \tag{14.2}$$

The last derivative can equivalently be obtained from a unit-vector coframe variation: $\partial_t^2 Q_a(r(e_\star + tv), 0)|_{t=0} = 2\beta_a \eta$. No extension to negative r is required.

At identity links and reference fields, let L_0, L_a be the unweighted and weighted graph Laplacians, with each edge counted once. The noncompact Hessians and an onsite fourth derivative are

$$H_e = (\kappa_e L_0 + m_e^2 I) \otimes I_{16}, \qquad H_\sigma = f^2 L_a + m_\sigma^2 f^2 I, \qquad \partial^4_{e_{v,i}} S_h = 6\lambda_e. \tag{14.3}$$

The mixed gauge energy vanishes at identity links. An off-diagonal edge entry of H_e identifies κ_e, and a row sum identifies m_e^2. A scalar edge entry with known positive weight identifies f^2; a row sum then identifies $m_\sigma^2 f^2$. Positivity fixes the square roots. This argument does not require a nondegenerate full gauge Hessian.

For temperature and mobility, let $p_h = \mathrm{d}\pi_h/\,\mathrm{d}\mu_h$ be the Gibbs density relative to the fixed volume and choose $S_h(x) \neq S_h(y)$. Then

$$\theta = -\frac{S_h(x) - S_h(y)}{\log p_h(x) - \log p_h(y)}, \qquad \frac{1}{2} \lim_{\Delta t \downarrow 0} \frac{\operatorname{Cov}(\Delta Y \mid Y_t = y)}{\Delta t} = \theta \Gamma_h(y). \tag{14.4}$$

The covariance uses the fixed local frame. Equivalently, the carré du champ, defined as $[\mathcal{L}_h(FG) - F\mathcal{L}_h G - G\mathcal{L}_h F]/2$, equals $\theta\langle \nabla F, \Gamma_h \nabla G\rangle$. These are ideal response and density probes; estimation from noisy finite observations remains a separate inverse problem.

PROPOSITION 14.1 (Finite response identifiability). *If the fixed graph has the stated link and edge probes and all responses are given in fixed units, the coefficients* $(\beta_a, \alpha, \eta, \kappa_e, m_e, \lambda_e, f, m_\sigma, \theta, \Gamma_h)$ *are uniquely determined by the preceding probes. The graph, reference fields, representations, and functional form are held fixed.*

Proof. Equation (14.2) recovers the gauge coefficients and shared couplings. Edge entries, row sums, and fourth derivatives in (14.3) recover the confinement and edge coefficients. Since $f > 0$, division recovers m_σ^2. Equation (14.4) then gives θ and Γ_h. Two registries with the same probes therefore coincide. This does not select the graph, vacuum, or group from primitive data. □

Absolute energy calibration is essential. For every $c > 0$,

$$(S_h, \theta, \Gamma_h) \longmapsto (cS_h, c\theta, \Gamma_h/c) \tag{14.5}$$

preserves both π_h and $\mathcal{L}_h$. It is realized within the registry by multiplying $\beta_a, \kappa_e, m_e^2, \lambda_e, f^2$ by c, leaving m_σ^2, α, η fixed, and changing θ, Γ_h as displayed. Probability laws alone cannot distinguish this family. One independent energy normalization removes this ambiguity; it does not prove unique selection of every constant by the mother theory.

For quadratic potentials one may instead use the Ornstein–Uhlenbeck relations $A_* = -\Gamma_h H_*$ and $C_* = \theta H_*^{-1}$. The covariance relation is not exact for a nonlinear Gibbs equilibrium. For example, $V(x) = m^2x^2/2 + \lambda x^4/4$ gives, by integration by parts, $m^2\mathbb{E}x^2 + \lambda\mathbb{E}x^4 = \theta$. For $\lambda > 0$, setting $\mathbb{E}x^2 = \theta/m^2$ is incorrect.

14.2. *Constraint tangency and the physical quotient.* A constraint selects admissible states; gauge symmetry identifies admissible states with the same physical meaning. A dynamics must respect both operations. Let $\mathcal{C} = (\mathcal{C}_1, \dots, \mathcal{C}_m)$ be C^3 on an open subset of $\mathbb{R}^n$, with $G = D\mathcal{C}$ of full row rank near $\mathcal{S} = \{\mathcal{C} = 0\}$. Set

$$P_T = I - G^{\mathsf{T}}(GG^{\mathsf{T}})^{-1}G, \qquad v = P_T b, \qquad B_k = P_T \sigma_k, \tag{14.6}$$

and assume sufficient smoothness for the local Stratonovich equation

$$\mathrm{d}Y_t = v(Y_t)\,\mathrm{d}t + \sum_k B_k(Y_t) \circ \mathrm{d}W_t^k. \tag{14.7}$$

Proposition 14.2 (Constraint preservation). *If $Y_0 \in \mathcal{S}$, the process remains in $\mathcal{S}$ until its lifetime or exit from the regular neighborhood. Its Itô drift is $v + \frac{1}{2}\sum_k DB_kB_k$.*

Proof. Since $GP_T = 0$, the Stratonovich chain rule gives $\mathrm{d}\mathcal{C}(Y_t) = 0$. For a direct Itô check, differentiate $D\mathcal{C}_i B_k = 0$ along B_k:

$$D^2\mathcal{C}_i[B_k, B_k] + D\mathcal{C}_i(DB_kB_k) = 0. \tag{14.8}$$

The curvature drift cancels the quadratic-variation term. Projecting only the noise in an Itô equation would generally omit this drift. □

Hamiltonian first-class closure is a separate requirement:

$$\{\mathcal{C}_\alpha, \mathcal{C}_\beta\} = f_{\alpha\beta}{}^{\gamma}\mathcal{C}_\gamma, \qquad \{\mathcal{C}_\alpha, H\} = u_\alpha{}^{\gamma}\mathcal{C}_\gamma. \tag{14.9}$$

It makes $J\nabla H$ tangent on $\mathcal{S}$. Enforcing tangency by a projection does not prove either bracket identity. For a smooth quotient $q : \mathcal{S} \to \mathcal{S}/\mathcal{G}$, physical evolution further requires

$$\mathcal{L}(f \circ q) = (\mathcal{L}_{\mathrm{phys}} f) \circ q \quad \text{for every smooth quotient function } f. \tag{14.10}$$

Gauge invariance of H and tangent ellipticity alone do not guarantee this: the diffusion and drift must respect gauge orbits. Nor does pure tangent noise preserve a Gibbs law without a matching dissipative drift and the appropriate surface and quotient volumes.

For a nonlinear example, take canonical coordinates (q_1, q_2, p_1, p_2) and

$$C = q_1 p_2 - q_2 p_1, \qquad H = \tfrac{1}{2}|p|^2 + \tfrac{\omega^2}{2}|q|^2 + \tfrac{\lambda}{4}|q|^4, \qquad \lambda \geq 0. \tag{14.11}$$

Direct differentiation gives $\{C, H\} = \{C, C\} = 0$ and $|DC|^2 = |q|^2 + |p|^2$. Away from the origin the constraint is regular. Simultaneous rotations of q, p are orthogonal, and P_T is equivariant. For $b = J\nabla H$ and isotropic ambient noise, the full projected generator commutes with rotations and descends to the regular quotient. On $q \neq 0$, the coordinates $r = |q|$, $p_r = q \cdot p/r$ give $H = p_r^2/2 + \omega^2 r^2/2 + \lambda r^4/4$ on $C = 0$. This verifies nonlinear tangency and projectability in a concrete model; its rotational constraint is not the ADM constraint system.

14.3. *The limit required for entropy dissipation.* Convergence of linear generators does not by itself control dissipation along nonlinear densities. Embed probabilities π_N in a common Polish space, with $\pi_N \Rightarrow \pi$. Let $\mathcal{E}_N$ be symmetric, strongly local diffusion forms, including the temperature coefficient. For $\rho_s^N = f_s^N \pi_N$, their chain rule gives

$$\mathcal{I}_N(\rho_s^N) = 4\mathcal{E}_N(\sqrt{f_s^N}, \sqrt{f_s^N}). \tag{14.12}$$

This expression is not asserted for arbitrary jump forms.

THEOREM 14.3 (Conditional transfer of entropy dissipation). *Fix $T > 0$. Assume the finite laws obey integrated entropy inequalities, their initial entropies converge to $D(\rho_0\|\pi) < \infty$, and $\rho_T^N \Rightarrow \rho_T$. Assume that for almost every $s \in (0, T)$ the limiting density $\rho_s = f_s\pi$ is identified and $\sqrt{f_s^N}$ converges to $\sqrt{f_s}$ in the weak comparison topology for the Mosco lower-bound condition. Then*

$$D(\rho_T\|\pi) + 4\int_0^T \mathcal{E}(\sqrt{f_s}, \sqrt{f_s})\, \mathrm{d}s \leq D(\rho_0\|\pi). \tag{14.13}$$

Proof. The variational formula $D(\rho\|\pi) = \sup_{g \in C_b}\{\int g\, \mathrm{d}\rho - \log \int e^g\, \mathrm{d}\pi\}$ gives joint lower semicontinuity at T. Square-root convergence and the Mosco lower bound give $\mathcal{E}(\sqrt{f_s}, \sqrt{f_s}) \leq \liminf_N \mathcal{E}_N(\sqrt{f_s^N}, \sqrt{f_s^N})$ almost everywhere in s. Fatou's lemma passes this through the integral. Add the lower bounds and use initial entropy convergence. □

For varying Hilbert spaces the comparison maps are part of the hypothesis; see [57]. Weak convergence of laws does not alone identify their square roots in this topology. The required compactness, or a direct integrated Fisher lower bound, must be established for the chosen sequence. The theorem specifies a passage to the limit; it does not supply uniform estimates for the full dynamical-coframe theory. It concerns thermal probability evolution, not quantum reconstruction.

14.4. *Positive quantum evolution at fixed spatial resolution.* Quantum positivity can be achieved constructively before taking a spatial limit. The following is an alternative temporal regularization: its time-crossing kernel replaces the temporal plaquette weight of (13.5). Equality of the two measures is not assumed. In particular, anchoring a weight to one vertex of a time-crossing plaquette need not preserve time reflection.

Fix a finite three-dimensional spatial lattice and set $Q_h = K^{\mathcal{E}_h^{\mathrm{sp}}} \times \mathbb{R}^{17|\mathcal{V}_h^{\mathrm{sp}}|}$, with product volume μ_h^{sp}. Let $V_h \geq 0$ be the spatial part of the finite action, including its shared interaction and confinement. Then $\int e^{-aV_h}\, \mathrm{d}\mu_h^{\mathrm{sp}} < \infty$ for every $a > 0$. Fix all field units and use $\hbar = 1$, so a has inverse-energy units. For a kinetic coefficient $\nu > 0$ with corresponding units, define on $\mathcal{H}_h = L^2(Q_h, \mu_h^{\mathrm{sp}})$

$$H_{0,h} = -\nu \Delta_{Q_h}, \qquad M_a = e^{-aV_h/2}, \qquad T_{a,h} = M_a e^{-aH_{0,h}} M_a. \tag{14.14}$$

The heat kernel propagates configurations between time slices; M_a assigns half the potential weight to each endpoint. This symmetric assignment yields positivity without assuming it for an arbitrary Gibbs weight.

Proposition 14.4 (An interacting quantum model with a spatial cutoff). *At fixed spatial lattice, $T_{a,h}$ is an injective positive self-adjoint trace-class contraction. It defines $H_{a,h} = -a^{-1} \log T_{a,h} \geq 0$ on a dense domain. Bounded positive-time cylinder observables on an even periodic time lattice satisfy reflection positivity, and the link-gauge- invariant subspace is preserved. Also, for every $t > 0$,*

$$(T_{t/n,h})^n \longrightarrow e^{-tH_h} \text{ strongly}, \qquad H_h = H_{0,h} \dotplus V_h, \tag{14.15}$$

where $\dotplus$ denotes the closed nonnegative form sum. The spatial regulator is fixed throughout this time-continuum limit.

Proof. Set $B = e^{-aH_{0,h}/2} M_a$. Then $T_{a,h} = B^* B$ and $\langle \psi, T_{a,h} \psi \rangle = \|B\psi\|^2 \geq 0$. Both factors are injective contractions. The heat kernel p_a has bounded diagonal on the compact group factor and constant diagonal $(4\pi\nu a)^{-d/2}$ on the Euclidean factor. Hence

$$\|B\|_{\mathrm{HS}}^2 = \int e^{-aV_h(x)} p_a(x,x)\, \mathrm{d}\mu_h^{\mathrm{sp}}(x) < \infty. \tag{14.16}$$

This makes $T_{a,h}$ trace class. Spectral calculus gives its densely defined self-adjoint nonnegative logarithmic Hamiltonian.

The transfer kernel is real, symmetric, and nonnegative. Reflect an even periodic time lattice through two opposite bonds. Multiplication by bounded observables and transfer along one half assemble into an operator A; integrating the reflected half gives the quadratic form

$$\mathrm{Tr}(A^* T_{a,h} A T_{a,h}) = \|T_{a,h}^{1/2} A T_{a,h}^{1/2}\|_{\mathrm{HS}}^2 \geq 0. \tag{14.17}$$

Linear combinations of cylinder observables give the corresponding linear combination of A. The normalization $\mathrm{Tr}(T_{a,h}^{2n})$ is finite and positive.

The finite site gauge group acts isometrically by left and right link multiplication. It preserves V_h: spatial plaquette traces are invariant, and e, σ are singlets in this model. Thus the group commutes with both transfer factors. Haar averaging projects orthogonally onto the invariant subspace, preserved by the transfer and Hamiltonian operators.

Table 3. Synthetic transfer calculation with 200 interior points on $[-6, 6]$. The reference is the unsplit matrix on the same grid; no continuum error bound is inferred.

a	Transfer ground energy	Absolute splitting error
0.200	0.557420583	1.568×10^{-3}
0.100	0.558593069	3.950×10^{-4}
0.050	0.558889138	9.896×10^{-5}
0.025	0.558963344	2.475×10^{-5}

Finally, $\nu \int |\nabla\psi|^2 \, \mathrm{d}\mu_h^{\mathrm{sp}} + \int V_h |\psi|^2 \, \mathrm{d}\mu_h^{\mathrm{sp}}$ is densely defined, closed, and nonnegative. On this complete product manifold the smooth nonnegative potential gives essential self-adjointness on smooth compactly supported functions. The contraction product formula [99] then yields (14.15), with symmetric half-potentials at the endpoints. No bound uniform in spatial lattice size has been used. □

This is interacting quantum mechanics of finitely many field coordinates, with a positive inner product and link gauge symmetry. It does not impose the gravitational Hamiltonian and momentum constraints. The selection of ν, V_h by mother data, and their matching to a physical Lorentzian action, remain separate questions. Removing the spatial regulator requires uniform estimates and renormalized limiting observables. Time reflection here acts on Euclidean time slices, not on the relaxation parameter of the earlier stochastic sampling process.

Positivity of a classical density is insufficient even if it is reflection symmetric. The density proportional to $\exp[-(x^2 + y^2 + 2cxy)/2]$, $0 < c < 1$, is positive and invariant under $x \leftrightarrow y$. For $F(x) = x$, however,

$$\mathbb{E}[(\Theta F)F] = \mathbb{E}[xy] = -\frac{c}{1 - c^2} < 0. \tag{14.18}$$

Truncation of F supplies bounded counterexamples as well. This explains why the transfer construction is a genuine extra requirement.

14.5. *Finite calculations and the next matching problem.* In a single-gauge-factor example, group the coordinates as $u = (\beta, \alpha, \eta, \kappa_e, m_e^2)$ and $v = (\lambda_e, f^2, m_\sigma^2, \theta, \gamma_1, \gamma_2, \gamma_3)$. The first five responses equal u; the remaining seven are $(6\lambda_e, f^2, f^2 m_\sigma^2, \theta^{-1}, \theta\gamma_1, \theta\gamma_2, \theta\gamma_3)$. Their Jacobian determinant is $-6f^2\theta \neq 0$. This checks the selected inverse map, not selection of primitive constants.

For a transfer calculation choose $H = -\frac{1}{2}\partial_x^2 + x^2/2 + 0.1x^4$ on $[-6, 6]$ with Dirichlet boundaries. A centered finite-difference kinetic matrix and its exact matrix exponential define T_a. We compare $-a^{-1} \log \lambda_{\max}(T_a)$ with the smallest eigenvalue of the unsplit Hamiltonian on the same grid, separating time-splitting from spatial discretization error. Units are dimensionless and data synthetic. The corresponding numerical values are reported in Table 3.

The corresponding numerical diagnostic is shown in Figure 13.

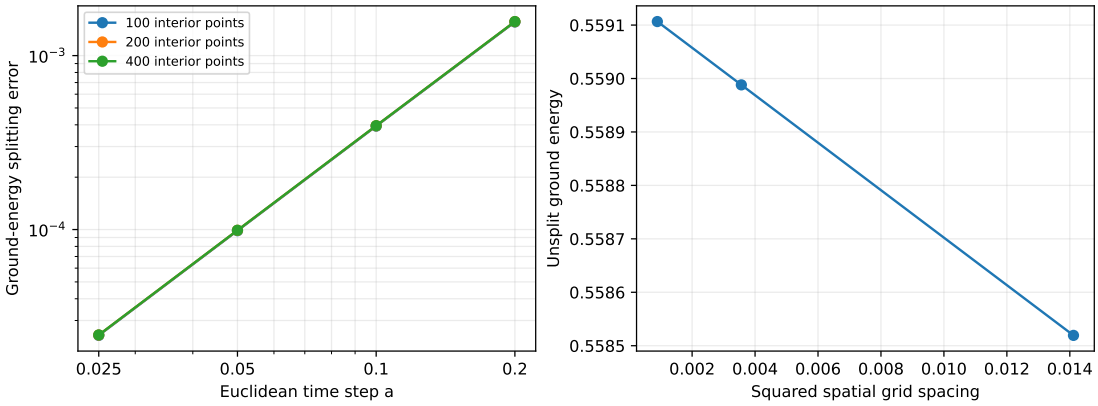


Figure 13. Synthetic quartic-oscillator calculation. Left: transfer energy error relative to the unsplit Hamiltonian on each identical grid. Right: spatial-grid variation of the unsplit energy. These finite diagnostics are not observations of gravity or a quantum-field spatial continuum limit.

Further work now has a definite order. First derive or independently calibrate the registry and freeze it before predicting a held-out observable. Next derive the actual Lorentzian constraints and prove propagation and projectability. Then establish uniform estimates and the nonlinear density convergence required by the entropy theorem. Finally match a positive quantum construction to that same Lorentzian branch and remove its spatial regulator. The finite results above provide components of this programme, with the remaining implications kept explicit.

14.6. *Matching a shared temporal weight to canonical quantum dynamics.* The positive transfer operator above leaves a specific matching question: which kinetic operator represents the same field-dependent weight as the regulated gauge action? A constant configuration-space diffusion does not in general answer that question. We can resolve it in a retained compact gauge mode coupled to the scalar. This calculation keeps a genuine shared interaction and makes the temporal normalization explicit.

Freeze the coframe coordinates at their reference values. Let $q \in S^1$ denote a retained $U(1)$ holonomy angle and shift the scalar reference to $\sigma_\star = 0$, absorbing the constant weight into both β and the temporal gauge inertia I. In fixed dimensionless reference units, with $\hbar = 1$, define

$$w(\sigma) = e^{-\alpha\sigma}, \qquad V(q,\sigma) = \beta w(\sigma)(1-\cos q) + \tfrac{1}{2}K_\sigma\sigma^2, \quad \beta, K_\sigma > 0. \tag{14.19}$$

Here K_σ is the scalar onsite coefficient $m_\sigma^2 f^2$ in the fixed normalization. Temporal coefficients require their own regulator scaling: write $I = \lim_{a\downarrow 0} a\beta_t(a) > 0$ for the gauge coefficient and $J > 0$ for the analogously normalized scalar inertia. These limits are matching conditions on temporal edge coefficients. The unscaled four-dimensional plaquette coefficient alone does not determine them without the spatial cell volume and field normalization.

The local Lorentzian mechanical action associated with these temporal coefficients is

$$L_L = \tfrac{1}{2} I w(\sigma) \dot{q}^2 + \tfrac{1}{2} J \dot{\sigma}^2 - V(q,\sigma), \qquad H_L = \frac{p_q^2}{2Iw(\sigma)} + \frac{p_\sigma^2}{2J} + V. \tag{14.20}$$

Both inertias are positive. The momenta are $p_q = Iw\dot{q}$ and $p_\sigma = J\dot{\sigma}$, so the Legendre map is invertible at every finite scalar value. Its Euler–Lagrange equations read

$$Iw\ddot{q} + Iw'\dot{\sigma}\dot{q} + V_q = 0, \qquad J\ddot{\sigma} - \tfrac{1}{2} Iw'\dot{q}^2 + V_\sigma = 0. \tag{14.21}$$

The two terms containing w' exchange energy between the retained gauge and scalar modes. Direct differentiation of H_L along the canonical equations gives $\dot{H}_L = 0$. The Wick substitution $t = -i\tau$ gives the positive kinetic Euclidean action $S_E = \int [Iw(q')^2/2 + J(\sigma')^2/2 + V] d\tau$. This is an explicit finite-mode continuation; it is not an analytic continuation theorem for the full fluctuating-coframe measure.

The kinetic mismatch and its correction. Choose flat canonical volume $dq\, d\sigma$ and the symmetric divergence ordering. The corresponding differential expression is

$$\mathsf{H} = -\frac{1}{2Iw(\sigma)} \partial_q^2 - \frac{1}{2J} \partial_\sigma^2 + V. \tag{14.22}$$

Since w is independent of q, the gauge kinetic term is exactly $-\partial_q[(2Iw)^{-1}\partial_q]$. There is no missing scalar drift in this chosen flat-volume ordering. A constant gauge coefficient $\nu = (2Iw(0))^{-1}$ instead changes the kinetic energy of a Fourier mode e^{inq} at a fixed scalar value by

$$\delta E_n(\sigma) = \frac{n^2}{2I} \big(w(\sigma)^{-1} - w(0)^{-1} \big). \tag{14.23}$$

Thus agreement at the reference vacuum does not imply agreement on the interacting branch. On $|\sigma| \le S$, $|n| \le N$, the exact operator norm of this kinetic difference is

$$\|\delta \mathsf{H}_q\| = \frac{N^2}{2I} (e^{\alpha S} - 1) \quad (\alpha \ge 0). \tag{14.24}$$

This is a kinetic norm bound on a declared finite Fourier band, not a bound for full gravitational field evolution.

A positive transfer operator with the corrected coefficient. First restrict the scalar to $(-S, S)$ with Dirichlet boundary conditions, keeping the angle periodic. This additional field-amplitude regulator makes the coefficient smooth and uniformly elliptic. Let $\mathsf{K}_q = -(2Iw)^{-1}\partial_q^2$ and $\mathsf{K}_\sigma = -(2J)^{-1}\partial_\sigma^2$. Define

$$\mathsf{T}_a = e^{-aV/2} e^{-a\mathsf{K}_\sigma/2} e^{-a\mathsf{K}_q} e^{-a\mathsf{K}_\sigma/2} e^{-aV/2}. \tag{14.25}$$

The gauge heat operator acts independently at each scalar value and has the explicit fiber kernel

$$p_a(q' - q; \sigma) = \frac{1}{2\pi} \sum_{n \in \mathbb{Z}} e^{-an^2/(2Iw(\sigma))} e^{in(q'-q)}. \tag{14.26}$$

Its Gaussian image representation has variance $a/(Iw)$ and includes the normalizing factor $(Iw/(2\pi a))^{1/2}$. Both the exponent and this field-dependent factor matter in comparison with a configuration integral.

PROPOSITION 14.5 (Matched positive evolution on the retained branch). *For fixed $S < \infty$, the operator (14.25) is an injective positive self-adjoint trace-class contraction. Its even periodic-time cylinder measure is reflection positive. For every $t > 0$, $\mathsf{T}_{t/n}^{n} \to e^{-t\mathsf{H}_S}$ strongly, where H_S is the Dirichlet realization of (14.22). After restoring $\hbar$ in the kinetic terms, its leading semiclassical symbol is the Hamiltonian in (14.20).*

Proof. Put $B = e^{-a\mathsf{K}_q/2}e^{-a\mathsf{K}_\sigma/2}e^{-aV/2}$. Every factor is an injective contraction, and $\mathsf{T}_a = B^*B$. For the trace, expand in angle Fourier modes and let $s_{a/2}$ be the Dirichlet scalar heat kernel. Since $V \geq 0$,

$$\|B\|_{\mathrm{HS}}^2 \leq \int_{-S}^{S}\int_{-S}^{S} |s_{a/2}(\sigma', \sigma)|^2 \sum_{n\in\mathbb{Z}} e^{-an^2/(2Iw(\sigma'))} d\sigma\, d\sigma' < \infty. \tag{14.27}$$

Boundedness above and below of w on this interval controls the Gaussian sum, and the scalar heat operator is Hilbert–Schmidt. The same folding argument as (14.17) proves reflection positivity because the kernel is nonnegative and $\mathsf{T}_a \geq 0$. The uniformly elliptic Dirichlet operator on the compact cylinder is self-adjoint, with the smooth Dirichlet functions as a core. The symmetric contraction product formula gives the stated time limit. Taking the principal symbol, or performing the Legendre calculation in (14.20), identifies the kinetic coefficient Iw. □

The amplitude restriction can also be removed for this two-coordinate Hamiltonian. On $S^1 \times \mathbb{R}$, close the nonnegative form

$$\mathfrak{q}[\psi] = \int \left[\frac{|\partial_q \psi|^2}{2Iw} + \frac{|\partial_\sigma \psi|^2}{2J} + V|\psi|^2 \right] dq\, d\sigma \tag{14.28}$$

initially on smooth functions with compact scalar support. Such a closure exists by local ellipticity and positivity. The increasing union of the finite-interval Dirichlet form domains is dense in this closed form by its definition. Monotone convergence of closed forms therefore gives strong resolvent, and then strong positive-time semigroup, convergence as $S \to \infty$, with the natural zero extensions. This constructs a positive Hamiltonian after removing an amplitude cutoff at fixed spatial and modal content. It does not remove a spatial field regulator or prove the remaining relativistic reconstruction requirements.

What normalization of a Wilson temporal link changes. The same matching can be checked against the actual compact-link interaction rather than only a quadratic approximation. At fixed σ the temporal Wilson factor and its row integral are

$$r_a(\delta; \sigma) = e^{-z(1-\cos\delta)}, \qquad z = \frac{Iw(\sigma)}{a}, \qquad c_a(\sigma) = 2\pi e^{-z} I_0(z). \tag{14.29}$$

Here $I_n(z) = (2\pi)^{-1}\int_{-\pi}^{\pi} e^{z\cos\delta}e^{-in\delta}d\delta$ is the modified Bessel coefficient. The normalized convolution r_a/c_a has positive Fourier multipliers $I_n(z)/I_0(z) \le 1$. For fixed Fourier band and a compact scalar interval, their energy satisfies, uniformly as $a \downarrow 0$,

$$-a^{-1}\log\frac{I_n(z)}{I_0(z)} = \frac{n^2}{2Iw} + \frac{an^2}{4I^2w^2} + O(a^2). \tag{14.30}$$

The fixed-order Bessel expansion is given in [79], formula 10.40.1 of its online companion. For completeness, the first two logarithmic terms follow by expanding $I_n(z) = e^z(2\pi z)^{-1/2}[1 - (4n^2 - 1)/(8z) + (4n^2-1)(4n^2-9)/(128z^2) + O(z^{-3})]$. Subtracting the logarithmic series for $n = 0$ gives $\log(I_n/I_0) = -n^2/(2z) - n^2/(4z^2) + O(z^{-3})$.

The unnormalized factor is not equivalent to the normalized one when σ fluctuates. Relative to the reference row integral, the additional multiplication factor can be written $e^{-aU_a(\sigma)}$, with

$$\begin{aligned} U_a(\sigma) &= -a^{-1}\log\frac{c_a(\sigma)}{c_a(0)}, \\ &= \frac{1}{2a}\log\frac{w(\sigma)}{w(0)} - \frac{1}{8I}\left(\frac{1}{w(\sigma)} - \frac{1}{w(0)}\right) + O(a). \end{aligned} \tag{14.31}$$

For the exponential weight the leading term is $-\alpha\sigma/(2a)$. This term is field dependent and generally divergent at fixed nonzero σ as $a \downarrow 0$. It cannot be discarded as a constant partition normalization. One must specify the temporal measure or a compensating local factor. The compact-interval asymptotic statement does not assert a limiting vacuum for the unnormalized full field model. Section 14.12 specifies a symmetric endpoint arrangement and calculates its exact compensating factor, including the finite term left by leading-power normalization alone.

Quantum ordering is a separate declared choice. The metric kinetic interpretation uses $ds_Q^2 = Iw(\sigma)dq^2 + Jd\sigma^2$. Its natural volume is proportional to $\sqrt{w}\,dq\,d\sigma$. Quantization by $-\Delta_Q/2 + V$, followed by the unitary map $\psi \mapsto w^{1/4}\psi$ to flat volume, gives

$$U(-\tfrac{1}{2}\Delta_Q + V)U^{-1} = \mathsf{H} + V_{\mathrm{ord}}, \qquad V_{\mathrm{ord}} = \frac{(\log w)''}{8J} + \frac{[(\log w)']^2}{32J}. \tag{14.32}$$

To check the formula, the scalar part of Δ_Q is $J^{-1}[\partial_\sigma^2 + \frac{1}{2}(\log w)'\partial_\sigma]$; conjugation removes the first derivative and gives the displayed potential. For $w = e^{-\alpha\sigma}$, $V_{\mathrm{ord}} = \alpha^2/(32J)$ is constant, so the two choices have identical energy gaps in this reduced example. For more general retained weights this need not be a constant. The classical action alone therefore does not settle the quantum ordering.

The nonabelian lattice extension and its exact Gauss constraints. The kinetic correction extends to the full compact link group at a fixed spatial graph. Keep e, σ as the gauge singlets specified in the finite branch, and choose positive temporal weights $w_\ell(e,\sigma)$ from the same retained weight. For source and target vertices $s(\ell), t(\ell)$, introduce a temporal gauge multiplier $A_{0,v}$ and the covariant velocity

$$D_tU_\ell = \dot{U}_\ell + A_{0,s(\ell)}U_\ell - U_\ell A_{0,t(\ell)}, \qquad L_g = \sum_\ell \frac{I_\ell w_\ell}{2}\|U_\ell^{-1}D_tU_\ell\|^2 - V_h. \tag{14.33}$$

Add the declared positive kinetic terms for the singlet variables. The group norm is bi-invariant. Under a time-dependent site transformation, $U_\ell \mapsto g_s U_\ell g_t^{-1}$ and $A_{0,v} \mapsto g_v A_{0,v} g_v^{-1} - \dot{g}_v g_v^{-1}$, the covariant velocity transforms as $D_t U_\ell \mapsto g_s (D_t U_\ell) g_t^{-1}$. Thus the spatial Wilson potential and the full kinetic expression are gauge invariant even when the weights fluctuate.

Let $\mathcal{G} = K^{\mathcal{V}_h^{\mathrm{sp}}}$ act by this link transformation. On the cotangent phase space, choose the equivariant moment-map convention $\{G[\xi], G[\zeta]\} = G[[\xi, \zeta]]$. The components of G are the sums of outgoing left and incoming minus right link momenta, with this fixed momentum convention. Variation of A_0 imposes $G_v^a = 0$.

Proposition 14.6 (Finite lattice Gauss closure and positive quantization). *For the continuous-time lattice action (14.33), the Gauss constraints are first class and preserved by its Hamiltonian:*

$$\{G_v^a, G_u^b\} = \delta_{vu} f^{ab}{}_c G_v^c, \qquad \{G_v^a, H_h\} = 0. \tag{14.34}$$

At a fixed finite scalar/coframe amplitude box with Dirichlet boundary, replace the constant link kinetic coefficient by

$$\mathsf{K}_g = -\sum_\ell \frac{1}{2 I_\ell w_\ell(e, \sigma)} \Delta_{K,\ell}. \tag{14.35}$$

The symmetric transfer construction using K_g, the singlet kinetic operator, and V_h is positive and preserves the gauge-invariant Hilbert subspace. On smooth gauge vectors, the quantum Gauss generators close without a central term.

Proof. The cotangent lift of a site action has the canonical moment map obtained by pairing each link momentum with the corresponding infinitesimal link variation. Left and right actions on the same link commute, actions on different links commute, and the action at a vertex has Lie bracket $[\xi_v, \zeta_v]$. The canonical moment-map brackets consequently give the first equation in (14.34). Invariance of the Hamiltonian gives the second. The covariant time action therefore preserves Gauss constraints; it is not an unconstrained evolution with an added numerical projection.

For quantization, let $\mathcal{U}(g)$ be the unitary pullback representation on product Haar and singlet volume. Define $\widehat{G}_v^a = i\, d\mathcal{U}(T_v^a)$, so that $\mathcal{U}(e^{tT_v^a}) = e^{-it\widehat{G}_v^a}$. Differentiating the representation identity gives $[\widehat{G}_v^a, \widehat{G}_u^b] = i\delta_{vu} f^{ab}{}_c \widehat{G}_v^c$ on smooth vectors. This calculation contains no central term. The bi-invariant link Laplacian, the singlet weights, and V_h commute with the site action. Each transfer factor therefore commutes with the Haar projection $\Pi_{\mathcal{G}} = \int_{\mathcal{G}} \mathcal{U}(g) dg$. Its range is precisely the invariant subspace, equivalently the joint kernel of the infinitesimal generators for the connected group used here. Positivity follows from the same B^*B factorization as (14.25). On the finite amplitude box the link diffusion coefficients have a common positive lower bound; the compact-group heat trace is uniformly finite. Together with the singlet Dirichlet heat trace this gives the trace-class estimate as in (14.27). □

This proves the full finite-graph internal Gauss algebra for this selected continuous-time action and its invariant quantum subspace. The lapse, shift, and dynamical spacetime coframe have not

Table 4. Synthetic coupled spectrum on 200 scalar interior points and angle modes $-6, \ldots, 6$. Parameters, potential, and discretization are identical in both rows. Grid and Fourier refinements are recorded separately.

Kinetic coefficient	Ground energy	First energy gap	$\langle\sigma\rangle_0$
Matched shared weight	0.96746453	0.89250524	0.01522086
Frozen at reference	0.96571572	0.86815162	0.07642631

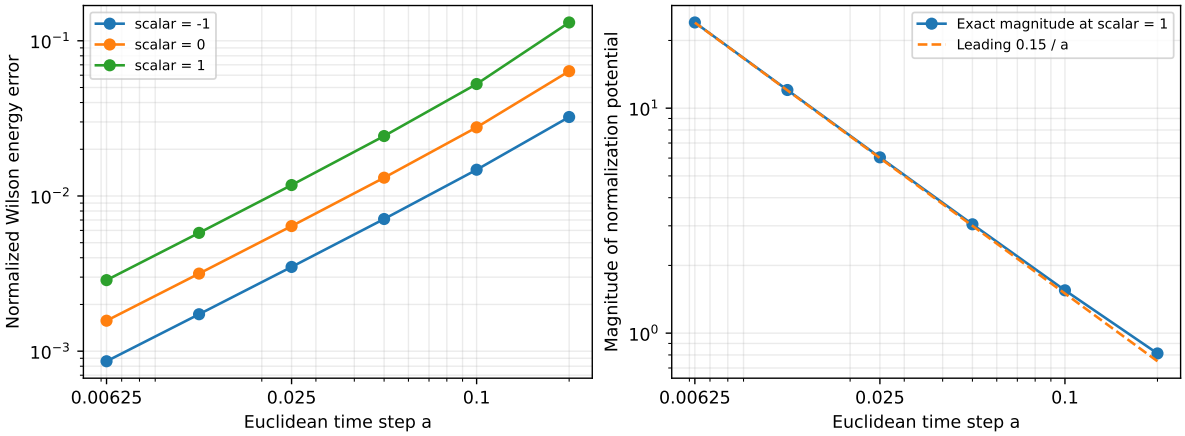


Figure 14. Synthetic retained-mode matching. Left: normalized Wilson-link energy error relative to the matched heat energy, for $n = 1$ and fixed scalar values. Right: the field-dependent normalization term at $\sigma = 1$ compared with its calculated leading divergence. These are tests of a finite shared-weight branch, not gravitational observations.

been introduced in this construction. Accordingly the hypersurface-deformation algebra of gravity, spatial regulator removal, and their quantum realization remain additional requirements.

Calculations with the same parameter registry. The following synthetic calculations fix $I = J = \beta = K_\sigma = 1$, $\alpha = 0.3$ and $\sigma_\star = 0$ before any comparison. Fourier modes $-N, \ldots, N$ represent the angle; centered scalar differences use Dirichlet data at $\sigma = \pm 6$. The matched kinetic operator and the reference-frozen constant coefficient use identical potentials and identical numerical spaces. No parameter is refitted between them. The scalar mean in the table is the quantum ground-state expectation, not a classical thermal mean. The corresponding numerical values are reported in Table 4.

The corresponding numerical diagnostic is shown in Figure 14.

The calculation resolves a specific part of the earlier matching problem: on this retained interacting branch the common temporal weight fixes the classical inertia and the principal quantum kinetic coefficient, and a positive transfer operator implements both. It also identifies the measure normalization and ordering data still required. Gravitational coframe variation, the full nonlinear constraint algebra, and a spatial quantum continuum are not supplied by freezing those degrees of freedom.

14.7. *Dynamical geometry, material clocks, and the physical inner product.* The retained gauge–scalar interaction provides a controlled setting in which to compare temporal measures and kinetic operators. A dynamical spacetime requires an additional distinction. A coframe determines lengths and causal cones, whereas a material reference system assigns readings to events. These roles can interact without being identified. We now give the local geometric construction, an exactly soluble constrained quantum example, and a sufficient estimate for taking limits of constraint products.

Geometry and reference readings. Use a, b for Lorentz indices, μ, ν for spacetime indices, and I, J for labels of four scalar reference fields. With signature $(-,+,+,+)$, an invertible coframe and its matrix inverse satisfy

$$g_{\mu\nu} = \eta_{ab} e^a{}_\mu e^b{}_\nu, \qquad g^{\mu\nu} = \eta^{ab} e_a{}^\mu e_b{}^\nu, \qquad e^a{}_\mu e_b{}^\mu = \delta^a_b. \tag{14.36}$$

The inverse is a matrix inverse; it is not obtained by raising an index with an independently prescribed background metric. Four scalar fields X^I do not replace this coframe. In particular, if $e^a = dX^a$ and the Jacobian has full rank, the X^a are local coordinates and $g = \eta_{ab}\, dX^a dX^b$ is locally flat. Thus this identification excludes general curved metrics. The statement concerns the equality $e^a = dX^a$: a common nonconstant factor $e^a = \Omega\, dX^a$ can give a curved, conformally flat metric. Also, $de^a = 0$ alone is not a torsion condition when an independent connection is present, since $T^a = de^a + \omega^a{}_b \wedge e^b$.

To use $T = X^0$ as a local clock, its level sets must be spacelike. On an injective reference chart the relevant conditions and normal are

$$\begin{aligned} g^{\mu\nu}\partial_\mu T \partial_\nu T < 0, \qquad & \det(\partial_\mu X^I) \neq 0, \\ n_\mu = -\frac{\partial_\mu T}{\sqrt{-g^{\alpha\beta}\partial_\alpha T \partial_\beta T}}, \qquad & h_{\mu\nu} = g_{\mu\nu} + n_\mu n_\nu. \end{aligned} \tag{14.37}$$

The sign of n is chosen to give the desired future orientation. The weaker condition $dT \neq 0$ allows both spacelike and null gradients: in Minkowski space $T = x^1$ and $T = t + x^1$ are elementary examples. If a clock ceases to define a chart, one may need another clock or another patch. Such failure does not by itself exclude the underlying physical configuration.

The inverse map $x = x(X)$ defines a relational scalar and metric by

$$O_{\mathrm{rel}}(X) = O(x(X)), \qquad g^{\mathrm{rel}}_{IJ}(X) = g_{\mu\nu}(x(X)) \frac{\partial x^\mu}{\partial X^I} \frac{\partial x^\nu}{\partial X^J}. \tag{14.38}$$

They are invariant under simultaneous spacetime diffeomorphisms of the fields, within the chosen chart. A coframe component evaluated at the same relational event still transforms under local Lorentz rotations. Its use as a fully invariant observable requires a frame choice or an additional Lorentz-invariant construction. Relational quantum descriptions can be related by reduction maps under specified clock and spectral assumptions [46]; this does not assert an equivalence for every gravitational constraint system.

Reference matter and its gravitational response. A physical clock carries energy. One explicit extension of the two-derivative gravitational branch is a scalar reference action

$$S_X = -\int \sqrt{-g}\left[\tfrac{1}{2}Q_{IJ}g^{\mu\nu}\partial_\mu X^I\partial_\nu X^J + U_X(X)\right] d^4x, \qquad Q_{IJ} = Q_{JI} > 0. \tag{14.39}$$

Here Q is constant. In four spacetime dimensions, with $c = \hbar = 1$, one may normalize X^I to have mass dimension one, Q to be dimensionless, and U_X to have dimension four. The readings X^I need not have the units of coordinate time or length. Positive Q gives ordinary healthy scalar kinetic terms; the Lorentz metric on coframes is not a target metric for these four scalars. This action is a declared matter extension. Identifying its coefficients with primitive mother data is a separate matching condition.

Variation gives $Q_{IJ}\Box_g X^J - \partial_I U_X = 0$ and

$$T^X_{\mu\nu} = Q_{IJ}\partial_\mu X^I\partial_\nu X^J - g_{\mu\nu}\left(\tfrac{1}{2}Q_{IJ}g^{\alpha\beta}\partial_\alpha X^I\partial_\beta X^J + U_X\right). \tag{14.40}$$

The ADM Legendre transform gives the two constraint contributions

$$\begin{gathered}\mathcal{H}_X = \frac{Q^{IJ}P_IP_J}{2\sqrt{h}} + \frac{\sqrt{h}}{2}Q_{IJ}h^{ij}\partial_i X^I\partial_j X^J + \sqrt{h}\,U_X,\\ \mathcal{H}_{i,X} = P_I\partial_i X^I.\end{gathered} \tag{14.41}$$

Indeed $P_I = \sqrt{h}\,Q_{IJ}(\dot{X}^J - N^i\partial_i X^J)/N$, so substitution into $P_I\dot{X}^I - \mathcal{L}_X$ gives $N\mathcal{H}_X + N^i\mathcal{H}_{i,X}$. For the Einstein–Hilbert branch this stress enters $M_{\mathrm{P}}^2(G_{\mu\nu} + \Lambda g_{\mu\nu}) = T^X_{\mu\nu} + T^{\mathrm{other}}_{\mu\nu}$. Reference matter therefore changes the constraints rather than merely labelling a pre-existing solution. Neither a free scalar action nor the ADM decomposition guarantees a globally valid clock, and the lapse, shift, and Lorentz gauge directions do not acquire independent physical momenta merely because a coframe is used.

Gauge averaging also affects how semiclassical geometry should be tested. Consider the four proper spatial rotations

$$\begin{aligned}R_0 &= \mathrm{diag}(1,1,1), \quad R_1 = \mathrm{diag}(1,-1,-1),\\ R_2 &= \mathrm{diag}(-1,1,-1), \quad R_3 = \mathrm{diag}(-1,-1,1).\end{aligned} \tag{14.42}$$

Each coframe $e_{(r)} = \mathrm{diag}(1, R_r)$ is invertible and induces the same Minkowski metric. Nevertheless, $\frac{1}{4}\sum_r e_{(r)} = \mathrm{diag}(1,0,0,0)$ is degenerate. A degenerate mean of a gauge-dependent coframe therefore need not signal degenerate physical geometry. Metric, volume, or relational observables give appropriate geometric tests. A semiclassical Einstein equation also requires a specified state, renormalized stress, and control of geometric fluctuations: in general $G(\langle e\rangle) \neq \langle G(e)\rangle$.

Ordering and a nontrivial test of constraint covariance. Coordinate covariance and a symmetric inner product restrict quantization but need not select it uniquely. On a compact smooth configuration manifold with metric γ and without boundary, the operators

$$\mathsf{H}_\xi = -\frac{\hbar^2}{2m}(\Delta_\gamma - \xi\mathcal{R}_\gamma) + V, \qquad \xi \in \mathbb{R}, \tag{14.43}$$

have the same principal symbol and are coordinate covariant. For smooth real V, each has a self-adjoint realization with domain H^2 in $L^2(d\,\mathrm{vol}_\gamma)$. The continuous curvature parameter is not fixed by these requirements. Earlier gravitational ordering analyses likewise distinguish ordering conditions from algebraic anomalies [16]. In a separate companion paper, Christodoulakis and Zanelli obtained a formally consistent constraint algebra using a minimal modification of canonical commutation relations [17]. That construction changes the algebraic input; it does not by itself provide a regulator-independent representation, a physical inner product, or a quantization of the present interacting mother action. Formal symmetry, self-adjoint realization, and a common invariant domain for products are separate requirements.

In the metric Einstein–Yang–Mills benchmark, let C_i denote the gauge-covariant momentum constraint, G_A the Gauss constraint with internal gauge label A, and $V_i = C_i + A_i^A G_A$ the ordinary spatial diffeomorphism constraint. With $G_A = -D_i E^i_A$ and the usual canonical Poisson bracket, the Hamiltonian bracket is

$$\{H[N], H[M]\} = C[Z] = V[Z] - G[Z^i A_i], \qquad Z^i = h^{ij}(N\partial_j M - M\partial_j N). \tag{14.44}$$

The right-hand side is a momentum constraint, with a field-dependent structure function. It is not another scalar Hamiltonian constraint. This distinction persists when a quantum representative and an ordering for the right-hand side are chosen.

Let Φ be a common invariant dense test domain on which the required products exist. If $\widehat{C}_\alpha\psi = 0$ for every constraint, then $[\widehat{C}_\alpha, \widehat{C}_\beta]\psi = 0$ already follows algebraically. Thus a calculation only on this common kernel cannot establish the required spacetime covariance. One must also establish a nonzero physical space and examine the commutator on a suitable domain, or its matrix elements in controlled semiclassical states, with the correct structure functions and regulator estimates. A term that adds independent restrictions may change the physical sector; its effect cannot be decided by simply discarding it on the kernel.

Changing canonical commutators is one possible additional hypothesis, not a consequence of the ordering problem. It must define a consistent adjoint algebra and a representation. For example, the proposal $[q_i, p_j] = i\hbar f(q)\delta_{ij}$ together with $[q_i, q_j] = [p_i, p_j] = 0$ gives the Jacobi expression

$$[p_i, [p_j, q_k]] + [p_j, [q_k, p_i]] + [q_k, [p_i, p_j]] = \hbar^2 f\big(\delta_{ik}\partial_j f - \delta_{jk}\partial_i f\big). \tag{14.45}$$

For nonconstant positive f in dimension at least two this generally fails. Alternative regulators, counterterms, reduced quantization, or other constraint constructions must be assessed on their own assumptions.

From a positive form to physical states. For a unitary representation of a compact internal gauge group, normalized Haar averaging gives an orthogonal projection $P_{\mathrm{inv}} = \int U(g)\, dg$. Hence

$$\begin{gathered} q(u,v) = \langle u, P_{\mathrm{inv}} v\rangle, \qquad q(u,u) = \|P_{\mathrm{inv}} u\|^2 \geq 0, \\ \mathcal{H}_{\mathrm{phys}} \simeq \mathcal{H}_{\mathrm{aux}}/\ker P_{\mathrm{inv}} \simeq \operatorname{Ran} P_{\mathrm{inv}}. \end{gathered} \tag{14.46}$$

Nonzero auxiliary vectors can have zero physical norm. The quotient removes these vectors and gives a positive definite inner product. For noncompact constraints, a rigging form instead requires a test space, a justified integral or distributional prescription, positivity, compatibility with physical observables, and completion of the null quotient. Uniqueness is an additional question. The Giulini–Marolf theorem assumes a finite-dimensional Lie group, an appropriate L^1 test space invariant under their group algebra, and a nonzero averaging form; under those conditions any compatible rigging map, if it exists, is proportional to group averaging [37]. Convergence alone is not that theorem. The field-dependent structure functions in (14.44) do not provide an ordinary constraint group with Haar measure for all gravitational constraints.

An explicit noncompact example shows both the construction and its scope. Set $\hbar = 1$, choose a Hermitian $d \times d$ matrix H_s, and take

$$\mathcal{H}_{\mathrm{aux}} = L^2(\mathbb{R}_T) \otimes \mathbb{C}^d, \qquad \Phi = \mathcal{S}(\mathbb{R}) \otimes \mathbb{C}^d, \qquad C = -i\partial_T + H_s. \tag{14.47}$$

In an orthonormal eigenbasis $H_s|\ell\rangle = E_\ell|\ell\rangle$, use the unitary Fourier transform in T. Group averaging is then exactly

$$\eta(u)[v] = \int_{\mathbb{R}} \frac{ds}{2\pi} \langle u, e^{isC} v\rangle = \sum_{\ell=1}^{d} \overline{\widetilde{u}_\ell(-E_\ell)}\, \widetilde{v}_\ell(-E_\ell). \tag{14.48}$$

For these test vectors the matrix coefficient is Schwartz in s, so the integral is absolutely convergent. Fourier inversion proves the displayed evaluation formula. It is positive semidefinite. Its null space consists precisely of the vectors for which all evaluations $\widetilde{u}_\ell(-E_\ell)$ vanish. Evaluation maps onto $\mathbb{C}^d$, since one may prescribe these finitely many values with Schwartz functions. The completed physical space is therefore $\mathbb{C}^d$. A corresponding history is $\Psi(T) = e^{-iH_s T}\chi$, and $C\Psi = 0$ follows by direct differentiation. For $\chi \neq 0$ this history is not square integrable in the clock variable, even though its physical norm $\|\chi\|$ is finite. This example realizes a deparametrized clock constraint; it does not realize the full gravitational hypersurface-deformation algebra.

The sign of an inner product must also be tied to its construction. For the relativistic mass-shell constraint $C = p_0^2 - |\mathbf{p}|^2 - m^2$, $m > 0$, put $\omega_{\mathbf{p}} = \sqrt{|\mathbf{p}|^2 + m^2}$. Averaging with $\delta(C)$ gives the

positive shell form

$$q(u,v) = \int \frac{d^3p}{2\omega_{\mathbf{p}}} \left[\overline{u(\omega_{\mathbf{p}}, \mathbf{p})} v(\omega_{\mathbf{p}}, \mathbf{p}) + \overline{u(-\omega_{\mathbf{p}}, \mathbf{p})} v(-\omega_{\mathbf{p}}, \mathbf{p}) \right]. \tag{14.49}$$

The conserved Klein–Gordon charge form has opposite signs on the two frequency sectors. These are different forms; positivity of one does not turn the other into a positive form. Enlarging a test space while retaining a negative-norm vector cannot remove that negative norm. Similarly, positivity of a temporal transfer operator $B^\dagger B$ does not identify its Hilbert space with a physical constraint quotient without a reconstruction or intertwining map.

Spatial refinement and products of constraints. Clock resolution, temporal step size, spatial field truncation, and amplitude cutoffs are different parameters. Finer clock readings do not add missing spatial field modes. A relational resolution can describe spatial refinement only after an explicit map to physical geometry and observables has been given. Projective consistency, a renormalization group fixed point, and convergence of a chosen sequence are also distinct properties. A fixed point is one possible route to a continuum theory; failure to find one in a truncation is not a nonexistence proof.

Even convergent matrix elements are insufficient for constraint products. Let $\{e_0, e_1, \dots\}$ be the standard basis of ℓ^2 and set

$$A_n = |e_0\rangle\langle e_n| + |e_n\rangle\langle e_0|, \qquad B_n = i\big(|e_n\rangle\langle e_0| - |e_0\rangle\langle e_n|\big). \tag{14.50}$$

Both self-adjoint sequences have norm one and converge weakly to zero. However, $[A_n, B_n] = 2i(P_0 - P_n)$ converges weakly to $2iP_0$, where $P_j = |e_j\rangle\langle e_j|$. Thus the commutator of the limits differs from the limit of the commutators.

The following stronger estimate gives a sufficient replacement.

PROPOSITION 14.7 (Control of commutators on a scale of spaces). *Let $V_2 \hookrightarrow V_1 \hookrightarrow V_0$ be Banach spaces. Suppose A_n, B_n, A, B act consistently on both successive levels $V_2 \to V_1$ and $V_1 \to V_0$, with every such operator norm at most M. If, on both levels, $\|A_n - A\| \le \epsilon_A(n)$ and $\|B_n - B\| \le \epsilon_B(n)$, then*

$$\|[A_n, B_n] - [A, B]\|_{V_2 \to V_0} \le 2M\big(\epsilon_A(n) + \epsilon_B(n)\big). \tag{14.51}$$

Proof. Write $A_nB_n - AB = (A_n - A)B_n + A(B_n - B)$. Composition between the successive spaces bounds this difference by $M(\epsilon_A + \epsilon_B)$. Apply the same argument to $B_nA_n - BA$ and use the triangle inequality. □

For changing Hilbert spaces the operators must first be transported by specified comparison maps. For unbounded gravitational constraints, the required domains and bounds remain to be established. The proposition is a conditional analytic criterion, rather than an estimate already proved for those constraints.

Quantization data and comparison of branches. The shared-weight example shows concretely why a path-integral measure and a kinetic expression must be matched. In general the quantization data also include the regulator, counterterms, boundary conditions, operator domains, and state preparation. A measure alone need not select an ordering. Terms of order $\hbar^2$ need not be negligible at low energy, and equations of motion need not uniquely select a boundary state or a reference-field preparation.

Agreement of one relational expectation value is not physical equivalence. For example, $H_1 = \operatorname{diag}(0,1)$ and $H_2 = \operatorname{diag}(0,2)$ have the same ground-state expectation of σ_z but different excitation gaps. Exact equivalence requires a unitary map W that preserves the physical observable representation and evolution:

$$W\pi_1(O)W^{-1} = \pi_2(O), \qquad WU_1(t) = U_2(t)W. \tag{14.52}$$

An effective low-energy comparison can instead specify a family of observables and states and bound their differences after comparison. Distinct vacua, superselection sectors, and inequivalent quantizations must be distinguished in that analysis. Their presence leaves the conditional branch constructions meaningful, while preventing a claim that the primitive mother data have already selected a unique physical quantum theory.

These results separate three tasks that a material-clock formulation must connect: dynamical geometric constraints, a positive physical state space, and spatial cutoff removal. The local reference construction and the clock model complete explicit parts of this connection. The full nonlinear gravitational operator algebra and its interacting continuum representation require additional constructions beyond the finite gauge sector.

14.8. *Logarithmic coframes and integrability near degenerate geometry.* An invertible coframe can approach a singular matrix while every matrix entry remains bounded. Inverse metric observables can therefore fail to be integrable even when the partition function is finite. Proposition 13.3 establishes this obstruction for the smooth positive matrix-entry density of the finite mother branch. Logarithmic coordinates locate the relevant tail precisely and provide an explicit alternative measure with finite inverse moments. The distinction between changing coordinates and changing the probability law is essential.

The polar change of variables. Work at one vertex in fixed dimensionless Euclidean coframe coordinates. If a dimensional coframe is used, it must first be divided by a specified reference scale. Every $e \in \mathrm{GL}^+(4,\mathbb{R})$ has the unique polar representation $e = R\exp S$, where $R \in \mathrm{SO}(4)$ and $S = S^{\mathsf{T}}$. Let dS_F be Lebesgue measure in the ten orthonormal Frobenius coordinates, namely S_{ii} and $\sqrt{2}S_{ij}$ for $i < j$, and normalize Haar measure dR to have mass one. For eigenvalues $\lambda_1, \dots, \lambda_4$ of S, the matrix-entry volume is

$$de = J(S)\, dR\, dS_F, \qquad J(S) = c_4 e^{4\,\mathrm{tr}\,S} \prod_{i<j} \frac{\sinh(\lambda_i - \lambda_j)}{\lambda_i - \lambda_j}. \tag{14.53}$$

Here $c_4 > 0$ depends only on the volume normalizations, and each ratio at a repeated eigenvalue has value one. To derive the formula, first write $e = RP$ with $P > 0$. At diagonal P with entries s_i, the differential $de = \Omega P + dP$, $\Omega^{\mathsf{T}} = -\Omega$, has Jacobian proportional to $\prod_{i<j}(s_i + s_j)$. Indeed the two off-diagonal entries for each pair (i, j) have determinant $s_i + s_j$. Next, the differential of $P = \exp S$ multiplies the diagonal direction i by e^{λ_i} and the symmetric direction (i, j) by $(e^{\lambda_i} - e^{\lambda_j})/(\lambda_i - \lambda_j)$. Multiplying these factors and using $e^{2\lambda_i} - e^{2\lambda_j} = 2e^{\lambda_i+\lambda_j} \sinh(\lambda_i - \lambda_j)$ gives (14.53).

In particular, $S = 0$ means $e = R$ and $\det e = 1$. No inverse-coframe singularity occurs there. The singular values of e are e^{λ_i}, so the dangerous direction is $\lambda_{\min} \to -\infty$. For the illustrative matrix Gaussian $d\mu \propto e^{-a \operatorname{tr}(e^{\mathsf{T}} e)} de$, $a > 0$, conditioned on positive orientation, integration over the angular coordinates gives the joint logarithmic singular-value density

$$p_a(\lambda) \propto e^{-a \sum_i e^{2\lambda_i}} e^{\sum_i \lambda_i} \prod_{i<j} |e^{2\lambda_i} - e^{2\lambda_j}|. \tag{14.54}$$

The ordinary real-symmetric spectral volume contributes $|\Delta(\lambda)| = \prod_{i<j} |\lambda_i - \lambda_j|$; these factors cancel the denominators in (14.53). The eigenvalues are not independent.

Keep $\lambda_2, \lambda_3, \lambda_4$ in compact disjoint intervals. As $\lambda_1 \to -\infty$, the density in (14.54) is bounded above and below by positive multiples of e^{λ_1}, uniformly on smaller such intervals. Both $(\det e)^{-r}$ and $\|e^{-1}\|_F^r$ then have a lower bound proportional to $e^{-r\lambda_1}$. Consequently their integrals contain

$$\int_{-\infty}^{-L} e^{(1-r)\lambda_1} \, d\lambda_1 = \infty, \qquad r \geq 1. \tag{14.55}$$

Thus the logarithmic change of variables preserves, and makes visible, the original divergence. In the interacting mother measure the exact pullback is instead $J(S) e^{-S_h(U, Re^S, \sigma)/\theta}$, with the remaining fields and angular variables retained. It need not have the factorized spectral form of (14.54).

For comparison, a bounded neighborhood of $S = 0$ gives an elementary finite integral. Ordering the four eigenvalues and integrating the Vandermonde polynomial yields

$$\int_{[0,\varepsilon]^4} |\Delta(\lambda)| \, d^4\lambda = \frac{\varepsilon^{10}}{1050}. \tag{14.56}$$

The power ten is the sum of four integration dimensions and the six Vandermonde factors. The coefficient follows from $4! \int_{0<x_1<x_2<x_3<x_4<1} \prod_{i<j}(x_j - x_i) \, d^4x = 1/1050$. For $r \geq 0$, inserting $e^{-r\sum_i \lambda_i}$ bounds the integral between $e^{-4r\varepsilon}\varepsilon^{10}/1050$ and $\varepsilon^{10}/1050$. Even without the Vandermonde factor the bounded integrand is integrable on this cube. A weight vanishing at $S = 0$ is therefore unnecessary for inverse-moment control and cannot repair the negative tail by its behavior at the origin alone.

A different measure with explicit inverse moments. Consider the declared logarithmic Gaussian law

$$d\nu_a(R, S) = \left(\frac{a}{\pi}\right)^5 e^{-a \operatorname{tr} S^2} \, dS_F \, dR, \qquad a > 0. \tag{14.57}$$

It is not the pullback of the matrix Gaussian above. Relative to matrix-entry volume its density contains $J(S)^{-1}$. This change suppresses nearly singular configurations rather than merely

renaming them. The Euclidean construction is invariant under fixed left and right SO(4) rotations. It is not, on that account, a Lorentz-invariant probability law or a solution of the gravitational constraints.

PROPOSITION 14.8 (Inverse moments of a logarithmic Gaussian coframe). *For* (14.57) *and every* $r \geq 0$,

$$\mathbb{E}_{\nu_a}(\det e)^{-r} = e^{r^2/a}, \qquad \mathbb{E}_{\nu_a}\|e^{-1}\|_F^r \leq 2^{r+5}e^{r^2/(2a)} < \infty. \tag{14.58}$$

If $d\nu_{a,W} = Z_W^{-1}e^{-W}d\nu_a$, *where* $W \geq -C$ *and* $0 < Z_W < \infty$, *each corresponding moment is at most* e^C/Z_W *times its value or bound under* ν_a.

Proof. The ten orthonormal matrix coordinates give the partition integral $(\pi/a)^5$. Since $\det e = e^{\operatorname{tr} S}$, complete the square:

$$-a\operatorname{tr} S^2 - r\operatorname{tr} S = -a\operatorname{tr}\left(S + \frac{r}{2a}I_4\right)^2 + \frac{r^2}{a}. \tag{14.59}$$

Translation invariance of dS_F proves the determinant formula. Moreover $\|e^{-1}\|_F \leq 2e^{\|S\|_F}$ and $r\rho \leq a\rho^2/2 + r^2/(2a)$. Integrating the resulting Gaussian with precision $a/2$ rather than a contributes 2^5, giving the second bound. Finally $e^{-W} \leq e^C$ proves the assertion for the tilt. □

The parameter a remains free: integrability holds for every $a > 0$. For example, $\mathbb{E}\operatorname{tr} S^2 = 5/a$ and $\operatorname{Var}(\log\det e) = 2/a$ offer possible calibration relations, but do not determine their observed values. A dynamical realization of the un-tilted law is equally explicit. If B_s^F is Brownian motion in the ten orthonormal symmetric coordinates, then

$$dS_s = -2\theta a S_s\,ds + \sqrt{2\theta}\,dB_s^F, \qquad \theta > 0, \tag{14.60}$$

has invariant density proportional to $e^{-a\operatorname{tr} S^2}$. An independent rotation diffusion with invariant Haar measure gives (14.57). Every finite-time sample has an invertible coframe. Here s is an auxiliary diffusion parameter; its identification with a physical clock requires further dynamics.

These estimates also explain the limit of a finite-lattice construction. For N_v vertices with marginal law (14.57), no independence assumption is needed for the union bound

$$\mathbb{P}\{\min_v \det e_v < \delta\} \leq \min\left\{1, N_v \exp\left[-\frac{a}{4}\left(\log\frac{1}{\delta}\right)^2\right]\right\}, \qquad 0 < \delta < 1. \tag{14.61}$$

Indeed Markov's inequality gives $N_v\delta^r e^{r^2/a}$, minimized at $r = (a/2)\log(1/\delta)$. The bound deteriorates as N_v grows. This loss of an upper bound is not itself evidence of degeneration. Section 14.13 compares different joint laws with the same marginals and proves a bound for a fixed list of averaged observations. Section 14.11 embeds the logarithmic reference in a finite locally rotation-covariant interaction, retaining the interaction-dependent normalization in its moment estimates. Individual inverse moments therefore do not establish a uniform nondegenerate continuum geometry; spatial regularity, correlations, and regulator-uniform estimates remain necessary.

Table 5. Synthetic inverse moments for a single logarithmic Gaussian coframe with $a = 1$. The matrix-entry Gaussian has divergent values in all four rows. Numerical values refer to the different law ν_1.

Observable	Value under ν_1	Evaluation
$(\det e)^{-1}$	$e = 2.7182818\ldots$	Exact Gaussian integral
$(\det e)^{-2}$	$e^4 = 54.5981500\ldots$	Exact Gaussian integral
$\|e^{-1}\|_F$	4.92466	Randomized quadrature
$\|e^{-1}\|_F^2$	31.11929	Gaussian quadrature

Finite-dimensional numerical illustration. Table 5 gives synthetic values for $a = 1$. The determinant moments are exact. For the second Frobenius moment, one can reduce the spectral integral to one-dimensional Gaussian quadratures. Define the antisymmetric matrix, with indices $0 \le i, j \le 3$,

$$A_{ij}(t) = \int_{x<y} (x^i y^j - y^i x^j) e^{-x^2-y^2} (1 + te^{-2x})(1 + te^{-2y})\, dx\, dy. \tag{14.62}$$

Expansion of the Vandermonde determinant on the ordered chamber gives $\mathcal{Z}(t) = 4! \operatorname{Pf} A(t)$, where $\operatorname{Pf} A = A_{01}A_{23} - A_{02}A_{13} + A_{03}A_{12}$. Thus $\mathcal{Z}(0) = 3\pi/2$ and

$$\mathbb{E}_{\nu_1} \|e^{-1}\|_F^2 = \frac{d}{dt} \log \mathcal{Z}(t)\Big|_{t=0} \simeq 31.1192891. \tag{14.63}$$

The substitution $x = u - v$, $y = u + v$, $v > 0$, factors each polynomial term into a full-line and a half-line Gaussian moment. The derivative in (14.63) is justified by Gaussian integrability; $\mathcal{Z}(t)$ is a generating polynomial near zero, not a claim of a positive density for negative t.

An independent calculation in matrix coordinates uses twelve scrambled Sobol replicates of 2^{17} points each. Writing $S = (q/2)I_4 + S_0$, with $\operatorname{tr} S_0 = 0$, $q \sim N(0, 1/2)$ independent of S_0, integrates the trace exactly: the factor for the rth inverse norm is $e^{r^2/16}$. The remaining nine-dimensional calculation gives 4.9246643 for the first moment and 31.1112707 for the second. Replicate-based standard error estimates are 0.0000451 and 0.002582, respectively. The second-moment difference from (14.63) is -0.0080184, approximately 0.026% or 3.1 estimated standard errors. The replicate estimates do not provide rigorous integration bounds. Figure 15 illustrates the different negative tails responsible for the integrability change.

14.9. *Constraint reduction and quantum consistency beyond moment bounds.* Finite inverse moments make geometric observables integrable. They do not determine the number of propagating degrees of freedom or the sign of a physical inner product. Those questions concern the action, its constraints, and its quantization. A finite mechanical example separates the constraint issue from the measure issue.

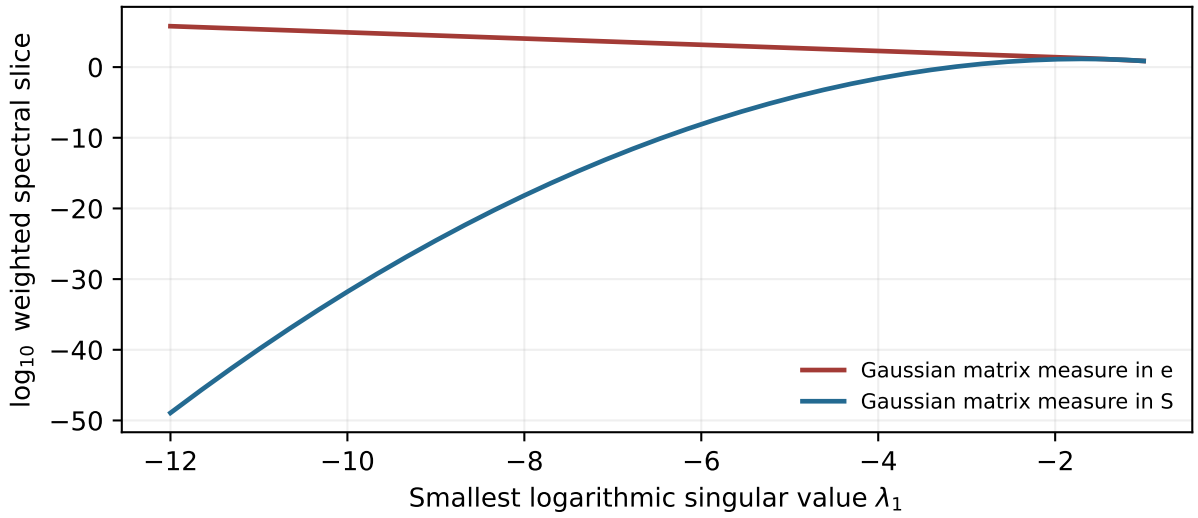


Figure 15. Synthetic conditional spectral slices, weighted by $e^{-2\lambda_1}$, with the other three logarithmic singular values fixed at $\log(1,2,3)$. Each unweighted slice is normalized to one at $\lambda_1 = -1$. The matrix-entry Gaussian grows after inverse-square weighting toward $\lambda_1 = -\infty$, whereas the logarithmic Gaussian decays. These slices are neither marginal densities nor observational data.

Second-class constraints can remove a higher-derivative mode. On a regular irreducible constraint stratum with N canonical pairs, F independent first-class constraints and S_c independent second-class constraints, the reduced number of canonical pairs is

$$N_{\mathrm{phys}} = N - F - \tfrac{1}{2}S_c. \tag{14.64}$$

Each first-class constraint removes one constraint direction and one gauge direction. Each second-class constraint removes one phase-space dimension. A degenerate velocity Hessian produces primary constraints, but preservation can generate further constraints or fix multipliers. The entire Dirac–Bergmann procedure, on a specified rank stratum, is needed before applying (14.64). The higher-derivative scalar–tensor analysis of Langlois and Noui provides a field-theoretic example of this distinction [58].

Consider the mechanical Lagrangian, with $\omega_x, \omega_y > 0$,

$$L = \tfrac{1}{2}(\dot{q} + \ddot{x})^2 + \tfrac{1}{2}\dot{x}^2 - \tfrac{1}{2}\omega_x^2 x^2 - \tfrac{1}{2}\omega_y^2 (q + \dot{x})^2. \tag{14.65}$$

Introduce $Q = \dot{x}$ and a multiplier enforcing this identity. After eliminating the multiplier's auxiliary canonical pair, the coordinates are (x, Q, q) and

$$H = \tfrac{1}{2}p_q^2 - \tfrac{1}{2}Q^2 + p_x Q + \tfrac{1}{2}\omega_x^2 x^2 + \tfrac{1}{2}\omega_y^2 (q + Q)^2, \qquad \phi = p_Q - p_q = 0. \tag{14.66}$$

The two momenta p_Q, p_q coincide because the Hessian in $(\dot{Q}, \dot{q})$ is the rank-one matrix with every entry equal to one. Canonical brackets give

$$\chi = \{\phi, H\} = Q - p_x, \qquad \{\phi, \chi\} = -1, \qquad N_{\mathrm{phys}} = 3 - 0 - 2/2 = 2. \tag{14.67}$$

Preserving χ fixes the multiplier of ϕ; it generates no gauge freedom. On the constraint surface put $y = q + Q$. The canonical one-form reduces to $p_x\,dx + p_q\,dy$, and the Hamiltonian becomes

$$H_{\mathrm{red}} = \tfrac{1}{2}(p_x^2 + p_q^2 + \omega_x^2 x^2 + \omega_y^2 y^2). \tag{14.68}$$

Two second-class constraints remove the extra pair and leave two stable oscillators, although there are no first-class constraints. For a coframe–connection action the analogous calculation must retain the independent connection until its constraints are classified. Elimination is justified by a map preserving the reduced symplectic structure and dynamics, not solely by equality of expressions after setting constraints to zero. Quantization adds domain and ordering requirements to this classical equivalence.

Real characteristic speeds are not a complete evolution estimate. Strong hyperbolicity of a first-order reduction requires a uniformly controlled diagonalization of its principal symbol, or an appropriate uniformly positive symmetrizer, in addition to real characteristic speeds. The constant system $\partial_t u = A\partial_x u$ with

$$A = \begin{pmatrix} 1 & 1 \\ 0 & 1 \end{pmatrix}, \qquad e^{ikAt} = e^{ikt}\left[I + ikt\begin{pmatrix} 0 & 1 \\ 0 & 0 \end{pmatrix}\right] \tag{14.69}$$

has real eigenvalues but growth proportional to $|k|t$, precluding a frequency-uniform estimate at the same Sobolev order. Gauge-dependent characteristic speeds can occur in legitimate gauge evolution equations. Their presence alone neither removes a mode nor proves a physical instability. Gauge fixing, the constraint subsystem, principal-symbol estimates, and boundary conditions must be considered together.

A vanishing physical expectation can miss an anomaly. Suppose provisionally that a physical subspace is represented by an orthogonal projection P in an auxiliary Hilbert space. Even vanishing of all compressed matrix elements only states $P\mathcal{A}P = 0$. For example,

$$P = \begin{pmatrix} 1 & 0 \\ 0 & 0 \end{pmatrix}, \qquad \mathcal{A} = \begin{pmatrix} 0 & 1 \\ 1 & 0 \end{pmatrix}, \qquad P\mathcal{A}P = 0, \quad \mathcal{A}\begin{pmatrix} 1 \\ 0 \end{pmatrix} = \begin{pmatrix} 0 \\ 1 \end{pmatrix}. \tag{14.70}$$

The operator takes a physical vector outside the physical subspace. Moreover, commutators vanish algebraically on a common constraint kernel whenever the products exist, and an empty physical space satisfies every such test vacuously. In refined algebraic quantization physical states can instead be distributions, as in (14.47); an auxiliary orthogonal projection onto their kernel is then not available.

A substantive sufficient estimate uses a common domain and the correct classical structure functions. For the benchmark (14.44), write, at fixed $\hbar > 0$,

$$\begin{aligned} \mathcal{A}_h[N, M] &= (i\hbar)^{-1}[\widehat{H}_h[N], \widehat{H}_h[M]] - \widehat{C[Z]}_h, \\ \|\mathcal{A}_h[N, M]\psi\|_{V_0} &\le \epsilon_h(N, M)\|\psi\|_{V_2}, \qquad \epsilon_h(N, M) \longrightarrow 0. \end{aligned} \tag{14.71}$$

The ordering of $\widehat{C[Z]}_h$ must include the metric dependence of Z. Comparison maps are needed when the regulated spaces differ. Proposition 14.7 supplies one sufficient product estimate, but not these gravitational bounds. This off-shell test must be accompanied by a nontrivial positive physical construction with the intended classical observables. An $O(\hbar)$ remainder can describe a semiclassical approximation; at fixed $\hbar$ it is not a vanishing cutoff error or a proof of exact anomaly cancellation.

Group averaging has similarly specific hypotheses. Under the Giulini–Marolf assumptions, including their L^1 test-space condition, invariance under the relevant group algebra, and a nonzero averaging form, a compatible rigging map is unique up to normalization if it exists [37]. Their integrability requirements include the specified modularly weighted measures for nonunimodular groups. Mere convergence of one Haar integral, or an arbitrary convergent regularization, does not supply these hypotheses. Louko and Molgado exhibit a convergent indefinite averaging form for the $(1, 1)$ oscillator representation; under the uniqueness hypotheses it rules out a rigging map for their chosen test space and observable structure [66]. This is not a universal nonexistence statement for every quantization of that classical system. Likewise, the relational trinity of [46] uses particular clock–system constraints and spectral assumptions; it is not a theorem for all ordinary Lie-group constraints, much less the full field-dependent gravitational algebra.

Higher-derivative poles, physical positivity, and effective theory. The BFV formulation organizes gauge constraints and their ghost sector. It does not by itself remove every negative-residue propagating mode. In the quadratic-gravity calculation of Bellorin, Bórquez, and Droguett, the stated sign choice gives a massive transverse-traceless tensor and one scalar with negative norm, while the massive transverse vector has positive norm [8]. These are statements about that calculation; classifying the present model requires its own constraint reduction and physical observables.

A fakeon prescription changes the quantization of selected poles rather than deriving their removal from the classical constraint algebra. Fakeons can contribute internally to tree and loop amplitudes, but are excluded from physical asymptotic states and the corresponding unitarity cuts. The construction uses a specified nonanalytic continuation, with average continuation across fake thresholds [2]. Its physical cutting equations sum over physical states. It therefore does not dispense with positive physical probabilities, nor does it supply a positive physical space for an arbitrary mother action. It also does not preserve ordinary microscopic causality: the one-loop gravity analysis explicitly finds a causality violation associated with the fakeon scale [3]. A perturbative fakeon construction and a reflection-positive Euclidean reconstruction impose different conditions; neither may be inferred merely by choosing a propagator pole.

The low-energy alternative admits a simple quantitative statement. For a Euclidean scalar polarization with $G_\ell(p) = [p^2(1 + \ell^2 p^2)]^{-1}$, let $G_\ell^{(n)}(p) = p^{-2} \sum_{j=0}^{n} (-\ell^2 p^2)^j$. At $p^2 > 0$, the finite

geometric-series identity gives

$$G_\ell - G_\ell^{(n)} = \frac{(-\ell^2 p^2)^{n+1}}{p^2(1+\ell^2 p^2)}, \qquad \frac{|G_\ell - G_\ell^{(n)}|}{|G_\ell|} \le (\ell^2\Lambda^2)^{n+1}, \quad 0 < p^2 \le \Lambda^2. \tag{14.72}$$

The bound is useful when $\ell\Lambda < 1$. It bounds this propagator expansion, not an interacting amplitude without further estimates, and not the negative part of a physical inner product. Treating higher-derivative operators perturbatively in an effective theory avoids using its truncated action as an exact high-energy propagator; it does not establish a positive ultraviolet completion of that propagator.

Power counting must use the actual high-momentum behavior. For a connected four-dimensional graph, with propagator decay p^{-r_e} on internal line e and d_v derivatives at vertex v,

$$D = 4L + \sum_v d_v - \sum_e r_e, \qquad L = I - V + 1. \tag{14.73}$$

Two-derivative Einstein power counting gives $D = 2L + 2$; if all relevant propagators decay as p^{-4} and all vertices carry at most four derivatives, it gives $D \le 4$. Mixed matter and gauge sectors require their own line and vertex counts. Neither estimate proves positive physical spectral weights. A negative component of a gauge-fixed auxiliary propagator also cannot alone decide physical unitarity: positivity tests concern physical observables under the stated spectral assumptions. Finally, a Euclidean renormalization-group fixed point does not supply Lorentzian constraint closure, causal reconstruction, or the physical inner product without the corresponding additional results.

14.10. *Constraint-preserving diffusions and pathwise clock readings.* The geometric constraint problem also appears before quantization: noise tangent to a curved surface produces a normal Itô drift. This drift is fixed by the curvature of the constraint surface. Keeping it explicit separates geometric invariance from the choice of an optimal approximation to an unconstrained stochastic model.

For a smooth regular constraint surface $\mathcal{M} = \{C_A = 0\}$ and an Itô diffusion $dZ = b\,ds + \sum_r \sigma_r\,dW^r$, Itô's formula gives the local invariance conditions on $\mathcal{M}$:

$$DC_A\sigma_r = 0, \qquad DC_A b + \tfrac{1}{2}\sum_r D^2C_A[\sigma_r,\sigma_r] = 0. \tag{14.74}$$

Under smooth local existence and uniqueness assumptions, these conditions ensure invariance up to the lifetime of the solution. They are independent of a particular projection convention. Stratonovich, Itô-vector and Itô-jet projections are all manifold-valued constructions when defined intrinsically. Armstrong, Brigo, and Ferrucci identify different local approximation criteria: in their setting the Itô-vector projection minimizes the stated leading weak error after fixing the diffusion approximation, whereas the Itô-jet projection minimizes the stated mean-square error relative to

the metric-projected process [4]. These criteria are distinct from constraint preservation. A numerical constraint residual can compare discretizations but cannot by itself choose a unique continuous projection.

On the unit sphere $\mathbb{S}^{d-1}$, $d \geq 2$, put $P_x = I - xx^{\mathsf{T}}$ and let U be smooth. The intrinsic Stratonovich diffusion and its equivalent Itô equation are

$$\begin{aligned} dX &= -P_X \nabla U \, ds + \sqrt{2\theta}\, P_X \circ dW, \\ dX &= [-P_X \nabla U - \theta(d-1)X] \, ds + \sqrt{2\theta}\, P_X \, dW. \end{aligned} \tag{14.75}$$

Here an arbitrary smooth ambient extension of U can be used; its projected gradient on the sphere is intrinsic. For the diffusion columns $V_r(x) = P_x e_r$, differentiation gives $\sum_r DV_r(x)V_r(x) = -(d-1)x$ on the sphere. Therefore the Stratonovich-to-Itô correction is $-\theta(d-1)x$. Since $x^{\mathsf{T}} P_x = 0$ and $\operatorname{tr} P_x = d - 1$,

$$d|X|^2 = [-2\theta(d-1) + 2\theta \operatorname{tr} P_X] \, ds = 0. \tag{14.76}$$

The generator is $\mathcal{L} = \theta \Delta_{\mathbb{S}} - \nabla_{\mathbb{S}} U \cdot \nabla_{\mathbb{S}}$. Integration by parts on the compact sphere gives the invariant law $Z^{-1} e^{-U/\theta} d \operatorname{vol}_{\mathbb{S}}$, and, for smooth f, g,

$$\int f \mathcal{L} g \, d\nu = -\theta \int \nabla_{\mathbb{S}} f \cdot \nabla_{\mathbb{S}} g \, d\nu. \tag{14.77}$$

This example verifies both the constraint and the Gibbs reference. A time-stepping rule must still be checked separately: a generic Euler step does not preserve the sphere exactly, and geometric projection of a step does not automatically preserve the invariant law.

Finally, a clock function $T(Z)$ has Itô differential and quadratic variation

$$dT = (\mathcal{L}T) \, ds + \sum_r DT\sigma_r \, dW^r, \qquad [T]_s = \int_0^s \sum_r |DT\sigma_r|^2 \, du. \tag{14.78}$$

A positive drift does not ensure increasing readings along individual paths: $T_s = s + \varepsilon W_s$ fails to be monotone for every $\varepsilon > 0$. A continuous monotone path has finite variation and zero quadratic variation. Thus monotone diffusion clocks necessarily satisfy $DT\sigma_r = 0$ almost everywhere along their paths. Together with $\mathcal{L}T \geq 0$, this condition is sufficient for nondecreasing readings; a uniform positive lower bound gives strictly increasing readings while the chart remains valid. The spacetime condition that dT is timelike, the probabilistic condition of pathwise monotonicity, and the identification of a physical clock with an auxiliary diffusion parameter are three separate requirements.

The finite calculations above give explicit measure, reduction, and stochastic-invariance results. Connecting them to an interacting quantum geometry requires a single action and measure to satisfy the complete gravitational constraints, regulator-uniform evolution and moment estimates, and a nontrivial positive physical quantum construction. Those connections are additional physical and analytic requirements; the logarithmic Gaussian example alone does not select them.

14.11. *A finite covariant extension with controlled inverse coframes.* The preceding constructions isolate three physical requirements: a coframe must transform with the local reference frame, inverse geometric observables must be integrable, and the time evolution must use the declared interaction. These requirements can be satisfied together in a finite Euclidean model. The construction below changes both the coframe representation and its probability law. It is an extension to be matched to the original mother branch, rather than a change of coordinates in that branch.

Take a fixed finite graph with oriented edges, a finite list of plaquettes, and four-dimensional internal Euclidean frames. At vertex v, set $e_v = R_v \exp S_v$, with $R_v \in \mathrm{SO}(4)$ and $S_v \in \mathrm{Sym}(4)$; let $\sigma_v \in \mathbb{R}$. On edge (v, w) take $U_{vw} \in \mathrm{SO}(4)$. For local rotations L_v, prescribe

$$R_v \mapsto L_v R_v, \qquad U_{vw} \mapsto L_v U_{vw} L_w^{-1}, \qquad S_v \mapsto S_v, \quad \sigma_v \mapsto \sigma_v. \tag{14.79}$$

Thus $e_v - U_{vw} e_w$ transforms as $L_v(e_v - U_{vw} e_w)$. The graph and coordinate column indices remain fixed: local internal rotations are being restored, not arbitrary changes of spacetime coordinates.

Normalize each Haar measure and put independent logarithmic Gaussians ν_a of (14.57) on the coframes, and normalized densities proportional to $e^{-b\sigma_v^2}$ on the scalars, with $a, b > 0$. Call the product reference measure $\nu_{a,b,h}$. For nonnegative κ, f^2, η and $\alpha \geq 0$, define

$$W_h = \frac{\kappa}{2} \sum_{(v,w)} \|e_v - U_{vw} e_w\|_F^2 + \sum_p \omega_{v(p)} k_p(U) + \frac{f^2}{2} \sum_{(v,w)} (\sigma_v - \sigma_w)^2, \tag{14.80}$$

$$\omega_v = e^{-\alpha\sigma_v} \left(1 + \eta \frac{\operatorname{tr} S_v^2}{1 + \operatorname{tr} S_v^2}\right), \qquad k_p(U) = 4 - \operatorname{tr} U_p.$$

Here $v(p)$ is a declared base vertex of each plaquette and U_p is its oriented holonomy. Since $U_p \in \mathrm{SO}(4)$, $k_p \geq 0$. All quantities in this construction are dimensionless after fixing a coframe scale, a scalar scale, and an energy unit.

Proposition 14.9 (A finite covariant Gibbs law). *The law $d\mu_h = Z_h^{-1} e^{-W_h} d\nu_{a,b,h}$ is well defined, locally* $\mathrm{SO}(4)$ *invariant, and has all positive inverse-coframe moments at each vertex. More precisely, for $r > 0$,*

$$0 < Z_h \leq 1, \qquad \mathbb{E}_{\mu_h} (\det e_v)^{-r} \leq Z_h^{-1} e^{r^2/a}, \qquad \mathbb{E}_{\mu_h} \|e_v^{-1}\|_F^r \leq Z_h^{-1} 2^{r+5} e^{r^2/(2a)}. \tag{14.81}$$

On the product Riemannian configuration space, its gradient Dirichlet form has a conservative reversible realization and only constants have zero Dirichlet energy. It therefore has a unique invariant probability density relative to μ_h.

Proof. Every summand of W_h is nonnegative and smooth. The integrand e^{-W_h} is strictly positive at every finite configuration, proving $0 < Z_h \leq 1$. Equation (14.79), orthogonal invariance of the Frobenius norm, and conjugation invariance of the plaquette trace give invariance of W_h. Left invariance of Haar measure gives invariance of the reference law. For a nonnegative observable F,

$\mathbb{E}_{\mu_h} F \le Z_h^{-1} \mathbb{E}_{\nu_{a,b,h}} F$. Apply the previously calculated logarithmic Gaussian moments to obtain (14.81).

Write $\Phi_h = a \sum_v \operatorname{tr} S_v^2 + b \sum_v \sigma_v^2 + W_h$. The smooth positive density proportional to $e^{-\Phi_h}$ defines the closed gradient form $\mathcal{E}_h(f,f) = \theta \int |\nabla f|^2 d\mu_h$. Choose smooth radial cutoffs in the noncompact coordinates, equal to one on a ball of radius R, vanishing outside radius $2R$, and with gradient bounded by C/R. They converge to one in $L^2(\mu_h)$ and their energies are at most $\theta C^2/R^2$. Hence the constant function belongs to the form domain with zero energy, and the associated symmetric Markov semigroup is conservative. A function of zero energy has zero weak gradient; connectedness and the strictly positive density imply that it is constant. This gives irreducibility and uniqueness of the invariant probability density. The generator on compactly supported smooth functions is

$$\mathcal{L}_h = \theta\Delta - \theta \nabla \Phi_h \cdot \nabla, \qquad \frac{d}{dt}\left[\theta \int f_t \log f_t \, d\mu_h\right] = -\theta^2 \int \frac{|\nabla f_t|^2}{f_t} \, d\mu_h. \tag{14.82}$$

The identity follows by integration by parts for positive smooth densities with finite dissipation; approximation extends the integrated inequality to the usual finite-entropy domain. □

The thermodynamic content of this model is specific. The reference energy is $E_h = \theta \Phi_h$, the chosen mobility is the identity in the specified product metric, and its covariance is 2θ times that mobility. Equation (14.82) is therefore a free-energy balance for this declared isothermal dynamics. Identification with measured bath entropy still uses the heat convention and local detailed balance developed earlier. Neither the equilibrium density alone nor local rotation invariance fixes the mobility, the clock, or a, b.

There is also an exact internal constraint statement. On the cotangent bundle, the infinitesimal site action now moves R_v as well as the links. With the moment-map convention of Proposition 14.6, its Gauss generator pairs the momenta with these variations:

$$G[\xi] = \sum_{(v,w)} p_{U_{vw}} (\xi_v U_{vw} - U_{vw} \xi_w) + \sum_v p_{R_v} (\xi_v R_v). \tag{14.83}$$

Cotangent-lift equivariance gives the same internal Lie algebra and any invariant Hamiltonian preserves $G = 0$. Omitting the second sum would omit the coframe charge. These are internal rotation constraints on a fixed graph; lapse and shift constraints have not been constructed here. Moreover, the positive Euclidean action above has not been derived by reducing the full mother group. Its matching, Lorentzian continuation, and regulator dependence remain distinct questions. In particular, Z_h^{-1} in (14.81) need not be uniformly bounded as the graph grows.

14.12. *Exact temporal normalization and the retained inertia.* A second connection concerns the time coordinate. A field-dependent normalization repeated at each time slice can change the limiting Hamiltonian, even when it seems harmless in a single integral. The retained $U(1)$ mode allows this effect to be computed without an expansion of the full field theory. Put $w = e^{-\alpha\sigma}$,

$w(0) = 1$, and let $\epsilon > 0$ denote the temporal spacing. The Wilson row integral is

$$c_\epsilon(\sigma) = \int_{-\pi}^{\pi} e^{-Iw(\sigma)(1-\cos q)/\epsilon}\, dq = 2\pi e^{-z} I_0(z), \quad z = \frac{Iw(\sigma)}{\epsilon}, \quad R_\epsilon = \frac{c_\epsilon(\sigma)}{c_\epsilon(0)}. \tag{14.84}$$

I_0 is the modified Bessel function. To specify how this row factor enters a transfer operator, consider the symmetric arrangement $T_{\mathrm{raw}} = R_\epsilon^{1/2} T_{\mathrm{norm}} R_\epsilon^{1/2}$, where each R_ϵ acts by multiplication. This is a declared kernel arrangement; an arbitrary mother kernel need not factor this way.

Proposition 14.10 (Endpoint compensation for one compact mode). *In this arrangement the exact compensating kernel multiplier is*

$$N_\epsilon(\sigma, \sigma') = R_\epsilon(\sigma)^{-1/2} R_\epsilon(\sigma')^{-1/2}. \tag{14.85}$$

Uniformly on each fixed compact scalar interval,

$$\log R_\epsilon = -\tfrac{1}{2} \log w + \frac{\epsilon}{8I}(w^{-1} - 1) + O(\epsilon^2). \tag{14.86}$$

Thus its leading endpoint multiplier is $w(\sigma)^{1/4} w(\sigma')^{1/4}$.

Proof. Multiplication by (14.85) cancels the two endpoint factors algebraically. The large-z formula $I_0(z) = e^z (2\pi z)^{-1/2}(1 + 1/(8z) + O(z^{-2}))$ gives (14.86), since w is bounded above and below on the specified interval. Taking minus one half of this logarithm gives the quarter power at each endpoint. □

For a constant scalar value, the uncompensated effective contribution $U_\epsilon = -\epsilon^{-1} \log R_\epsilon$ is

$$U_\epsilon = -\frac{\alpha\sigma}{2\epsilon} - \frac{e^{\alpha\sigma} - 1}{8I} + O(\epsilon). \tag{14.87}$$

A half power of w at each endpoint overcompensates and leaves the opposite divergence $+\alpha\sigma/(2\epsilon)$. A quarter power at each endpoint cancels the divergence but leaves the finite term $-(e^{\alpha\sigma} - 1)/(8I)$. Exact compensation cancels the entire declared row factor. For d independent Gaussian kinetic coordinates with the same scalar weight, the leading endpoint exponent is $d/4$; with a general kinetic matrix it is the corresponding determinant factor. The exponent must therefore be computed for the retained variables.

For example, the synthetic values $I = 1$, $\alpha = 0.3$, $\sigma = 1$ give the following direct Bessel evaluations. The last column concerns only the row contribution, not the complete Hamiltonian.

ϵ	$\epsilon U_{\mathrm{raw}}$	$\epsilon U_{1/2}$	$U_{1/4}$
0.10000	−0.15501838	0.14498162	−0.05018378
0.05000	−0.15232871	0.14767129	−0.04657415
0.02500	−0.15112701	0.14887299	−0.04508030
0.01250	−0.15055487	0.14944513	−0.04438996
0.00625	−0.15027536	0.14972464	−0.04405726
Limit	−0.15	0.15	−0.04373235

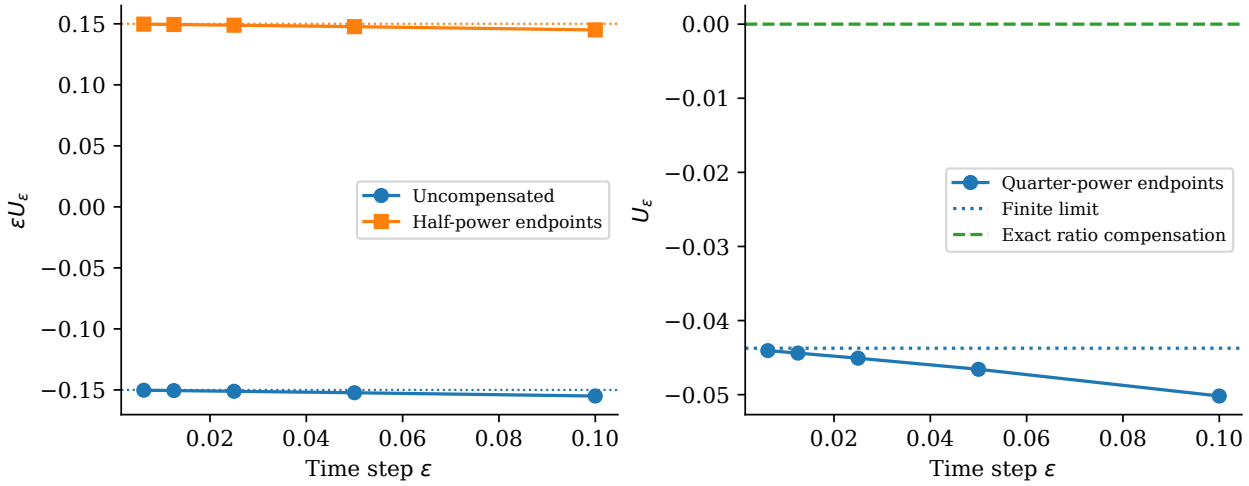


Figure 16. Synthetic normalization calculation for one retained compact mode. Left: the uncompensated and half-power choices have opposite divergent potentials. Right: quarter-power compensation leaves a finite potential, whereas the exact Bessel ratio removes the declared row factor.

The corresponding numerical diagnostic is shown in Figure 16.

Normalization does not remove the matched inertia $Iw(\sigma)$ in (14.20). Rescaling the angle by a scalar-dependent factor would change its periodicity and introduce mixed derivatives when the scalar moves. Nor does the factor $J(\Delta\sigma)^2/(2\epsilon)$ in a short-time action imply a Hamiltonian inertia proportional to ϵ^{-1}: the factor ϵ^{-1} arises from integrating a squared velocity over a time step. Temporal normalization, kinetic matching, and spatial regulator removal are separate operations.

14.13. *Nondegeneracy at a stated observation scale.* An observation averages fields over a finite region. This gives a useful nondegeneracy question that is weaker than controlling the smallest coframe determinant at every regulator vertex. Fix the coordinate reference volume used to define $D_v = \det e_v > 0$, and deterministic weights $b_{jv} \geq 0$ with $\sum_v b_{jv} = 1$ for $j = 1, \dots, M$. Define $\bar{D}_j = \sum_v b_{jv} D_v$; these are averages of a density relative to that fixed volume, not coordinate-independent scalars without an observation prescription.

Proposition 14.11 (Finite-resolution determinant bound). *Suppose, for every $r > 0$ and vertex v, $\mathbb{E}D_v^{-r} \leq C_h e^{r^2/a}$, with $C_h \geq 1$. Then, for $0 < \delta < 1$,*

$$\mathbb{E}\bar{D}_j^{-r} \leq C_h e^{r^2/a}, \qquad \mathbb{P}\{\min_j \bar{D}_j < \delta\} \leq \min\{1, MC_h e^{-a\log^2(1/\delta)/4}\}. \tag{14.88}$$

No independence assumption is required.

Proof. Convexity of $x \mapsto x^{-r}$ gives $\bar{D}_j^{-r} \leq \sum_v b_{jv} D_v^{-r}$. Markov's inequality and a union bound then give $MC_h\delta^r e^{r^2/a}$. Its exponent $r\log\delta + r^2/a$ is minimized at $r = (a/2)\log(1/\delta)$, proving the assertion. □

For the product logarithmic law, $C_h = 1$. For the interacting model of Proposition 14.9, $C_h = Z_h^{-1}$ is available and must be retained. If $\bar{D}(x)$ is also defined for continuously located observations, assume its Lipschitz constant is at most K_L outside an event of probability ζ. An η-net with $M(\eta)$ centers then gives, for every $r > 0$,

$$\mathbb{P}\{\inf_x \bar{D}(x) < \delta\} \le \min\{1, \zeta + M(\eta) C_h (\delta + K_L \eta)^r e^{r^2/a}\}. \tag{14.89}$$

Indeed an observation below δ has a net center below $\delta + K_L\eta$ on the Lipschitz event. Spatial regularity and uniform control of C_h would still have to be proved for a continuum claim.

The need for joint control can be seen without asymptotics. Under the one-vertex logarithmic law, $\log D$ is Gaussian with variance $2/a$. For $a = 1$ and $\delta = 0.1$, the one-vertex probability is approximately 0.05174405. For $N = 10$ independent vertices the minimum falls below δ with probability 0.41216455; for $N = 100$ the probability is 0.99507328. Perfectly correlated copies keep the one-vertex probability for every N. The same marginals therefore do not determine the large-graph event. A union upper bound that grows beyond one proves neither degeneration nor nondegeneration. Finally, $e = \mathrm{diag}(z, z^{-1}, 1, 1)$ has determinant one while $\|e^{-1}\|_F^2 = z^2 + z^{-2} + 2$ diverges as $z \to \infty$. Determinant control must be supplemented by shape control when inverse metrics are the observable of interest.

14.14. *Equilibrium preservation does not select a physical clock.* The equilibrium reference constrains admissible dynamics, but a reference density does not determine the rate of physical evolution. This is particularly relevant when a thermodynamic model is matched to a field-theoretic clock. Let $\pi \propto e^{-U/\theta}$, and write the reversible diffusion generator in fixed Euclidean coordinates as

$$Lf = \theta \pi^{-1} \nabla \cdot (\pi \Gamma \nabla f) = \theta \nabla \cdot (\Gamma \nabla f) - \Gamma \nabla U \cdot \nabla f. \tag{14.90}$$

Here Γ is symmetric positive definite. Under the time change $dt = r(X_s)ds$, with smooth $0 < c \le r \le C$, the new generator and stationary law are

$$L_r = r^{-1} L, \qquad d\pi_r = Z_r^{-1} r \, d\pi, \qquad Z_r = \int r \, d\pi. \tag{14.91}$$

To verify stationarity, integrate $L_r f$ against π_r and cancel r. More explicitly, choose $\Gamma_r = \Gamma/r$ and $U_r = U - \theta \log r$. The derivative of r^{-1} in the divergence term cancels the derivative of $-\theta \log r$ in the drift, leaving L/r. The Dirichlet form becomes $\mathcal{E}_r = \mathcal{E}/Z_r$. Although U_r represents the new occupation density, this algebra does not show that a mechanical energy has changed solely because a clock has been relabelled. Physical heat and work must use the calibrated generator and the declared bath model.

For a concrete obstruction, take $L_a = \theta \partial_y^2 - 2\theta a y \partial_y$ and $r(y) = e^{-(a'-a)y^2}$ with $a, a' > 0$. The stationary density after time change is still Gaussian, proportional to $e^{-a'y^2}$, but its diffusion coefficient is $\theta/r(y)$ and is nonconstant if $a' \neq a$. Thus the Gaussian Gibbs family is preserved while the constant-diffusion Ornstein–Uhlenbeck family is not. Although this r need not be bounded,

its stationary mean is finite and positive; ergodicity of the original process gives $\int_0^s r(X_u)du \to \infty$, so the time change remains conservative. Even a constant r leaves a global clock-scale freedom. Selecting a physical time therefore requires a dynamical matching or a clock observable beyond membership in a Gibbs family.

14.15. *Backreaction from the same shared weight.* The retained mechanical model now gives a quantitative test of how a common weight affects an observable. A changing scalar changes both the gauge kinetic energy and its restoring force. The leading frequency at a fixed scalar value is consequently independent of that weight, while energy exchanged with a moving scalar gives an amplitude-dependent correction. This distinction determines which experiment the model would require.

Write $K = K_\sigma > 0$, $x = \sigma - \sigma_0$, and $w_0 = e^{-\alpha\sigma_0}$. The previous branch has $\sigma_0 = 0$; a displaced reference requires an explicitly included preparation or stabilizing potential $K(\sigma - \sigma_0)^2/2$. With $\omega_0^2 = \beta/I$ and $\Omega^2 = K/J$, the exact equations are

$$\ddot{q} - \alpha\dot{x}\dot{q} + \omega_0^2 \sin q = 0, \tag{14.92}$$

$$J\ddot{x} + Kx = \alpha w_0 e^{-\alpha x}[\beta(1 - \cos q) - I\dot{q}^2/2]. \tag{14.93}$$

Their conserved energy is

$$E = \tfrac{1}{2} I w_0 e^{-\alpha x}\dot{q}^2 + \tfrac{1}{2} J\dot{x}^2 + \beta w_0 e^{-\alpha x}(1 - \cos q) + \tfrac{1}{2} K x^2. \tag{14.94}$$

The scalar source contains a potential contribution and a kinetic contribution with opposite signs. Substitution of $q = A\cos\omega_0 t$ gives $F\cos 2\omega_0 t$ to order A^2, where

$$F = \tfrac{1}{2}\alpha\beta w_0 A^2, \qquad \Delta = K - 4J\omega_0^2, \qquad B = F/\Delta. \tag{14.95}$$

Its mean vanishes at this order. For $\Delta \neq 0$, the periodic particular solution is $B\cos 2\omega_0 t$, whereas zero scalar position and velocity initially give

$$x_a(t) = B(\cos 2\omega_0 t - \cos \Omega t). \tag{14.96}$$

At $\Omega = 2\omega_0$, direct resonant forcing instead gives

$$x_a(t) = \frac{\alpha\beta w_0 A^2}{8J\omega_0}\, t \sin 2\omega_0 t.$$

The static denominator K cannot replace Δ in an oscillatory response, and proximity to resonance requires a different approximation.

For a smooth small-amplitude periodic branch admitting a regular expansion, the order-A^3 equation for q contains the fundamental forcing $\omega_0^2 A^3/8 + \alpha B A \omega_0^2$. The first term follows from $\cos^3 t = (3\cos t + \cos 3t)/4$; the second follows from $2\sin 2t \sin t = \cos t - \cos 3t$ in $\alpha\dot{x}\dot{q}$. Removing

the secular fundamental term therefore gives the coefficient

$$\frac{\omega-\omega_0}{\omega_0}=-\frac{A^2}{16}-\frac{\alpha^2\beta w_0A^2}{4\Delta}+O(A^4). \tag{14.97}$$

This coefficient calculation presumes such a regular branch and excludes the displayed resonance. It does not establish its global existence or a uniform remainder for arbitrary preparations. A finite-time estimate for an explicitly prepared trajectory can, however, be proved directly.

Proposition 14.12 (Finite-time response estimate). *Assume $I,J,\beta,K,w_0>0$, $\alpha\ge 0$, $0<A<\pi$ and $\Delta\neq 0$. Let the exact solution start at $(q,\dot q,x,\dot x)=(A,0,0,0)$, and set $y_a=(A\cos\omega_0 t,-A\omega_0\sin\omega_0 t,x_a,\dot x_a)$. Define $E_0=\beta w_0(1-\cos A)$ and*

$$\begin{aligned}&S_e=\sqrt{2E_0/K}, && w_-=w_0e^{-\alpha S_e}, && Q_e=\arccos(1-E_0/(\beta w_-)),\\ &V_e=\sqrt{2E_0/(Iw_-)}, && Z_e=\sqrt{2E_0/J}, && S_a=2|B|,\quad Z_a=|B|(2\omega_0+\Omega).\end{aligned} \tag{14.98}$$

Require $E_0<2\beta w_-$ and put

$$\begin{aligned}&Q=\max(Q_e,A),\quad V=\max(V_e,A\omega_0),\quad S=\max(S_e,S_a),\\ &Z=\max(Z_e,Z_a),\qquad w_+=w_0e^{\alpha S}.\end{aligned} \tag{14.99}$$

In the norm $\|y\|_E^2=\omega_0^2q^2+v^2+\Omega^2x^2+z^2$, the exact error obeys, for every finite $t\ge 0$,

$$\|y(t)-y_a(t)\|_E\le\eta\frac{e^{L_Et}-1}{L_E}, \tag{14.100}$$

with the continuous interpretation ηt if $L_E=0$, where

$$\begin{aligned}\eta_v&=\omega_0^2A^3/6+\alpha Z_aA\omega_0,\\ \eta_z&=\frac{\alpha\beta w_0}{J}\left[\frac{A^2}{2}(e^{\alpha S_a}-1)+e^{\alpha S_a}\frac{A^4}{24}\right],\qquad \eta=(\eta_v^2+\eta_z^2)^{1/2},\\ L_E^2&=\left(\frac{\omega_0Q^2}{2}\right)^2+(\alpha Z)^2+(\alpha V)^2+\left(\frac{\alpha\beta w_+Q}{J\omega_0}\right)^2\\ &\quad+\left(\frac{\alpha Iw_+V}{J}\right)^2+\left[\frac{\alpha^2w_+(\beta Q^2+IV^2)}{2J\Omega}\right]^2.\end{aligned} \tag{14.101, 14.102}$$

Proof. Energy conservation gives $|x|\le S_e$, $|\dot x|\le Z_e$ and $|\dot q|\le V_e$. A continuous trajectory from $A\in(0,\pi)$ cannot reach either $q=\pi$ or $q=-\pi$, because its potential energy there is at least $2\beta w_->E_0$. On this connected potential well it therefore satisfies $|q|\le Q_e$. The approximate trajectory lies in the enlarged box (14.99), so every line segment between the two trajectories lies in that box. These bounds also prevent finite-time escape of the exact solution.

Separate the first-order vector field as $\dot y=\mathsf{A}y+N(y)$, where A is the direct sum of the two harmonic oscillators and

$$N(y)=\left(0,\alpha zv+\omega_0^2(q-\sin q),0,\frac{\alpha w_0e^{-\alpha x}}{J}[\beta(1-\cos q)-Iv^2/2]\right). \tag{14.103}$$

The linear group is an isometry in $\|\cdot\|_E$. The six possibly nonzero entries of the weighted Jacobian of N have the bounds whose squares appear in (14.102). Here one uses $|\sin q| \le |q|$ and $1-\cos q \le q^2/2$. Their Frobenius norm bounds the operator norm, giving a Lipschitz constant L_E on the box.

Only the velocity equations have a residual at y_a. The bound $|q - \sin q| \le |q|^3/6$ gives η_v. For the scalar equation,

$$\beta(1-\cos q_a) - Iv_a^2/2 = \tfrac{1}{2}\beta A^2 \cos 2\omega_0 t + \rho(t), \qquad |\rho(t)| \le \beta A^4/24. \tag{14.104}$$

Multiply by $e^{-\alpha x_a}$ and use $|e^{-\alpha x_a} - 1| \le e^{\alpha S_a} - 1$ to obtain η_z. Variation of constants then bounds the error by $\int_0^t (L_E \|y(s) - y_a(s)\|_E + \eta) ds$. Gronwall's inequality gives (14.100) because the initial error is zero. □

The estimate controls a complete trajectory in fixed time units, not only the scalar amplitude. It can be conservative over long observation windows because it grows exponentially. A small frequency correction therefore still needs a phase-error estimate, a sufficiently long calibrated measurement, and detector noise below the signal. In particular, (14.100) supplies no automatic experimental resolution.

Synthetic comparisons without changing the parameters. Fix $I = J = \beta = 1$, $K = 9$, $\alpha = 0.3$, and $\sigma_0 = 0$. For zero scalar initial data, integrate the complete equations (14.92)–(14.93) for $T = 2\pi$. An eighth-order DOP853 calculation uses relative tolerance $2 \cdot 10^{-12}$, absolute tolerance $2 \cdot 10^{-14}$, and maximum step 0.025. The table compares the largest error on 2001 equally spaced samples with the analytic bound at T, which also bounds all earlier times.

A	L_E	Sampled maximum error	Bound at T
0.05	0.03015577	$5.26033 \cdot 10^{-5}$	$1.83037 \cdot 10^{-4}$
0.10	0.06072202	$4.20385 \cdot 10^{-4}$	$1.61928 \cdot 10^{-3}$
0.20	0.12368627	$3.34897 \cdot 10^{-3}$	$1.60915 \cdot 10^{-2}$

The maximum sampled relative energy drift is below $7.5 \cdot 10^{-14}$. This is a numerical conservation check; floating-point integration is not an interval enclosure of the exact trajectory.

A separate long-time calculation uses the same coefficients and $(q, \dot q, x, \dot x) = (A, 0, B, 0)$, which matches the periodic preparation through order A^2. DOP853 tolerances are $2 \cdot 10^{-11}$ and $2 \cdot 10^{-13}$, the maximum step is 0.15, and the duration is 240π; frequency is measured from successive peaks after 40π. For $A = 0.05, 0.10, 0.20$, respectively, the measured frequencies are 0.999832510370, 0.999330165599, and 0.997322636213. Equation (14.97) gives 0.999832500000, 0.999330000000, and 0.997320000000. The coefficients approach $(1-\omega)/A^2 = 0.067$, whereas the frozen-scalar pendulum has leading coefficient $1/16 = 0.0625$. Its exact comparator is $\pi/[2\mathsf{K}(\sin^2(A/2))]$, where $\mathsf{K}(m) = \int_0^{\pi/2} (1 - m\sin^2 u)^{-1/2} du$. No coefficient is fitted between these comparisons. The two initial preparations must be distinguished: the finite-time theorem above addresses the zero-scalar preparation, not the long-time peak estimator. The corresponding numerical diagnostic is shown in Figure 17.

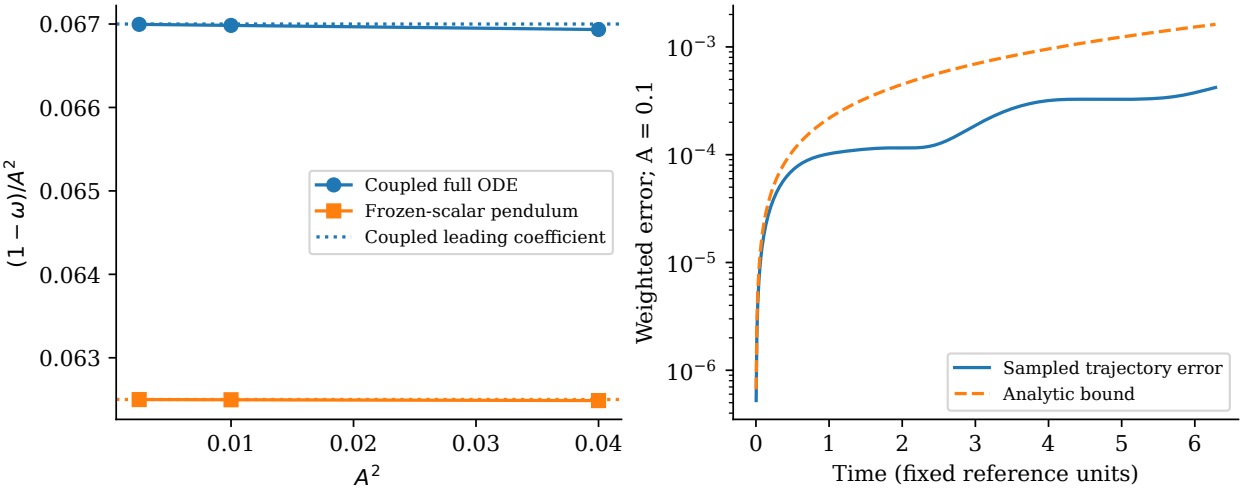


Figure 17. Synthetic shared-weight response. Left: frequencies from the coupled equations, compared with the frozen-scalar pendulum and the perturbative coefficient, using the same registered parameters. Right: the zero-scalar preparation at $A = 0.1$, compared with the analytic finite-time error bound. These simulations are finite-model calculations, not observations of a new interaction.

14.16. *What the finite construction requires of the field theory.* The finite results give concrete tests for an extension to fluctuating geometry. Such an extension must identify its independent fields and reduce their complete constrained spectrum. Up to ten broken symmetry directions can be represented in a vierbein in suitable spontaneous Lorentz- and diffeomorphism-breaking models [9]; this is not a count of ten propagating massless particles. Gauge directions, first- and second-class constraints, and kinetic degeneracies change the physical count. Massive negative-norm or tachyonic modes must be tested as well as massless polarizations. The teleparallel equivalent of general relativity is equivalent to GR under its defining assumptions [70]; extra modes in modified teleparallel theories cannot be assigned to TEGR itself. An independent Palatini connection can be auxiliary. Its spectrum depends on its action and cannot be inferred from a universal "two plus five" count.

Constraint closure must likewise refer to the specified generators. Loll's lattice calculation concerns the spatial diffeomorphism commutator in a particular construction and its small-spacing behavior [64]. It does not preclude exact finite internal Gauss closure, and it does not supply the missing Hamiltonian and mixed brackets of the present mother theory. If a deformed gravitational algebra is used, its generators, structure functions, Jacobi identities, error topology, and common continuum limit must all be specified. These requirements cannot be replaced by the fact that a finite symmetry exists.

Finally, a local one-loop expansion cannot decide a far negative log-coframe tail without a uniform remainder and a coercive estimate there. Nor does a nonzero projection of a constraint onto a Hessian nullspace establish ghost removal: the full reduced Hamiltonian and its inner product

are needed. A fakeon prescription is a distinct physical choice involving analytic continuation and microscopic causality [2] and [3]. Discrete spatial momentum alone is not a no-go theorem for that prescription; lattice dispersion functions can have analytic extensions and time can remain continuous. Conversely, the present finite construction does not implement such a prescription. The earlier negative-residue reflection test for the unchanged higher-derivative tensor kernel remains applicable. A positive transfer operator for the retained compact model cannot remove that obstruction in a different physical sector. The new finite estimates identify what can be matched and calculated now, while leaving a precise spectral and dynamical task for the complete theory.

14.17. *Which conservation laws are recovered.* A common variational origin is useful only if the projected equations retain the corresponding balance laws. Three statements must be distinguished: pathwise constancy of a quantity, constancy of its expectation, and a balance in which resolved energy is exchanged with other fields or a bath.

Stochastic Noether theory in optimal control relates suitable contact symmetries of a sufficiently regular HJB equation to local martingales along optimal states [24]. The Itô criterion below tests a proposed charge; it does not construct a symmetry by itself. Its drift cancellation must follow from the actual symmetry theorem or from a direct calculation for the specified dynamics.

For a regular classical Lagrangian $L(q,\dot q,t)$ and an infinitesimal configuration symmetry $\delta q = \xi(q)$ at fixed time, suppose $\delta L = dB/dt$. On an Euler–Lagrange solution, writing $p = \partial_{\dot q} L$ gives

$$\frac{d}{dt}(p\cdot\xi - B) = (\dot p - \partial_q L)\cdot\xi + \delta L - \frac{dB}{dt} = 0.$$

This is the classical Noether charge. Time translation of an autonomous regular Lagrangian gives conservation of $H = p\cdot\dot q - L$; spatial translation and rotation give the corresponding momentum and angular momentum when external fields and boundaries share those symmetries. The recovery requires an identified mechanical action and the relevant symmetry, not only a noise coefficient tending to zero.

Proposition 14.13 (Stochastic charge and pathwise criterion). *Let $dX_t = b\,dt + \sigma\,dW_t$ be a well-posed finite-dimensional Itô diffusion and $Q \in C^{1,2}$ with $\mathbb{E}|Q(0,X_0)| < \infty$. Up to localization,*

$$dQ(t,X_t) = \left(\partial_t Q + b\cdot\nabla Q + \tfrac{1}{2}\sigma\sigma^{\mathsf T} : D^2 Q\right)dt + (\sigma^{\mathsf T}\nabla Q)\cdot dW_t.$$

If the drift vanishes, $Q(t,X_t)$ is a local martingale. It is a martingale, with constant expectation, when its stochastic integral is square integrable and its initial value is integrable. It is pathwise constant if both the drift and $\sigma^{\mathsf T}\nabla Q$ vanish along the trajectories. Conversely pathwise constancy forces these two terms to vanish almost everywhere along the trajectories.

Proof. Itô's formula gives the decomposition. Its quadratic variation is $\int_0^t |\sigma^\top \nabla Q|^2 \, ds$. A constant process has zero quadratic variation and zero finite-variation part; uniqueness of the semimartingale decomposition gives necessity. The zero-integrand conditions give sufficiency. Square integrability upgrades the local stochastic integral to a true martingale. □

For a time-independent charge in a Stratonovich Hamiltonian realization, $dQ = \{Q, H_0\}dt + \sum_k \{Q, H_k\} \circ dW^k$, a charge commuting with every H_k, including H_0, is pathwise conserved. A symmetry of the drift Hamiltonian alone is insufficient. For a time-independent charge, a state-dependent positive clock divides LQ by its rate and the stochastic coefficient by its square root; it preserves their vanishing when the time-change theorem applies. An explicitly time-dependent charge requires changing the time coordinate of the augmented process as well: replacing $Q(s, x)$ by $Q(t, x)$ without this transformation need not preserve a martingale. A vanishing-noise limit recovers a classical charge only if the actions, symmetries, coefficients, solutions, and relevant moment bounds converge. Classical Noether theory is therefore contained in a matched conservative limit, rather than in every deterministic limit.

Proposition 14.14 (A finite-time conservative limit). *On $\mathbb{R}^{2n}$ let $b_0 = J\nabla H$ be globally Lipschitz, where J is the canonical symplectic matrix. Let r_ϵ and σ_ϵ be uniformly bounded and globally Lipschitz coefficients, and let $0 < \epsilon \le 1$. Couple*

$$dX_t^\epsilon = [b_0(X_t^\epsilon) + \epsilon r_\epsilon(X_t^\epsilon)]\, dt + \sqrt{\epsilon}\, \sigma_\epsilon(X_t^\epsilon)\, dW_t, \qquad \dot{x}_t = b_0(x_t).$$

If $\mathbb{E}|X_0^\epsilon - x_0|^2 \le C_0\epsilon$, then for every finite T there is C_T independent of ϵ such that

$$\mathbb{E} \sup_{t \le T} |X_t^\epsilon - x_t|^2 \le C_T \epsilon.$$

Every continuous classical conserved charge Q therefore satisfies

$$\sup_{t \le T} |Q(X_t^\epsilon) - Q(x_0)| \longrightarrow 0 \quad \textit{in probability.}$$

Convergence of the corresponding expectations additionally requires uniform integrability.

Proof. Write the difference as the initial error, the integral of the b_0 difference, the ϵr_ϵ integral, and a martingale. If the Lipschitz constant of b_0 is L and the coefficient bounds are R, S (the latter in Hilbert–Schmidt norm), Cauchy–Schwarz, the inequality $|\sum_{i=1}^4 z_i|^2 \le 4 \sum_i |z_i|^2$, and Doob's L^2 inequality give, for $t \le T$,

$$F(t) \le 4C_0\epsilon + 4TL^2 \int_0^t F(s)\, ds + 4\epsilon^2 T^2 R^2 + 16\epsilon T S^2,$$
$$F(t) = \mathbb{E} \sup_{v \le t} |X_v^\epsilon - x_v|^2.$$

Gronwall's inequality proves the estimate. Continuity of Q and the continuous-mapping theorem on finite-time path space give the last assertion, since $Q(x_t) = Q(x_0)$. Uniform integrability is the extra condition needed to pass to expectations. □

These assumptions describe a finite-dimensional conservative branch. For locally Lipschitz physical forces the same estimate is first localized; a uniform exit or moment estimate is needed to remove the stopping time. Neither an arbitrary long-time limit nor removal of the field regulator follows from this finite-T argument. In particular, leaving a nonzero friction term as $\epsilon \to 0$ changes the limiting equation and need not preserve mechanical energy.

14.18. *A stochastic Hamiltonian example with exact conservation.* Take $X = (q, p)$, $H(X) = |X|^2/2$, and the canonical matrix $J = \left(\begin{smallmatrix} 0 & 1 \\ -1 & 0 \end{smallmatrix}\right)$. For a scalar Brownian motion and constant β,

$$dX = JX\,dt + \beta JX \circ dW = \left(JX - \frac{\beta^2}{2}X\right) dt + \beta JX\,dW.$$

Both driving Hamiltonians are multiples of H. Directly,

$$LH = -\frac{\beta^2}{2}|X|^2 + \frac{\beta^2}{2}|JX|^2 = 0, \qquad (\beta JX)\cdot\nabla H = 0.$$

Thus $H(X_t) = H(X_0)$ on every sample path. Equivalently $X_t = \exp[J(t + \beta W_t)]X_0$ is an orthogonal rotation. Omitting the Itô drift correction changes the model: for $dX = JX\,dt + \beta JX\,dW$ one instead obtains $dH = \beta^2 H\,dt$. This example identifies the precise cancellation needed for conservation; it also shows why stochasticity alone does not imply mechanical dissipation.

14.19. *Dissipation is compatible with a total energy balance.* Consider the isothermal Langevin momentum $dp = -(\gamma/m)p\,dt + \sqrt{2\gamma k_B T}\,dW_t$, with $E = p^2/(2m)$. Itô's formula yields

$$dE = \left(-\gamma p^2/m^2 + \gamma k_B T/m\right) dt + (p/m)\sqrt{2\gamma k_B T}\,dW_t.$$

The positive trace term must accompany the random work. If heat delivered to the reservoir is defined by the model's first-law convention,

$$dQ_{\text{bath}} = \left(\gamma p^2/m^2 - \gamma k_B T/m\right) dt - (p/m)\sqrt{2\gamma k_B T}\,dW_t,$$

then $dE + dQ_{\text{bath}} = 0$. At the Gibbs variance $\mathbb{E}p^2 = mk_BT$, the mean energy injection and friction loss cancel. This is the open-system energy ledger under a specified bath model, not a derivation of that bath's microscopic dynamics.

14.20. *Fluid, geometric, and gauge balances.* For an orthogonal, divergence-free Fourier–Galerkin projection on a periodic domain, let

$$du_N = [-\Pi_N((u_N\cdot\nabla)u_N) + \nu\Delta u_N + f_N]\,dt + G_N\,dW_t.$$

The kinetic-energy pairing gives

$$d\frac{\|u_N\|_2^2}{2} = \left[-\nu\|\nabla u_N\|_2^2 + \langle f_N, u_N\rangle + \frac{1}{2}\|G_N\|_{\text{HS}}^2\right] dt + \langle u_N, G_N\,dW_t\rangle.$$

The nonlinear term vanishes because orthogonality removes Π_N from the pairing and $\int u_N\cdot(u_N\cdot\nabla)u_N\,dx = \int\nabla\cdot(|u_N|^2u_N/2)\,dx = 0$. If the zero Fourier mode is included, spatial integration gives

$d\int u_N\,dx = (\int f_N\,dx)dt + \int G_N\,dW_t$. Thus momentum is conserved pathwise when both integrated sources vanish. If a mean-zero subspace is imposed instead, its prescribed mean is fixed as part of the phase space. Kinetic energy is conserved in the unforced inviscid deterministic branch; viscosity converts it into unresolved or internal energy in a thermodynamic completion. For a compressible smooth branch, $\partial_t\rho + \nabla\cdot(\rho u) = 0$ conserves total mass under periodic or impermeable boundaries. A proposed projection must retain this conservative form, or explicitly account for its mass source.

For interacting relativistic fields, diffeomorphism invariance of the complete matched action and the on-shell matter equations give the covariant total-stress balance. In an Einstein representation with higher-curvature terms consistently retained or placed in an effective stress tensor, it has the form $\nabla_\mu T^{\mu\nu}_{\mathrm{tot}} = 0$. Individual sectors can obey $\nabla_\mu T_i^{\mu\nu} = Q_i^\nu$ with $\sum_i Q_i^\nu = 0$. Local covariant balance does not imply a globally defined conserved energy in an arbitrary spacetime. A Killing symmetry and suitable boundary flux conditions provide such a charge; dynamical geometries require the corresponding boundary or asymptotic construction. Indeed, for symmetric T_{tot} and a Killing field ξ,

$$\nabla_\mu(T^{\mu\nu}_{\mathrm{tot}}\xi_\nu) = T^{\mu\nu}_{\mathrm{tot}}\nabla_{(\mu}\xi_{\nu)} = 0.$$

The divergence theorem then equates the charges on two spacelike slices when the intervening boundary flux vanishes.

Likewise the matched gauge equations imply a covariant current identity $D_\mu J^\mu = 0$ on shell under the appropriate gauge symmetry. For $D_\mu F^{\mu\nu} = g_{\mathrm{YM}}^2 J^\nu$ with a constant coupling, antisymmetry gives $D_\nu D_\mu F^{\mu\nu} = \frac{1}{2}[D_\nu, D_\mu]F^{\mu\nu} = 0$: the spacetime curvature contractions are symmetric–antisymmetric contractions, and the gauge-curvature contraction is proportional to $[F_{\nu\mu}, F^{\mu\nu}] = 0$. A field-dependent coupling instead requires differentiating the full gauge displacement in its field equation. The scalar and interaction terms cannot be dropped. An anomaly-free quantum realization and a well-defined boundary charge are additional requirements. The two-fluid internal-force cancellation, MHD Lorentz exchange, and conservative GP particle balance are concrete instances of this common bookkeeping principle. Controls, reservoirs, and unresolved modes must appear in the balance whenever they exchange the relevant quantity.

14.21. *What Remains Open.* Several extensions are intentionally left open rather than hidden behind formal notation:

(i) deriving a unique universal microscopic stochastic law from more primitive physics;
(ii) proving a universal action-to-generator principle beyond specified variational classes;
(iii) obtaining sharp hypocoercive entropy rates for broad molecular potentials;
(iv) proving a physical-time moving-history coercivity theorem in a general infinite-dimensional setting;
(v) obtaining a general uniform LSI for the full nonlinear infinite-dimensional 2D stochastic Navier-Stokes invariant law under colored forcing;

(vi) extending the framework consistently to nonisothermal, chemically reactive, quantum, relativistic, or gauge-field systems without importing unjustified analogies.

These are research problems, not premises of the proved second-law theorem.

14.22. *One coupled realization of equilibrium and maintained heat transport.* The physical interpretation of an entropy inequality can be verified in a finite model without changing its couplings between experiments. Let

$$H_{\mathrm{f}}(q,p)=\tfrac{1}{2}p^{T}p+\tfrac{1}{2}q^{T}K_{\mathrm{f}}q,\qquad K_{\mathrm{f}}=\begin{pmatrix}2&0&-\eta_{\mathrm{f}}\\0&3&-0.6\eta_{\mathrm{f}}\\-\eta_{\mathrm{f}}&-0.6\eta_{\mathrm{f}}&5\end{pmatrix},\qquad |\eta_{\mathrm{f}}|<\sqrt{5/0.62}.$$

Take unit masses, fixed dimensionless units, $k_B=1$, and

$$dq=p\,dt,\qquad dp=(-K_{\mathrm{f}}q-\Lambda_{\mathrm{f}}p)\,dt+\sqrt{2\Lambda_{\mathrm{f}}\Theta_{\mathrm{f}}}\,dW,\quad \Lambda_{\mathrm{f}}=\mathrm{diag}(0.7,0.9,0.8).$$

The three positive reservoir temperatures are the entries of Θ_{f}. The full finite proof in the mother paper [50] establishes a unique nondegenerate Gaussian law from a Hurwitz drift and controllability. This is an explicit thermal model, with supplied reservoirs and reversal $(q,p)\mapsto(q,-p)$.

The heat entering from reservoir i is

$$dQ_i=\gamma_i(\Theta_i-p_i^2)\,dt+\sqrt{2\gamma_i\Theta_i}\,p_i\,dW_i,\qquad dH_{\mathrm{f}}=\sum_i dQ_i.$$

This formula follows by applying Itô's rule to the stated energy; its constant term is the noise injection. At stationarity, $\dot{Q}_i=\gamma_i(\Theta_i-C_{p_ip_i})$ and $\sum_i\dot{Q}_i=0$. For the Gaussian density ρ_{f}, define the dissipative momentum currents $j_i=-\gamma_i(p_i\rho_{\mathrm{f}}+\Theta_i\partial_{p_i}\rho_{\mathrm{f}})$. Integration by parts gives

$$\sigma_{\mathrm{f}}=-\sum_i\frac{\dot{Q}_i}{\Theta_i}=\sum_i\int\frac{j_i^2}{\gamma_i\Theta_i\rho_{\mathrm{f}}}\geq 0.$$

The integration is over all positions and momenta. To check the equality, expand the squares and use $\int p_i\partial_{p_i}\rho_{\mathrm{f}}=-1$. The remaining Fisher terms sum to $\sum_i\gamma_i$, by stationarity of Shannon entropy. For a connected coupling graph, vanishing current requires equal temperatures: zero currents give $\rho_{\mathrm{f}}=f(q)e^{-\sum_i p_i^2/(2\Theta_i)}$, while Hamiltonian stationarity forces $\nabla\log f=-\Theta_{\mathrm{f}}^{-1}K_{\mathrm{f}}q$. Its Hessian is symmetric only when temperatures coincide along every nonzero coupling edge.

Equal temperatures therefore give a Gibbs equilibrium with zero stationary entropy production. Unequal temperatures give maintained heat transport with strictly positive entropy production when $\eta_{\mathrm{f}}\neq 0$. The same mechanical energy and couplings occur in both experiments. The difference is the supplied reservoir condition, not a reinterpretation of every random motion as irreversible.

For synthetic generating value $\eta_{\mathrm{f}}=0.7$, calibration at equal temperature 0.8 uses the exact relation $\eta_{\mathrm{f}}=2C_{q_1q_3}/C_{q_3q_3}$. Independent Gaussian calibration gives $\widehat{\eta}_{\mathrm{f}}=0.69559058$, with standard error 0.01076504. Freezing this parameter predicts entropy rates $0.00479634, 0.01558864, 0.04138724$

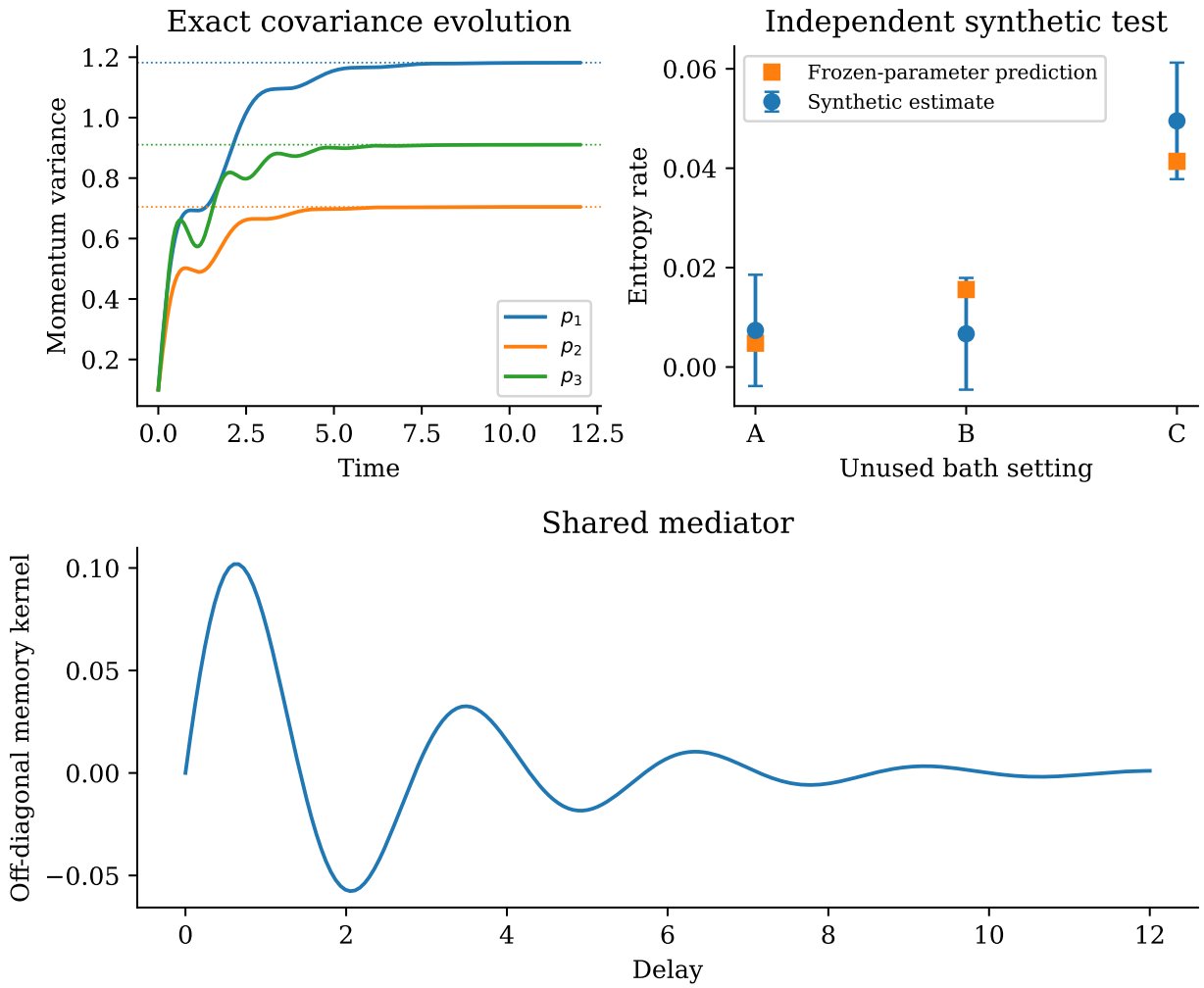


Figure 18. One fixed coupling connects covariance relaxation, reservoir entropy production and a retarded interaction. Error bars are 1.96 combined asymptotic standard errors from independent synthetic calibration and target samples. The lower panel retains the memory generated by eliminating the mediator.

at reservoir settings $(1.2, 0.7, 0.9)$, $(1.4, 0.5, 0.9)$, and $(1.6, 0.3, 0.9)$. Independent synthetic estimates are $0.00736950, 0.00668704, 0.04951965$; the combined first-order standard errors are $0.00571119, 0.00573660, 0.00598202$. The weakest setting is poorly resolved at this sample size. These are finite model comparisons, not experimental observations.

The corresponding numerical diagnostic is shown in Figure 18.

14.23. *A dimension-independent decay rate with a non-tight equilibrium family.* An additional condition is needed to transfer the finite theorem to a continuum. The energy and volume conditions used in the finite thermal model are also central to [103]. Let $u \in \mathbb{R}^N$, and suppose

$$du = (-\nu A_N u - B_N(u))dt + \sqrt{2\nu\Theta A_N}\, dW, \quad A_N \succeq \lambda_1 I, \quad u \cdot B_N(u) = 0, \quad \operatorname{div} B_N = 0.$$

At fixed N, smooth locally Lipschitz coefficients and the energy estimate give nonexplosion; nondegenerate noise gives the usual local elliptic smoothing. The invariant Gaussian is $\pi_N = N(0, \Theta I_N)$, since $\operatorname{div}(B_N \pi_N) = 0$. The nonlinear contribution to the derivative of $D(\rho\|\pi_N)$ is zero, and Gaussian logarithmic Sobolev gives

$$D(\rho_t\|\pi_N) \le e^{-2\nu\lambda_1 t} D(\rho_0\|\pi_N).$$

In detail, dissipation is $\nu\Theta \int \rho |\nabla \log(\rho/\pi_N)|^2_{A_N}$; the Gaussian inequality is $D(\rho\|\pi_N) \le \frac{\Theta}{2} \int \rho |\nabla \log(\rho/\pi_N)|^2$. Their combination proves the displayed rate without an N-dependent constant.

However, for every fixed energy radius R,

$$\pi_N\{|u|^2 \le R\} = \mathbb{P}\{\chi^2_N \le R/\Theta\} \longrightarrow 0.$$

This follows from $\mathbb{E}\chi^2_N = N$ and $\operatorname{Var}(\chi^2_N) = 2N$. Compact sets in the energy Hilbert space are bounded, so the orthogonally embedded family π_N is not tight in that space. A uniform relaxation rate is not a uniform energy bound. A different forcing covariance, temperature scaling or distribution-valued state space may give a different limit, but its invariant measure and thermodynamic interpretation must be established anew. This finite example exposes the additional compactness requirement without asserting a universal continuum second law.

15. **Cross-sector response and independent validation**

A common origin becomes predictive when its reduction maps constrain observables that have not been used to select the model. This section specifies that requirement at a finite regulator. It distinguishes a calculation within a specified model from a derivation of that model's physical coefficients. In particular, eliminating unresolved variables usually introduces memory; the resulting static stiffness is not by itself a Kerr propagation operator.

15.1. *Shared hypotheses, parameters, and observable consequences.* A shared reduction starts from one specified state space, action, residual metric, mobility, path cost, reference law, and projection. Its consequences depend on matching the action, generator, covariance, boundaries, and clock in the physical branch. The curvature-sourced scalar response provides one example: its massless charge relation uses the topological result of Prabhu and Stein [87], while the common-weight hypothesis relates its coefficient to coefficients in the other retained terms.

The numerical weights, invariant-form normalizations, physical projections, scalar mass, and constitutive maps are supplied or independently matched data unless a separate selection argument determines them. In particular, $(S, \theta, M) \mapsto (aS, a\theta, M/a)$, $a > 0$, leaves the finite diffusion law unchanged. Uniqueness of a stationary response for fixed coefficients does not remove this freedom. The following identifiability calculation determines precisely which observations are unchanged by that scaling.

The stationary scalar boundary problem and cross stress determine part of the gravitational reduction. Tensor resonance coefficients $C_{\ell m}(a/M)$ additionally require the coupled metric calculation. A non-vacuum accretion observable $D(a/M, \dot{M}, \ldots)$ requires its transport and radiation map. The Kerr companion supplies selected leading tensor coefficients on an explicitly matched massless vacuum branch by normalizing published coupled spectral results. This does not evaluate the general massive tensor response. A separate massive zero-spin calculation now supplies the local surface-flux response of a prescribed steady test thin disc, including the leading conformal matter contribution. It does not supply a rotating radiative accretion flow or a detector map. For a strictly positive scalar mass, a separate coercive stationary problem gives a unique finite-energy weak scalar response and a residual-controlled numerical susceptibility. Its shared-weight amplitude still needs an independently constrained curvature scale; calibrating the elementary force strength and scalar mass alone leaves that scale free. Their use in prediction requires a parameter vector fixed from independent calibration, followed by propagation of source, instrument, and model uncertainty.

Numerical refinement and symbolic residuals test the specified equations. An observational comparison instead uses the full forward map and the held-out protocol in Section 15.13. GWOSC strain, NICER timing and spectra, and EHT interferometry require their respective instrument likelihoods; JHTDB supplies numerical fluid data. Access to those products alone establishes neither a fit nor a common-parameter validation.

15.2. *Identifiability theorem for the present mother data.* The coupling question can be settled rigorously at the level of the present finite diffusion data. Let $\mathscr{L}_{S,\theta,M,c}$ denote the law of

$$\mathrm{d}X_t = \big[-M\nabla S + \theta\ \mathrm{div}\, M + c\big](X_t)\ \mathrm{d}t + \sqrt{2\theta M}\ \mathrm{d}W_t,$$

with fixed domain, reference measure, boundary condition, and a unique martingale problem. For every $a > 0$, define

$$T_a(S, \theta, M, c) = (aS, a\theta, M/a, c).$$

Then

$$-\frac{M}{a}\nabla(aS) + a\theta\ \mathrm{div}(M/a) + c = -M\nabla S + \theta\ \mathrm{div}\, M + c, \qquad 2(a\theta)(M/a) = 2\theta M.$$

The Gibbs exponent is also unchanged: $(aS)/(a\theta) = S/\theta$. Hence

$$\mathscr{L}_{T_a(S,\theta,M,c)} = \mathscr{L}_{S,\theta,M,c}$$

for every path observable defined in the declared physical time. The map from these coefficients to the state-path law is therefore non-injective. No estimator based only on that law can distinguish two points on this normalization orbit. In particular, its likelihood cannot select the absolute normalization without independent thermodynamic calibration. An HJB value or a Noether charge is a law-only statistic only after its cost and observable definitions have also been fixed. For example, the same uncontrolled state process with running costs 1 and a, zero terminal cost, and horizon T

has values $T-t$ and $a(T-t)$. Thus equality of state-path laws alone does not imply equality of externally normalized costs or charges.

There is a second obstruction after this normalization is fixed. For a direct sum of r compact simple ideals, every invariant positive form has

$$h=\sum_{i=1}^{r} c_i h_i, \qquad c_i>0.$$

One linear trace normalization removes at most one degree of freedom; the admissible coefficient set still has local dimension $r-1$. The matrices

$$H_h=\begin{pmatrix} 1 & h \\ h & 1 \end{pmatrix}, \qquad |h|<1,$$

give an elementary finite counterfamily with distinct cross-couplings, strict positivity, normalizable Gibbs laws, and well-posed linear diffusions. Thus positivity, Gibbs invariance, finite HJB well-posedness, and stochastic symmetry identities do not imply unique relative couplings.

The first calculation establishes non-identifiability of absolute normalization from the state-path law. The second establishes that positivity, invariance, and well-posedness do not select the relative couplings. These are different conclusions. Once the normalization orbit has been quotiented out, a relative coupling can still be identifiable from data. For example, the diffusion with drift $-H_h x$ and covariance $2\theta I$ has stationary covariance

$$C_h=\frac{\theta}{1-h^2}\begin{pmatrix} 1 & -h \\ -h & 1 \end{pmatrix}, \qquad h=-\frac{(C_h)_{12}}{(C_h)_{11}}.$$

Thus its exact stationary law determines h, even when the common variance scale is unknown. This identification does not derive the value of h from positivity or invariance. One route to an independently selected coupling is a functional F_{sel} on the physical quotient with the existence and strictness properties stated below. It is a sufficient route, not the only possible selection mechanism. Introducing such a functional to reproduce a desired value adds model data rather than deriving it from the existing Gibbs, HJB, or Noether conditions.

The scaling calculation exhibits a nontrivial equivalence orbit of the coefficient-to-law map; it does not classify its entire kernel. The relative weight example separately disproves selection from positivity and invariance alone. Additional measurements can distinguish relative weights, but they do not turn those weights into deductions of the original premises.

15.3. *Conditional coupling-selection theorem.* The normalization obstruction does not prevent a conditional selection theorem once the missing physical data are supplied. Let Θ be the admissible parameter space and let $\sim$ identify gauge, normalization, and operationally indistinguishable descriptions. Assume that the quotient $\Theta/\sim$ carries the declared topology and that the energy, temperature, and physical-time units have been fixed independently. Suppose the mother model

derives a functional

$$F_{\mathrm{sel}} : \Theta/\!\sim \longrightarrow \mathbb{R} \cup \{+\infty\}$$

THEOREM 15.1 (Conditional unique-coupling selection). *Assume that the quotient has a fixed metrizable realization, that F_{sel} is proper, bounded below, and lower semicontinuous, and that every finite sublevel set is compact. For uniqueness, assume either that its effective domain is identified with a convex subset of a real vector space on which it is strictly convex, or that an explicitly identified candidate ϑ_0 satisfies $F_{\mathrm{sel}}(\vartheta) - F_{\mathrm{sel}}(\vartheta_0) \geq \delta > 0$ for every other admissible class. In the latter case the gap must be established by a separate calculation. Then there is one and only one equivalence class*

$$\vartheta_* = \operatorname*{arg\,min}_{\vartheta \in \Theta/\!\sim} F_{\mathrm{sel}}(\vartheta).$$

Proof. A minimizing sequence is eventually contained in a compact sublevel set and therefore has a convergent subsequence; lower semicontinuity attains the infimum. If two distinct minimizers existed, strict convexity would make the value at their midpoint strictly smaller. In the strict-gap case the strict gap gives the same contradiction. The selected representative is unique only if an additional gauge or normalization convention selects exactly one representative of that equivalence class. □

This theorem is conditional. It becomes a deduction of the mother model only if the displayed F_{sel}, the quotient, the units, and the coercivity/strictness estimates are derived independently from that model. Adding F_{sel} solely to obtain a preferred numerical coupling would instead add a new physical postulate. The normalization obstruction and the failure of positivity alone to select relative weights remain in force; neither excludes identification from additional observations.

15.4. *Declared mother-cost selection principle.* To turn the conditional selection theorem into a testable model extension, we declare the following additional principle explicitly. After fixing the energy, temperature, and physical-time units and passing to $\Theta/\!\sim$, let π_ϑ denote the stationary law of the specified regulated generator whenever it exists. For a dimensionless joint residual q_ϑ and a fixed positive residual metric $\mathsf{H}_{\mathrm{ref}}$, define

$$\Phi_\kappa(q) = \begin{cases} (e^{\kappa q} - 1 - \kappa q)/\kappa^2, & \kappa \neq 0, \\ q^2/2, & \kappa = 0, \end{cases} \qquad \Phi_\kappa(q) \geq 0,$$

and

$$F_{\mathrm{sel}}([\vartheta]) := \limsup_{T\to\infty} \frac{1}{T} \mathbb{E}_{\pi_\vartheta}\left[\int_0^T \left\{\frac{1}{2} R_\vartheta^{\mathsf{T}} \mathsf{H}_{\mathrm{ref}}^{-1} R_\vartheta + \eta_{\mathrm{sel}} \Phi_{\kappa_{\mathrm{risk}}}(q_\vartheta)\right\} \mathrm{d}t\right].$$

Here $\eta_{\mathrm{sel}} \geq 0$ is a separately declared dimensionless penalty weight, and $\kappa_{\mathrm{risk}} \geq 0$ is the dimensionless risk parameter. Neither symbol redefines the original exponential-cost coefficient κ_{cost}. The residual metric, residuals, and score must descend to the quotient; otherwise the minimization is not a well-defined operation on physical equivalence classes. The *mother-cost selection principle*

(SP) chooses the equivalence class that minimizes this dimensionless long-time cost, subject to the exact positivity, conservation, gauge, parity, and generator-matching constraints. The subtraction $1+\kappa q$ makes the risk term continuous at $\kappa = 0$; no sign or convexity claim is made for a dimensional q before its normalization is declared.

SP is a new, explicitly declared physical postulate unless a microscopic derivation of this stationary score from the mother action is supplied. Consequently the conditional theorem above proves uniqueness only when SP's functional is independently shown to be lower semicontinuous, coercive, and strictly convex (or separated by a certified discrete gap) on the quotient. The finite construction below tests SP directly. These analytic properties and a unique numerical physical coupling have not been established for the full continuum theory.

15.4.1. *Stationary averaging, integrability, and parameter sensitivity.* Let $c_\vartheta(x)$ denote the nonnegative integrand in SP, with $\mathsf{H}_{\mathrm{ref}} > 0$ and $\eta_{\mathrm{sel}} \geq 0$. For a stationary initial law, Tonelli's theorem gives, for every $T > 0$,

$$\frac{1}{T}\mathbb{E}_{\pi_\vartheta}\int_0^T c_\vartheta(X_t)\,\mathrm{d}t = \int c_\vartheta\,\mathrm{d}\pi_\vartheta.$$

Thus the stated long-time score is exactly a one-time stationary expectation, including the possibility of the value $+\infty$. No ergodic theorem is needed for this equality. Almost-sure estimation from a single trajectory additionally requires ergodicity and integrability. For positive risk, finite polynomial moments do not suffice: the score requires the relevant exponential moment. For example, if a residual is quartic in a nondegenerate Gaussian state, its positive exponential moment is generally infinite. A nonempty finite-score domain must be established before applying the selection theorem.

This stationary expectation must also be distinguished from the path cumulant rate

$$\Lambda_\vartheta(k) = \lim_{T\to\infty} T^{-1}\log\mathbb{E}\exp\left(k\int_0^T c_\vartheta(X_t)\,\mathrm{d}t\right).$$

SP, as defined above, is not this cumulant rate or a path relative entropy. The two functions have different integrability and spectral requirements. Calling the stationary penalty informational does not identify it with a Girsanov likelihood or a large-deviation rate function.

A useful conditional existence result is elementary. Suppose the parameter quotient is represented by a compact metric space K, the state space is fixed and Polish, $\vartheta \mapsto \pi_\vartheta$ is weakly continuous, and the continuous costs c_ϑ converge uniformly on compact state sets as the parameter converges. Suppose also that the stationary laws are uniformly tight and the costs are uniformly integrable under these laws. Truncation to a compact set followed by bounded continuous convergence shows that $\pi_\vartheta(c_\vartheta)$ is continuous. Compactness then gives a minimum. For unbounded costs, the tail estimate is an essential part of this argument. These conditions give existence; they do not give strict convexity or uniqueness.

Even strict convexity of the integrand in the parameter need not survive averaging against a parameter-dependent law. To see this, let

$$\mathrm{d}X_t = -[X_t - (v + \sin v)]\,\mathrm{d}t + \sqrt{2}\,\mathrm{d}W_t, \qquad c_v(x) = (v - x)^2, \qquad v \in [-\pi, \pi].$$

The unique stationary law is $N(v + \sin v, 1)$. Although $\partial_v^2 c_v(x) = 2$, its averaged score is $F(v) = 1 + \sin^2 v$, with three minimizers at $-\pi, 0, \pi$. This is a counterexample to inferring uniqueness of the selection score from convexity of the residual penalty alone.

For a differentiable stationary family, the missing derivative can be computed. Assume that differentiation under stationary integration is justified and that the centered Poisson problem has a solution in a common generator domain:

$$\mathcal{L}_\vartheta u_\vartheta = c_\vartheta - F(\vartheta), \qquad \pi_\vartheta(u_\vartheta) = 0.$$

Differentiating $\pi_\vartheta \mathcal{L}_\vartheta = 0$, and using $\partial_i \pi_\vartheta(1) = 0$, gives

$$\partial_i F = \pi_\vartheta(\partial_i c_\vartheta) - \pi_\vartheta((\partial_i \mathcal{L}_\vartheta) u_\vartheta).$$

The second term is the stationary-law response. Omitting it generally changes both the stationary point and the Hessian. A strong-convexity certificate therefore concerns the complete derivative, in the tangent directions of the constrained quotient.

There is also a temporal identifiability limitation. If different circulation drifts preserve the same π_ϑ, and if c_ϑ does not depend on those drifts, SP gives them the same score. For an isotropic Gaussian law, the diffusions with drift $-x + \omega J x$, $J^{\mathsf{T}} = -J$, illustrate this freedom. Choosing a stationary distribution alone therefore does not select a nonzero stationary current or an arrow of time. Those require the generator, parity convention, and appropriate path observables.

15.4.2. *A selection problem solved without an assumed convexity claim.* The following finite example tests what the new principle actually selects. Fix the noise scale $\theta > 0$, the reference residual metric $\mathsf{H}_{\mathrm{ref}} = I$, and all units. Let

$$H_g = \begin{pmatrix} 1 & g \\ g & 1 \end{pmatrix}, \qquad \mathrm{d}X_t = -H_g X_t\,\mathrm{d}t + \sqrt{2\theta}\,\mathrm{d}W_t, \qquad |g| < 1.$$

The solution is a Gaussian Ornstein–Uhlenbeck process. Since the drift eigenvalues are $1 \pm g > 0$, its invariant law is uniquely $\pi_g = N(0, \theta H_g^{-1})$, and its mean and covariance converge to that law. Declare the residual $R_g = gJX$, where $J = \left(\begin{smallmatrix} 0 & 1 \\ 1 & 0 \end{smallmatrix}\right)$, and put $q_g = |R_g|^2/2 = g^2|X|^2/2$. These residual choices are additional model data; they are not consequences of invariance. Orthogonal diagonalization gives independent coordinates with variances $\theta/(1+g)$ and $\theta/(1-g)$. Hence

$$m_g := \mathbb{E}_{\pi_g} q_g = \frac{\theta g^2}{1 - g^2}, \qquad M_g(k) := \mathbb{E}_{\pi_g} e^{k q_g} = \prod_{\sigma \in \{-1,1\}} \left(1 - \frac{k\theta g^2}{1 + \sigma g}\right)^{-1/2}.$$

For $k > 0$, the last expression is finite exactly when $k\theta g^2 < 1 - |g|$. The score is therefore

$$F(g) = m_g + \frac{\eta_{\mathrm{sel}}}{k^2}[M_g(k) - 1 - km_g]$$

on this finite-moment domain. With positive η_{sel}, it is $+\infty$ outside the domain. If $\eta_{\mathrm{sel}} = 0$, the risk term is absent rather than interpreted as $0 \cdot \infty$. At $k = 0$, Gaussian fourth moments instead give

$$F(g) = \frac{\theta g^2}{1 - g^2} + \frac{\eta_{\mathrm{sel}}\theta^2 g^4(2 + g^2)}{2(1 - g^2)^2}.$$

These expressions follow directly by integrating the two Gaussian marginals; they do not use fitted coefficients.

PROPOSITION 15.2 (A unique but vanishing cross coupling). *For the displayed residual model, $g_* = 0$ is the unique global minimizer of SP for $\theta > 0$, $\eta_{\mathrm{sel}} \geq 0$, and $k \geq 0$, with the finite-score convention above.*

Proof. The inequality $e^z \geq 1 + z$ makes the risk contribution nonnegative. At $g = 0$, the residual vanishes identically, so $F(0) = 0$. At any $g \neq 0$ in the finite-score domain, $F(g) \geq m_g > 0$. Infinite scores cannot minimize it. This proves global uniqueness without an unverified global Hessian condition. □

For $(\theta, k, \eta_{\mathrm{sel}}) = (0.7, 0.5, 0.3)$, the computed scores at $g = (0, 0.2, 0.5, 0.7)$ are respectively 0, 0.0294309860515, 0.254795800047, and 1.00268822460. Independent Gaussian quadrature agrees with the closed exponential moments to less than 10^{-12} in these cases. This is a numerical check of the finite example, not a measurement of a physical coupling. At zero noise the attracting stationary law is δ_0 for every g, and every score vanishes. Thus uniqueness in this example is not uniform in the zero-noise limit. A nonzero selected physical coupling needs independently justified competing terms or constraints; it cannot be inferred from the name of the selection principle.

The corresponding numerical diagnostic is shown in Figure 19.

15.5. *Perturbative tensor response and observable matching.* For the matched action used in the Kerr branch, a consistent tensor prediction requires the following background and perturbation equations. Let $h^{(2)}$ solve

$$M_{\mathrm{P}}^2\, \delta G^{\mathrm{K}}_{ab}[h^{(2)}] = T^{\varphi}_{ab}[\varphi_1] + T^{\mathrm{int}}_{ab}[\varphi_1]$$

with a specified gauge, regular future-horizon data, fixed asymptotic mass and spin, and no unlisted homogeneous perturbation. Let Π_{phys} be the corresponding constraint and gauge projection and $G^{\mathrm{stat}}_{\mathrm{K}}$ an inverse, on the chosen stationary source and solution spaces, of $M_{\mathrm{P}}^2 \delta G^{\mathrm{K}}$ after those zero modes are removed. Existence of this inverse is an additional analytic hypothesis; it is not supplied by the scalar boundary problem. The first backreaction is then

$$h^{(2)} = G^{\mathrm{stat}}_{\mathrm{K}} \Pi_{\mathrm{phys}}\big(T^{\varphi}[\varphi_1] + T^{\mathrm{int}}[\varphi_1]\big).$$

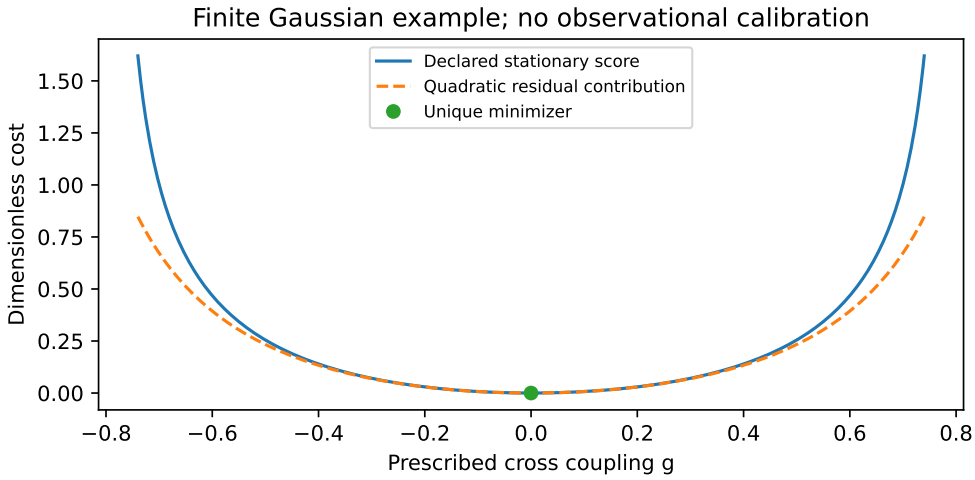


Figure 19. The exactly specified Gaussian selection example at $\theta = 0.7$, $\kappa_{\mathrm{risk}} = 0.5$, and $\eta_{\mathrm{sel}} = 0.3$. The risk penalty increases the cost away from zero, while the minimum is already fixed by the declared quadratic residual. The curve is a finite-model computation.

After differentiating the complete operator, including the background change, direct metric terms, scalar-mediated term, and the boundary domain, the first nonzero resonant correction must have the form

$$\mathcal{N}_{\ell m} := \big\langle v_{\ell m}, \big(\mathcal{L}^{[p]}_{\mathrm{direct}} + \mathcal{L}^{[p]}_{\mathrm{bg}}[h^{(2)}] + \mathcal{L}^{[p]}_{\mathrm{scalar}}\big) u_{\ell m} \big\rangle,$$

$$C_{\ell m} := -\frac{\mathcal{N}_{\ell m}}{\langle v_{\ell m}, \partial_{\widehat{\omega}} \mathcal{L}_{\mathrm{Kerr}} u_{\ell m} \rangle}, \qquad M\Delta\omega_{\ell m} = \varepsilon^p C_{\ell m} + o(\varepsilon^p).$$

The stationary correction is an argument of the background-dependent operator; that operator acts on the oscillating right mode, not on the stationary correction itself. The left and right resonant states, their bilinear pairing, the boundary variation, and the order p must all be supplied. A scalar profile, static Schur complement, or mass–spin diffusion does not determine these objects. A reliable computation requires that (i) the coupled boundary-value solve converges under radial and angular refinement, (ii) the constraint residual converges in the same gauge, (iii) the result is invariant under an allowed gauge change, and (iv) the same frozen ϑ_* is used in every held-out observable.

For an accretion observable, the response requires the non-vacuum equations

$$\nabla_a T^{ab}_{\mathrm{total}} = 0, \qquad T_{\mathrm{total}} = T_{\mathrm{fluid}} + T_{\mathrm{EM}} + T_{\mathrm{rad}} + T_{\mathrm{cross}},$$

an equation of state and closure, radiation transport, boundary and initial data, and an instrument map. For nonzero reference observable $\mathcal{D}_0$, define its dimensionless leading response at a declared positive integer order q_D by

$$\mathcal{D}(\varepsilon) = \mathcal{D}_0[1 + \varepsilon^{q_D} D + o(\varepsilon^{q_D})].$$

All lower derivatives must vanish if $q_D > 1$; a vanishing linear derivative is not evidence for the absence of a quadratic signal. The coefficient is determined only after those equations are solved with the same frozen ϑ_*. It cannot be recovered from T^{ab}_{cross} alone.

15.6. *Frozen-parameter validation is a reproducible procedure.* The no-refit claim is accepted only if the following sequence is recorded:

(1) Freeze the action, regulator, units, clock, projection, and nuisance parameterization.
(2) Select ϑ_* using only $\mathcal{D}_{\mathrm{cal}}$ and exact structural constraints.
(3) Publish hashes of source code, input data, and the frozen parameter file.
(4) Open the held-out data only after the preceding steps.
(5) Evaluate the complete forward map and likelihood without refitting ϑ_*.
(6) Report uncertainty, model discrepancy, nuisance treatment, baseline comparison, and a predeclared decision rule.

Application to the gravitational branch requires independently calibrated λ_3, m_φ, the backreacted tensor waveform, and the complete accretion forward map. Those physical inputs and calculations remain necessary before this procedure yields an observational test.

15.7. *Parameter definitions and selection.* For every coefficient, the model record must specify its defining equation, units, regulator and renormalization scale, physical clock, admissible range, and origin: prescribed, derived, or independently calibrated. In particular, the following symbols have different meanings:

Symbol	Definition	Present role
κ_{cost}	Coefficient multiplying the residual cost in an exponential	Input; $\kappa_{\mathrm{cost}} q$ must be dimensionless
κ_P	Coefficient of the declared curvature term	Branch coefficient, with units fixed by the action convention
κ_H	Surface gravity of the normalized horizon generator	Derived geometric quantity, not a universal coupling
κ_{trap}	Stiffness in a specified physical displacement coordinate	Local experimental coefficient
$\bar{\kappa}$	Normalized common perturbation parameter	Requires an independent selection or calibration map
η_{sel}	Weight of the additional stationary selection penalty	New SP input; not selected by naming the score
κ_{risk}	Exponent parameter in $\Phi_\kappa(q)$	New dimensionless SP input; requires exponential integrability

This list distinguishes the original five symbols and the two SP inputs; it does not identify them. The rest of the record includes the energy coefficients, mobility, covariance, observation maps, reference measure, boundary data, and clock. Derived quantities such as $\kappa_H(M, a)$ are not counted

again as free coordinates. A function-valued coefficient requires either a fixed function or a declared finite basis, not an unrecorded fit.

A unique minimizer for a fixed cost is not a unique physical parent theory. For example, all matrices

$$H_h = \begin{pmatrix} 1 & h \\ h & 1 \end{pmatrix}, \qquad |h| < 1,$$

define strictly positive quadratic energies and well-posed reversible diffusions with identity mobility and normalizable Gibbs laws. Their cross-couplings differ. Thus positivity, Gibbs invariance, and well-posedness alone do not select a common weight. Additional symmetry or variational restrictions must actually eliminate this freedom.

A sufficient finite-dimensional selection theorem would specify a convex admissible coefficient set and an independently fixed, coercive, strictly convex objective on it. Existence and strict convexity would then give a unique minimizer within that class. Gauge-equivalent representations must first be quotiented out. Selection of a physical projection requires, in addition, its operational definition and generator-matching identity. These hypotheses have not been established for all physical couplings and all projections of the unified field programme.

There is an exact normalization freedom even before physical selection. For any positive constant a, the simultaneous replacement

$$(S_r, \theta, M_r) \longmapsto (aS_r, a\theta, M_r/a)$$

leaves S_r/θ, the drift $-M_r\nabla S_r + \theta \operatorname{div} M_r + c_r$, and the covariance $2\theta M_r$ unchanged, with the same reference measure, domain, and c_r. The same conclusion holds for a weighted divergence. Thus it leaves the state-path law unchanged whenever the martingale problem is unique. Absolute energy and temperature units, or independently measured thermodynamic responses, can fix this normalization; the state trajectory alone cannot. This is a redundancy of this diffusion identification, not a statement that every independently defined control cost is invariant.

Nor does removing this normalization fix all relative weights. For a direct sum of r compact simple ideals, invariant positive forms can have r independent positive coefficients. One trace normalization leaves an $(r-1)$-dimensional open simplex. Minimizing over the fields does not vary these external coefficients. A penalty favoring equal coefficients would be additional model data unless derived from a stated microscopic selection problem.

15.8. *Constrained linearization and exact elimination.* All matrices below are expressed in fixed physical coordinates after constraint reduction. If constraints $G_j(Y) = 0$ are imposed before linearization, the energy Hessian on an orthonormal tangent basis Q at a constrained critical point is

$$H_* = Q^{\mathsf{T}} \left(D^2 S_r + \sum_j \lambda_j D^2 G_j \right) Q, \qquad \nabla S_r + \sum_j \lambda_j \nabla G_j = 0.$$

It is generally not the unrestricted Hessian. A nonlinear state reduction also contributes an Itô drift correction. Those terms, the transformed reference measure, and boundary conditions must be included before forming a reduced generator.

In the resulting coordinates, write the mother drift as $b = -M_r \nabla S_r + \theta \operatorname{div} M_r + c_r$. Its differential in a direction v is

$$Db(Y_*)v = -M_* H_* v - (DM_r(Y_*)[v])\nabla S_r(Y_*) + \theta D(\operatorname{div} M_r)(Y_*)v + Dc_r(Y_*)v. \tag{15.1}$$

The simpler expression $B_* = -M_* H_* + C_*$ applies when $\nabla S_r(Y_*) = 0$, with $C_* = \theta D(\operatorname{div} M_r)(Y_*) + Dc_r(Y_*)$. An expansion about a constant deterministic background also requires $b(Y_*) = 0$. Existence of a stationary probability law does not imply either of these pointwise conditions.

Partition the retained fluctuation into $Y = (\xi, \eta)$ and set

$$H_* = \begin{pmatrix} H_{\xi\xi} & H_{\xi\eta} \\ H_{\eta\xi} & H_{\eta\eta} \end{pmatrix}, \qquad M_* = \begin{pmatrix} M_{\xi\xi} & M_{\xi\eta} \\ M_{\eta\xi} & M_{\eta\eta} \end{pmatrix}, \qquad B_* = Db(Y_*). \tag{15.2}$$

For the additive-noise linear realization $dY = B_* Y\, dt + \Sigma_*\, dW$, variation of constants gives

$$\begin{aligned} \eta_t &= e^{tB_{\eta\eta}}\eta_0 + \int_0^t e^{(t-s)B_{\eta\eta}} B_{\eta\xi}\xi_s\, ds + \int_0^t e^{(t-s)B_{\eta\eta}}\Sigma_\eta\, dW_s, \\ d\xi_t &= \left[B_{\xi\xi}\xi_t + \int_0^t K(t-s)\xi_s\, ds + B_{\xi\eta}e^{tB_{\eta\eta}}\eta_0 + \zeta_t\right] dt + \Sigma_\xi\, dW_t, \\ K(t) &= B_{\xi\eta}e^{tB_{\eta\eta}}B_{\eta\xi}, \qquad \zeta_t = B_{\xi\eta}\int_0^t e^{(t-s)B_{\eta\eta}}\Sigma_\eta\, dW_s. \end{aligned} \tag{15.3}$$

This is exact for the specified linear model. The inherited colored noise, its correlation with retained noise, and the initial transient cannot be deleted while claiming the same reduced stochastic law. For nonlinear multiplicative noise, the additive model itself is an additional approximation.

For z outside the spectrum of $B_{\eta\eta}$, the corresponding deterministic response pencil is

$$\mathcal{P}(z) = zI - B_{\xi\xi} - B_{\xi\eta}(zI - B_{\eta\eta})^{-1}B_{\eta\xi}. \tag{15.4}$$

Only at zero frequency does this reduce to

$$B_{\mathrm{eff}}(0) = B_{\xi\xi} - B_{\xi\eta}B_{\eta\eta}^{-1}B_{\eta\xi}. \tag{15.5}$$

If $A = B_{\eta\eta}$ is invertible and $|z|\|A^{-1}\| < 1$, the resolvent identity and a Neumann series yield

$$\|(zI - A)^{-1} + A^{-1}\| \le \frac{|z|\|A^{-1}\|^2}{1 - |z|\|A^{-1}\|}.$$

Multiplication by the two off-diagonal block norms bounds the error in replacing the full response by its static approximation. This condition controls both frequency and possible nonnormal amplification.

15.9. *Perturbation order and the Kerr identification.* Let $\varepsilon = \bar{\kappa}$ be a declared dimensionless parameter. A response coefficient is a derivative, not the entire finite-coupling difference:

$$\mathcal{L}_{\mathrm{cross}}(z) := \partial_\varepsilon \mathcal{P}(z;\varepsilon)|_0\,, \qquad \mathcal{P}(z;\varepsilon) = \mathcal{P}(z;0) + \varepsilon \mathcal{L}_{\mathrm{cross}}(z) + O(\varepsilon^2). \tag{15.6}$$

The background, blocks, projectors, and boundary conditions that depend on ε must all be differentiated. If $R = (zI - B_{\eta\eta})^{-1}$, then $R' = RB'_{\eta\eta}R$, and

$$\mathcal{P}' = -B'_{\xi\xi} - B'_{\xi\eta}RB_{\eta\xi} - B_{\xi\eta}RB'_{\eta\xi} - B_{\xi\eta}RB'_{\eta\eta}RB_{\eta\xi}.$$

If both off-diagonal drift blocks are $O(\varepsilon)$ and the diagonal blocks have no first-order correction, the first nonzero elimination term is $O(\varepsilon^2)$. A nonzero linear signal cannot be assumed.

For example, take the fully specified two-coordinate energy and mobility

$$S = \tfrac{1}{2}a_0x^2 + \varepsilon g_0 xy + \tfrac{1}{2}b_0y^2, \qquad M = \mathrm{diag}(\mu,\nu),$$
$$a_0, b_0, \mu, \nu > 0, \quad a_0b_0 > \varepsilon^2 g_0^2.$$

The process with drift $-M\nabla S$ and covariance $2\theta M$ has

$$\mathcal{P}(z;\varepsilon) = z + \mu a_0 - \frac{\mu\nu\varepsilon^2 g_0^2}{z + \nu b_0}, \qquad \mathrm{Var}(x) = \frac{\theta}{a_0 - \varepsilon^2 g_0^2/b_0}. \tag{15.7}$$

The second identity follows by integrating out y in the Gibbs density. The first follows directly by substituting the four drift blocks into (15.4). Thus $\partial_\varepsilon \mathcal{P}|_0 = 0$, although the finite-coupling response and equilibrium covariance change. The pole $-\nu b_0$ also shows why a static Schur complement is not a full dynamical description. This is a finite mathematical benchmark, not a black-hole prediction.

For the prescribed dimensionless values $(a_0, b_0, g_0, \varepsilon, \mu, \nu, \theta) = (2, 3, 0.4, 0.6, 0.8, 1.4, 0.7)$, the effective static stiffness is 1.9808 and the exact variance is 0.3533925687. An independent sample of 50,000 Gaussian equilibrium draws gives variance 0.3547202593, with theoretical standard error 0.0022350732 for the unbiased sample variance. Solving the full Lyapunov equation agrees with θH_*^{-1} to a maximum entrywise error of 2.3×10^{-16}. These results check the specified finite realization; none of its coefficients has been inferred from observations.

The corresponding numerical diagnostic is shown in Figure 20.

To apply the construction to Kerr, a separate field identification must show that the physical perturbation pencil at zero coupling is the declared Kerr operator, with its gauge conditions, physical time, and ingoing and outgoing boundary conditions. A mass–spin label diffusion does not establish that identification. In units $G = c = 1$, put $\widehat{\omega} = M\omega$ and $\chi = a/M$. If that identification and a simple resonance perturbation theory hold, one may write

$$\mathcal{L}_{\mathrm{BH}}(\widehat{\omega}, \chi; \varepsilon) = \mathcal{L}_{\mathrm{Kerr}}(\widehat{\omega}, \chi) + \varepsilon^p \mathcal{L}^{[p]}_{\mathrm{cross}}(\widehat{\omega}, \chi) + o(\varepsilon^p),$$
$$C_{\ell m}(\chi) = -\frac{\langle v_{\ell m}, \mathcal{L}^{[p]}_{\mathrm{cross}} u_{\ell m}\rangle}{\langle v_{\ell m}, \partial_{\widehat{\omega}} \mathcal{L}_{\mathrm{Kerr}} u_{\ell m}\rangle}, \qquad M\Delta\omega_{\ell m} = \varepsilon^p C_{\ell m} + o(\varepsilon^p). \tag{15.8}$$

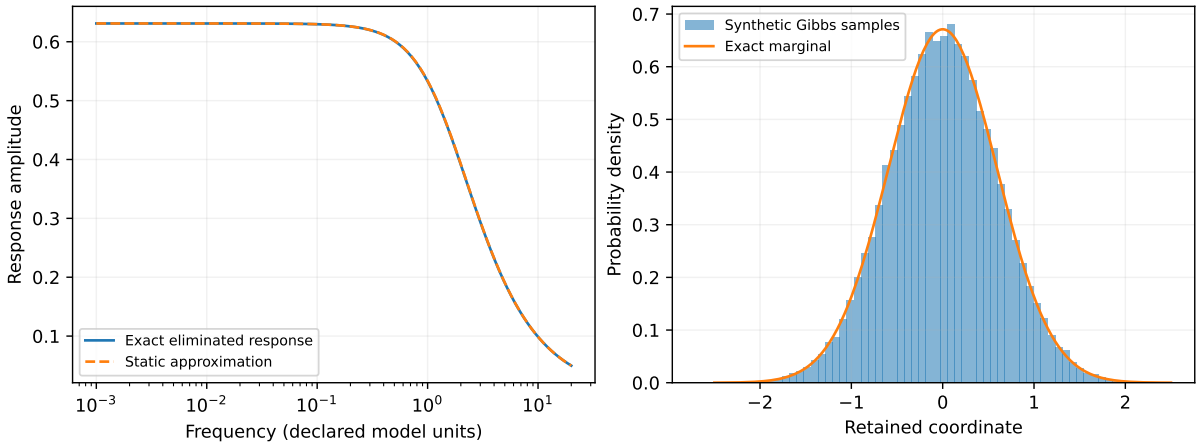


Figure 20. Finite synthetic benchmark for the prescribed two-coordinate model. Left: exact frequency response and its zero-frequency elimination approximation. Right: independent equilibrium samples and the analytical Gaussian marginal. The agreement concerns the declared mathematical model and is not an astronomical or laboratory validation.

Here p is the first nonzero order. The left and right resonant modes and their pairing must be defined in the specified spectral realization; ordinary square-integrable normalization is generally unavailable for outgoing resonances. The denominator must be nonzero. Differentiating the eigenequation and pairing with the left null vector removes the unknown mode derivative and gives the displayed formula. Perturbations of the boundary domain must be included in the differentiated operator.

15.10. *Resonance perturbation under fixed analytic hypotheses.*

THEOREM 15.3 (Conditional existence and uniqueness of the Kerr coefficient). *Let the horizon and infinity conditions be represented on fixed complex Banach spaces X, Y after a specified analytic change of domain. If scalar or auxiliary fields are eliminated, assume that their elimination is analytic and retains every contribution at the stated order. Assume that the resulting gauge-fixed tensor operator is analytic in $(\widehat{\omega}, \varepsilon)$, is Fredholm of index zero, and has the operator-norm expansion*

$$\mathcal{L}(\widehat{\omega}, \varepsilon) = \mathcal{L}_0(\widehat{\omega}) + \varepsilon^p \mathcal{L}_p(\widehat{\omega}) + O(\varepsilon^{p+1}), \qquad p \geq 1.$$

Require $\mathcal{L}_0(\widehat{\omega}) = \mathcal{L}_{\mathrm{Kerr}}(\widehat{\omega}, \chi) : X \to Y$ in this same boundary and gauge realization. The equality of the unperturbed operators is part of the hypothesis; properties of a different Kerr operator do not suffice. Assume that the gauge-fixed Kerr boundary-value operator $\mathcal{L}_{\mathrm{Kerr}}(\widehat{\omega}, \chi)$ is an analytic Fredholm family of index zero near a simple resonance $\widehat{\omega}_0$, with right and left null vectors $u_{\ell m}$ and $v_{\ell m}$. Assume that the kernel and cokernel are both one dimensional and that

$$\left\langle v_{\ell m}, \partial_{\widehat{\omega}} \mathcal{L}_{\mathrm{Kerr}}(\widehat{\omega}_0, \chi) u_{\ell m} \right\rangle \neq 0.$$

Then, for sufficiently small ε, there is a unique resonance branch $\widehat{\omega}_{\ell m}(\varepsilon)$ near $\widehat{\omega}_0$, modulo the declared mode normalization, and

$$\widehat{\omega}_{\ell m}(\varepsilon) = \widehat{\omega}_0 + \varepsilon^p C_{\ell m}(\chi) + O(\varepsilon^{p+1}),$$

where $C_{\ell m}$ is the quotient in (15.8). A bound uniform over a compact spin interval additionally requires uniform operator bounds, a uniformly bounded inverse on the complementary subspaces, a uniform lower bound on the displayed nonzero pairing, and isolation from other resonances. Being away from extremality alone does not establish those conditions.

Proof. Write $T_0 = \mathcal{L}_0(\widehat{\omega}_0)$, $u_0 = u_{\ell m}$, and let $v_0 = v_{\ell m} \in Y^*$ annihilate the range of T_0. Choose a bounded functional $\ell \in X^*$ with $\ell(u_0) = 1$. Then $X = \operatorname{span}\{u_0\} \oplus X_1$, where $X_1 = \ker \ell$. Since the range is closed with codimension one, $Y_1 = \operatorname{ran} T_0 = \ker v_0$. Choose $y_0 \in Y$ with $v_0(y_0) = 1$, and set $Qy = y - v_0(y)y_0$. The restriction $T_0 : X_1 \to Y_1$ is a bounded bijection and has a bounded inverse.

Apply the analytic implicit-function theorem to

$$Q\mathcal{L}(\widehat{\omega}, \varepsilon)(u_0 + w) = 0, \qquad w \in X_1.$$

Its w-derivative at the base point is the preceding bijection. It therefore determines a unique analytic $w = w(\widehat{\omega}, \varepsilon)$ nearby. The remaining equation is the scalar equation

$$g(\widehat{\omega}, \varepsilon) = v_0(\mathcal{L}(\widehat{\omega}, \varepsilon)[u_0 + w(\widehat{\omega}, \varepsilon)]) = 0.$$

At the base point,

$$\partial_{\widehat{\omega}} g = v_0((\partial_{\widehat{\omega}} \mathcal{L}_0)u_0),$$

because $v_0 T_0 = 0$. This derivative is nonzero by hypothesis, so a second analytic implicit-function theorem gives the unique local resonance branch with normalization $\ell(u) = 1$.

The operator expansion has no positive powers below p. Successively comparing these powers in the normalized equation forces the corresponding frequency and mode coefficients to vanish. At order p the equation is

$$T_0 u_p + C_{\ell m}(\partial_{\widehat{\omega}} \mathcal{L}_0)u_0 + \mathcal{L}_p u_0 = 0.$$

Applying v_0 removes u_p and proves the quotient. Analyticity gives the local remainder. The stated uniform inverse, pairing, and isolation bounds are additionally needed to control that remainder uniformly in spin. □

The theorem is a conditional closure statement. It does not manufacture $\mathcal{L}^{[p]}_{\mathrm{cross}}$: all same-order curvature operators, metric backreaction, scalar mass, gauge, horizon data, and asymptotic conditions must be supplied before a numerical $C_{\ell m}$ can be reported.

15.10.1. *The dynamical scalar elimination and its range of validity.* The operator entering the frequency quotient can be identified more precisely before computing its matrix elements. After fixing the action, field normalizations, gauge, and frequency-dependent boundary conditions, suppose the coupled perturbation pencil has the block expansion

$$\begin{pmatrix} L_g(\widehat{\omega}) + \varepsilon^2 A_2(\widehat{\omega}) + O(\varepsilon^3) & \varepsilon B_1(\widehat{\omega}) + O(\varepsilon^2) \\ \varepsilon C_1(\widehat{\omega}) + O(\varepsilon^2) & L_s(\widehat{\omega}) + O(\varepsilon) \end{pmatrix} \begin{pmatrix} u \\ v \end{pmatrix} = 0.$$

Here A_2 includes the change of the metric background, direct tensor terms, and the pulled-back change of the boundary domain. This expansion assumes that no retained operator produces a first-order tensor term. It must be derived from the specified action, not from a stationary Hessian alone. All compositions below are between the stated function spaces and must be bounded in the chosen operator topology.

If $L_s(\widehat{\omega})$ has a holomorphic inverse near the tensor resonance, the scalar equation gives

$$v = -\varepsilon L_s^{-1} C_1 u + O(\varepsilon^2), \qquad L_{\mathrm{eff}} = L_g + \varepsilon^2 \underbrace{(A_2 - B_1 L_s^{-1} C_1)}_{L^{[2]}_{\mathrm{cross}}} + O(\varepsilon^3).$$

The minus sign follows from solving the scalar equation and substituting it into the tensor equation. The inverse must carry the actual horizon and outgoing-wave conditions. A zero-frequency elliptic inverse generally cannot replace it. The background contribution within A_2 is $(D_g L_g)[h^{(2)}]$; it acts on the right resonant mode u.

With the left functional w annihilating the range of $L_g(\widehat{\omega}_0)$, the leading coefficient is

$$C = -\frac{\langle w, (A_2 - B_1 L_s^{-1} C_1) u \rangle}{\langle w, \partial_{\widehat{\omega}} L_g \, u \rangle}.$$

Differentiating the frequency dependence of the Schur term contributes at the next order: its prefactor is already ε^2, whereas $\Delta\widehat{\omega} = O(\varepsilon^2)$. The zeroth-order denominator is therefore correct in the isolated simple-mode problem. If a scalar resonance coincides with the tensor resonance, L_s^{-1} has a pole and this elimination fails. One must retain the coupled resonant subspace; an $O(\varepsilon)$ splitting can then occur.

An elementary complex matrix checks the algebra without claiming a Kerr computation. Set

$$L = \begin{pmatrix} \widehat{\omega} - w_g + \varepsilon^2 a & \varepsilon b \\ \varepsilon c & \widehat{\omega} - w_s \end{pmatrix}, \qquad C = -a + \frac{bc}{w_g - w_s}.$$

For $w_g = 0.37 - 0.09i$, $w_s = 0.50 - 0.10i$, $a = 0.03 + 0.02i$, $b = 0.08 - 0.01i$, and $c = 0.11 + 0.015i$, direct solution of the quadratic determinant gives $C = -0.0983823529412 - 0.0260294117647i$. For $\varepsilon = 0.1, 0.05, 0.025, 0.0125$, the absolute errors after subtracting $w_g + \varepsilon^2 C$ are 5.292×10^{-6}, 3.338×10^{-7}, 2.091×10^{-8}, and 1.308×10^{-9}. Their fourth-order scaling follows here from the exact even dependence of this matrix on the coupling. These values are a finite algebraic benchmark, not values of $C_{\ell m}$ for a black hole.

15.10.2. *What a numerical coefficient would certify.* Small residuals alone are insufficient near a nonnormal resonance. Let N and d be the exact numerator and denominator of the frequency quotient. If independent bounds satisfy

$$|N-\widetilde{N}|\le\delta_N,\qquad |d-\widetilde{d}|\le\delta_d<|\widetilde{d}|,$$

then elementary subtraction of the two quotients yields

$$\left|C+\frac{\widetilde{N}}{\widetilde{d}}\right|\le\frac{\delta_N}{|\widetilde{d}|-\delta_d}+\frac{|\widetilde{N}|\delta_d}{|\widetilde{d}|(|\widetilde{d}|-\delta_d)}.$$

Obtaining δ_N,δ_d requires errors in the background, both resonant modes, operator matching, and the regularized pairing. The inverse on the complementary spectral subspace converts equation residuals into mode errors. Grid refinement is useful numerical evidence, but does not supply that inverse bound by itself. No such certified full Kerr computation is asserted here.

15.11. *Covariant cross stress.* A state-space quadratic cost is not automatically a covariant spacetime action. Suppose an independent reduction supplies a differentiable, diffeomorphism-invariant action $S_{\rm phys}=S_0+\varepsilon S_1+O(\varepsilon^2)$. With signature $(-+++)$ and variation of the covariant metric, define

$$\delta_g S_1=\frac{1}{2}\int\sqrt{-g}\,T^{\mu\nu}_{\rm cross}\delta g_{\mu\nu}\,d^4x,\qquad T^{\mu\nu}_{\rm cross}=\frac{2}{\sqrt{-g}}\frac{\delta S_1}{\delta g_{\mu\nu}}.\tag{15.9}$$

Equivalently, $T^{\rm cross}_{\mu\nu}=-2(\sqrt{-g})^{-1}\delta S_1/\delta g^{\mu\nu}$. The sign changes when the varied metric is inverted. Metric dependence of the volume, contractions, field operators, and projections must all be varied, including boundary terms.

As a convention check, a prescribed scalar cross action $S_1=-h_0\int\sqrt{-g}\,g^{\alpha\beta}\partial_\alpha\phi\partial_\beta\psi\,d^4x$ gives

$$T^{\mu\nu}_{\rm cross}=h_0\big(\nabla^\mu\phi\nabla^\nu\psi+\nabla^\nu\phi\nabla^\mu\psi-g^{\mu\nu}\nabla_\alpha\phi\nabla^\alpha\psi\big).$$

This follows from $\delta\sqrt{-g}=\frac{1}{2}\sqrt{-g}g^{\mu\nu}\delta g_{\mu\nu}$ and $\delta g^{\alpha\beta}=-g^{\alpha\mu}g^{\beta\nu}\delta g_{\mu\nu}$. It illustrates the variation; it does not select this interaction or its coefficient from the mother model. Only the total stress is conserved on the coupled field equations; the cross contribution can exchange energy and momentum with other sectors. Dissipative contributions from eliminated reservoirs require their own covariant constitutive construction.

For a specified accretion observable $\mathcal{D}$, the fractional response at linear order $q_D=1$ is

$$\mathcal{D}(\varepsilon)=\mathcal{D}_0[1+\varepsilon D+o(\varepsilon)],\qquad D=\mathcal{D}_0^{-1}\frac{\partial\mathcal{D}}{\partial\varepsilon}\bigg|_0,\qquad \mathcal{D}_0\neq0.\tag{15.10}$$

This derivative requires the coupled fluid, electromagnetic, radiation, and observation equations at fixed independently specified boundary data. If the leading order is higher, the expansion must be changed accordingly. It cannot be computed from a stress symbol alone.

Theorem 15.4 (Conditional accretion-response closure). *Suppose a covariant initial–boundary value problem for* $T^{ab}_{\rm total}=T^{ab}_{\rm fluid}+T^{ab}_{\rm EM}+T^{ab}_{\rm rad}+T^{ab}_{\rm cross}$ *is well posed in a Banach space,* $\nabla_a T^{ab}_{\rm total}=0$

holds, and the equation of state, radiation closure, source data, and detector map are fixed independently of ε. Write its equations, constraints, and lifted boundary conditions as $\mathscr{F}(U,\varepsilon)=0$, a C^2 map between specified Banach spaces, with $\mathscr{F}(U_0,0)=0$. Assume that $A_0=D_U\mathscr{F}(U_0,0)$ is a bounded isomorphism after gauge and constraint reduction. Let the observation map $\mathcal{D}(U,\varepsilon)$ be C^2, with $\mathcal{D}_0=\mathcal{D}(U_0,0)\neq 0$. Then D in (15.10) exists and is unique. Its value is obtained by solving the linearized coupled conservation, constitutive, and instrument equations with the same boundary data; changing any of those inputs changes the response problem.

Proof. The implicit-function theorem supplies the local solution branch and

$$U_1=-A_0^{-1}\partial_\varepsilon\mathscr{F}(U_0,0),\qquad D=\frac{D_U\mathcal{D}(U_0,0)[U_1]+\partial_\varepsilon\mathcal{D}(U_0,0)}{\mathcal{D}_0}.$$

This proves the stated uniqueness and gives the computation. Ordinary nonlinear well-posedness alone does not imply invertibility of its linearization. Shocks, changing domains, marginal stability, and long-time limits therefore require separate estimates. If the first nonzero response is quadratic, the parameter in this theorem may instead be the declared squared coupling, with the corresponding smoothness checked. □

This theorem is conditional on the complete non-vacuum forward model. The present manuscripts have not supplied that model and therefore do not report a numerical accretion coefficient.

For a quadratic leading response, the same assumptions give a more explicit formula without presuming an even reparameterized solution. Write

$$U(\varepsilon)=U_0+\varepsilon U_1+\varepsilon^2U_2+o(\varepsilon^2),$$

where $U_2=\frac{1}{2}\partial_\varepsilon^2U(0)$. Taylor expansion of $\mathscr{F}(U(\varepsilon),\varepsilon)=0$ gives

$$\begin{aligned}U_1&=-A_0^{-1}\mathscr{F}_\varepsilon,\\ U_2&=-A_0^{-1}\left\{\tfrac{1}{2}\mathscr{F}_{UU}[U_1,U_1]+\mathscr{F}_{U\varepsilon}[U_1]+\tfrac{1}{2}\mathscr{F}_{\varepsilon\varepsilon}\right\}.\end{aligned}$$

Every derivative on the right is evaluated at $(U_0,0)$, and includes the fixed constraint and boundary realization. If the linear observable coefficient vanishes, its coefficient D at $q_D=2$ is therefore

$$D=\mathcal{D}_0^{-1}\left\{\mathcal{D}_U[U_2]+\tfrac{1}{2}\mathcal{D}_{UU}[U_1,U_1]+\mathcal{D}_{U\varepsilon}[U_1]+\tfrac{1}{2}\mathcal{D}_{\varepsilon\varepsilon}\right\}.$$

This expansion retains the direct observable response and the change of the state at both orders. The first-order scalar state may be nonzero even when the first-order tensor or luminosity response vanishes. Consequently a substitution $\delta=\varepsilon^2$ is justified only for a reduced problem that is smooth in δ, not for an arbitrary coupled scalar–metric state with an odd scalar component.

15.12. *Which constraints actually remove free parameters?* Work in one ambient parameter vector $\alpha\in\mathbb{R}^d$ containing the independent sector coefficients. Let $F_0(\alpha)=0$ encode the within-sector

constraints and $C(\alpha) = 0$ encode proposed additional cross-sector relations. At a feasible regular point, define

$$J_0 = DF_0, \qquad J_{\text{joint}} = \begin{pmatrix} DF_0 \\ DC \end{pmatrix}, \qquad \Delta r = \operatorname{rank} J_{\text{joint}} - \operatorname{rank} J_0. \tag{15.11}$$

With constant ranks in a neighborhood, the solution manifold dimensions are $d - \operatorname{rank} J_0$ and $d - \operatorname{rank} J_{\text{joint}}$. Their difference is Δr. If N_0 spans $\ker J_0$, then $\Delta r = \operatorname{rank}(DC\, N_0)$: one restricts the new constraints to directions left free by the old ones. This proves precisely what is removed. A stacked shared-parameter Jacobian and a block-diagonal Jacobian with duplicated parameter columns are not comparable by a direct rank subtraction.

For instance, $F_0(\alpha) = \alpha_1 + \alpha_2 + \alpha_3 - s_0$ has rank one. Adding $C = (\alpha_1 - \alpha_2, \alpha_2 - \alpha_3)$ gives total rank three and removes two local degrees of freedom. This is a transparent algebraic example. It is a physical result only after the two equalities are derived from the specified mother model, not imposed for the calculation.

Observational identifiability is a separate test. If N spans the tangent space of the fully constrained parameter set, $D_\alpha \mathcal{O}$ is the observable derivative, $D_\beta \mathcal{O}$ the nuisance derivative, and W a fixed whitening matrix, use

$$J_{\text{obs}}^{\text{phys}} = (I - P_\beta) W (D_\alpha \mathcal{O}) N,$$

where P_β is the orthogonal projector onto $\operatorname{range}(W D_\beta \mathcal{O})$. Full column rank is a sufficient regular local test for distinguishing all allowed physical directions from nuisance directions. Rank deficiency is an infinitesimal degeneracy, not a proof of global non-identifiability. Singular values, dimensionless scaling, tolerance, and numerical derivative errors must be reported.

15.13. *Frozen calibration and the status of the data.* Let ϑ parameterize the admissible model after structural constraints are imposed. Exact constraints are enforced as constraints, not silently replaced by a soft penalty:

$$\vartheta_* \in \operatorname*{arg\,min}_{\vartheta \in \Theta,\, \mathcal{C}(\vartheta) = 0} \| \mathcal{O}_{\text{cal}}(\vartheta) - D_{\text{cal}} \|^2_{\Sigma_{\text{cal}}^{-1}}. \tag{15.12}$$

Approximate constraints require independently justified residual bounds. A nonunique minimizer requires a declared selection rule or propagation of the entire allowed set. It must not be chosen with the validation data.

For branch b, independently specified source and instrument data $\mathcal{I}_b$ define

$$\widehat{\mathcal{O}}_b = \mathcal{P}_b(\vartheta_*; \mathcal{I}_b), \qquad R_{\text{test}} = \| \widehat{\mathcal{O}}_b - D_{\text{test}} \|^2_{\Sigma_{\text{pred}}^{-1}}. \tag{15.13}$$

The prediction covariance includes measurement noise, propagated calibration uncertainty, and specified model discrepancy. Gaussian quadratic statistics are used only when their sampling assumptions apply. Event-count likelihoods and visibility likelihoods generally require different statistical models. Instrument processing, data exclusions, nuisance estimation, and rejection thresholds are fixed before opening the held-out observations. No-refit refers to shared theory parameters; new

sources can still require independently constrained masses, spins, viewing angles, or accretion rates. Baseline GR/Kerr, GRMHD, and sector-specific models must use comparable nuisance treatment.

The public sources have different evidential roles:

- GWOSC supplies measured detector strain. Public posterior products incorporate their original waveform models and priors; they are not independent raw data from which an arbitrary new likelihood follows.
- HEASARC/NICER products require event filtering, background estimation, instrument responses, and source selection before a timing or spectral test.
- Released EHT observational products must be distinguished from EHT GRMHD code-comparison simulations; the latter test forward models.
- JHTDB is a direct-numerical-simulation benchmark for fluid statistics, not an astronomical or laboratory observation.

A GW150914 H1 4-kHz, 32-s strain file is archived with SHA-256

```
C5EA87BECED5094B56B4D694F3A36E6D59F7
4D3A46E546B980A6A199D1F252A9.
```

The two lines concatenate to one hash. Archiving the file does not constitute a frozen-parameter test. A data-access route is likewise not a completed NICER, EHT, or JHTDB validation.

Keeping the physical couplings as supplied inputs, as in the conditional branch used here, permits forward calculations over those inputs. It does not create an independently selected parameter vector. In particular, using the published GW150914 remnant posterior to set mass and spin and then calling the same event an independent ringdown test would require accounting for the data reused in that posterior. Independent calibration must be independent of the tested statistic, or the shared likelihood must explicitly account for the dependence. A second detector does not by itself remove this issue if the calibration posterior already used both detectors.

For a fixed detector template $h(\vartheta)$, Gaussian noise with a separately estimated covariance Σ would give

$$-2\log\mathscr{L}(\vartheta) = (d-h(\vartheta))^{\mathsf{T}}\Sigma^{-1}(d-h(\vartheta)) + \log\det\Sigma + \text{constant}.$$

The covariance and template must describe the same filtering and sampling. The normalized stationary scalar profile is not h. Without the tensor waveform, source-to-detector projection, and declared nuisance model, this formula has no computable theory likelihood. Assigning a parameter value or a likelihood merely because a raw file is available would supply uncomputed physical information.

15.14. *A conditional local curvature response.* The companion Kerr analysis makes a local field response explicit. Suppose the matched Lorentzian metric action retains $f_3(\varphi)R^2_{\alpha\beta\gamma\delta}$, with a canonical scalar of mass m_φ, and suppose the other operators of the retained order are controlled. Put

$\lambda_3 = f_3'(0)$. On a Ricci-flat Kerr background the leading scalar equation is

$$(\Box_{\mathrm{K}} - m_\varphi^2)\varphi_1 = -\lambda_3 R^{\mathrm{K}}_{\alpha\beta\gamma\delta} R_{\mathrm{K}}^{\alpha\beta\gamma\delta}.$$

Horizon regularity, axis regularity, and decay at infinity give at most one stationary axisymmetric response for $m_\varphi^2 \geq 0$ under the stated finite-energy conditions. In the massless case, direct integration of the monopole equation gives

$$Q_{\mathrm{BH}} = 8\lambda_3 \kappa_H, \qquad \varphi_1 = Q_{\mathrm{BH}}/r + O(r^{-2}).$$

This recovers the known curvature-induced scalar-charge mechanism [87]. Its relation to the common-weight branch is $\lambda_3 = -\bar{\alpha}_3\gamma = -2\bar{\alpha}_3 a_{\mathrm{m}}$, where $f_3(0) = \bar{\alpha}_3$, $\gamma = -\partial_\varphi \log B_\gamma|_0$, and $a_{\mathrm{m}} = \partial_\varphi \log A|_0$. These signed relations require matched common weights and constant elementary Jordan masses; they are not general consequences of Gibbs invariance.

For the specified curvature interaction, metric variation gives an explicit covariant cross stress; on the Ricci-flat background its leading form is

$$T^{\mathrm{int}}_{ab} = -8\lambda_3 R^{\mathrm{K}}_{acbd} \nabla^c \nabla^d \varphi_1.$$

Its divergence cancels the scalar stress exchange on the sourced scalar equation. The full expression, the nonvacuum terms, and the scalar–metric differential coupling are given in the Kerr companion. The charge formula applies to the massless response; a positive scalar mass changes the asymptotics. These calculations determine a conditional exterior field response and its source. On their own they do not evaluate a tensor resonance shift or a disk luminosity. The separate coupled spectral matching in the Kerr companion supplies leading tensor coefficients only under its additional massless vacuum conditions.

With geometrical mass $\mathcal{M} = G_N M$, the dimensionless backreaction scale is $\lambda_3^2/(M_{\mathrm{P}}^2 \mathcal{M}^4)$. One universal dimensionful λ_3 therefore produces different dimensionless strengths for different source masses. The mass, canonical normalization, curvature coefficient, and physical matter coupling must all be fixed before a shared-parameter observational comparison.

The unaltered tree-level Cartan potential imposes a further restriction: with $|\bar{\alpha}_3|/M_{\mathrm{P}}^2 = \ell^2/8$ and $m_\varphi^2 \ell^2 \geq 6\alpha_\varphi$,

$$\frac{\lambda_3^2}{M_{\mathrm{P}}^2 \mathcal{M}^4} \leq \frac{(m_\varphi \mathcal{M})^2}{192} \left(\frac{\ell}{\mathcal{M}}\right)^6.$$

Thus a light scalar and a controlled curvature expansion suppress this particular branch's tensor backreaction. An exactly massless scalar with these unaltered coefficients has zero coupling. The nonzero massless charge calculation is a reference for other matched branches, not an additional prediction obtained by discarding that constraint.

15.15. *Logical status.* The finite-regulator Gibbs and relative-entropy identities hold under the stated analytic hypotheses. The block elimination, perturbation-order calculation, metric-variation

convention, and rank identity above are finite mathematical results. Classical mechanics and the geometric, gauge, and fluid branches require their stated projections, generator matching, scalings, and boundary conditions. In particular, finite Galerkin energy balance alone is not a proof of a thermodynamic entropy-production formula; the invariant measure and projected generator must also be matched.

The solved massless zero-spin reference branch further supplies the first exterior metric backreaction and a circular-orbit binding diagnostic. At fixed ADM mass, its minimally coupled fractional efficiency coefficient is $D_{\mathrm{geo}} = 0.420800563657\ldots$ per unit $\zeta = \lambda_3^2/(M_{\mathrm{P}}^2\mathcal{M}^4)$. With the stated Jordan matter projection, a separate term $-2.64578589957\ldots\, a_{\mathrm{m}}\lambda_3/\mathcal{M}^2$ appears in the fractional binding efficiency at the same retained level. The Schwarzschild and Kerr companion calculations give the derivation and normalization. This orbit-energy quantity is not the full radiation and instrument-dependent accretion response D, and the nonzero massless reference is unavailable in an unaltered potential that forces its coupling to vanish.

A single independently fixed physical parameter vector, the general massive tensor response, a closed accretion and radiation model, and their joint independent observational validation have not been obtained by these identities. The Kerr companion now gives 60 source-attributed, normalized leading tensor coefficients for three fundamental modes, two parities and ten spins in a specified massless vacuum branch. They are inherited coupled spectral results, not newly solved tensor equations or uniquely selected physical constants.

A fixed conditional likelihood has also been evaluated on real GW150914 H1 and L1 strain, with off-source noise calibration. Its supplied coupling scenarios have negligible discrimination: the joint log likelihood contrast is about 1.22×10^{-4} even for the declared $\sqrt{|\alpha|} = 10\,\mathrm{km}$ scenario. Source and excitation priors remain inputs; this comparison is not a common-parameter validation of thermodynamics, fluids and gravity. The one-mode mass–spin–coupling degeneracy and the conditional two-mode rank calculation specify what additional information is needed. Neither a physical $\bar{\kappa}_*$ nor a radiative D is selected by these calculations. The continuum and quantum limits remain separate problems.

15.16. *Invariant-measure claims: existence, uniqueness, and convergence.* Claims about a stationary law require three logically separate questions. For a regulated Markov generator $\mathcal{L}_N$ on a state space $\mathcal{X}_N$, existence means that at least one probability π_N satisfies

$$P_t^{N,*}\pi_N = \pi_N \quad (t \geq 0), \qquad \Longrightarrow \qquad \int_{\mathcal{X}_N} \mathcal{L}_N f \, \mathrm{d}\pi_N = 0$$

for integrable functions in the generator domain. The converse requires a conservative realization for which the weak stationary equation determines a stationary solution, for example uniqueness of the corresponding forward equation in the stated measure class. Uniqueness means that no other probability has this property. Convergence means that $P_t^{N,*}\nu$ tends to that particular π_N in a

declared topology for the stated class of initial laws ν. Existence alone implies neither uniqueness nor convergence, and uniqueness alone does not supply convergence or a rate.

For a reversible gradient branch, the calculation is explicit. If

$$\mathcal{L}_N f = \theta_N p_N^{-1} \nabla \cdot \big(p_N M_N \nabla f\big),$$
$$\pi_N(\,\mathrm{d}x) = p_N(x)\,\mathrm{d}x, \qquad p_N(x) = Z_N^{-1} e^{-S_N(x)/\theta_N} m_N(x), \quad Z_N < \infty.$$

then integration by parts and the declared zero-flux or reflecting boundary condition give

$$\int \mathcal{L}_N f \,\mathrm{d}\pi_N = \theta_N \int_{\partial \mathcal{X}_N} p_N M_N \nabla f \cdot n \,\mathrm{d}\sigma = 0.$$

For the conservative semigroup associated with the closed, reflecting Dirichlet form, this calculation gives invariance. It does not prove uniqueness. Uniqueness requires, for example, strong Feller regularisation together with topological irreducibility, or a separately verified Harris or contraction theorem. Likewise, a quantitative convergence statement requires a mixing estimate. For instance, a Poincaré inequality

$$\mathrm{Var}_{\pi_N}(f) \le C_{P,N} \int (\nabla f)^T M_N \nabla f \,\mathrm{d}\pi_N$$

combined with the symmetric generator yields

$$\mathrm{Var}_{\pi_N}(P_t^N f) \le e^{-2\theta_N t / C_{P,N}} \,\mathrm{Var}_{\pi_N}(f),$$

with the rate changed according to the normalization of $\mathcal{L}_N$. An invariant density, a free-energy minimizer, or a positive diffusion coefficient alone does not supply either of the latter two conclusions.

For a nonreversible nonequilibrium stationary state, the same existence and uniqueness questions remain, but the stationary current need not vanish and the invariant law need not have Gibbs form. Thus path-space irreversibility and stationarity must not be identified with failure of existence or with nonuniqueness. In the finite Galerkin branch, a coercive Lyapunov estimate and the Feller property give existence by tight occupation measures; uniqueness and convergence are conditional on the stated irreducibility, smoothing, or weak-Harris hypotheses. In the Schwarzschild one-dimensional reflected diffusion, normalisability, ellipticity, reflection, and irreducibility give the unique reversible law, while a Poincaré estimate supplies exponential relaxation. In the bounded reflected Kerr mass–spin model, the weighted Poincaré estimate gives the positive spectral gap and hence uniqueness and L^2 relaxation for that regulated label process. These are theorems for the declared generators; they are not global uniqueness theorems for the continuum spacetime, arbitrary turbulent flow, or quantum theory.

Accordingly, stationary-law claims in this programme distinguish the following properties: (E) existence of an invariant probability, (U) uniqueness for the fixed generator and boundary data, or (C) convergence in a specified metric. A claim states which properties have been established; thermodynamic equilibrium does not require uniqueness among all stationary laws or attraction

from all initial states. Its physical interpretation requires the declared energy, reservoir conditions, temperature, parity, and time calibration, including absence of maintained entropy-producing currents under the physical reversal. For example, a canonical harmonic oscillator is an equilibrium stationary ensemble although its Hamiltonian flow has many invariant laws and does not relax from a displaced point mass. Existence, uniqueness, attraction, and the thermodynamic interpretation therefore retain their separate hypotheses.

Conditional closure theorem and proof. The following implication is used whenever a branch is labelled "conditional." Assume (A1) that the fixed-regulator martingale problem is well posed and its Markov semigroup P_t^N is Feller; (A2) that a nonnegative Lyapunov function V_N has compact sublevel sets and satisfies

$$\mathcal{L}_N V_N \le -c_N V_N + C_N, \qquad c_N > 0;$$

(A3) that either strong Feller regularisation and topological irreducibility hold, or a stated Harris/weak-Harris contraction holds; and (A4), for a quantitative rate, that the displayed Poincare inequality or the corresponding Harris/hypocoercive estimate holds. Then the fixed-regulator process has an invariant probability; it is unique under (A3), and it converges to that law in the metric specified by (A4).

Indeed, Dynkin's formula and Gronwall's inequality give

$$\mathbb{E}_x V_N(X_t) \le e^{-c_N t} V_N(x) + \frac{C_N}{c_N}(1 - e^{-c_N t}).$$

Averaging this estimate over $0 \le t \le T$ gives a T-independent bound on the mass of the occupation measure outside each compact sublevel set. The occupation measures are therefore tight. Every weak limit of a Krylov–Bogoliubov subsequence is invariant because the Feller property allows $P_t^N f$ to pass to the limit for bounded continuous f. This proves existence.

If two invariant probabilities existed, the strong Feller and irreducibility assumptions in (A3) would make the semigroup positivity improving; the standard Doob argument then gives equality of the two measures. In the alternative Harris route, the contraction estimate applied to both invariant measures gives a zero distance and hence equality. This proves uniqueness without using a free-energy minimum as a substitute for mixing.

Finally, in the symmetric gradient case, set $u_t = P_t^N f - \int f \, d\pi_N$. Integration by parts gives

$$\frac{d}{dt}\|u_t\|^2_{L^2(\pi_N)} = -2\theta_N \int (\nabla u_t)^T M_N \nabla u_t \, d\pi_N.$$

Applying (A4) and Gronwall yields

$$\|u_t\|^2_{L^2(\pi_N)} \le e^{-2\theta_N t / C_{P,N}} \|u_0\|^2_{L^2(\pi_N)}.$$

The nonsymmetric case uses the declared Harris or hypocoercive estimate in the same final step. Thus the proof establishes exactly the conditional existence, uniqueness, and convergence claim and no stronger continuum statement.

15.17. *Structural-selection axiom and conditional coupling closure.* The entropy-production inequality constrains admissible dynamics but does not by itself determine every absolute or relative coupling. We therefore state the proposed extension as a new postulate.

The selection principle does not determine the reservoir temperature, the reference measure or a thermodynamic clock; those quantities remain part of the physical calibration data.

Let $\bar{\Theta} = \Theta/\sim$ quotient gauge and normalization-equivalent descriptions after the physical energy, temperature, and clock units have been fixed. For a frozen finite probe set, collect dimensionless intertwining, positivity, boundary, entropy-balance, and regulator residuals in $R_\alpha(\bar{\vartheta})$ and define

$$F_{\mathrm{sel}}(\bar{\vartheta}) = \frac{1}{2}\sum_{\alpha} \|R_\alpha(\bar{\vartheta})\|_\alpha^2, \qquad \bar{\vartheta}_* \in \arg\min_{\bar{\vartheta}\in\bar{\Theta}} F_{\mathrm{sel}}. \tag{15.14}$$

Assumption 15.5 (Structural-selection principle). The physical coupling is the minimizing class; a degenerate minimum is reported as non-identifiability and is not removed by holdout-data fitting.

THEOREM 15.6 (Conditional existence and uniqueness). *Completeness of the quotient, proper lower semicontinuity with compact sublevels, and strong convexity of F_{sel} on a geodesically convex admissible quotient domain imply existence and uniqueness of the selector.*

Proof. The direct method proves attainment on a compact sublevel set, while strong convexity excludes two distinct minimizers. □

This is a conditional statement for the extended model. It becomes a consequence of the original mother model only after an independent derivation of the score and its convexity. Numerical uniqueness must be accompanied by quotient-Jacobian, Hessian, and regulator-refinement certificates.

15.18. *Selection after solving the nuisance field equations.* A consistency condition tests whether a proposed field solves its equations. A selection condition must also distinguish physical parameter values after the fields have been solved. These are different questions. Let ξ denote coordinates on a smooth gauge-fixed chart of the admissible parameter quotient, and let Y collect the background fields, projected states and boundary data that are solved for at a given ξ.

PROPOSITION 15.7 (Vanishing profiled residuals do not select a coupling). *Suppose $R(\xi, Y)$ is C^2 into a finite-dimensional inner-product space and a C^2 solution family $Y(\xi)$ satisfies $R(\xi, Y(\xi)) = 0$ on an open parameter set U. Then*

$$F_{\mathrm{prof}}(\xi) = \tfrac{1}{2}\|R(\xi, Y(\xi))\|^2 = 0, \qquad DF_{\mathrm{prof}} = 0, \qquad D^2F_{\mathrm{prof}} = 0 \quad \text{on } U.$$

Neither strict convexity nor an isolated selected parameter follows from these residuals. In particular, full rank of $\partial_\xi R$ while holding Y fixed is not a rank certificate for the profiled problem.

Proof. The composite residual is identically zero, so the asserted derivatives vanish. The chain rule gives

$$J_{\mathrm{prof}} = \partial_\xi R + \partial_Y R\, D_\xi Y = 0.$$

At zero residual, differentiating its squared norm gives $D^2 F_{\mathrm{prof}} = J_{\mathrm{prof}}^\top J_{\mathrm{prof}} = 0$. As an explicit example, $R(\xi, Y) = Y - \xi$, $Y(\xi) = \xi$ has $\partial_\xi R = -1$ but $J_{\mathrm{prof}} = 0$. □

There is a useful form when the fields are obtained by a local least-squares solve rather than an exact prescribed family. Let J_Y be full column rank after removing its gauge kernel. At a zero residual, elimination of the field variation gives the reduced quadratic form

$$H_{\mathrm{prof}} = J_\xi^\top (I - P_Y) J_\xi, \qquad P_Y = J_Y (J_Y^\top J_Y)^{-1} J_Y^\top. \tag{15.15}$$

Indeed, minimizing $\|J_\xi v + J_Y w\|^2$ over w gives $w = -(J_Y^\top J_Y)^{-1} J_Y^\top J_\xi v$ and the value $v^\top H_{\mathrm{prof}} v$. If an exact field family absorbs a parameter variation, then $J_\xi v$ lies in $\operatorname{Ran} J_Y$ and the reduced curvature in that direction is zero. Equation (15.15) is local; it does not prove global uniqueness and assumes an interior smooth chart with the stated rank.

Thus the conditional selector theorem applies only to residuals or an additional physical functional that remain parameter-sensitive after field elimination. An independently specified off-shell mother matching condition could supply such information, but its reduced rank and global selection property must be established. Equations solved separately for each coupling do not do so. A new selection postulate is legitimate if stated explicitly; its physical objective and weights require independent justification. Choosing a quadratic penalty centred at a desired coupling would prescribe that coupling rather than derive it.

All global strong-convexity statements here require a geodesically convex admissible domain, or an ordinary convex coordinate domain with its stated metric. Completeness alone does not supply a joining geodesic. Existence uses properness, lower semicontinuity and compact sublevels, with a finite lower bound or an equivalent exclusion of descent to $-\infty$; for the nonnegative squared-residual score the lower bound is automatic. Coercivity must mean compact sublevels, or be combined with a proper metric/finite-dimensional closed-domain assumption that ensures them. A positive global gap on a continuous parameter space can be asserted outside a fixed neighbourhood of an isolated minimizer, not between the minimizer and every arbitrarily close point.

The parameter-freezing operation used in a statistical analysis remains distinct from this selection theorem. Freezing an input or a posterior mixture prevents subsequent parameter adjustment; it does not change the source of that input or prove a unique physical coupling.

15.19. *Selection by information projection of a fixed mother path law.* A candidate field can satisfy its equations at many different couplings. To select among those couplings, the comparison must contain information that is held fixed while the candidate is varied. We now supply such a

comparison at a finite regulator. It uses a specified mother path law, a specified physical projection, and calibrated units. It does not use a target observation or a penalty centred at a desired answer.

The change-of-measure identity is the standard Girsanov construction [36]; the hidden linear filter below uses the Kalman–Bucy covariance equation [53]. The physical interpretation is a new conditional principle: among a declared family of effective dynamics, use the member that loses the least information about the fixed projected mother dynamics. The resulting mathematical minimizer is derived below. Calling that minimizer a physical coupling additionally requires this principle and the coefficient-to-coupling map as physical hypotheses. The reference law itself cannot be changed when the candidate coupling changes.

15.19.1. *Path laws, covariance matching, and the new principle.* Let X be a stationary, finite-dimensional mother diffusion on a fixed probability space, and let $Y = \Pi(X)$ take values in $\mathbb{R}^n$. Fix the physical energy, temperature and clock units, the map Π, and the time-reversal parity of all coordinates. Suppose that, in its own filtration, the projected process has the semimartingale representation

$$dY_t = \beta_t\, dt + \sigma(Y_t)\, dW_t^Y, \qquad Q(y) = \sigma(y)\sigma(y)^\top > 0. \tag{15.16}$$

The drift β_t may depend on the observed past. Thus this hypothesis does not assume that projection removes memory. Assume a stationary current law π_Y and a measurable function $\bar\beta$ such that

$$\mathbb{E}[\beta_t \mid Y_t] = \bar\beta(Y_t) \quad \text{for almost every } t. \tag{15.17}$$

For a smooth projection of a stationary Itô diffusion, this identity follows from conditional expectation of $D\Pi\, b + \frac{1}{2} Q_X : D^2\Pi$, provided the projected covariance is the function $Q(Y)$ appearing in (15.16) and the indicated semimartingale representation is valid.

Represent a gauge-fixed physical parameter chart by a nonempty closed convex set $K \subset \mathbb{R}^d$. Introduce nuisance drift coordinates $\eta \in \mathbb{R}^q$. They are coefficients of specified drift features, not an unrestricted family of background fields. The candidate dynamics are

$$dY_t = [b_0(Y_t) + \Phi(Y_t)\xi + \Psi(Y_t)\eta]dt + \sigma(Y_t)dW_t, \qquad \xi \in K. \tag{15.18}$$

Here b_0, the $n \times d$ matrix Φ, and the $n \times q$ matrix Ψ are fixed before minimization. The initial law of every candidate is π_Y. Assume nonexplosion and well-posedness for the declared candidate laws. On each finite time interval assume the change of drift satisfies the Girsanov martingale and integrability conditions, so that the projected reference law $\mathbb{R}_T$ is absolutely continuous with respect to the candidate law $\mathbb{P}_{\xi,\eta,T}$ and has finite relative entropy. These analytic conditions are separate from parameter identifiability. The chart identifies distinct points with distinct declared physical equivalence classes. Global uniqueness on the entire admissible quotient requires that this chart cover that quotient; otherwise the conclusion is global only on the declared branch K.

The covariance in (15.18) is the same as that in (15.16). This is essential: for two different constant covariances, the sets of continuous paths with quadratic variation tQ_1 and tQ_2 are disjoint.

Their diffusion path laws are mutually singular, and a drift-only relative-entropy formula cannot compare them.

Assumption 15.8 (Fixed-reference information projection). The effective coefficients minimize

$$F_T(\xi,\eta) = T^{-1} D(\mathbb{R}_T \| \mathbb{P}_{\xi,\eta,T}), \qquad T > 0,$$

over the declared family. The mother law, units, covariance, projection, features, nuisance family and coefficient-to-physical-coupling map are fixed independently of target data. If these primitive inputs still contain an unselected fundamental parameter, the minimization does not select that parameter without further information.

15.19.2. *Derivation and elimination of nuisance directions.* All expectations below use the reference law. Write $\delta_t = \beta_t - b_0(Y_t)$ and define

$$\begin{aligned} H &= \mathbb{E}_{\pi_Y}[\Phi^\top Q^{-1}\Phi], & B &= \mathbb{E}_{\pi_Y}[\Phi^\top Q^{-1}\Psi], \\ V &= \mathbb{E}_{\pi_Y}[\Psi^\top Q^{-1}\Psi], & h &= \mathbb{E}_{\pi_Y}[\Phi^\top Q^{-1}(\bar\beta - b_0)], \\ g &= \mathbb{E}_{\pi_Y}[\Psi^\top Q^{-1}(\bar\beta - b_0)]. \end{aligned} \tag{15.19}$$

Assume these quantities and $c_T = (2T)^{-1}\mathbb{E}\int_0^T \delta_t^\top Q^{-1}\delta_t dt$ are finite. When $q > 0$, assume V is positive definite after redundant nuisance coordinates have been removed. When $q = 0$, all expressions involving Ψ, V, B, g are absent.

Theorem 15.9 (Conditional unique effective coupling). *Under the preceding hypotheses, the relative-entropy score has the exact form*

$$F_T = c_T + \frac{1}{2}\xi^\top H\xi + \xi^\top B\eta + \frac{1}{2}\eta^\top V\eta - h^\top\xi - g^\top\eta. \tag{15.20}$$

Eliminating the nuisance coordinates gives

$$\begin{aligned} \eta_*(\xi) &= V^{-1}(g - B^\top\xi), \\ F_T^{\mathrm{red}}(\xi) &= c_T - \tfrac{1}{2}g^\top V^{-1}g + \tfrac{1}{2}\xi^\top H_{\mathrm{red}}\xi - h_{\mathrm{red}}^\top\xi, \\ H_{\mathrm{red}} &= H - BV^{-1}B^\top, \qquad h_{\mathrm{red}} = h - BV^{-1}g. \end{aligned} \tag{15.21}$$

If $H_{\mathrm{red}} \geq \lambda I$ for some $\lambda > 0$, this score has one and only one minimizer on K. It is independent of T. If $H_{\mathrm{red}}^{-1}h_{\mathrm{red}} \in K$, then

$$\xi_* = H_{\mathrm{red}}^{-1}h_{\mathrm{red}}. \tag{15.22}$$

Otherwise it is the unique point satisfying $\langle H_{\mathrm{red}}\xi_* - h_{\mathrm{red}}, \xi - \xi_*\rangle \geq 0$ for every $\xi \in K$. A fixed physical map $k(\xi)$ then assigns the unique conditional coupling $k(\xi_*)$.

Proof. Let $u_t = \sigma(Y_t)^{-1}[\beta_t - b_0 - \Phi\xi - \Psi\eta]$; for a rectangular noise factor the same argument uses its minimum-norm right inverse. The assumed Girsanov identity and martingale integrability

give

$$D(\mathbb{R}_T\|\mathbb{P}_{\xi,\eta,T}) = \frac{1}{2}\mathbb{E}\int_0^T |\beta_t - b_0 - \Phi\xi - \Psi\eta|^2_{Q^{-1}}dt.$$

The stochastic integral in the log likelihood has zero reference expectation. The identical initial laws give no initial entropy term. Expanding the square proves (15.20); stationarity fixes the quadratic terms, and (15.17) fixes the linear terms. The constant c_T may depend on T because the observed filter can retain memory, but it has no parameter dependence.

Differentiate with respect to η to obtain $V\eta + B^\top\xi - g = 0$. Positive definiteness of V gives the displayed nuisance minimizer. Substitution and completion of the square give (15.21). Its Hessian is exactly H_{red}; there is no parameter-dependent reference measure whose derivative was omitted. The inequality $H_{\mathrm{red}} \geq \lambda I$ gives

$$F_T^{\mathrm{red}}(\xi) \geq c_T - \tfrac{1}{2}g^\top V^{-1}g + \tfrac{\lambda}{2}|\xi|^2 - |h_{\mathrm{red}}|\,|\xi|.$$

Thus sublevel sets on the closed finite-dimensional set K are compact. A minimizing sequence converges along a subsequence and continuity gives attainment. Strict convexity on the convex domain gives uniqueness. Differentiation gives the variational inequality and, at an admissible unconstrained critical point, (15.22). The T-dependent constant does not change this minimizer. □

The hypothesis on the reduced matrix has a concrete meaning. In the Hilbert space of drift features with norm $\|f\|^2 = \mathbb{E}_{\pi_Y} f^\top Q^{-1} f$,

$$v^\top H_{\mathrm{red}} v = \inf_{w\in\mathbb{R}^q} \|\Phi v + \Psi w\|^2. \tag{15.23}$$

Indeed, expanding this norm and minimizing gives $w = -V^{-1}B^\top v$. Hence positive reduced rank means that no nonzero physical parameter direction can be absorbed by the declared nuisance drifts. Full rank before this elimination is insufficient.

If the quotient needs finitely many disjoint branch charts K_j, use the same reference law and time interval in every score. Suppose each branch satisfies the theorem and has minimum score m_j. If one branch j_* has $m_j - m_{j_*} \geq \delta > 0$ for every $j \neq j_*$, the minimizer on their union is unique: every other branch has strictly larger score, and the selected branch has a unique minimizer. The positive gap is an extra comparison of branch minima, not a gap to arbitrarily nearby points in a continuous chart. Branch-dependent constants in the entropy score must be retained in this comparison. Without this coverage or strict branch comparison, chart uniqueness is not quotient uniqueness.

15.19.3. *Stability of the selected coefficients under refinement.* The information projection also supplies an error estimate. Suppose $H_r \geq \lambda I$ and $H \geq \lambda I$ are reduced matrices on the same closed

convex K, with linear coefficients h_r, h and minimizers ξ_r, ξ_*. The two variational inequalities imply

$$|\xi_r - \xi_*| \le \frac{\|H_r - H\|\,|\xi_*| + |h_r - h|}{\lambda}. \tag{15.24}$$

To prove it, use ξ_* as a comparison in the first inequality and ξ_r in the second. Subtracting gives $\lambda|\xi_r-\xi_*|^2 \le |(H_r-H)\xi_*-(h_r-h)|\,|\xi_r-\xi_*|$. Cancel the nonzero distance; the zero case is immediate. Uniform reduced rank and convergent reference Gram integrals therefore imply convergence of the conditional selector. They do not establish removal of a physical field regulator unless those integrals and their physical matching also converge.

15.19.4. *A finite mother model with an explicit nonzero selected drift.* Consider the dimensionless, fully specified example

$$dX = -AX\,dt + \sqrt{2}\,dW, \qquad A = \begin{pmatrix} 1 & 0.25 & 0.15 \\ -0.15 & 1.4 & 0.2 \\ 0.1 & -0.2 & 2 \end{pmatrix}, \qquad Y = (X_1, X_2). \tag{15.25}$$

The symmetric part of A is positive definite, so every eigenvalue has positive real part. The unique Gaussian invariant covariance is

$$C_X = 2\int_0^\infty e^{-At}e^{-A^\top t}dt, \qquad AC_X + C_X A^\top = 2I.$$

Write $C = (C_X)_{YY}$, $a = A_{Y3}$ and $r = (C_X)_{3Y}C^{-1}$. Gaussian conditional expectation gives

$$\bar\beta(y) = -[A_{YY} + ar]y =: -B_* y.$$

The candidate damping matrix is $B_\xi = \left(\begin{smallmatrix} k_1 & g-\omega_c \\ g+\omega_c & k_2 \end{smallmatrix}\right)$. Take $K = \mathbb{R}^4$ and no nuisance coordinates. Every candidate is a nonexplosive linear diffusion on a finite time interval; it need not have an invariant law for the path comparison to be defined. The reference observation and its conditional hidden mean form an augmented linear filter with bounded deterministic coefficients on each such interval. Replacing the observation drift by $-B_\xi Y$ leaves this augmented system linear. Localization of the change-of-drift exponential therefore gives shifted laws with uniform finite-time second-moment bounds. Their probability of reaching a localization radius R is $O(R^{-2})$, so no mass is lost when the radius tends to infinity and the exponential has mean one. This proves the finite-time Girsanov martingale condition here; Gaussian second moments also give the required entropy integrability. Its four independent linear features and $Q_Y = 2I$ give a positive Gram matrix: a nonzero matrix difference D has $\mathbb{E}|DY|^2 = \operatorname{tr}(DCD^\top) > 0$ since $C > 0$. Thus the theorem uniquely selects B_*. The YY block of the covariance equation gives $B_*C + CB_*^\top = 2I$, which also proves stability of B_*.

This selection does not make the projected process Markovian. For the hidden coordinate, stationary filtering has variance P satisfying

$$0 = -2A_{33}P + 2 - \tfrac{1}{2}|a|^2P^2, \qquad P = \frac{2}{A_{33} + \sqrt{A_{33}^2 + |a|^2}}.$$

This follows from the scalar Kalman–Bucy covariance equation after observing $dY + A_{YY}Y dt = -aX_3 dt + \sqrt{2}dW_Y$; the hidden noise is independent of the observation noise. Conditioning on the full past leaves P, whereas conditioning on the current Y leaves $v_0 = (C_X)_{33} - (C_X)_{3Y}C^{-1}(C_X)_{Y3}$. The limiting minimum path entropy rate is

$$F_{\min} = \tfrac{1}{4}|a|^2(v_0 - P) \geq 0. \tag{15.26}$$

It follows from the conditional variance of $\mathbb{E}[X_3 \mid Y_{(-\infty,t]}] - rY_t$ and the same Girsanov formula. The finite-time filter initialized from Y_0 converges to the positive stationary Riccati root; its transient contribution vanishes in the entropy rate. A nonzero minimum records unresolved memory rather than an exact generator intertwining.

Solving the covariance equation in exact rational arithmetic gives

$$B_* \simeq \begin{pmatrix} 0.991086457297 & 0.251978689569 \\ -0.161884723605 & 1.402638252758 \end{pmatrix}.$$

The selected coefficients are approximately

$$k_1 = 0.991086457297, \quad k_2 = 1.402638252758,$$
$$g = 0.045046982982, \quad \omega_c = -0.206931706587.$$

The four Gram eigenvalues are approximately 0.356056, 0.505232, 0.712284 and 1.010710; exact positive leading minors also establish its positive definiteness. If a nuisance feature duplicates the circulation feature, the reduced rank is three and that parameter is not selected. The memory floor in (15.26) is $3.470142914 \times 10^{-5}$ per declared time unit. These are exact-formula finite-model quantities rounded for display, not physical measurements.

For any real s, the alternatives $B_s = B_* + sJC^{-1}$, $J = \left(\begin{smallmatrix} 0 & -1 \\ 1 & 0 \end{smallmatrix}\right)$, have exactly the same stationary covariance. Their excess path score is $\mathrm{tr}[(B_s - B_*)^\top (B_s - B_*)C]/4$, strictly positive for $s \neq 0$. This illustrates why a stationary density alone misses circulation information. All numbers in this example are mother-model inputs or derived effective drift coefficients. None is a determination of λ_3, m_φ or a universal physical coupling.

15.19.5. *What the conditional selection closes.* The result replaces an assumed convexity assertion by a derived quadratic functional and an explicit reduced-rank condition. It closes the selection problem for a specified projected reference law and a specified effective feature family. Applying it to the unified physical model requires its parameter-independent primitive reference, physical projection and coefficient map. If changing ξ also changes that reference, or if all physical features lie in the nuisance span, the theorem does not apply. Thus adding its conditions is mathematically sufficient, while verifying those conditions in the full physical branch remains a separate task.

15.20. *Frozen prediction and an exact condition for statistical separation.* A frozen prediction is a distribution for new data, not a promise that those data will support the theory. This distinction

can be expressed without a particular detector. Let $\mathcal{C}$ contain every calibration datum and every design choice. Conditional on $\mathcal{C}$, freeze the physical parameters, source treatment, forward map, detector response, noise model, analysis window and decision rule. The test likelihood is the sampling law conditional on this calibration record. New test outcomes are not used to choose the frozen inputs. Conditional independence of test events is imposed only where stated; integrating one uncertain shared parameter can make those events dependent. A retrospectively chosen split of previously inspected data does not acquire this property merely by being renamed a holdout set.

Write $p_*(d \mid i)$ for the frozen prediction, $p_0(d \mid i)$ for a specified baseline, and $q(d \mid i)$ for the actual test distribution. Here i denotes independently supplied source or instrument inputs. Assume common dominating measures, positive model densities on the support of q, and integrable log density ratios. For the relative-entropy identity, also require both conditional relative entropies to be finite with finite averages over I; otherwise their difference could be the undefined expression $\infty - \infty$. All statements below are conditional on the frozen calibration record.

PROPOSITION 15.10 (Expected predictive advantage). *The mean test log ratio obeys*

$$\mathbb{E}_q \log \frac{p_*(D \mid I)}{p_0(D \mid I)} = \mathbb{E}_I \left[D(q(\cdot \mid I) \| p_0(\cdot \mid I)) - D(q(\cdot \mid I) \| p_*(\cdot \mid I)) \right]. \tag{15.27}$$

If $q = p_*$, this quantity is nonnegative and is strictly positive exactly when the frozen and baseline distributions differ on a set of source inputs of positive probability. For independent identically distributed test pairs with an integrable log ratio, the sample average converges almost surely to this expectation.

Proof. For fixed i, subtract the two integrals $\int q \log(q/p_0)$ and $\int q \log(q/p_*)$. The terms $\log q$ cancel and leave $\int q \log(p_*/p_0)$. Average over I to obtain (15.27). Relative entropy is nonnegative, with equality precisely for equal probability distributions. The convergence statement is the strong law applied to the integrable independent log ratios. □

The same identity explains a negative result: an incorrect frozen prediction can be farther from q than the baseline. Theorem-level mathematical consistency does not fix q. Moreover, a free source nuisance parameter that reproduces the physical response can eliminate observable separation even when the physical coefficients were selected uniquely.

15.20.1. *A finite-sample result with specified detector noise.* An explicit power calculation is possible when each test event has a fixed finite detector vector, an independently fixed positive covariance Σ_e, and two fully specified mean vectors $\mu_{*,e}, \mu_{0,e}$. Assume independent Gaussian noise with this same covariance under both models. Put

$$s_e = \mu_{*,e} - \mu_{0,e}, \qquad v_e = s_e^\top \Sigma_e^{-1} s_e, \qquad V = \sum_{e=1}^{n} v_e. \tag{15.28}$$

These means include the physical detector map. A field amplitude, a mode frequency or a source catalogue entry alone is not a detector mean vector.

THEOREM 15.11 (Conditional finite-sample detection power). *For $V > 0$, the summed log likelihood ratio*

$$L = \sum_e \left[s_e^\top \Sigma_e^{-1} (D_e - \mu_{0,e}) - \tfrac{1}{2} v_e \right]$$

has law $N(V/2, V)$ under the frozen model and $N(-V/2, V)$ under the baseline. A threshold $h_\alpha = -V/2 + \sqrt{V}\, z_{1-\alpha}$ has false-positive probability α and frozen-model power

$$1 - \Phi_{\mathrm{N}}(z_{1-\alpha} - \sqrt{V}). \tag{15.29}$$

Here Φ_{N} is the standard normal cumulative distribution function and $z_p = \Phi_{\mathrm{N}}^{-1}(p)$. For $0 < \alpha, \beta < 1/2$, power at least $1 - \beta$ is equivalent to $V \geq (z_{1-\alpha} + z_{1-\beta})^2$.

Proof. Expanding the two Gaussian quadratic forms cancels their common covariance normalization and gives the displayed expression for L. Under the frozen model, $D_e = \mu_{0,e} + s_e + \varepsilon_e$, so the event contribution is $v_e/2 + s_e^\top \Sigma_e^{-1} \varepsilon_e$. The random term has mean zero and variance v_e. Under the baseline, the mean is instead $-v_e/2$ and the variance is unchanged. Independence adds means and variances, proving both normal laws. Standardizing the baseline gives the threshold and its false-positive rate. Standardizing the frozen-model distribution gives (15.29). Finally $1 - \Phi_{\mathrm{N}}(z_{1-\alpha} - \sqrt{V}) \geq 1 - \beta$ is equivalent to $\sqrt{V} \geq z_{1-\alpha} + z_{1-\beta}$. □

For example, $\alpha = \beta = 0.05$ requires $V \geq 10.822174$. This is a design sensitivity criterion for the specified Gaussian experiment, not an observed significance. If $V = 0$, both distributions are identical and no test based on these vectors can distinguish them. Unknown covariance, fitted nuisance parameters, non-Gaussian noise, selection effects and posterior mixtures change the likelihood calculation; they cannot be absorbed into this fixed-mean theorem without derivation.

15.20.2. *Independent checks across several physical branches.* For independent branch data, log likelihood ratios and their expected advantages add. A joint test must use the same frozen shared physical parameters in every branch, with declared branch-specific source inputs. If the physical parameter is represented by a frozen posterior mixture rather than a single value, its joint predictive density is

$$p_*(D_1, \ldots, D_n) = \int \prod_{e=1}^{n} p(D_e \mid \vartheta, I_e)\, \Pi_{\mathrm{cal}}(d\vartheta).$$

The common parameter is integrated once after multiplying event likelihoods. Multiplying separately mixed event predictions generally corresponds to independent parameters and does not test the shared-coupling model.

These results close the mathematical definition, expectation and sensitivity of a conditional independent test. They do not establish that real GWOSC, NICER, EHT or turbulence observations follow the proposed distribution. That conclusion requires the completed forward map and an

actual frozen-data comparison. In particular, the existing retrospective strain calculation retains its recorded unresolved preference and is not upgraded by this theorem.

15.21. *Common physical parameters and propagated prediction errors.* A common dynamical description becomes restrictive when one parameter choice determines several measurable responses. This requires more than using the same symbol in several equations. The physical units, projection, source data, and nuisance parameters must be fixed before a comparison. We give quantitative conditions for this interpretation. The results apply to a specified physical branch; an unevaluated observation map remains an additional input.

15.21.1. *Physical constraints and observable directions.* Let ϑ belong to a gauge-fixed p-dimensional physical chart, and let $C(\vartheta) = 0$ be a set of derived cross-sector constraints. At a regular point where DC has constant rank r, the constant-rank theorem gives a local admissible manifold of dimension $p-r$. Its tangent space is $\ker DC$. This count is local and does not compare disconnected branches. A constraint obtained by fitting the observation being tested does not supply independent predictive information.

Choose a matrix Z whose columns span $\ker DC$. For a differentiable observation map $\mathcal{O}(\vartheta, \eta)$ with nuisance parameter η and a fixed positive observation covariance Σ, put

$$J_\vartheta = \Sigma^{-1/2} D_\vartheta \mathcal{O}\, Z, \qquad J_\eta = \Sigma^{-1/2} D_\eta \mathcal{O}, \qquad P_\eta = J_\eta J_\eta^{+}.$$

The superscript + denotes the Moore–Penrose inverse. The locally profiled information matrix is

$$I_{\mathrm{phys}} = J_\vartheta^T (I - P_\eta) J_\vartheta. \tag{15.30}$$

Indeed, minimizing $\|J_\vartheta v + J_\eta w\|^2$ over w removes the orthogonal projection onto the nuisance range and leaves $v^T I_{\mathrm{phys}} v$. Positivity of this matrix means that no nonzero allowed infinitesimal physical change can be absorbed by the declared nuisance parameters. It does not imply global identifiability or internal selection of the physical parameter.

15.21.2. *A quantitative error bound for a conditional selector.* Suppose a fixed-reference reduction gives the quadratic objective $F(\xi) = \frac{1}{2}\xi^T H \xi - h^T \xi + c$, after eliminating nuisance directions. All reference inputs are held fixed. Let $H \succeq \gamma I$, $\gamma > 0$, and suppose the unconstrained minimizer belongs to the interior of the allowed chart.

Proposition 15.12 (Perturbation of a selected effective coefficient). *Let $\widehat{H} = H + E$ be symmetric, $\|E\| \le e < \gamma$, and $\widehat{h} = h + f$, $\|f\| \le d$. If both minimizers are interior, then*

$$\|\widehat{\xi} - \xi_*\| \le \frac{d + e\|\xi_*\|}{\gamma - e}, \qquad \xi_* = H^{-1}h, \quad \widehat{\xi} = \widehat{H}^{-1}\widehat{h}.$$

For a physical map K with Lipschitz constant L_K on the segment joining these points, the physical-coefficient error is at most L_K times this bound.

Proof. The eigenvalue bound gives $\widehat{H} \succeq (\gamma - e)I$. Subtracting the two normal equations yields $\widehat{H}(\widehat{\xi} - \xi_*) = f - E\xi_*$. Apply the inverse norm bound $(\gamma - e)^{-1}$ and the triangle inequality. The last claim is the defining Lipschitz estimate for K. □

An a posteriori variant is $\|\widehat{\xi} - \xi_*\| \le (d + e\|\widehat{\xi}\|)/\gamma$, obtained by multiplying the difference by H. Statistical and discretization contributions to d, e must be included. A boundary minimizer requires a variational-inequality estimate; the displayed interior formula cannot be used across an active-set change. Neither estimate fixes a fundamental parameter that is still free in the reference law or in K.

15.21.3. *Dimensionful matching across source scales.* On the specified curvature–scalar branch, let M be the geometrized source mass, M_P the Planck normalization, m_φ the physical scalar mass, and λ_3 its curvature coupling. In units $c = \hbar = 1$, M has length dimension, M_P and m_φ have inverse-length dimension, and λ_3 has length dimension. Define

$$\mu(M) = m_\varphi M, \qquad \epsilon(M) = \frac{\lambda_3}{M_P M^2}, \qquad \zeta(M) = \epsilon(M)^2. \tag{15.31}$$

Thus a fixed physical parameter pair gives $\mu(M_2)/\mu(M_1) = M_2/M_1$ and $\zeta(M_2)/\zeta(M_1) = (M_1/M_2)^4$. Fixing the same nonzero μ independently at different masses changes m_φ. For cosmological sources, the mass in μ is the source-frame mass; the product of detector-frame mass and observed frequency equals the corresponding source-frame product under the stated redshift convention.

For the isolated action with linear $\lambda_3\varphi\mathcal{G}$ and a quadratic scalar potential, the transformation $(\lambda_3, \varphi) \mapsto (-\lambda_3, -\varphi)$ leaves the action invariant. Even metric responses therefore cannot identify the sign of λ_3 independently of this field convention. Additional matter couplings may make relative signs measurable, but they must be specified.

Suppose two dimensionless responses on the same source satisfy

$$X = \zeta C + R_X, \qquad Y = \zeta D + R_Y, \qquad |R_X| \le A_X\zeta^2, \quad |R_Y| \le A_Y\zeta^2.$$

Then elimination of the common amplitude gives the exact bound

$$|DX - CY| \le (|D|A_X + |C|A_Y)\zeta^2. \tag{15.32}$$

The proof is the identity $DX - CY = DR_X - CR_Y$ and the triangle inequality. This form remains meaningful if C is small or vanishes. For numerical coefficients and responses, their additional errors must also be propagated. The relation becomes a physical prediction only after C, D, their matching, and their remainders have been calculated.

15.21.4. *From field residuals to a detector likelihood.* For a specified linear boundary realization $Ak = s$, an inverse estimate $\|A^{-1}\| \le K_A$ gives $\|k - k_N\| \le K_A\|s - Ak_N\|$. A discretization requires separate consistency and boundary errors. A small matrix residual is not, by itself, a bound for a

continuum inverse. The same distinction applies when the observable depends on a derivative of k or on a poorly conditioned resonance.

For a finite detector vector, take one fixed positive covariance Σ and the norm $\|v\|_\Sigma^2 = v^T\Sigma^{-1}v$. Let the exact prediction be h, the computed prediction $h + \delta h$, and the residual $r = d - h$. The Gaussian log likelihood obeys

$$|\log L(h + \delta h) - \log L(h)| \le \|r\|_\Sigma \|\delta h\|_\Sigma + \tfrac{1}{2}\|\delta h\|_\Sigma^2. \tag{15.33}$$

To prove this, expand $-\frac{1}{2}(\|r - \delta h\|_\Sigma^2 - \|r\|_\Sigma^2)$ and use Cauchy–Schwarz. The covariance and normalization must be the same in the two likelihoods. Noise-model and parameter-integration errors are additional contributions.

There is also a useful bound for a common frozen calibration posterior Π. Suppose event likelihoods are positive and $|\log \widehat{L}_e(\vartheta) - \log L_e(\vartheta)| \le b_e$ uniformly on its support. Multiplication followed by integration gives

$$e^{-\sum_e b_e} \int \prod_e L_e \, d\Pi \le \int \prod_e \widehat{L}_e \, d\Pi \le e^{\sum_e b_e} \int \prod_e L_e \, d\Pi.$$

Hence the joint predictive log likelihood has error at most $\sum_e b_e$. The posterior is integrated once for the shared parameter. Changing it between test events invalidates this bound for a common-parameter test.

These estimates connect conditional mathematical control to observable accuracy. They neither select the data-generating law nor guarantee a favorable comparison. An independent test requires untouched data, specified source and detector maps, and a predicted separation larger than the relevant numerical and systematic uncertainties.

15.22. *Calibrated parameters and the scope of empirical evidence.* A predictive physical branch may contain constants determined by measurement. Internal selection of every constant is a stronger claim than predictive adequacy. Once an identifiable parameter vector has been calibrated, an effective theory is tested by carrying that vector, its uncertainty and the same observation map to a different measurement. The distinction is between parameters fixed before prediction and parameters adjusted to its outcome. An internally unique coupling is therefore not a prerequisite for a useful test. Conversely, identifying a coupling from data does not prove that the mother model selects it without physical inputs.

Let ϑ denote shared physical parameters and let η_b denote independently specified experimental conditions and nuisance parameters in branch b. A joint prediction has the form

$$p(D_{\text{test}} \mid D_{\text{cal}}) = \int p(D_{\text{test}} \mid \vartheta, \eta_{\text{test}}) p(\vartheta, \eta_{\text{test}} \mid D_{\text{cal}}) \, d\vartheta \, d\eta_{\text{test}}. \tag{15.34}$$

Here the distribution of test conditions is specified from the experimental design or independent auxiliary measurements. It is not inferred from the test responses whose prediction is being assessed. In a frequentist implementation the analogous calculation propagates calibration and instrument

uncertainty through a fixed forward map. In either approach, changing a common parameter to improve a held-out response invalidates that response as a test of the previously fixed prediction.

A finite stochastic example supplies a precise warning. A projected Ornstein–Uhlenbeck process and its optimal stationary Markov approximation can have exactly the same invariant covariance while having different frequency responses and time correlations. Thus agreement with an equilibrium distribution does not establish agreement with dynamical observations. The response difference must also exceed the uncertainty of the chosen observation protocol. Independent numerical implementations test an implementation; independent noise realizations test sampling; experimental observations test a physical observation map. These are distinct uses of independence.

For the present family, thermal response and finite-regulator entropy provide accessible branch tests. Neither a successful thermal test nor a downloaded black-hole data set supplies the missing gravitational waveform. A massive rotating calculation still requires the coupled tensor, scalar and constraint sectors, the physical boundary conditions, and a controlled detector response. Likewise, a turbulence test requires the actual nonlinear projected generator, forcing covariance and observation filter. A common parameter establishes a cross-sector prediction only after these maps have been derived and the same dimensionful parameter has been used in each sector.

15.23. *A fixed finite mother process and its stationary law.* A hidden degree of freedom can store information about the earlier state of an observed system. Eliminating that degree of freedom therefore changes more than the equal-time distribution. To examine this effect without introducing an uncontrolled continuum approximation, consider the declared, dimensionless process

$$dX_t = (-AX_t + Gf(t))\,dt + \sqrt{2}\,dW_t,$$

$$A = \begin{pmatrix} 1 & .25 & .15 \\ -.15 & 1.4 & .2 \\ .1 & -.2 & 2 \end{pmatrix}, \qquad G = \begin{pmatrix} 1 \\ 0 \\ 0 \end{pmatrix}. \tag{15.35}$$

Here W is a three-dimensional standard Brownian motion, $X = (Y, Z)$, $Y = (X_1, X_2)$, and $P = (I_2\ 0)$ is the observation projection. The entries of A, the noise strength and the time unit are inputs. They are neither measured thermal constants nor curvature couplings. The forcing is deterministic and the unforced stationary law is used as the initial distribution for the response experiment.

The symmetric part of A is

$$A_s = \begin{pmatrix} 1 & .05 & .125 \\ .05 & 1.4 & 0 \\ .125 & 0 & 2 \end{pmatrix}.$$

For a real vector v, the inequality $2|v_iv_j| \le v_i^2+v_j^2$ gives $v^TA_sv \ge .825|v|^2$. Consequently $\|e^{-At}\|_2 \le e^{-.825t}$. In particular,

$$C = 2\int_0^\infty e^{-At}e^{-A^Tt}\,dt, \qquad AC + CA^T = 2I_3 \tag{15.36}$$

exists and is positive definite: its quadratic form is the integral of $2|e^{-A^Tt}v|^2$, which is strictly positive for $v \neq 0$. Differentiating the integrand proves the Lyapunov equation. Conversely, the difference H between any two solutions satisfies $e^{-At}He^{-A^Tt} = H$ and must vanish as $t \to \infty$.

The explicit solution with $f = 0$ is $X_t = e^{-At}X_0 + \sqrt{2}\int_0^t e^{-A(t-s)}dW_s$. It proves invariance of $N(0, C)$ and convergence in distribution from every fixed initial point. It also proves uniqueness of the invariant probability without a moment assumption: if ϕ is the characteristic function of an invariant law, then

$$\phi(k) = \phi(e^{-A^Tt}k)\exp\{-\tfrac{1}{2}k^T(C - e^{-At}Ce^{-A^Tt})k\}.$$

Continuity of ϕ at zero and $t \to \infty$ give $\phi(k) = \exp(-k^TCk/2)$. With finite second moments, synchronous coupling also gives a Wasserstein contraction factor $e^{-.825t}$. This is a theorem for the specified finite model, not for every branch of the unified theory.

The computed covariance and stationary Markov drift are

$$C \simeq \begin{pmatrix} 1.010676204 & -.006617615 & -.060145331 \\ -.006617615 & .712178430 & .009787776 \\ -.060145331 & .009787776 & .503986044 \end{pmatrix}, \tag{15.37}$$

$$B = A_{yy} + A_{yz}C_{zy}C_{yy}^{-1} \simeq \begin{pmatrix} .991086457 & .251978690 \\ -.161884724 & 1.402638253 \end{pmatrix}. \tag{15.38}$$

Indeed, Gaussian conditioning gives $\mathbb{E}[Z \mid Y] = C_{zy}C_{yy}^{-1}Y$. The upper-left block of (15.36) implies $BC_{yy} + C_{yy}B^T = 2I_2$. Thus $d\bar{Y} = -B\bar{Y}\,dt + \sqrt{2}\,dW_y$ has the correct stationary covariance. This conditional drift does not make Y an exact Markov process, and its unforced selection does not establish exact driven response.

15.24. *Exact elimination produces memory and colored noise.* Write $a = A_{zz} = 2$ and partition A into observed and hidden blocks. Variation of constants in the hidden equation gives

$$\begin{aligned} Z_t = e^{-at}Z_0 - \int_0^t e^{-a(t-s)}A_{zy}Y_s\,ds + \int_0^t e^{-a(t-s)}G_zf(s)\,ds \\ + \sqrt{2}\int_0^t e^{-a(t-s)}dW_z(s). \end{aligned} \tag{15.39}$$

Substitution into the Y equation yields a positive-sign memory term $\int_0^t A_{yz}e^{-a(t-s)}A_{zy}Y_s\,ds$, an initial contribution $-A_{yz}e^{-at}Z_0$, and a colored random force $-\sqrt{2}A_{yz}\int_0^t e^{-a(t-s)}dW_z(s)$, in addition to the direct drift, forcing and white noise. The sign follows from the two minus signs in the original off-diagonal drifts. It must not be replaced by an assumed dissipative sign. Stability follows here from the full matrix estimate, not from the memory kernel alone.

For a stationary realization on the entire time axis, the lower integration limit is $-\infty$. The hidden noise contribution then has covariance

$$\mathbb{E}[\xi_z(t)\xi_z(s)^T] = a^{-1}e^{-a|t-s|}A_{yz}A_{yz}^T. \tag{15.40}$$

This follows by the Itô isometry and $2\int_{-\infty}^{\min(t,s)} e^{-a(t+s-2u)}du = a^{-1}e^{-a|t-s|}$. The driving white noises in the two blocks are independent. The hidden initial state in a finite-time stationary experiment is correlated with Y_0 and cannot be replaced by an independent draw without changing transient correlations.

15.25. *Response and fluctuation spectra obey the same elimination.* Use the forcing convention $f(t) = \operatorname{Re} e^{i\omega t}$. The complex susceptibility, defined by the steady mean response per unit forcing amplitude, is

$$\begin{aligned} H(\omega) &= (A + i\omega I_3)^{-1}, \qquad \chi(\omega) = PH(\omega)G, \\ R_z(\omega) &= (a + i\omega)^{-1}, \\ R(\omega) &= [A_{yy} + i\omega I_2 - A_{yz}R_zA_{zy}]^{-1}, \\ \chi(\omega) &= R(\omega)[G_y - A_{yz}R_zG_z]. \end{aligned} \tag{15.41}$$

To verify the last identity, solve the hidden row of $(A + i\omega I)x = G$ for $z = R_z(G_z - A_{zy}y)$ and substitute into the observed row. Invertibility follows from stability of A and $a > 0$. This derivation also displays the hidden forcing correction, which happens to vanish for the declared G.

Define the two-sided spectrum by $S_Y(\omega) = \int_{\mathbb{R}} e^{-i\omega t}\mathbb{E}[Y_tY_0^T]dt$, so that $C_{yy} = (2\pi)^{-1}\int S_Y(\omega)d\omega$. The white-noise spectrum is $2I_3$. Fourier transformation gives

$$\begin{aligned} S_Y(\omega) &= PH(\omega)(2I_3)H(\omega)^\dagger P^T \\ &= R(\omega)[2I_2 + 2|R_z(\omega)|^2A_{yz}A_{yz}^T]R(\omega)^\dagger. \end{aligned} \tag{15.42}$$

The dagger denotes conjugate transpose. The second equality follows by eliminating the hidden white-noise input with the same block inverse used for the forcing. Retaining the memory correction in R but omitting the colored-noise term changes the fluctuation law. Neither equality is an equilibrium fluctuation–dissipation theorem: the declared matrix includes stationary circulation.

For the selected memoryless model, the corresponding susceptibility is $(B+i\omega I_2)^{-1}G_y$. The two lag covariances are $Pe^{-At}CP^T$ and $e^{-Bt}C_{yy}$ for $t \geq 0$. They agree at $t = 0$ but generally not at positive lags. Thus invariant-law recovery, response recovery and path-law recovery are separate mathematical requirements.

15.26. *Entropy decay and stationary irreversibility are distinct.* For the unforced diffusion, let $\pi = N(0, C)$ and $u(x) = (-A + C^{-1})x$. The stationary probability current is $j_*(x) = u(x)\pi(x)$ and satisfies $\nabla \cdot j_* = 0$ by (15.36). If $p = f\pi$ is a smooth positive density with sufficiently decaying

boundary terms, its evolution is

$$\partial_t(f\pi) = -\nabla\cdot(uf\pi) + \nabla\cdot(\pi\nabla f).$$

Multiply by $1+\log f$ and integrate. The circulation contribution is $\int u\cdot\nabla f\, d\pi = 0$ and the diffusion contribution is negative. Hence

$$\frac{d}{dt}\int f\log f\, d\pi = -\int \frac{|\nabla f|^2}{f}\, d\pi \le 0. \tag{15.43}$$

This statement extends to finite relative entropy initial laws by regularization and lower semicontinuity. It does not assert monotonicity of the differential Shannon entropy or positivity on every trajectory.

Assign all three coordinates even parity under time reversal. The stationary reversed drift is $b^R = -b + 2\nabla\log\pi$ with $b = -Ax$. Consequently $b - b^R = 2u$. The stationary path relative entropy per unit time, from the drift change formula at diffusion covariance $2I_3$, is

$$\sigma_{\text{path}} = \frac{1}{4}\mathbb{E}_\pi|b-b^R|^2 = \operatorname{tr}[(-A+C^{-1})^T(-A+C^{-1})C] \simeq 0.1194617975. \tag{15.44}$$

The finite-time change-of-measure identity can be justified first for stopped linear diffusions and then by Gaussian integrability and localization. Its stationary rate is finite because C is finite. It vanishes exactly when $A = C^{-1}$, which is detailed balance in this even-parity setting. Different physical reversal parities require a different reversed process. Identification of this information-theoretic rate with reservoir entropy additionally requires a physical energy, reservoir temperatures and local detailed balance. In particular, relative entropy can cease changing at stationarity while the stationary path entropy rate remains positive.

15.27. *Frozen response calculations and their resolving power.* For $X_0 \sim N(0, C)$ and $f(t) = \cos(\omega t)$, direct integration gives

$$m(t) = \operatorname{Re}\{[e^{i\omega t}I_3 - e^{-At}](A + i\omega I_3)^{-1}G\}. \tag{15.45}$$

Differentiating this expression verifies $\dot m = -Am + G\cos\omega t$ and $m(0) = 0$. Deterministic forcing leaves the covariance equal to C. At step length h, define $F = e^{-Ah}$ and $Q_h = C - FCF^T = 2\int_0^h e^{-As}e^{-A^Ts}ds$. The exact update uses independent $N(0, Q_h)$ increments and forcing increment

$$\operatorname{Re}\{e^{i\omega t}(e^{i\omega h}I_3 - F)(A + i\omega I_3)^{-1}G\}.$$

It introduces no Euler time-discretization bias for this linear model.

The calculation used $h = .05$, duration 30, frequencies $.3, 1, 3$, and 8192 independent replicas at each frequency. Inputs and noise seeds were fixed before drawing the trajectories. A separate adaptive ordinary differential equation solver checked the mean formula. These are synthetic observations generated under declared parameters.

Frequency	Mean ODE discrepancy	Monte Carlo mean RMS error
.3	$1.46\,10^{-12}$	.01033
1	$1.40\,10^{-12}$	.01157
3	$6.96\,10^{-13}$	.01124

The tabulated discrepancies round the computed bounds upwards. Over 160 logarithmically spaced frequencies in $[.03, 30]$, the block-inverse and full-system susceptibilities differed by at most $4.45\,10^{-16}$, and their spectral matrices by $1.78\,10^{-15}$. The largest relative susceptibility difference between the full and memoryless models on that grid was .0041702. This maximum is a grid result, not a certified supremum over frequencies.

At times $2, 5, 10, 20, 30$, the coordinate standard errors are exactly $\sqrt{C_{ii}/8192}$. A Bonferroni simultaneous 95% bound for 30 scalar checks uses $z = 3.14398$ and does not require independence among the checks. All selected snapshot means were within this bound. The shaded envelope in the response plot is calibrated at these snapshots; it is not a simultaneous confidence band for the entire curve. The corresponding numerical diagnostic is shown in Figure 21.

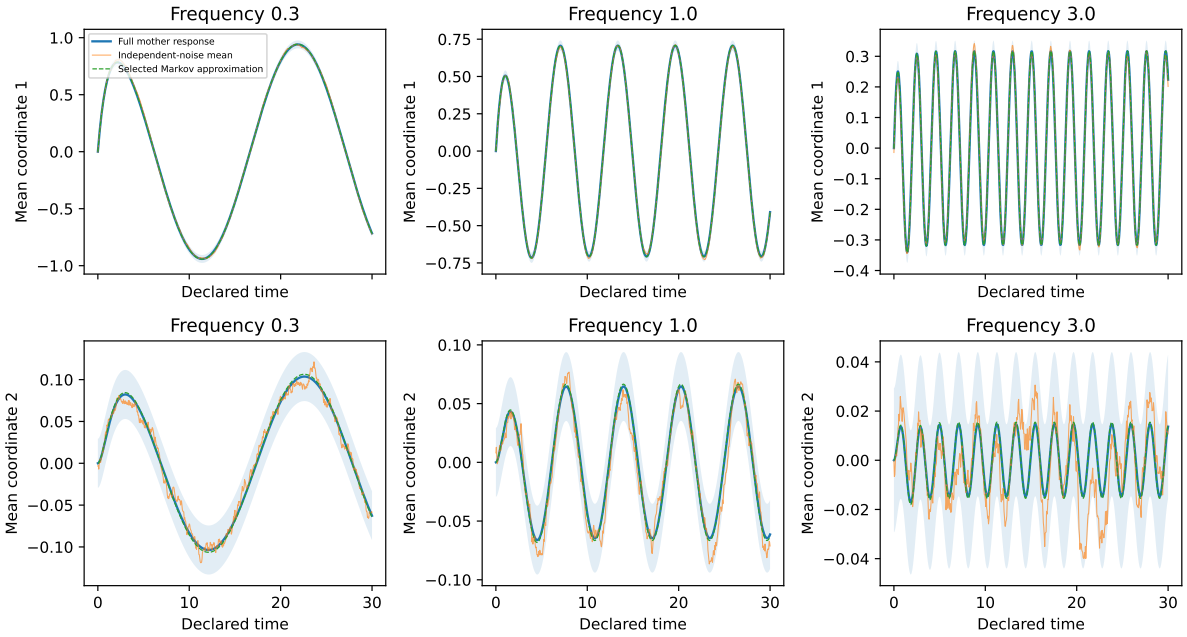


Figure 21. Synthetic mean response at three fixed frequencies. The independent-noise average is compared with the exact mother response and its stationary Markov approximation. The displayed uncertainty envelope is calibrated only for the declared snapshot checks.

The difference between the predicted models is smaller than the observed sampling error. Its detectability can be quantified without treating successive observations from one trajectory as independent. Stack both coordinates at the five snapshot times. The single-replica covariance is

the positive definite block matrix

$$K_{ij} = Pe^{-A(t_i - t_j)}CP^T \quad (t_i \geq t_j), \qquad K_{ji} = K_{ij}^T. \tag{15.46}$$

Let $\delta = m_1 - m_0$ be the stacked difference between two prescribed mean responses. In the mean-only comparison with common stipulated covariance K/R, the statistic

$$T = \frac{\delta^T K^{-1}(\bar{Y} - m_0)}{\sqrt{\delta^T K^{-1}\delta / R}}$$

has law $N(0,1)$ under the first mean and $N(\sqrt{Rq}, 1)$ under the second, where $q = \delta^T K^{-1}\delta$. Thus a one-sided test of size α has power $\Phi(\sqrt{Rq} - z_{1-\alpha})$, and power at least $1 - \beta$ requires

$$R \geq (z_{1-\alpha} + z_{1-\beta})^2 / q. \tag{15.47}$$

This result follows directly from the mean and variance of a linear Gaussian functional. It is not the likelihood-ratio test between the two full path laws, whose covariance matrices differ.

The computed q values at the three frequencies are $4.39940\,10^{-5}$, $2.72290\,10^{-5}$ and $5.35454\,10^{-6}$. Pooling the independent frequency experiments adds their q values. At 8192 replicas per frequency the resulting power is .19688. For $\alpha = \beta = .05$, the mean-only design requires 141324 replicas per frequency. This is a prospective calculation made after the first simulation, not a predeclared success criterion. It excludes measurement noise and calibration uncertainty, both of which can alter the required sample size. It explains why agreement of the initial synthetic curves cannot establish resolved memory effects.

The corresponding numerical diagnostic is shown in Figure 22.

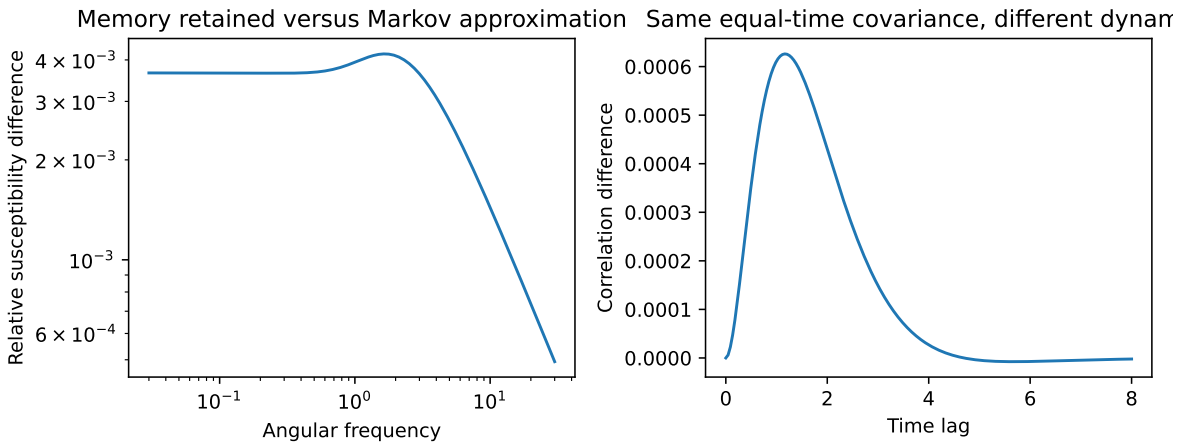


Figure 22. Dynamic differences despite equal stationary covariance. Left: relative susceptibility difference on the evaluated frequency grid. Right: difference in the first-coordinate lag covariance.

15.28. *An openly available experimental benchmark.* Liao, Ang, Lai and Jun studied a colloidal Brownian gyrator in a hybrid thermal and active bath [63]. Their model makes the active Ornstein–Uhlenbeck noise an explicit hidden variable. It is therefore directly relevant to the distinction between observed dynamics and complete energetic accounting. The physical mechanism and experimental discovery belong to that work. They are not new predictions of the present framework.

The public workbook [62] contains both theoretical curves and experimental summaries. Figure 9 of the source paper identifies the 10 ms persistence-time experiment and six measured quantities: total work rate, hot-bath heat rate, efficiency, entropy production rate, work diffusion and the thermodynamic uncertainty ratio. The reported uncertainties are bootstrap standard deviations from 17 experimental trajectories, with 10^4 bootstrap samples. The workbook has 12 control settings for each quantity. The summaries do not establish statistical independence across quantities or control settings, and 10^4 bootstrap samples are not independent experiments.

We compare the experimental means in columns A–C of the six corresponding sheets with the published 10 ms theoretical curve in columns D and F, without adjusting parameters. Linear interpolation is restricted to the tabulated control interval. At each experimental setting, define the descriptive residual $r_i = (y_i - y_i^{\mathrm{pub}})/s_i$, where s_i is the published bootstrap standard deviation. The first rows and column descriptions were examined before this comparison was chosen. It is a retrospective reanalysis, not a blind calibration–test split.

Observable	Points	RMS of r_i	$\lvert r_i\rvert \le 2$
Total work rate	12	1.338	11
Hot-bath heat rate	12	.707	12
Efficiency	12	1.065	11
Entropy production rate	12	2.351	8
Work diffusion	12	1.592	9
Uncertainty ratio	12	28.949	10

These summaries retain all six panels. The largest residual in the entropy-production panel is 4.940 reported standard deviations. The largest descriptive uncertainty-ratio residual is 100.222 at $\epsilon = 25$ pN/μm, where the published theoretical ratio is approximately 10498.22, while the experimental summary is 40.83 ± 104.34. This is a ratio containing the squared mean work in the denominator, which becomes small near stall. A Gaussian significance interpretation of this residual is unjustified. A different averaging order, finite observation time and uncertainty in the near-zero denominator can matter strongly. No point is removed to improve agreement.

In particular, no global chi-square probability is assigned: the six observables share trajectories and their joint covariance is not provided by these figure summaries. A more stable test near stall uses the primitive current, current variance and entropy-production estimates jointly, rather than assuming a normal distribution for their ratio. The workbook's reported entropy-production means are positive at all twelve settings. That observation is compatible with the source model's

thermodynamic accounting; it does not prove a universal entropy theorem from experiments. The corresponding numerical diagnostic is shown in Figure 23.

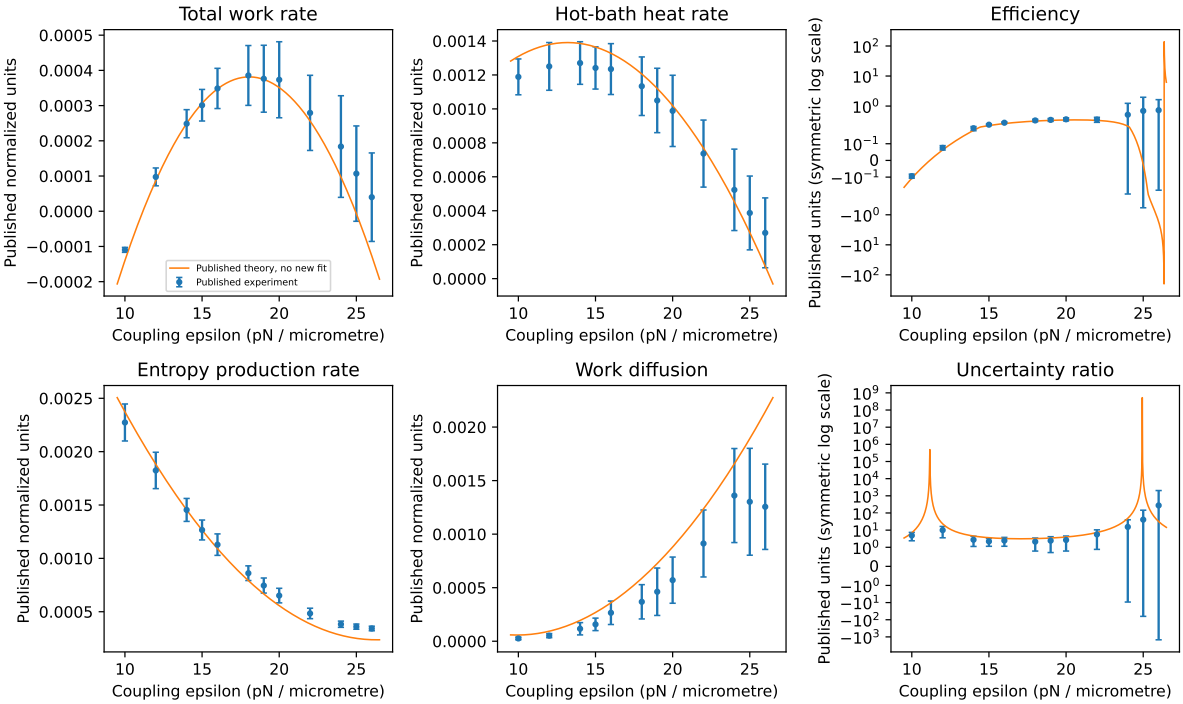


Figure 23. Retrospective reproduction of published experimental summaries and theoretical curves for the 10 ms active-bath experiment [63] and [62]. Error bars are the source's bootstrap standard deviations. The plotted curves are shown on symmetric logarithmic axes for efficiency and the uncertainty ratio to retain their near-pole behavior without hiding other points. The curves are the source's theory, with no new fit. They are not predictions from the three-coordinate example of (15.35).

15.29. *From a benchmark to a discriminating physical test.* The dimensionless matrix in (15.35) cannot be identified with a colloidal trap by relabelling its coordinates. A physical reduction must specify the force calibration, mobility, thermal reservoirs, active-noise correlation time and readout units. In particular, a generalized Langevin reduction must retain the same memory kernel in its response and the corresponding hidden noise in its fluctuation spectrum. These requirements produce testable compatibility conditions once the physical mapping is fixed.

For a linear readout with transfer matrix $H_{\mathrm{det}}(\omega)$ and independent stationary detector noise spectrum S_n, the continuous-time measured spectrum is

$$S_{\mathrm{meas}}(\omega) = H_{\mathrm{det}}(\omega) S_Y(\omega) H_{\mathrm{det}}(\omega)^\dagger + S_n(\omega). \tag{15.48}$$

The deterministic response uses $H_{\mathrm{det}}\chi$, not χ alone. If observations are sampled at interval h, their discrete spectrum, under the convention $\sum_k \Gamma_k e^{-ik\Omega}$, is

$$S_{\mathrm{sample}}(\Omega) = \frac{1}{h}\sum_{n\in\mathbb{Z}} S_{\mathrm{meas}}\left(\frac{\Omega+2\pi n}{h}\right), \quad -\pi \le \Omega \le \pi. \tag{15.49}$$

This identity follows by substituting the inverse Fourier integral for the covariance at lag kh and applying the Fourier comb identity. It requires an integrable effective continuous spectrum; finite exposure or filtering must precede sampling of ideal white detector noise. Independent discrete readout noise instead contributes its constant discrete spectrum directly.

For a physical test, fit a designated calibration block using this observation model, and preserve its parameter uncertainty. Then freeze the physical parameters, preprocessing and discrepancy statistic before evaluating an independent forcing frequency, bath condition or experiment. Compare a memory-retaining reduction with a specified alternative under the same instrument model. If both descriptions reduce to the same ordinary stochastic thermodynamics in that experiment, agreement supports their shared branch and cannot identify the proposed unification uniquely. An independent cross-sector test needs an additional derived relation between the physical parameters of different sectors; no such relation follows from the numerical entries of A alone.

15.30. *Exact physical projection and the scope of entropy recovery.* To recover a branch from a mother process, specifying its variables is not sufficient. Their future law must also close. This subsection makes that requirement explicit and derives the entropy statement that follows from it. The result applies to a finite regulator; a regulator limit requires its own uniform estimates and identification argument.

Let E, F be standard Borel state spaces, $R : E \to F$ a measurable physical projection, and P_t, Q_t Markov semigroups on bounded measurable functions. Assume the exact intertwining identity

$$P_t(f \circ R) = (Q_t f) \circ R \quad (t \ge 0) \tag{15.50}$$

for every bounded measurable f. This is an assumption on the physical projection and the dynamics, not a consequence of writing variables in one vector. It can be established from generator matching on a suitable determining domain, provided the associated martingale problem is well posed and the domain and integrability conditions permit passage from generators to transition laws.

Proposition 15.13 (Invariant laws and entropy under an exact projection). *Suppose π is an invariant probability for P_t and (15.50) holds. Then $\nu = R_{\#}\pi$ is invariant for Q_t, and for any initial law ρ_0, $R_{\#}(P_t^*\rho_0) = Q_t^*(R_{\#}\rho_0)$. For $\rho \ll \pi$,*

$$D(R_{\#}\rho\|\nu) \le D(\rho\|\pi).$$

If the mother entropy satisfies $D(P_t^*\rho\|\pi) \le e^{-\lambda t}D(\rho\|\pi)$ for all finite-entropy initial laws, then

$$D(Q_t^*\sigma\|\nu) \le e^{-\lambda t}D(\sigma\|\nu) \tag{15.51}$$

for every $\sigma \ll \nu$ of finite entropy.

Proof. Integrate (15.50) against ρ_0; equality against every bounded measurable f proves the equality of projected laws. Setting $\rho_0 = \pi$ proves invariance of ν. If $h = d\rho/d\pi$, disintegration gives the projected density $\bar{h}(Rx) = \mathbb{E}_\pi[h \mid R](x)$. Convexity of $z \log z$ and conditional Jensen give

$$\int_F \bar{h} \log \bar{h} \, d\nu \le \int_E h \log h \, d\pi.$$

The inequality extends to infinite entropy by standard nonnegative relative-entropy approximations. To prove the final assertion, let $g = d\sigma/d\nu$ and choose the particular lift $d\rho_0 = (g \circ R)d\pi$. Then $R_\# \rho_0 = \sigma$ and $D(\rho_0 \| \pi) = D(\sigma \| \nu)$. Apply projected-law equality, conditional Jensen and mother entropy decay successively. This yields (15.51) with no unobserved initial entropy term. □

For a general lift of σ, the microscopic initial entropy can be larger. Substituting the macro initial entropy into that particular trajectory's microscopic bound would therefore require the preceding choice of lift or a separate argument. Exact intertwining makes this choice harmless for the macro law. Without it, different hidden-state preparations can give different macro dynamics and memory cannot be discarded.

For example, in an isothermal finite-dimensional realization with symmetric positive mobility M and invariant density π, let

$$Lf = \frac{\theta}{\pi} \nabla \cdot (\pi \mathsf{M} \nabla f) + c \cdot \nabla f, \qquad \nabla \cdot (\pi c) = 0.$$

Assume sufficient smoothness, finite entropy and the integrability needed below. On a bounded domain impose $\pi \mathsf{M} \nabla h \cdot n = 0$ and $c \cdot n = 0$ for $h = \rho/\pi$; on an unbounded domain require the corresponding boundary terms to vanish in an exhaustion. Then

$$\partial_t h = \frac{\theta}{\pi} \nabla \cdot (\pi \mathsf{M} \nabla h) - c \cdot \nabla h.$$

Multiplication by $(1 + \log h)\pi$ and integration by parts give

$$\frac{d}{dt} D(\rho_t \| \pi) = -\theta \int \rho_t \, \nabla \log h_t^T \mathsf{M} \nabla \log h_t \, dx \le 0. \tag{15.52}$$

The current term vanishes because it is the integral of $-\pi c \cdot \nabla(h \log h)$. An entropy–dissipation inequality bounding the last integral below by $\lambda D/\theta$ supplies exponential decay. Invariance and this calculation alone do not supply existence of a conservative process, normalizability, or uniqueness among every invariant law. Those hypotheses must be established in the chosen state space. If a finite Galerkin branch satisfies the exact projection identity with matched covariance, the proposition transfers the proved entropy statement to that branch.

15.30.1. *Path reversal is a separate comparison.* Let $\mathbb{P}_T$ be a stationary path law over $[0, T]$, and let $\mathcal{R}_E$ reverse time and apply the prescribed parity to odd variables. Let $\widehat{R}$ act pointwise on paths, and require $\widehat{R}\mathcal{R}_E = \mathcal{R}_F \widehat{R}$. The data-processing inequality, proved by the same conditional

Jensen argument on path space, gives

$$D(\widehat{R}_{\#}\mathbb{P}_T\|\mathcal{R}_{F\#}\widehat{R}_{\#}\mathbb{P}_T) \le D(\mathbb{P}_T\|\mathcal{R}_{E\#}\mathbb{P}_T).$$

This includes infinite relative entropies in the extended sense. If the mother stationary law is reversible, the right-hand side is zero, so its exact observed stationary path law is reversible as well. This conclusion does not require Markov closure of the observed process. Thus exact observation of a reversible stationary process cannot, by itself, create positive stationary path-reversal entropy. Relaxation from a nonequilibrium preparation, maintained irreversible currents, discarded memory, and an incorrectly specified reversal operation are different mechanisms and must not be conflated. Relative-entropy decay and a physical stationary time arrow remain distinct statements.

For an isothermal experiment, the physical clock, temperature, mobility and reversal parities are fixed before response data are compared. Relative-entropy contraction alone cannot identify those parameters: many distinct generators share the same invariant density. Relaxation rates and path asymmetry therefore enter the observation map separately.

15.31. *A coupled positive-coordinate realization with proved convergence.* The coordinates in this example represent nonnegative block energies. A physically admissible diffusion must remain in the positive region, not merely have a formally normalizable density there. We therefore establish boundary behavior before using the invariant law. A square-root coordinate change then makes the noise constant and exposes the curvature responsible for entropy convergence; its Jacobian must be retained when the density is transformed.

A logarithmic state penalty and an invariant density answer different questions. The penalty may be integrable along trajectories that reach a boundary. Likewise, an invariant density does not by itself prove attraction. The following finite realization makes the boundary mechanism, invariant law and convergence estimate consequences of one specified generator. Its coordinates are declared positive variables. Their identification with fluid density or internal energy would additionally require the physical projection and covariance matching established elsewhere in this programme.

Let $y \in (0,\infty)^n$, $s_y = \sum_i y_i$, and fix

$$d > 0, \qquad b > 0, \qquad g \ge 0, \qquad k_i \ge 1.$$

The letter b here is a scalar confinement coefficient, not a drift vector. Define the dimensionless potential and density

$$V_+(y) = bs_y + \tfrac{1}{2}gs_y^2, \tag{15.53}$$

$$\pi_+(y) = Z_+^{-1}\exp[-V_+(y)]\prod_i y_i^{k_i-1}, \tag{15.54}$$

$$L_+f = d\sum_i \{y_i\partial_{ii}f + [k_i - y_i(b+gs_y)]\partial_i f\}. \tag{15.55}$$

Thus the mobility is $d\,\mathrm{diag}(y_i)$ and the covariance is twice that matrix. The equation is

$$dY_i = d[k_i - Y_i(b + gs_Y)]\,dt + \sqrt{2dY_i}\,dW_i.$$

All coefficients are model inputs; they are not selected constants of the full field theory. The off-diagonal coupling comes from the common potential through gs_y, rather than from a separately appended dissipation term.

PROPOSITION 15.14 (Positive paths, invariant law and entropy contraction). *For every strictly positive initial point the displayed stochastic equation has a pathwise unique, nonexplosive solution that stays in $(0,\infty)^n$. Its unique invariant probability is (15.54). For initial densities with finite relative entropy, its semigroup satisfies*

$$D(\rho_t\|\pi_+) \le e^{-dbt} D(\rho_0\|\pi_+). \tag{15.56}$$

The entropy identity and its bound first hold on the regular form domain and extend by approximation. Point-mass initial conditions are allowed in the path statement but are not assigned finite initial relative entropy.

Proof. On any compact subset of the open orthant the coefficients are locally Lipschitz and the covariance is positive definite. Local strong existence and uniqueness therefore hold up to exit. Consider the sum s_Y:

$$L_+ s_y = d\sum_i k_i - dbs_y - dgs_y^2 \le d\sum_i k_i - dbs_y.$$

The stopped first-moment estimate bounds the probability of an upper exit before any fixed time by a constant divided by the exit level. Hence there is no finite-time explosion once lower boundary exits are excluded.

Stop when s_Y reaches a fixed upper level R. Before that stopping time, the ith drift is bounded below by $d[k_i - (b+gR)Y_i]$. Compare Y_i, with the same Brownian motion, to the one-dimensional square-root diffusion

$$dZ_i = d[k_i - (b+gR)Z_i]dt + \sqrt{2dZ_i}\,dW_i.$$

For this diffusion the scale derivative is, up to a positive constant, $z^{-k_i}e^{(b+gR)z}$. Its integral diverges at zero when $k_i \ge 1$; the lower endpoint is inaccessible from a positive starting point. The one-dimensional comparison theorem for the common square-root coefficient gives $Y_i \ge Z_i$ before the upper stop. Exhausting the upper levels proves absence of lower exits. Local uniqueness then gives global pathwise uniqueness. No discrete projection or cutoff appears in this argument.

Normalizability follows from $b > 0$, $g \ge 0$ and $k_i > 0$. In divergence form,

$$L_+ f = \pi_+^{-1}\sum_i \partial_i(dy_i\pi_+\partial_i f), \qquad \int f L_+ h\,\pi_+ dy = -d\sum_i \int y_i f_i h_i\,\pi_+ dy.$$

The conservative natural-boundary realization of this form agrees with the unique stochastic equation. It follows that π_+ is invariant and reversible. Interior ellipticity and the localized transition kernel give strong Feller regularity and irreducibility on the connected open orthant. Nonexplosion and lower-boundary inaccessibility permit exhaustion by compact interior domains. Consequently there cannot be two invariant probabilities. This uniqueness argument concerns a fixed generator, not a choice of its physical parameters.

To obtain a quantitative bound, put $z_i = 2\sqrt{y_i}$. Itô's formula gives constant covariance $2dI$ and the gradient generator

$$\widetilde{L}_+ = d(\Delta_z - \nabla W_+ \cdot \nabla), \qquad W_+(z) = b\frac{|z|^2}{4} + \frac{g}{2}\left(\frac{|z|^2}{4}\right)^2 - \sum_i (2k_i - 1)\log z_i.$$

The Jacobian $dy = \prod_i (z_i/2)dz$ is included in this transformed density; omitting it would give the wrong logarithmic coefficient. More precisely, write $\pi_z(z) = \pi_+(z_1^2/4, \dots, z_n^2/4)\prod_i (z_i/2) = Z_z^{-1} e^{-W_+(z)}$, and let ρ^z be the corresponding pushforward density of ρ. Thus $D(\rho^z \| \pi_z) = D(\rho \| \pi_+)$; densities in the two coordinate systems are different even though relative entropy is invariant. Writing $s_z = |z|^2/4$ gives the explicit Hessian

$$\nabla^2 W_+ = \frac{b}{2} I + g\left(\frac{s_z}{2} I + \frac{zz^\top}{4}\right) + \operatorname{diag}\left(\frac{2k_i - 1}{z_i^2}\right) \succeq \frac{b}{2} I. \tag{15.57}$$

The Bakry–Emery logarithmic Sobolev estimate on this convex domain [7] gives

$$D(\rho^z \| \pi_z) \le \frac{1}{b} \int |\nabla_z \log(\rho^z/\pi_z)|^2 \, \rho^z \, dz.$$

It can be obtained on convex truncated orthants with reflecting boundaries; their curvature lower bound is independent of the truncation. Passing to the natural form realization gives the displayed estimate. Entropy differentiation in the same coordinates yields

$$\frac{d}{dt} D(\rho_t^z \| \pi_z) = -d \int |\nabla_z \log(\rho_t^z/\pi_z)|^2 \rho_t^z \, dz \le -dbD(\rho_t^z \| \pi_z).$$

Gronwall's inequality proves (15.56). □

For a smooth initial law with finite entropy, Pinsker's inequality also gives convergence in total variation with the explicit bound

$$\|\rho_t - \pi_+\|_{\mathrm{TV}} \le \sqrt{D(\rho_0 \| \pi_+)/2}\, e^{-dbt/2}.$$

Strict state admissibility, uniqueness of a probability law and convergence have thus been proved separately. The stationary process is reversible: free-energy relaxation of a displaced law does not imply persistent stationary entropy production. A nonreversible extension must specify its additional current, parity and reservoir interpretation.

15.31.1. *An exact microscopic ancestor for half-integer shapes.* For $k_i = n_i/2$ with integers $n_i \ge 2$, the generator above follows from an explicit smooth Euclidean microscopic model. Let

$x_i \in \mathbb{R}^{n_i}$, set $y_i = |x_i|^2/4$, and use

$$U(x) = \frac{b}{4}|x|^2 + \frac{g}{32}|x|^4, \qquad dX = -d\nabla U(X)dt + \sqrt{2d}\, dW.$$

The microscopic generator is $d(\Delta_x - \nabla U \cdot \nabla_x)$. For $f(y(x))$, the exact chain rule gives

$$\Delta_{x_i} f = y_i f_{ii} + \frac{n_i}{2} f_i, \qquad \nabla_{x_i} U \cdot \nabla_{x_i} f = y_i(b + g s_y) f_i.$$

It therefore projects exactly to (15.55) with $k_i = n_i/2$. The radial Jacobian of Euclidean volume is proportional to $\prod_i y_i^{n_i/2-1} dy$, which gives the same invariant law. Both the normal diffusion and inward drift are thus derived together. In this subclass the threshold $k_i \geq 1$ is the microscopic dimension condition $n_i \geq 2$, not a logarithmic penalty added after projection.

The ancestor also has $\nabla^2 U = (b/2 + g|x|^2/8)I + gxx^\top/4 \succeq bI/2$. Its entropy contraction passes to the radial branch by taking initial densities whose ratio to the microscopic invariant density depends only on the radii. The chain rule above applies to every smooth radial test function, including functions that couple the two blocks. The numerical shapes $(1.2, 1.8)$ used below are not half-integers and are not assigned this particular Euclidean ancestor. This exact finite microscopic projection is a separate constructive witness; it does not identify these blocks with the unconstructed compressible fluid or Cartan-field continuum.

15.31.2. *Why finite logarithmic costs do not protect a boundary.* Set $g = 0$ and $n = 1$. The stationary distribution is gamma with shape k and rate b. For every $k > 0$,

$$\int |\log y| \pi_+(dy) < \infty, \qquad \mathbb{E}_{\pi_+}[-\log Y] = \log b - \psi_{\mathrm{dg}}(k),$$

where ψ_{dg} is the digamma function. Nevertheless zero is attainable for $0 < k < 1$ in the conservative square-root realization. For a stationary path, Tonelli's theorem gives finite expected integrated absolute logarithmic cost on each finite interval. The same path law can therefore hit the boundary even though this cost is finite. Inaccessibility comes from the drift–normal-covariance threshold $k \geq 1$, not from the integrability of $-\log y$ or from an interior ellipticity statement. This counterexample is also why positivity at discrete sampling times cannot prove that a continuous path has avoided zero between them.

15.31.3. *A compatible stationary arrow with the same invariant law.* Attraction and stationary irreversibility can coexist. In the transformed two-coordinate model let η be a nonconstant smooth compactly supported function inside the positive orthant, and let

$$J = \begin{pmatrix} 0 & 1 \\ -1 & 0 \end{pmatrix}, \qquad Q = e^{W_+} J \nabla \eta.$$

Replace the transformed drift by $-d\nabla W_+ + Q$. Since $\mathrm{div}(e^{-W_+}Q) = \mathrm{div}(J\nabla\eta) = 0$, the same π_z remains invariant in the z coordinates. The current is bounded, supported away from every boundary, and therefore leaves the nonexplosion and boundary arguments intact. Its contribution

to relative-entropy differentiation is

$$\int \pi_z Q \cdot \nabla(\rho^z/\pi_z)\, dz = 0.$$

Consequently the same contraction estimate holds. On the other hand, with both coordinates declared even under reversal, the reversed stationary drift is $-d\nabla W_+ - Q$. Girsanov's formula with covariance $2dI$ gives

$$\frac{1}{T} D(\mathbb{P}_{[0,T]} \| \mathbb{P}^{\mathrm{rev}}_{[0,T]}) = \frac{1}{d} \int |Q|^2 \pi_z \, dz > 0. \tag{15.58}$$

The initial law is stationary and common to both experiments; bounded Q supplies the finite-time change-of-measure condition. The result proves a stationary statistical arrow for this declared extension. Identification with heat and thermodynamic reservoir entropy needs local detailed balance and work bookkeeping; it is not implied by the path likelihood alone.

This stationary current also has an exact microscopic realization in the two-block subclass $k_i = n_i/2$, $n_i \geq 2$. Write $z_i = |x_i|$ and set

$$v_i(x) = \frac{x_i}{z_i} Q_i(z), \qquad dX = (-d\nabla U + v)dt + \sqrt{2d}\, dW.$$

Extend v by zero wherever a block radius vanishes. The support of Q is a compact subset of the positive radial quadrant, so this extension is smooth and bounded on the Euclidean state space. Let $w(z) = \prod_i z_i^{n_i - 1}$. The radial divergence identity gives

$$\begin{aligned} \mathrm{div}_x(e^{-U} v) &= \frac{1}{w(z)} \sum_i \partial_{z_i} [w(z) e^{-U(z)} Q_i(z)] \\ &= \frac{1}{w(z)} \mathrm{div}_z(e^{-W_+} Q) = 0. \end{aligned}$$

Thus the microscopic invariant law remains proportional to $e^{-U} dx$. For a radial test function $f(z)$, $v \cdot \nabla_x f = Q \cdot \nabla_z f$; the radial projection has precisely the current used above. Since $|v(x)|^2 = \sum_i |Q_i(z)|^2$, the two stationary reversal rates agree:

$$\frac{1}{d} \int |v|^2 \pi_x \, dx = \frac{1}{d} \int |Q|^2 \pi_z \, dz > 0.$$

Here all microscopic coordinates and radial coordinates are declared even, and π_z is the pushforward of π_x. In this constructed branch the radial observation therefore retains the entire stationary reversal cost. With Q replaced by ξQ, the invariant law is unchanged and this rate is multiplied by ξ^2; $\xi \to 0$ recovers the reversible law. This supplies a finite microscopic example of compatible relaxation and a stationary arrow. The current and its amplitude remain specified model data, and their physical origin is not selected by the construction.

For the synthetic parameters $k = (1.2, 1.8)$, $b = 1$, $g = 0.2$, $d = 0.7$, take

$$\eta(z) = 0.05\, h((z_1 - 1.5)/0.6)\, h((z_2 - 2)/0.6), \qquad h(u) = \begin{cases} e^{-1/(1-u^2)}, & |u| < 1, \\ 0, & |u| \geq 1. \end{cases}$$

This specifies the extra current independently of the reversible simulation below. Its entropy-rate integral is evaluated with 96 and 144 Gauss nodes per coordinate. The computed rate is 3.9304128×10^{-5}; refining the quadrature changes it by less than 7.5×10^{-19}. This comparison is a floating-point quadrature check, not an interval-certified error bound. It is not a fitted physical time-arrow parameter, and the synthetic trajectories below retain $Q = 0$.

15.31.4. *A positive splitting calculation.* The generator splits into independent square-root components and the deterministic coupled flow. Both subflows preserve positive coordinates. For a step h, the independent component has the exact transition

$$Y_i' = c_h \, \chi'^2_{2k_i}(\lambda_i), \quad c_h = \frac{1 - e^{-dbh}}{2b}, \quad \lambda_i = \frac{Y_i e^{-dbh}}{c_h}.$$

The coupled subflow is exactly $Y_i' = Y_i/(1+dgs_Y h)$. Half a coupled step, a full independent step and half a coupled step define a symmetric splitting without clipping. Exact positivity of the subflows does not establish exact invariance of their composed discrete chain. No uniform weak-order or numerical entropy theorem is inferred from this finite experiment.

For $k = (1.2, 1.8)$, $b = 1$, $g = 0.2$, $d = 0.7$, the invariant density is integrated by separating s_Y and the Dirichlet proportions. Its means are $(0.79913806, 1.19870709)$, and its covariance is

$$\begin{pmatrix} 0.46374871 & -0.05599308 \\ -0.05599308 & 0.66762652 \end{pmatrix}.$$

The exact one-dimensional integral gives $\int L_+ s_Y \, d\pi_+$ and $\int L_+ s_Y^2 \, d\pi_+$ with numerical residuals below 3.2×10^{-15}. Starting at $(0.05, 0.10)$, three independently seeded sets of 12,000 synthetic paths are advanced to time 12:

h	mean Y_1	standard error	mean Y_2	standard error
0.100	0.799610	0.006222	1.193806	0.007390
0.050	0.795789	0.006272	1.203903	0.007460
0.025	0.784132	0.006000	1.183319	0.007472

The last realization differs from the invariant means by about 2.50 and 2.06 Monte Carlo standard errors. All runs are reported. The error bars describe sampling uncertainty only; they do not include finite-time bias or splitting error. These samples are not a convergence-order certificate. The corresponding numerical diagnostic is shown in Figure 24.

The construction provides verifiable sufficient conditions for a finite positive-state branch. Applying it to compressible turbulence would require deriving the distance variables, their Itô drift and their normal covariance from the actual mother projection, while preserving mass and energy exchange. It is not a proof of that presently unspecified fluid identification.

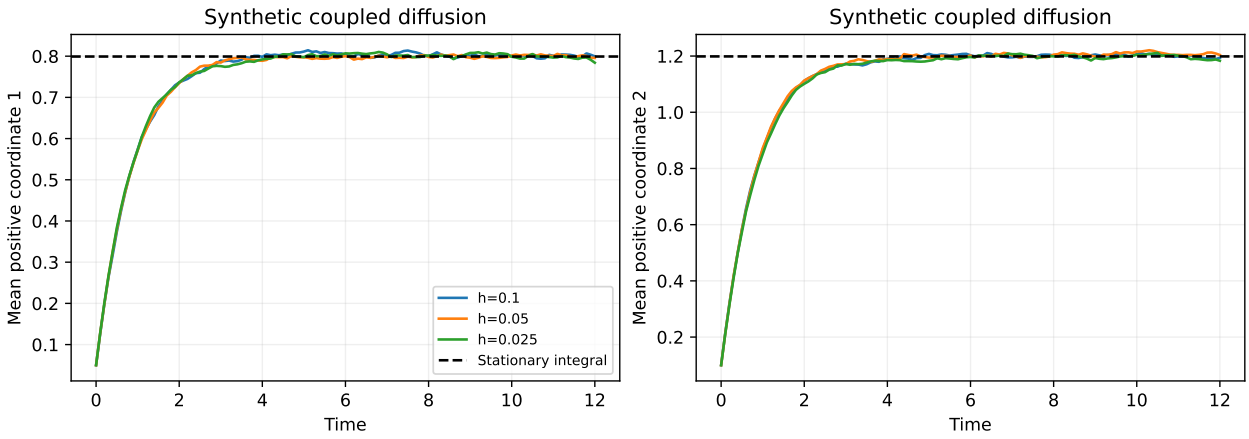


Figure 24. Synthetic moment evolution under positive subflow splitting. The dashed levels are stationary integrals of the continuous generator. The analytic state-boundary and entropy results concern the continuous model, whereas the plotted trajectories use a discrete split law.

16. **Three-layer invariant-measure and regulator-limit theorem**

An invariant law describes an ensemble that does not change in time. Uniqueness asks whether the fixed dynamics admit another such ensemble; convergence asks what happens to a specified initial preparation. These properties require different estimates. A further question arises when the number of retained degrees of freedom increases: can probability or energy escape into unresolved scales? We state the finite-level existence, uniqueness, and convergence results first, then identify the compactness and generator conditions needed to pass to a continuum law.

16.1. *Existence by Feller–Lyapunov compactness.* Let E be a Polish state space, $(P_t)_{t\ge 0}$ a Markov semigroup, and X_t its Markov realization. Let $V : E \to [0,\infty]$ be lower semicontinuous with compact sublevel sets.

Assumption 16.1 (Existence hypotheses). The semigroup is Feller, the stopped Dynkin formula is valid for V, and there are $c > 0$ and $C < \infty$ such that

$$LV \le -cV + C$$

in the extended-generator sense. The initial law has finite V-moment.

Proposition 16.2 (Invariant-measure existence). *Under Assumption 16.1, there exists at least one invariant probability measure π satisfying*

$$P_t^*\pi = \pi \qquad (t \ge 0).$$

Proof. The stopped Dynkin formula and the Lyapunov inequality give

$$\sup_{T\ge 1} \frac{1}{T} \int_0^T \mathbb{E}V(X_s)\, \mathrm{d}s < \infty.$$

For the occupation measures

$$\bar{\nu}_T = \frac{1}{T}\int_0^T \mathrm{Law}(X_s)\ \mathrm{d}s,$$

compact sublevels of V imply tightness. Let $\bar{\nu}_{T_k} \Rightarrow \pi$. For bounded continuous f and $r > 0$,

$$|\bar{\nu}_T(P_r f) - \bar{\nu}_T(f)| \le \frac{2r\|f\|_\infty}{T}.$$

The Feller property permits passage to the weak limit, giving $\pi(P_r f) = \pi(f)$. Since r is arbitrary, $P_r^*\pi = \pi$ for every $r \ge 0$. □

16.2. *Uniqueness by smoothing and accessibility.*

Assumption 16.3 (Uniqueness hypotheses). The invariant-measure candidate from Proposition 16.2 exists, and either:

(U1) P_t is strong Feller and topologically irreducible; or

(U2) for a skeleton $P := P_\tau$, there are a measurable finite $W : E \to [1, \infty)$, $0 < a < 1$, $b \ge 0$, and $R > 2b/(1-a)$ such that

$$PW \le aW + b, \qquad P(x, \cdot) \ge \varepsilon\nu(\cdot) \quad \text{whenever } W(x) \le R,$$

where $\varepsilon > 0$ and ν is one probability measure. The drift bound holds on the whole state space and the same minorising measure is used throughout the indicated sublevel set.

THEOREM 16.4 (Uniqueness of the invariant probability). *Under Assumption 16.3, the invariant probability measure is unique.*

Proof. In case (U1), strong Feller regularisation and irreducibility imply that two invariant probabilities cannot be mutually singular; the standard invariant measure separation argument then forces equality: distinct ergodic invariant probabilities would be mutually singular, whereas strong Feller smoothing and irreducibility preclude that separation. In case (U2), the displayed global drift and common sublevel minorisation are a geometric Harris criterion, with the quantitative sublevel threshold included [43] and [71]. They give uniqueness of the invariant probability for the skeleton chain. A minorisation on an unreachable set alone would not suffice. Any full-semigroup invariant probability is invariant for that skeleton and must therefore equal the unique skeleton invariant probability. No invariance of the full semigroup is inferred from skeleton invariance alone. □

16.3. *Convergence by Harris, spectral, or hypocoercive estimates.*

Assumption 16.5 (Convergence hypotheses). In addition to uniqueness, assume one of the following quantitative mechanisms:

(C1) a geometric Harris estimate for a skeleton chain, in a specified finite weight $W \ge 1$, together with $\sup_{0 \le s \le \tau} P_s W \le C_W W$ to pass to physical time;

(C2) a Poincaré or logarithmic Sobolev inequality for a reversible generator; or

(C3) a hypocoercive modified entropy or L^2 estimate for the kinetic generator.

Initial laws must belong to the class controlled by the chosen estimate: finite W-moment in (C1), an $L^2(\pi)$ density for an L^2 spectral estimate, finite relative entropy for an entropy estimate, or finite specified modified entropy in (C3). These are distinct classes. A point mass is not generally an $L^2(\pi)$ density; convergence from that point requires an additional entrance or smoothing estimate.

THEOREM 16.6 (Quantitative convergence). *Under Assumption 16.5, the unique invariant measure is the limit of the evolved initial laws in the class and topology supplied by the chosen estimate. For example, a geometric Harris condition with the interpolation bound in* (C1) *gives*

$$\|P_t(x,\cdot)-\pi\|_W \le C\,W(x)e^{-\gamma t}.$$

Here $\|\zeta\|_W = \sup_{|f|\le W} |\int f \,\mathrm{d}\zeta|$. *Writing* $t = n\tau + s$, *the skeleton bound is applied to* $P_s f$, *whose absolute value is at most* $C_W W$; *invariance then gives the displayed continuous-time estimate. A reversible Poincaré estimate instead yields, for an initial density* $h_0 \in L^2(\pi)$,

$$\|h_t - 1\|_{L^2(\pi)} \le e^{-\lambda t}\|h_0 - 1\|_{L^2(\pi)}.$$

Logarithmic Sobolev and hypocoercive estimates give their corresponding entropy or modified-entropy bounds on their stated initial classes. These conclusions do not extend a density estimate to every deterministic initial state without the additional regularisation just specified.

Remark 16.7. The positive relaxation statement is made only on a fixed-mean sector when a zero Fourier mode is conserved. On the full state space, a nonconstant function of the conserved mode has positive variance and zero Dirichlet energy, which rules out a positive global Poincaré constant.

16.4. *Regulator-uniform limit.* Let E_N be finite or regularised state spaces embedded in a common Polish space E, let P_t^N be their embedded semigroups, and let π_N satisfy

$$(P_t^N)^*\pi_N = \pi_N.$$

Assumption 16.8 (Uniform regulator hypotheses). There is a coercive lower-semicontinuous $V : E \to [0,\infty]$ with compact sublevels such that

$$\sup_N \int_E V \,\mathrm{d}\pi_N < \infty.$$

Choose a complete metric d generating the topology of E. The embedded processes have continuous paths. For the stationary initial laws π_N, require on every finite interval $[0,T]$:

(R1) for every $\epsilon > 0$ there is a compact $K \subset E$ with

$$\sup_N \mathbb{P}(X_s^N \notin K \text{ for some } s \le T) < \epsilon;$$

(R2) for every $\epsilon > 0$,

$$\lim_{\delta \downarrow 0} \sup_N \mathbb{P}\left(\sup_{\substack{s,t \le T \\ |t-s| \le \delta}} d(X_t^N, X_s^N) > \epsilon \right) = 0;$$

(R3) for every f in a probability-determining core $\mathcal{C}_{\mathrm{core}} \subset C_b(E)$, the function Lf is continuous. There are bounded generator-domain lifts $f_N : E_N \to \mathbb{R}$, with $\sup_N \|f_N\|_\infty < \infty$, such that on every compact K,

$$\sup_{x \in K \cap E_N} |f_N(x) - f(x)| \to 0, \qquad \sup_{x \in K \cap E_N} |L_N f_N(x) - Lf(x)| \to 0.$$

The corresponding Dynkin martingales are valid. For some $r_f > 1$,

$$\sup_N \mathbb{E} \int_0^T \left(|L_N f_N(X_s^N)|^{r_f} + |Lf(X_s^N)|^{r_f} \right) \, \mathrm{d}s < \infty.$$

The limiting martingale problem on this core is well posed for the initial laws under consideration and defines a conservative Markov semigroup. For convergence from other initial laws $\nu_N \Rightarrow \nu$, require the same three conditions for those laws as well. Stationary estimates alone are not assumptions about a process started from a prescribed point. A negative-space estimate can be used to prove these conditions only after its topology and compact embedding into E have been specified.

THEOREM 16.9 (Regulator-limit theorem). *Under Assumption 16.8, the family $\{\pi_N\}$ is tight. Every weakly convergent subsequence $\pi_{N_k} \Rightarrow \pi$ is invariant for the limiting semigroup:*

$$\pi_{N_k} \Rightarrow \pi, \qquad P_t^* \pi = \pi.$$

For any additional initial laws $\nu_N \Rightarrow \nu$ satisfying (R1)–(R3)*, the path laws converge in $C([0,T]; E)$ for every finite T. In particular, for $x_N \in E_N$ with $x_N \to x$,* provided these conditions hold for initial laws δ_{x_N},

$$P_t^N(x_N, \cdot) \Rightarrow P_t(x, \cdot).$$

If the limiting semigroup has a unique invariant probability, then the whole sequence converges:

$$\pi_N \Rightarrow \pi.$$

Proof. The uniform V-moment and compact sublevels give tightness of $\{\pi_N\}$ by Markov's inequality and Prokhorov's theorem. Conditions (R1)–(R2) give path-space tightness by the metric-space Arzela–Ascoli criterion. Consider a weakly convergent path subsequence. For $s < t$, multiply the increment of

$$f_N(X_t^N) - f_N(X_0^N) - \int_0^t L_N f_N(X_r^N) \, \mathrm{d}r$$

by a bounded continuous cylinder function of the path at times at most s. Its expectation is zero. On compact path ranges the two local uniform convergence statements in (R3) pass the endpoint and generator terms to the limit. The uniform bound on f_N controls the endpoint tails.

Holder's inequality, the r_f-moment bound, and (R1) make the integrated generator tails tend to zero uniformly as the compact-containment error tends to zero. The continuous Lf then identifies the limiting integral, with the same moment bound passed by truncation. A monotone-class argument extends the cylinder identity to the past sigma-field. Thus every limit solves the stated martingale problem with its limiting initial law.

For stationary starts, evaluation at any fixed time is continuous on $C([0,T];E)$; every limiting marginal equals the same weak limit π. Well-posedness identifies this stationary process with the semigroup of L, hence $P_t^*\pi = \pi$. For another specified sequence of initial laws, the additional (R1)–(R3) give the same argument and well-posedness makes all subsequential path limits identical. Evaluation at time t proves the asserted transition convergence for $x_N \to x$. Finally, uniqueness of the limiting invariant probability makes every stationary subsequential limit equal to π, proving $\pi_N \Rightarrow \pi$ for the full sequence. □

Both lift consistency and the initial-law qualification are substantive. For example, on $E = \{0,1\}$, take every regulated generator to be $L_N = \left(\begin{smallmatrix} -1 & 1 \\ 1 & -1 \end{smallmatrix}\right)$. Choosing the inconsistent "lifts" $f_N \equiv 0$ would make $L_N f_N = Lf = 0$ for the proposed limiting generator $L = 0$, for every test f. Nevertheless, from 0 the actual transition probability of state 1 is $(1 - e^{-2t})/2$, whereas the $L = 0$ process stays at 0. Generator expressions alone therefore cannot replace $f_N \to f$. Likewise, tightness of stationary paths does not, by itself, supply tightness for every deterministic initial state.

Remark 16.10. Finite Galerkin entropy contraction, finite-state stationarity, or a finite-dimensional spectral gap does not establish $\pi_N \Rightarrow \pi$ without the uniform hypotheses above. In particular, the regulator limit must include the energy estimate, path-space tightness, generator identification, and zero-mode restriction in the same theorem.

17. **Spatial correlation, inverse geometry, and an interacting mode limit**

A field describes values at neighboring points, not merely a list of one-point distributions. This distinction matters for fluctuating geometry. A positive determinant at each point does not by itself control an inverse metric uniformly over space. Nor do finite inverse moments at individual lattice sites establish such control as the lattice grows. We therefore construct a spatially correlated example in which these questions can be answered directly. The construction isolates a useful geometric mechanism: summable fluctuations of the logarithm of a coframe give a common bound on its size, its inverse, and their truncation errors.

The reference covariance is specified as part of this model. Its smooth mode tail is retained in the limit; it is not derived from the full gravitational action. Thus the limit below removes a mode truncation of a chosen spatial random field. It does not remove a physical ultraviolet scale from an interacting Lorentzian quantum theory.

17.1. *A correlated logarithmic reference.* Let K be a compact spatial domain with a Borel volume measure m of total mass one. One example is the three-dimensional torus with normalized coordinate volume. Let $F_k : K \to \mathrm{Sym}(4)$ be continuous, $\|F_k\|_{\infty,\mathrm{op}} \le 1$, and let $a_k \ge 0$ satisfy $A = \sum_{k\ge1} a_k \in (0,\infty)$. On a common probability space with independent standard real Gaussian variables ξ_k, define

$$S_N(x) = \sum_{k=1}^{N} a_k \xi_k F_k(x), \qquad M = \sum_{k\ge1} a_k|\xi_k|, \qquad A_{>N} = \sum_{k>N} a_k. \tag{17.1}$$

Choose a deterministic continuous $R : K \to SO(4)$ and put $e_N = R \exp S_N$. This is a Euclidean coframe model. The use of $SO(4)$ here does not assert Lorentzian local symmetry. The rotation is fixed, and the matrix exponential acts pointwise.

The matrices represent coframe coefficients in a fixed reference trivialization. For $K = \mathbb{T}^3$, they can be interpreted as four-dimensional coframe data restricted to one slice of $\mathbb{R} \times \mathbb{T}^3$, relative to its product frame. They are not four independent one-forms on a three-dimensional tangent space. The norms and volume measure used below refer to that declared reference.

The elementary Gaussian estimates needed below have constants independent of N. Tonelli's theorem gives $\mathbb{E}M = \sqrt{2/\pi}A < \infty$, so $M < \infty$ almost surely. For $t \ge 0$ and every real $p \ge 1$, Jensen's inequality with weights a_k/A gives

$$\mathbb{E}e^{tM} \le 2e^{t^2A^2/2}, \qquad \mathbb{E}M^p \le A^p \mathbb{E}|\xi_1|^p, \qquad \mathbb{E}M_{>N}^2 \le A_{>N}^2, \tag{17.2}$$

where $M_{>N} = \sum_{k>N} a_k|\xi_k|$. To see the first estimate, use $\mathbb{E}e^{u|\xi_1|} = 2e^{u^2/2}\Phi(u) \le 2e^{u^2/2}$, where Φ is the standard normal distribution function. For a finite sum the unused weight can be assigned to zero; monotone convergence then justifies the infinite sum. Applying the same argument to its tail gives the last estimate. In particular, $\mathbb{E}M^4 \le 3A^4$.

17.2. *Uniform nondegeneracy and a nonlinear interacting measure.* The interaction is chosen before the truncation is removed:

$$\begin{aligned} W_N &= g\int_K \|S_N(x)\|_F^4 \, dm(x), \qquad Z_N = \mathbb{E}e^{-W_N}, \\ d\mu_N &= Z_N^{-1} e^{-W_N}\, d\mathbb{P}, \qquad g \ge 0. \end{aligned} \tag{17.3}$$

It couples the Gaussian mode amplitudes through their common spatial field. It is a nonlinear spatial interaction, rather than a product law over sites. All tilted measures are first defined on the same sequence space; their coframe laws are then obtained by evaluating e_N.

THEOREM 17.1 (A correlated interacting coframe limit). *Under the preceding assumptions, S_N converges almost surely uniformly to a continuous symmetric field S. The coframes e_N and their inverses converge uniformly to $e = R\exp S$ and e^{-1}. Set $W = g\int_K \|S\|_F^4\, dm$, $Z = \mathbb{E}e^{-W}$, and*

$d\mu = Z^{-1}e^{-W}d\mathbb{P}$. *With* $z_* = \exp(-48gA^4)$, *one has*

$$Z_N, Z \geq z_* > 0, \qquad \|\mu_N - \mu\|_{\mathrm{TV}} \leq \min\{1, 192gz_*^{-1}A^3A_{>N}\}, \tag{17.4}$$

$$\mathbb{E}_{\mu_N}\|e_N^{-1}\|_{\infty,\mathrm{op}}^r \leq 2z_*^{-1}e^{r^2A^2/2}, \qquad r \geq 0,$$

$$\mathbb{E}_{\mu}\|e^{-1}\|_{\infty,\mathrm{op}}^r \leq 2z_*^{-1}e^{r^2A^2/2}, \tag{17.5}$$

$$\mathbb{E}_{\mu}\sup_{x\in K}(\det e(x))^{-r} \leq 2z_*^{-1}e^{8r^2A^2}. \tag{17.6}$$

Almost surely, $\inf_{x\in K}\sigma_{\min}(e(x)) \geq e^{-M} > 0$. *The same inverse-moment and determinant estimates hold for every finite truncation. Total variation in* (17.4) *compares the tilted measures on the common sequence space, not coframe laws supported on different finite-dimensional subspaces.*

Proof. The Weierstrass bound $\|S - S_N\|_{\infty,\mathrm{op}} \leq M_{>N} \to 0$ gives uniform convergence and continuity. Symmetry gives real eigenvalues with absolute values at most M. Consequently

$$\|e^{\pm S}\|_{\infty,\mathrm{op}} \leq e^M, \qquad \det e = e^{\operatorname{tr} S} \geq e^{-4M}. \tag{17.7}$$

The smallest singular value is at least e^{-M} because R is orthogonal. For any two symmetric matrices B, C, differentiating $e^{(1-t)B}e^{tC}$ and integrating gives

$$\|e^B - e^C\|_{\mathrm{op}} \leq \|B - C\|_{\mathrm{op}}e^{\max(\|B\|_{\mathrm{op}},\|C\|_{\mathrm{op}})}. \tag{17.8}$$

This argument requires no commutativity of B and C. Applying it to S_N, S and to $-S_N, -S$ proves uniform convergence of both coframes and inverses, with error at most $e^M M_{>N}$ for each.

For a 4×4 symmetric matrix, $\|S\|_F \leq 2\|S\|_{\mathrm{op}}$. It follows that $0 \leq W_N, W \leq 16gM^4$ and $\mathbb{E}W_N, \mathbb{E}W \leq 48gA^4$. Jensen's inequality applied to the convex function e^{-u} yields the common lower bound z_*. The quartic difference obeys

$$|W_N - W| \leq 64gM^3M_{>N}, \qquad \delta_N := \mathbb{E}|W_N - W| \leq 192gA^3A_{>N}. \tag{17.9}$$

Indeed $|u^4 - v^4| \leq 4\max(u,v)^3|u-v|$, and Hölder's inequality gives

$$\mathbb{E}(M^3M_{>N}) \leq (\mathbb{E}M^4)^{3/4}(\mathbb{E}M_{>N}^4)^{1/4} \leq 3A^3A_{>N}.$$

Since e^{-u} is one-Lipschitz on $[0,\infty)$, $|Z_N - Z| \leq \delta_N$. Splitting the difference of normalized densities gives an $L^1(\mathbb{P})$ bound $2\delta_N/z_*$ and hence the stated total-variation bound, with the convention $\|\nu - \rho\|_{\mathrm{TV}} = \frac{1}{2}\int|d\nu - d\rho|$. Finally, multiplication by the tilted density costs at most z_*^{-1}. Combining (17.7) with (17.2) proves the inverse and determinant moments, uniformly in N. □

Proposition 17.2 (An observable error bound). *For a functional* Ψ *of a coframe and its inverse, suppose* $|\Psi| \leq B_\Psi$ *and* Ψ *is Lipschitz with constant* L_Ψ *for the maximum of the two uniform operator norms. Then*

$$\left|\mathbb{E}_{\mu_N}\Psi(e_N, e_N^{-1}) - \mathbb{E}_{\mu}\Psi(e, e^{-1})\right|$$

$$\le z_*^{-1}\left(\sqrt{2}L_\Psi e^{A^2}+384gB_\Psi A^3\right)A_{>N}. \quad (17.10)$$

Proof. First change the field at fixed measure μ_N, and then change the measure at fixed field (e,e^{-1}). The first error is at most $L_\Psi z_*^{-1}\mathbb{E}(e^M M_{>N})$. Cauchy–Schwarz and (17.2) bound this by $\sqrt{2}L_\Psi z_*^{-1}e^{A^2}A_{>N}$. The second error is at most $2B_\Psi\|\mu_N-\mu\|_{\mathrm{TV}}$. □

17.3. *A compatible finite-mode stochastic dynamics.* The interacting reference also admits an explicit finite-mode dynamics. This supplies a useful connection with dissipation, while keeping the choice of an evolution rate visible. Let $z=(\xi_1,\dots,\xi_N)$ and write $W_N(z)$ for the quartic interaction above. Its probability density with respect to Lebesgue measure is

$$q_N(z)=\mathcal{Z}_N^{-1}e^{-V_N(z)},\qquad V_N(z)=\tfrac{1}{2}|z|^2+W_N(z),\qquad \mathcal{Z}_N=(2\pi)^{N/2}Z_N. \quad (17.11)$$

Proposition 17.3 (Finite-mode evolution and entropy balance). *For $\gamma>0$ and square-integrable initial data, the diffusion*

$$dZ_s=-\gamma\nabla V_N(Z_s)ds+\sqrt{2\gamma}\,dB_s \quad (17.12)$$

has a unique nonexplosive strong solution. Its invariant density is q_N. For a smooth positive normalized evolving density p_s with finite relative entropy, sufficient decay, and justified differentiation and integration by parts, one has

$$\frac{d}{ds}D(p_s\|q_N)=-\gamma\int_{\mathbb{R}^N}p_s\left|\nabla\log\frac{p_s}{q_N}\right|^2dz\le 0. \quad (17.13)$$

The invariant law is independent of γ; its evolution rate is not.

Proof. The quartic interaction is a nonnegative homogeneous polynomial of degree four in z. Its drift is locally Lipschitz. For the generator $\mathcal{L}_N=\gamma(\Delta-\nabla V_N\cdot\nabla)$, Euler's homogeneity identity gives

$$\mathcal{L}_N|z|^2=2\gamma N-2\gamma|z|^2-8\gamma W_N(z)\le 2\gamma N-2\gamma|z|^2. \quad (17.14)$$

The stopped Itô estimate bounds the probability of reaching radius R before time T by $(\mathbb{E}|Z_0|^2+2\gamma NT)/R^2$. Letting $R\to\infty$ excludes finite-time explosion; local strong existence and pathwise uniqueness therefore extend globally. The density e^{-V_N} has Gaussian decay and its gradient is a polynomial times that decay. Its current $\nabla q_N+q_N\nabla V_N$ vanishes. Equivalently, the symmetric divergence generator with this finite confining potential preserves its normalized measure, giving invariance.

The Fokker–Planck current for p is $j=-\gamma(\nabla p+p\nabla V_N)=-\gamma p\nabla\log(p/q_N)$. Differentiating relative entropy, using normalization to remove its constant derivative term, and integrating the continuity equation $\partial_s p=-\nabla\cdot j$ by parts gives (17.13). The assumed decay removes the boundary term. Multiplying the generator by γ changes time without changing its zero-current density. □

The normalization and geometric estimates above are uniform in the number of modes. In contrast, the Lyapunov bound for the unweighted Gaussian coordinate norm contains N, as it must. The proposition does not assert a dimension-uniform bound for $|Z|^2$ or construct an infinite-dimensional stochastic evolution. Moreover, identifying its relative-entropy loss with physical heat requires a reservoir, energy scale, and time calibration. A chosen reversible generator establishes compatibility with the reference; it does not prove that the mother theory uniquely selects this generator.

If K is a compact smooth domain or manifold and $\sum_k a_k \|F_k\|_{C^j} < \infty$ for an integer $j \geq 1$, the same Weierstrass argument gives $S_N \to S$ almost surely in C^j. When R is also C^j, the coframes and inverses converge in that topology. These are additional regularity assumptions. With $a_k = 2^{-k}$, the uniform tail in (17.10) is 2^{-N}. By contrast, $e_\varepsilon = \operatorname{diag}(\varepsilon, \varepsilon^{-1}, 1, 1)$ has determinant one and inverse norm tending to infinity. The singular-value estimate above supplies precisely the shape control missing from a determinant-only condition.

The construction supplies an infinite-mode, nonlinear spatial random geometry with explicit inverse-observable bounds. It also identifies the remaining physical matching problem. A complete gravitational theory would have to produce a suitable reference or a replacement uniform estimate from its own action, include the independent connection and matter fields, and establish physical-time dynamics and positivity. Neither the chosen summable covariance nor the nonnegative quartic tilt implies the Hamiltonian constraint, reflection positivity, or Lorentzian unitarity.

17.4. *A fixed spatial test with nonlinear mode coupling.* For a reproducible example take $K = \mathbb{T}^3$, $R = I$, $a_k = 2^{-k}$, and $g = 0.02$. Enumerate the nonzero integer wavevectors by increasing squared length and then lexicographic order, keeping the sign for which the first nonzero component is positive. Use $F_k(x) = D_k \cos(n_k \cdot x)$, where D_k cycles through the four diagonal matrix units and the six matrices $E_{ij} + E_{ji}$, ordered lexicographically by $i < j$. Each has operator norm one. Thus $A = 1$, $A_{>N} = 2^{-N}$, and $z_* = e^{-0.96} = 0.38289289$.

The observable is $\Psi = \tanh \max_{x \in G} \|e^{-1}(x) - I\|_{\mathrm{op}}$ on the fixed 9^3-point equally spaced torus grid G. It is bounded by one and has Lipschitz constant one for the norm in Proposition 17.2. The analytic error bound is therefore $30.09779354\, 2^{-N}$. The grid defines this observable; it does not replace the continuous supremum in Theorem 17.1.

Eight independently scrambled Sobol replicates, each with 512 Gaussian samples and dimension 24, estimate the normalized interacting expectations. Within a replicate the same coefficients are used at all truncations. The Gaussian variables are the inverse normal transforms of the Sobol coordinates. The largest component frequency among these 24 modes is two. Consequently the 9^3-point quadrature integrates the quartic interaction exactly in exact arithmetic: its trigonometric degree in each coordinate is at most eight and no nonzero such frequency is a multiple of nine. A comparison with an 11^3 grid for two samples differs by less than $4 \cdot 10^{-19}$ in floating-point arithmetic.

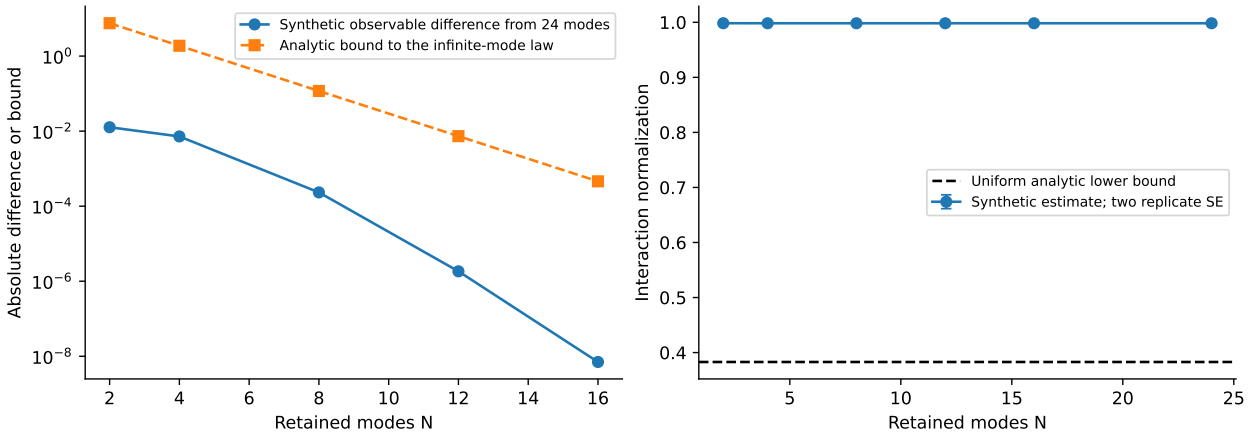


Figure 25. Synthetic convergence for the prescribed correlated coframe model. Left: the absolute paired observable difference from 24 retained modes, together with a conservative analytic bound to the infinite-mode law. Right: estimated interaction normalizations and the common lower bound. Error bars show two standard errors across randomized replicates; they are not rigorous confidence bounds. The data test a specified spatial model and are not observations of quantum gravity.

N	Z_N	$\mathbb{E}_{\mu_N}\Psi$	Δ_N	B_N
2	0.99836845	0.46273720	$-1.270 \cdot 10^{-2}$	$7.524 \cdot 10^{0}$
4	0.99830132	0.46821304	$-7.221 \cdot 10^{-3}$	$1.881 \cdot 10^{0}$
8	0.99829261	0.47520098	$-2.329 \cdot 10^{-4}$	$1.176 \cdot 10^{-1}$
12	0.99829258	0.47543203	$-1.836 \cdot 10^{-6}$	$7.348 \cdot 10^{-3}$
16	0.99829258	0.47543387	$7.039 \cdot 10^{-9}$	$4.593 \cdot 10^{-4}$
24	0.99829258	0.47543386	0	$1.794 \cdot 10^{-6}$

Here Δ_N is the signed paired difference from 24 modes and B_N is the analytic bound to the infinite law. The standard error across independent replicate estimates is approximately $2.07 \cdot 10^{-5}$ for Z_{24} and $1.69 \cdot 10^{-4}$ for its normalized observable. For the paired difference at $N = 16$ it is $1.03 \cdot 10^{-8}$, exceeding the absolute difference displayed in the table. That small difference is therefore not evidence for a resolved nonzero truncation effect. The analytic bound from 24 modes to the infinite law is $1.794 \cdot 10^{-6}$; it does not remove sampling error. Importance-weight effective sample sizes exceed 511.98 out of 512 within every replicate. This favorable overlap does not make the randomized quadrature an interval certificate.

The corresponding numerical diagnostic is shown in Figure 25.

18. **Equilibrium, evolution, and the calibration of time**

An equilibrium distribution answers how often a state is occupied. A clock answers how rapidly a transition occurs. These are different measurements. Their distinction is especially useful in a framework that uses an equilibrium reference to organize stochastic and quantum dynamics. We

give a finite quantum example in which the ambiguity and its resolution can both be computed, and then explain the corresponding classical time change.

18.1. *What the KMS condition fixes.* Let H be a self-adjoint matrix, $\beta > 0$ an inverse energy, and $\hbar > 0$. Define

$$\rho_\beta = \frac{e^{-\beta H}}{\operatorname{tr} e^{-\beta H}}, \qquad \alpha_t(B) = e^{itH/\hbar} B e^{-itH/\hbar}, \qquad \omega_\beta(B) = \operatorname{tr}(\rho_\beta B). \tag{18.1}$$

Here $\beta = (k_B T)^{-1}$ when a physical temperature T has been specified. All matrix observables are entire analytic in t. Direct trace cyclicity gives the Kubo–Martin–Schwinger boundary identity

$$\omega_\beta(\alpha_t(A)B) = \omega_\beta(B\alpha_{t+i\beta\hbar}(A)). \tag{18.2}$$

For example, in an energy basis the (i, j) term on the left has weight $e^{-\beta E_i} e^{it(E_i - E_j)/\hbar}$; on the right the same weight is $e^{-\beta E_j} e^{-\beta(E_i - E_j)} e^{it(E_i - E_j)/\hbar}$. This verifies both the sign and the factor $\hbar$. The imaginary-time shift has units of time.

The transformation $H \mapsto aH + E_0 I$, $\beta \mapsto \beta/a$, with $a > 0$, leaves the Gibbs density unchanged. The scalar E_0 cancels from both this density and the Heisenberg evolution, whereas a changes the evolution rate. KMS is a condition on a state together with a specified evolution. It does not determine an absolute rate from the density alone. Failure of KMS may also describe a driven state; it does not by itself invalidate the clock used to observe that state.

18.2. *Removing the scale ambiguity by an independent transition.*

Proposition 18.1 (Population and frequency calibration). *Let $H = E_0 I + cH_*$, where the finite-dimensional self-adjoint matrix H_* is known and dimensionless, c has units of energy, and $\Delta = \varepsilon_j - \varepsilon_i > 0$ is an ordered gap of H_*. Suppose $c, \beta > 0$, the state is ρ_β, and its populations p_i, p_j are measured in this known eigenbasis. The population ratio determines only*

$$b = -\frac{\log(p_j/p_i)}{\Delta} = \beta c. \tag{18.3}$$

If the angular transition frequency ω_{ji} is also measured relative to an independently calibrated time unit, then

$$c = \frac{\hbar \omega_{ji}}{\Delta}, \qquad \beta = \frac{b}{c}. \tag{18.4}$$

These measurements do not determine E_0. Suppose estimates obey $|\widehat{b} - b| \le \epsilon_b$ and $|\widehat{\omega} - \omega_{ji}| \le \epsilon_\omega$. If $\epsilon_c = \hbar\epsilon_\omega/\Delta < c$, then

$$|\widehat{c} - c| \le \epsilon_c, \qquad |\widehat{\beta} - \beta| \le \frac{\epsilon_b}{c - \epsilon_c} + \frac{b\epsilon_c}{c(c - \epsilon_c)}, \qquad \widehat{\beta} = \widehat{b}/\widehat{c}. \tag{18.5}$$

Proof. The ratio of Gibbs populations is $p_j/p_i = \exp[-\beta c(\varepsilon_j - \varepsilon_i)]$. The same pair of energy levels gives angular frequency $c\Delta/\hbar$. These are two independent relations for b and c. The frequency

estimate gives the first bound. Since $\widehat{c} \geq c - \epsilon_c > 0$,

$$\left| \frac{\widehat{b}}{\widehat{c}} - \frac{b}{c} \right| \leq \frac{|\widehat{b} - b|}{\widehat{c}} + \frac{b|\widehat{c} - c|}{c\widehat{c}},$$

which proves the second. An additive scalar in H cancels from every displayed observable, proving its nonidentifiability here. □

For example, take $\hbar = 1$, $H_* = \mathrm{diag}(0, 1, 3)$, $c = 1.7$, and $\beta = 0.8$. The three populations are approximately $(0.78519546, 0.20152888, 0.01327567)$, and $b = 1.36$. The pair $c' = 3.4$, $\beta' = 0.4$ gives exactly the same populations. For the first gap the angular frequencies are 1.7 and 3.4, respectively. With $\epsilon_b = 0.002$ and $\epsilon_\omega = 0.001$, the bound in (18.5) is approximately 0.00164803. These are synthetic examples in declared units. They illustrate identifiability and are not measurements of a new interaction.

The independent time unit is essential. An unknown apparatus Hamiltonian or an unknown common frequency standard would introduce another scale ambiguity. The proposition therefore supplies an operational matching test, rather than selecting a preferred clock from equilibrium alone.

18.3. *The corresponding stochastic time change.* Let L be a Markov generator with invariant law π. For the time change $dt = r(X_s)ds$, assume r is positive, bounded above and below, and integrable against π. The new generator and invariant law are

$$L_r = r^{-1}L, \qquad d\pi_r = \frac{r\, d\pi}{\int r\, d\pi}. \tag{18.6}$$

Indeed integrating $L_r f$ against π_r cancels r and leaves a constant multiple of $\int Lf\, d\pi = 0$. In the constant case $r = r_0$, the invariant law is unchanged, while every decay rate is divided by r_0. For an overdamped harmonic mode $dX_s = -\kappa X_s ds + \sqrt{2\theta\gamma}\, dW_s$ with $\kappa = \gamma k > 0$, the stationary variance is θ/k and the stationary correlation is $(\theta/k)e^{-\kappa|s|}$. In the new time it is $(\theta/k)e^{-\kappa|t|/r_0}$. Thus a variance measurement fixes an equilibrium combination, while a time correlation tests the mobility relative to a clock.

For a normalized density p at a corresponding state and a reversible model, $d\mathcal{F}/dt = r_0^{-1} d\mathcal{F}/ds$. Physical heat and work rates transform in the same way if the bath and energy are held fixed. Their integrated values over the same trajectory segment are unchanged. For a state-dependent r, the occupation law itself changes as in (18.6); assigning physical heat then requires the declared reservoir model. An arbitrary change of an occupation potential is not a derivation of a new mechanical energy.

19. **Conclusion**

The microscopic interpretation is now explicit at both starting points. A primitive stochastic generator may contain a stationary reversal defect; a reversible Hamiltonian reservoir instead realizes a conditional effective law. Neither distinction replaces the proof of free-energy dissipation, which follows from thermal calibration, invariance, and the positive diffusion form. Equilibrium reversibility and nonequilibrium relaxation can therefore coexist without identifying a reverse trajectory with an equilibrium-preserving recovery map.

The covariant finite extension makes another part of the interface explicit. Its reference measure controls inverse coframes, and its positive generator gives the free-energy dissipation identity with a specified energy and temperature. Observation-scale determinant bounds identify the additional normalization and spatial regularity needed beyond a finite graph. Equilibrium-family preservation alone does not select a clock or a mobility: both change under state-dependent time reparametrization. The retained shared-weight calculation therefore matches the temporal normalization and the kinetic coefficient before computing backreaction. Its finite-time bound controls a prepared trajectory, while the separate frequency comparison exhibits the role of scalar motion. Future applications must retain these preparation, clock, and heat conventions when matching the finite balance to physical reservoirs and fluctuating geometry.

The current-contraction result makes the reduction problem quantitative. The observed mobility is the contracted positive form, while a residual conditional force measures the part of the microscopic thermodynamic force that the observation has not closed. When this defect vanishes and the projected generator is autonomous, the same variational and entropy statements hold for the observed diffusion. When the defect remains, the derived bound specifies how much observed free-energy increase it can produce. The Gaussian examples test both cases with analytic formulas and reproducible synthetic sampling.

The complete observation balance also includes the change in transport under conditional averaging. Its defect B_ρ bounds possible observed free-energy recovery even when the instantaneous averaged transport does not preserve the marginal reference. The transport-only Gaussian experiment attains the recovery bound, while the stationary zero-defect experiment retains memory. Together these examples separate an observed density balance from autonomy of the observed paths. The conditional mean-force limit agrees with established effective-dynamics estimates; the physical synthesis here concerns the stated reservoir, current contraction, transport, preparation and observation conditions.

Future progress requires physical derivations of these compatibility conditions in broader interacting reservoirs and constrained dynamical models, together with estimates uniform in the regulator. Such work can strengthen the microscopic basis and the predictive scope of the proposed reconstruction. The finite results already identify the quantities that must be measured or

derived: mobility, equilibrium weights, conditional forces, clock calibration, and the appropriate reverse experiment.

An ideal cross-sector force–frequency inverse can identify the shared scalar and curvature parameters under its resolved-data assumptions. It does not determine the reservoir temperature, the reference measure or a thermodynamic clock. The entropy results here retain their own generator and exchange conditions; their physical use with the same calibration requires a derived projection rather than an identification of unrelated parameters by notation.

The explicit positive-state realization closes existence, uniqueness, admissibility and convergence at its stated finite level. Its reversible branch relaxes in law without stationary entropy production; the compact current extension has a stationary statistical arrow under the specified even parity. Identification of that arrow with reservoir entropy requires the physical work and local-detailed-balance conditions already separated in this paper. Neither result supplies an unconditional continuum law.

The coupled reservoir example derives heat and entropy production from one stated energy and generator. Its equilibrium and nonequilibrium experiments use the same mechanical coupling. The separate Galerkin example shows that even a uniform entropy rate does not provide the compactness needed to remove the regulator: stationary energy can escape every fixed energy ball. These calculations identify both a realizable finite thermodynamic model and a precise limit obstruction.

Physical duration and statistical time asymmetry remain distinct. For a bounded positive state-dependent clock, the invariant density is reweighted by the clock rate and stationary path entropy is measured per unit of the new time. The calibrated Poincare estimate makes the corresponding relaxation bound explicit. These facts refine the thermodynamic interpretation without identifying entropy production with proper time. Dissipation of a resolved subsystem is compatible with the full energy ledger when reservoir heat and stochastic work are included consistently. The harmonic-reservoir realization in Section 4 derives constant-mobility Euclidean and periodic branches from specified reversible microscopic dynamics. Its covariance and retarded response determine the metric and the variational sign, while its preparation and scale limits remain physical inputs. Equilibrium alone does not uniquely specify a generator or an absolute cosmological time orientation. General field mobilities, circulating drifts, and constrained or continuum reservoirs require additional realizations.

The common-origin calculation in Section 11.2 adds a precise interface to the unified variational programme. It specifies the running cost that selects a given Gibbs drift, the hidden entropy of a projection, and the field constraints a stochastic realization must preserve. For a rotating gravitational reservoir it retains angular-momentum work. These links extend the applications of the thermodynamic result without changing its autonomous isothermal physical hypotheses.

The analysis establishes a precise hierarchy of statements that are often conflated under the phrase "derivation of the second law." The most general theorem is information theoretic: an invariant probability measure of a Markov evolution is a reference relative to which Kullback-Leibler divergence cannot increase. Under a diffusion or closed Dirichlet-form structure, this contraction admits an entropy-dissipation identity. Under an independently established Gibbs thermodynamic identification, relative entropy becomes excess free energy divided by $k_B T$, so autonomous isothermal free energy decreases and total entropy production is nonnegative.

The minimum-cost principle required by the physical programme is formulated not as the false assertion that every noisy microscopic path globally minimizes one classical action, but as a variational statement for the dissipative probability current. In the overdamped constant-mobility class this current is the unique minimizer of an explicit Rayleighian and is compatible with a weighted Wasserstein minimizing-movement scheme. In the kinetic molecular class the generator naturally splits into Hamiltonian transport and degenerate thermal dissipation; convergence is then hypocoercive rather than uniformly elliptic.

This structure clarifies the classical paradoxes. Loschmidt's reversed microscopic construction is not denied mathematically; rather, strict probability-law contraction excludes a positive invariant-measure-preserving Markov inverse. Poincare recurrence is not dismissed by appealing to infinite dimensionality; instead, strict contraction excludes exact recurrence of a non-equilibrium probability law, while sample-path recurrence and equilibrium recurrence remain logically possible. The absence of a flat locally finite translation-invariant measure on an infinite-dimensional Banach space is a separate geometric fact, not the principal recurrence theorem.

A finite-window Gibbs measure relative to a Gaussian reference is defined under normalizability; its finite-term variational principle also requires the stated cost moment. Its canonical symmetric sampler need not be the physical moving-history process. For a fixed window of an endpoint Markov process, the exact segment-law factorization proves that history entropy equals the oldest endpoint entropy. Thus the explicit quadratic kinetic bound transfers after one memory window. Delayed feedback, growing windows, and infinite histories remain outside that theorem.

The 2D stochastic Navier-Stokes equation further demonstrates which parts of the theory are dimension free and which are not. Markov relative-entropy contraction with respect to any invariant law is unconditional once the semigroup is well defined. Differential Fisher-information identities require a closed-form domain theory, and uniform LSI statements cannot be imported from Gaussian equivalence alone. The energy and enstrophy estimates, the correct covariance of the OU reference process, and the weighted-divergence condition for convective antisymmetry provide explicit structural checks.

The resulting theorem architecture can be summarized as

$$\boxed{\begin{aligned}&\text{thermally calibrated microscopic stochastic dynamics}\\ &\quad\Longrightarrow \text{conservative transport } A+ \text{ dissipative sector } S,\\ &\quad\Longrightarrow \text{Gibbs invariance and Markov relative-entropy contraction},\\ &\quad\Longrightarrow \text{free-energy dissipation and } \dot{S}_{\mathrm{tot}} \geq 0,\\ &\quad\Longrightarrow \text{equilibrium convergence when coercivity/hypocoercivity holds.}\end{aligned}} \tag{19.1}$$

Within the explicit assumptions of the model class, this chain is non-circular: the equilibrium law, the dissipative variational structure, the information contraction theorem, and the convergence mechanism are separate mathematical ingredients whose roles are stated transparently.

Appendix A. Notation and Variational Identities

The notation and units used throughout the paper are listed first. The remaining subsections give the full Gibbs and Rayleighian calculations underlying Section 6.

A.1. *Notation.* To prevent the symbol overload that commonly occurs in stochastic thermodynamics, the following notation is used consistently.

Symbol	Meaning
$\mathcal{H}(q,p)$	Molecular Hamiltonian.
$\mathcal{H}$	Hilbert state space in infinite-dimensional sections.
ν_t	Probability law at physical time t.
μ	Generic invariant probability measure.
μ_{eq} or π_{eq}	Thermodynamic equilibrium measure.
$f_t = \mathrm{d}\nu_t/\,\mathrm{d}\mu$	Density relative to the chosen invariant reference measure.
P_t	Markov transition semigroup.
L	Backward Markov generator on observables.
$L^{\dagger_\mu}$	Adjoint of L in $L^2(\mu)$.
S_μ and A_μ	Symmetric dissipative and antisymmetric transport parts of L w.r.t. μ.
Θ	Physical time-reversal involution, including parity of odd variables.
Γ_L	Carré du champ associated with L.
$\Gamma_{2,L}$	Iterated carré du champ.
$\mathcal{E}_{S,\mu}$	Closed symmetric Dirichlet form generated by S_μ.
$\mathcal{I}_\mu$	Relative Fisher information/dissipation functional.
$F[\nu]$	State-space thermodynamic free energy.
Φ	Dimensionless trajectory cost when a path Gibbs measure is used.
$\mathcal{F}_\Omega$	Trajectory-space Gibbs free-energy functional.
G	Molecular friction matrix; deliberately distinct from Γ_L.
K	Mobility matrix in overdamped dynamics.
A_{St}	Positive Stokes operator in the Navier-Stokes section.
ρ_γ	Reference Gaussian Bakry-Emery curvature.
κ	Hessian lower bound constant.
μ_{NS}	Navier-Stokes invariant measure.
μ_G	Navier-Stokes Gaussian reference measure.

A.2. *Symbols and Physical Units.* The following conventions are used globally. They are repeated here because several standard notations collide in stochastic thermodynamics.

Object	Symbol	Type or units	Collision avoided
Mobility	K	length squared per energy per time	Not the mass matrix.
Mass matrix	M	mass	Not mobility and not sample count.
Diffusion tensor	D	length squared per time	Not KL divergence.
KL divergence	$D(\nu\|\mu)$	dimensionless	Not a diffusion coefficient.
State relative entropy	$H(t)$	dimensionless	Not physical entropy.
Physical entropy	S	energy per temperature	Not the symmetric generator.
Dimensionless entropy-production rate	Σ or σ_{tot}	inverse time	Physical rate is $k_B\Sigma$.
Probability current	j_t, scalar ring current J	density times velocity	Not every current is denoted by J.
Independent trajectory count	R	positive integer	Not M.
Stationary density	π	density	Not a reference constant.
Constant density reference	r_0	density	Not a nonconstant stationary law.

A.3. *Detailed Proof of the Gibbs Free-Energy Identity.* This appendix provides a fully expanded derivation of the Gibbs free-energy identity Equation (6.68). Every algebraic step is shown explicitly, and no normalisation factors are suppressed.

A.3.1. *Setup and Notation.* Let m be a fixed reference measure on the state space $\mathcal{X}$. Let ν be a probability measure absolutely continuous with respect to m, with density

$$r(x) := \frac{d\nu}{dm}(x). \tag{A.1}$$

The Gibbs measure is defined as

$$\pi(dx) = Z^{-1} e^{-\beta \mathcal{H}(x)} m(dx), \tag{A.2}$$

where

$$Z := \int_{\mathcal{X}} e^{-\beta \mathcal{H}(x)} m(dx) < \infty \tag{A.3}$$

by Theorem 6.3.

The free-energy functional is

$$F[\nu] := \int_{\mathcal{X}} \mathcal{H}(x)\,\nu(dx) + k_B T \int_{\mathcal{X}} r(x)\log r(x)\,m(dx). \tag{A.4}$$

Equivalently, since $\nu(dx) = r(x)m(dx)$,

$$F[\nu] = \int_{\mathcal{X}} \mathcal{H}(x)r(x)\,m(dx) + k_B T \int_{\mathcal{X}} r(x)\log r(x)\,m(dx). \tag{A.5}$$

A.3.2. *Step 1: Compute the Radon-Nikodym Derivative.* We first compute $\frac{d\nu}{d\pi}$ in terms of r, $\mathcal{H}$, and Z.

By the chain rule for Radon-Nikodym derivatives,

$$\frac{d\nu}{d\pi}(x) = \frac{d\nu}{dm}(x)\cdot\frac{dm}{d\pi}(x). \tag{A.6}$$

Now $\frac{dm}{d\pi}(x)$ is the reciprocal of $\frac{d\pi}{dm}(x)$. From the definition of π,

$$\frac{d\pi}{dm}(x) = Z^{-1}e^{-\beta\mathcal{H}(x)}. \tag{A.7}$$

Therefore,

$$\frac{dm}{d\pi}(x) = Ze^{\beta\mathcal{H}(x)}. \tag{A.8}$$

Hence,

$$\frac{d\nu}{d\pi}(x) = r(x)\cdot Ze^{\beta\mathcal{H}(x)} = Zr(x)e^{\beta\mathcal{H}(x)}. \tag{A.9}$$

This is a key intermediate result.

A.3.3. *Step 2: Take the Logarithm.* Taking the logarithm of both sides,

$$\log\frac{d\nu}{d\pi}(x) = \log Z + \log r(x) + \beta\mathcal{H}(x). \tag{A.10}$$

This is the expression used in the main text.

A.3.4. *Step 3: Integrate Against ν.* By definition of the Kullback-Leibler divergence,

$$D(\nu\parallel\pi) = \int_{\mathcal{X}} \frac{d\nu}{d\pi}(x)\log\frac{d\nu}{d\pi}(x)\,\pi(dx). \tag{A.11}$$

Equivalently, using the change of measure $\nu(dx) = \frac{d\nu}{d\pi}(x)\,\pi(dx)$,

$$D(\nu\parallel\pi) = \int_{\mathcal{X}} \log\frac{d\nu}{d\pi}(x)\,\nu(dx). \tag{A.12}$$

Substituting the expression from Step 2,

$$\begin{aligned} D(\nu\parallel\pi) &= \int_{\mathcal{X}} \left[\log Z + \log r(x) + \beta\mathcal{H}(x)\right]\nu(dx) \\ &= \log Z\int_{\mathcal{X}}\nu(dx) + \int_{\mathcal{X}}\log r(x)\,\nu(dx) + \beta\int_{\mathcal{X}}\mathcal{H}(x)\,\nu(dx). \end{aligned} \tag{A.13}$$

Since ν is a probability measure, $\int_{\mathcal{X}} \nu(dx) = 1$. Also, $\log r(x)\, \nu(dx) = r(x) \log r(x)\, m(dx)$ because $\nu(dx) = r(x)m(dx)$. Therefore,

$$D(\nu \parallel \pi) = \log Z + \int_{\mathcal{X}} r(x) \log r(x)\, m(dx) + \beta \int_{\mathcal{X}} \mathcal{H}(x)\, \nu(dx). \tag{A.14}$$

A.3.5. *Step 4: Multiply by $k_B T$.* Multiplying both sides by $k_B T$:

$$k_B T\, D(\nu \parallel \pi) = k_B T \log Z + k_B T \int_{\mathcal{X}} r(x) \log r(x)\, m(dx) + k_B T \beta \int_{\mathcal{X}} \mathcal{H}(x)\, \nu(dx). \tag{A.15}$$

Using the relation $k_B T \beta = 1$, which follows from $\beta = (k_B T)^{-1}$, we obtain

$$k_B T\, D(\nu \parallel \pi) = k_B T \log Z + k_B T \int_{\mathcal{X}} r(x) \log r(x)\, m(dx) + \int_{\mathcal{X}} \mathcal{H}(x)\, \nu(dx). \tag{A.16}$$

A.3.6. *Step 5: Identify the Free Energy.* The right-hand side is exactly $F[\nu] + k_B T \log Z$, because

$$F[\nu] = \int \mathcal{H}\, d\nu + k_B T \int r \log r\, dm. \tag{A.17}$$

Therefore,

$$k_B T\, D(\nu \parallel \pi) = F[\nu] + k_B T \log Z. \tag{A.18}$$

A.3.7. *Step 6: Evaluate at $\nu = \pi$.* When $\nu = \pi$, the relative entropy vanishes: $D(\pi \parallel \pi) = 0$. Substituting into the previous equation,

$$0 = F[\pi] + k_B T \log Z. \tag{A.19}$$

Hence,

$$F[\pi] = -k_B T \log Z. \tag{A.20}$$

A.3.8. *Step 7: Rearrange the Identity.* Using $F[\pi] = -k_B T \log Z$ from Step 6, the identity in Step 5 can be rearranged directly:

$$F[\nu] - F[\pi] = F[\nu] + k_B T \log Z = k_B T\, D(\nu \parallel \pi). \tag{A.21}$$

Therefore,

$$\boxed{F[\nu] - F[\pi] = k_B T\, D(\nu \parallel \pi).} \tag{A.22}$$

This completes the derivation.

A.3.9. *Remark on the Reference Measure.* The reference measure m appears in both $F[\nu]$ and $F[\pi]$ through the entropy term $\int r \log r \, \mathrm{d}m$. The statement that a change of reference measure only changes the free energy by an additive constant is correct only for a constant rescaling of the reference measure, or when the Hamiltonian is transformed at the same time. Indeed, if $\tilde{m} = e^{-\chi} m$, then

$$\frac{\mathrm{d}\nu}{\mathrm{d}\tilde{m}} = e^{\chi} \frac{\mathrm{d}\nu}{\mathrm{d}m}. \tag{A.23}$$

Consequently,

$$\int \frac{\mathrm{d}\nu}{\mathrm{d}\tilde{m}} \log \frac{\mathrm{d}\nu}{\mathrm{d}\tilde{m}}\, \mathrm{d}\tilde{m} = \int r \log r\, \mathrm{d}m + \int \chi\, \mathrm{d}\nu. \tag{A.24}$$

The last term is not a constant in ν unless χ is constant. Thus the invariant free-energy difference must be stated relative to one fixed reference measure, or the Hamiltonian must be changed from $\mathcal{H}$ to $\mathcal{H} - k_B T\chi$ so that the Gibbs density represents the same physical measure.

A.4. *Detailed Derivation of the Overdamped Minimum-Dissipation Structure.* This appendix provides a complete derivation of the overdamped minimum-dissipation variational principle, including the computation of the functional derivative, the first variation, the second variation, and the resulting free-energy dissipation rate.

A.4.1. *Setup: Free Energy and Its Functional Derivative.* We consider the free-energy functional

$$F[\rho] = \int_{\mathbb{R}^n} U(x)\rho(x)\,dx + k_B T \int_{\mathbb{R}^n} \rho(x)\log\rho(x)\,dx. \tag{A.25}$$

We compute its functional derivative with respect to ρ.

Let η be a perturbation with $\int \eta\,dx = 0$ (to preserve total mass). Define $\rho_\varepsilon := \rho + \varepsilon\eta$. Then

$$\frac{d}{d\varepsilon}F[\rho_\varepsilon]\bigg|_{\varepsilon=0} = \frac{d}{d\varepsilon}\int U(\rho+\varepsilon\eta)\,dx\bigg|_{\varepsilon=0} + k_B T\frac{d}{d\varepsilon}\int (\rho+\varepsilon\eta)\log(\rho+\varepsilon\eta)\,dx\bigg|_{\varepsilon=0}. \tag{A.26}$$

The first term is

$$\frac{d}{d\varepsilon}\int U(\rho+\varepsilon\eta)\,dx\bigg|_{\varepsilon=0} = \int U\eta\,dx. \tag{A.27}$$

For the second term, we use the derivative of $s\log s$:

$$\frac{d}{ds}(s\log s) = \log s + 1. \tag{A.28}$$

Therefore,

$$\frac{d}{d\varepsilon}\int (\rho+\varepsilon\eta)\log(\rho+\varepsilon\eta)\,dx\bigg|_{\varepsilon=0} = \int (\log\rho + 1)\eta\,dx. \tag{A.29}$$

Thus,

$$\frac{d}{d\varepsilon}F[\rho_\varepsilon]\bigg|_{\varepsilon=0} = \int \left[U + k_B T(\log\rho + 1)\right]\eta\,dx. \tag{A.30}$$

By definition of the functional derivative,

$$\frac{\delta F}{\delta\rho} = U + k_B T(\log\rho + 1). \tag{A.31}$$

A.4.2. *Step 1: From Functional Derivative to Gradient Flow.* Taking the gradient:

$$\nabla\frac{\delta F}{\delta\rho} = \nabla U + k_B T\nabla\log\rho. \tag{A.32}$$

Using $\nabla\log\rho = \frac{\nabla\rho}{\rho}$,

$$\nabla\frac{\delta F}{\delta\rho} = \nabla U + k_B T\frac{\nabla\rho}{\rho}. \tag{A.33}$$

Multiplying by $\rho\mathsf{K}$:

$$\rho\mathsf{K}\nabla\frac{\delta F}{\delta\rho} = \rho\mathsf{K}\nabla U + k_B T\mathsf{K}\nabla\rho. \tag{A.34}$$

The right-hand side is exactly the flux term in the Fokker-Planck equation:

$$\partial_t \rho = \nabla \cdot \left[\mathsf{K} \left(\rho \nabla U + k_B T \nabla \rho \right) \right]. \tag{A.35}$$

Hence,

$$\partial_t \rho = \nabla \cdot \left[\rho \mathsf{K} \nabla \frac{\delta F}{\delta \rho} \right]. \tag{A.36}$$

A.4.3. *Step 2: Rayleighian Definition.* The continuity equation is $\partial_t \rho + \nabla \cdot j = 0$. The Rayleighian is defined as

$$\mathcal{R}_\rho[j] = \frac{1}{2} \int \frac{j^{\mathsf{T}} \mathsf{K}^{-1} j}{\rho} \, dx + \int j \cdot \nabla \frac{\delta F}{\delta \rho} \, dx. \tag{A.37}$$

The first term is the dissipation cost (kinetic energy in the Wasserstein metric); the second term is the driving force.

A.4.4. *Step 3: First Variation of the Rayleighian.* Let $j_\varepsilon = j + \varepsilon h$, where h is an admissible variation with $h = 0$ on $\{\rho = 0\}$. Then

$$\begin{aligned} \frac{d}{d\varepsilon} \mathcal{R}_\rho[j_\varepsilon] \bigg|_{\varepsilon=0} &= \frac{1}{2} \int \frac{2 j^{\mathsf{T}} \mathsf{K}^{-1} h}{\rho} \, dx + \int h \cdot \nabla \frac{\delta F}{\delta \rho} \, dx \\ &= \int h^{\mathsf{T}} \left(\frac{\mathsf{K}^{-1} j}{\rho} + \nabla \frac{\delta F}{\delta \rho} \right) dx. \end{aligned} \tag{A.38}$$

Setting this to zero for all admissible h gives the Euler-Lagrange equation:

$$\frac{\mathsf{K}^{-1} j}{\rho} + \nabla \frac{\delta F}{\delta \rho} = 0. \tag{A.39}$$

Multiplying by $\rho \mathsf{K}$:

$$j = -\rho \mathsf{K} \nabla \frac{\delta F}{\delta \rho}. \tag{A.40}$$

Thus, the minimizer is

$$j_\star = -\rho \mathsf{K} \nabla \frac{\delta F}{\delta \rho}. \tag{A.41}$$

A.4.5. *Step 4: Second Variation and Uniqueness.* The second variation is

$$\frac{d^2}{d\varepsilon^2} \mathcal{R}_\rho[j + \varepsilon h] \bigg|_{\varepsilon=0} = \int \frac{h^{\mathsf{T}} \mathsf{K}^{-1} h}{\rho} \, dx. \tag{A.42}$$

Since $\mathsf{K}^{-1} > 0$ and $\rho > 0$ on the support, the second variation is strictly positive for any nonzero h. Therefore, the Rayleighian is strictly convex, and the minimizer $j_\star$ is unique.

A.4.6. *Step 5: Free-Energy Dissipation Rate.* Using the continuity equation and the minimizer $j_\star$:

$$\begin{aligned}\frac{dF}{dt} &= \int \frac{\delta F}{\delta \rho} \partial_t \rho \, dx \\ &= -\int \frac{\delta F}{\delta \rho} \nabla \cdot j_\star \, dx \\ &= \int j_\star \cdot \nabla \frac{\delta F}{\delta \rho} \, dx.\end{aligned} \tag{A.43}$$

Substituting $j_\star = -\rho \mathsf{K} \nabla(\delta F/\delta \rho)$:

$$\frac{dF}{dt} = -\int \rho \left(\nabla \frac{\delta F}{\delta \rho}\right)^{\mathsf{T}} \mathsf{K} \left(\nabla \frac{\delta F}{\delta \rho}\right) dx. \tag{A.44}$$

Since $\mathsf{K} > 0$, the integrand is nonnegative, so

$$\frac{dF}{dt} \leq 0. \tag{A.45}$$

Equality requires $\nabla(\delta F/\delta \rho) = 0$ almost everywhere where $\rho > 0$. For a positive density on a connected state domain, with the stated Gibbs free energy and no boundary flux, this identifies ρ with the normalized Gibbs law. On disconnected invariant components the proportionality constants can differ, according to the conserved mass in each component. Entropy dissipation alone does not select those component masses.

Appendix B. Supplementary Entropy and Convergence Arguments

These arguments supply the equality condition, kinetic decomposition, and distinctions among existence, uniqueness, convergence, and smoothing used in Sections 7 and 8.

B.1. *Detailed Proof of the Markov Equality Criterion.* The conditional-expectation representation of the output density gives the equality criterion in Theorem 7.2.

B.1.1. *Setup and Notation.* Let P be a Markov kernel on a measurable space $\mathcal{X}$, and let μ be a probability measure invariant under P, i.e.,

$$\mu P = \mu. \tag{B.1}$$

Let ν be another probability measure with $\nu \ll \mu$. Define

$$f(x) := \frac{d\nu}{d\mu}(x). \tag{B.2}$$

Assume that $D(\nu \parallel \mu) < \infty$.

Define the joint measure on $\mathcal{X} \times \mathcal{X}$:

$$R(dx, dy) := \mu(dx) P(x, dy). \tag{B.3}$$

This is the stationary joint law: the first marginal is μ, and the conditional distribution of Y given $X = x$ is $P(x, \cdot)$.

B.1.2. *Step 1: Define the Conditional Expectation.* Define the function

$$g(y) := \mathbb{E}_R[f(X) \mid Y = y]. \tag{B.4}$$

This is the conditional expectation of $f(X)$ given the output variable Y. This function is well-defined μ-a.e.

B.1.3. *Step 2: Show That g Is the Density of νP with Respect to μ.* For any bounded measurable function $\varphi : \mathcal{X} \to \mathbb{R}$,

$$\int_{\mathcal{X}} \varphi(y)\,(\nu P)(dy) = \int_{\mathcal{X}} \varphi(y) \int_{\mathcal{X}} f(x) P(x, dy)\,\mu(dx). \tag{B.5}$$

This can be written as an integral with respect to the joint measure R:

$$\int_{\mathcal{X}} \varphi(y)\,(\nu P)(dy) = \int_{\mathcal{X}\times\mathcal{X}} \varphi(y) f(x)\,R(dx, dy). \tag{B.6}$$

By the tower property of conditional expectation,

$$\mathbb{E}_R[\varphi(Y) f(X)] = \mathbb{E}_R\big[\varphi(Y)\mathbb{E}_R[f(X) \mid Y]\big] = \int_{\mathcal{X}} \varphi(y) g(y)\,\mu(dy). \tag{B.7}$$

Therefore,

$$\int_{\mathcal{X}} \varphi(y)\,(\nu P)(dy) = \int_{\mathcal{X}} \varphi(y) g(y)\,\mu(dy). \tag{B.8}$$

Since this holds for all bounded measurable φ, we conclude that

$$g = \frac{d(\nu P)}{d\mu}. \tag{B.9}$$

B.1.4. *Step 3: Express the Relative Entropies.* Define $\Psi(r) := r \log r$ for $r > 0$, with $\Psi(0) := 0$. This function is convex on $[0, \infty)$ because

$$\Psi''(r) = \frac{1}{r} > 0 \quad \text{for } r > 0. \tag{B.10}$$

The input relative entropy is

$$D(\nu \parallel \mu) = \int_{\mathcal{X}} \Psi(f(x))\,\mu(dx) = \mathbb{E}_R[\Psi(f(X))]. \tag{B.11}$$

The output relative entropy is

$$D(\nu P \parallel \mu) = \int_{\mathcal{X}} \Psi(g(y))\,\mu(dy) = \mathbb{E}_R[\Psi(g(Y))]. \tag{B.12}$$

B.1.5. *Step 4: Apply Conditional Jensen.* By conditional Jensen's inequality, since Ψ is convex,

$$\Psi(\mathbb{E}[f(X) \mid Y]) \le \mathbb{E}[\Psi(f(X)) \mid Y]. \tag{B.13}$$

That is,

$$\Psi(g(Y)) \le \mathbb{E}[\Psi(f(X)) \mid Y]. \tag{B.14}$$

Taking expectations with respect to R:

$$\mathbb{E}_R[\Psi(g(Y))] \leq \mathbb{E}_R[\mathbb{E}[\Psi(f(X)) \mid Y]]. \tag{B.15}$$

By the tower property, the right-hand side equals $\mathbb{E}_R[\Psi(f(X))]$. Therefore,

$$D(\nu P \parallel \mu) \leq D(\nu \parallel \mu). \tag{B.16}$$

B.1.6. *Step 5: Determine the Equality Condition.* Equality in Jensen's inequality holds if and only if the random variable inside the conditional expectation is almost surely equal to its conditional expectation. That is,

$$f(X) = \mathbb{E}[f(X) \mid Y] \quad R\text{-almost surely.} \tag{B.17}$$

But $\mathbb{E}[f(X) \mid Y] = g(Y)$. Therefore, equality holds if and only if

$$f(X) = g(Y) \quad R\text{-almost surely.} \tag{B.18}$$

Equivalently, there exists a measurable function h such that

$$f(X) = h(Y) \quad R\text{-almost surely.} \tag{B.19}$$

This means that the initial density f is completely determined by the output Y; i.e., f is measurable with respect to the σ-algebra generated by Y.

B.1.7. *Remark on the Equality Condition.* The equality condition means that P preserves the relative information in this particular input law exactly when its density f is determined by the output Y. An invertible deterministic kernel has this property. Excluding equality for every $\nu \neq \mu$ requires an additional strict entropy-contraction result. Ordinary non-increase of entropy, satisfied by every μ-preserving Markov kernel, does not imply that strictness.

B.2. *Detailed Kinetic Generator Decomposition.* The following integration-by-parts calculation identifies the symmetric and antisymmetric differential expressions on a common test domain. Hilbert-space adjoint identities additionally require specified closed realizations. Proposition 9.4 supplies a conservative realization when the Hamiltonian flow is complete; the dissipative realization is obtained from its closed nonnegative Dirichlet form.

B.2.1. *Setup: The Kinetic Generator.* The kinetic generator is decomposed as $L = L_{\text{cons}} + L_{\text{diss}}$, where

$$L_{\text{cons}} = \mathsf{M}^{-1} p \cdot \nabla_q - \nabla U \cdot \nabla_p, \tag{B.20}$$

$$L_{\text{diss}} = -\mathsf{G}\mathsf{M}^{-1} p \cdot \nabla_p + k_B T\, \mathsf{G} : \nabla_p^2. \tag{B.21}$$

B.2.2. *Step 1: Verify That $L_{\text{cons}}^* \pi = 0$.* The formal Lebesgue adjoint of L_{cons} is

$$L_{\text{cons}}^* f = -\mathsf{M}^{-1} p \cdot \nabla_q f + \nabla U \cdot \nabla_p f. \tag{B.22}$$

This follows from integration by parts and the fact that the Hamiltonian vector field has zero divergence:

$$\nabla_q \cdot (\mathsf{M}^{-1}p) + \nabla_p \cdot (-\nabla U) = 0. \tag{B.23}$$

Now compute $L^*_{\text{cons}}\pi$. Using $\pi = Z^{-1}e^{-\beta\mathcal{H}}$:

$$\nabla_q \pi = -\beta \nabla U\, \pi, \qquad \nabla_p \pi = -\beta \mathsf{M}^{-1} p\, \pi. \tag{B.24}$$

Then,

$$\begin{aligned} L^*_{\text{cons}}\pi &= -\mathsf{M}^{-1}p \cdot (-\beta \nabla U\, \pi) + \nabla U \cdot (-\beta \mathsf{M}^{-1} p\, \pi) \\ &= \beta(\mathsf{M}^{-1}p \cdot \nabla U)\pi - \beta(\nabla U \cdot \mathsf{M}^{-1}p)\pi \\ &= 0. \end{aligned} \tag{B.25}$$

The two terms cancel because $\mathsf{M}^{-1}p \cdot \nabla U = \nabla U \cdot \mathsf{M}^{-1}p$ (the dot product is commutative).

B.2.3. *Step 2: Verify That $L^*_{\text{diss}}\pi = 0$.* The formal Lebesgue adjoint of L_{diss} is

$$L^*_{\text{diss}}\rho = \nabla_p \cdot \left(\mathsf{G}\mathsf{M}^{-1}p\, \rho + k_B T \mathsf{G} \nabla_p \rho\right). \tag{B.26}$$

Then,

$$\begin{aligned} L^*_{\text{diss}}\pi &= \nabla_p \cdot \left(\mathsf{G}\mathsf{M}^{-1}p\, \pi + k_B T \mathsf{G} \nabla_p \pi\right) \\ &= \nabla_p \cdot \left(\mathsf{G}\mathsf{M}^{-1}p\, \pi - k_B T \beta \mathsf{G}\mathsf{M}^{-1}p\, \pi\right). \end{aligned} \tag{B.27}$$

Since $k_B T\beta = 1$,

$$\mathsf{G}\mathsf{M}^{-1}p\, \pi - k_B T\beta \mathsf{G}\mathsf{M}^{-1}p\, \pi = \mathsf{G}\mathsf{M}^{-1}p\, \pi - \mathsf{G}\mathsf{M}^{-1}p\, \pi = 0. \tag{B.28}$$

Therefore, $L^*_{\text{diss}}\pi = 0$.

Combining Steps 1 and 2, we have $L^*\pi = 0$, so π is invariant.

B.2.4. *Step 3: Verify Antisymmetry of L_{cons} in $L^2(\pi)$.* For $f, g \in \mathcal{C}_{\text{core}}$, consider $\langle f, L_{\text{cons}} g\rangle_\pi$. By integration by parts:

$$\begin{aligned} \langle f, L_{\text{cons}} g\rangle_\pi &= \int f \left(\mathsf{M}^{-1}p \cdot \nabla_q g - \nabla U \cdot \nabla_p g\right) \pi\, dq\, dp \\ &= \int f \mathsf{M}^{-1}p \cdot \nabla_q g\, \pi\, dq\, dp - \int f \nabla U \cdot \nabla_p g\, \pi\, dq\, dp. \end{aligned} \tag{B.29}$$

For the first term, integrate by parts in q:

$$\int f \mathsf{M}^{-1}p \cdot \nabla_q g\, \pi\, dq\, dp = -\int g \mathsf{M}^{-1}p \cdot \nabla_q (f\pi)\, dq\, dp. \tag{B.30}$$

Now $\nabla_q(f\pi) = \nabla_q f\, \pi + f\, \nabla_q \pi = \nabla_q f\, \pi - \beta f \nabla U\, \pi$. Thus,

$$\int f \mathsf{M}^{-1}p \cdot \nabla_q g\, \pi = -\int g \mathsf{M}^{-1}p \cdot \nabla_q f\, \pi\, dq\, dp + \beta \int g f \mathsf{M}^{-1}p \cdot \nabla U\, \pi\, dq\, dp. \tag{B.31}$$

For the second term, integrate by parts in p:

$$-\int f \nabla U \cdot \nabla_p g\, \pi\, dq\, dp = \int g \nabla U \cdot \nabla_p (f\pi)\, dq\, dp. \tag{B.32}$$

Now $\nabla_p(f\pi) = \nabla_p f\,\pi + f\nabla_p\pi = \nabla_p f\,\pi - \beta f \mathsf{M}^{-1}p\,\pi$. Thus,

$$-\int f\nabla U\cdot\nabla_p g\,\pi = \int g\nabla U\cdot\nabla_p f\,\pi\,dq\,dp - \beta\int gf\nabla U\cdot\mathsf{M}^{-1}p\,\pi\,dq\,dp. \tag{B.33}$$

Adding the two contributions, the β terms cancel exactly because

$$\mathsf{M}^{-1}p\cdot\nabla U = \nabla U\cdot\mathsf{M}^{-1}p. \tag{B.34}$$

Therefore,

$$\langle f, L_{\text{cons}}g\rangle_\pi = -\int g\mathsf{M}^{-1}p\cdot\nabla_q f\,\pi\,dq\,dp + \int g\nabla U\cdot\nabla_p f\,\pi\,dq\,dp = -\langle L_{\text{cons}}f, g\rangle_\pi. \tag{B.35}$$

Thus the formal weighted adjoint satisfies $L_{\text{cons}}^{\dagger_\pi} = -L_{\text{cons}}$ on these test functions. Equality of the closed operator domains is a separate requirement.

B.2.5. *Step 4: Verify Symmetry of L_{diss} in $L^2(\pi)$.* For $f, g \in \mathcal{C}_{\text{core}}$,

$$\langle f, L_{\text{diss}}g\rangle_\pi = \int f\left(-\mathsf{G}\mathsf{M}^{-1}p\cdot\nabla_p g + k_BT\mathsf{G}:\nabla_p^2 g\right)\pi\,dq\,dp. \tag{B.36}$$

The verification of symmetry follows from two integrations by parts in p, using the fact that π is Gaussian in p. The result is

$$\langle f, L_{\text{diss}}g\rangle_\pi = \langle L_{\text{diss}}f, g\rangle_\pi. \tag{B.37}$$

Thus L_{diss} is symmetric on the test domain. Its self-adjoint realization is the negative of the nonnegative operator associated with the closed dissipative form; symmetry of the test-domain expression alone does not establish self-adjointness.

B.2.6. *Step 5: Conclude.* On the common test domain the decomposition of the differential expression is uniquely determined by its formal weighted adjoint:

$$S_\pi = \frac{1}{2}(L + L^{\dagger_\pi}) = L_{\text{diss}}, \tag{B.38}$$

$$A_\pi = \frac{1}{2}(L - L^{\dagger_\pi}) = L_{\text{cons}}. \tag{B.39}$$

These identities concern restrictions to that domain. They do not assert that the adjoint of an arbitrary unbounded operator sum is the sum of the adjoints on their maximal domains.

B.3. *Existence, Uniqueness, and Global Attraction Are Distinct Questions.* This appendix clarifies the distinction between existence, uniqueness, and convergence to an invariant measure. These are separate mathematical properties that should not be conflated.

B.3.1. *Existence via Foster-Lyapunov Conditions.* Let the conservative Markov semigroup be Feller on a Polish state space, in the sense that P_t preserves bounded continuous functions. Take $V \geq 1$ with compact sublevel sets, finite $V(x)$, and enough extended-generator regularity and integrability to justify the stopped Dynkin formula and its limiting inequality. A Foster–Lyapunov

condition with $c > 0$ and $C \geq 0$ has the form

$$LV \leq -cV + C \tag{B.40}$$

Then Dynkin's formula gives, in the integrated sense or almost everywhere when the expectation is absolutely continuous,

$$\frac{d}{dt}\mathbb{E}_x[V(X_t)] \leq -c\mathbb{E}_x[V(X_t)] + C. \tag{B.41}$$

By Gronwall's inequality,

$$\mathbb{E}_x[V(X_t)] \leq e^{-ct}V(x) + \frac{C}{c}(1 - e^{-ct}). \tag{B.42}$$

For $\bar{\nu}_T = T^{-1}\int_0^T P_t(x,\cdot)\,dt$, integration of the drift inequality gives

$$\bar{\nu}_T(V) \leq \frac{V(x)}{cT} + \frac{C}{c}, \qquad \bar{\nu}_T\{V > R\} \leq \frac{V(x)/(cT) + C/c}{R}.$$

Thus the averages are tight as $T \to \infty$. Let a subsequence converge weakly to π. For bounded continuous f and fixed $s > 0$,

$$|\bar{\nu}_T(P_s f) - \bar{\nu}_T(f)| \leq \frac{2s\|f\|_\infty}{T}.$$

The Feller property permits passage to the weak limit in both terms, giving $\pi P_s = \pi$. This supplies the invariance step in the Krylov–Bogoliubov argument; tightness by itself would not identify an invariant limit.

B.3.2. *Uniqueness via Strong Feller and Irreducibility.* Uniqueness of the invariant measure can follow from:

1. **Strong Feller property.** The semigroup maps bounded measurable functions to continuous functions.
2. **Irreducibility.** For every nonempty open set O and every initial condition x, there exists $t > 0$ such that $\mathbb{P}_x(X_t \in O) > 0$.

Under these conditions there is at most one invariant probability. Its existence must still be established independently, for example by the preceding argument.

B.3.3. *Convergence Requires Additional Mixing.* Uniqueness alone does not guarantee convergence from every initial distribution. The following are distinct sufficient routes, each with its own initial-law class and norm:

1. **Aperiodic positive Harris recurrence.** For a skeleton chain, this gives total-variation convergence on the stated Harris class. A geometric rate requires additional quantitative drift and minorization conditions [71].
2. **A coercive L^2 estimate.** If $-\operatorname{Re}\langle f, Lf\rangle_\pi \geq \lambda\|f\|^2_{L^2(\pi)}$ for mean-zero functions in the generator domain, with $\lambda > 0$, differentiation of $\|P_t f\|_2^2$ and Gronwall's inequality give $\|P_t f\|_2 \leq e^{-\lambda t}\|f\|_2$. The statement is initially about the L^2 class, not arbitrary singular initial laws.

3. **Hypocoercive decay.** A modified functional comparable to a declared norm and satisfying $\mathcal{H}'(t) \leq -\lambda\mathcal{H}(t)$ gives decay in that norm. Smoothing or a commutator condition without the accompanying coercive estimates does not supply this conclusion.

Recurrence alone cannot replace the aperiodicity hypothesis. For the two-state discrete-time kernel $P = \left(\begin{smallmatrix} 0 & 1 \\ 1 & 0 \end{smallmatrix}\right)$, the unique stationary law is $(1/2, 1/2)$ and both states recur infinitely often. Nevertheless $P^{2n} = I$, $P^{2n+1} = P$, and the law from either fixed initial state remains at total-variation distance $1/2$ from stationarity. Thus existence, uniqueness, recurrence and convergence require separate arguments.

B.4. *Why LSI Does Not Mean Ultracontractivity.* This appendix clarifies the relationship between logarithmic Sobolev inequalities and ultracontractivity. These are distinct functional inequalities with different implications.

B.4.1. *Logarithmic Sobolev Inequality.* A logarithmic Sobolev inequality (LSI) is of the form

$$\mathrm{Ent}_\mu(g^2) \leq \frac{2}{\rho}\mathcal{E}_{S,\mu}(g, g). \tag{B.43}$$

It implies:

1. **Hypercontractivity.** The semigroup P_t satisfies

$$\|P_t f\|_{L^p(\mu)} \leq \|f\|_{L^q(\mu)} \tag{B.44}$$

for suitable $p > q$ and t large enough.

2. **Exponential decay of relative entropy.** In the compatible convention, $D(f_t\mu\|\mu) \leq e^{-2\rho t} D(f_0\mu\|\mu)$.

B.4.2. *Ultracontractivity.* Ultracontractivity is the stronger property

$$P_t : L^1(\mu) \to L^\infty(\mu) \tag{B.45}$$

for $t > 0$. This means that the semigroup instantly smooths any integrable function to a bounded function. This is much stronger than hypercontractivity.

B.4.3. *Counterexample: Ornstein-Uhlenbeck Semigroup.* The Gaussian Ornstein–Uhlenbeck semigroup satisfies Gross's LSI [41] but is not ultracontractive in the invariant-measure scale. Its hypercontractive bound relates $L^p(\mu)$ and $L^q(\mu)$ for $p > 1$ and the appropriate relation between p, q, and time. It does not imply a bounded $L^1(\mu)$-to-$L^q(\mu)$ map for arbitrary $q > 1$ at finite positive time.

For example, the Mehler kernel's $L^q(\mu)$ norm at a fixed source point becomes unbounded as that source point tends to infinity, for every $q > 1$ and finite time. An LSI therefore does not imply ultracontractivity. On a compact domain, appropriate ellipticity and heat-kernel bounds can instead provide ultracontractivity; those are separate hypotheses.

Appendix C. Infinite-Dimensional Geometry and Fluid Estimates

The first argument concerns reference measures in infinite dimensions; the second gives the two-dimensional bilinear estimate used in the fluid equation. Their assumptions and conclusions are independent.

C.1. *Detailed Proof of the Infinite-Dimensional No-Lebesgue Theorem.* This appendix provides the complete proof of the non-existence of a nonzero locally finite translation-invariant Borel measure on an infinite-dimensional separable Banach space. The proof is broken into five steps, with each step fully justified. A preliminary geometric lemma is also proved.

C.1.1. *Preliminary Lemma: Infinitely Many Disjoint Balls.*

Lemma Statement. Let X be an infinite-dimensional normed space. For every open ball $B \subset X$ of radius $R > 0$, there exists a sequence of pairwise disjoint open balls $\{B_n\}_{n=1}^{\infty}$ such that:

1. All B_n have the same radius $r > 0$.
2. $B_n \subset B$ for every $n \in \mathbb{N}$.

Proof of the Lemma.

Step 1: Construct infinitely many separated unit vectors. Choose any unit vector $u_1 \in X$ with $\|u_1\| = 1$. Since X is infinite-dimensional, the subspace $Y_1 := \operatorname{span}\{u_1\}$ is a proper closed subspace.

By Riesz's lemma [90], there exists a unit vector $u_2 \in X$ such that

$$\|u_2 - y\| \geq \frac{1}{2} \quad \text{for all } y \in Y_1. \tag{C.1}$$

In particular, $\|u_2 - u_1\| \geq \frac{1}{2}$. The non-strict estimate is sufficient for the disjointness argument below.

Now suppose $u_1, \ldots, u_n$ have been constructed with pairwise distances at least $\frac{1}{2}$. Let $Y_n := \operatorname{span}\{u_1, \ldots, u_n\}$, a finite-dimensional, hence closed, proper subspace. By Riesz's lemma again, there exists a unit vector $u_{n+1} \in X$ such that

$$\|u_{n+1} - y\| \geq \frac{1}{2} \quad \text{for all } y \in Y_n. \tag{C.2}$$

Thus, $\|u_{n+1} - u_k\| \geq \frac{1}{2}$ for each $k = 1, \ldots, n$. By induction, we obtain a sequence $(u_n)_{n=1}^{\infty}$ of unit vectors satisfying

$$\|u_n - u_m\| \geq \frac{1}{2} \quad \text{for all } n \neq m. \tag{C.3}$$

Step 2: Scale and center the balls. Let $B = B(x_0, R)$ be the given open ball. Define

$$x_n := x_0 + \frac{R}{2} u_n, \qquad r := \frac{R}{8}. \tag{C.4}$$

Then each x_n lies in B since

$$\|x_n - x_0\| = \frac{R}{2}\|u_n\| = \frac{R}{2} < R. \tag{C.5}$$

Consider the open balls $B_n := B(x_n, r)$. For $n \neq m$,

$$\|x_n - x_m\| = \frac{R}{2}\|u_n - u_m\| \geq \frac{R}{2} \cdot \frac{1}{2} = \frac{R}{4} = 2r. \tag{C.6}$$

Hence $B_n \cap B_m = \emptyset$, since if there were a point $z \in B_n \cap B_m$, the triangle inequality would give

$$\|x_n - x_m\| \leq \|x_n - z\| + \|z - x_m\| < r + r = 2r, \tag{C.7}$$

contradicting $\|x_n - x_m\| \geq 2r$.

Step 3: Verify containment in B. For any $y \in B_n$,

$$\|y - x_0\| \leq \|y - x_n\| + \|x_n - x_0\| < r + \frac{R}{2} = \frac{R}{8} + \frac{R}{2} = \frac{5R}{8} < R. \tag{C.8}$$

Thus, $y \in B$. Therefore, $B_n \subset B$ for every n. This completes the proof of the lemma.

C.1.2. *The Main Theorem.*

Theorem Statement. Let X be an infinite-dimensional separable Banach space. There is no nonzero locally finite translation-invariant Borel measure on X.

Proof. Assume for contradiction that λ is a nonzero locally finite translation-invariant Borel measure on X.

Step 1: Existence of a finite-measure ball. Since λ is locally finite, for each point there exists an open neighbourhood of finite measure. The family of all such finite-measure neighbourhoods covers X. Because X is separable and hence Lindelof, there is a countable subcover $\{U_j\}_{j\geq 1}$ with $\lambda(U_j) < \infty$ for every j. Since λ is nonzero, at least one such set, say U_{j_0}, has positive measure. A separable metric space has a countable base of open balls; therefore U_{j_0} is the countable union of basis balls contained in U_{j_0}. If all those balls had zero measure, countable subadditivity would give $\lambda(U_{j_0}) = 0$, a contradiction. Hence there is an open ball $B(x_0, R) \subset U_{j_0}$ with

$$0 < \lambda(B(x_0, R)) < \infty. \tag{C.9}$$

By translation invariance, the translated ball $B(0, R) = B(x_0, R) - x_0$ also satisfies

$$0 < \lambda(B(0, R)) < \infty. \tag{C.10}$$

This is the finite positive reference ball used in the contradiction.

Step 2: Every positive-radius ball has positive measure. We claim that for every $r > 0$,

$$\lambda(B(0, r)) > 0. \tag{C.11}$$

Suppose to the contrary that $\lambda(B(0, r)) = 0$ for some $r > 0$. Since X is separable, there exists a countable dense set $\{z_j\}_{j=1}^{\infty} \subset X$. Then

$$X = \bigcup_{j=1}^{\infty} B(z_j, r). \tag{C.12}$$

By translation invariance, $\lambda(B(z_j, r)) = \lambda(B(0, r)) = 0$ for every j. By countable subadditivity,

$$\lambda(X) \leq \sum_{j=1}^{\infty} \lambda(B(z_j, r)) = 0, \tag{C.13}$$

contradicting non-triviality. Hence the claim holds.

Step 3: Apply the geometric lemma. By the preliminary lemma applied to the ball $B(0, R)$, there exists a sequence of pairwise disjoint open balls $\{B_n\}_{n=1}^{\infty}$, all of the same radius $r > 0$, such that

$$B_n \subset B(0, R) \quad \text{for all } n. \tag{C.14}$$

By translation invariance,

$$\lambda(B_n) = \lambda(B(0, r)) =: c > 0, \tag{C.15}$$

where the positivity follows from Step 2.

Step 4: Countable additivity yields the contradiction. Since the balls B_n are pairwise disjoint,

$$\lambda\left(\bigcup_{n=1}^{\infty} B_n\right) = \sum_{n=1}^{\infty} \lambda(B_n) = \sum_{n=1}^{\infty} c = \infty. \tag{C.16}$$

But $\bigcup_{n=1}^{\infty} B_n \subset B(0, R)$, so by monotonicity,

$$\lambda(B(0, R)) \geq \lambda\left(\bigcup_{n=1}^{\infty} B_n\right) = \infty, \tag{C.17}$$

contradicting the finite measure of $B(0, R)$ from Step 1.

Therefore, no such measure exists.

C.1.3. *Corollary: Consequences for Infinite-Dimensional Analysis.* The theorem has the following consequences:

1. **No analogue of Lebesgue measure.** In an infinite-dimensional separable Banach space, there is no locally finite translation-invariant measure. Thus, one cannot define a "Lebesgue measure" on such spaces.
2. **No densities with respect to a flat measure.** Since no reference measure of Lebesgue type exists, one cannot define probability densities with respect to a flat measure on the full space.
3. **Gaussian and Gibbs measures.** Instead of a flat Lebesgue measure, one must use Gaussian measures, such as the Wiener measure on path space, or Gibbs measures of the form $d\mu = Z^{-1}e^{-\Phi}d\gamma$, where γ is a Gaussian reference measure.
4. **Poincare recurrence is unaffected.** The non-existence of Lebesgue measure is not the reason for the absence of Poincare recurrence. Poincare recurrence depends only on the existence of a finite invariant measure, not on the existence of a Lebesgue measure.

C.2. *Detailed Two-Dimensional Navier-Stokes Bilinear Estimate.* This appendix provides the detailed derivation of the bilinear estimate for the convective term in the two-dimensional Navier-Stokes equations.

C.2.1. *Setup: Trilinear Form.* For divergence-free functions u, v, w, define

$$b(u, v, w) := \int_{\mathbb{T}^2} (u \cdot \nabla) v \cdot w \, dx. \tag{C.18}$$

We aim to prove that for $u, v, w \in V = H^1_{\sigma,0}(\mathbb{T}^2; \mathbb{R}^2)$,

$$|b(u, v, w)| \leq C \|u\|_V \|v\|_V \|w\|_V . \tag{C.19}$$

C.2.2. *Step 1: Hölder's Inequality.* By Hölder's inequality,

$$|b(u, v, w)| \leq \|u\|_{L^4} \|\nabla v\|_{L^2} \|w\|_{L^4}. \tag{C.20}$$

C.2.3. *Step 2: Ladyzhenskaya Inequality in 2D.* In two dimensions, the Ladyzhenskaya inequality states that there exists a constant C such that for all $z \in H^1(\mathbb{T}^2)$,

$$\|z\|_{L^4} \leq C \|z\|_{L^2}^{1/2} \|\nabla z\|_{L^2}^{1/2}. \tag{C.21}$$

Applying this to u and w:

$$\|u\|_{L^4} \leq C \|u\|_{L^2}^{1/2} \|\nabla u\|_{L^2}^{1/2}, \tag{C.22}$$

$$\|w\|_{L^4} \leq C \|w\|_{L^2}^{1/2} \|\nabla w\|_{L^2}^{1/2}. \tag{C.23}$$

C.2.4. *Step 3: Combine the Estimates.* Substituting these bounds into the Hölder estimate:

$$|b(u, v, w)| \leq C \|u\|_{L^2}^{1/2} \|\nabla u\|_{L^2}^{1/2} \|\nabla v\|_{L^2} \|w\|_{L^2}^{1/2} \|\nabla w\|_{L^2}^{1/2}. \tag{C.24}$$

C.2.5. *Step 4: Use Poincare's Inequality.* On the mean-zero torus, Poincare's inequality gives

$$\|u\|_{L^2} \leq C \|\nabla u\|_{L^2}, \qquad \|w\|_{L^2} \leq C \|\nabla w\|_{L^2}. \tag{C.25}$$

Therefore,

$$|b(u, v, w)| \leq C \|\nabla u\|_{L^2} \|\nabla v\|_{L^2} \|\nabla w\|_{L^2}. \tag{C.26}$$

In the notation $\|\cdot\|_V = \|\nabla \cdot\|_{L^2}$,

$$|b(u, v, w)| \leq C \|u\|_V \|v\|_V \|w\|_V . \tag{C.27}$$

C.2.6. *Step 5: Conclude Continuity.* The estimate shows that for fixed $u, v \in V$, the map $w \mapsto b(u, v, w)$ is continuous on V with respect to the V-norm. Therefore, there exists an element $B(u, v) \in V^*$ such that

$$\langle B(u, v), w \rangle_{V^*, V} = b(u, v, w). \tag{C.28}$$

Thus, $B(u, v) \in V^*$ for $u, v \in V$.

Appendix D. Perturbation Expansion for the Driven Ring

This appendix provides the detailed perturbation expansion for the periodically driven ring model, including the first-order density correction and the second-order entropy production change.

D.1. *Setup: The Perturbed Equation.* The stochastic differential equation on the ring is

$$dX_t = [b + \varepsilon_r \sin(kX_t)]\,dt + \sqrt{2D}\,dW_t \pmod{L}. \tag{D.1}$$

The perturbation is single-valued on the ring only when the wave number is compatible with the circumference:

$$k = \frac{2\pi n}{L} \quad \text{for some integer } n \geq 1. \tag{D.2}$$

The stationary density is expanded as

$$\rho_{\varepsilon_r}(x) = \pi_0 + \varepsilon_r \rho_1(x) + \varepsilon_r^2 \rho_2(x) + O(\varepsilon_r^3), \tag{D.3}$$

where $\pi_0 = 1/L$ is the unperturbed stationary density.

The stationary current is expanded as

$$J_{\varepsilon_r}(x) = J_0 + \varepsilon_r J_1(x) + \varepsilon_r^2 J_2(x) + O(\varepsilon_r^3), \tag{D.4}$$

where $J_0 = b/L$ is the unperturbed stationary current.

D.2. *Step 1: First-Order Stationary Equation.* The Fokker-Planck equation in stationary form is $\nabla \cdot J = 0$, i.e., J is constant. The current is

$$J = b\rho + \varepsilon_r \sin(kx)\rho - D\rho'. \tag{D.5}$$

At first order in ε_r:

$$J_1 = b\rho_1 + \pi_0 \sin(kx) - D\rho_1'. \tag{D.6}$$

Since J_1 is constant, integrating Equation (D.6) over one period gives

$$LJ_1 = b\int_0^L \rho_1(x)\,dx + \pi_0 \int_0^L \sin(kx)\,dx - D\int_0^L \rho_1'(x)\,dx. \tag{D.7}$$

The first integral is zero because the expansion preserves the normalization of the probability density order by order, the second integral is zero by Equation (D.2), and the third integral is zero by periodicity. Hence $J_1 = 0$. Thus,

$$b\rho_1 + \pi_0 \sin(kx) - D\rho_1' = 0. \tag{D.8}$$

This is the first-order stationarity equation.

D.3. *Step 2: Solve the First-Order Equation.* Assume a solution of the form

$$\rho_1(x) = C_1 \cos(kx) + C_2 \sin(kx). \tag{D.9}$$

Then

$$\rho_1'(x) = -kC_1 \sin(kx) + kC_2 \cos(kx). \tag{D.10}$$

Substituting into the first-order equation:

$$b(C_1 \cos + C_2 \sin) + \pi_0 \sin - D(-kC_1 \sin + kC_2 \cos) = 0. \tag{D.11}$$

Collecting coefficients of $\cos(kx)$ and $\sin(kx)$:

$$\cos: \quad bC_1 - DkC_2 = 0, \tag{D.12}$$

$$\sin: \quad bC_2 + \pi_0 + DkC_1 = 0. \tag{D.13}$$

Solving this linear system:

$$C_1 = -\frac{\pi_0 Dk}{b^2 + D^2k^2}, \qquad C_2 = -\frac{\pi_0 b}{b^2 + D^2k^2}. \tag{D.14}$$

Therefore,

$$\rho_1(x) = -\frac{\pi_0}{b^2 + D^2k^2} \left[Dk \cos(kx) + b \sin(kx) \right]. \tag{D.15}$$

D.4. *Step 3: Entropy Production Functional.* The total entropy production is

$$\Sigma_{\varepsilon_r} = \int_0^L \frac{J_{\varepsilon_r}^2}{D\rho_{\varepsilon_r}} \, dx. \tag{D.16}$$

Expand the reciprocal density:

$$\frac{1}{\rho_{\varepsilon_r}} = \frac{1}{\pi_0 + \varepsilon_r \rho_1 + \varepsilon_r^2 \rho_2 + O(\varepsilon_r^3)} = \frac{1}{\pi_0} - \varepsilon_r \frac{\rho_1}{\pi_0^2} + \varepsilon_r^2 \left(\frac{\rho_1^2}{\pi_0^3} - \frac{\rho_2}{\pi_0^2} \right) + O(\varepsilon_r^3). \tag{D.17}$$

Also,

$$J_{\varepsilon_r}^2 = J_0^2 + 2\varepsilon_r J_0 J_1 + \varepsilon_r^2 (J_1^2 + 2J_0 J_2) + O(\varepsilon_r^3). \tag{D.18}$$

Since $J_1 = 0$, this simplifies to

$$J_{\varepsilon_r}^2 = J_0^2 + 2\varepsilon_r^2 J_0 J_2 + O(\varepsilon_r^3). \tag{D.19}$$

D.5. *Step 4: Compute the Second-Order Entropy Production Change.* Substituting into the entropy production functional:

$$\Sigma_{\varepsilon_r} = \int_0^L \frac{1}{D} \left(J_0^2 + 2\varepsilon_r^2 J_0 J_2 + O(\varepsilon_r^3) \right) \left(\frac{1}{\pi_0} - \varepsilon_r \frac{\rho_1}{\pi_0^2} + \varepsilon_r^2 \left(\frac{\rho_1^2}{\pi_0^3} - \frac{\rho_2}{\pi_0^2} \right) + O(\varepsilon_r^3) \right) dx. \tag{D.20}$$

The first-order term vanishes because $\int \rho_1 \, dx = 0$. Here $\Delta\Sigma^{(2)}$ denotes the second-order contribution, rather than the full finite-perturbation difference. For fixed $D, L > 0$ and a nonzero allowed wave number, translation by π/k changes ε_r to $-\varepsilon_r$, so the exact stationary rate is even in ε_r. Its analytic quadrature therefore gives $\Sigma_{\varepsilon_r} - \Sigma_0 = \Delta\Sigma^{(2)} + O(\varepsilon_r^4)$. The second-order contribution is

$$\Delta\Sigma^{(2)} = \frac{\varepsilon_r^2}{D} \int_0^L \left[\frac{2J_0 J_2}{\pi_0} + \frac{J_0^2 \rho_1^2}{\pi_0^3} - \frac{J_0^2 \rho_2}{\pi_0^2} \right] dx. \tag{D.21}$$

The term involving ρ_2 integrates to zero because ρ_2 has zero mean by normalization. Using $J_0 = b/L$ and $\pi_0 = 1/L$, the remaining two contributions are

$$\Delta\Sigma^{(2)} = \frac{\varepsilon_r^2}{D}\left[2bLJ_2 + b^2L\int_0^L \rho_1^2\,dx\right]. \tag{D.22}$$

The second-order current is determined by averaging the order-ε_r^2 stationarity equation

$$J_2 = b\rho_2 + \sin(kx)\rho_1 - D\rho_2'. \tag{D.23}$$

Since $\int_0^L \rho_2\,dx = 0$ and $\int_0^L \rho_2'\,dx = 0$, this gives

$$J_2 = \frac{1}{L}\int_0^L \sin(kx)\rho_1(x)\,dx = -\frac{b}{2L(b^2 + D^2k^2)}. \tag{D.24}$$

Using the explicit form of ρ_1:

$$\begin{aligned}\int_0^L \rho_1^2\,dx &= \frac{\pi_0^2}{(b^2 + D^2k^2)^2}\int_0^L \left[Dk\cos(kx) + b\sin(kx)\right]^2\,dx \\ &= \frac{1}{L^2(b^2 + D^2k^2)^2}\cdot\frac{L}{2}(b^2 + D^2k^2) \\ &= \frac{1}{2L(b^2 + D^2k^2)}.\end{aligned} \tag{D.25}$$

Therefore,

$$\begin{aligned}\Delta\Sigma^{(2)} &= \frac{\varepsilon_r^2}{D}\left[2bL\left(-\frac{b}{2L(b^2 + D^2k^2)}\right) + b^2L\frac{1}{2L(b^2 + D^2k^2)}\right] \\ &= -\frac{b^2\varepsilon_r^2}{2D(b^2 + D^2k^2)}.\end{aligned} \tag{D.26}$$

For $b \neq 0$, the baseline $\Sigma_0 = b^2/D$ is positive and the relative second-order correction is

$$\frac{|\Delta\Sigma^{(2)}|}{\Sigma_0} = \frac{\varepsilon_r^2}{2(b^2 + D^2k^2)}. \tag{D.27}$$

At $b = 0$, both the exact stationary rate and its correction are zero; the ratio in Equation (D.27) is then undefined. At $k = 0$, the perturbation is identically zero and all its current corrections vanish; the nonzero-mode coefficient formulas must not be used.

Use of AI tools

OpenAI's ChatGPT assisted with mathematical exposition, selected computational calculations and scripts, language editing, and LaTeX preparation. DeepSeek was used for language polishing and revision of selected passages. The author checked all mathematical statements, computational results, citations, and final typeset files and assumes full responsibility for the content of this manuscript.

References

[1] S. Adams, N. Dirr, M. A. Peletier, and J. Zimmer, "From a Large-Deviations Principle to the Wasserstein Gradient Flow: A New Micro-Macro Passage," *Communications in Mathematical Physics* **307** (2011), 791–815. DOI: 10.1007/s00220-011-1328-4.

[2] D. Anselmi, Fakeons and Lee–Wick models, *Journal of High Energy Physics* **02** (2018), 141. https://doi.org/10.1007/JHEP02(2018)141.

[3] D. Anselmi and M. Piva, Quantum gravity, fakeons and microcausality, *Journal of High Energy Physics* **11** (2018), 021. https://doi.org/10.1007/JHEP11(2018)021.

[4] J. Armstrong, D. Brigo, and E. Ferrucci, Projections of SDEs onto submanifolds, *Information Geometry* **7**, Suppl. 1 (2024), S397–S427. https://doi.org/10.1007/s41884-022-00093-7.

[5] D. G. Aronson, "Bounds for the fundamental solution of a parabolic equation," *Bulletin of the American Mathematical Society*, vol. 73, pp. 890–896, 1967.

[6] D. Bakry and M. Émery, "Diffusions hypercontractives," in *Séminaire de Probabilités XIX*, Lecture Notes in Mathematics, vol. 1123, pp. 177–206, Springer, 1985.

[7] D. Bakry, I. Gentil, and M. Ledoux, *Analysis and Geometry of Markov Diffusion Operators*. Springer, 2014.

[8] J. Bellorin, C. Bórquez, and B. Droguett, Batalin–Fradkin–Vilkovisky quantization of quadratic gravity, *Physical Review D* **113** (2026), 106006. https://doi.org/10.1103/c22r-2v5h.

[9] R. Bluhm and V. A. Kostelecký, Spontaneous Lorentz violation, Nambu–Goldstone modes, and gravity, *Physical Review D* **71** (2005), 065008. https://doi.org/10.1103/PhysRevD.71.065008.

[10] S. G. Bobkov and P. Tetali, "Modified logarithmic Sobolev inequalities in discrete settings," *Journal of Theoretical Probability*, vol. 19, no. 2, pp. 289–336, 2006. doi: 10.1007/s10959-006-0016-3.

[11] V. I. Bogachev, *Gaussian Measures*, Mathematical Surveys and Monographs, vol. 62. American Mathematical Society, 1998.

[12] L. Boltzmann, "Weitere Studien über das Wärmegleichgewicht unter Gasmolekülen," *Sitzungsberichte der Kaiserlichen Akademie der Wissenschaften*, vol. 66, pp. 275–370, 1872.

[13] H. B. Callen and T. A. Welton, "Irreversibility and generalized noise," *Physical Review*, vol. 83, pp. 34–40, 1951.

[14] P. Caputo, P. Dai Pra, and G. Posta, "Convex entropy decay via the Bochner–Bakry–Emery approach," *Annales de l'Institut Henri Poincaré, Probabilités et Statistiques*, vol. 45, no. 3, pp. 734–753, 2009. doi: 10.1214/08-AIHP183.

[15] P. Cattiaux, G. Conforti, I. Gentil, and C. Léonard, "Time reversal of diffusion processes under a finite entropy condition," *Annales de l'Institut Henri Poincaré, Probabilités et Statistiques*, vol. 59, no. 4, pp. 1844–1881, 2023. doi: 10.1214/22-AIHP1320.

[16] T. Christodoulakis and J. Zanelli, Operator ordering in quantum mechanics and quantum gravity, *Nuovo Cimento B* **93** (1986), 1–21. https://doi.org/10.1007/BF02728299.

[17] T. Christodoulakis and J. Zanelli, Consistent algebra for the constraints of quantum gravity, *Nuovo Cimento B* **93** (1986), 22–35. https://doi.org/10.1007/BF02728300.

[18] R. Clausius, "Über die bewegende Kraft der Wärme und die Gesetze, welche sich daraus für die Wärmelehre selbst ableiten lassen," *Annalen der Physik*, vol. 79, pp. 368–397 and 500–524, 1850.

[19] J. Coe, M. Hairer, and L. Tolomeo, "Quasi-Gaussianity of the 2D stochastic Navier-Stokes equations," arXiv:2510.13460, 2025.

[20] G. E. Crooks, "Entropy production fluctuation theorem and the nonequilibrium work relation for free energy differences," *Physical Review E*, vol. 60, pp. 2721–2726, 1999. doi: 10.1103/PhysRevE.60.2721.

[21] L. Da Costa and G. A. Pavliotis, "The entropy production of stationary diffusions," *Journal of Physics A: Mathematical and Theoretical*, vol. 56, no. 36, 365001, 2023. doi: 10.1088/1751-8121/acdf98.

[22] G. Da Prato and J. Zabczyk, *Stochastic Equations in Infinite Dimensions*. Cambridge University Press, 1992.

[23] G. Da Prato and J. Zabczyk, *Ergodicity for Infinite Dimensional Systems*. Cambridge University Press, 1996.

[24] F. C. De Vecchi, E. Mastrogiacomo, M. Turra, and S. Ugolini, Noether theorem in stochastic optimal control problems via contact symmetries, *Mathematics* **9** (2021), 953. DOI: 10.3390/math9090953.

[25] M. Ding and M. E. Cates, "Hamiltonian Heat Baths, Coarse-Graining and Irreversibility: A Microscopic Dynamical Entropy from Classical Mechanics," arXiv:2503.11334v1 (2025). https://arxiv.org/abs/2503.11334v1.

[26] M. Doi, "Onsager's variational principle in soft matter," *Journal of Physics: Condensed Matter*, vol. 23, no. 28, 284118, 2011. doi: 10.1088/0953-8984/23/28/284118.

[27] M. H. Duong, A. Lamacz, M. A. Peletier, A. Schlichting, and U. Sharma, "Quantification of coarse-graining error in Langevin and overdamped Langevin dynamics," *Nonlinearity* **31** (2018), 4517–4566. DOI: 10.1088/1361-6544/aaced5.

[28] M. Erbar, "Gradient flows of the entropy for jump processes," *Annales de l'Institut Henri Poincaré, Probabilités et Statistiques*, vol. 50, no. 3, pp. 920–945, 2014. doi: 10.1214/12-AIHP537.

[29] P. Español, "Embedding memory in coarse-grained Hamiltonian systems," *Physical Review Research*, vol. 8, 033133, 2026. doi: 10.1103/dlzj-gtx3.

[30] M. Esposito and C. Van den Broeck, "Three faces of the second law. I. Master equation formulation," *Physical Review E*, vol. 82, 011143, 2010. doi: 10.1103/PhysRevE.82.011143.

[31] Y. Etzioni, B. Horovitz, and P. Le Doussal, "Rings and Coulomb boxes in dissipative environments," *Physical Review B* **86** (2012), 235406. DOI: 10.1103/PhysRevB.86.235406.

[32] G. W. Ford, M. Kac, and P. Mazur, "Statistical Mechanics of Assemblies of Coupled Oscillators," *Journal of Mathematical Physics*, vol. 6, pp. 504–515, 1965. doi: 10.1063/1.1704304.

[33] M. I. Freidlin and A. D. Wentzell, *Random Perturbations of Dynamical Systems*, 3rd ed. Springer, 2012.

[34] M. Fukushima, Y. Oshima, and M. Takeda, *Dirichlet Forms and Symmetric Markov Processes*, 2nd revised and extended ed. De Gruyter, 2011.

[35] Q. Gao, H.-M. Chun, and J. M. Horowitz, "Thermodynamic constraints on the nonequilibrium response of one-dimensional diffusions," *Physical Review E*, vol. 105, L012102, 2022. doi: 10.1103/PhysRevE.105.L012102.

[36] I. V. Girsanov, On transforming a certain class of stochastic processes by absolutely continuous substitution of measures, *Theory of Probability and Its Applications* **5** (1960), 285–301. doi:10.1137/1105027.

[37] D. Giulini and D. Marolf, A uniqueness theorem for constraint quantization, *Class. Quantum Grav.* **16** (1999), 2489–2505. https://doi.org/10.1088/0264-9381/16/7/322.

[38] S. Goldstein and J. L. Lebowitz, "On the (Boltzmann) entropy of non-equilibrium systems," *Physica D* **193** (2004), 53–66. DOI: 10.1016/j.physd.2004.01.008.

[39] M. Grmela and H. C. Öttinger, "Dynamics and thermodynamics of complex fluids. I. Development of a general formalism," *Physical Review E*, vol. 56, pp. 6620–6632, 1997. doi: 10.1103/PhysRevE.56.6620.

[40] L. Gross, "Abstract Wiener spaces," in *Proceedings of the Fifth Berkeley Symposium on Mathematical Statistics and Probability*, vol. II, part 1, pp. 31–42, University of California Press, 1967.

[41] L. Gross, "Logarithmic Sobolev inequalities," *American Journal of Mathematics*, vol. 97, no. 4, pp. 1061–1083, 1975.

[42] M. Hairer and J. C. Mattingly, "Ergodicity of the 2D Navier-Stokes equations with degenerate stochastic forcing," *Annals of Mathematics*, vol. 164, no. 3, pp. 993–1032, 2006.

[43] M. Hairer and J. C. Mattingly, "A theory of hypoellipticity and unique ergodicity for semilinear stochastic PDEs," *Electronic Journal of Probability*, vol. 16, pp. 658–738, 2011.

[44] D. Hartich and A. Godec, "Violation of local detailed balance upon lumping despite a clear timescale separation," *Physical Review Research*, vol. 5, L032017, 2023. doi: 10.1103/PhysRevResearch.5.L032017.

[45] U. G. Haussmann and E. Pardoux, "Time reversal of diffusions," *The Annals of Probability*, vol. 14, no. 4, pp. 1188–1205, 1986. doi: 10.1214/aop/1176992362.

[46] P. A. Höhn, A. R. H. Smith, and M. P. E. Lock, Trinity of relational quantum dynamics, *Phys. Rev. D* **104** (2021), 066001. https://doi.org/10.1103/PhysRevD.104.066001.

[47] R. Holley and D. W. Stroock, "Logarithmic Sobolev inequalities and stochastic Ising models," *Journal of Statistical Physics*, vol. 46, pp. 1159–1194, 1987.

[48] S. Hottovy, A. McDaniel, G. Volpe, and J. Wehr, "The Smoluchowski–Kramers Limit of Stochastic Differential Equations with Arbitrary State-Dependent Friction," *Communications in Mathematical Physics*, vol. 336, pp. 1259–1283, 2015. doi: 10.1007/s00220-014-2233-4.

[49] S. Hu, *Stationary Action and Effective Equilibrium on the Moduli Space of Static Schwarzschild Exteriors: Singularity Diagnostics and Identification Limits*, unpublished manuscript, revised October 25, 2026.

[50] S. Hu, *A Finite-Regulator Variational–Stochastic Programme: Geometry, Gauge Fields, Matter, and the Arrow of Time*, unpublished manuscript, revised October 25, 2026.

[51] C. Jarzynski, "Nonequilibrium equality for free energy differences," *Physical Review Letters*, vol. 78, pp. 2690–2693, 1997. doi: 10.1103/PhysRevLett.78.2690.

[52] R. Jordan, D. Kinderlehrer, and F. Otto, "The variational formulation of the Fokker-Planck equation," *SIAM Journal on Mathematical Analysis*, vol. 29, no. 1, pp. 1–17, 1998. doi: 10.1137/S0036141096303359.

[53] R. E. Kalman and R. S. Bucy, New results in linear filtering and prediction theory, *Journal of Basic Engineering* **83** (1961), 95–108. doi:10.1115/1.3658902.

[54] A. Kolchinsky, A. Dechant, K. Yoshimura, and S. Ito, "Generalized free energy and excess/housekeeping decomposition in nonequilibrium systems: From large deviations to thermodynamic speed limits," *Physical Review Research*, vol. 8, 023025, 2026. doi: 10.1103/r48t-dghl.

[55] R. Kraaij, A. Lazarescu, C. Maes, and M. A. Peletier, "Deriving GENERIC from a Generalized Fluctuation Symmetry," *Journal of Statistical Physics* **170** (2018), 492–508. DOI: 10.1007/s10955-017-1941-5.

[56] R. Kubo, "The fluctuation-dissipation theorem," *Reports on Progress in Physics*, vol. 29, pp. 255–284, 1966.

[57] K. Kuwae and T. Shioya, Convergence of spectral structures: a functional analytic theory and its applications to spectral geometry, *Communications in Analysis and Geometry* **11** (2003), 599–673. https://doi.org/10.4310/CAG.2003.v11.n4.a1.

[58] D. Langlois and K. Noui, Hamiltonian analysis of higher derivative scalar-tensor theories, *Journal of Cosmology and Astroparticle Physics* **07** (2016), 016. https://doi.org/10.1088/1475-7516/2016/07/016.

[59] J. C. Latorre, G. A. Pavliotis, and P. R. Kramer, "Corrections to Einstein's relation for Brownian motion in a tilted periodic potential," *Journal of Statistical Physics*, vol. 150, pp. 776–803, 2013. doi: 10.1007/s10955-013-0692-1.

[60] J. L. Lebowitz and H. Spohn, "A Gallavotti-Cohen-type symmetry in the large deviation functional for stochastic dynamics," *Journal of Statistical Physics*, vol. 95, pp. 333–365, 1999.

[61] F. Legoll and T. Lelièvre, "Effective dynamics using conditional expectations," *Nonlinearity* **23** (2010), 2131–2163. DOI: 10.1088/0951-7715/23/9/006.

[62] Y.-H. Liao, Second Law-abiding account of heat engines in active bath, Zenodo data release (2025). DOI: 10.5281/zenodo.17681574.

[63] Y.-H. Liao, J. V. Ang, P.-Y. Lai, and Y. Jun, Second law-abiding-account of heat engines in active bath, *Physical Review Research* **8** (2026), 023136. DOI: 10.1103/2yzz-mq4r.

[64] R. Loll, On the diffeomorphism commutators of lattice quantum gravity, *Classical and Quantum Gravity* **15** (1998), 799–809. https://doi.org/10.1088/0264-9381/15/4/008.

[65] J. Loschmidt, "Über den Zustand des Wärmegleichgewichtes eines Systems von Körpern mit Rücksicht auf die Schwerkraft," *Sitzungsberichte der Kaiserlichen Akademie der Wissenschaften*, vol. 73, pp. 128–142, 1876.

[66] J. Louko and A. Molgado, Group averaging in the (p, q) oscillator representation of $\mathrm{SL}(2, \mathbb{R})$, *Journal of Mathematical Physics* **45** (2004), 1919–1943. https://doi.org/10.1063/1.1689001.

[67] J. Maas, "Gradient flows of the entropy for finite Markov chains," *Journal of Functional Analysis*, vol. 261, pp. 2250–2292, 2011.

[68] S. Machlup and L. Onsager, "Fluctuations and irreversible process. II. Systems with kinetic energy," *Physical Review*, vol. 91, pp. 1512–1515, 1953.

[69] C. Maes and K. Netočný, "Time-Reversal and Entropy," *Journal of Statistical Physics* **110** (2003), 269–310. DOI: 10.1023/A:1021026930129.

[70] J. W. Maluf, The teleparallel equivalent of general relativity, *Annalen der Physik* **525** (2013), 339–357. https://doi.org/10.1002/andp.201200272.

[71] S. P. Meyn and R. L. Tweedie, *Markov Chains and Stochastic Stability*, 2nd ed. Cambridge University Press, 2009.

[72] A. Mielke, M. A. Peletier, and D. R. Michiel Renger, "On the Relation between Gradient Flows and the Large-Deviation Principle, with Applications to Markov Chains and Diffusion," *Potential Analysis* **41** (2014), 1293–1327. DOI: 10.1007/s11118-014-9418-5.

[73] A. Mielke, M. A. Peletier, and J. Zimmer, "Deriving a GENERIC system from a Hamiltonian system," *Archive for Rational Mechanics and Analysis* **249** (2025), article 62. DOI: 10.1007/s00205-025-02119-7.

[74] A. T. Mohite and H. Rieger, "Thermodynamic length in stochastic thermodynamics of far-from-equilibrium systems: Unification of fluctuation relation and thermodynamic uncertainty relation," *Physical Review E*, vol. 114, 014103, 2026. doi: 10.1103/fmlt-px9y.

[75] H. Mori, "Transport, collective motion, and Brownian motion," *Progress of Theoretical Physics*, vol. 33, pp. 423–455, 1965.

[76] Y. Murashita, K. Funo, and M. Ueda, "Nonequilibrium equalities in absolutely irreversible processes," *Physical Review E*, vol. 90, 042110, 2014. doi: 10.1103/PhysRevE.90.042110.

[77] E. Nelson, "Derivation of the Schrodinger equation from Newtonian mechanics," *Physical Review*, vol. 150, pp. 1079–1085, 1966.

[78] M. E. J. Newman and G. T. Barkema, *Monte Carlo Methods in Statistical Physics*. Oxford University Press, 1999.

[79] F. W. J. Olver, D. W. Lozier, R. F. Boisvert, and C. W. Clark (eds.), *NIST Handbook of Mathematical Functions*, Cambridge University Press, Cambridge, 2010. Online companion: *NIST Digital Library of Mathematical Functions*, Sections 10.32 and 10.40. https://dlmf.nist.gov/10.40.

[80] L. Onsager, "Reciprocal relations in irreversible processes. I," *Physical Review*, vol. 37, pp. 405–426, 1931.

[81] L. Onsager, "Reciprocal relations in irreversible processes. II," *Physical Review*, vol. 38, pp. 2265–2279, 1931.

[82] L. Onsager and S. Machlup, "Fluctuations and irreversible processes," *Physical Review*, vol. 91, pp. 1505–1512, 1953.

[83] H. C. Öttinger, "General projection operator formalism for the dynamics and thermodynamics of complex fluids," *Physical Review E*, vol. 57, pp. 1416–1420, 1998. doi: 10.1103/PhysRevE.57.1416.

[84] H. C. Öttinger and M. Grmela, "Dynamics and thermodynamics of complex fluids. II. Illustrations of a general formalism," *Physical Review E*, vol. 56, pp. 6633–6655, 1997. doi: 10.1103/PhysRevE.56.6633.

[85] G. A. Pavliotis, *Stochastic Processes and Applications: Diffusion Processes, the Fokker-Planck and Langevin Equations*. Springer, 2014.

[86] H. Poincaré, "Sur le probleme des trois corps et les equations de la dynamique," *Acta Mathematica*, vol. 13, pp. 1–270, 1890.

[87] K. Prabhu and L. C. Stein, Black hole scalar charge from a topological horizon integral in Einstein-dilaton-Gauss-Bonnet gravity, *Phys. Rev. D* **98** (2018), 021503. https://doi.org/10.1103/PhysRevD.98.021503.

[88] I. Prigogine, "Moderation et transformation irreversible des systemes ouverts," *Bulletin de la Classe des Sciences, Academie Royale de Belgique*, vol. 31, pp. 600–606, 1945.

[89] P. Reimann, C. Van den Broeck, H. Linke, P. Hänggi, J. M. Rubí, and A. Pérez-Madrid, "Diffusion in tilted periodic potentials: Enhancement, universality, and scaling," *Physical Review E*, vol. 65, 031104, 2002. doi: 10.1103/PhysRevE.65.031104.

[90] F. Riesz, "Über lineare Funktionalgleichungen," *Acta Mathematica*, vol. 41, pp. 71–98, 1916. doi: 10.1007/BF02422940.

[91] H. Risken, *The Fokker–Planck Equation: Methods of Solution and Applications*, 2nd ed., Springer Series in Synergetics, vol. 18. Springer, 1996. doi: 10.1007/978-3-642-61544-3.

[92] M. Röckner and B. Schmuland, "Quasi-regular Dirichlet forms: examples and counterexamples," *Canadian Journal of Mathematics*, vol. 47, pp. 165–200, 1995.

[93] D. Santolin, N. Freitas, M. Esposito, and G. Falasco, "Bridging Freidlin–Wentzell large deviations theory and stochastic thermodynamics," *Physical Review E*, vol. 111, 024106, 2025. doi: 10.1103/PhysRevE.111.024106.

[94] U. Seifert, "Entropy production along a stochastic trajectory and an integral fluctuation theorem," *Physical Review Letters*, vol. 95, 040602, 2005. doi: 10.1103/PhysRevLett.95.040602.

[95] U. Seifert, "Stochastic thermodynamics, fluctuation theorems and molecular machines," *Reports on Progress in Physics*, vol. 75, 126001, 2012. doi: 10.1088/0034-4885/75/12/126001.

[96] M. H. Stone, "On one-parameter unitary groups in Hilbert space," *Annals of Mathematics*, vol. 33, no. 3, pp. 643–648, 1932. https://doi.org/10.2307/1968538.

[97] R. L. Stratonovich, *Topics in the Theory of Random Noise*, vol. II, revised English ed., translated by R. A. Silverman. Gordon and Breach, 1967.

[98] D. W. Stroock and S. R. S. Varadhan, "On the support of diffusion processes with applications to the strong maximum principle," in *Proceedings of the Sixth Berkeley Symposium on Mathematical Statistics and Probability*, vol. III, pp. 333–359, University of California Press, 1972.

[99] H. F. Trotter, On the product of semi-groups of operators, *Proceedings of the American Mathematical Society* **10** (1959), 545–551. https://doi.org/10.1090/S0002-9939-1959-0108732-6.

[100] C. Van den Broeck and M. Esposito, "Three faces of the second law. II. Fokker-Planck formulation," *Physical Review E*, vol. 82, 011144, 2010. doi: 10.1103/PhysRevE.82.011144.

[101] H. Vaquero del Pino, F. Gay-Balmaz, H. Yoshimura, and L. Y. Chew, "Variational formulation of stochastic thermodynamics: Finite-dimensional systems," *Physical Review E*, vol. 113, 054107, 2026. doi: 10.1103/xrbh-7fhd.

[102] C. Villani, *Hypocoercivity*, Memoirs of the American Mathematical Society, vol. 202, no. 950. American Mathematical Society, 2009.

[103] Z.-W. Wang and S. L. Braunstein, "Logarithmic Sobolev inequality and hypercontractivity for the Navier-Stokes Fokker-Planck operator," arXiv:2606.03182, 2026.

[104] X. Xing, "Foundation for Stochastic Thermodynamics via the Microcanonical Ensemble," *Journal of Statistical Physics* **193** (2026), article 26. DOI: 10.1007/s10955-026-03580-8.

[105] J. Yong and X. Y. Zhou, *Stochastic Controls: Hamiltonian Systems and HJB Equations*. Springer, 1999.

[106] E. Zermelo, "Über einen Satz der Dynamik und die mechanische Warmetheorie," *Annalen der Physik*, vol. 57, pp. 485–494, 1896.

[107] Q. Zhang and Y. Lu, "Entropy production rate and time-reversibility for general jump diffusions on $\mathbb{R}^n$," *Chaos*, vol. 35, 103104, 2025. doi: 10.1063/5.0293862.

[108] R. Zwanzig, "Memory effects in irreversible thermodynamics," *Physical Review*, vol. 124, pp. 983–992, 1961.

[109] R. Zwanzig, "Nonlinear generalized Langevin equations," *Journal of Statistical Physics*, vol. 9, pp. 215–220, 1973. doi: 10.1007/BF01008729.

Shipei Hu

College of Finance and Mathematics, West Anhui University, Lu'an, Anhui 237012, China

E-mail: hushipei@126.com